

2003

Hidden in the sands of time: geoarchaeology of sandstone landscapes in the Keep River region, Northern Territory, Australia

Ingrid A. Ward
University of Wollongong

Follow this and additional works at: <https://ro.uow.edu.au/theses>

University of Wollongong

Copyright Warning

You may print or download ONE copy of this document for the purpose of your own research or study. The University does not authorise you to copy, communicate or otherwise make available electronically to any other person any copyright material contained on this site.

You are reminded of the following: This work is copyright. Apart from any use permitted under the Copyright Act 1968, no part of this work may be reproduced by any process, nor may any other exclusive right be exercised, without the permission of the author. Copyright owners are entitled to take legal action against persons who infringe their copyright. A reproduction of material that is protected by copyright may be a copyright infringement. A court may impose penalties and award damages in relation to offences and infringements relating to copyright material.

Higher penalties may apply, and higher damages may be awarded, for offences and infringements involving the conversion of material into digital or electronic form.

Unless otherwise indicated, the views expressed in this thesis are those of the author and do not necessarily represent the views of the University of Wollongong.

Recommended Citation

Ward, Ingrid A, Hidden in the sands of time: geoarchaeology of sandstone landscapes in the Keep River region, Northern Territory, Australia, PhD thesis, School of Geosciences, University of Wollongong, 2003. <http://ro.uow.edu.au/theses/352>

**HIDDEN IN THE SANDS OF TIME:
GEOARCHAEOLOGY OF SANDSTONE LANDSCAPES
IN THE KEEP RIVER REGION,
NORTHERN TERRITORY, AUSTRALIA.**

**A thesis submitted in fulfilment of the
requirements for the award of the degree**

Doctor of Philosophy

From

UNIVERSITY OF WOLLONGONG

By

Ingrid Alexandra Kirsten Ward, M.A, M.Sc, Grad. Dip.

School of Geosciences

2003



CERTIFICATION

I, Ingrid Alexandra Kirsten Ward, declare that this thesis, submitted in fulfilment of the requirements for the award of Doctor of Philosophy, in the School of Geosciences, University of Wollongong, is wholly my own work unless otherwise referenced or acknowledged. The document has not been submitted for qualifications at any other academic institution.

Ingrid Alexandra Kirsten Ward

February 2003

TABLE OF CONTENTS

Table of Contents	iii
List of Figures	xi
List of Tables	xxvii
Abstract	xxx
Acknowledgements	xxxii

CHAPTER ONE

Introduction

1.1	Geoarchaeology of the Keep River Region	1
1.2	Regional Geoarchaeological Context	2
1.3	Geographical Context	5
1.4	Local Archaeological Context	7
1.5	Research Strategy and Thesis Aims	12

CHAPTER TWO

Literature Review: Perspectives on a Geoarchaeological Approach to Current Issues in Australian Archaeology

2.1	Introduction	14
2.2	History of Geoarchaeology in Australian Archaeology	15
2.3	Quantifying Change	17
2.3.1	Cosmogenic Isotope Dating	18
2.3.2	Luminescence Dating	20
2.3.3	Radiocarbon Dating	22
2.4	Identifying Change	23
2.4.1	Sediment Characterisation	23

2.4.2	Bioturbation	25
2.5	Interpreting Change	27
2.5.1	Cultural versus Natural Processes and Deposits	27
2.5.2	Rock shelters	31
2.5.3	Open sites	33
2.6	Geoarchaeology of Northern Australia	35
2.6.1	Geoarchaeological problems in the Keep River Region	36
2.7	Conclusions	37

CHAPTER THREE

Regional Setting

3.1	Introduction	38
3.2	Geological Setting	38
3.2.1	Bedrock Geology	38
3.2.2	Soils and Sediments	42
3.3	Geomorphological Setting	44
3.3.1	Late Pleistocene (100 – 10 ka)	44
3.3.1.1	Last Glacial Maximum (25 – 18 ka)	44
3.3.2	Holocene (10 – present)	46
3.3.3	Present	47
3.4	Vegetation	49
3.5	Palaeoclimate	50
3.5.1	Late Pleistocene (100 – 10 ka)	51
3.5.1.1	Last Glacial Maximum (25 – 18 ka)	53
3.5.2	Holocene (10 ka - present)	54
3.5.3	Present	57
3.6	Topographic Setting and Study Area	58
3.6.1	Local Topography	58

3.6.2	Aerial Photography	59
3.7	Sampling Strategy	62
3.8	Conclusion	63

CHAPTER FOUR

In Situ Cosmogenic Isotope Dating of Escarpment and Sand Sheets

4.1	Introduction	64
4.2	<i>In Situ</i> Cosmogenic Isotope Dating	64
4.2.1	Exposure Dating – Theory and Equations	65
4.2.2	Burial Dating – Theory and Equations	70
4.2.3	Modelling Accumulation (Partially Shielded Burial)	71
4.2.4	<i>In Situ</i> Cosmogenic Dating and Sand Sheet Formation	76
4.3	Methodology	78
4.3.1	Field Sampling	78
4.3.2	Sample Chemistry and AMS Measurement	81
4.4	Results	83
4.4.1	Bedrock	83
4.4.2	Sand Sheet Sediments	85
4.5	Discussion	90
4.5.1	Landscape Weathering over the Past 200 ka	90
4.5.2	Sand Sheet Evolution	94
4.6	Validating Erosion and Accumulation Rates from Cosmogenic Dating	97
4.7	Geoarchaeological Implications	99
4.8	Conclusions	100

CHAPTER FIVE

Sediment Characterisation and Site Formation

5.1	Introduction	102
5.2	Methodology	104
5.3	Results	108
5.3.1	Sediment Macrostratigraphy	108
5.3.1.1	Rock shelters	108
5.3.1.2	Sand sheets	112
5.3.1.3	Creeks	116
5.3.2	Sediment Micromorphology	120
5.3.2.1	Bedrock	120
5.3.2.2	Sand Sheets	121
5.3.2.3	Creeks	126
5.3.3	Sediment Geochemistry	129
5.3.3.1	Bedrock and Rubble Geochemistry	129
5.3.3.2	Rock Shelter Geochemistry	131
5.3.3.3	Sand sheet Geochemistry	131
5.3.3.4	Creek Geochemistry	133
5.4	Discussion	134
5.4.1	Depositional Processes – Source and Transport Processes	134
5.4.2	Environment of Deposition (Site Formation)	137
5.4.3	Post-Depositional (Diagenetic) Processes	139
5.4.3.1	Sediment Colour	139
5.4.3.2	Mottles and Concretions	143
5.5	Conclusion	146

CHAPTER SIX

Luminescence Dating

6.1	Introduction	148
6.2	Geoarcheological Application of Luminescence Dating in the Keep River Region	148
6.3	Luminescence Dating Theory	151
6.3.1	Determining Palaeodose	152
6.3.2	Determining Dose Rate	154
6.4	Methodology	156
6.4.1	Field Work	156
6.4.2	Laboratory Work	157
6.4.2.1	Palaeodose	158
6.4.2.2	Dose Rate Measurements	159
6.5	Results	169
6.5.1	Thermoluminescence (TL) dating	160
6.5.2	Optically Stimulated Luminescence (OSL) dating	166
6.5.2.1	Palaeodose	166
6.5.2.2	Dose Rate	177
6.5.3	Comparison of TL and OSL results	179
6.5.4	U-series dating of pisolites	184
6.5.5	Age-depth Curves	185
6.6	Discussion	187
6.6.1	Sedimentation Rates and Processes	187
6.6.2	Chronostratigraphy	189
6.6.2.1	Chronostratigraphy of the Sand Sheets	189
6.6.2.2	Chronostratigraphy of Karlinga Creek and Sandy Creek	194
6.6.2.3	Chronostratigraphy of the Rock shelter excavations	196
6.7	Conclusions	199

CHAPTER SEVEN

Connecting the Local and Regional Records

7.1	Introduction	200
7.2	Quantifying Change - Comparison of Chronological Records	200
7.2.1	Comparison of <i>in situ</i> Cosmogenic and Luminescence Dating Results	201
7.2.2	Comparison of Radiocarbon and Luminescence Dating Results	203
7.3	Identify Change	206
7.3.1	Depositional Resolution	206
7.4	Interpreting Change	209
7.4.1	Cultural versus Natural Processes - The Stone Tool Record	209
7.4.2	Rock Shelters - The Rock Art Record	213
7.4.3	Open Sites – The Climatic Record	215
7.5	Continuity and Discontinuity in the Keep River Region	217
7.6	Placing the Keep River Record into a Regional Perspective	219
7.6.1	Age-depth Curves for the Kimberley and Arnhem Land region	219
7.6.2	The Holocene Record and Intensification	221
7.6.3	The Pleistocene Record and the east Kimberley Refuge	224
7.7	Conclusions	226

CHAPTER EIGHT

Conclusions and Suggestions for Further Research

8.1	Introduction	228
8.2	Summary and Major Conclusions	228
8.3	Suggestions for Further Research	233
8.3.1	Regional Environment	233
8.3.2	<i>In Situ</i> Cosmogenic Dating	234

8.3.3	Luminescence Dating	235
8.3.4	Sediment Characterisation	236
8.3.5	Archaeological Comparisons	237

REFERENCES		238
-------------------	--	-----

APPENDIX

A1	SURVEYING	
A1.1	Surveying	A1
A2	COSMOGENIC ISOTOPE DATING	
A2.1	ANSTO Sample Forms	A2
A2.2	Chemistry Results	A5
A2.3	AMS Radioisotope Results for ¹⁰ Be for all Bedrock and Sediment Samples	A6
A2.4	AMS Radioisotope Results for ²⁶ Al for all Bedrock and Sediment Samples	A6
A3	SEDIMENT CHARACTERISATION	
A3.1	Petrographic Descriptions	A8
A3.2	Soil Micromorphology	A14
A3.2.1	Chemical Mapping (SEM/EDXA)	A15
A3.3	Mineralogy (XRD)	A15
A3.4	Grain size Analyses	A16
A3.4.1	Methods	A16
A3.4.2	Grain Size Results	A17
A3.4.3	Statistical Analysis of Grain size Results	A23
A3.5	Geochemistry	A25
A3.5.1	X-ray Fluorescence (XRF) Results	A25
A3.5.2	Statistical Analysis of Geochemistry Results	A27

A3.5.3	Graphical Comparison of Grain Size and Geochemistry.	A34
A4	LUMINESCENCE DATING	
A4.1	Field Sampling	A38
A4.2	Thermoluminescence (TL) Determinations	A39
A4.3	Optically Stimulated Luminescence (OSL) Determinations	A41
A4.3.1	Preparatory grain-size separation and grain-mounting	A41
A4.3.2	Palaeodose Determinations	A41
A4.3.3	OSL Results	A46
A4.4	Dose Rate Determinations	A82
A4.4.1	Methods	A82
A4.4.2	Raw Results for U and Th Analyses	A83
A4.4.3	U-series dating of pisolites	A84
A5	ARCHAEOLOGY	
A5.1	Radiocarbon Analyses	A88
A5.2	Stone Artefact Records	A89
A6	PUBLICATIONS	
A6.1	Ward, I. and Larcombe, P. (2003) A Process-Orientated Approach to Archaeological Site Formation: Application to Semi-Arid Northern Australia. <i>Journal of Archaeological Science</i> , 30, 1223-1236.	A92

LIST OF FIGURES

CHAPTER ONE

Figure 1.1	Possible migration routes into Australia based on earliest evidence of Homo sapiens from archaeological sites and evidence for impact on the vegetation in palaeoecological sites from southeast Asian and northern Australia (from Kershaw et al., 2002), showing location of the Keep River region. Extended landmass shaded to -150 m contour.	3
Figure 1.2	Location of Keep River (red) and other major archaeological and rock-shelter sites throughout northern Australia.	4
Figure 1.3	NASA Satellite image of the Keep River region, including Lake Argyle (sourced from http://eol.jsc.nasa.gov/ Image No. STS41C-52-2562).	5
Figure 1.4	Location of the three main archaeological sites (Jinmium, Goorurarmum, and Karlinga) and the non-archaeological site (Sandy Creek Gorge) along the Keep River catchment, and bounded by the larger catchments of the Ord River and Victoria River.	6
Figure 1.5	Location of the archaeological site areas in relation to the expanding Ord River Irrigation Area (ORIA).	7
Figure 1.6	Path of the Djibigun dreaming track through the Keep River region, which begins in the north-west at Biwinjar, passes through Granilpi, across the Keep River and Sandy Creek to Jinmium where it ends.	8
Figure 1.7	Examples of different styles of paintings found in the Keep River region, including (a) “Keep River Bradshaw” (Tacon et al., 1999) at Karlinga, (b) animal stencils at Granilpi, (c) figures at Granilpi, and (d) superimposed figures at Karlinga.	10
Figure 1.8	Examples of different styles of pictographs found in the Keep River region, including (a) rings or circles at Karlinga, (b) scratches at Karlinga, (c) cupules at Jinmium, and (d) pecks depicting animal figures at Karlinga.	11

CHAPTER TWO

- Figure 2.1 Dynamic denudation model modified from Johnson (2002: 18, his Figure 1), wherein biotic processes, together with geomorphic and anthropogenic processes, contribute to landform evolution. Artefacts are depicted as filled shapes. Examples of processes that may disturb the distribution of artefacts include: (i) erosion of surface soils, leading to redistribution downslope of sediment and artefact material, (ii) constant subsurface bioturbations, (iii) intermittent mound building and upward displacement of sediments and artefacts, (iv) hydrological translocation processes within the sediment, (v) formation and integration of artefacts into stone lines, and (vi) disturbance of surface and buried artefacts by tree fall or decay. 25
- Figure 2.2 Alternative interpretation of trends in time-series graphs, presented in comparison to (a) the original graph of apparent stratigraphic unconformities in northern Australian rock-shelters by Smith and Sharp (1993). Such a trend is also typical of a bioturbation profile, as presented by (b) Du et al. (1998), their Fig. 2, and (c) artefact and gastroliths depth profiles from western Illinois (after Van Nest, 2002, her Fig. 5). 26

CHAPTER THREE

- Figure 3.1 Drainage basins in north-central and north-western Australia around 18 ky BP, showing the Keep River region flanked by the adjacent Kimberley and Arnhem Land regions (from Lewis, 1988, his Map 4). 39
- Figure 3.2 Geology of the Keep River region, combining the Cambridge Gulf (Sheet 5214, BMR 1970) and Auverne (Sheet 5215, BMR 1975) 1: 250 000 mapsheets. Project area and major site locations are marked. 40
- Figure 3.3 The dominant escarpment of Walujapi, a female black-headed Python (*Aspidites melanocephalus*). 42
- Figure 3.4 Location of the Keep River (indicated by arrow) in relation to the changing shoreline around the Joseph Bonaparte Gulf at 18 ¹⁴C kyr BP (LGM), 12 ¹⁴C kyr BP, and 6 ¹⁴C kyr BP (from Yosukame et al., 2001; their Fig. 5).

	Bathymetric and topographic contours are indicated by changes in colour scheme, and show the depth increase from 0 m, to 25 m to 50 m depth near the mouth of the Keep River.	45
Figure 3.5	Submarine topography of Joseph Bonaparte Gulf, determined from high resolution aeromagnetic surveys as part of the North West Margins Project at AGSO (http://www.agso.gov.au/marine/nws/).	46
Figure 3.6	Photograph of small delta fan in the north-west corner of the Goorurarmum amphitheater, made obvious by the new growth of Spinifex grass after the 2000 wet season. Aerial photo of Goorurarmum, Jinnium and Sandy Creek Gorge.	48
Figure 3.7	Cross-sections across the planned Ord River Irrigation Area, showing a stratigraphic section from the Keep River to Sandy Creek (T - T'), and from Border Creek to the Keep River (S - S'). Although oversimplified, these depictions indicate that the average thickness of the sand sheet is less than 5 m thick, and are laterally discontinuous.	48
Figure 3.8	Palaeoclimatic and palaeoenvironmental information for northern Australia, modified from White (1994) and based on information from 1. Bowler et al (2001), 2. Chen et al. (1995), 3. DeDeckker (1986), 4. Head (1996), 5. Kershaw (1995), 6. McConnell and O'Connor (1997), 7. Schulmeister (1992), 8. Tacon and Brockwell (1995), and 9. van der Kaars (1991).	52
Figure 3.9	Palaeoclimatic data for the period prior to and following the Pleistocene-Holocene transition in northern Australia and New Guinea, modified from CLIMANZ (http://rses.anu.edu.au/enproc/AQUADATA/archive.html).	54
Figure 3.10	Average rainfall and temperature for Kununurra (sourced from http://www.bom.gov.au/climate/averages/ , 2001).	57
Figure 3.11	Topographic map of Keep River region indicating the project area and major site locations. Enlargement of the Karlinga and of the Jinnium-Sandy Creek catchment area is given in Figure 3.12.	58
Figure 3.12	Topographic map of project area showing major site locations of Karlinga, Jinnium, Goorurarmum and Sandy Creek Gorge.	59
Figure 3.13a	Aerial photo of the area around the archaeological site of Goorurarmum, and the non-archaeological sites of Sandy Creek, and Sandy Creek Gorge.	60

Figure 3.13b	Aerial photo of the Weaber Ranges, showing location of the archaeological sites or Karlinga (KR36), Karlinga North, and the creek site near KR99.	62
 CHAPTER FOUR		
Figure 4.1	Theoretically calculated variation in the ratios of ^{10}Be and ^{26}Al concentration as a function of ^{10}Be concentration for unit nuclide production rates (atom/g/yr) (modified from Lal, 1991). Surfaces with different erosion rates plot in the shaded area, termed the <i>steady-state erosion island</i> . Lines running diagonally represent lines of burial such that with sufficient burial there is zero production ($P = 0$). Samples which have undergone cyclic periods of burial and exposure fall below the curve in the complex exposure zone.	68
Figure 4.2	Possible exposure histories for rocks sampled for in situ cosmogenic dating studies (modified from Dorn and Phillips, 1991), including (a) multiple cycles of exposure through erosion and burial, (b) constant centimetre-scale erosion of exposed landforms through physical weathering processes, (c) episodic large-scale mass wasting of exposed landforms, and (d) human abrasion of exposed rocks, such as engraving or tool making.	70
Figure 4.3	Theoretical patterns of nuclide depth profiles assuming (a) zero sedimentation ($C_{0(x=0)}$), (b) varying erosion rate, and (c) varying sedimentation rate (modified from Fink et al., 2000; Phillips, 2000). The model curves assume values for production of ^{10}Be and ^{26}Al scaled to the latitude (15.43°S) and altitude (10 m) of the Keep River region. Refer text for explanation.	74
Figure 4.4	Ratio of muon and neutron input for the extremes of zero erosion ($E = 0 \text{ mm.ka}^{-1}$) and high erosion ($E = 200 \text{ mm.ka}^{-1}$), indicating the dominance of muon-induced production (i.e. $C_{\text{muons}}/C_{\text{neutrons}} > 1$) only over depths greater than about 5 m (shown by arrows) (from David Fink, pers. comm., 2002).	76
Figure 4.5	Location map of cosmogenic sample sites, including bedrock samples (COS-G2, G4, J1, J2, K1 and K5) and sediment samples from the Jinmium sand sheet (JG1 and JG2).	79

Figure 4.6	Photograph of three of the bedrock samples (a) COS-J1, (b) COS-G2, and (c) COS-K1 collected for <i>in situ</i> cosmogenic dating. Samples were taken from horizontal surfaces with different forms of weathering.	80
Figure 4.7	$^{26}\text{Al}/^{10}\text{Be}$ ratio diagram indicating position of bedrock samples generally within the steady-state erosion island (see text for further explanation).	84
Figure 4.8	Plot of $^{26}\text{Al} / ^{10}\text{Be}$ ratios for bedrock samples, and sediment samples from auger cores JG1 and JG2 on steady-state erosion island diagram. The position of the auger samples below the steady-state curve indicates that cores samples have not undergone cycles of burial and exposure.	85
Figure 4.9	Measured radionuclide concentrations for (a) ^{10}Be and (b) ^{26}Al for the two cores JG1 and JG2, plotted against model profiles for sedimentation rates of 5, 10, 20 and 50 mm.k^{-1} , using C_0 calculated from the average bedrock erosion rate (E_{ave}). Refer text for explanation.	89
Figure 4.10	Landslip off the Goorurarmum escarpment that occurred sometime after the 2000 wet season, looking towards Sandy Creek Gorge.	92
Figure 4.11	Seepage of water through several metres of bedrock was evident several months after the end of the 2000 wet season, indicating the likely gradual saturation and disintegration of the bedrock through chemical weathering.	93
Figure 4.12	Hypothetical reconstruction of sand sheet evolution. Initial accretion of sand sheets over an exposed pediment occurs through deep weathering and erosion of the escarpment. Subsequent vertical accretion may occur through (a) gradual accumulation of sand, (b) episodic events of erosion and sand deposition, or (c) autochthonous weathering. Human occupation may occur during any period of relative landscape stability or instability. Refer text for further explanation.	96

CHAPTER FIVE

Figure 5.1	(a) Location of sample sites around Jinnium, Goorurarmum and Sandy Creek Gorge, (contours from topographic maps) and (b) detailed map and contour survey of the Goorurarmum sand sheet and main rock shelter site (KR31). Areas shaded in brown, pink and blue represent bedrock, scree slope and swampland respectively.	105
Figure 5.2	(a) Location of sample sites around Karlinga (contours from topographic map), and (b) detailed map and contour survey of the sand sheet and main rock-shelter site (KR36). Areas shaded in brown and pink represent bedrock and scree slope respectively.	106
Figure 5.3	Photograph of slumped material over the top of horizontal stratigraphic horizons at the site of KR99CP.	107
Figure 5.4	Profiles for the Jinnium C1 rock shelter. Dates are sourced from Fullagar et al. (1996) and Roberts et al. (1998a), and artefact numbers were kindly supplied by R. Fullagar (pers. comm., 2001).	109
Figure 5.5	Profiles for the Goorurarmum, the rock shelter excavation. Luminescence dates are derived from Chapter Six, and radiocarbon dates are detailed in Chapter Seven. Artefact numbers were kindly supplied by R. Fullagar (pers. comm., 2001).	110
Figure 5.6	Profiles for the Karlinga rock shelter excavation. Luminescence dates are derived from Chapter Six, and radiocarbon dates are detailed in Chapter Seven. Artefact numbers were kindly supplied by R. Fullagar (pers. comm., 2001).	111
Figure 5.7	Profiles for the Goorurarmum sand sheet excavation. Luminescence dates are derived from Chapter Six, and radiocarbon dates are detailed in Chapter Seven. Artefact numbers were kindly supplied by R. Fullagar (pers. comm., 2001).	113
Figure 5.8	Profiles for the Karlinga sand sheet excavation. Luminescence dates are derived from Chapter Six, and radiocarbon dates are detailed in Chapter Seven. Artefact numbers were kindly supplied by R. Fullagar (pers. comm., 2001).	114

Figure 5.9	Profiles of the creek near the site of KR99. Luminescence dates are derived from Chapter Six.	117
Figure 5.10	Profiles of the creek at Sandy Creek Gorge. Luminescence dates are derived from Chapter Six.	118
Figure 5.11	An indurated silicate horizon situated adjacent to the main creek bank profile at Sandy Creek Gorge (refer text for further description).	119
Figure 5.12	Thin section of escarpment bedrock sampled from (a and b) Goorurarmum, (c - e) Karlinga and (f) Jinmium (scale bar = 250 μ m).	120
Figure 5.13	Thin section of Goorurarmum (Goor-1) sand sheet sediments, taken at 75 cm, 120 cm, and 175 cm respectively (scale bar = 100 μ m).	122
Figure 5.14	Thin section of the Karlinga (Karl-3) sand sheet sediments, taken at 100 cm and 240 cm respectively (scale bar = 100 μ m). Inset shows limonite staining in sediment matrix, which may indicate the process of rubefaction (reddening).	123
Figure 5.15	Post depositional formation of iron-clay cutans as evidenced from the contrasting images of quartz grains (a) before burial, and (b) after burial. Inset of (b) shows a cross-section of a quartz grain highlighting the Fe ₂ O ₃ - and Al ₂ O ₃ - rich cutan.	124
Figure 5.16	General observation of deterioration of quartz grains from with burial depth in sand sheet profiles.	124
Figure 5.17	Example of shard-like grains sampled from the Karlinga (Karl-3) and Goorurarmum (Goor-1) excavations.	125
Figure 5.18	Cross section of pisolitic material taken from the base of the profile of auger JG4, near Jinmium. The sample has a thin crust and a matrix of poorly sorted quartz and clay.	126
Figure 5.19	Cross section of pisolitic material taken from the base of the profile of Sandy Creek Gorge. The sample has a thick crust, and a matrix of poorly sorted quartz and clay minerals.	126
Figure 5.20	Magnification (x 50) of indurated silicate material adjacent to Sandy Creek Gorge profile, showing the fine grained, iron-stained quartz surrounding larger degraded opaline-like clasts (scale bar = 100 μ m).	127

Figure 5.21	Thin section of the KR99CP sediments, taken at 95 cm, 180 cm, 255 cm and 340 cm respectively (scale bar = 100µm).	128
Figure 5.22	Triplot of major elements Al_2O_3 - Na_2O + CaO - K_2O for each of the four major sites and bedrock samples indicating obvious discrimination of the Sandy Creek Gorge sediments on the basis of high relative K_2O concentration. The enrichment of K_2O reflects the process of illitisation and is typical of clayey palaeosols (Retallack, 1990).	133
Figure 5.23	Grain size map, indicating typical grain size distribution for the different depositional sand sheet and mud flat environments.	135
Figure 5.24	Throughout the Keep River region, large slabs of bedrock can be observed in the process of mass exfoliation; this example has a petroglyph on the surface.	138
Figure 5.25	Salt (gypsum) weathering within the Goorurarmum (Goor-2) rock shelter, effecting mass exfoliation and disintegration of the shelter walls. The frequency of mass exfoliation of these sandstone surfaces may provide some indication of the age of the engraving.	139
Figure 5.26	Examples of the coloured sands found throughout the Keep River region, including the red sands around Jinmium (JG-1) and yellow sands overlying a red pisolitic horizon around Karlinga (KN-7).	142
Figure 5.27	Hypothetical interpretation of the present sedimentary features observed at Sandy Creek Gorge. A soil horizon(s) formed (a) initially under an ancient rainforest or vine thicket community undergoes (b) post-depositional burial gley of organic matter, dehydration of ferric oxyhydroxides, compaction and illitisation of smectite clay (modified from Retallack, 1990).	145

CHAPTER SIX

Figure 6.1	Stratigraphic sections of the north (C1/II and C1/III) and south (C1/III) faces of the Jinmium pit, adapted from Fullagar et al. (1996, Figs. 5 and 6). Crosses indicate TL dates (Fullagar et al., 1996), dots indicate single-grain OSL dates (Roberts et al., 1998a).	150
Figure 6.2	Stratigraphic section of the excavation pit C1/IV and auger hole 4 (A4) at Jinmium. Adapted from Fullagar et al. (1996, Fig. 7). Crosses indicate TL	

	dates (Fullagar et al., 1996).	150
Figure 6.3	Schematic diagrams illustrating theoretical OSL signal histories including (a) in situ decay of unbleached saprolite, (b) deposition of well-bleached over unbleached sediment sands, (c) deposition of well-bleached transported sediment, and (d) deposition of partially-bleached sediment (modified from Frederick et al., 2002). An understanding of the geomorphological context remains critical to differentiating luminescence history.	153
Figure 6.4	Examples of the temperature plateau for Goor-1 samples taken at 95 cm (W3033) and 155 cm (W3034). Note the foreshortened temperature plateau in W3033, which is similar to those found in samples from the original Jinnium rock shelter excavation (Fullagar et al., 1996).	162
Figure 6.5	Examples of differing second glow curves for Goorurarmum (W3033 and W3034), indicating differing provenance of the sedimentary material.	162
Figure 6.6	Examples of differing glow curves for auger samples KN-2 (W2973) and KN-3 (W2974), indicating a different provenance for sediments from these two sites.	164
Figure 6.7	Example of the stepped temperature plateau that is typical of the Sandy Creek sediments, this sample (W3044) was taken from Sandy Creek Gorge at 57 cm.	165
Figure 6.8	(a) Test dose OSL (T_r/T_n) ratios and (b) palaeodose estimates obtained at preheat temperatures ranging from 160 – 300°C using an SAR protocol applied to 24 single aliquots of quartz from the Goorurarmum rock shelter, and from four different depths (50, 100, 150, 220 cm) of the Goorurarmum sand sheet excavation. The dashed line in (a) corresponds to a unit test dose OSL ratio ($T_r/T_n = 1$) that indicates no change in sensitivity between the natural and regenerative cycles. The dashed lines in (b) correspond to the average palaeodose for each sample.	167
Figure 6.9	Radial plot of palaeodose estimates for the Goorurarmum rock shelter at 20 cm depth. Inset shows palaeodose estimates for a double-regenerative test using a single regenerative dose of 0.4 Gy on 12 aliquots using a mask size of 0.5 mm.	168

Figure 6.10	Radial plots of palaeodose estimates for the Goorurarmum sand sheet samples at 50, 100, 175 and 220 cm. Inset shows palaeodose estimates for double-regenerative test using a single regenerative dose of 1.5 Gy at 50 cm, 6.7 Gy at 175 cm, and 17.5 Gy at 220 cm.	169
Figure 6.11	Radial plot of palaeodose estimates for the Karlinga (Karl-1) rock shelter. Circles represent estimated palaeodose values using a single regenerative value ($D_e = R_1$), and the diamonds estimated palaeodose values using bracketed regenerative values ($R_1 < D_e < R_2$) for the SAR protocol. Inset shows palaeodose estimates for a double-regenerative test using a single regenerative dose of 18 Gy on 12 aliquots using a mask size of 0.5 mm.	171
Figure 6.12	As for 6.10, for samples from the Karlinga rock shelter (Karl-1 at 27 cm) and Karlinga sand sheet excavation (Karl-3) from depths of 90, 150, 210 and 240 cm.	172
Figure 6.13	Radial plot of palaeodose estimates for the Karlinga (Karl-3) sand sheet excavation. Circles represent estimated palaeodose values using a single regenerative value ($D_e = R_1$), and the diamonds estimated palaeodose values using bracketed regenerative values ($R_1 < D_e < R_2$) for the SAR protocol. Inset shows palaeodose estimates for a double-regenerative test for a regenerative dose of 25 Gy at 210 cm and 40 Gy at 240 cm.	173
Figure 6.14	Radial plot of palaeodose estimates for the Karlinga Creek site (KR99CP) at (a) 95 cm and (b) 320 cm.	174
Figure 6.15	As for 6.10, for samples taken from depths of 57, 126, 321 and 357 cm at Sandy Creek Gorge.	175
Figure 6.16	As for Figure 6.13 for samples from Sandy Creek Gorge at (a) 57, (b) 126, (c) 321 and (d) 357 cm. A regenerative dose of 4.7 Gy at 57 cm, 24.4 Gy at 321 cm and 40 Gy at 357 cm was used for double-regenerative tests (shown inset).	176
Figure 6.17	Comparison of TL and OSL palaeodose estimates. Samples should plot along the equilibrium line if there is a good correspondence between the two methods.	179
Figure 6.18	Palaeodose 'plateau test' for aliquots of sample KTL167 processed under red (filled triangle) and yellow (open circle) light from Roberts (1997: 854,	

	his figure 9(b)). Note the “double” or stepped plateau and partial erasure of 325°C peak under yellow illumination, compared to the full plateau under red illumination.	180
Figure 6.19	Comparative glow curves for two samples (a) Goor-1 at 220 cm and (b) SCG at 321 cm, exposed to red (red curve) and yellow light (yellow curve) for 3 hours. The latter sample has an initial stepped TL plateau. After 3 hours exposure to yellow illumination the 325°C peak is diminished relative to the sample exposed under red illumination. Refer text for details.	181
Figure 6.20	Results of exposure test undertaken on a sample from (a) Goor-1 at 220 cm and (b) SCG at 321 cm. Samples were exposed to yellow illumination for 1, 10, 100, 1000 and 10,000 seconds, respectively, and compared to a control sample exposed to red illumination for 10,000 seconds. A significant decrease in the palaeodose value is measured after 10,000 seconds exposure to yellow illumination. Refer text for details.	182
Figure 6.21	Isochron plot of U-series dating of pisolitic material from Jinmium and Sandy Creek Gorge, indicating an open and closed system for the former and latter sites respectively.	184
Figure 6.22	Age-depth curve for the sand sheets at Karlinga (Karl-3), Goorurarmum (Goor-1), Jinmium (Auger 4 and 5, from Fullagar et al., 1996), and for Sandy Creek Gorge. A line of best fit for all data shows a progressive increase in sedimentation from about 30 ka.	185
Figure 6.23	Age-depth curve combining all present and previously published (Fullagar et al., 1996) luminescence and U-series ages from the Keep River region. A line of best fit is drawn for the original Jinmium (C1) excavation, and another for all other data using (refer text for explanation).	186
Figure 6.24	Ages and archaeological evidence from the three sand sheet excavations with occupation records in the Keep River region, including Karlinga (Karl-3), Goorurarmum (Goor-1) (this study) and Jinmium (Auger 4) (Fullagar et al., 1996).	189
Figure 6.25	Chronostratigraphy of Jinmium - Goorurarmum transect (including dates from Fullagar et al., 1996).	192
Figure 6.26	Chronostratigraphy of Karlinga to Karlinga North transect.	193

Figure 6.27	Chronostratigraphy of Sandy Creek Gorge and Sandy Creek transect. It should be noted that the TL age estimates are mainly derived from stepped plateaux and therefore represent maximum values.	195
Figure 6.28	Ages and archaeological evidence from five rock-shelter excavations from past and present research in the Keep River region, including Karlinga (Karlinga-1), Goorurarmum (Goor-2) (this study), Punipunil (PP1), Granilpi (G1) (Atchison, 2000, Atchison et al., in prep.), and Jinmium (C1) (Fullagar et al., 1996; Roberts et al., 1998; Atchison et al., in prep.). The OSL ages for the Jinmium profile represent central age estimates from single-grain dating (from Roberts et al., 1998).	197

CHAPTER SEVEN

Figure 7.1	Equivalent plot to the regional age-depth curve depicted in Figure 6.23 (excluding Jinmium rock shelter ages), using a logarithmic axis for age (ka). The plot indicates a trend towards lower accumulation rates over longer term timescales.	202
Figure 7.2	Comparison of luminescence dates and radiocarbon dates (including Atchison, 2000; Roberts et al., 1998) for archaeological sites in the Keep River region over the past 20 ka. Note, radiocarbon ages do not exceed beyond 150 cm.	205
Figure 7.3	Profiles of (a) mean grain size and artefact (2 – 4 mm) numbers with depth in the Goorurarmum (Goor-1) sand sheet. Both these trends may reflect natural processes.	208
Figure 7.4	Plot of artefact accumulation rate against sedimentation rate (litres/100 years) for the archaeological excavation site of Goor-1. Artefact accumulation is measured both as the number of artefacts per unit time (closed diamonds) and density per unit time (open diamonds) and normalized against total volume of sediment. Numbers refer to the lowest age (ky BP) of each sediment interval. The circled points indicate the large	

	differences where there are low artefact numbers but a high artefact density (e.g. a single core stone).	210
Figure 7.5	As for Figure 7.4, for the archaeological excavation site of Karl-3. Note, for clarity, the rate of sedimentation is plotted on a log scale. Numbers refer to the lowest age (ky BP) of each sediment interval. The circled points indicate the large differences where there are low artefact numbers but a high artefact density (e.g. a single core stone).	211
Figure 7.6	Possible scenarios for sedimentation and rock art dating. Horizon 'w' represents a sterile surface, over which is deposited an archaeological horizon 'x' that is contemporaneous with the rock art surface. In scenario A, the archaeological horizon is eroded and a younger horizon 'z' is subsequently deposited over a now partially bleached horizon 'w'. Both horizons are distinct from the age of the rock art, and luminescence dating would result in the underestimation of its age. In scenario B, the younger horizon 'z' is deposited immediately over horizon 'x' but is subsequently eroded re-exposing horizon 'x'. Luminescence dating would again underestimate the age of the rock art.	214
Figure 7.7	Age-depth data for archaeological sites (rock-shelters and sand sheets) in the Kimberley and Arnhem Land regions (data from Atchison, 2000; Balme, 2000; Dortch and Roberts, 1996; Harrison and Frink, 2000; Morwood and Hobbs, 1995; McConnell and O'Connor, 1997; O'Connor, 1996).	220
Figure 7.8	Dated archaeological sites in the Kimberley and Arnhem Land region (data from Atchison, 2000; Balme, 2000; Dortch and Roberts, 1996; Harrison and Frink, 2000; Morwood and Hobbs, 1995; McConnell and O'Connor, 1997; O'Connor, 1996 and Walsh, 2000 and references therein). All ages are calibrated ¹⁴ C ages, or are marked by subscript as luminescence age (TL or OSL). Chronological gaps (stippled line) are defined as a cultural hiatus according to the authors, or as a question mark if unknown. The yellow band marks the period (~ 17 to 12 ky BP) where no ages have apparently been registered for northwest Australia (Veth, 1995: 744). The dated introduction of stone points (P) and adzes (A) are marked.	222

Figure 7.9	Location of the Keep River region in the context of the biogeographic refuge, defined by Veth (1989: 81) as an extensive system of piedmont/montane uplands and riverine gorges which provided reliable networks of water during the climatic oscillations of the last 40 ka.	225
------------	---	-----

APPENDIX FIGURES

Figure A3.1	Petrographic description of (a) auger cores (Gu-1 to 4) and excavation pits (Goor-1 and 2) taken within the Goorurarmum amphitheatre, and (b) auger cores (Gu-6 to 8) taken at ~ 1 km intervals north towards the coast.	A9
Figure A3.2	Petrographic description of auger cores taken north-west of Jinmium (JN-1 to 4) and between Jinmium and Goorurarmum (JG-1 to 5).	A10
Figure A3.3	Petrographic description of (a) the creek bank profile excavated adjacent to the archaeological site of KR99, and (b) auger cores (Ka-1 to 4) and excavation pit (Karl-1) taken within the Karlinga ampitheatre.	A11
Figure A3.4	Petrographic description of auger cores (KN-1 to 8) and the sand sheet excavation (Karl-3) taken north of Karlinga.	A12
Figure A3.5	Petrographic description of (a) auger cores (SC-1 to 3) taken adjacent to Sandy Creek, and (b) creek bank profile excavated at Sandy Creek Gorge.	A13
Figure A3.6	Sampling of sand sheet sediments using Kubiena tin pressed into soaked excavation pit wall (Goor-1).	A14
Figure A3.7	Profiles of grain size mode (black), < 60 µm (blue) and < 10 µm (red) and major element chemistry SiO ₂ (black), Al ₂ O ₃ (blue), K ₂ O (blue dashed), and LOI (black dashed) in (a) Goor-2 rock shelter excavation, (b) Goor-1 sand sheet excavation and (c) auger core JG-4.	A34
Figure A3.8	Profiles of grain size mode (black), < 60 µm (blue) and < 10 µm (red) and major element chemistry SiO ₂ (black), Al ₂ O ₃ (blue), K ₂ O (blue dashed), and LOI (black dashed) in (a) Jinmium (CI/1) rock shelter excavation and auger cores (b) Auger 5, and (c) JG-2.	A35

Figure A3.9	Profiles of grain size mode (black), < 60 μm (blue) and < 10 μm (red) and major element chemistry SiO_2 (black), Al_2O_3 (blue), K_2O (blue dashed), and LOI (black dashed) in the (a) Karl-1 rock shelter excavation, (b) Karl-3 sand sheet excavation, and (c) KR99 creek profile.	A36
Figure A3.10	Profiles of grain size mode (black), < 60 μm (blue) and < 10 μm (red) and major element chemistry SiO_2 (black), Al_2O_3 (blue), K_2O (blue dashed), and LOI (black dashed) in the (a) auger core SC-1 and (b) Sandy Creek Gorge (SCG) creek bank profile.	A37
Figure A4.1	Collection of luminescence samples involved gently hammering a PVC or steel tube (both depicted) into the excavation pit wall.	A38
Figure A4.2	Typical IR test result indicating no presence of peaks that would otherwise result from feldspar or heavy mineral contamination.	A42
Figure A4.3	Example of MARA plot (KARL-1-27), before and after sun bleaching, showing extrapolation of curve back to x-axis to estimate true palaeodose.	A43
Figure A4.4	Illustration of a radial plot with two hypothetical points that have different palaeodoses and associated uncertainties (from Galbraith et al., 1999: 356).	A46
Figure A4.5	OSL results for Goor-2 rock shelter excavation at 20 cm, including: (a) MARA test, (b) preheat plateau test, (c) sensitivity test, and (d) double-regenerative test.	A49
Figure A4.6	OSL results for Goor-1 sand sheet excavation at 50 cm, including: (a) MARA test, (b) preheat plateau test, (c) sensitivity test, and (d) double-regenerative test.	A51
Figure A4.7	OSL results for Goor-1 sand sheet excavation at 100 cm, including: (a) MARA test, (b) preheat plateau test, and (c) sensitivity test.	A53
Figure A4.8	OSL results for Goor-1 sand sheet excavation at 175 cm, including: (a) MARA test, (b) preheat plateau test, (c) sensitivity test, and (d) double-regenerative test.	A55
Figure A4.9	OSL results for Goor-1 sand sheet excavation at 220 cm, including: (a) MARA test, (b) preheat plateau test, (c) sensitivity test, and (d) double-regenerative test.	A57

Figure A4.10	OSL results for Karl-1 rock shelter excavation at 27 cm, including: (a) MARA test, (b) preheat plateau test, (c) sensitivity test, and (d) double-regenerative test.	A59
Figure A4.11	OSL results for Karl-3 sand sheet excavation at 90 cm, including: (a) MARA test, (b) preheat plateau test, (c) sensitivity test, and (d) double-regenerative test.	A62
Figure A4.12	OSL results for Karl-3 sand sheet excavation at 150 cm, including: (a) MARA test, (b) preheat plateau test, and (c) sensitivity test.	A64
Figure A4.13	OSL results for Karl-3 sand sheet excavation at 210 cm, including: (a) MARA test, (b) preheat plateau test, (c) sensitivity test, and (d) double-regenerative test.	A66
Figure A4.14	OSL results for Karl-3 sand sheet excavation at 240 cm, including: (a) MARA test, (b) preheat plateau test, (c) sensitivity test, and (d) double-regenerative test.	A68
Figure A4.15	OSL results for creek profile near KR99 at 95 cm, including: (a) MARA test, (b) preheat plateau test, and (c) sensitivity test.	A69
Figure A4.16	OSL results for creek profile near KR99 at 320 cm, including: (a) MARA test, (b) preheat plateau test, and (c) sensitivity test.	A71
Figure A4.17	OSL results for the creek bank profile at Sandy Creek Gorge at 57 cm, including: (a) MARA test, (b) preheat plateau test, (c) sensitivity test, and (d) double-regenerative test.	A73
Figure A4.18	OSL results for the creek bank profile at Sandy Creek Gorge at 126 cm, including: (a) MARA test, (b) preheat plateau test, and (c) sensitivity test.	A75
Figure A4.19	OSL results for the creek bank profile at Sandy Creek Gorge at 321 cm, including: (a) MARA test, (b) preheat plateau test, (c) sensitivity test, and (d) double-regenerative test.	A77
Figure A4.20	OSL results for the creek bank profile at Sandy Creek Gorge at 357 cm, including: MARA test, (b) preheat plateau test, and (c) sensitivity test.	A79

LIST OF TABLES

Table 1.1	Primarsy study components in this study of the geoarchaeology of the Keep River region.	13
Table 3.1	Summary of field sampling strategy undertaken in July 1999 and July 2000, which provides a continuum from human occupation sites to those where there is no indication of human activity.	62
Table 4.1	Summary of apparent exposure age and maximum erosion rate estimated from ^{26}Al and ^{10}Be isotope concentrations in six bedrock samples from the Keep River region. Note that the exposure age does not represent the geological age of the bedrock.	83
Table 4.2	Mean concentrations and ratios of ^{10}Be and ^{26}Al radioisotopes determined from successive analyses of target samples, taken from various depths in three different burial profiles near Jinmium.	86
Table 5.1	Summary (mean and standard deviation, SD) of sediment geochemistry for each location, and for all combined sediment samples compared to bedrock (in bold). Results indicate the very similar geochemistry of all samples.	130
Table 5.2	Pigmentation of sediments is due mainly to the nature and grain size of iron oxide and hydroxide minerals, and may provide information on the pedoenviroment (from Schwertmann, 1993: 54).	140
Table 6.1	Thermoluminescence (TL) age estimates, grouped according to location. All palaeodose estimates are calculated from the 375°C peak, except those marked with an asterix (*). The latter are derived from stepped plateaux (using the 325°C peak), hence the corresponding age determinations should be considered maximum values.	160
Table 6.2	OSL age determinations, grouped according to location, and calculated using central age palaeodose and dose rate determined from thick-source alpha-counting (TSAC) and high-resolution gamma spectrometry for the two rock-shelter samples(*).	166
Table 7.1	Comparison of radiocarbon dating results with measured and extrapolated luminescence age estimates for equivalent depths in the rock shelter and adjacent sand sheets at Goorurarmum and Karlinga. Radiocarbon samples	

with a 'Wk.' lab code comprise < 125 um material, whereas samples with an 'OZ' lab code comprise finer grained or degraded carbon material.	203
---	-----

APPENDIX TABLES

Table A1.1	Location details for cosmogenic bedrock samples and sediment auger hole sites as determined by GPS.	A1
Table A2.1	ANSTO Sample Forms.	A2
Table A2.2	Chemistry results for Al and Be.	A5
Table A2.3	AMS ¹⁰ Be measurement results.	A6
Table A2.4	AMS ²⁶ Al measurement results.	A6
Table A3.1	Grain size analyses for samples taken around Jinmium.	A17
Table A3.2	Grain size analyses for samples taken around Goorurarmum.	A18
Table A3.3	Grain size analyses for samples taken around Karlinga.	A20
Table A3.4	Grain size analyses for samples taken around Sandy Creek Gorge.	A21
Table A3.5	Summary of all grain size analyses for each of the site areas.	A22
Table A3.6	Statistical analyses of grain size results.	A23
Table A3.7	Major element chemistry for Keep River samples (AAC Job No. 4148)	A25
Table A3.8	Major element chemistry for Keep River samples (AAC Job No. 3923).	A26
Table A3.9	Statistical analyses of geochemistry results.	A27
Table A4.1	Thermoluminescence (TL) results.	A40
Table A4.2	Summary of OSL analyses.	A48
Table A4.3	SAR analyses for Goorurarmum rock shelter (Goor-2) excavation.	A50
Table A4.4	SAR analyses for Goorurarmum sand sheet excavation (Goor-1) at 50 cm.	A52
Table A4.5	SAR analyses for Goorurarmum sand sheet excavation (Goor-1) at 100 cm.	A54
Table A4.6	SAR analyses for Goorurarmum sand sheet excavation (Goor-1) at 175 cm.	A56
Table A4.7	SAR analyses for Goorurarmum sand sheet excavation (Goor-1) at 220 cm.	A58
Table A4.8	(a) SAR analyses for the Karlinga rock shelter excavation (Karl-1) at 27 cm.	A60
Table A4.8	(b) Bracketed SAR analysis for the Karlinga rock shelter excavation (Karl-1) at 27 cm, analysed with the "Analyst" program.	A61
Table A4.9	SAR analyses for the Karlinga sand sheet excavation (Karl-3) at 90 cm.	A63

Table A4.10	SAR analyses for the Karlinga sand sheet excavation (Karl-3) at 150 cm.	A65
Table A4.11	SAR analyses for the Karlinga sand sheet excavation (Karl-3) at 210 cm.	A67
Table A4.12	SAR analyses for the creek bank profile near KR99 at 95 cm depth.	A70
Table A4.13	SAR analyses for the creek bank profile near KR99 at 320 cm depth.	A72
Table A4.14	SAR analyses for creek bank profile at Sandy Creek Gorge at 57 cm depth.	A74
Table A4.15	SAR analyses for creek bank profile at Sandy Creek Gorge at 126 cm depth.	A76
Table A4.16	SAR analyses for creek bank profile at Sandy Creek Gorge at 321 cm depth.	A78
Table A4.17	(a) SAR analyses for the creek bank profile at Sandy Creek Gorge at 357 cm depth	A80
Table A4.17	(b) Bracketed SAR analyses for creek bank profile at Sandy Creek Gorge at 357 cm, analysed with the “Analyst” program.	A81
Table A4.18	Alpha spectrometry and gamma spectroscopy results (supplied by ANSTO).	A83
Table A5.1	Results of radiocarbon analyses. Charcoal samples were prepared by Dr. John Head, and analysed at Waikato Dating Laboratory (‘Wk’ lab codes) and at ANSTO, Lucas Heights (‘OZG’ lab codes).	A88
Table A5.2	(a) Artefact analyses for Jinmium and Goorurarmum excavations (provided by R. Fullagar, pers. comm., 2002).	A89
Table A5.2	(b) Artefact analyses for Karlinga excavations (provided by R. Fullagar, pers. comm., 2002).	A90

ABSTRACT

This geoarchaeological study aims to establish the geomorphic context of Aboriginal cultural landscapes and archaeological sites in the Keep River region, Northern Territory, over the Late Quaternary. The geomorphic focus of the thesis is concentrated on the sand sheets, which occur at the base of the sandstone escarpments. Sample locations include the occupation (rock-shelter and sand sheet) sites of Goorurarmum, Jinmium and Karlinga, and non-occupation (creek) sites at Karlinga and Sandy Creek Gorge. The thesis presents five interrelated studies, including (i) an assessment of the theoretical relevance of geoarchaeology in northern Australia; and three studies at different timescales, evaluating (ii) long-term landscape processes over timescales of millenia using *in situ* cosmogenic dating, (iii) sedimentary processes over timescales of centuries to millenia using luminescence dating, and (iv) sedimentary processes over decadal timescales. A fifth study integrates the results of the above four studies with existing archaeological data.

Measurement of *in-situ* cosmogenic ^{10}Be and ^{26}Al concentrations from the local escarpment bedrock has revealed denudation rates of 4 - 7 mm.ka⁻¹ over $10^3 - 10^5$ year timescales, consistent with similar studies in other parts of semi-arid Australia. Calculated bedrock denudation rates were used to model burial profiles up to 6 m deep from the Jinmium sand sheet. Measured concentrations of ^{10}Be and ^{26}Al in two profiles, provided vertical accretion rates of ~10 - 20 mm.ka⁻¹ over the past few hundred thousand years.

Grain size, micromorphology, mineralogy and geochemistry indicate that the sand-sheet sediments are locally sourced. The rock-shelter sediments have higher relative concentrations of CaO, P₂O₅ and greater LOI, than the surrounding sand-sheet sediments, reflecting higher levels of charcoal, guano and organic matter. Post-depositional reddening of the sediments reflects groundwater variation rather than any proxy for depositional age.

A total of 33 thermoluminescence (TL) and 15 optically stimulated luminescence (OSL) dates were obtained from the rock-shelters, sand sheets and creek embankments. U- and Th-series

analyses indicate relative equilibrium, with slightly higher dose rates ($3.0 \pm 0.83 \text{ Gy.ky}^{-1}$) for mottled sediments than elsewhere ($1.3 \pm 0.29 \text{ Gy.ky}^{-1}$). Foreshortened TL plateaux in some sand sheet sediments at Goorurarmum and Jinmium, and stepped TL plateaux in the sediments alongside Sandy Creek are indicative of episodic rapid deposition events. Basal OSL ages for the Goorurarmum rock shelter and adjacent sand sheet excavation are $0.3 \pm 0.07 \text{ ky BP}$ and $14.3 \pm 0.4 \text{ ky BP}$ respectively, and near-basal OSL ages for the Karlinga rock shelter and more distant sand sheet excavation are $18.4 \pm 5.4 \text{ ky BP}$ and $18.0 \pm 0.6 \text{ ky BP}$ respectively. The 18 ka age for the Karlinga rock shelter is uncertain, and a much younger basal radiocarbon age of $\sim 4 \text{ ka}$ is preferred. The deepest OSL ages for the Karlinga creek profile (KR99CP) and Sandy Creek Gorge profile is $8.6 \pm 0.3 \text{ ky BP}$ and $13.9 \pm 0.4 \text{ ky BP}$ respectively. An increase in the sand sheet accumulation rates from $\sim 100 \text{ mm.ka}^{-1}$ in the late Pleistocene to over 200 mm.ka^{-1} in the Holocene is interpreted to reflect enhanced monsoonal activity following postglacial marine transgression rather than human activity.

The preceding results are integrated with information from radiocarbon analyses, regional archaeology, and local palaeobotanical, stone artefact and rock-art studies. Chronological results support initial evidence of seed processing, stone point production, and rock art around 3 – 4 ka. However, it is questioned whether these trends reflect ‘intensification’ or preservation and sorting of the archaeological records. The combined chronological data from the Keep River region indicates that although there is evidence of occupation from the Last Glacial Maximum (LGM), the majority of occupation deposits in the Keep River region are Holocene in age. However, this is biased by the greater number of rock shelter sequences sampled and by the poor preservation potential of the semi-arid monsoonal climate which favours younger sediment sequences. Better preservation of older sequences is found in open sites. The overall geoarchaeological history describes a relatively insensitive sedimentary record of the comparatively sensitive Aboriginal occupation of the sandstone landscapes in the Keep River region. Scope remains for further multi-disciplinary geoarchaeological investigations in similar semi-arid monsoonal environments.

Acknowledgements

The field work and partial laboratory work for this project was funded from an ARC Large Research Grant (A59905957) awarded to Assoc. Prof. Lesley Head and Dr. Richard Fullagar. I thank them for providing me the partial scholarship and for all their help and supervision throughout the candidature. I also wish to thank the Aboriginal people of Marralam Community – particularly Paddy Carlton and Biddy Simon. For assistance in the field, I thank Jenny Atchison, Richard Fullagar, Lesley Head, Ken Mulvaney, Gerald Nanson and Alan Watchman.

A significant part of the laboratory work, including the cosmogenic dating and U-series dating, was funded by an AINSE post-graduate award. A huge thank-you goes to Dr. David Fink for helping me to even begin to understand the complicated theory and equations of cosmogenic dating. Thanks also to David Child, Charles Misfud and Melissa Thomas for help in the ANSTO labs. Dr. David Price kindly provided and helped decipher the many results of thermoluminescence (TL) dating. The early stages of the optically-stimulated luminescence (OSL) dating would not have been possible without the help of CSIRO, and specifically Jon and Jacqui Olley. The latter stages of OSL luminescence dating were significantly aided by Dr. Bert Roberts and Hiro Yoshida. I also thank my fellow PhD colleagues Martine Coupel, Tim Peitch and Tim Cohen for their enlightened help! I am grateful to the Advanced Analytical Centre (AAC) at James Cook University (JCU) for the geochemistry analyses, and their ongoing support. Advice was obtained from various people, including Dr. Alan Watchman, Prof. Bob Carter, Dr. Ross Coventry, Assoc. Prof. John Chappell, Dr. Tony Barham, Dr. Patrick DeDeckker, Drs. Bob and Ann Young, David Carrie and Aivars Deepers.

Thanks to both my supervisors Assoc. Profs. Gerald Nanson and Lesley Head for putting up with the many long-distance communications. Thanks to my partner, Piers Larcombe, for the same. Finally, I wish to give a particular dedication to the three bikes that have carried me over

the past three or so years, particularly my KHS which remains true to its name a nomad, and sadly missed.



The three bicycles that have transported me over the years of my PhD include the Park-Pre (2000), KHS Nomad (2001) and Marin Bear-Valley (2002).

CHAPTER ONE

Introduction

If we want to understand the dream, we had better learn something of the past from which it sprang. -Eisenberg (1998, xx).

1.1 Geoarchaeology of the Keep River Region

Eisenberg's (1998) quote can be interpreted from an Australian perspective that in order to understand Aboriginal Dreaming we need to learn something of the past landscape from which it evolved. Prehistoric people lived on a landscape that was dynamic and continually changed and in which the record of their activities was differentially preserved and destroyed; hence an understanding of the archaeological record requires a full understanding of the geological processes that have shaped that record (Waters and Khuen, 1996). This research is aimed specifically at establishing the geomorphic context of archaeological sites in the Keep River region. From a geoarchaeological perspective, the aim is to use an earth-science approach to define the evolving landscape context of human occupation. This work forms part of a larger study which integrates archaeological excavation and analysis, rock art studies, ethnography and biogeography to explore relationships between the changing environment, the archaeological record and human marking of the landscape (Fullagar et al., 2000: 45).

Questions of change are one of the key contemporary issues of Australian (and world) archaeology (Lourandos, 1996), and the Keep River region is of particular interest because it is geographically and culturally midway between the adjacent Kimberley District to the west and Victoria River District (VRD) to the east (Taçon et al., 1999). It is hoped that the geoarchaeological record within the Keep River region can provide a unique but regionally comparative record. This study uses geochronological and geological methods to consider temporal and spatial changes in the Keep River region from the processes operating in the sedimentary and archaeological record. Particular interest is given to the sandstone escarpments and sand sheets, which form the main archaeological contexts.

The aim is to illustrate how variations in the processes and rates of landscape evolution may help understand the archaeological context. A major problem is that in the extreme arid and semi-arid monsoonal climate of northwest Australia formation processes tend to result in a fragmented environmental and archaeological record. Rather than just treating formation processes as problems to be overcome in order to reconstruct the past, an understanding of formation processes is essential to interpretations of the archaeological record (Barton et al., 2002: 186). Although this thesis includes a study of geomorphic dating techniques, it is also a study of methodology and a geoarchaeological approach to archaeological problems. The relevance of geoarchaeology to broader debates within archaeology is reviewed in Chapter Two, and the specific geochronological and sedimentary methods used in this study are outlined in the relevant chapters.

1.2 Regional Geoarchaeological Context

Due to its proximity to the northwest shelf, the archaeology of the Keep River region is potentially of interest to debates about the early human settlement of the Australian continent (Fig. 1.1). Most researchers consider the initial occupation of Sahul occurred sometime between 40 and 70 ky BP (Veth, et al., 1998), when sea level was between 50 and 90 m below its present position (Chappell, 1994). During this period the Keep River region, which presently lies approximately 100 km south of the Joseph Bonaparte Gulf, would have been a further 200 - 300 km inland. Although the area explored in this study of the Keep River presently inland of any coastal influence, previous changes in sea-level and climate are an important part of the regional context. The archaeological record along other parts of the northwest coastline is outlined by Veth (1999).

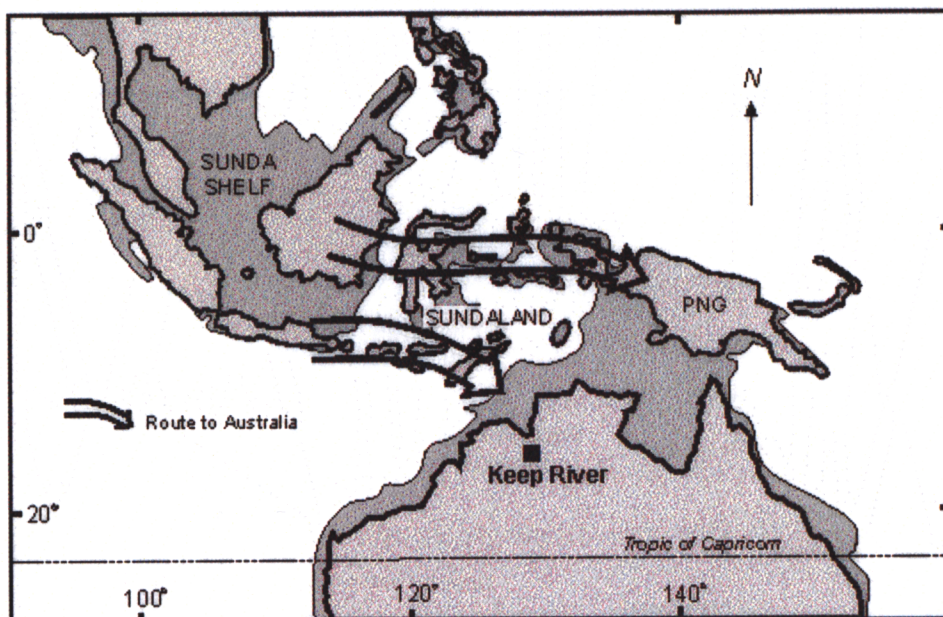


Figure 1.1 Possible migration routes into Australia based on earliest evidence of *Homo sapiens* from archaeological sites and evidence for impact on the vegetation in palaeoecological sites from southeast Asian and northern Australia (from Kershaw et al., 2002), showing location of the Keep River region. Extended landmass shaded to -150 m contour.

Well over half of the archaeological study sites in Australia are rock-shelter sites (Smith and Sharp, 1993) and a large body of theory on Australia's prehistory (e.g. initial occupation, intensification, human-land interactions) has developed from studies of them. Although enclosed rock-shelter sites, offer the potential for long, relatively well-stratified sequences (Lourandos and David, 1998), the stratigraphy and consequent archaeological interpretation may be complicated by various geomorphic factors. In addition, ethnographic evidence suggests that rock shelters were only rarely used as habitation sites (Mulvaney and Kamminga, 1999) and indeed more arid parts, such as the Western Desert, are devoid of caves and rock shelters and people must have occupied more open areas (Peterson, 1971). Despite this, few Australian studies have attempted to directly compare excavated deposits from rock shelters and open sites in the same area (Morwood, 1981, 1986, Mardaga-Campbell and Campbell, 1985). The focus of this study is on the sand sheets, which not only represent the landscape on which people lived over the Quaternary and prior to the period of occupation, but are also the link between the escarpments and rock shelters.

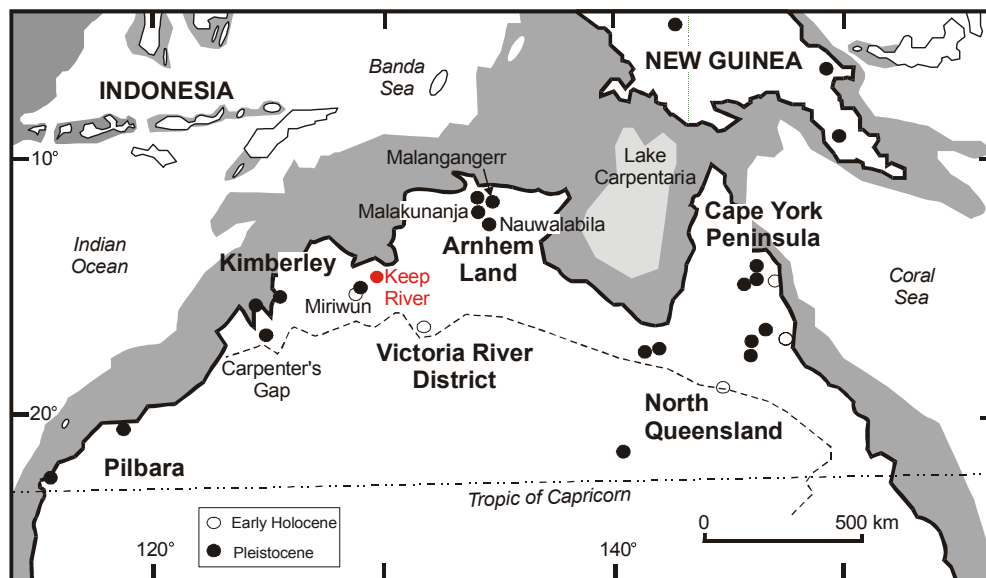


Figure 1.2 Location of Keep River (red) and other major archaeological and rock-shelter sites throughout northern Australia.

Previous archaeological investigations within the Keep River region have included both open sites and rock shelter sites (Fullagar et al., 1996; Head and Fullagar, 1997; Atchison, 2000). Other excavations in the region have mainly concentrated on rock shelters and include the Miriwun and Monsmont Shelters in the nearby Ord Valley, east Kimberley (Fig. 1.2). The Miriwun site attests to the use of riverine resources during the LGM through to the late Holocene (Dortch and Roberts, 1996). Other rock shelters in the region such as Kununurra and Pincombe Range have provided recent ages falling between *ca.* 3.5 and > 1.0 ky BP (Veth, 1995: 743). Radiocarbon determinations for many of archaeological sites in north-west Australia are listed in Veth (1995: 736-7), and the combined chronology of sites in the Keep River region and in other parts of the Kimberley and adjacent regions is given in Chapter Seven (refer 7.2.2). Along with current dating of archaeological sites in the Keep River region, the regional chronology is considered to be indicative of ‘intensification’ during the Holocene, i.e. increased social and economic complexity, defined by more intensive use of sites and increased numbers of sites (Lourandos, 1996).

Possibly related to 'intensification' is the development of the 'Australian Small Tool Tradition' (Gould, 1969), characterised by presence of stone points (including unifacial and bifacial points) and dating from mid Holocene to present. Although the exact date is contested between 4.5 ky BP (Bowdler and O'Connor, 1991) and 5.7 ky BP (Jones and Johnson, 1985: 206), the introduction of points into the archaeological record can theoretically be used as a chronological marker in the northern Australian sequences. In the Keep River region, the introduction of points is dated to around 3 ky BP (Attenbrow et al., 1995; Fullagar et al., 1996: 764). An earlier industry in northern Australia dates from late Pleistocene to mid Holocene and is generally characterized by cores, scrapers, and edge ground axes (Dortch, 1977; O'Connor, 1999).

1.3 Geographical Context

The Keep River (129.2°E, 15.4°S) is situated near the border of Western Australia and the Northern Territory, between the Ord and Victoria Rivers (Fig. 1.3).

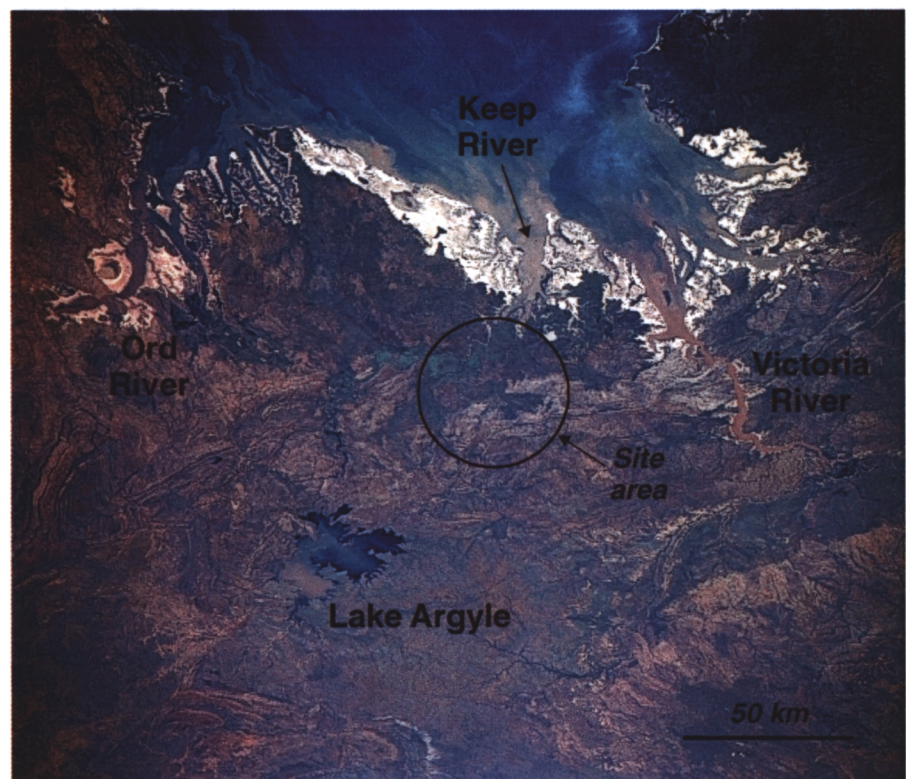


Figure 1.3 NASA Satellite image of the Keep River region, including Lake Argyle (sourced from <http://eol.jsc.nasa.gov/> Image No. STS41C-52-2562).

Research is concentrated at three sites within the Keep River region, namely Jinmium, Goorurarmum and Karlinga (Fig. 1.4). These archaeological sites were linked to an adjacent non-archaeological site of Sandy Creek Gorge (Fig. 1.4) in order to obtain a sedimentary record essentially independent of any significant anthropogenic signature.

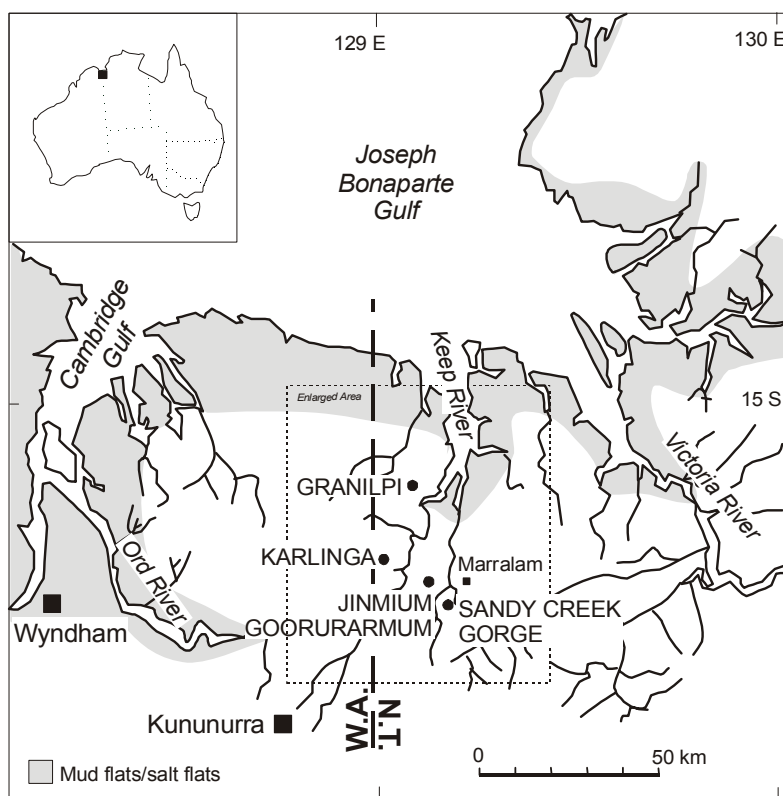


Figure 1.4 Location of the three main archaeological sites (Jinmium, Goorurarmum, and Karlinga) and the non-archaeological site (Sandy Creek Gorge) along the Keep River catchment, and bounded by the larger catchments of the Ord River and Victoria River.

The archaeological sites investigated in this study border on parts of the Ord River Irrigation Area (ORIA) (Fig. 1.5). Since 1995 much of the Keep River region is being progressively engulfed in the expansion of ORIA Stage II (<http://www.nt.gov.au/majorprojects/ord.shtml>). The Stage II development of the ORIA will use the waters of Lake Argyle to expand the scheme's current irrigated area of 13,000 ha (5000 km²) by a further 50,000 ha (20 000 km²) for broad-acre cropping and some 15,000 ha (6000 km²) for intensive horticulture (<http://www.nt.gov.au/agri/factsheets/area.shtml>). Details of Stage I and II of ORIA are outlined in an environment review and management program (Kinhill, 2001). An estimated 8 %

of the land area proposed for development in the ORIA Project is considered to have archaeological sensitivity to these people. Head (1999a, b) outlines the conceptual influence of the past and proposed development on Aborigines, environment and agriculture by ORIA.

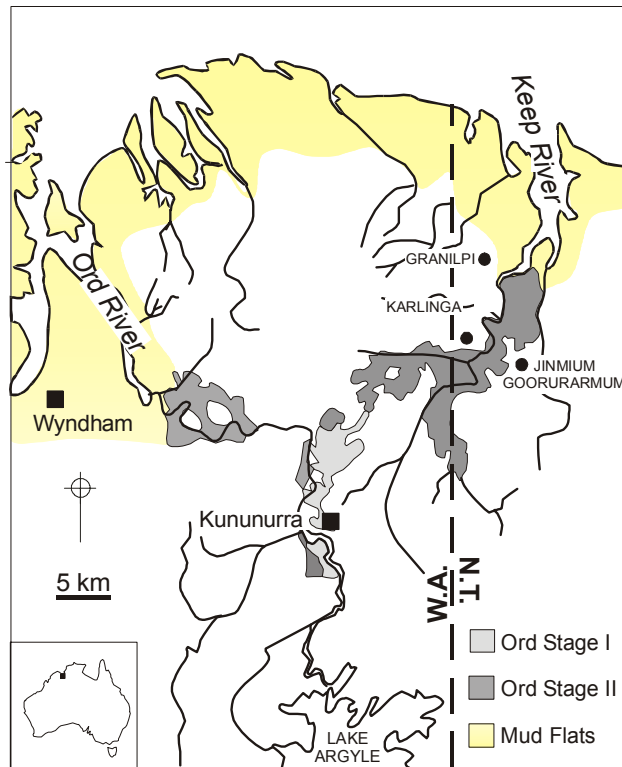


Figure 1.5 Location of the archaeological site areas in relation to the expanding Ord River Irrigation Area (ORIA).

1.4 Local Archaeological Context

The Keep River region provides an opportunity to compare physical, chronological and cultural patterns (e.g. rock art, stone artefact, ethnographic, etc.) within northwest Australia. Research indicates that the area has preserved a unique record of art (and hence culture) overlapping in both age and style that of the adjacent Kimberley District to the west and VRD to the east (Taçon et al., 1999), and possibly also related to that of Arnhem Land (Lewis, 1988). The relative age of the Keep River region compared to these adjacent cultural provinces, however, remains in contention (Roberts et al., 1997). The Miriuwung and Gajerrong people have close links to the land in this region, and many of the sites investigated in this study are incorporated

into their present-day Aboriginal Dreaming. One of these Dreaming tracks, depicted in Fig. 1.6, include a number of rocky outcrops that link Granilpi, Jinmium and Sandy Creek (Fullagar, et al., 1996; Taçon et al., 1997).

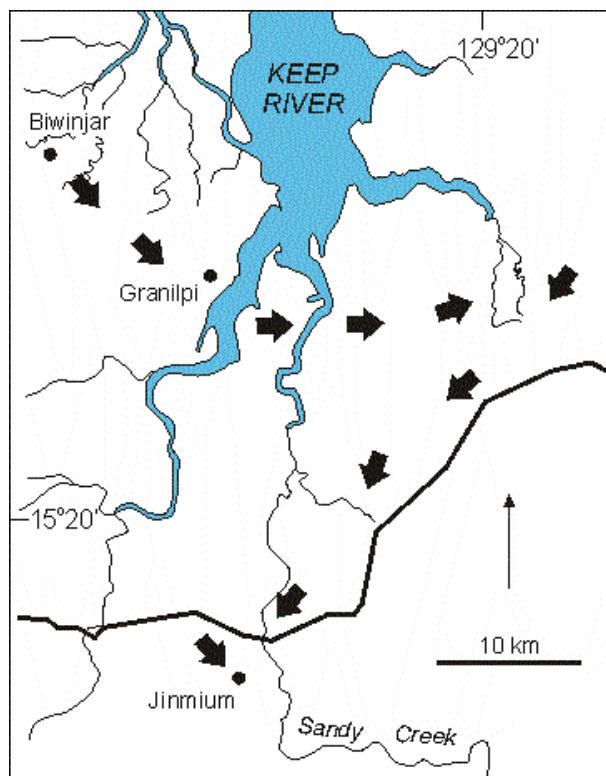


Figure 1.6 Path of the Djibigun dreaming track through the Keep River region, which begins in the north west at Biwinjar, passes through Granilpi, across the Keep River and Sandy Creek to Jinmium where it ends.

Previous work to date in the Keep River region has considered hunter-gatherer use of fire and its impact on vegetation (Head, 1996; Atchison, 2000); reopened debate on initial colonisation and the relative merits of dating techniques (Fullagar et al., 1996; Roberts et al., 1997; Watchman et al., 2000); highlighted rapid cultural change in the post-European contact period (Fullagar and Head, 1999; Head and Fullagar, 1997; Mulvaney, 1996); documented ethnographic and prehistoric subsistence tools (Atchison and Fullagar, 1998; Boer-Mah, 2002; Head et al., 2002); and documented a seven stage sequence in the rock art (Taçon et al., 1997). Aboriginal people have been central to the research, communicating extensive mythological traditions throughout these areas. There are some questions relating to the timing and pattern of these various

archaeological records both in the Keep River region and more generally in semi-arid monsoonal sandy sites of northern Australia (Chapter Two). The following geoarchaeological study aims to help resolve some of these questions by focusing on the sedimentary context, and predominantly on sedimentation rates and processes.

In July 1999, when this research project began, a total of 43 rock art sites previously unknown to non-Aboriginal people were recorded: 19 in the Weaber Range and 21 in Goorurarmum, the hills to the east of Jinmium; another three were recorded elsewhere. (A coding system was established by Dr. Paul Taçon of the Australian Museum to record the rock art sites as sequential 'KR' numbers in sequence of which they have been recorded). Since 1987, eleven Aboriginal archaeological sites and 76 art sites have been recorded by Dr. Taçon on the Legune 1:100 000 mapsheet, and excavations have been undertaken at five localities within the Keep River area. The discovery of archaeological deposits (through a comprehensive augering strategy) in open sites close to rock shelters in the Keep River indicates that the rock shelters may represent cultural 'nodes' for occupation (Boer-Mah, 2002: 78). Whilst the potential exists for older and deeper archaeological sequences to be found in open sites throughout the Keep River region, the challenge lies in linking the sedimentary and archaeological deposits to those found within the rock shelters.

Several of the rock art sites found in 1999 contain panels with figures resembling the 'Bradshaws' of the Kimberley region to the west (Figure 1.7). Together with two previously recorded figures in the Granilpi area, these are the easternmost Bradshaw figures known (Taçon et al., 1997; 1999), and are significant because of style (Taçon et al., 1999; Walsh, 2000) as well as their contentious antiquity (Lewis, 1997; Roberts et al., 1997). Roberts et al. (1997) have obtained an age of 17.5 ± 1.8 ky BP for a so-called Bradshaw figure, whilst Watchman (2001) considers 3.9 ± 0.11 ky BP is a more reliable age for this art (Watchman et al., 1997). Bednarik (2002) also dismisses the older 17 ky BP estimation of the Kimberley figure, noting that a Pleistocene painting tradition has not survived anywhere else in the world in such large numbers outside of caves.

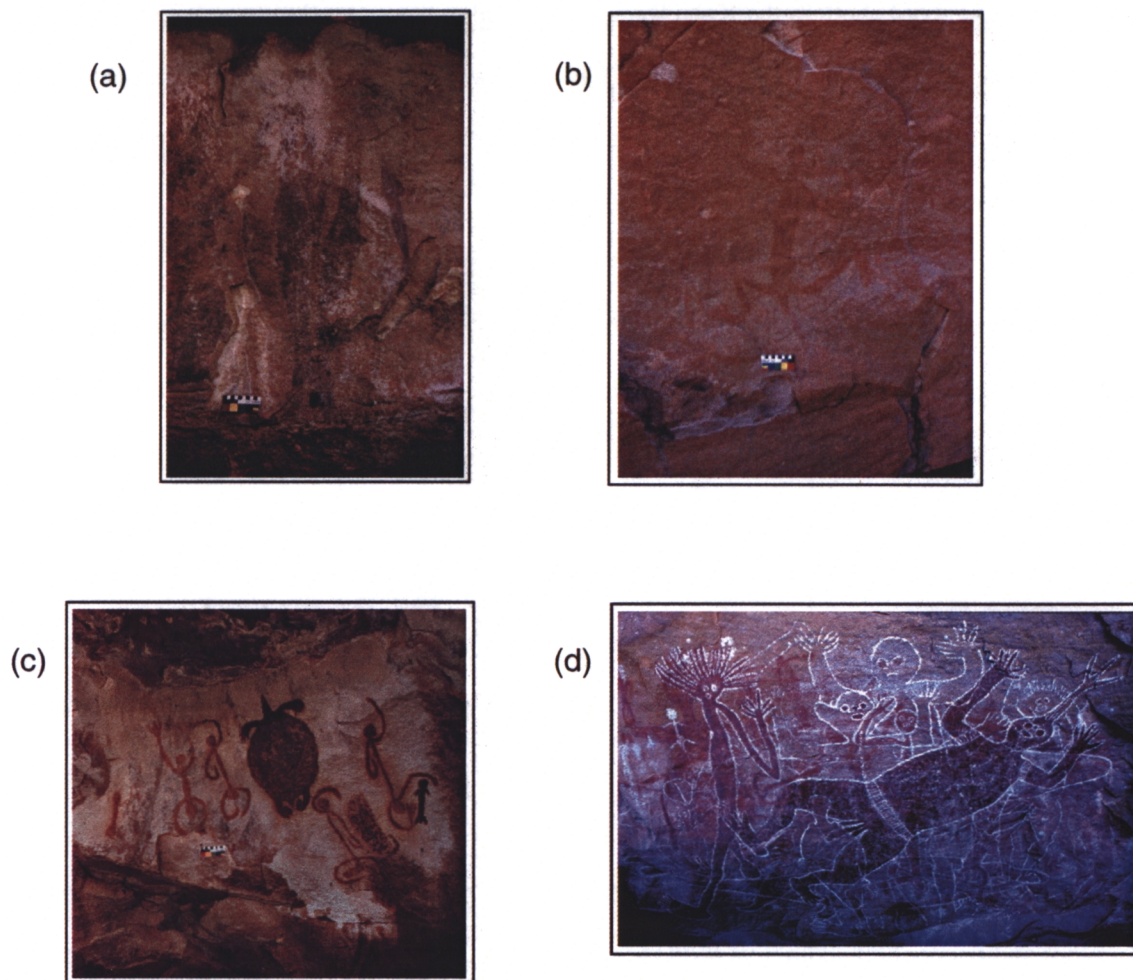


Figure 1.7 Examples of different styles of paintings found in the Keep River region, including (a) “Keep River Bradshaw” (Tacon et al., 1999) at Karlinga, (b) animal stencils at Granilpi, (c) figures at Granilpi, and (d) superimposed figures at Karlinga.

Additional to the paintings are numerous rock engravings, some of which have been described by Fullagar et al. (1996) and Taçon et al. (1997). Found most commonly on boulders or rock-shelter walls (Taçon et al., 1997), the engravings take the form of cup-shaped marks or ‘cupules’ and are recognised as the oldest surviving form of rock-art in northern Australia (Chaloupka, 1993; Flood, 1997; Taçon et al., 1997). Direct dating of oxalate-crust surfaces formed over the cupules give minimum ages ranging from 2.2 ± 0.05 ka at Jinmium to 4.3 ± 0.08 ky BP at Granilpi (Watchman, 2001). The estimate for Jinmium oxalate-crust accords with the OSL age of the sediments that covered a spalled rock fragment bearing weathered cupule marks (Roberts et al., 1998). The 1999 field season also uncovered an ancient bird track

engraving in the Weaber ranges, which was interpreted to represent the genus *Genyornis newtoni* (Ouzman et al., 2002). Ouzman et al. (2002) argue that this engraving is no more than a few thousand years old, indicating that *Genyornis* became extinct much later than the 25 and 50 ky BP age proposed by Miller et al. (1999). As such, Ouzman et al. (2002) suggest that the engraved bird track has both recent and ancient referents, sustained over many tens of millennia of changing cultural and environmental circumstances. The following study is a consideration of those environmental circumstances both in relation to the rock art of the Keep River region and to the archaeological record in general.

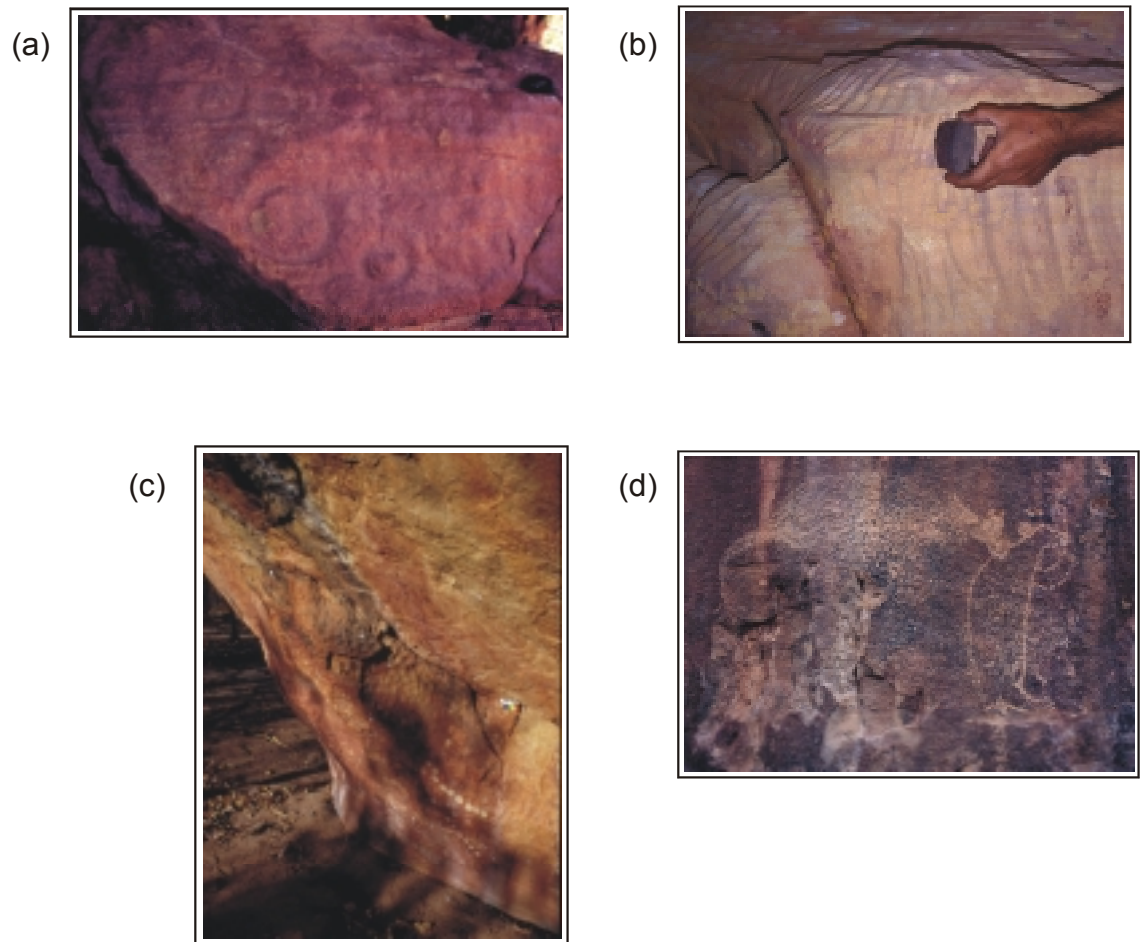


Figure 1.8 Examples of different styles of pictographs found in the Keep River region, including (a) rings or circles at Karlinga, (b) scratches at Karlinga, (c) cupules at Jinmium, and (d) pecks depicting animal figures at Karlinga.

1.5 Research Strategy and Thesis Aims

The broad aim of this study is directed towards understanding the geomorphic and sedimentary context of archaeological sites in the Keep River region in order to provide the temporal and spatial resolution for interpreting the remaining archaeological record. The thesis begins with a literary compilation of the regional geological, environmental and climatic background. The research then progresses from the general geochronological and geoarchaeological context by using the techniques of *in situ* cosmogenic isotope dating and luminescence dating, to the more specific sedimentary and archaeological site contexts, using the sedimentary and archaeological features within the sand sheet and rock shelter sediments (Table 1.1). An attempt is made to link the observations of modern day processes with those of the older landscape.

The multidisciplinary nature of this research cannot provide an independent and exhaustive examination of any of the separate radiometric, sedimentary or archaeological elements. A predominantly empirical approach is designed to evaluate data both from within and outside this study, and illustrate how a geoarchaeological approach can contribute to our understanding of site formation sandy environments of northern Australia. Ideally this work can in future be linked with information on biota, demography, and material culture in order to generate a more integrated geoarchaeological model of prehistoric settlement and subsistence patterning for the Keep River region. It is also intended that this work should provide an introduction, not only to geoarchaeological research in Australia, but also in similar semi-arid monsoonal environments worldwide.

The specific objectives of this thesis are to:

- (i) Review the importance of a geoarchaeological approach to studies of archaeological site formation in Australia.
- (ii) Outline the regional geological, geomorphological, palaeoclimatic and ecological context of the Keep River region as a background to subsequent geoarchaeological interpretations.

- (iii) Obtain an estimate of the rate of escarpment erosion from various sites within the Keep River region using *in situ* cosmogenic dating.
- (iv) Obtain an estimate of the rate sand sheet accumulation in the Keep River region using both *in situ* cosmogenic dating and luminescence dating techniques.
- (v) Investigate the processes of sedimentation and weathering within the sand sheets of the Keep River region using techniques of geochemistry and micromorphology.
- (vi) Discern the chronological and contextual relationship between the landscape and its archaeological record at the site specific and regional level.

Table 1.1 Primary study components in this study of the geoarchaeology of the Keep River region.

<i>Theoretical Context</i>	Chapter Two: Relevance of geoarchaeology to current issues in Australian archaeology
<i>Landscape Context</i>	
Regional environment, landform and topographic setting	Chapter Three: Regional environment
Landscape processes	Chapter Four: Cosmogenic dating of escarpments
<i>Site Formation</i>	
Geomorphic agents Cultural and natural processes Post-depositional processes	Chapter Five: Sedimentary description and analysis
<i>Stratigraphic Context</i>	
Site processes and chronology	Chapter Six: Luminescence Dating of sand sheets
<i>Archaeological Context</i> Landscape and site modification	Chapter Seven: Archaeological record

CHAPTER TWO

Literature Review: Perspectives on a Geoarchaeological Approach to Current Issues in Australian Archaeology

Close co-operation among sedimentologists, archaeologists, and other specialists during planning, excavation, and interpretative stages is crucial to a successfully integrated study.

- Farrand (2001:537).

2.1 Introduction

The field of geoarchaeology is generally defined as the application of concepts and methods of the geosciences to archaeological research (Waters, 1992). In Australia, geoarchaeological research has often been carried out under the broad themes of ‘landscape’, ‘spatial’ or ‘environmental archaeology’ (Hughes and Sullivan, 1982). Whilst providing a means for reconstructing prehistoric and ancient landscapes, depositional environments, and paleoclimatic regimes, such studies have often fallen short of linking broader-scale landscape change to archaeological evidence, especially at the temporal and physical scales at which groups of prehistoric people may have interacted with the landscape (White and O’Connell, 1982).

The majority of archaeological remains throughout Sahul’s prehistory derive from *small, short-term*, open encampments; with little *persistent* data beyond a hearth, some stone artefacts and food remains. Once *abandoned*, this material was usually *disturbed and transported* over a considerable area before being *buried* and partly *preserved* in sand or alluvial clay. Each cluster of remains is likely to represent only *one part of a much larger* camp that was *discontinuously* spread over many locally different *geomorphic* units, the exact *correlation* of which is difficult if not impossible.

- White and O’Connell (1982: 34; my emphasis)

The above quote notes some of the potential problems associated with determining and correlating geochronology and stratigraphic sequences, and preservation of materials in many

archaeological sites in Australia. Like many geoarchaeological issues, these problems relate specifically to the nature of basic physical, chemical, biological and human properties and processes to morphological and sedimentological changes on timescales ranging from months to millennia, and at spatial scales ranging from tens of metres to tens of kilometres.

In addition to reviewing these issues, this chapter outlines the history and present status of geoarchaeology in northern Australia, where there is emerging some of the oldest evidence of human-environmental interactions (Dodson, 1992; Head, 2000). In considering the history of geoarchaeology, this review argues for a renewed emphasis on the physical context to archaeological research. Changes in time and space are key contemporary issues in Australian archaeology (Lourandos, 1996; Sullivan, 1996), hence the following considers the problems and potential application of geoarchaeological concepts and methods to identifying and quantifying change in the cultural and natural deposits of semi-arid and monsoonal northwestern Australia. The geoarchaeological issues for the Keep River region are also outlined.

2.2 History of Geoarchaeology in Australian Archaeology

For over two centuries archaeologists have been investigating the prehistory of Australia. The historical paradigm of “an unchanging people in an unchanging land” (Pulleine, 1928) has since evolved to the opposite contemporary interpretation of archaeology within a dynamic Australian landscape (Lourandos, 1996; Sullivan, 1996; Head, 2000). In the nineteenth century, natural scientists, studying the earliest periods of human occupancy of Australia, made a plea for conducting archaeology on geological rather than archaeological grounds (White and O’Connell, 1982: 23), and many natural scientists continue to do so (Mulvaney, 1972; Hughes and Sullivan, 1982; Bowler, 1998). In addition to defending a stratigraphic approach to unearthing evidence of human occupation, such pleas allude to cultures and landscapes operating over geological time scales. In this regard, a close interdisciplinary relationship has long existed between the earth sciences and archaeology, but in Australia, geoarchaeology has

yet to be generally acknowledged, as it has in Europe (Davidson and Shackley, 1976; Rapp and Hill, 1998) and America (Butzer, 1982; Waters, 1992; Waters and Khuen, 1996; Stein, 2001), as an integral part of archaeology.

Many concepts in Australian research have been founded in studies of more temperate and northern hemisphere climates (White and O'Connell, 1982), even though there has been longstanding research in the southern Pacific region (Bowler et al., 1976; Dickinson, et al., 1998; Dodson, 1992; Veth et al., 1998). Even within Australia a great majority of archaeological studies have been undertaken in the southern temperate region (Mulvaney and Kamminga, 1999), despite the fact that the arid and semi-arid monsoonal zone occupies over two-thirds of the continental land surface. Considerable scope exists to explore and expand the consideration of human-environmental interactions to semi-arid monsoonal regions of Australia. Such was the aim of a recent conference on the archaeology and environmental history of southern hemisphere deserts which included Australia, South America and South Africa (Smith, 2003).

Geoarchaeology has always been primarily concerned with the temporal contexts of sites through the application of stratigraphy and geochronology (Renfrew, 1976) and geochronology is integral to a range of active debates in Australian archaeology. Many of these geochronological aspects have been previously discussed (Frankel, 1995; Morwood and Hobbs, 1995), and include arrival and colonisation of the Sahul continent (Allen, 1989; Webb, 1998; Roberts et al., 1994b, Veth et al., 1998; Roberts and Jones, 2001), and human impacts thereon, particularly through the use of fire (Head, 1996; Kershaw et al., 1997, 2000), and on the timing of megafaunal extinctions (Flannery, 1994; Miller et al., 1999; Roberts et al., 2001).

Investigations of human impacts often base the case for an anthropogenic cause strongly on temporal association, but far more evidence is needed before human and climatic roles can be disentangled (Ross, 1982).

Changes in the natural environment also have impacts upon humans and on the preservation of archaeological material (i.e. natural site formation processes). Rather than tackling archaeological questions through specific geoarchaeological research, archaeological research often derives physical and environmental context from related studies, such as the CLIMANZ records (<http://rses.anu.edu.au/enproc/AQUADATA/archive.html>) that, although useful, are not necessarily aimed at answering any specific archaeological problem. Site formation processes have generally been considered from taphonomic archaeological studies, which have broadened to recognise the wider importance of processes involved in archaeological, palaeontological and geological sites (Hiscock, 1990). Only a few studies have been directed specifically towards investigating site formation processes, and examples concern rock art (MacLeod et al., 1997; Ward et al., 1999), palaeobotany (McConnell, 1997) and maritime archaeology (Ward et al., 2000). Hughes (1983a) outlined some basic geoarchaeological field and laboratory techniques to improve understanding of archaeological site history. The potential exists for targeted geoarchaeological investigations to provide a more contextual and quantifiable link between the regional long-term evidence, and local or site specific short-term evidence.

2.3 Quantifying Change

Changes in time and space are a key contemporary issue for Australian (and world) archaeology (Lourandos, 1996; Sullivan, 1996), and studies of change require a focus upon the *processes* which influence the archaeological record, and what that record tells us about human-environment relationships (Lourandos, 1996). Conversely, recent emphasis on change has also drawn introspection on questions of continuity and stasis (Frankel, 1995; Terberger and Street, 2002). Early recognition of cultural change in Australia was based on stratigraphic differentiation (Mulvaney, 1961) but with the advance of absolute dating techniques (Roberts and Jones, 2001), the chronostratigraphy (rather than the nature of the stratigraphy), has become the main basis for identifying change. However, premature adoption of poorly evaluated analytical techniques and their preliminary results has perhaps given archaeology, and its related disciplines, a reputation of being method driven (Dincauze, 2000). With recent

advances in luminescence dating, and with problems in Pleistocene radiocarbon determinations still unresolved, the observation of Allen (1994) that we are undergoing another significant but controversial dating revolution, is probably still valid. Whilst acknowledging these problems, the following discussion considers the use of *in situ* cosmogenic dating, luminescence dating and radiocarbon dating techniques to quantify processes over longer and shorter timescales.

2.3.1 *In-situ* cosmogenic dating

Long-lived cosmogenic radionuclides ^{10}Be ($T_{1/2}=1.5$ Ma), ^{26}Al (0.7 Ma) and ^{36}Cl (0.3 Ma) are produced from the interaction of secondary cosmic-ray particles within the upper metre or so of the Earth's crust and in exposed surface rocks. The accumulation of these radionuclides can be utilised as radiometric clocks to elucidate the exposure history of geomorphic formations and previously unexposed surfaces. *In situ* cosmogenic dating has the potential to be useful to many geoarchaeological studies (Nishiizumi et al., 1993; Bierman, 1994; Cerling and Craig, 1994; Harbor, 1999), as the concentration of isotopes is based on physical processes that can be quantitatively determined over timescales of ~2 ka to 5 Ma (Granger and Muzikar, 2001) that are appropriate to the development of most landscapes (Dorn and Phillips, 1991; Nishiizumi et al., 1993) particularly in Australia (Nishiizumi et al., 1993; Bierman and Turner, 1995; Bierman and Caffee, 2002). The different half-lives of each these radionuclides represent different time windows into the past.

Used initially in glacial geochronology (Lal et al., 1987; Brown et al., 1991; Nishiizumi et al., 1991), *in situ* cosmogenic isotope dating continues to be applied to an increasing breadth and complexity of geomorphic contexts including the development of raised river terraces and paleo-beach ridges (Pavich et al., 1986; Trull et al., 1995), soil formation (Heimseth et al., 1999; 2000), basin wide aggregate erosion (Chappell et al., 2001), sediment burial (Granger and Muzikar, 2001) and as shown in this thesis, modelling of sediment accumulation (Fink et al., 2000). Dating sediment deposition over long-term timescales is important in many areas of

geology, geomorphology, and palaeoanthropology (Nishiizumi et al., 1993; Granger and Muzikar, 2001).

Watchman and Twidale (2002) argue that cosmogenic methods are presently only useful to geologically recent events partly because of changes in climate and tectonism. Yet, the application of cosmogenic dating to the study of geologically recent archaeological and geoarchaeological contexts is virtually undeveloped, as evidenced from a recent conference workshop on the application of cosmogenic nuclides to geoarchaeology (http://www.rekihaku.ac.jp/e_news/workshop/ams.html). One such relevant study is the use of ^{10}Be to estimate denudation rates in Arnhem Land (Nott and Roberts, 1996). Obtaining minimum exposure ‘ages’ of exposed archaeological constructs, such as rock art (e.g. Phillips et al., 1997), pyramids, the Sphinx, and Stonehenge (e.g. Williams-Thorpe et al., 1995) is theoretically possible. In practice, care must be taken in interpreting exposure age results. In the particular study of the engravings of the Coa Valley, Portugal (Phillips et al., 1997), the calculated weathering rate was greater than that which would preserve the observed engraving (Watchman, 1998). A particular problem for rock art surfaces is that the penetration of radiogenic particles is vastly greater than the thickness of the art itself, and the isotopic concentrations in the surface are too small to be detected without laboriously analysing many kilograms of rock. Moreover, the cosmogenic ‘age’ does not define the exact age that a surface was exposed to the atmosphere, but like luminescence and radiocarbon dating, defines a range or period (Lal, 1991). Importantly, however, the CRN method adds a radiometric quantitative measure to all assumptions and theories of landscape evolution and the concept of age is not changed.

A different application of cosmogenic exposure age dating has been used for dating of prehistoric cave sediments in Israel (Boaretto et al., 2000), and exposure dating of chert artefacts of known typological age (Late Acheulean to early Middle Paleolithic) near Luxor, Egypt (Ivy-Ochs et al., 2001). These studies require a measure of the ^{26}Al radionuclide concentration which can be complicated by the matrix material of the artefacts themselves (e.g.

flint, chert). A more recent use of CRN methods is not only in surficial material but material which has undergone a process of transport and redeposition, and involves a measure of the timescales of these processes. By estimating the accumulation rate of sediments it is possible to place any discovered artefacts into the temporal context of the stratigraphic profile.

Depth profiles of *in situ* produced cosmogenic nuclides can be used to study surficial processes, quantify denudation and burial rates and elucidate mechanisms involved in landform evolution and soil formation. These sorts of studies began in the lateritic sediments in Africa by Brown et al. (1994) and more recently by Braucher et al. (2000). Subsequently in Central Africa, archaeological investigations of human artefacts (Schwartz, 1996) were complemented by cosmogenic studies of pebbly laterites that occurred in the archaeological stratigraphy (Braucher et al., 1998). Other applications include the comparison of *in situ* produced ^{10}Be in fluvial sediments between an agricultural and an undisturbed watershed in Puerto Rico to confirm the anthropogenic origin of the high modern denudation (Brown et al., 1998). All these studies provide the foundation for this study of lateritic sediments in the Keep River region. A comprehensive presentation of the *in situ* model, methods and application of cosmogenic exposure dating is given by Lal (1991) and Gosse and Phillips (2001).

2.3.2 Luminescence Dating

Luminescence dating is still a relatively new chronological technique, allowing quartz and feldspar rich sediments, which are otherwise undatable by conventional radiocarbon methods, to be absolutely dated ($\pm \sim 10\%$) within a range of 100 to 200 ka (Aitken, 1989). The method is based upon the fact that many naturally occurring minerals are able to act as dosimeters, recording the amount of ionizing radiation that they are exposed to. This radiation principally comes from the radioactive decay of uranium, thorium and potassium in the sediments surrounding a sample (Aitken, 1989). This stored dose can be evicted by heating to 500°C (thermoluminescence, TL) or by stimulating with light of a particular wavelength (optically stimulated luminescence, OSL). The calculated age represents the time elapsed since last

bleaching or heating and is an absolute age which does not need to be referred to any secondary calibration.

While much is made of the crucial role of luminescence dating in determining the chronology of the initial colonisation of Australia (Allen, 1994; Roberts and Jones, 1991; Roberts et al., 1994b; Head, 2000), major questions have arisen regarding the relationship between radiocarbon and luminescence ages (Allen, 1994; Webb, 1998) and between thermoluminescence (TL) and optically-stimulated luminescence (OSL) determinations (Roberts et al., 1999; McCoy et al., 2000). Part of the problem of discrepancies between dating results is that different dating techniques measure “time” using different materials that yield different ages (Frankel, 1990) or, more correctly, age ranges (Webb, 1998). In the future, single-grain OSL dating may allow a variety of contentious issues to be addressed, such as the presence and impacts of bioturbation on archaeological deposits (Bateman et al., 2002), and the identification of so-called “contaminant” grains (Roberts et al., 2000). Other major problems concern the understanding of sedimentary factors that relate directly to interpretations of dating results (e.g. Fullagar et al., 1996).

There remains an unresolved dispute surrounding the dating of sediments obtained from the Jinmium site (Spooner, 1998, Roberts et al., 1998a). Apparent sediment accumulation rates inside the rock-shelter are an order of magnitude slower than those of the adjacent escarpment-base sand sheets (Fullagar et al., 1996), and Roberts et al. (1998a) argued that this difference, along with differences of sediment colour, indicated that the TL ages were incorrect. Whilst some studies have focused on reviewing the TL and OSL analyses on quartz grains from the Jinmium rock-shelter excavation (Roberts et al., 1999; McCoy et al., 2000), little attempt has been made to define and differentiate the processes that influence net sedimentation, and reddening of sediments over time, either within the shelters or on the exposed sand sheets. Why sediment accumulation rates and colour should necessarily be similar in these two different environments has not been argued, and the archaeological significance, if any, is therefore unknown. Jinmium is now one of the most dated archaeological sites in Australia, but

the age of the deposits and their archaeological significance will remain unclear until there is careful and targeted research designed to improve understanding of sedimentary processes and products in these arid sandy environments.

2.3.3 Radiocarbon Dating

The limitations associated with radiocarbon dating of archaeological sites in Australia, particularly those of Pleistocene age, have been variously discussed by Allen (1994), Roberts et al. (1994a), Allen and Holdaway (1995), Chappell et al. (1996), Webb (1998) and more recently by Turney and Bird (2002). These limitations include problems of calibration of various source materials (e.g. charcoal, wood, peat, shell, coral), and of sample contamination either through post-depositional processes or during recovery and subsequent processing. Allen and Holdaway (1995) suggest that there is a significant difference in the oldest radiocarbon ages obtained from archaeological and geological sites, but do not ascribe this to any difference in cultural versus natural site formation, or in source material despite a sevenfold greater percentage analysis of charcoal from archaeological sites.

As in other archaeologically-relevant dating techniques (Wintle, 1996), some advance is being made in radiocarbon dating methods in the ability to use small samples of specific carbon-bearing extractions with improved precision (e.g. Bird et al., 1999). The greater potential for contamination of small samples is generally outweighed by the analytical (precision) benefits and the reduced impact on culturally sensitive material. In her archaeobotanical studies in the Keep River region, Atchison (2000) obtained more reliable radiocarbon results from larger seed fractions (> 2 mm) arguing that finer carbon fractions may have moved in the sediment profile. Roberts et al. (1998a) also argued for a more reliable radiocarbon and luminescence chronology at Jinmium from the > 125 µm fraction. These results contrast with studies within a similar sandstone rock shelter in New South Wales, which indicated the smaller the artefact the more likely that it has retained its original depositional position (Balme and Beck, 2002). Balme and Beck (2002) also found that the processes affecting the distribution of plant (starch and

charcoal) remains were different from those affecting stone artefacts. Thus for each study there remains a need to assess the material being dated and its landscape context.

2.4 Identifying Change

In the unconsolidated sandy profiles typical of much of northern Australia, the relationship between the geochronology, sediment stratigraphy, and archaeological stratigraphy is not always apparent (Hiscock and Kershaw, 1992). However, the limits of resolution for interpreting past physical changes in such sandy sediments are set not only by the limits of the chronological methods used, but also by the paucity in our knowledge of physical processes acting in these landscapes, and problems of interpreting past changes of conditions and processes from stratigraphic and geomorphic evidence (Chappell, 1978).

2.4.1 Sediment Characterisation

Sedimentologists and geomorphologists have been involved in many archaeological field studies, but the published record of sedimentary analyses in the archaeological literature rarely goes beyond descriptions of the basic colour and textural information. Whilst these are useful, data such as petrographic descriptions, compositional analyses (eg. grain size analyses, mineralogy, organic, heavy mineral and/or carbonate content) are generally required in order to establish a clear and reliable stratigraphy. For example, in an attempt to derive a master sequence spanning both the Holocene and Pleistocene, Bowdler and O'Connor (1991) combined the sequences and ages from two shelters at Widgingarri, in the western Kimberley. Whilst acknowledging the problematic transference of ages (see Frankel, 1993: 28), Bowdler and O'Connor's (1991) inference of a ~ 10 ka hiatus in occupation derives from a master stratigraphy defined only by Munsell soil colour and texture (degree of compaction). If this were the case, then the Keep River and Malakunanja I archaeological sites, which are similarly composed of poorly sorted fine, medium and coarse-grained (red) siliceous sands (Roberts et al., 1999), would arguably be of similar (Pleistocene) age.

Specific mineral components (e.g. authigenic phosphates, calcite, iron and/or manganese oxides), and physicochemical properties (eg. pH, redox) can also provide potential information on palaeoclimatic or palaeoenvironmental conditions, and whether important anthropogenic materials such as bones, phytoliths, eggshells, pollen or flint tools have or have not been preserved or were never present (Weiner et al., 2002). Part of the problem is that archaeologists often have a poor grounding in modern soil science techniques and hence only a partial understanding of how advanced analytical techniques can be used to approach or solve geoarchaeological problems (R. Gilkes, pers. comm., 2002). The importance of basic sediment description in Australian archaeology has been previously argued (Mulvaney, 1972; Keeley and Macphail, 1981; Hughes, 1983a; Webb, 1992; Barham et al., 1995), but it is not yet a common feature of many published archaeological studies.

Micromorphology – the study in thin section of resin impregnated unconsolidated sediments - has rarely been used within Australia despite the benefits of such micromorphological studies to geochronological and geoarchaeological research (Courty et al., 1989; Macphail et al., 1990; Davidson et al., 1992; Matthews et al., 1997; Goldberg and Arpin, 1999; Goldberg, 2002).

Micromorphology is generally used to qualify initial hypotheses derived from field examination, and in particular to identify sediment type, anthropogenic features, nature of disturbance during occupation, and post-depositional disturbance (Davidson et al., 1992). The latter may be especially important to reliable chronological determinations. In Meadowcroft rockshelter, Pennsylvania, Goldberg and Arpin (1999) used micromorphology to confirm that groundwater contamination (and inclusion of humates or coal particulates) had not contributed to falsely early radiocarbon ages. Goldberg and Arpin (1999) also identified subtle changes in colour and texture within the rock shelter sediments which not only indicated the palaeodripline but also changes in the rock shelter configuration. Similar micromorphological analyses would be invaluable in many northern Australian rock shelters. Unfortunately, there is little or no groundwork characterising either the natural and cultural features of sandy sediments in these semi-arid monsoonal environments.

2.4.2 Bioturbation

Bioturbation is acknowledged as one of the major problems in identifying processes and features in archaeological deposits, and in the possible distribution of artefacts (Fig. 2.1). Recent reviews have stressed the significant effects of earthworm activity on archaeological stratigraphy (Johnson et al., 2002; Canti, 2003). In more arid and monsoonal environments, such as northern Australia, termites essentially fill the role of earthworms (McBeaty, 1990). McBeaty (1990) provides one of the few studies of termites as agents of post-depositional disturbance on archaeological sites but there remains no equivalent study in Australia.

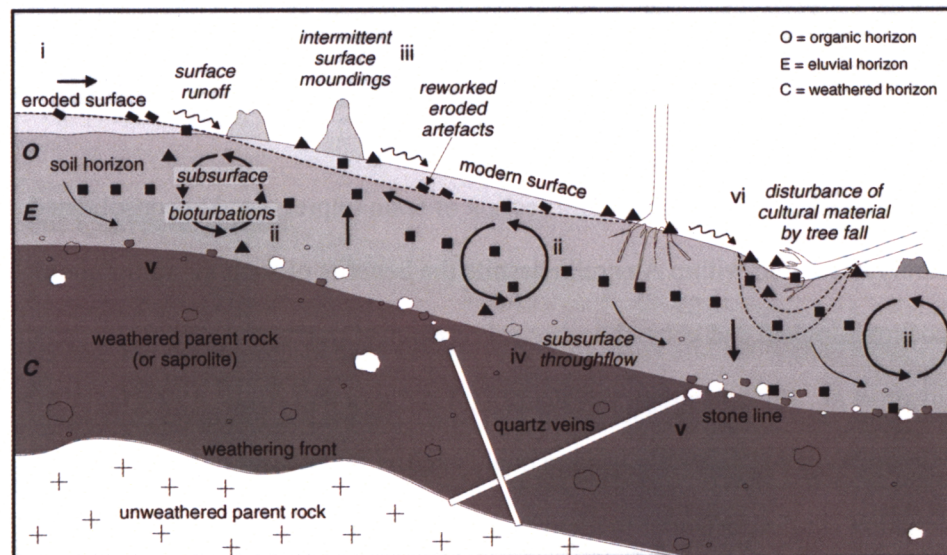


Figure 2.1 Dynamic denudation model modified from Johnson (2002: 18, his Fig. 1), wherein biotic processes, together with geomorphic and anthropogenic processes, contribute to landform evolution. Artefacts are depicted as filled shapes. Examples of processes that may disturb the distribution of artefacts include: (i) erosion of surface soils, leading to redistribution downslope of sediment and artefact material, (ii) constant subsurface bioturbations, (iii) intermittent mound building and upward displacement of sediments and artefacts, (iv) hydrological translocation processes within the sediment, (v) formation and integration of artefacts into stone lines, and (vi) disturbance of surface and buried artefacts by tree fall or decay.

Whilst it may not be possible to attribute specific products to specific processes in archaeological sites, it is important to try to identify the scales at which bioturbation processes overlap with other depositional processes. Canti (2003), for example, defines the depth of artefact burial due to worm activity to 10 – 25 cm. Grave and Kealhofer (1999) used a combination of soil morphology and phytolith analyses to estimate the disturbance scale of bioturbation to be between 0.2 and 5 cm. The undisturbed pattern of natural or cultural processes may only be represented deeper in the sequence as biotic influences decrease (see also Nkem et al., 2000).

Consequently, consideration should be given to the many environmental and/or cultural processes that produce similar signatures, particularly in the upper sediment horizons, before any archaeological or geoarchaeological implications are made. Consider, for example, interpretations of settlement patterns throughout Australia presented by Smith and Sharp (1993) using time-series graphs of site use (Fig. 2.2a). In the absence of any normalisation to non-occupied sites, depth, or some other measure of frequency, the apparent cultural trend could equally be representative of natural processes. The shape of the curve, for example, is typical of bioturbation as identified by Du et al. (1998, Fig. 2.2b) and Van Nest (2002, Fig. 2.2c).

An alternative explanation for the apparent trend may include the poor preservation of older carbon (Fifield et al., 2001), particularly in deep sequences which are subject to fluctuating groundwater levels (refer also 7.2.1). If the frequency of sites at *a particular depth* is plotted against age, then the pattern of site numbers (irrespective of the presence of unconformities) simply reflects the greater occurrence of younger sites in shallower sequences and visa-versa for older sites.

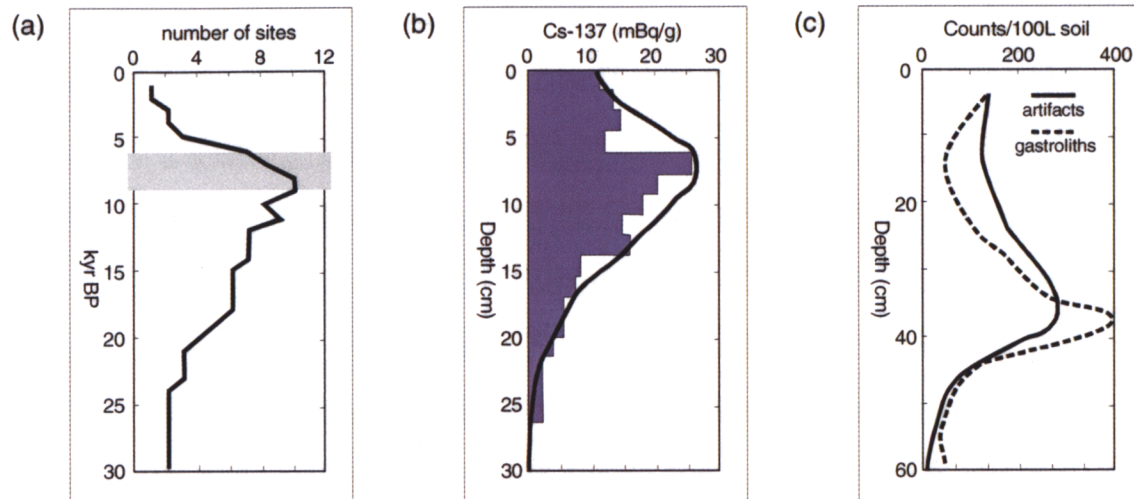


Figure 2.2 Alternative interpretation of trends in time-series graphs, presented in comparison to (a) the original graph of apparent stratigraphic unconformities in northern Australian rock-shelters by Smith and Sharp (1993). Such a trend is also typical of a bioturbation profile, as presented by (b) Du et al. (1998), their Fig. 2, and (c) artefact and gastroliths depth profiles from western Illinois (after Van Nest, 2002, her Fig. 5).

2.5 Interpreting Change

The following discussion considers some of the problems of deciphering cultural and natural deposits, and interpreting the stratigraphic and geomorphic evidence in both rock-shelter and open environments.

2.5.1 Cultural versus Natural Processes and Deposits

An ongoing debate in archaeology is that regarding the continuity of the archaeological record (Farrand, 1993; Frankel, 1995), and of the significance of those sediment layers which contain no evidence of human activity (O'Connor et al., 1999). Archaeological rock-shelter sites across northern Australia typically have mid- to late Holocene units (~ 8 – 3 ky BP) immediately overlying units dating from the last period of glacial aridity (~ 20 ky BP) (Morwood and Hobbs, 1995; O'Connor et al., 1999) indicating a major chronological hiatus. In order to explain the gaps in occupation records in a sedimentary sequence (i.e. a 'cultural

hiatus'), cultural processes have been invoked as 'first-order explanations' (Veth, 1995; O'Connor et al., 1999). The major thesis of O'Connor et al. (1999) is that the absence or loss of cultural deposits results from behavioural changes (i.e. abandonment or higher mobility) rather than erosion and removal of the previous phases of accumulation as postulated by Smith and Sharp (1993).

Whilst in some circumstances at a local level it may be possible or appropriate to consider cultural changes as a prime reason for the absence of preserved cultural materials (e.g. Holdaway et al., 2002), it cannot be taken as the general case (i.e. it cannot be a 'first-order explanation'). In the absence of any relevant geoarchaeological research, the justification of cultural hiatuses remains, on environmental grounds, dubious. Why, for example, do chronological hiatuses also exist in some non-occupation sites (e.g. Bowler, 1998, Nott and Price, 1999)? There are simply too few records of non-occupation sequences available for effective comparison of their nature and stratigraphy with those sites which possess occupation sequences. Moreover, many rock art sites may have little or no sediment deposits or evidence of occupation other than the rock art itself. In the Koolburra Plateau in north Queensland, Flood (1987) noted that 64% of rock art sites had little or no sediment deposits and, of these, only 4% had stone tools. Hence, it may be difficult to assign a sequence as cultural even where sediments are present.

The non-cultural explanation for incomplete stratigraphy within rock shelters of northern Australia (Smith and Sharp, 1993) is based on a graph showing the temporal distribution of stratigraphic unconformities within them (Fig. 2.2a). The graph shows a pattern interpreted to show widespread erosion of rock-shelter deposits in the period 9 - 6 ky BP. The data for the graph have previously been criticised for reasons which include the extrapolation of ages, the similar treatment of data from rock-shelters and caves, and poorly defined stratigraphy (O'Connor et al., 1999). It could also be argued that such a pattern of occurrence of unconformities might occur for many types of sedimentary site, and whether occupied or not. Thus, in the absence of a comparative non-occupation record, the justification of widespread

erosion of rock-shelter deposits in the terminal Pleistocene/early Holocene (Smith and Sharp, 1993) is also questionable.

Smith and Sharp (1993: 55) themselves doubt whether the excavation methods used to obtain the rock-shelter records are adequate to detect erosional surfaces. For young and/or shallow deposits, particularly the unconsolidated sandy sediments typical across northern Australia, the stratigraphy is less readily defined (Ward and Larcombe, 2003). Both brief pauses in sediment accumulation and more significant erosional events may be difficult to detect when either the particle size distribution acts against the development of stratification, or if primary sequences are disturbed by secondary mixing processes (Barham et al., 1995). Consequently, there will be instances where occupation occurred but for which we cannot find any discernable evidence, or infer any regional event or process, until the resolution for correlating chronostratigraphic sequences and unravelling their depositional and post-depositional history has improved.

In some instances, higher resolution dating may be the key. By obtaining numerous AMS ^{14}C radiocarbon ages from an apparently homogeneous and continuous stratigraphic sequence in Okuzini Cave, Southwest Turkey, Otte et al., (2002) were able to interpret a straightforward link between the observed cultural changes with sedimentary lacunae, erosion, or changes in rates of sedimentary processes, and rule out any break in human occupation, or anthropogenic alteration. In other instances, it may be through serendipity or intention that a site is discovered which challenges a perceived hiatus in occupation (Terberger and Street, 2002). For many rock-shelter sites the lithostratigraphic units may be finer than the artefact stratigraphy (ethnostratigraphy) or the chronostratigraphy, thus the characteristics of the sediments themselves and the recognition of hiatuses based on weathering criteria must be utilised (Farrand, 2001: 549).

Dortch and Roberts (1996: 33) argue that occupational or depositional hiatuses in cave and rock-shelter deposits could just as likely result from site-specific developments or localised changes as from regional shifts in physical conditions, population movements, or other large-

scale trends. For example, for sites which relate to mobile hunter-gatherer groups, site formation is likely to result from a complex mix of cultural and natural processes that vary across the landscape, and are differentially preserved within it. The concept of temporally and spatially variable occupation is similar to the geomorphological concept of dynamic depositional environments (e.g. as a consequence of changes in sea-level or climate), in which sedimentary environments and facies shift position through time. Discontinuity that is primarily spatial is thus masked by variation that is primarily temporal (Tipper, 1998). The discontinuous use of place over time provides the basis for surface archaeological studies (Holdaway et al., 2000, 2002), and such studies should be extrapolated into the stratigraphic record by acknowledging that all archaeological sites now buried were once surface scatters (Dunnell and Dancey, 1983). Thus, if archaeological excavations are extended laterally there is an increased chance that time gap(s) will be filled and the overall stratigraphic record will be more complete (Farrand, 1993; Stern, 1994).

Similarly, it is important that any geoarchaeological study include (non-archaeological) areas adjacent to archaeological deposits to, “allow an even finer resolution of geomorphic events and of the relationships between these events and Aboriginal use of sites and their surrounds” (Hughes and Sullivan, 1986: 131). Not only is it important to fill in the gaps between archaeological and adjacent deposits, but also, where possible, to fill in the periods between abandonment and occupation, which, as discussed above, do not necessarily equate with a cultural hiatus. Although many archaeologists have difficulty with the notion that non-archaeological data might provide evidence of human activity (Head, 1994), the converse that archaeological data might provide evidence of natural processes is also true. Consequently, interpretation of both natural and cultural records will be advantaged when approached through multidisciplinary studies.

2.5.2 Rock-shelters

Whilst coastal environments in northern Australia may contain well-preserved mid to late Holocene archaeological sites (Woodroffe et al., 1988; Veth, 1995), research of older sites, or those in non-coastal regions, has mainly focused on rock-shelter sites (O'Connor, 1995; Roberts et al., 1994a; Veth, 1995). Despite the focus given to rock-shelter sites (Smith and Sharp, 1993), few detailed geomorphological investigations of Australian rock-shelters and caves have been undertaken (David and Lourandos, 1999) and hence there is little empirical evidence to support many of the geoarchaeological interpretations made from these sites. Whereas open sites tend to more reflect regional environmental conditions, rock-shelters and caves are idiosyncratic and often have their own microclimates and localised sediment sources (Farrand, 2001). Correlation of deposits from outside shelters with those within are necessary to support chronological comparisons, although they may be complicated where rock-shelter deposits are endogenous or polygenetic, or show poor soil development (Dincauze, 2000). Barton and Clake (1993) have argued that the diversity of geomorphic processes affecting rock-shelters requires that each site be approached individually, and in much the same way that these processes are (or should be) treated at open sites.

For rock-shelter studies, the links between site-specific conditions, patterns of site-use and abandonment, and regional trends have not always been clearly justified. The apparent high correlation between the intensity of human occupation and the sediment accumulation rate, argued from a number of Australian rock-shelters (Hughes and Lampert, 1982; Hughes and Sullivan, 1981, 1982), continues to be cited to support the argument that Aboriginal use of fire increased rates of erosion (e.g. Veth, 1995:745). Within these rock-shelters the apparent correlation between apparent increased intensity of site usage with accelerated accumulation of sediment (apparently from roof-fall) was considered to result from 'quasi-natural' processes including changes in local temperature and humidity (Hughes, 1983; Hughes and Sullivan, 1982). However, first, whether the intensity of human occupation can be effectively measured from the amount of preserved archaeological material is in itself questionable (Hiscock, 1981;

1990), and second, there has been little research to substantiate the original argument for human accelerated erosion. The essence is that the natural processes need to be defined before the cultural interpretation becomes widespread and accepted. In a later paper, Hughes and Sullivan (1986: 130) themselves specified four lines of sedimentological and geoarchaeological investigation which were required to test the hypothesised links but this paper has not received due attention.

Outside rock-shelters, on surrounding sandstone slopes Hughes and Sullivan (1981) argued that Aboriginal burning of the landscape resulted in increased rates of erosion (measured against ‘natural’ firing regimes) in the mid to late Holocene, through increasing instances of the removal of ground-covering grasses and shrubs above ‘natural’ levels. Their argument of increased erosion is based upon coincidence of the commencement of occupation with the onset of sediment accumulation (Hughes and Sullivan, 1981: 277, see also Hope et al., 1995: 231). This premise fails to account for the limitations in the identification and dating of either event, or that in the absence of net sediment accumulation, there may be no clear means of preserving and evidence of occupation. Although increased sedimentation in caves and rock-shelters due to human processes is not unheard of (e.g. Farrand, 1993, 2001), some circumspection would be appropriate when using sedimentation rates in interpreting human-environment interactions until more detailed studies of the processes of sedimentation associated with such sites are undertaken. The following research in the Keep River region attempts to do this.

Overall, despite the attention given to rock-shelter sites throughout Australia, too few archaeological studies follow-up field stratigraphic and sedimentary surveys with laboratory analyses selected to reveal those attributes most relevant to the interpretations, and unfortunately some uncorroborated interpretations persist in the literature. Scope exists for developing an integrated geoarchaeological approach to Australian studies, like those used in America (Farrand, 1985; 1993; 2001), and Europe and the Near East (Barton and Clark, 1993)

which leads to an understanding of site-formation processes during human occupation, and, in some cases, to a reconstruction of local and regional paleoclimates.

2.5.3 Open sites

Aboriginal activity was not restricted to rock shelters, so it is surprising that few studies extend their archaeological excavations out to the adjacent sediments. The main rationale in doing so is to distinguish site-specific trends from cultural and depositional sequences characteristic of the wider area. A few studies have restricted attention of open sites to the (present) dripline (Morwood, 1981, 1986; Mardaga-Campbell and Campbell, 1985), and attempted to explain the distribution of artefacts due to cultural (e.g. stone working, caching and discard) or natural processes (e.g. preferential removal through runoff). In addition to challenging the geomorphological assumption that the palaeodripline has not been altered, these studies would also benefit from empirical studies assessing the hydrological disturbance of archaeological materials (e.g. Schick, 1987). A number of excavations have extended beyond the dripline but the comparison of cultural deposits (e.g. Flood, 1970; Smith, 1989) and comparison of sediments and chronology (e.g. Jones and Johnson, 1985; Morwood et al., 1995) between the rock-shelter and outside areas have been minimal; hence the site formation history remains incomplete.

The consideration of open archaeological sites in Australia can be extended to those associated with sand sheets and source-bordering dunes, lunettes, alluvial terraces, and wetlands (Smith and Sharp, 1993). The importance of the availability of water is apparent in all these sedimentary environments and appears to be reflected in common regional responses to long-term climatic fluctuations (Morwood and Hobbs, 1995). However, at the site specific scale, human responses are more likely to vary according to local environmental conditions and available resources. Thus, even in the absence of specific archaeological surveys, geoarchaeological studies which explore the dynamics of coasts, palaeo-lakes and rivers provide important information regarding the nature and potential for long-term human use of

these environments. The Tsodilo Hills, in the Kalahari Desert, is one of the few sites of palaeoenvironmental and archaeological significance that have yielded composite proxies of both dry (from palaeodunes) and wet (from palaeolakes) conditions during phases of occupation (Thomas et al., 2003). Recent work in the Eastern Sahara has also shown that the combination of changes in the palaeolakes and rivers (as interpreted from sedimentological and geochemical data) used in conjunction with archaeological results, reveals the importance of natural and cultural links during the Holocene (Hoelzmann et al., 2001). In this case, changing water resources reflected in a shift in migration routes, until the area became too arid and was completely abandoned.

Unravelling the prehistory of arid Australia, especially of the sand deserts and their associated chaotic drainage systems, is a complex task (Hughes and Sullivan, 1982). To date, few detailed studies of arid-zone rivers exist to aid palaeoenvironmental reconstructions (Nanson and Tooth, 1999). The studies of Ferring (1992), Gladfelter (1985), Hassan (1985), and Howard and Macklin (1999) have all promoted the integration of archaeological and geomorphological evidence in alluvial environments. These studies are useful in building models of potential archaeological preservation and erosion, and also illustrate how landscape archaeology depends on understanding formation processes and change in the underlying physical landscape. There are contrasting records of past rivers, lakes and even rainfall distribution for northern Australia, and they may produce a range of signatures of prehistoric human activity (Morwood and Hobbs, 1995) as well as site preservation. For instance, the archaeological response to increased aridity and changing sea-level during the Pleistocene-Holocene transition differed in relation to reliable networks of water, with groups focusing on riverine systems and having more sedentary encampments along the coast (Veth, 1995). In a study of settlement patterns in the Ord-Victoria River region, Gregory (1998) concluded that the biggest taphonomic impact upon site preservation is fluvial processes and that these processes are likely to have a similar impact on sites elsewhere in northern Australia.

2.6 Geoarchaeology of Northwestern Australia

As in southern Africa, America, India, Canada and part of Europe (Straus et al., 1996), the human-land story in Australia reflects how humans adapted their foraging lifeways to deal with significant changes in environments and resource structures, such as during the climatic fluctuations of the Pleistocene-Holocene transition (Allen and O'Connell, 1995). The recent view that gatherers and hunters did not live in perfect in harmony with the environment but in fact have long been the world's great destabilisers (Goudie, 1986), has raised issues of what is natural and the role of humans as instigators of change (Head, 2000), and how this is manifest in the geoarchaeological record (Ross, 1982). Theoretically, if Aboriginal people did have an important influence on geomorphic events, it should be possible to compare rates of geomorphic change over time between areas with similar natural environments but different anthropological influences, assuming the latter can be identified and quantified.

Savanna landscapes, particularly those in northern Australia, Atchison (2000: 23) argues have maintained a large spatial and long temporal hunter-gatherer presence. Historically savanna ecosystems have been described as stable or steady state (Skarpe, 1992), but subsequent researchers have argued for a more complex dynamic equilibrium in which the only perception of change, both cultural and natural, in such environments is in effect a function of the spatial and temporal scale (Friedel, 1994). In theory, Aboriginal people act in non-equilibrium systems alongside other disturbance processes (Atchison, 2000: 38), and it is these processes that need to be defined and quantified. The semi-arid monsoonal environment of northern Australia offers the opportunity to review aspects of landscape archaeology and site formation that have had foundations in more temperate climates (White and O'Connell, 1982). Consequently, it is hoped that this study of the Keep River region adds as much value to geoarchaeological studies throughout Australia, as it does to other semi-arid and monsoonal continents such as Africa, and America.

2.6.1 Geoarchaeological Problems in the Keep River Region

Geoarchaeology is not strictly one discipline and, accordingly, this study includes techniques of *in situ* cosmogenic dating, luminescence dating and sediment geochemistry to explore the Keep River region over different temporal and spatial scales. These geoarchaeological investigations are intended as a framework in which to consider the analyses of the archaeological excavations and rock art studies in the Keep River region. The sedimentary and geoarchaeological contexts of the rock shelters and sand sheets are initially defined within the regional climatic-geological environment in Chapter Three, for which there is still very limited information.

Consideration is given to long-term rates of plateau denudation using *in situ* cosmogenic dating. One of the major limitations of *in situ* cosmogenic dating is the cost of analysis, which limits the number of samples that can be processed. However, with careful sampling, a reasonable estimate of regional erosion rates in the Keep River region can be obtained and compared to other parts of northern Australia. Whilst useful in providing long-term estimates of plateau denudation, *in situ* cosmogenic dating is limited in terms of the defining variability of erosion between specific rock formations or archaeological surfaces throughout the Keep River region. The denudation history of the Keep River landscape complements the genetically linked depositional chronology, determined using a combination of *in situ* cosmogenic and luminescence dating techniques. Burial dating using *in situ* cosmogenic isotopes can potentially differentiate between erosion, accumulation, and bedrock disintegration over the long-term, which has been a speculative issue in previous discussion of the Jinnium site. Cosmogenic isotope dating cannot, however, distinguish brief, episodic events. Thus in keeping with the aim of relating the broader landscape processes to the specifics within individual sites, a more detailed chronostratigraphy of the sand sheets is investigated using luminescence dating. Similar dating combinations have (Markewich et al., 1998) and should continue to provide better resolution and accuracy in geomorphological studies (Watchman and Twidale, 2002).

The Keep River region has been presented in the light of previous problems in the dating and geomorphology of the sandstone deposits. In this light it is clear that a regional geochronology for rates of land-surface change both within and beyond any immediate archaeological sites is required. Using multiple dating techniques, further research is needed to explore the geomorphological context of site deposition and attempt to relate these to the archaeological and rock art records (Fullagar et al., 1996), particularly given the conflicting age relationships between the visible rock art and the cultural deposits at Jinmium (refer 2.3.2). This study attempts to do this.

Given that TL and OSL dating techniques inherently relate to depositional processes, it is important to understand the physical processes within and between the escarpment and sand sheets. It is the depositional and post-depositional processes which ultimately influence the relationship between archaeological materials and the sedimentary matrix. Consideration is given to the geochemical character and micro-scale features of the sediments at specific sites. The attempts in this study to obtain thin sections of the stratigraphy from resin impregnated sediments involve a certain degree of experimentation, particularly in the absence of any comparable micromorphological research in such sandy sediments, many of which are heavily bioturbated. The taphonomic implications of this research are relevant to many sandy sites common across northern Australia.

2.7 Conclusion

Australia's ancient landscapes and cultures are inextricably linked in the evolving paradigms of archaeological research, but the associated studies of earth sciences and archaeology have yet to be effectively linked in Australian geoarchaeology. There is need for the development of geoarchaeological concepts and techniques based in semi-arid monsoonal (sandy) environments in Australia and elsewhere –the following research is a step towards this.

CHAPTER THREE

Regional Setting

The land is my foundation. – Fox (1983: 27).

3.1 Introduction

Situated in the far north western corner of the Northern Territory, the Keep River region is a good example of an ancient landscape in a presently semi-arid monsoonal environment. Superimposed over the ancient landscape features are the more recent (Quaternary) geomorphic features that bear the human-land record. The following discussion outlines the regional geological and environmental setting of the Keep River region, and summarises the modest amount of available palaeoclimatic information for this part of northern Australia. As implied by Fox (1983), the geological, geomorphological, ecological and climatic background provides the foundation for subsequent local geochronologic and geoarchaeological interpretations.

3.2 Geological Setting

3.2.1 Bedrock Geology

The Keep River region is geologically younger than both the Kimberley to the west and the Victoria River District (VRD) to the east (Whitehead and Fahey, 1985) (Fig. 3.1). The geology of the Keep River region is dominated by a basement of sandstone, shale and conglomerate, overlain by alluvial sediments deposited by the Ord and Keep Rivers (Kinhill, 2001). Whilst some consider the Keep River region more typical of the eastern Kimberley than northwestern Victoria River and Arnhem Land (Tacon et al., 1999), others argue that the Keep River region is neither (culturally?) part of East Kimberley, nor is the bedrock as durable as that in the north west Kimberley (Walsh, 2000).

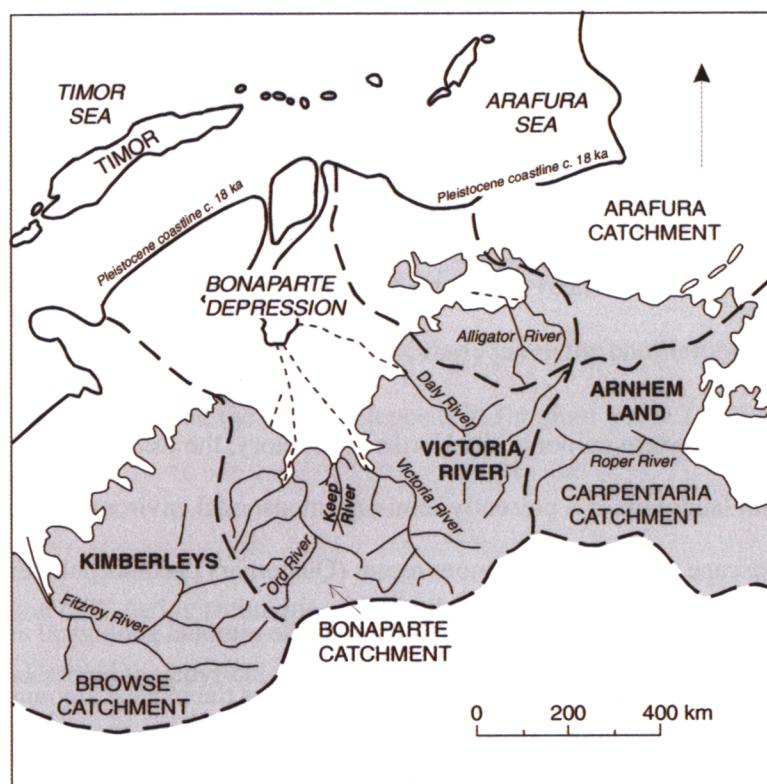


Figure 3.1 Drainage basins in north-central and north-western Australia around 18 ky BP, showing the Keep River region flanked by the adjacent Kimberley and Arnhem Land regions (from Lewis, 1988, his Map 4).

In the study area the geology takes the form of extensively weathered sandstone bluffs and low sandy ridges, separating red earth and black soil (cracking clay) plains (Fig. 3.2). These plains include the Keep River Plain, Weaber Plain and Knox Creek Plain, which are to be developed under ORIA Stage II (Fig. 1.3). Detailed descriptions of the geology of the Ord River area can be found in Traves et al. (1970), Dow and Gemuts (1969), Mory and Beere (1988), and of the Keep River National Park in Whitehead and Fahey (1985).

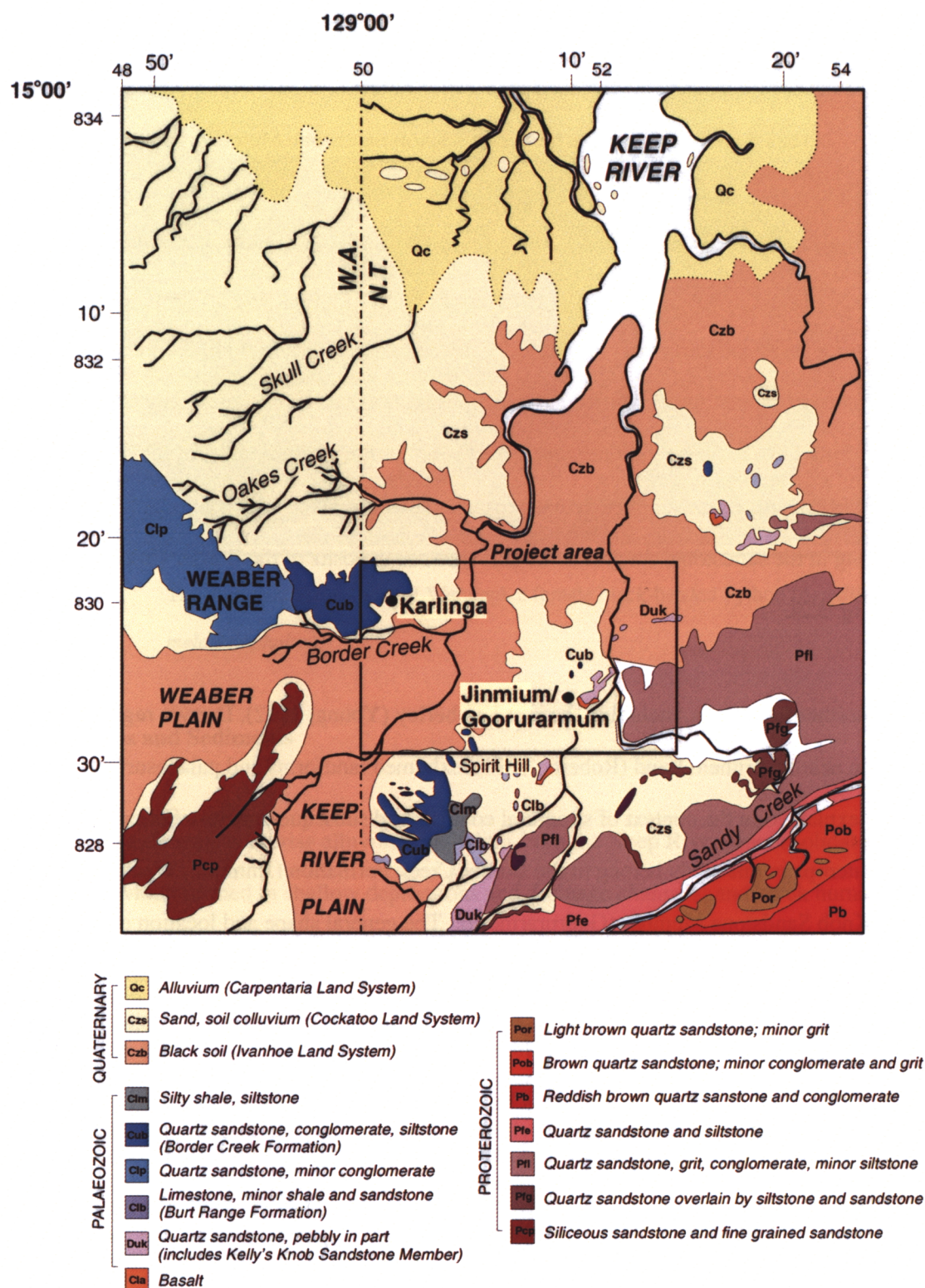


Figure 3.2 Geology of the Keep River region, combining the Cambridge Gulf (Sheet 5214, BMR 1970) and Auverne (Sheet 5215, BMR 1975) 1: 250 000 mapsheets. Project area and major site locations are marked.

The overall depositional environment of the Keep River region has changed from a continental-fluvial environment in the Palaeozoic to a terrestrial environment in the Quaternary (Whitehead and Fahey, 1985). The basal members, such as the Kelly's Knob Sandstone Member, comprise conglomerate and pebbly quartz sandstone (Fig. 3.2) formed in a near-shore shallow marine environment during the Devonian. Subsequent deposition of different sediments was determined by varying influxes of terrigenous material, reflecting the continued faulting and uplift of various source areas throughout the Early Carboniferous. Calcareous sediments (dolomite, limestone) were deposited in an environment with significant terrigenous input (shale, sandstone) to make up the Burt Range Formation. Between the Early and Late Carboniferous further uplift of the southeast portion of the Bonaparte Basin supplied coarse terrigenous sediments to river valleys, channels and plains, resulting in the sandstone, conglomerate and siltstone deposits of the Border Creek Formation (Fig. 3.2).

Throughout northern Australia, including the east Kimberley (Young, 1992), Darwin region (Nott, 1994b), and in nearby Arnhem Land (Roberts, 1991), exhumed landforms and palaeosurface remnants are explained in the context of structural controls and subsequent deep-weathering. The major rock outcrops in this study belong to the Border Creek Formation (Jinmium, Weaber Range) and Kelly's Knob Sandstone Member (Goorurarmum). The general shape and location of these outcrops are considered to be manifestations of spirit figures which crossed the landscape during the 'dreaming' (Atchison, 2000). One of the more dominant outcrops is the escarpment (Fig. 3.3) at Wulurungu (eastern Weaber Ranges) which represents Walujapi, a female Black-headed Python (*Aspidites melanocephalus*). The rock shelters situated along the Keep River escarpments are a feature relict of a landscape that has undergone dramatic changes in sea level (Woodroffe, 1993) and climate (Lees, 1992b; Nott and Price, 1994, 1999; Schulmeister, 1992) over tens of thousands of years.



Figure 3.3 The dominant escarpment of Walujapi, a female black-headed Python (*Aspidites melanocephalus*).

3.2.2 Soils and Sediments

Quaternary sediments comprise alluvium, including from the Keep River; unconsolidated sediments, which formed in shallow depressions and drainage channels; and black humic soils, which form on poorly drained floodplains (Whitehead & Fahey, 1985). Indications from analogous sand sheets in Arnhem Land are that the development of the sand sheets over the past quarter of a million years has been cyclical with periodic accumulation during periods of high sea level and extensive gullying and denudation during periods of low sea level (Roberts, 1991). At any particular glacial maximum, gullies will erode some sites more than others to leave aprons with a mosaic of sediments of different basal ages (Roberts, 1991: 303). The present sand sheets in the Keep River region are probably representative of the most recent phase of sand accumulation. Uncertainty regarding the geomorphological foundations of the sand sheets is considered in Chapter Four.

The two archaeological site areas of Karlinga (Wulurungu) and Goorurarmum are part of the Cockatoo Land System, and are separated by sediments of the Ivanhoe Land System (Fig. 3.2). The Cockatoo Land System represents former landscape remnants that comprise red-brown earths (Bonaparte) and red-earth (Weaber). The sediments can be described as oxisols (Stace, 1968), with deeply weathered soils having uniform profiles dominated by resistant minerals, particularly quartz, and some deeply weathered mottled horizons (plinthite). Typically these soils are vegetated by eucalypt woodland to open forests but, as in Arnhem Land (Roberts, 1991), most of these sediments have little organic matter due to loss of plant material in the dry season fires and the rapid decay of organics in this tropical climate. The Ivanhoe Land System comprises cracking clays (gilgai) considered to be of Holocene origin (Aldrick and Moody, 1977). The vegetation on these soils is variable; common communities include open grassland (*Themeda australis* and *Sehima nervosum*), and open *Acacia* shrubland.

Soil distribution is also influenced by the course of present and prior streams, with soils adjacent to freshwater creeks and abandoned channels, such as those alongside Sandy Creek, more typical of quartz-rich spodosols. According to Aldrick and Moody (1977) soil distribution is most apparent in the succession of vegetation with a progression toward treelessness as the soil conditions become less favourable as a result of increasing salinity or aridity. The succession is thought to have occurred under the influence of dynamic changes in soils and fluvial hydrology, and later, to anthropogenic influences associated with fire and overgrazing. Further details of soil studies relevant to ORIA Stage I and II can be found in the draft Environmental Impact Study (EIS) of Kinhill (2001).

3.3 Geomorphological Setting

Modern coastal and offshore geomorphology contains strong elements of Quaternary inheritance, with topography closely resembling that of the adjacent landmass (Van Andel and Veevers, 1967; Woodroffe et al., 1992). Detailed reconstruction of the modern coast and adjacent Joseph Bonaparte Gulf thus provides an important background for geoarchaeological research.

3.3.1 Late Pleistocene

The Keep River region lies within the Ord-Victoria geomorphic region outlined by Paterson (1970). The basement rock underlying the Keep River and Weaber Plain is for the most part undifferentiated Permo-Carboniferous sandstone, over which lie the erosional and alluvial plains (5 - 25 m deep) of the Cambridge Gulf Lowlands (Kinhill, 2001). The ancient course of the Ord River is postulated to have flowed north-east beneath the Weaber Plain and then roughly along the course of the present day Keep River (Kinhill, 2001), although the timing of separation of the two rivers is unknown. It is postulated that some time after the capture of the Ord River, deposition of material from the Keep River and Sandy Creek reduced tidal range in the Keep River region to 3.7 m, compared to 5.2 m in the adjacent Gulf (Aldrick and Moody, 1977).

3.3.1.1 Last Glacial Maximum (25 – 18 ka)

Prior to the Holocene marine transgression, all major rivers of the region drained into the marine lagoon that is now the Bonaparte Depression (Fig. 3.1). The present shoreline lies approximately 100 km south of Joseph Bonaparte Gulf (Fig. 3.4). At the Last Glacial Maximum (LGM), the shoreline would have been a further 600 km offshore at approximately 130 m depth, and marine cores taken to the north and south of the Bonaparte Depression reveal micro-palaeontological indicators of increasingly marine conditions (Yosukame, 2001).

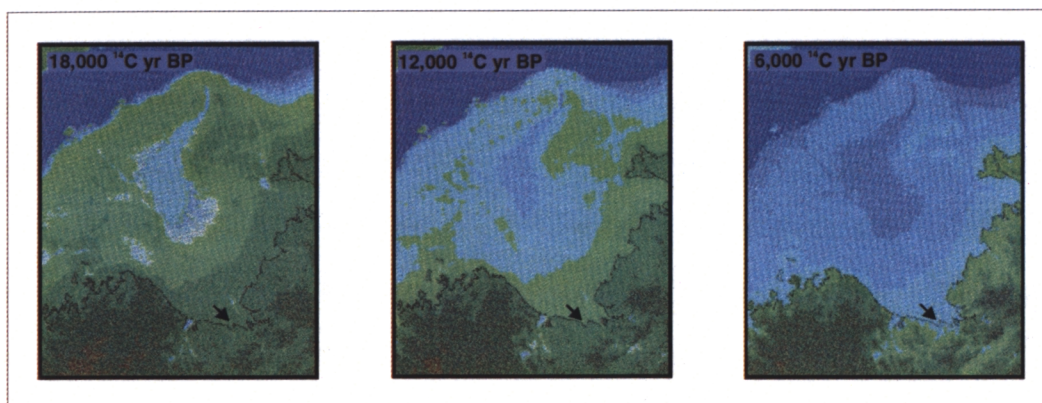


Figure 3.4 Location of the Keep River (indicated by arrow) in relation to the changing shoreline around the Joseph Bonaparte Gulf at 18 ¹⁴C kyr BP (LGM), 12 ¹⁴C kyr BP, and 6 ¹⁴C ky BP (from Yosukame et al., 2001; their Fig. 5). Bathymetric and topographic contours are indicated by changes in colour scheme, and show the depth increase from 0 m, to 25 m to 50 m depth near the mouth of the Keep River.

Van Andel and Veevers (1967: 38) indicate that the submarine topography of the Joseph Bonaparte Gulf resembles that of the adjacent land (Fig. 3.5). Geomorphological studies on land in the nearby Coburg Peninsula, northeast of the Keep River, also indicate a strong element of Quaternary inheritance that has evolved through the reoccupation of previous intertidal levels (Woodroffe et al., 1992). The Keep Plains now stand several metres above sea level and there is no evidence to indicate that they have formed under marine or estuarine conditions (Aldrick and Moody, 1977). However, the seaward side of the Keep Plain was observed to comprise highly calcareous silty clays typical of marine deposits.

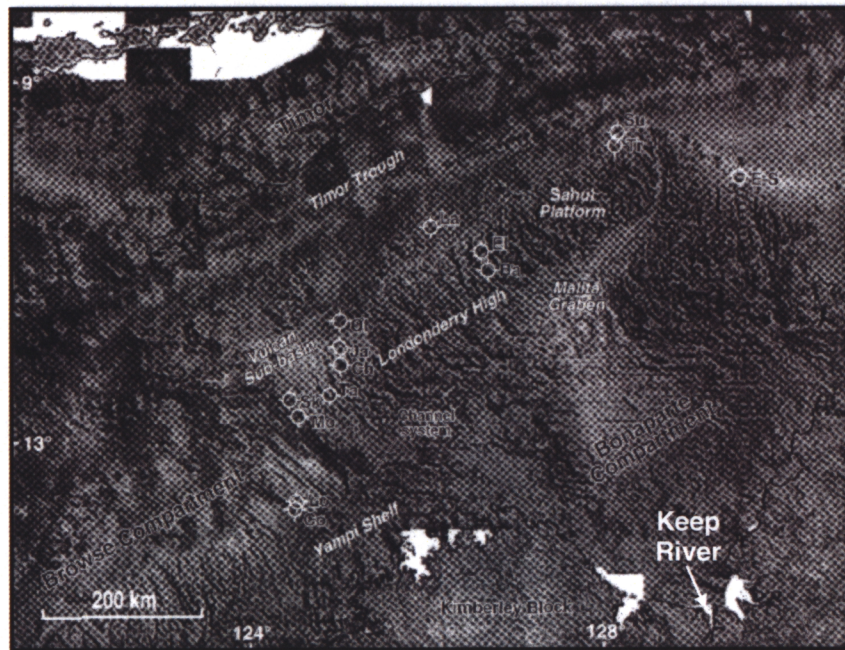


Figure 3.5 Submarine topography of Joseph Bonaparte Gulf, determined from high resolution aeromagnetic surveys as part of the North West Margins Project at AGSO (<http://www.agso.gov.au/marine/nws/>).

3.3.2 Holocene (10 ka - present)

Extensive geomorphological studies in northern Australia (Woodroffe et al., 1987; 1989; 1992) have revealed the rapid rise of sea level from about -12 m AHD to its present elevation between 8 and 6 ky BP, with indications from bedded beach deposits that about 5 - 6 ky BP relative sea level was 0 - 1 m above present (Woodroffe, et al., 1992). From 7 to 3.5 ¹⁴C ky BP, much of northern Australia formed part of the “Big Swamp” until subsequent freshwater sedimentation led to the establishment of a more terrestrial environment. The pattern of sea level rise appears to have lagged slightly behind that in eastern Australia, and also indicates that the extreme north of Australia may be undergoing gradual subsidence (Woodroffe et al., 1992). From about 3 ky BP the modern landform with freshwater lagoons and swamps, estuarine and salt-marsh areas, dry land communities on the plains and plateaux were essentially established (Lewis, 1988: 63).

Geomorphological evidence has shown that large macrotidal rivers in northern Australia were diverted or blocked while their coastal plains were prograding as a result of an unusually dry climatic period sometime between 3.5 and 2 ky BP (Chappell, 2000).

3.3.3 Present

The approximate catchment area of the Keep River is 5000 km², which is approximately equivalent to 8% of the Ord River catchment (Kinhill, 2001). The major rivers draining the uplands and plateaux are the Keep River and Sandy Creek (Fig. 3.2). During the wet season, a number of intermittent water courses discharge from the hills onto the surrounding plains, including Cockatoo Creek, Knox Creek, Border Creek and Oakes Creek (Fig. 3.2). This water spreads out as indistinct sheet flow and only at the extremity of the plains is there defined drainage (Kinhill, 2001, 5-7). Rivers and creeks incise the topography of the plains only locally and to a maximum depth of 5 m (Kinhill, 2001, 4-2), although some minor ephemeral creek systems may generate small delta fans and shallow gullies (Fig. 3.6). Alongside many of the larger creeks, there are small semi-permanent billabongs and sandy strips which are primarily associated with old meanders. Groundwater generally occurs about 20 - 25 m AHD, which is approximately 5 m below ground surface (Kinhill, 2001).

Figure 3.7 shows two cross sections determined for parts of the Ord River Stage II, flanked by the main archaeological sites of Karlinga and Granilpi to the west, and Jinmium and Goorurarmum to the east. The cross sections indicate that the profile observed at Sandy Creek Gorge underlies but is not necessarily contemporaneous with the uppermost sediment horizons. The uppermost silty-clay horizon is also unconformable with older horizons and is laterally discontinuous. The sand sheets are likely to be similarly discontinuous.



Figure 3.6 Photograph of small delta fan in the north-west corner of the Goorurarmum amphitheatre, made obvious by the new growth of Spinifex grass after the 2000 wet season.

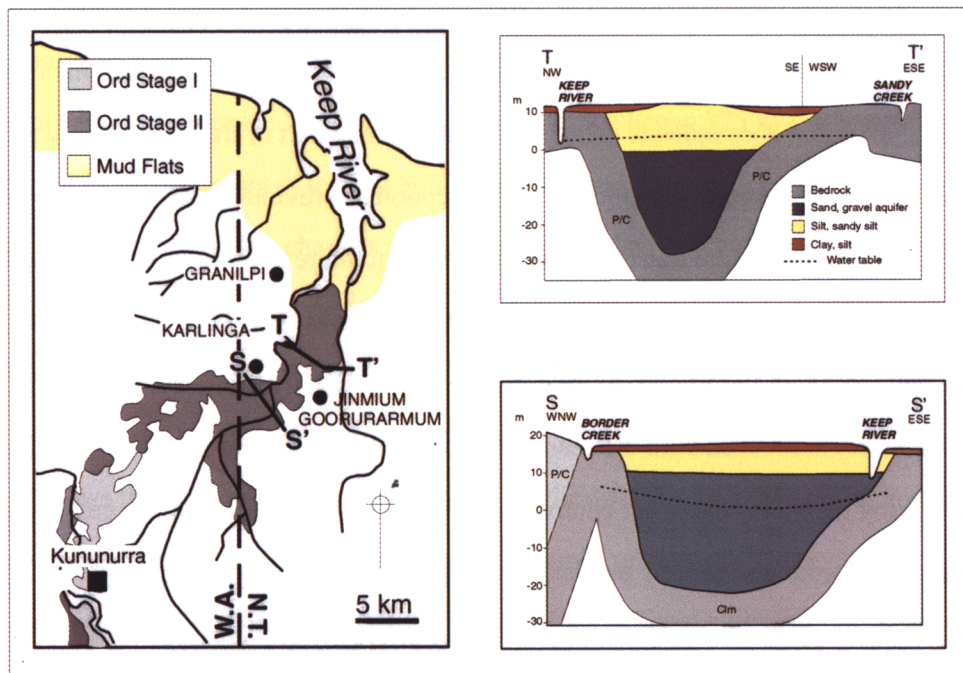


Figure 3.7 Cross-sections across the planned Ord River Irrigation Area, showing a stratigraphic section from the Keep River to Sandy Creek (T - T'), and from Border Creek to the Keep River (S - S') (from Kinhill, 2001). Although oversimplified, these depictions indicate that the average thickness of the upper sediment horizons are less than 5 m thick, and are laterally discontinuous.

3.4 Vegetation

The Keep River region occurs in the general biogeographic province known as the Tropical (Torresian) Zone, which encompasses the humid tropical and subtropical regions of northern Australia (Hope, 1984). The variety of vegetation types found in this region range from remnant tropical-subtropical rainforests in northeastern Australia, to dry sclerophyll and grassland in northern Australia, with mangrove forest established along much of the coastline. The appearance of modern environmental patterns and vegetation communities (and fire regime) probably had its origins in the early Pleistocene and developed during the Pleistocene – Holocene transition (Hope, 1984), as a result of positive feedback between fire, vegetation, soil, nutrient status and water balance (Kershaw et al., 1997).

In a history of fire in Australia, Kershaw et al. (2002) continue to debate whether climate rather than human activity has exerted the major control over both fire activity and vegetation change. Anthropological evidence does indicate that fire was an essential part of the Aboriginal way of life, but the impact of people was predominantly in the disruption of previous vegetation-environmental relationships, possibly such as the transition from rainforest to more open savannah-type woodland at about 120 ky BP (Kemp, 1981; Kershaw et al., 2000). Discussions by Head (1989; 1996) argue that anthropogenic influence on preservation or demise of wet and dry rainforest in northern Australia is intimately associated with the seasonality of its climate during the Holocene, and possibly also during the Pleistocene, but continuous palaeoecological records from central and northern Australia are required to fully evaluate the magnitude of human impact.

More specifically the Keep River region is situated within the Victoria-Bonaparte biogeographic region (Whitehead and Fahey, 1985), with a range of vegetation types from open savannah to tall grassland. Open woodlands (*Eucalyptus* spp.) occur on the plains and rocky areas, and low woodland on sandy soils (*Tristania*, *Grevillea*, *Banksia* spp.). *Pandanus* is dominant along waterholes and dry annual creeks beds, while freshwater mangroves and tall perennial grasses

dominate along more permanent streams (Whitehead & Fahey, 1985). Detailed vegetation and flora surveys conducted for ORIA (Kinhill, 2001) indicate the most numerous families in the area are Poaceae (grasses), Myrtaceae (eucalypts and paperbarks), Cyperaceae (sedges and rushes), Mimosaceae (wattles), Asteraceae (daisies), Papilionaceae (peas) and Combretaceae (*Terminalia* spp.). Aquatic plants include mixed rushes and grasses, waterlilies (*Nymphaea* spp.), bladderwort (*Utricularia australis*) and algae. Head et al. (2002) document the past and present use of many of these plants by Aborigines, including the burning of Cypress Pine (*Callitris intratropica*) to keep away mosquitoes, the collection of seeds of *Cathormium umbellatum* for making necklaces, and the harvesting of various other edible and non-edible fruits, seeds and roots including species of figs (*Ficus* spp.), yams (*Dioscorea* spp.) and water lily (*Nymphaea* spp.).

3.5 Palaeoclimate

Large glacial-interglacial oscillations of global climate have, with periods of 40 – 100 ka have occurred for several millennia. The last glacial cycle, which began 125 kya, was not significantly different from its predecessors of the last 800 ka and differed only moderately from those of the preceding 2 million years. The changes of climate over the last 100 ka lie within the last of a long series of climatically comparable cycles. A general outline of palaeoclimatic trends for Australia from 100 ky BP to the present is depicted in Fig. 3.8 and discussed below.

Figure 3.9 shows the existing palaeoclimatic data, synthesised from CLIMANZ archives (<http://rses.anu.edu.au/enproc/AQUADATA/archive.html>), prior to and following the Pleistocene-Holocene transition in northern Australia and New Guinea. Climatic differences between the northeast and northwest regions relate to the presence of the coastal escarpment (The Great Dividing Range) and highlands of New Guinea, which influence both orographic rainfall and exposure to westerly winds. In the northwest, the absence of many physical or thermal barriers means that the main stress has been changing aridity (Hope, 1994), which has partly been a result of changes in sea level, and resultant continental (low sea-level) or maritime (high sea-level)

conditions depending on distance from the coast (Ross et al., 1992). The other major influencing factor is the relative strength and shifting of the Australian monsoon, which in turn is affected by the El Nino/Southern Oscillation (ENSO) (Schulmeister, 1999). A broader discussion of Australia's monsoonal palaeoclimates has been summarised by Van der Kaars (1991) and Johnson et al., (1999).

3.5.1 Late Pleistocene (100 - 10 ka)

There is very little palaeoclimatic or palaeoenvironmental information for northwestern Australia in the early Pleistocene, with the first direct evidence of regional trends being provided from pollen records off the north Australian coast (van der Kaars, 1991; van der Kaars et al., 2000; Wang et al., 1999). These records indicate a decrease in temperatures and rainfall from the early part of isotope Stage 5, followed by a cooler and drier climate during Stage 4, becoming wetter during Stage 3 (van der Kaars et al., 2000), when it is argued that the Australian monsoon was at full strength (Johnson et al., 1999).

A similar story emerges from geomorphological and palaeohydrological studies in the east Kimberley Plateau (Wende et al., 1997), Lakes Woods and Lake Gregory in northwestern Australia (Miller et al., 1999; Bowler, et al., 2001), and other regions of monsoonal Australia (Nanson et al., 1992) including the Magela Creek catchment in Northern Arnhem Land (Nanson et al., 1993).

These studies spanning the last 300 ka, indicate a trend of increased aridity towards the late Pleistocene, with pluvial events broadly corresponding to interglacial phases (Stages 1, 3, 5 and 7), and intervening dry periods (including the LGM) characterised by dune expansion (Fig. 3.8). Thus across northern Australia and Papua New Guinea there evidence of oscillating wet and dry conditions corresponding with glacial and interglacial cycles prior to 25 ky BP.

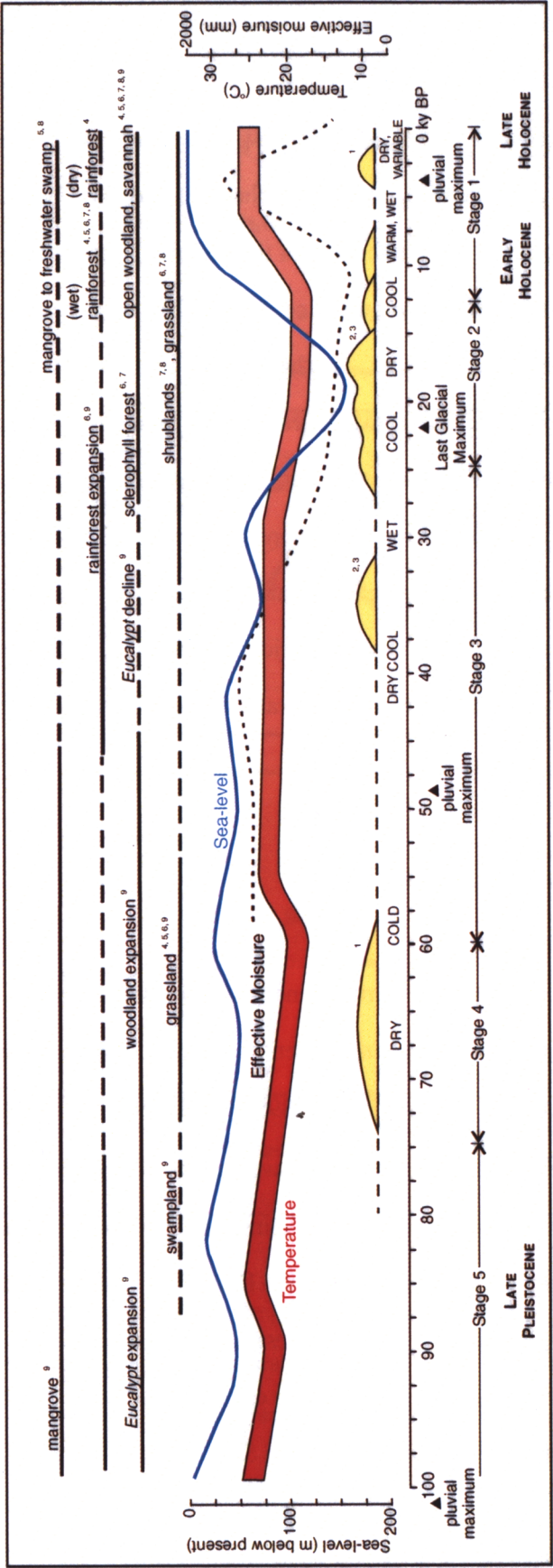


Figure 3.8 Palaeoclimatic and palaeoenvironmental information for northern Australia, modified from White (1994) and based on information from 1. Bowler et al. (2001), 2. Chen et al. (1995), 3. DeDecker (1986), 4. Head (1996), 5. Kershaw (1995), 6. McConnell and O'Connor (1997), 7. Schulmeister (1992), 8. Tacon and Brockwell (1995) and 9. van der Kaars (1991).

From about 40 ky BP, the palaeoclimatic and palaeoenvironmental record is geographically and temporally more contradictory. CLIMANZ records indicate wetter conditions in the northwest and cooler, drier conditions in the northeast of Australia and New Guinea around this period (Fig. 3.8). Higher terrace levels surrounding plunge pools in Kakadu National Park have been interpreted to indicate wetter conditions as a result of a strengthening of the northwest monsoon in this part of northern Australia around 25 to 18 ky BP (Nott and Price, 1994). This evidence contrasts with the general consensus that this was a very dry period. In other parts of northern Australia, perhaps due to the coincident period of occupation, climatic (Miller et al., 1999) and environmental changes (van der Kaars et al., 2000; Wallis, 2001) have questionably attributed to human impact. It has not yet been demonstrated that human impacts have had a more significant effect on the climate of northern Australia than the regional changes in sea-level and concomitant ocean circulation off the north coast. Rather because the northern region was so arid, small climatic changes may have had large impacts locally, indicating the need for more temporally and spatially constrained paleoenvironmental studies in this region.

3.5.1.1 Last Glacial Maximum (25 – 18 ka)

During the LGM, the Australian monsoon was virtually non-existent (Johnson et al., 1999), although the seasonal wet/dry regime was operating (Allen and Barton, 1989). Mountain and coastal areas of PNG were at least 6 °C cooler (Hope, 1989; Aharon, 1983), while slightly cooler (-1.5 °C) and possibly warmer sea-surface temperatures have been indicated for northern Australia at this time (Schulmeister, 1999). From a retrodiction of climates across Australia at 18 ky BP, Hubbard (1995) indicated that only the extreme north of the Kimberley and the Northern Territory would have received monsoonal precipitation. Even in these areas summer rainfall is likely to have been diminished due to the increased landmass and closure of the Torres Strait that blocked the easterly warm current (Bowler, et al., 1976; Hubbard, 1995; Schulmeister, 1999).

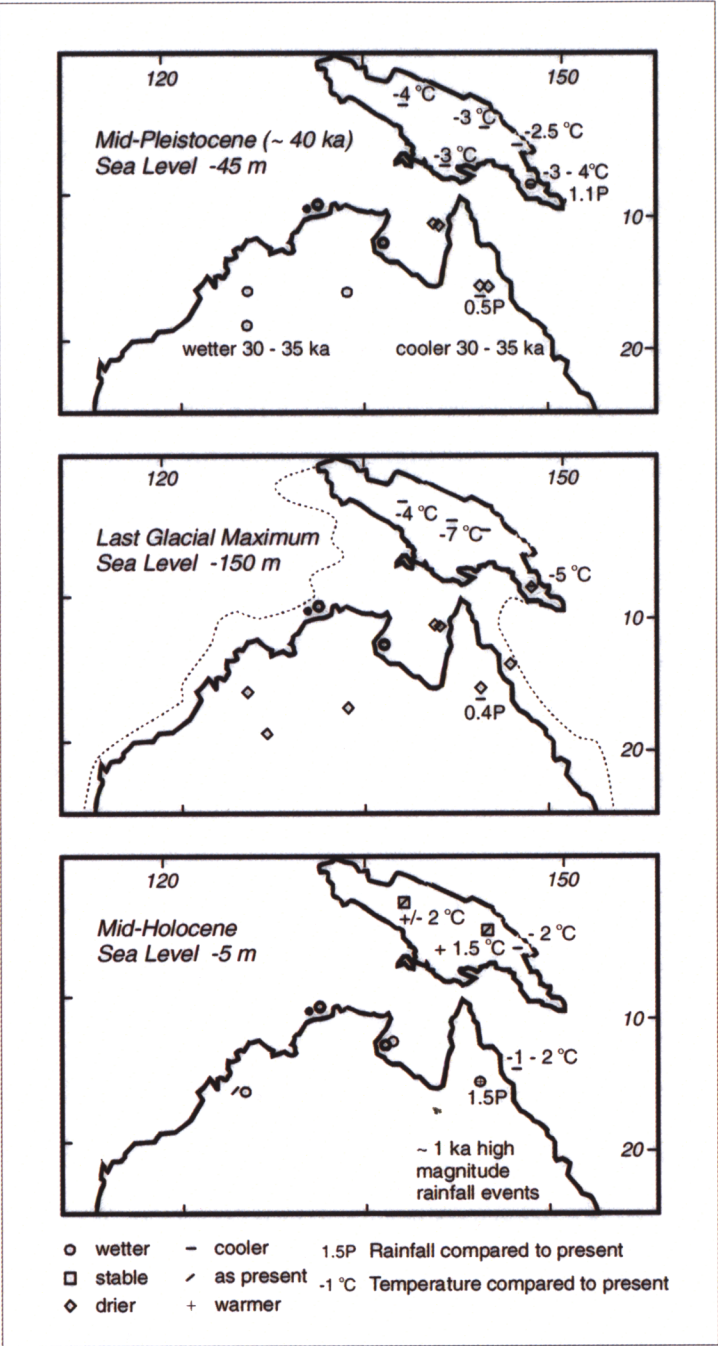


Figure 3.9 Palaeoclimatic data for the period prior to and following the Pleistocene-Holocene transition in northern Australia and New Guinea, modified from CLIMANZ (<http://rses.anu.edu.au/enproc/AQUADATA/archive.html>).

Although moisture in the form of precipitation and streams had decreased, sufficient moisture was apparently available to support perennial grasses and shrubs in parts of the southern Kimberley (McConnell and O'Connor, 1997; Wallis, 2001). The low effective precipitation and sparse vegetation cover facilitated a major phase of dune building in the north (Lees et al., 1990; Wende et al., 1997; Bowler et al., 2001) and in other parts of Australia (Chen et al., 1995; DeDeckker, 1986) (Fig. 3.8). In the archaeological record there is a decline in site occupation at this time (Shulmeister, 1992), except along the arid shoreline where it is evident that humans utilised both coastal and hinterland resources during the Pleistocene (Veth, 1999). Site use increases toward the terminal Pleistocene as climate ameliorated (Schulmeister, 1992; Veth, 1999), with definitive evidence for re-establishment of the monsoon regime in northern Australia from about 14 ky BP (Wyrwoll and Miller, 2001).

3.5.2 Holocene (10 ka - present)

As can be seen from CLIMANZ maps (Fig. 3.9), only a small number of Holocene palaeoclimatic studies have been undertaken in northern Australia (Lees, 1992a; Wende et al., 1997; Wyrwoll et al., 1986, 1992; Nott and Price, 1999; Nott et al., 1999; Schulmeister, 1999; Bowler et al., 2001). Early evidence was thought to indicate that the climate of the Ord and Keep River region has remained broadly similar for the last 8 ka (Aldrick and Moody, 1977), but evidence outlined below is slowly emerging of a less stable climate with locally significant effects. A comparative palaeoenvironmental record for the Holocene from interior and southeastern Australia is provided by Holdaway et al. (2002), which show regionally similar trends to the northwest but with some exceptions, as outlined below.

The early Holocene climate history of Northern Australia is dominated by the effects of the marine post-glacial transgression that flooded the extensive continental shelf around 7 ky BP and a gradual return of the summer monsoon (Shulmeister, 1999). In parts of northwestern Australia, the establishment and use of archaeological sites continued to increase in accordance with climatic

amelioration (Schulmeister, 1992), although up to 10 m of land per year was being lost in the Pleistocene-Holocene transition (Woodroffe, 1993). The available evidence from pollen (Schulmeister, 1992; Kershaw, 1986) and palaeohydrological records (Nanson et al., 1993; Nott and Price, 1994; 1999; Bowler et al., 2001) all point toward significantly wetter conditions in the early/middle Holocene (~ 10 - 5 ky BP) than in the late Holocene. Nott et al. (1999) question whether the increase in precipitation to the pluvial maximum was gradual, or whether it was interrupted by short, intense phases of aridity or cooling around 8 - 6 ky BP, as evidenced from activation of dune fields in tropical northern Australia.

The pluvial maximum occurred around 4 ky BP (Schulmeister, 1999), at least 1000 years later than in southern and northeast Australia (e.g. Holdaway et al., 2002). This hypsothermal is thought to be a result of increased ENSO activity that generated a stronger but more latitudinally confined summer monsoon (Moss and Kershaw, 2000; Schulmeister, 1999). A drier phase followed the wet phase from 2.8 ky BP (Ross et al., 1992; Bowler et al., 2001), with coastal dune sequences indicating reduced wet season precipitation from 2.7 – 1.8 ka (Lees et al., 1990; 1992). A rise of rainfall from 1.4 ky BP in northeast Australia is not recorded in the northwest (Ross et al., 1992), perhaps because of lack of indicative sites. Although such evidence points to increased climatic variability during the Holocene, under what Johnson et al. (1999) argue was a moderately effective monsoon, climatic variability may have been as great or greater under the stronger monsoonal climate of the Pleistocene.

3.5.3 Present

The present regional climate of the Keep River region is semi-arid, with a distinct monsoon season during which much of the annual rain (*ca.* 900 mm) falls (Fig. 3.10). The atmospheric circulation in this area is dominated by the monsoon and trade winds, with a southeast circulation dominating during the winter and northwest monsoon and southwest trades dominating during the summer. Average maximum temperatures exceed 30 °C, and mean annual evaporation (*ca.* 2000 mm) is highest in June and during the summer monsoon (Bureau Meteorology, 1996). The rivers of northwestern Australia flow seasonally, leading to constant changes in the local importance of erosion, transport, and deposition.

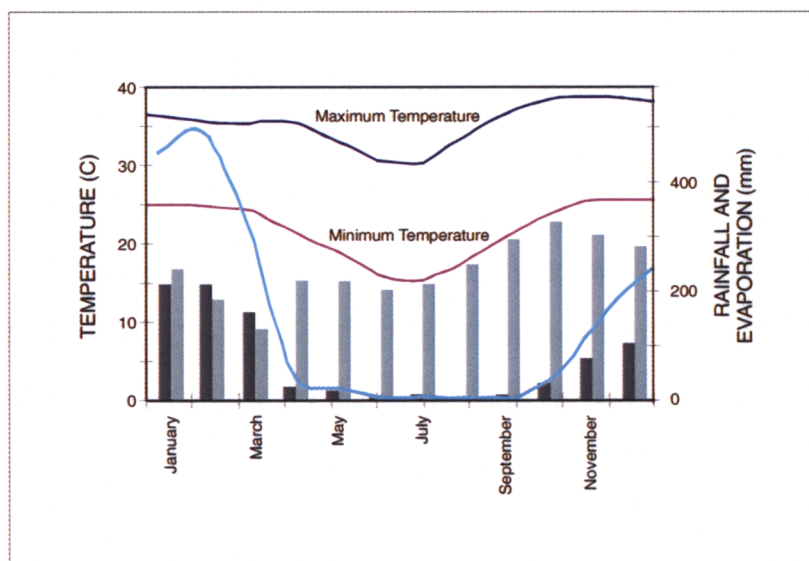


Figure 3.10 Average rainfall and temperature for Kununurra (sourced from <http://www.bom.gov.au/climate/averages/>, 2001).

3.6 Topographic Setting and Study Area

3.6.1 Local Topography

The project area of Keep River region (inset of Fig. 3.11) occupies the northwest corner of the Auvergne and Legune mapsheets. The area consists of dissected plateaux that rise over 200 m above the surrounding low lying alluvial plains. The elevation of the Keep River Plain varies from 20 m AHD in the south-west to 10 m AHD in the north-west (Kinhill, 2001). Details are given below.

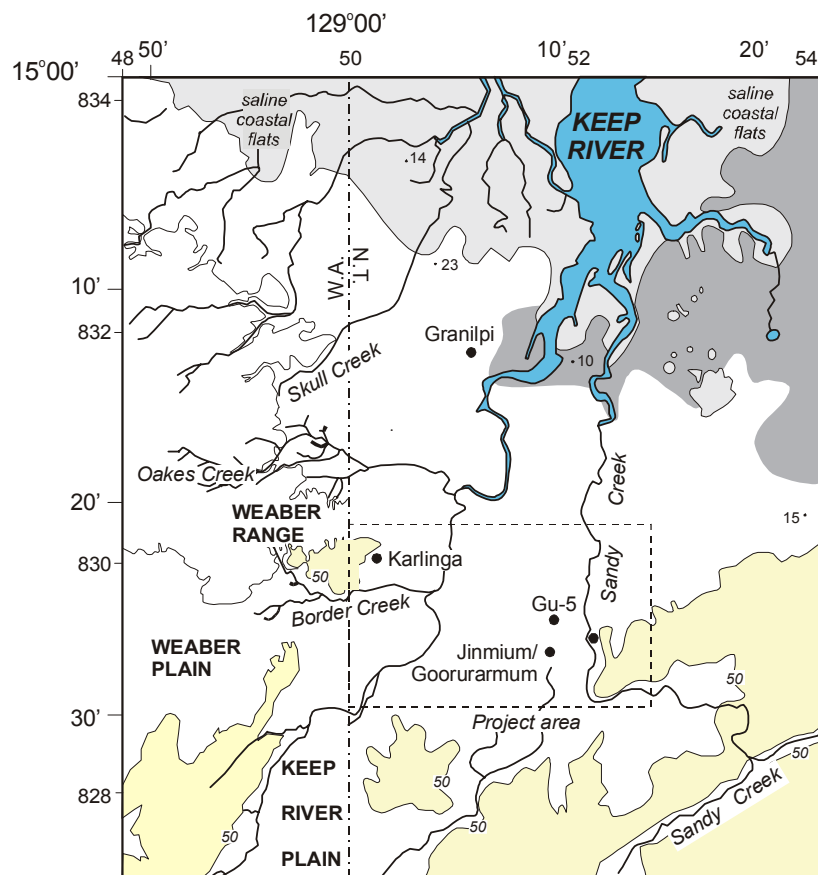


Figure 3.11 Topographic map of Keep River region indicating the project area and major site locations. Enlargement of the Karlinga and of the Jinmium-Sandy Creek catchment area is given in Figure 3.12.

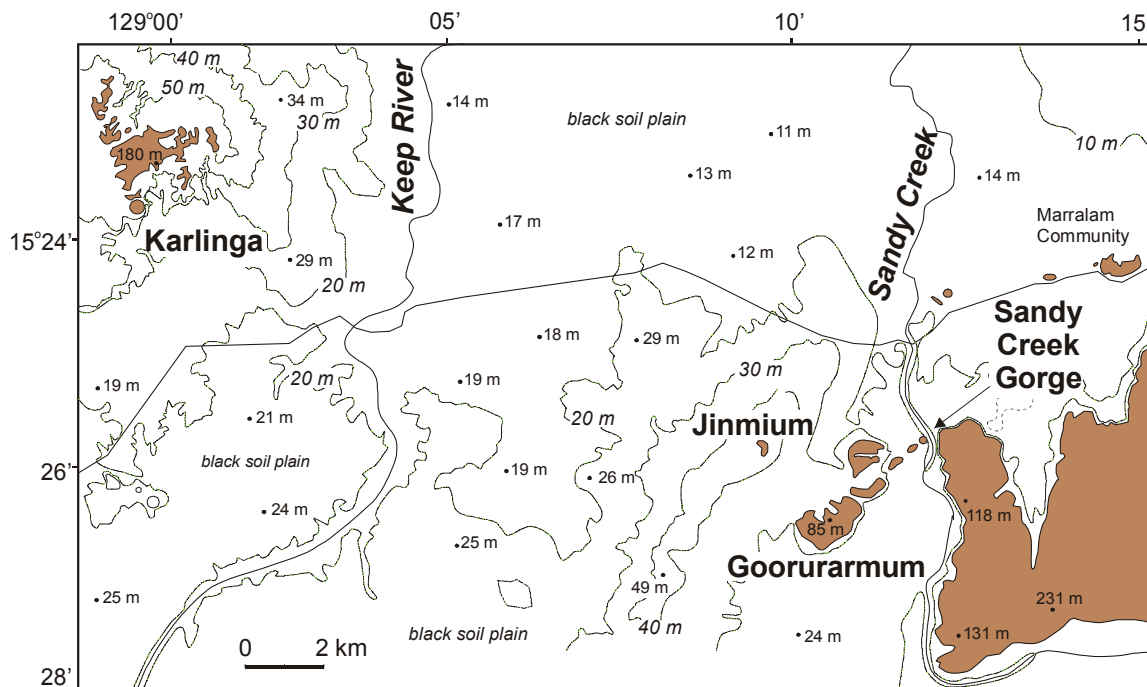


Figure 3.12 Topographic map of project area showing major site locations of Karlinga, Jinmium, Goorurarmum and Sandy Creek Gorge.

3.6.2 Aerial Photography

Aerial photos show the protrusion of the isolated sandstone escarpments above the surrounding sandy plains, such as those around Goorurarmum (Fig. 3.13a), which themselves are dissected by the ephemeral Sandy Creek and its tributaries. Little or no change in the rivers or surrounding plains is evident between aerial photos taken in 1992 and in 1999, indicating the geomorphic processes over this time period are relatively stable. Goorurarmum and Sandy Creek Gorge are situated less than 2 km apart but their topographic relationship has yet to be determined from surveys.

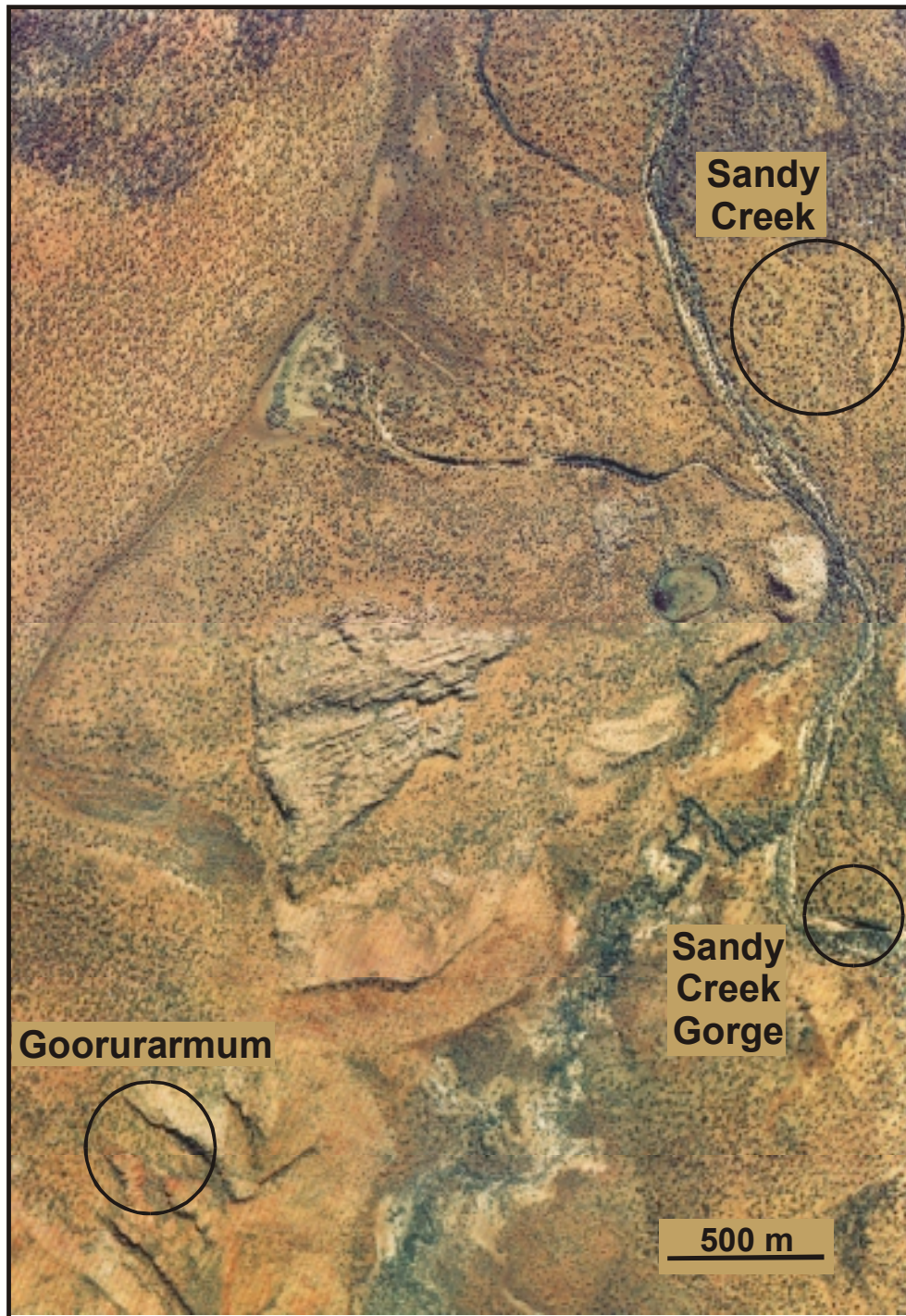


Figure 3.13a Aerial photo of the area around the archaeological site of Goorurarmum, and the non-archaeological sites of Sandy Creek, and Sandy Creek Gorge.

The majority of site locations in this study occur below 100 m AHD. The bedrock escarpment between Goorururumum and Sandy Creek peaks at a little over 85 m (Fig. 3.12), and dips about 20° southeast to the base of the sand sheets. At the base of the escarpments, there is an abrupt change of slope to the subdued relief of the sand sheets. The sand sheets about the escarpment directly where the dip of the bedrock is upward, and are interposed by a scree slope on the downward dip. The sites of Jinmium and Goorurarmum are situated approximately 1 km apart at the same relative level of *ca.* 50 m AHD. About 18 m lower than these two topographic highs in the landscape, is a dry swamp. North of the main Jinmium site, the landscape drops around 20 m over a distance of 1.5 km to another swampland.

Aerial photos of the Weaber Ranges (Fig. 3.13b) reveal the heavily dissected plateaux, which form the maze of beehive-like formations evident at ground level. The escarpment range represented by Walajupi is one of the highest points in the landscape around Karlinga at around 180 m AHD (Fig. 3.12). The bedrock escarpment between the two main excavation sites (Karl-1 and Karl-3) peaks at a little over 75 m, and the bedding dips more gently about 10° to the south. The surrounding sand plains form a series of terraces, which dip gently about 2 - 5° towards the Keep River. Field surveys indicate a relative drop in elevation of about 5 m between the main Karlinga escarpment to the rock outcrop at Karlinga North, and a further drop of 2.5 m less than 200 m further south into swamp sediments. In the south-west, the site of KR99 is clearly seen in the river-course draining from the upper plateaux to the well forested sand plains below (Fig. 3.13b).

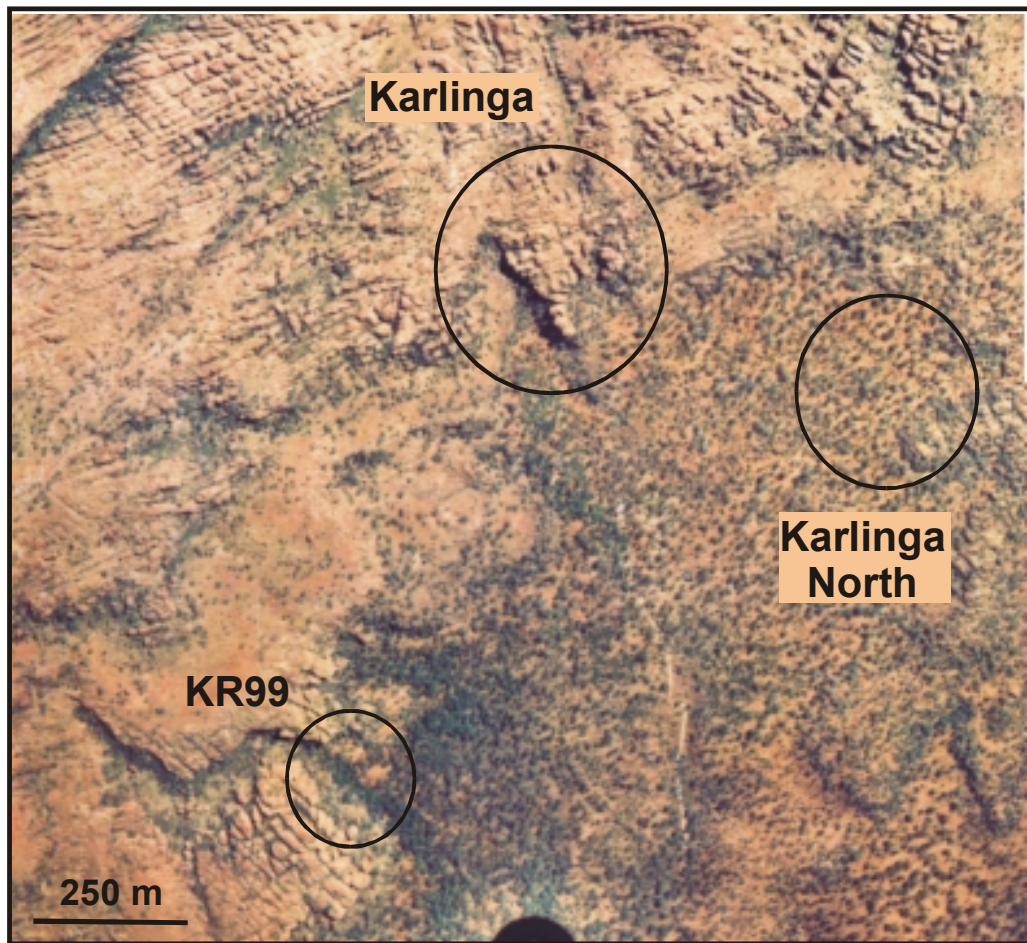


Figure 3.13b Aerial photo of the Weaber Ranges, showing location of the archaeological sites or Karlinga (KR36), Karlinga North, and the creek site near KR99.

3.7 Sampling Strategy

From the physical layout of the Keep River region, a conceptual layout of the site sampling strategy (Table 3.1) is proposed with the aim of linking the major archaeological and landscape contexts of the sandstone escarpments and adjacent sand sheets. Representative sampling is focused towards a geological continuum from supposed source (escarpment bedrock) to sink (rock-shelter, sand sheet, creek profiles), and a cultural continuum from occupied, intermediate to non-occupied sites.

Source	SANDSTONE ESCARPMENTS	
	Karlinga, Jinmium, Goorurarmum	
	(12 samples)	
<i>Sediment pathways</i>		
Sink	NON-OCCUPATION SITES	
	SAND SHEETS	CREEKS
<i>Environmental Inputs/Modifications</i>	Karlinga, Jinmium, Goorurarmum	Karlinga, Sandy Creek
	(2 excavation sites)	(2 sections)
	(20 auger core sites)	
<i>Anthropogenic Inputs/Modifications</i>	OCCUPATION SITES	
<i>Environmental Inputs/Modifications</i>	Karlinga, Goorurarmum (2 rock shelter sites)	

Table 3.1 Summary of field sampling strategy, which provides a continuum from human occupation sites to those where there is no indication of human activity.

3.8 Conclusion

Although the palaeoclimate and palaeoenvironment record for northwest Australia is scant, there is emerging evidence of a changing landscape over long term millennial scales and during short periods of rapid alteration. The question of continuity and change in the Keep River region can be addressed from a geoarchaeological perspective (Chapter 2), using chronology (Chapters 4 and 6), sediment stratigraphy (Chapter 5), and archaeology (Chapter 7). The regional and local environmental and climatic background outlined above provides important contextual information for each of the following geoarchaeological studies.

CHAPTER FOUR

In Situ Cosmogenic Isotope Dating of Sandstone Bedrock and Sand Sheets

As the physical processes shaping the land can be seen to unfold over hundreds and thousands of years, so can the .. processes which are evident in the archaeological data.

– Gosden and Head (1994: 113)

4.1 Introduction

This chapter aims to outline and model the broader geomorphic processes of landscape evolution in the Keep River region, including quantifying rates of plateau denudation using *in situ*-produced cosmogenic radionuclides, ^{10}Be and ^{26}Al . The denudation history of the plateaux is complemented with the depositional chronology of the genetically linked sand sheets determined from profiles of ^{10}Be and ^{26}Al concentrations. The innovative use and geoarchaeological application of cosmogenic radionuclides to measure sediment accumulation involves some experimentation; hence the theoretical background and accumulation models are outlined below. The long-term sand sheet chronology is subsequently compared to the chronology determined by luminescence dating techniques in Chapter Six.

4.2 *In Situ* Cosmogenic Isotope Dating

As indicated in Chapter Two (refer 2.4.1), the accumulation of cosmic radionuclides can be utilised as radiometric clocks to elucidate the erosion rate (ϵ) of geomorphic formations or exposure age of a previously unexposed surface (t_{exp}). A decade ago, Lal (1991) presented the first definitive publication for modelling exposure dating and defining the cosmic radionuclide (CRN) method. The general theory and model equations are outlined here in increasing order of complexity; first for exposure age dating, second for burial dating, and finally, sediment accumulation. The latter is the major focus of this chapter.

4.2.1 Exposure Dating - Theory and Equations

The cosmogenic radionuclides ^{26}Al ($T_{1/2} = 0.71 \text{ Ma}$) and ^{10}Be ($T_{1/2} = 1.5 \text{ Ma}$) are produced by reactions of two main types of cosmic-ray secondary particles, nucleons and muons, with silicon and oxygen target atoms in quartz (Tuniz et al., 1998). The accumulation of cosmogenic radionuclides in the Earth's lithosphere occurs as a function of time and depth below surface, and as such, is sensitive to the denudation rate of that surface. Only about a million atoms of cosmogenic radioisotopes are produced *in situ* within a ten thousand year exposure period per gram of surface rock, hence the technique of Accelerator Mass Spectrometry (AMS) is needed to measure this signal (Tuniz et al., 1998). An exposure history refers to an estimate of the length of time (t in years) the rock was exposed to cosmic rays and the average erosion rate (ϵ in centimetres per year) experienced during exposure. On the assumption of an ideal surface undergoing zero erosion, the build-up in concentration of *in-situ* produced radionuclides can be expressed by the following equation:

$$C_0 = P (1 - e^{-\lambda t}) / \lambda \quad (1)$$

Where C_0 = concentration (atoms per gram of SiO_2) at the present rock surface,
 λ = radioisotope decay constant ($= \ln 2 / t_{1/2} \text{ years}^{-1}$), and
 P = production rate at the sample site (atoms per gram of SiO_2 per year)
as a function of latitude, θ , and altitude, A .

For a constant production rate, the concentration (C) of radionuclides increases with time during cosmic-ray exposure, at first linearly and then more slowly until, after a few half-lives, the system reaches a secular equilibrium in which production equals decay. By knowing the rate of production (P) and measuring the surface concentration it is possible to estimate a surface exposure age from:

$$T_{\text{exp}} = - \ln (1 - \lambda C_0 / P) / \lambda \quad (2)$$

Assuming zero erosion, model exposure ages are necessarily minimum ages and for younger surfaces (< 20 ka), denudation rates effectively have little influence. For surfaces older than many tens of thousands of years, denudation becomes increasingly important. In the presence of a constant erosion rate, given by ϵ , equation (1) becomes (Lal, 1991):

$$C = P (1 - e^{-(\lambda + \epsilon \rho / \Lambda) t}) / (\lambda + \epsilon \rho / \Lambda) \quad (3)$$

Where C is the measured surface radioisotope value at time t ,
 ρ = density of the material (grams per cubic centimetre), and
 Λ = attenuation length of cosmic-rays.

The attenuation length is defined as the thickness of material (i.e. rock) which is required to reduce the intensity of cosmic ray flux to a value which is $1/e$ (~ 0.4) of the surface (or original) intensity. The depth profile of the flux is given by $P(x) = P_{(x=0)} e^{-x/\Lambda}$ and hence Λ determines the effective penetration depth of active cosmic rays, which for the average rock density of 3 g.cm^{-3} represents a distance of $\sim 50 \text{ cm}$ depth (or equivalently $\sim 150 \text{ g.cm}^{-2}$). In effect the denominator term $(\lambda + \epsilon \rho / \Lambda)$ can be interpreted as the residency time radionuclides within the first 50 cm of the rock surface. The time required to remove a thickness of rock equivalent to the mean attenuation length Λ of cosmic rays is equivalent to the mean effective or apparent exposure age (t_{app}). By comparing equations (1) and (3), it is possible to define an apparent age, t_{app} , which essentially incorporates the surface denudation rate and radionuclide decay to give an “effective half-life”:

$$t_{\text{app}} = 1/(\lambda + \epsilon \rho / \Lambda) = 1/\lambda_{\text{app}} \quad (4)$$

For sufficiently long exposures, cosmogenic concentrations saturate; at which point production is balanced by the sum of decay and removal by erosion. Thus for very small ϵ , where $t \gg t_{1/2}$, an expression for the denudation rate can be obtained, as follows:

$$\varepsilon = \Lambda/\rho (P_0/ C_\varepsilon - \lambda) \quad (5)$$

Under these conditions, the maximum saturation concentration at the rock surface is dictated by the magnitude of the denudation rate. The larger the value of ε , the smaller the allowed saturation value. Increasing denudation rates imply that a surface has been uncovered rapidly, and correspondingly surface saturation concentrations are decreasing. For the surface to achieve erosional equilibrium, the model erosion rate is necessarily a maximum one (ε_{\max}) (Nishiizumi et al., 1991) which alternatively corresponds with a model interpretation of minimum exposure age.

Using two radionuclides with different half-lives in principle allows a better simultaneous estimate of the denudation rate and exposure age variables. A plot of the concentration ratio of $^{26}\text{Al}/^{10}\text{Be}$ against ^{10}Be , shows the limiting curves for denudation and exposure age, which define the *steady-state erosion island* (Fig. 4.1) (Lal, 1991). Theoretically, samples that plot on the upper curve (or the minimum exposure line) have undergone no burial or erosion ($\varepsilon = 0$) during the current or finite exposure, the duration of which is indicated by the distance along the curve (Fig. 4.1). Samples with ratios plotting on the lower curve (or maximum erosion line) represent erosional equilibrium conditions of exposure ($t = \infty$) (Nishiizumi et al., 1991). Samples plotting within the erosion island theoretically represent a unique and quantifiable combination of denudation and exposure but in practice, resolution (defined in terms of cumulative errors, technique sensitivity, precision, etc.) limits quantification to minimum exposure (t_{\min}) and maximum erosion (E_{\max}). Samples plotting below the steady-state erosion island would indicate a more complicated exposure history of burial (see 4.2.2) (Fig. 4.1), and in the absence of independent information, a minimum exposure is assumed (Gosse and Phillips, 2001). Samples plotting above the erosion island indicate measurement error (or sample contamination), except in the case where a sample received prior exposure at a site where the nuclide production rate was higher, such as through uplift (Lal, 1991; Brook, 1995).

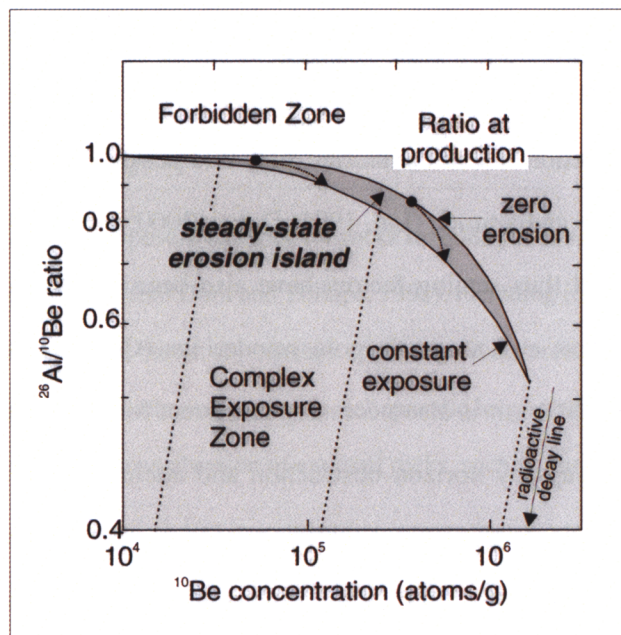


Figure 4.1. Theoretically calculated variation in the ratios of ^{10}Be and ^{26}Al concentration as a function of ^{10}Be concentration for unit nuclide production rates (atom/g/yr) (modified from Lal, 1991). Surfaces with different erosion rates plot in the shaded area, termed the *steady-state erosion island*. Lines running diagonally represent lines of burial such that with sufficient burial there is zero production ($P = 0$). Samples which have undergone cyclic periods of burial and exposure fall below the curve in the complex exposure zone.

Although the removal and radioactive decay of *in-situ* cosmogenic radionuclides is well understood, the precision and accuracy of exposure histories depends primarily on the accuracy to which the rate of production of radionuclides can be determined. Production rates of *in-situ* cosmogenic radionuclides are measured from sites whose exposure age is independently known (Nishiizumi et al., 1989; Clark et al., 1995). Radiocarbon dating is typically used for age control and thus production rate calibration is usually not available past ~20 ka, or for simplicity is otherwise assumed to have remained constant over the whole period of exposure (Nishiizumi et al., 1989; Bierman et al., 1996; Tuniz et al., 1998). Another method is to determine production rates experimentally, by exposing target materials to cosmic radiation at high latitudes for a number of years (e.g. Nishiizumi et al., 1996; Brown et al., 2000).

The cosmic ray flux changes as a function of latitude and altitude (Lal, 1991; Nishiizumi et al., 1991). Hence scaling factors are needed to obtain a relative cosmic ray flux for unknown sample locations. Using the known production rate at calibration sites it is possible to scale production to the location of an unknown latitude and altitude (Lal, 1991; Dunai, 2000; Stone, 2000). Production rates are not time independent and thus scaling factors have also been developed to account for geomagnetic field intensity variations and magnetic pole wanderings (Clarke et al. 1995; Dunai, 2000; Masarik et al., 2001). In addition, it is also necessary to correct for site specific effects such as geometric shielding of cosmic rays by horizon obstruction and attenuation on sloped surfaces (Dunne et al., 1999). The effects of topography and shielding by local vegetation are site specific, and for the dry savannah of the Keep River region these effects are negligible. In this study, the production rates from Stone (2001) are used. Specifically these are 5.1 at/g/yr for ^{10}Be and 30.1 at/g/yr for ^{26}Al at sea-level (SL) and high latitude (HL), with quoted errors of 6 – 8 %. No additional uncertainty is included, and no correction is made for geometric field variation. A full review of production rates for ^{10}Be and ^{26}Al is given by Kubik et al. (1998) and Gosse and Phillips (2001).

Whilst *in situ* cosmogenic isotope dating has the potential for solving many geomorphological and archaeological problems, it is important to acknowledge that the measured radioisotope concentration does not necessarily define a geological age. For recent or stochastic events, where correction factors are minimal, cosmogenic dating can provide an age effectively equivalent to a true age. For longer term processes of evolving landscape surfaces, cosmogenic dating provides an erosion rate which can be used to estimate the mean apparent age. Depth profiles of the concentrations of radionuclides, ratios of different radionuclides in the rock, and concentrations of radionuclides in the sediments produced by erosion can all provide measures of the rate of erosion (Harbor, 1999). *The challenge is to correctly interpret the model results according to the geomorphic and geoarchaeological setting* (e.g. Fig. 4.2).

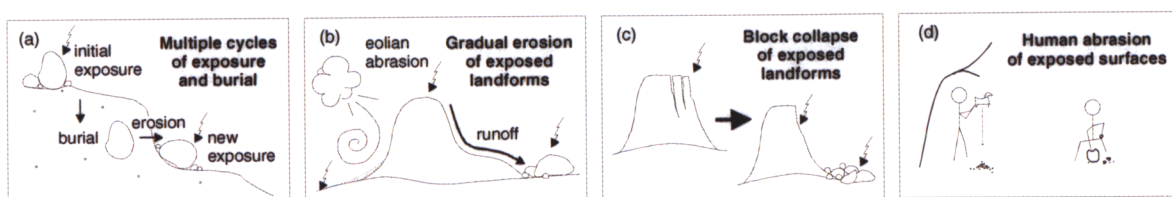


Figure 4.2 Possible exposure histories for rocks sampled for *in situ* cosmogenic dating studies (modified from Dorn and Phillips, 1991), including (a) multiple cycles of exposure through erosion and burial, (b) constant centimetre-scale erosion of exposed landforms through physical weathering processes, (c) episodic large-scale mass wasting of exposed landforms, and (d) human abrasion of exposed rocks, such as engraving or tool making.

The measurement of more than one radioisotope offers the potential to differentiate phases of combined geomorphological processes, because each radioisotope has a half-life that dictates the time scale of its sensitivity as a chronometer (Lal, 1991). From *in situ* cosmogenic nuclide concentrations, exposure ages may be determined in the order of 5 ka – 5 Ma, and erosion rates in the order of ~ 0.1 mm to 100 mm.k^{-1} . Whilst the upper age limit is set by radionuclide saturation, the lower age limit is set more by the practical limitations of analysing kilograms of material rather than the present sensitivity of AMS.

4.2.2 Burial Dating – Theory and Equations

Burial dating was first proposed by Lal and Arnold (1985). It is similar to surface exposure dating in that both rely on the *in situ* production of cosmogenic radionuclides that necessarily decrease with depth below surface. However, the methods differ both in how they measure time intervals and in the problems they are useful for (Granger and Muzikar, 2001). In contrast to surface exposure dating, which measures accumulation from time zero (or event time), burial dating measures the relative decay of a reserve of radioactive radionuclides in buried sediments. The most straightforward case of burial dating assumes that material, whose initial radionuclide concentration is known, has been rapidly buried (e.g. washed into a deep cave, or covered by several metres of overburden), so that cosmogenic production effectively ceases (Granger and Muzikar, 2001). The

situations in which production does not completely cease upon burial, and which is the main subject of this chapter, is considered below (refer 4.2.3).

^{26}Al and ^{10}Be are particularly useful for burial dating because the ratio of their production rates is well known, and roughly independent of factors such as latitude, altitude, and depth (Granger and Muzikar, 2001). As ^{26}Al decays more rapidly than ^{10}Be , the $^{26}\text{Al}/^{10}\text{Be}$ ratio decreases exponentially with burial time. Pre-burial concentrations and hence erosion rates can be inferred from simple models of cosmogenic nuclide accumulation at the surface. This study also makes use of plateau denudation rates from *in situ* cosmogenic dating. The age range of burial dating for ^{10}Be and ^{26}Al in quartz is in the order of 200 ka to 5 Ma (Granger and Muzikar, 2001), which accords within the depositional age provided by luminescence dating of the sand sheet sediments surrounding the Jinmium site (Fullagar et al., 1996).

4.2.3 Modelling Accumulation (Partially Shielded Burial)

The model of *in situ* cosmogenic isotope depth profiles follows the methods of Lal et al. (1987) for determining accumulation rates, S (mm.k^{-1}) in ice cores from Antarctica. For modelling purposes it is assumed that sediment accumulation has been constant for long periods, and has not been instantaneously or repeatedly buried (e.g. migrating sand dunes). For accumulating sediment sequences, production does not cease upon burial, and is referred to here as partially ‘shielded burial’. For an accumulating profile, or for partial burial of surface, the cosmogenic nuclide concentrations may increase as long as the buried surface remains shallow enough (i.e. low accumulation rates) that production outweighs decay (Braucher et al., 1998; 2000), after which the shape of the profile is dependent on the accumulation rate. Hence it is possible to model theoretical patterns of nuclide depth profiles assuming different initial concentrations and transport of source material and re-deposition or accumulation. This study considers an accumulating surface where deposition outweighs removal.

Under constant accumulation, depth (X , cm) can be used as a proxy for time (years), and the concentration (C_{TOT} , atoms per gram) as a function of depth is given by the following equation:

$$C_{TOT}(x) = C_0(E_0)e^{-\lambda x/S} + P_0(e^{-\lambda x/S} - e^{-\rho x/\Lambda})/(\rho S/\Lambda - \lambda) \quad (\text{Equation 6})$$

Where C_0 is the nuclide concentration (atoms per gram) of the transported sediment (i.e. $x = 0$),
 E_0 is the erosion rate of the contributing bedrock source (mm per year),
 P_0 is the nuclide production rate (atoms per gram per year) at $x = 0$,
 ρ is the density (grams per cubic centimetre),
 Λ is the cosmic ray absorption mean free path (grams per square centimetre),
 λ is the decay constant of the nuclide (units of inverse years), and
 S is the sediment accumulation rate (centimetres per year).

The initial surface concentrations of ^{10}Be and ^{26}Al in deposited sand are assumed to be related to the average erosional equilibrium concentration, C_0 , of the bedrock source (Fink et al., 2000). In this study, the value of C_0 is given by the average CRN concentrations, C_i , of the all the bedrock plateaux samples. For any given value of C_i it is possible to estimate a corresponding maximum model erosion rate, E_i , according to equation (7):

$$C_i = P_i(0)/(\lambda + \rho E_i / \Lambda) \quad (\text{Equation 7})$$

This equivalence assumes that all the eroding bedrock surfaces contribute equally to the accumulation of sediment in a particular region, and here specifically the Keep River region. The mean erosion rate can then be determined from the average of all the E_i .

Modelling of *in situ* cosmogenic depth profiles can be determined using equation (6), outlined above, for a range of erosional equilibrium concentrations (C_0) of source material and estimated

accumulation rates (S) for both ^{10}Be and ^{26}Al . For zero accumulation (including autochthonous weathering), samples from any given depth will have maintained their relative shielding per unit time (i.e. the surface level remains constant) and the cosmogenic profile should appear similar to a bedrock core with close to exponential decay. On a log scale, nuclide depth profiles show steadily decreasing nuclide concentrations (Fig. 4.3a).

For a depositional profile where the sediment accumulation rate (S) is constant, the picture is more complex. It is assumed that the bedrock erosion rate, characterised by C_0 (or E_0) is the only source of transported sediment. With decreasing bedrock erosion rate (increasing initial radionuclide concentrations), the shape of the nuclide depth profiles become more parallel (Fig. 4.3b). For the case where the initial radionuclide concentration of transported sediment is constant, the radionuclide depth profiles typically decrease with depth and become more flat with increasing sedimentation rate (Fig. 4.3c). The aim is to fit an envelope of modelled profiles to the measured nuclide concentrations from a sand sheet profile, whereby the point where $x = 0$ is fixed by the initial erosional equilibrium concentration (C_0) and different values of sedimentation rate (S) are used to match the shape. The complexities of radionuclide inheritance, accumulation, erosion and decay mean that it is better to focus on the entire profile rather than individual points (Brown and Bourles, 2002).

In this way the evolution of ^{10}Be or ^{26}Al concentrations as a function of depth for a profile can allow quantification of sedimentation (S) and erosion (E). Moreover it can differentiate various patterns of erosion and burial (Phillips, 2000), including that resulting from *in-situ* (autochthonous) conversion of bedrock to soil or regolith and constant accumulation of transported (allochthonous) sediments (Brown et al., 1998; Braucher et al., 1998; 2000; Heimsath et al., 1999). Examples of burial dating include the origin of stone-lines in lateritic environments (Braucher et al., 1998, 2000; Brown et al., 1994), and the evolution of desert sand-dunes and sand plains in arid Australia (Fink et al., 2000). Further details and synopsis of burial dating can be found in Lal (1991), Phillips, (2000) and Granger and Muzikar (2001).

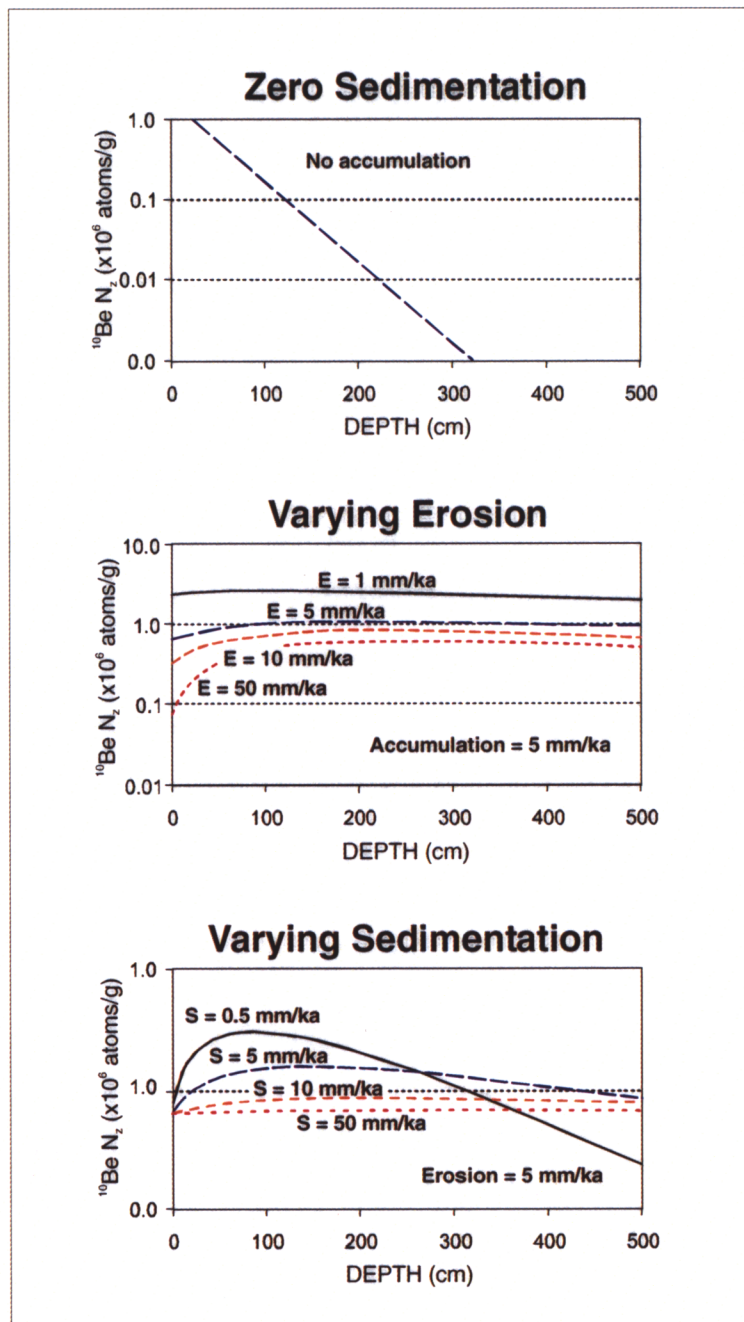


Figure 4.3 Theoretical patterns of nuclide depth profiles assuming (a) zero sedimentation ($C_{0(x=0)}$), (b) varying erosion rate, and (c) varying sedimentation rate (modified from Fink et al., 2000; Phillips, 2000). The model curves assume values for production of ^{10}Be and ^{26}Al scaled to the latitude (15.43°S) and altitude (10 m ASL) of the Keep River region. Refer text for explanation.

Bioturbation buffers the average cosmogenic nuclide concentrations in surface soils against short-term changes in erosion (Brown et al., 1995), hence the effects of bioturbation may need to be considered in the determination of burial rates of sand sheet sediments. In theory, bioturbation will homogenise the nuclide concentration throughout its region of activity to a value similar to that of a surface unaffected by bioturbation, and hence can be used to differentiate the bioturbated zone from lower layers unaffected by bioturbation (Brown et al., 1995; Bracher et al., 2000). In reality all surfaces are affected by bioturbation, but the ideal profile of the model remains valid. In the Keep River region, the greatest bioturbating influence is likely to come from prevalent termite activity, with rates of topsoil reworking estimated from 25 mm.ka⁻¹ (Holt et al., 1980) to 200 mm.ka⁻¹ (Hart, 1995). From studies of stoneline profiles in southwest Australia, Colin et al. (2001) derive similar rates of termite excavation in the order of 20 mm.ka⁻¹ using *in situ* produced ¹⁰Be. Termite activity is generally restricted to above the water table, which in a monsoonal environment may be extremely variable. Further consideration of the effects of bioturbation on stratigraphic integrity is given in Chapter Six in relation to luminescence dating, and any microstratigraphic evidence of bioturbation is investigated Chapter Five.

The two main types of cosmic-ray particles, nucleons and muons, have different attenuation lengths. The effective attenuation length of neutrons is short (~ 150 g cm⁻²) relative to that of muons (~ 750 g cm⁻²) (Brown et al., 1995; Granger and Smith, 2000). This effectively means that neutron-induced production dominates near the surface whilst muon-induced production only becomes significant for solid bedrock profiles > 10 m (Fig. 4.4). Samples taken in the Keep River region are neither deep enough nor old enough (refer 4.3.1) for muon contribution to be significant.

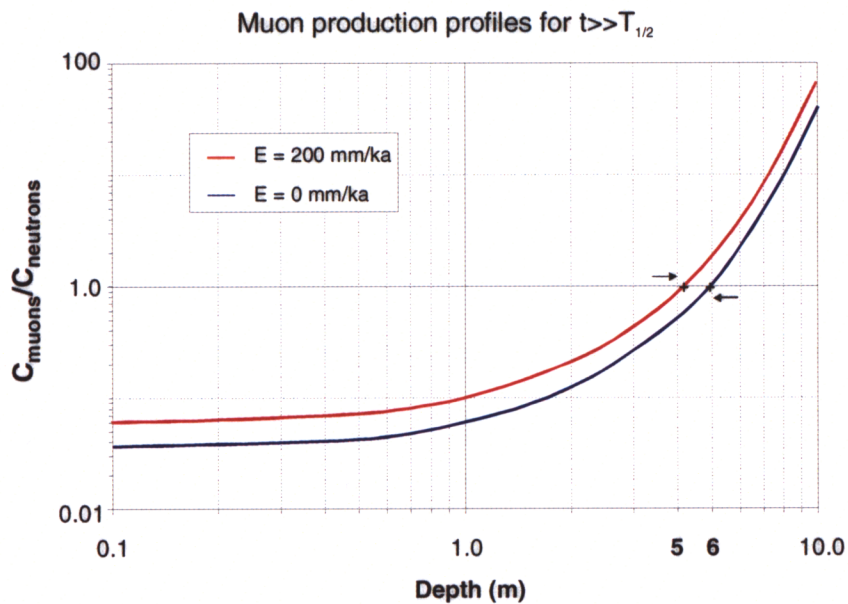


Figure 4.4 Ratio of muon and neutron input for the extremes of zero erosion ($E = 0 \text{ mm.k}^{-1}$) and high erosion ($E = 200 \text{ mm.k}^{-1}$), indicating the dominance of muon-induced production (i.e. $C_{\text{muons}}/C_{\text{neutrons}} > 1$) only over depths greater than about 5 m (shown by arrows) (from David Fink, pers. comm., 2002).

4.2.4 *In situ* Cosmogenic Dating and Sand Sheet Formation

Sand terrains comprising ergs, dunes and sand sheets occur in the arid and semi-arid and monsoonal environments of the Sahara, Arabia, central Asia, southern Africa and Australia, yet the origin of many of these sand terrains remains uncertain (Newsome, 2000). In western Arnhem Land, it has been argued that sand deriving from the nearby sandstone plateau began accumulating at the same time as the initiation of human occupation around 50 - 60 ky BP (Roberts et al., 1994b), whether as a result of human firing practices (e.g. Hope et al., 1985; Jones, 1985) or as a response to climate (e.g. Ross et al., 1992). There is some question over the justification of the coincidence of commencement of occupation and sediment accumulation (refer 2.5.2). Nevertheless, these observations imply that the sand sheet sediments have accumulated over the top of an exposed pediment. Further evidence is required to differentiate the evolution history of the sand sheets from a number of possible options, including: (i) the *in situ* (autochthonous) conversion of the underlying

saprolite (Mory and Beere, 1988), (ii) long-distance transport of aeolian sediments (Pye and Gardner, 1981; Ross et al., 1992), (iii) long-distance transport of colluvial sediments (Nanson et al., 1988), or (iv) local accumulation of detrital material from the escarpment face and intervening scree slope (Young, 1988; Roberts, 1991).

In situ cosmogenic dating of the bedrock outcrops and profiles within the adjacent sand sheets may help to understand the processes of landscape evolution of sandstone landscapes in the Keep River region. More specifically, measurement of *in situ* cosmogenic nuclides in depth profiles can differentiate between extremes of autochthonous (*in situ*) and allochthonous formation of the sand sheets. Broad regional comparisons can be made between climatic parameters and landform assemblages (Derbyshire, 1976), and between long-term environmental and archaeological trends (Lourandos and David, 1998: 110). While the long-term archaeological trends for the Keep River region are yet to be determined, the inferred geomorphic environment can begin to provide a context for interpreting these trends.

The following application of *in situ* cosmogenic isotope dating in the Keep River region aims to:

- determine the denudation rate of the bedrock plateaux based on a direct model interpretation of bedrock cosmogenic ^{10}Be and ^{26}Al radionuclide concentrations,
- model the accumulation rate of the sand sheets from depth profiles of measured ^{10}Be and ^{26}Al radionuclide concentrations,
- compare and contrast estimated values of denudation and sedimentation with other semi-arid and monsoonal sandstone environments, and
- discuss the geoarchaeological implications of the above results.

4.3 Methodology

4.3.1 Field Sampling

Bedrock

A measure of maximum plateau denudation was determined for the bedrock outcrops which are considered to represent the source for the sand sheets in each of the site areas of Jinmium, Goorurarmum and Karlinga. Unfortunately, it was not feasible in this study to measure vertical erosion rates directly using *in situ* cosmogenic dating. Rather the main use of the plateau denudation rates is in the modelling and burial dating of the adjacent sand sheets. A total of 15 bedrock samples were collected in July 2000 (recorded sequentially for each site as a COS-number). Approximately 1 kg of rock was removed from well-exposed, apparently stable, horizontal surfaces along the plateaux of the three main bedrock escarpments (Fig. 4.6). Samples were primarily chosen according to the principle of elevation such that the higher the surface the older it is. Different weathering surfaces (e.g. tafoni, case hardening) were sampled in order to give an estimate of the variation of denudation rates within a particular lithology and catchment area. The height of the plateau above the sand sheets was estimated from topographic surveys and the location of each sample site was determined from a Global Positioning System (GPS) (Fig. 4.5). Two bedrock samples from each site catchment (total of 6) were used for subsequent analyses. Details of each sample and location are given in Appendix A2.1.

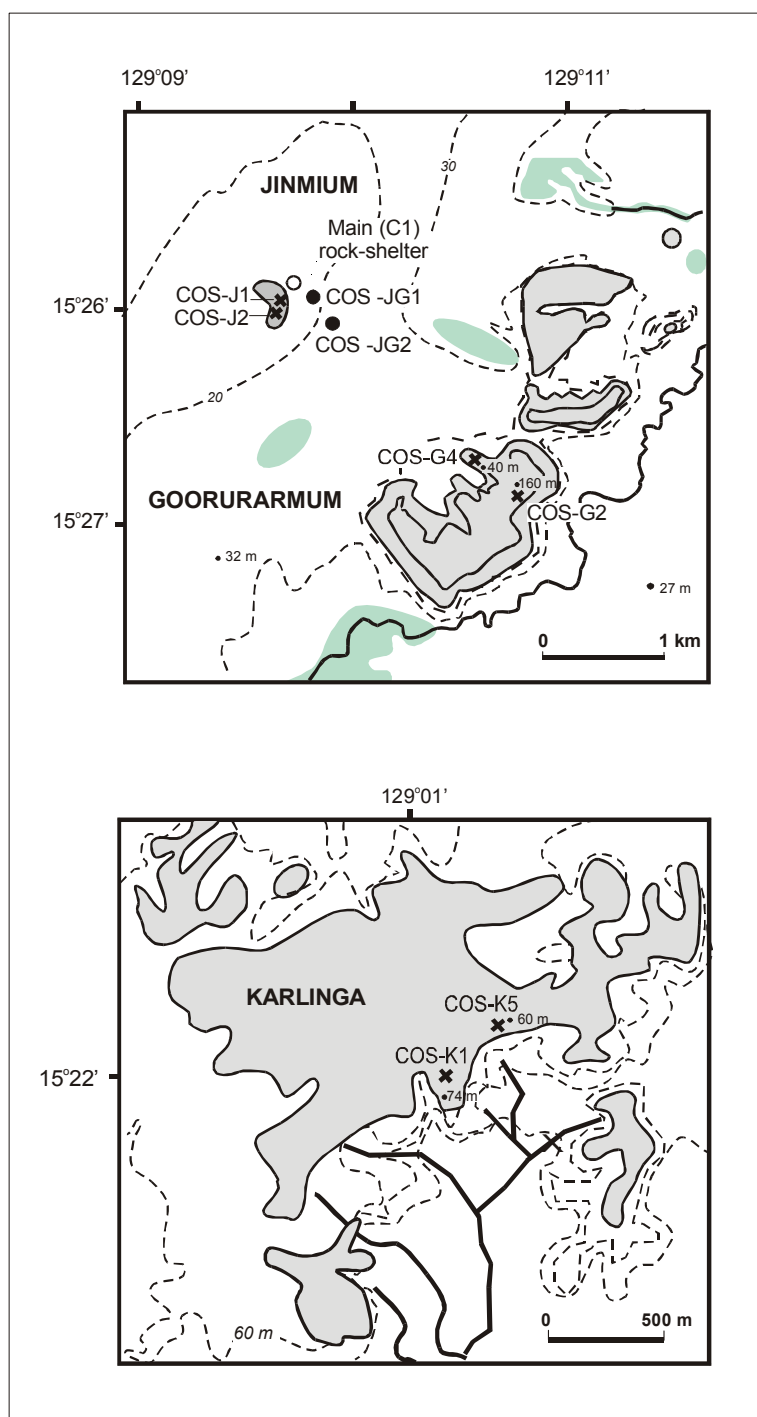


Figure 4.5 Location map of cosmogenic sample sites, including bedrock samples (COS-G2, G4, J1, J2, K1 and K5) and sediment samples from the Jinmium sand sheet (JG1 and JG2).

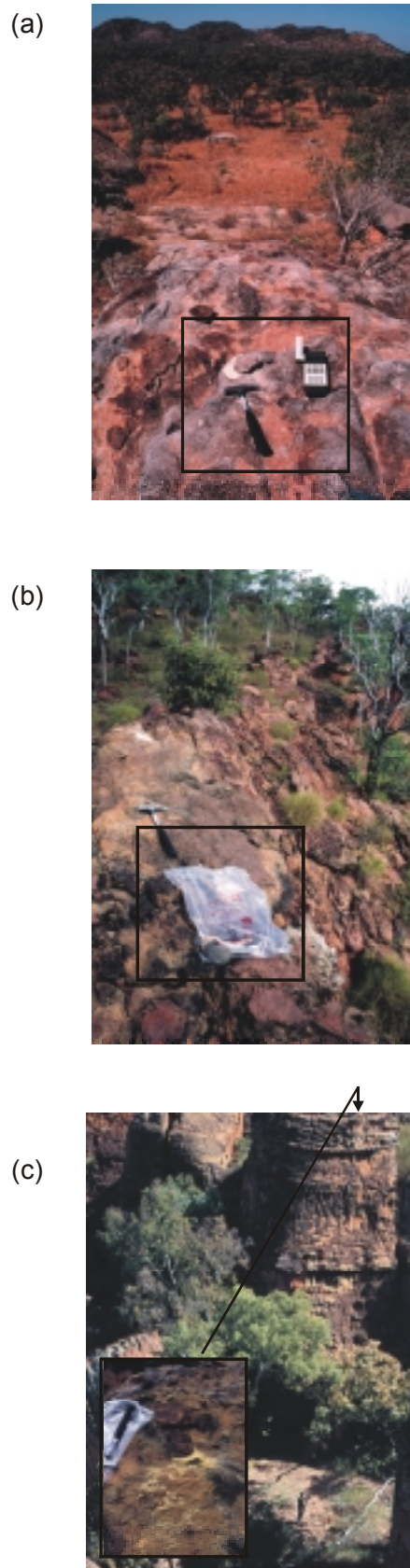


Figure 4.6 Photograph of three of the bedrock samples (a) COS-J1, (b) COS-G2, and (c) COS-K1, collected for *in situ* cosmogenic dating. Samples were taken from horizontal surfaces with different forms of weathering.

Sand Sheets

In order to obtain a measure of the corresponding deposition history of the sand sheet sediments, two sediment cores were obtained from the Jinmium sand sheet. The Jinmium site was chosen as previous luminescence dating of a nearby auger site (Fullagar et al. 1996) indicated both the necessary antiquity (*ca.* 103 ± 14 ky BP) and depth (*ca.* 5 m) required for a ^{10}Be and ^{26}Al profile which may exhibit a shallow subsurface maximum and decay at depth. The first core (JG1) was limited to a depth of 3 m by a pisolitic sandstone base (refer A3.1). The second core (JG2) was augered to a depth of 6 m, which was the limit of the auger with no basal contact. Samples were taken at 30 cm intervals with a maximum depth error of ± 5 cm. Eight of the 10 samples were analysed from the 3 m core, and 10 of the possible 18 from the 6 m core, being a sufficient number to allow derivation of an accumulation rate. Permission to sample the plateaux and sand sheets was obtained from traditional custodians and no samples were taken from art surfaces. Details of each sample location are given in Appendix A2.1 and sediment descriptions given in Appendix A3.1.

4.3.2 Sampling Chemistry and AMS Measurement

Typically, only about a million atoms of ^{10}Be and ^{26}Al are produced *in situ* within a ten thousand year exposure period per gram of surface rock, hence the technique of Accelerator Mass Spectrometry (AMS) is needed to measure this signal. All bedrock and sediment samples were processed at ANSTO, following a three-stage process of sample preparation, AMS measurement, and data analysis (modelling) and interpretation. An overview of AMS techniques, laboratory practices, and discussion of exposure age applications is given by Tuniz et al. (1998).

Sample processing follows the ANTARES methods detailed in Child et al. (2000), which is based on a modification of Kohl and Nishiizumi (1992) and Brown et al. (1991). Raw sample masses ranging from 0.2 to 1 kg were used to obtain 50 – 100 grams of final pure quartz after chemical treatment. Following the sieved extraction of the 200 – 700 μm fraction from crushed bedrock or

sediment, samples were subjected to systematic selective leaching in dilute HF to obtain pure quartz as a closed system for *in situ* produced ^{10}Be and ^{26}Al . Selective leaching eliminates the potential atmospheric ^{10}Be contamination and reduces the concentration of aluminium sourced from contaminant mineral fractions outside and within each quartz grain. Excess aluminium in etched quartz decreases the $^{26}\text{Al}/^{27}\text{Al}$ ratio and hence sensitivity of ^{26}Al as a chronometer. Constant ^{10}Be concentrations were obtained after $\sim 30\%$ etching, after which the residual quartz was completely dissolved in HF. The high purity of quartz meant there was no need for any heavy liquid separation of other contaminant minerals. The sample and HF mixture was then spiked with $\sim 0.3 - 0.5\text{ mg}$ ^9Be carrier, but no Al carrier as there were adequate concentrations in the clean quartz. ICP-AE results for Al range from 93 to 270 ppm, with typical errors of 2 – 4%. Be and Al were isolated, in the form of oxide, by solvent extraction as outlined in the flowchart by Child et al. (2000). The final pure powder samples were mixed with Nb powder and loaded into holders for AMS isotopic analyses.

Isotopic concentrations of ^{10}Be and ^{26}Al were measured using the ANTARES AMS spectrometer. Several measurements are made on any single target sample, and the weighted mean concentration is used to determine the denudation rate. An outline of the ANTARES AMS setup are given by Lawson et al. (2000), and details of AMS techniques and laboratory practices is given by Tuniz et al. (1998). The final AMS measurement errors depend predominantly on statistical errors of total ^{10}Be and ^{26}Al counts. Final quoted ratios are the weighted ratios of 4 – 6 independent repeat measurements. For $^{10}\text{Be}/^9\text{Be}$ ratios these are typically $< 5\%$ for younger samples ($\sim 15\text{ ka}$) and $< 2\%$ for older samples ($> 100\text{ ka}$) based on counting statistics, variability in measurement of standards, and uncertainty in blank corrections. For ^{26}Al the errors are larger, around 5 – 10 %, due to lower ^{26}Al count rates.

4.4 Results

4.4.1 Bedrock

The results of all AMS determinations for the six bedrock samples are given in Appendix A2.3 for ^{10}Be and A2.4 for ^{26}Al , along with the calculated isotopic concentrations, calculated site production rates, and denudation rates. A summary of the results is given in Table 4.1, and discussed further below.

Table 4.1 Summary of apparent exposure age and maximum denudation rate estimated from ^{26}Al and ^{10}Be isotope concentrations in six bedrock samples from the Keep River region. Refer 4.2.1 for definition of apparent exposure age (t_{app}). Results were calculated using a production rate of 5.1 at.g^{-1} for ^{10}Be and 31.1 at.g^{-1} for ^{26}Al at sea-level and high latitude (from Stone, 2000), and scaled to the relevant latitude and altitude using the scaling factors of Lal (1991).

Bedrock sample	Altitude (m)	^{10}Be $\times 10^6$ (atom.g $^{-1}$)	^{26}Al $\times 10^6$ (atom.g $^{-1}$)	$^{26}\text{Al}/^{10}\text{Be}$	^{10}Be t_{app} (ka)	^{26}Al t_{app} (ka)	^{10}Be erosion rate (mm.ka $^{-1}$)	^{26}Al erosion rate (mm.ka $^{-1}$)
JIN1	10	0.360	2.38	6.61	114.6	126.4	4.72	4.13
JIN2	20	0.247	1.61	6.50	77.3	82.7	7.06	6.45
KAR1	74	0.512	2.96	5.79	152.2	147.1	3.52	3.51
KAR5	60	0.304	1.55	5.09	90.1	75.0	6.04	7.13
GUR2	160	0.314	2.11	6.72	88.6	98.4	6.14	5.37
GUR4	40	0.706	3.92	5.56	223.3	210.2	2.36	2.38
Ave		0.41	2.42	6.04	124.4	123.3	4.83	4.97
SD		0.070	0.386	0.270	22.6	20.60	0.743	0.727

The apparent exposure age, or the time required to remove ~ 500 mm of these geological surfaces, ranges from 75 to 210 ka for ^{26}Al and 75 to 210 ka for ^{10}Be (average ~ 125 ky BP). The average denudation rate is about $5.0 \pm 0.7 \text{ mm.ka}^{-1}$ for ^{26}Al and $4.8 \pm 0.7 \text{ mm.ka}^{-1}$ for ^{10}Be , and values range from 2.4 mm.ka^{-1} (GUR4) to $\sim 7.0 \text{ mm.ka}^{-1}$ (JIN2). The mean bedrock concentration of $4.9 \pm 0.7 \text{ mm.ka}^{-1}$ is taken as the mean bedrock denudation rate over the past few Ma. With the exception of KAR5, and within the 10 % margin of error, the remaining five bedrock samples plot within the island between ‘constant exposure’ and ‘steady erosion’ (Fig. 4.7), indicating that they have undergone continual exposure with little or no burial or shielding of these bedrock samples. The position of KAR5 below the ‘constant exposure’ line may indicate some prior shielding.

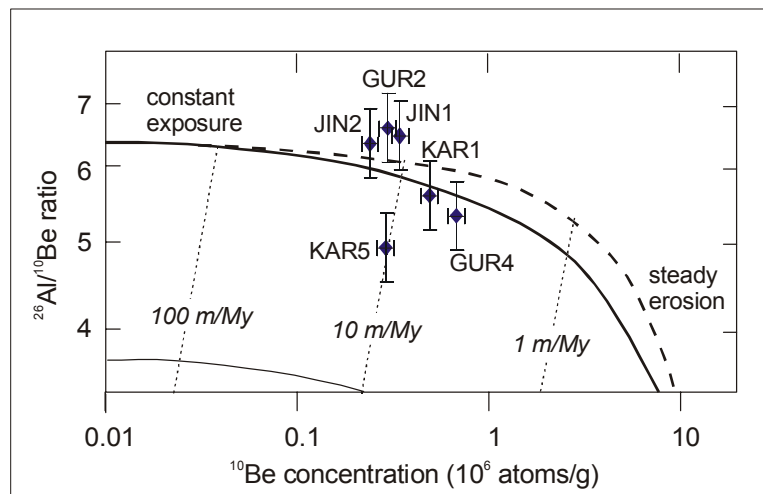


Figure 4.7 $^{26}\text{Al}/^{10}\text{Be}$ ratio diagram indicating position of bedrock samples in relation to the steady-state erosion island (see text for further explanation).

4.4.2 Sand Sheet Sediments

Raw results

The average ^{26}Al and ^{10}Be concentrations and $^{26}\text{Al} / ^{10}\text{Be}$ ratio per depth for cores JG1 and JG2 are given in Table 4.2 and shown graphically below (Fig. 4.8). Full results of all ^{10}Be and ^{26}Al analyses are detailed in Appendix A2.4 and A2.5 respectively.

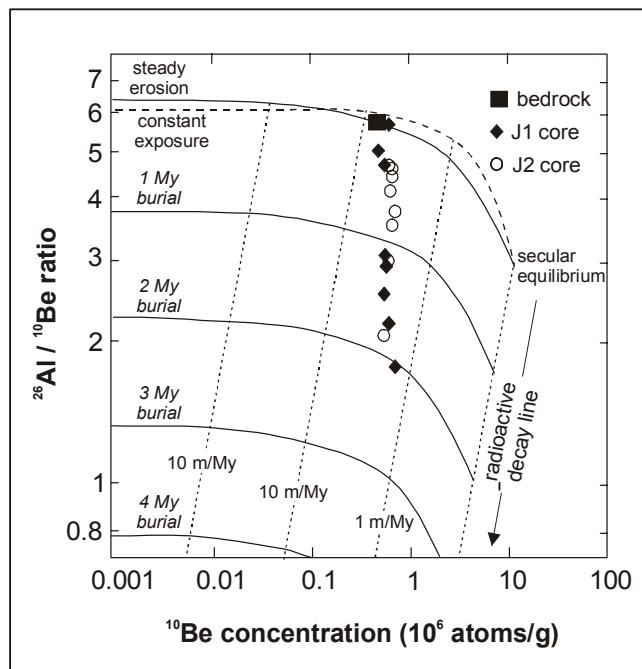


Figure 4.8 Plot of $^{26}\text{Al} / ^{10}\text{Be}$ ratios for bedrock samples, and sediment samples from auger cores JG1 and JG2 on steady-state erosion island diagram. The position of the auger samples below the steady-state curve indicates that cores samples have not undergone cycles of burial and exposure.

Table 4.2 Concentrations and ratio of ^{10}Be and ^{26}Al radionuclides determined from successive analyses of target samples, taken from various depths in the two burial profiles (JG1 and JG2) near Jinmium. The high concentration of ^{10}Be at 300 cm in the JG1 core (italicised) may represent a buried pediment surface (refer text for explanation).

Profile Sample	Depth (cm)	^{10}Be (10^6 atoms/g)	^{26}Al (10^6 atoms/g)	$^{26}\text{Al} / ^{10}\text{Be}$
JG1	30	0.534	2.180	4.34
JG1	60	0.476	2.354	4.94
JG1	90	0.526	2.006	3.82
JG1	150	0.599	1.947	3.25
JG1	180	0.545	1.799	3.30
JG1	210	0.539	2.154	3.99
JG1	270	0.591	1.699	2.88
<i>JG1</i>	<i>300</i>	<i>0.705</i>	<i>1.644</i>	<i>2.33</i>
JG2	30	0.584	2.775	4.75
JG2	60	0.629	2.827	4.49
JG2	90	0.634	2.958	4.67
JG2	150	0.632	2.829	4.47
JG2	210	0.685	2.579	3.77
JG2	300	0.599	2.508	4.19
JG2	360	0.589	2.456	4.17
JG2	450	0.627	2.224	3.55
JG2	540	0.584	1.716	3.46
JG2	600	0.526	1.086	3.17

In the burial profiles of JG1 and JG2, the $^{26}\text{Al}/^{10}\text{Be}$ ratio decrease steadily with depth (Table 4.2). The mean concentration of ^{26}Al and ^{10}Be in the shallow surface (< 100 cm) is $\sim 2.5 \times 10^6$ at.g $^{-1}$ and $\sim 0.56 \times 10^6$ at.g $^{-1}$ respectively. These values are similar to the mean bedrock concentrations (Table 4.1), supporting the assertion that the local bedrock is the main source of sediment to the sand

sheets. The consequent mean ratio of $^{26}\text{Al}/^{10}\text{Be}$ in the shallow surface is ~ 4.5 and is less than the mean bedrock $^{26}\text{Al}/^{10}\text{Be}$ ratio. The shorter JG1 profile shows an irregular increase of ^{26}Al at 210 cm (Table 4.2). The base of JG1 comprised pisolitic sandy sediments, which differed to the unconsolidated red sands above. The comparatively elevated concentration of ^{10}Be at the base (300 cm) of the JG1 profile (Table 4.2), may represent inheritance preserved in a previously exposed surface or pediment, with comparable cosmogenic isotope concentrations to the presently exposed bedrock. For the longer JG2 profile, the concentrations of $^{10}\text{Be}/^{26}\text{Al}$ ratio shows a gradual decrease with depth.

Estimating E_0 and S

For the two auger cores JG1 and JG2, sedimentation rate is determined by using the weighted mean of measured ^{10}Be and ^{26}Al concentrations as the initial value for deposition and modelled with depth profiles using eq. (7) with a range of approximated accumulation rates (S) (refer 4.2.3). Model results were calculated using a value for $P(0)$ of $3.79 \text{ at.g.yr}^{-1}$ and $19.90 \text{ at.g.yr}^{-1}$ for ^{10}Be and ^{26}Al respectively (15.43°S , 10 m altitude), a density of 1.66 g.cm^{-3} , an attenuation length of 150 g.cm^{-2} , and a decay constant of $4.59 \times 10^{-7} \text{ y}^{-1}$ for ^{10}Be and $9.89 \times 10^{-7} \text{ y}^{-1}$ for ^{26}Al . In order to match measured concentration with modelled profiles for ^{10}Be and ^{26}Al , the best correspondence was obtained by using the average concentrations of $0.41 \times 10^6 \text{ at.g}^{-1}$ and $2.42 \times 10^6 \text{ at.g}^{-1}$ respectively, rather than the minimum or maximum bedrock concentration (from 4.4.1).

Fig. 4.9 shows the profiles for sedimentation rates of 5, 10, and 20 mm.ka^{-1} for ^{10}Be . With the exception of the sample at 60 cm (disturbance) and 300 cm (which may represent buried bedrock), the measured ^{10}Be concentrations in JG1 correspond to a sedimentation rate between 8 and 15 mm.ka^{-1} . For the deeper core JG2, the measured profile indicates a sedimentation rate between 5 and 10 mm.ka^{-1} . In summary, the measured concentrations for both ^{10}Be profiles are bracketed by the model curves with accumulation rates of $5 - 20 \text{ mm.ka}^{-1}$. Any lower sedimentation rates (S)

would predict a larger maximum and sharper fall off at depth, while any higher S would lie well below all the data points, effectively invariant with depth.

For ^{26}Al the correspondence between the measured concentrations and the model curves for JG2 is acceptable but is poorer for JG1. The measured concentrations in the JG1 core fall below any of the model curves and are difficult to explain. The profile for JG2 corresponds to a sedimentation rate between 10 mm.k^{-1} and 20 mm.k^{-1} , which is larger than that determined from ^{10}Be . Attempts to force a better fit to the profiles of JG1 and JG2 (using an equivalent S of $5 - 10 \text{ mm.k}^{-1}$ for ^{10}Be), using a lower initial ^{26}Al concentration (C_0) are unsuccessful. For $S > 20 \text{ mm.k}^{-1}$, the curves are flat and require a much higher initial ^{26}Al concentration (C_0). Thus using ^{26}Al the average rate of sedimentation is also estimated to be $10 - 20 \text{ mm.k}^{-1}$.

It is also necessary to consider the possible effects of bioturbation on the burial profiles. Using the theory of homogenisation (Braucher et al., 2000) the extent of bioturbation is estimated to be less than 100 cm. This is supported by comparable mean concentrations of ^{26}Al and ^{10}Be over this depth and the source bedrock, and by the relatively poor fit of the model profiles over this depth. Beyond this depth the measured concentrations, although scattered, do show some decay with depth. However, the cosmogenic data show two features which indicate that vertical mixing may be significant: (i) more scatter than predicted from theory (compare Figs. 4.3 and 4.9) and (ii) depressed $^{26}\text{Al}/^{10}\text{Be}$ ratios (4.3 – 4.8) in near-surface samples given their inferred sedimentation rate ($\sim 10 \text{ mm.k}^{-1}$).

In summary, although the measured concentrations provide a relatively flat curve, they typically show weak subsurface maxima and tail off at depths below 300 cm. The cosmogenic data are sensitive to prior erosion rate ($\sim 5 \text{ mm.k}^{-1}$), which provides a representative accumulation rate of $10 - 20 \text{ mm.k}^{-1}$ for the sand sheets. Maximum errors have been integrated into the cosmogenic data, but there remains some uncertainty regarding the sedimentation rate. Ironically, burial dating becomes less precise with increasing erosion rates.

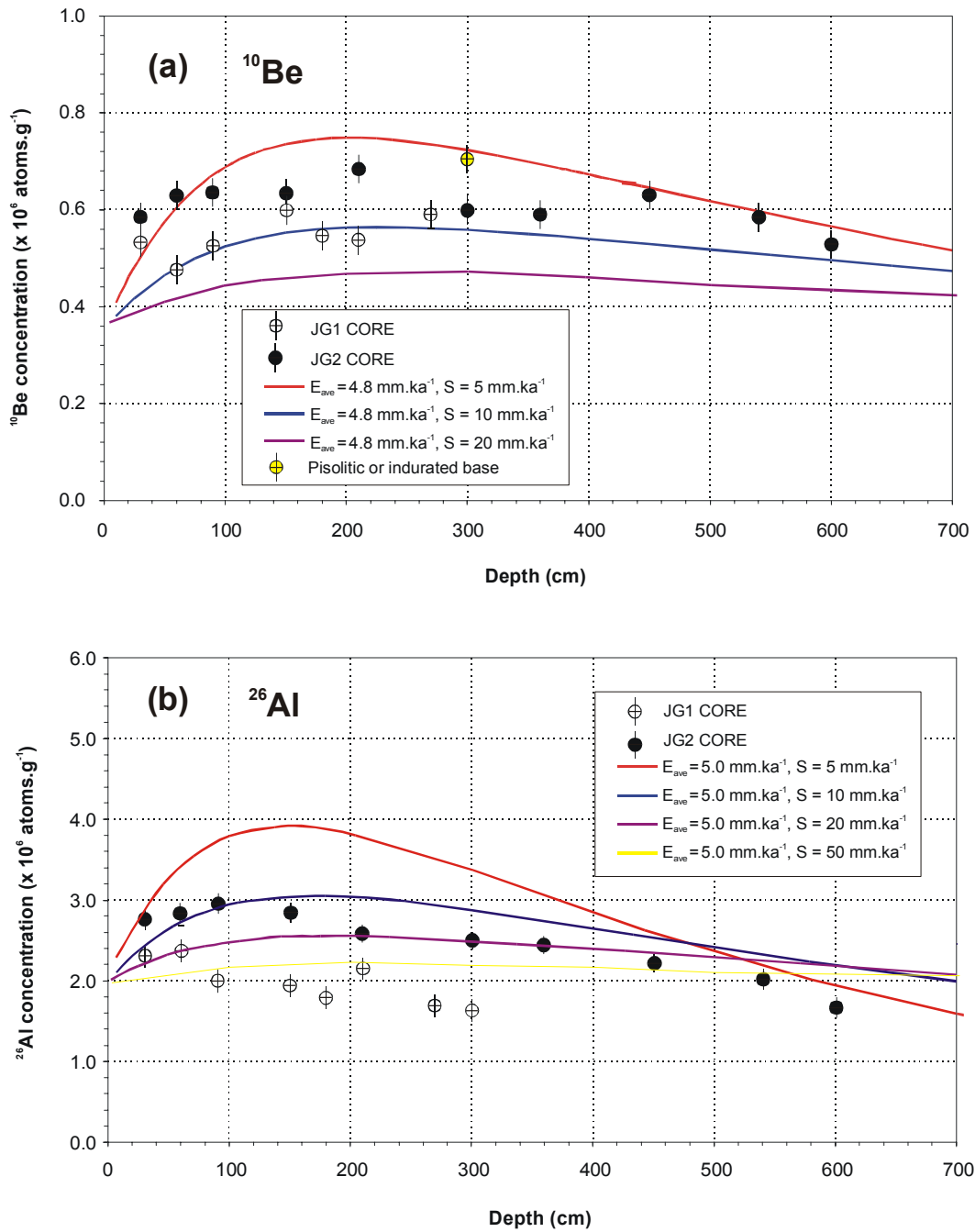


Figure 4.9 Measured radionuclide concentrations for (a) ^{10}Be and (b) ^{26}Al for the two cores JG1 and JG2, plotted against model profiles for sedimentation rates of 5, 10, 20 and 50 mm.ka^{-1} , using C_0 calculated from the average bedrock erosion rate (E_{ave}). Refer text for explanation.

4.5 Discussion

The use of cosmogenic radionuclides to determine sedimentary processes in buried sediments follows the concept developed by Brown et al. (1994) on buried laterite. The work also complements *in situ* cosmogenic isotopic studies already being undertaken by Fink et al. (2000), and by other researchers in Arnhem Land (Nott and Roberts, 1996), and Flinders Ranges (Heimsath et al., 2000). The following discusses the estimates of bedrock denudation and sand sheet accumulation in the Keep River region, in the context of landscape weathering and sand sheet evolution. A hypothetical model of sand sheet evolution dominated by long-term deep weathering is proposed, with the aim of providing a context for interpreting the archaeological trends for the Keep River region.

4.5.1 Landscape Weathering over the Past 200 ka

As outlined in Chapter Three, the climatic environment since the early Pleistocene has changed from being cool and wet, to one that was increasingly arid up to the time of the Last Glacial Maximum (LGM), to the semi-arid monsoonal climate of today. Changing environmental conditions have been critical to the formation and differential erosion of sandstone assemblages, but the manifest erosional variation within sandstone assemblages is generally greater than that between similar rock-types under different climatic regimes (Young and Young, 1992). In the Keep River region, the measured ratios of ^{10}Be and ^{26}Al in the six bedrock samples fall near the expected steady-state values, indicating continual exposure of unshielded bedrock resulting in erosional equilibrium conditions. As argued for Arnhem Land (Roberts, 1991), the weathering rate of the escarpment sandstone in the Keep River region is apt to be slow and reasonably constant under any climatic regime.

Model minimum exposure ages of the bedrock plateaux in the Keep River average around 125 ka, and in the context of exposure age modelling, corresponds to the time taken to denude

approximately 500 mm of bedrock (refer 4.2.1). The period of denudation extends back to the last interglacial period of the early Pleistocene. The measured denudation rate over this time period averages about 5 mm.k^{-1} , regardless of the presence of case-hardened surfaces or otherwise, indicating that there is little temporal or spatial variation in denudation rate at this scale of analysis. It should also be remembered that denudation rates based on cosmogenic radionuclides average several hundred thousand years of exposure and erosion and are buffered against short term changes in denudation rates (Brown et al., 1995). Cosmogenic nuclide concentrations thus reflect pre-anthropogenic erosional conditions (Brown et al., 1998).

Recent work by Bierman and Caffee (2002) indicate that denudation rates are slightly higher (i.e. radionuclide concentrations are lower) in northern Australia than in other parts of Australia, inferring that surface stability is inversely related to mean annual precipitation. The denudation rates calculated from over 60 exposed bedrock surfaces ranged from 0.3 mm.k^{-1} from granite inselbergs to 5.7 mm.k^{-1} on sandstones (Bierman and Caffee, 2002). The estimates of plateau denudation for the Keep River region are similar to those estimated from *in situ* cosmogenic dating in the Arnhem Land plateau (Roberts, 1991; Nott and Roberts, 1996), Victoria Plateau (Fink et al., 2000), Flinders, Macdonnell and Mt Isa Ranges (Heimsath et al., 2000), Eyre Peninsula (Bierman and Turner, 1995; Bierman and Caffee, 2002), and also in the climatically similar environment of South Africa (Flemming et al., 1999). These cosmogenic-based erosion rates also correspond to estimates for semi-arid climates obtained from a review of numerous sources by Young (1983), which range from about 10 mm.k^{-1} under humid temperate climates, 1 mm.k^{-1} for semi-arid, and 0.01 mm.k^{-1} for arid climates. Thus the estimated denudation rates for Keep River are regionally consistent.

Erosion of landscape locally and over shorter periods (decades to millenia) may be more erratic and based on stochastic events rather than through a slow process of weathering of the bedrock surface. After the 2000 wet season, which had over 250 mm of rainfall, evidence of a landslide or rock fall was visible on the Goorurarmum escarpment (Fig. 4.10). The effect of such a brief episodic event

can outweigh the mass transport resulting from continuous spalling of the escarpments and rock-fall debris, but generally only where such events are both numerous and the evidence is obvious (Saunders and Young, 1983). The *block-wise* denudation of landscapes is presently being considered by Chappell et al. (2001) in the sandstone terrain of the Flinders Ranges, and give apparent erosion rates that are slightly greater (mean $E_{app} = 166 \text{ mm.ka}^{-1}$) than those estimated from long-term uniform erosion (mean $E_{app} = 143 \text{ mm.ka}^{-1}$). Thus erosion rates in some parts of the Keep River region may easily be greater than $10 - 20 \text{ mm.ka}^{-1}$.

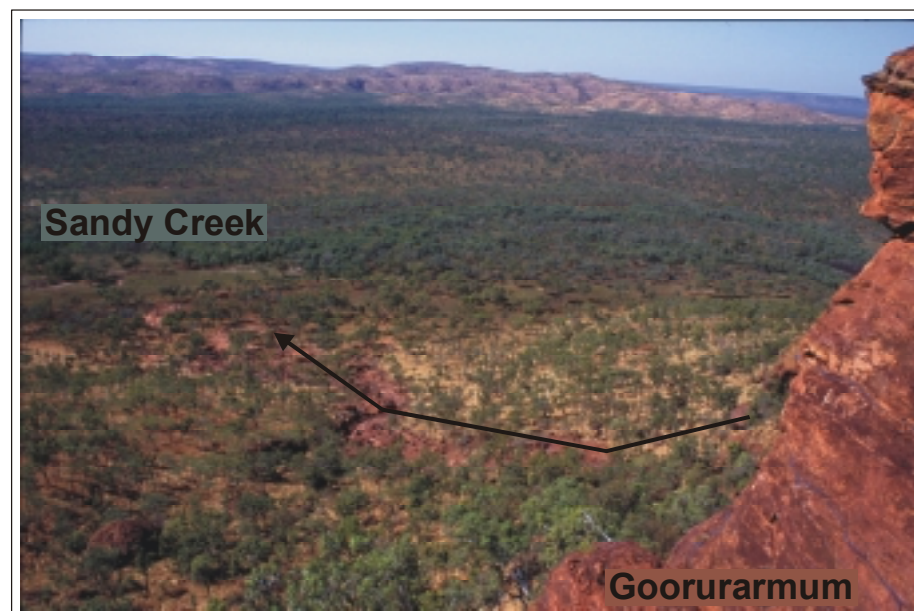


Figure 4.10 Landslip off the Goorurarmum escarpment that occurred sometime after the 2000 wet season, looking towards Sandy Creek Gorge.

Many months after the end of the 2000 wet season there was evident seepage from the escarpment faces (Fig. 4.11), indicating the likely saturation and chemical disintegration of the bedrock through loss of silicate clay minerals (Young and Young, 1992). Removal of intergranular cement can reduce the mechanical strength, while case hardening through re-deposition of silica or iron oxides near the surface may increase strength (Young and Young, 1992).

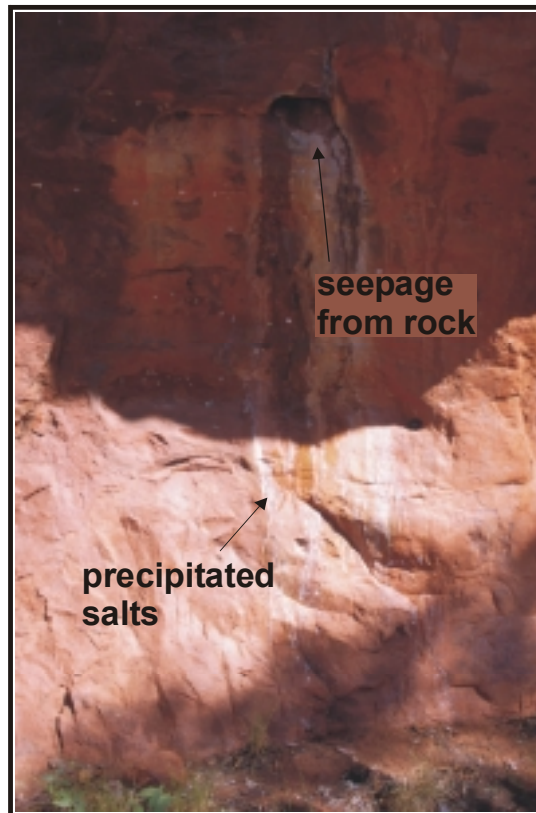


Figure 4.11 Seepage of water through several metres of bedrock was evident several months after the end of the 2000 wet season, indicating the likely gradual saturation and disintegration of the bedrock through chemical weathering.

This differential cycle of disintegration and stabilization is evident from the deeply etched stratigraphic units, exfoliating slabs, tafoni, and case-hardened and lateritic surfaces throughout the Keep River region. Although permanence was not the purpose of most Aboriginal art (Mulvaney and Kamminga, 1999), it is possible that Aboriginal people deliberately chose to place their art on more stable surfaces. These surfaces would also have been subject to differential erosion and preservation. Consequently, the erosion rate of any local rock-art surface may not be represented by regional estimates of vertical or horizontal denudation, nor should the age of the art be reckoned from these regional estimates.

4.5.2 Sand Sheet Evolution

The cosmogenic depth profiles for ^{10}Be and ^{26}Al (Fig. 4.9) are clearly more typical of (allochthonous) accumulating sediments rather than a burial profile developed from *in situ* (autochthonous) weathering. Furthermore, the correlation between the cosmogenic isotopic concentration of the bedrock and surface sediment samples support the assumption that the sand sheet sediments are locally derived. Thus the results from *in situ* cosmogenic dating support the formation of the sand sheets from local accumulation of detrital material from the escarpment face and intervening scree slope in line with Young (1988) and Roberts (1991).

The higher basal concentration of ^{10}Be at the base of the JG1 profile is interpreted to represent a previously exposed palaeosurface upon which later sediments accumulated. Interpolating the estimated accumulation rate of $10 - 20 \text{ mm.k}^{-1}$ of the sand sheet sediments to a minimum age of the inferred palaeosurface at 300 cm in JG1, gives an estimated age of 300 – 150 ka respectively. This is not unreasonable given previous TL ages for these sand sheet sediments in the order of 100 ka (Fullagar et al., 1996).

A hypothetical reconstruction of long-term sand sheet evolution in the Keep River region is illustrated in Fig. 4.12, with the model illustrating the initial accretion of sand sheets over a previously exposed palaeosurface. The accumulation of sand over this palaeosurface is likely to be discontinuous with earlier (older) sediments filling and being preferentially preserved in depositional lows compared to later (younger) sediments. Maxwell and Haynes (2001) describe a comparable formation history for the evolution of the Selima sand sheet, in Egypt. In both cases, older archaeological sequences are more likely to be represented in these topographic lows.

Subsequent accumulation of the sand sheets may occur through gradual and continuous processes, or may occur through major catastrophic events of accretion and partial denudation, akin to the ‘episodic disequilibrium’ described by Nanson (1986). In parts of Australia, periodic expansion of

sand dunes and sand sheets occurs through aeolian activity during acutely arid glacial stages (Bowler, 1976; Pye and Gardner, 1981; Ross et al., 1992; Wasson, 1983, 1986; Wende et al., 1997), whilst in other parts, expansion has occurred as a result of alluvial activity during interglacials (Nanson et al., 1988). At Cabbage Creek, approximately 150 km south of Kununurra, evidence of enhanced alluvial activity is indicated from dated overbank deposits at 37 ka, and between 12 and 6 – 5 ka (Wende et al., 1997). Thus it is quite possible that some expansion of sand sheets also occurred in the Keep River region in association with these wetter interglacial periods.

Contrasting episodes of sand sheet denudation are indicated from geomorphological studies on the Arnhem Land plateau and Magela Creek catchment (Roberts, 1991; Nanson et al., 1993) and in the nearby Koolpin Gorge (Walsh, 1993). All these studies indicate major episodes of alluvial stripping occurred prior to Stage 5, with later events of partial stripping since 100 ky BP, particularly during Stage 3. Geomorphological studies in the Arnhem Land region indicate that these periods of enhanced denudation most likely resulted from dramatic changes in sea-level and/or more frequent rainfall events and floods (Nott and Price, 1994, 1999; Nott and Roberts, 1996). Situated much closer to the coast than Arnhem Land, the Keep River region would have been even more vulnerable to such erosional events, resulting in more frequent and/or extensive episodes of sand removal over the past 100 ka and possibly throughout the entire Quaternary.

During periods of relative stability or where accumulation is more gradual and continuous, soil-forming processes may allow distinct horizons to form. In the White Paintings rock shelter, in the northwest Kalahari Desert, soil A-horizon development not only delimited particular sand units but also correlated with significant peaks in artefact materials (Robbins et al., 2000). However, in northern Australia quartz-rich sands in the form of dunes and sand plains have often been found unfavourable for the formation and preservation of any internal sedimentary structures (Mulvaney and Kamminga, 1999; Newsome, 2000) or palaeosol horizons (Bowler et al., 2001). Field observations in the Keep River region indicate that this is also true of the quartz-rich sand sheets.

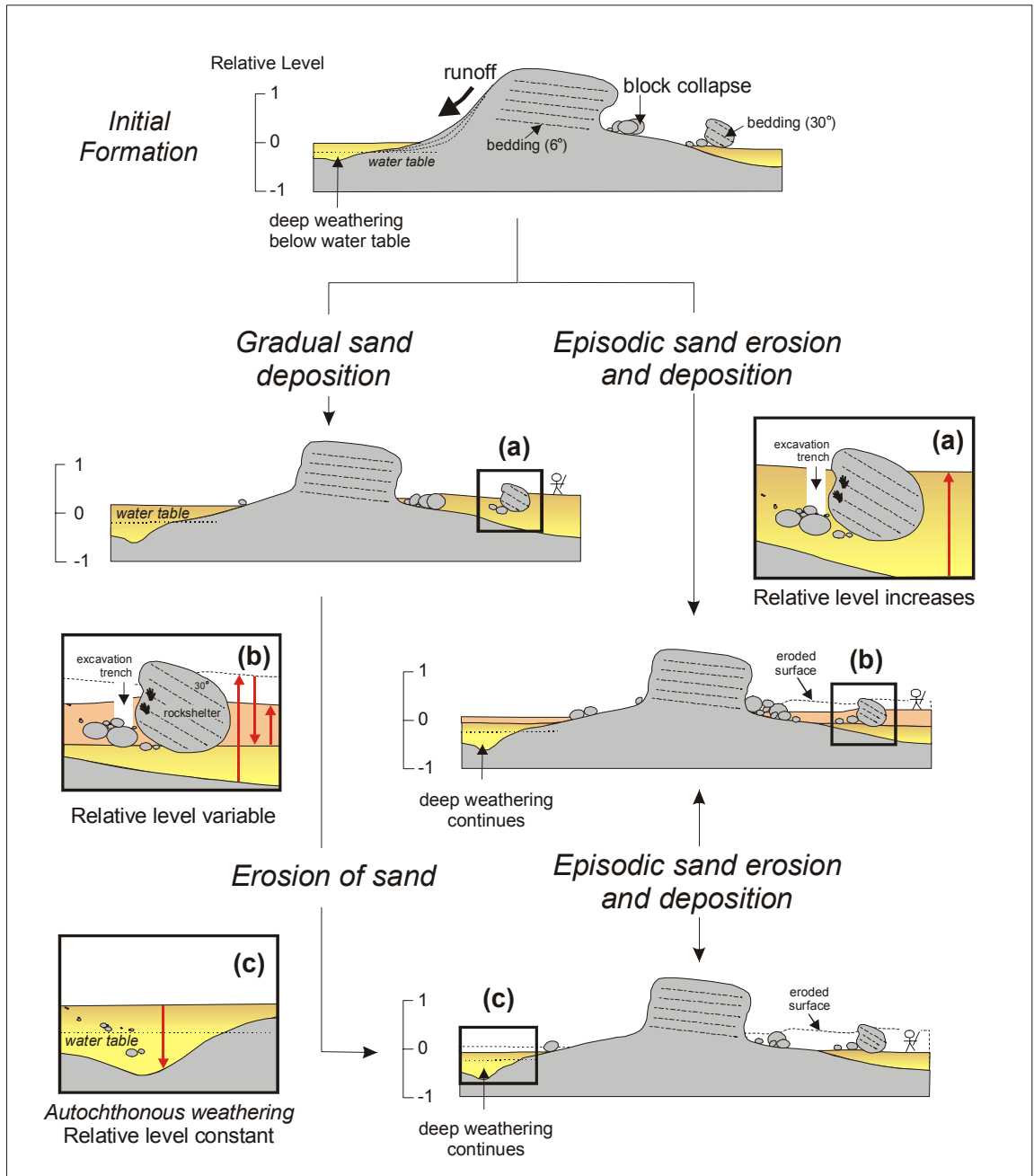


Figure 4.12 Hypothetical reconstruction of sand sheet evolution over timescales of several millennia. Initial accretion of sand sheets over an exposed pediment occurs through deep weathering and erosion of the escarpment. Subsequent vertical accretion may occur through (a) gradual accumulation of sand, (b) episodic events of erosion and sand deposition, or (c) autochthonous weathering. Human occupation may occur during any period of relative landscape stability or instability. Refer text for further explanation.

Thus over time, net deposition may occur with or without obvious major facies and/or stratigraphic boundaries, which may only be determined from the chronostratigraphy or micromorphology. Unfortunately, the chronostratigraphic resolution from *in situ* cosmogenic dating is not favourable, in these relatively young and shallow sequences because the estimated sedimentation rate (S) is a mean for the entire period of sand sheet accumulation. Overall, the results of *in situ* cosmogenic dating indicate that the evolution of the sand-sheets in the Keep River region over the past several hundred thousand years has been gradual (10 - 20 mm.ka⁻¹), involving local derivation of weathered materials and colluvial reworking and bioturbation.

4.6 Validating Denudation and Accumulation Rates from Cosmogenic Dating

The estimated rate of plateaux denudation from exposure dating (~ 5 mm.ka⁻¹) is less than the estimated rate of sediment accumulation from burial dating (10 - 20 mm.ka⁻¹) in the adjacent sand sheets. However, the two measures are not directly comparable. Studies in Arnhem Land indicate that only 5% of the volume of the sand sheets comprises sand denuded from the plateau surface and the remaining 95% derives from the escarpment face (Roberts, 1991). From ¹⁰Be and ²⁶Al cosmogenic dating, calculated denudation rates for the Arnhem Land plateaux of 4 mm.ka⁻¹ (Nott and Roberts, 1996) contrast with scarp retreat rates estimated from volumetric calculations of 20 to 200 mm.ky⁻¹ (Roberts, 1991). On the Drakensberg escarpment, SE South Africa, Fleming et al. (1999) used cosmogenic ³⁶Cl abundances to measure plateaux denudation rates of 5 mm.ka⁻¹ and scarp retreat rates of 50 – 95 mm.ka⁻¹. Weathering of these basalt escarpments also occurred through regular spalling of thin sheets or individual grains and/or the periodic loss of half-metre blocks. Comparable estimates of plateau denudation of 5 mm.ka⁻¹ (Heimsath et al., 2000) and block-wise retreat of 166 mm.ka⁻¹ (Chappell et al., 2001) are obtained from sandstone landforms in the Flinders Ranges. Thus assuming similar ratios also exist in the Keep River region, it is possible to infer escarpment erosion rates in the order of 50 - 100 mm.ka⁻¹.

Correspondingly, sediment accumulation (S_{area}) can be estimated according to the relative areas of supply (A_{bed}) and deposition (A_{ss}), assuming that these bedrock outcrops (E_{bed}) are the only source for the adjacent sand sheets:

$$S_{\text{area}} = \frac{\text{Erosion rate } (E_{\text{bed}}) \times \text{Area of bedrock } (A_{\text{bed}})}{\text{Area of sand sheet } (A_{\text{ss}})}$$

The area of contributing escarpment in each of the catchment areas of Karlinga and Goorurarmum is estimated from topographic maps (refer Fig. 4.5) to be in the order of 2 km². Converting the bedrock to its granular equivalent by adding 20 % for inter-granular porosity (Roberts, 1991) increases the effective area of the bedrock source to 2.4 km². The adjacent sand sheets in each local catchment area can be approximated a length and breadth of 4 km (refer Fig 3.5), giving an areal extent (A_{ss}) of 16 km². Assuming an erosion rate of 100 mm.ka⁻¹ gives an estimated sedimentation rate (S_{area}) of around 14 mm.ka⁻¹, which is comparable to sedimentation rates estimated from cosmogenic burial dating (S_{cosmo}). The equivalence of the sedimentation rate estimated by cosmogenic dating (S_{cosmo}) and from geometric determinations (S_{area}) supports the assumption that the local bedrock outcrops are the main or only source of material to the adjacent sand sheets. These assumptions are given further credence in the following chapters on luminescence dating and sediment characterisation.

4.7 Geoarchaeological Implications

Modelling, measuring and comparing regional archaeological trends have presented problems for the archaeologist (Lourandos and David, 1998). Modelling, measuring and comparing regional geological processes are perhaps first steps towards defining the dynamics of the human landscape. As the physical processes shaping the land can be seen to unfold over hundreds and thousands of years, so can the social processes which are evident in the archaeological data (Gosden and Head, 1994: 113). Geomorphodynamics in dry savanna environments can often have both anthropogenic and climatic causes (Heinrich and Moldenhauer, 2002).

In a recent program on the Kimberley rock art, an allusion was made to the weathering rate of the sandstone bedrock. It was stated that:

“In the Kimberley, and in Arnhem Land, the rock is so hard, you can actually see paintings that are 40 to 50 thousand years old still on the surface.”

(M. Morwood on ‘Australian Story’ ABC, 14 October 2002).

The statement implies that the erosion rate of the sandstone bedrock is less than the thickness of the paintings, or less than 1 – 2 mm per 50 ka or 0.05 mm.ka⁻¹. Such notional statements highlight the need for more empirical quantification of denudation and erosion rates of sandstone surfaces throughout the Kimberley and Arnhem Land. In the Keep River region, as in other parts of northern Australia (refer 4.5.1), *in situ* cosmogenic isotope dating provides an estimation of plateau denudation that is 1 – 2 orders of magnitude greater than the above implied erosion rate of the escarpment faces upon which the rock art occurs. However, it should be remembered that *in situ* cosmogenic dating averages processes occurring over million year timescales and not the hundred or thousand year timescales over which local weathering of rock art occurs. In other words, higher resolution dating techniques may provide better estimates of weathering of local rock art surfaces (see also Bednarik, 2002; Watchman and Twidale, 2002).

The results from *in situ* cosmogenic isotope dating indicate that the physical processes shaping the sandstone landscapes in the Keep River region date well beyond 100 ky BP, and compares with the archaeological history of northern Australia with occupation dates around 60 ky BP (Roberts et al., 1994b; Turney et al., 2001). Although burial dating necessarily assumes gradual accumulation of the sand sheets, a hypothetical model proposes that sand sheet formation occurs episodically, with sediment and associated archaeological deposits preserved accordingly. In both the physical and human landscape are shorter term dynamics. The shorter term landscape dynamics of the Keep River region are the subject of the following chapters on luminescence dating and sediment characterisation.

4.8 Conclusions

Using *in situ* cosmogenic nuclide dating, the estimated rate of plateau denudation is 5 mm.ka⁻¹ over the past 500 ka, which corresponds well to regional estimates. However, greater resolution is required to accommodate recent catastrophic events (e.g. rock falls) or estimate erosion at specific site locations, particularly for surfaces where rock art observed.

The bedrock denudation rates are used to model depth profiles of ¹⁰Be and ²⁶Al concentrations through the sand sheets. The results support the formation of sand sheets through local accumulation of detrital material from the escarpment face and intervening scree slope rather than from *in situ* conversion of the underlying saprolite or long-distance transport of aeolian sediments. The local sourcing of material to the sand sheets is indicated from the correspondence between the isotopic concentration in the bedrock and surface sediments. Burial dating indicates that over the past several hundred thousand years, accumulation of sand in the sand-sheets has been greater than erosion with a net sedimentation rate of 10 - 20 mm.ka⁻¹. However, the resolution from these sediments cannot discern intermediate changes in accumulation rate or episodes of erosion over shorter timescales.

CHAPTER FIVE

Sediment Characterisation and Site Formation

It is important to recognise that the sediment constitutes the site!

– Farrand, 2001: 537.

5.1 Introduction

To geoarchaeologists the concept of formation processes means the search for processes of formation associated with the archaeological context (Stein, 2001). The depositional context is characterised through objective description of the sedimentary characteristics and formation processes. These processes include cultural and natural formation processes, which may be evident within the archaeological deposit itself and/or within deposits which reflect more regional influences. Deposit characterisation provides the basis for the interpretation of formation processes. Identification of both natural and cultural component begins with a consideration of sedimentation, which is a function of four factors (1) source, (2) transportation mechanism, (3) environment of deposition (comprises site-formation processes), and (4) post-depositional environment (Stein, 1985:5). Here, the physical and geochemical properties of escarpment bedrock and sediment samples from the rock-shelters, sand sheets and creeks are characterised and used to identify and understand the nature of these factors.

This study couples field observations with laboratory analyses to provide, first, the necessary basic description of the sediments and, second, an interpretation of the environment of sedimentation. Present understanding and empirical data on site formation processes in sandy deposits across northern Australia is limited; consequently the following sedimentary analyses are exploratory rather than comprehensive. The characterisation of bedrock and sand sheet sediments at the macro-scale (including petrography, grain size and morphology, sediment colour, etc.) provide a first-order indication of the composition (mineralogy) of the sandstone material. The geochemical analysis of sediments may indicate discrete groups that relate particular sediment sources or sinks, or to stratigraphic or taphonomic processes (Reynolds and

Catt, 1987). Phosphate minerals, for example, are particularly favourable for identification of inputs of human or animal wastes (Parnell et al., 2002).

Microscopic and micro-morphological analysis of sediments offers the potential for examination of cultural and non-cultural processes that might otherwise be undetected from field observations or bulk analyses (Courty et al., 1989; Davidson et al., 1992; Goldberg et al., 1994; Goldberg and Arpin, 1999; Matthews et al., 1997; Macphail et al., 1990). The necessarily small sample size means that these methods are only really effective when dealing with questions refined from larger-scale stratigraphic problems (French and Whitelaw, 1999). The appropriate resolution of individual depositional events and processes in the sandy sediments throughout northern Australia is poorly understood and hence poorly defined. Here, an attempt is made to reveal both the larger-scale stratigraphy and micro-stratigraphy of the sand sheets and rock shelters of the Keep River region. These studies can lead to an understanding of site-formation processes during human occupation, and eventually to a reconstruction of local and, in some cases, regional paleoclimates. Furthermore, sediment study is essential for intra-site correlation, independent of archaeological and chronological techniques.

The characterisation of the sediments in the Keep River region is aimed at answering the following questions:

- What do the characteristics of the bedrock, sand sheet, rock-shelter and creek sediments indicate about source and transport processes? Is it possible to correlate or differentiate sediment sources and sinks within and between (archaeological) site locations?
- What do the physical and geochemical characteristics of the sand sheet, rock-shelter and creek sediments indicate about post-depositional processes?
- Is there any distinct anthropogenic signature in any of the rock-shelter or sand sheet sediments?
- How might the above influence interpretations of the archaeological record?

5.2 Methodology

Six of the bedrock samples used for cosmogenic analyses (Chapter Four), were used to provide a compositional range of sandstone source material. In the absence of buried bedrock material, four rubble samples were retrieved from samples collected at the base of the excavation pits at Jinmium (original C1 trench), Goorurarmum (Goor-1 and 2) and Karlinga (Karl-1). Nearly 100 sediment samples were analysed in order to identify local chemical processes within the sand sheets. This included 4 of the samples used for cosmogenic isotope analysis (Chapter Four), 40 samples used for luminescence dating (Chapter Six), 8 samples from the original Jinmium trench, and ~ 50 selected samples (including pisolitic deposits) from other indicative sites.

Sediment sampling of the sand sheets surrounding Goorurarmum and Jinmium (Fig. 5.1), and Karlinga (Fig. 5.2) was undertaken over two separate field trips in 1999 and 2000 as part of the main archaeological field seasons. A key strategy was to compare rockshelter occupation deposits with occupation deposits on the adjacent sand plains. Two pits were excavated at Goorurarmum (KR31), one in the main rock shelter (Goor-2) and one ~ 25 m in front on the sand sheet (Goor-1) (Fig. 5.1). Archaeological pits were excavated at three separate sites in the Karlinga site area, one within the KR36 rock shelter (Karl-1), one within the elevated (~ 80 m) rock shelter (Karl-2), and another on the sand sheet adjacent to a small overhanging shelter (Karl-3). The elevated and sheltered location Karl-2 less directly relates to the sedimentary deposits of the sand sheets and was not used in this study.

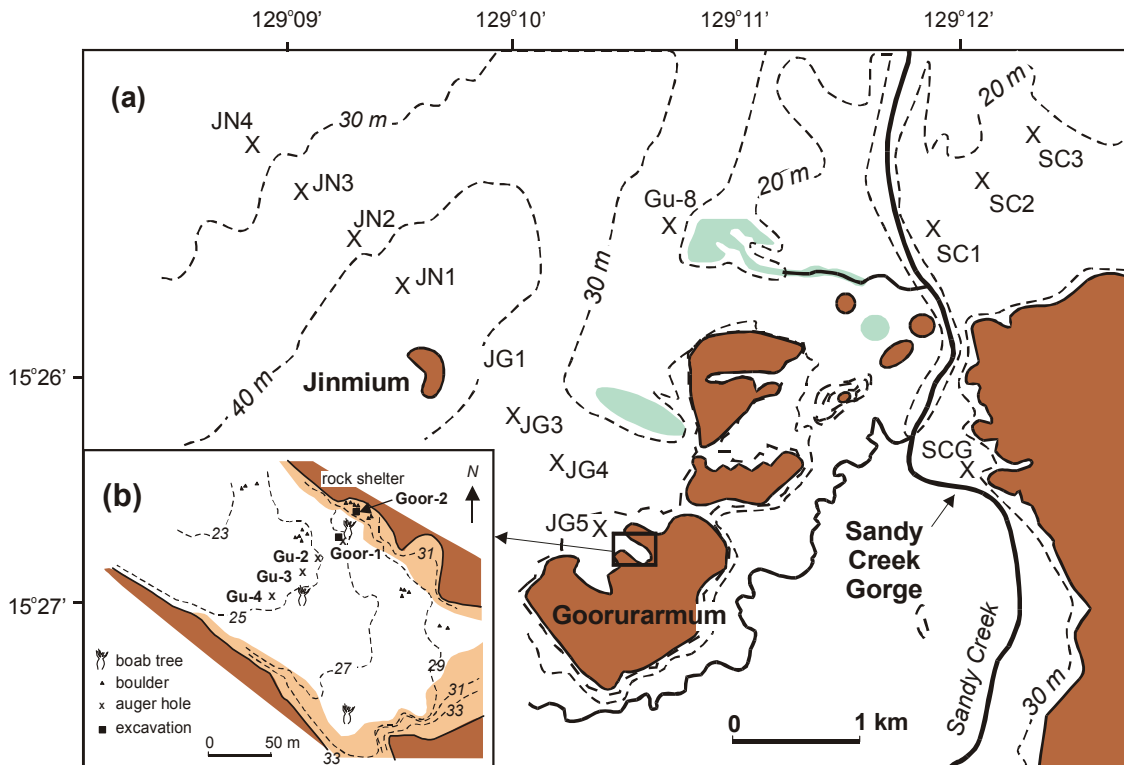


Figure 5.1 (a) Location of sample sites around Jinmium, Goorurarmum and Sandy Creek Gorge, (contours from topographic maps) and (b) detailed map and contour survey of the Goorurarmum sand sheet and main rock shelter site (KR31). Areas shaded in brown, pink and blue represent bedrock, scree slope and swampland respectively.

In addition to the excavation pits, auger hole transects were cored across several of the sand sheets, 14 between Jinmium and Goorurarmum, 3 at Sandy Creek (Fig. 5.1), 14 cores at Karlinga (Fig. 5.2), and 4 at other sites in the Keep River region. This was presumed to provide a non-occupation sedimentary comparison to the archaeological sites. The absence of artefacts was confirmed from a selection sieved (using 2 mm sieve) auger samples in the field. Sediments included uniform red sands, mottled red and yellow sands, streaky red and grey sands, and pisolitic material, thus providing a range of moderate to intensively leached sites from a range of depths across the sand sheets. Where possible, samples were carefully taken to reflect obvious stratigraphic variations (in grain size or colour), which may correspond to changes in sedimentation. More easily accessible profiles of the sand sheet stratigraphy were obtained from two creek sections, one at Sandy Creek Gorge (Fig. 5.1) and another near the rock shelter KR99 (Fig. 5.2). These sites were chosen in order to provide the most extensive

and representative section within each creek. Digging vertical sections in steps, and removing slumped material revealed *in situ* horizontal stratigraphic horizons (Fig. 5.3).

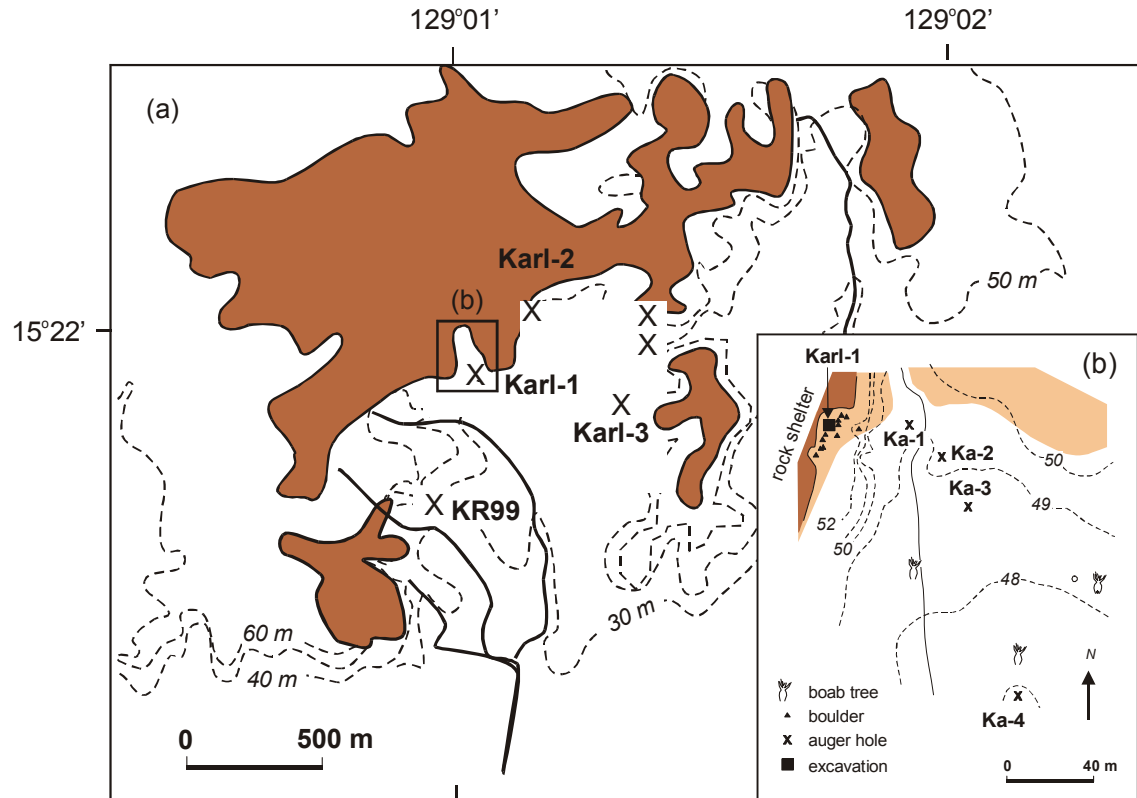


Figure 5.2 (a) Location of sample sites around Karlinga (contours from topographic map), and (b) detailed map and contour survey of the sand sheet and main rock-shelter site (KR36). Areas shaded in brown and pink represent bedrock and scree slope respectively.

In situ sub-samples of sediment profiles were collected using Kubiena tins from two excavation pits, Goor-1 and Karl-3, and at the creek section near site KR99. Although only half the sample was successfully impregnated with the low-viscosity resin, it did provide enough material to prepare standard thin-sections and resin-mounted stubs. Significant expansion occurred in at least one sample (Goor-2-120 cm), thus the porosity present in the thin section will be partly artificial. Despite repeated attempts, the hydrophobic nature of the rock-shelter sediments (due to the high concentration of charcoal) prevented sampling of these sites. Details of sampling and thin section preparation are outlined in Appendix A3.2.

Descriptions of bedrock samples, sand sheet and rock-shelter sediments included petrography, grain size, and colour. Grain size variations were accurately obtained using two Long Bed Malvern Master Sizer, laser particle sizers, housed at James Cook University (JCU) and the University of Wollongong (UOW) (Appendix A3.4.1). Mineralogy was determined from petrographic observations, and using X-ray Diffraction (XRD) at UOW. Major element geochemistry was determined using X-Ray Fluorescence (XRF) at JCU. In order to present all aspects of the sedimentary micro-fabric, thin sections were observed at a range of scales, using the optical microscope, and electron microscopy. Detailed chemical mapping by SEM/EDXA provides elemental characterisation of single grains, surface coatings and interstitial material, which may also reflect sedimentary processes. SEM/EDXA analyses were undertaken at the Advanced Analytical Centre (AAC) at JCU, and details of the SEM/EDXA setup are outlined in Appendix A3.2.1.



Figure 5.3 Photograph of slumped material over the top of horizontal stratigraphic horizons at the site of KR99CP.

5.3 Results

Core diagrams including petrographic descriptions, grain size and artefact density with depth, and luminescence dating results (from Chapter Six) are given below for the initial Jinmium (C1/III) excavation (Fig. 5.4), the rock-shelter excavation at Goorurarmum (Fig. 5.5) and at Karlinga (Fig. 5.6), the sand sheet excavation at Goorurarmum (Fig. 5.7) and at Karlinga (Fig. 5.8), and for the creek profile near the site of KR99 (Fig. 5.9), and at Sandy Creek Gorge (Fig. 5.10). Core diagrams and sediment descriptions for all auger cores and excavation profiles are given in Appendix A3.1, for Goorurarmum and Jinmium (Fig. A3.2), Karlinga (Fig. A3.3) and Sandy Creek (Fig. A3.4). Results of grain size and major element analyses of bedrock and sedimentary material from each of the four main sites of Goorurarmum, Jinmium, Karlinga and Sandy Creek Gorge are outlined below. Full details and statistical analyses of grain size are given in Appendix 3.4.2 and 3.4.3 respectively, and for geochemistry in Appendix 3.5.2 and 3.5.3 respectively.

5.3.1 Sediment Macro-stratigraphy

5.3.1.1 Rock shelters

The original Jinmium (C1) rock-shelter excavation is summarized in Fig. 5.4 for comparison with the more recent excavation profiles described below. Original diagrams are depicted in Figs 6.1 and 6.2 and a full description is provided by Fullagar et al. (1996). The rock-shelter deposits are generally comprised of moderately sorted, medium-coarse (~ 400 µm), red-yellow (7.5YR 5/4) to dark brown (5YR 2.5/2) sands, with sandstone rubble increasing towards the base of the 1- 2 m profiles. Charcoal (1 – 5%) and artefacts, present in the upper parts of the stratigraphy, were absent at the base of all the excavations.

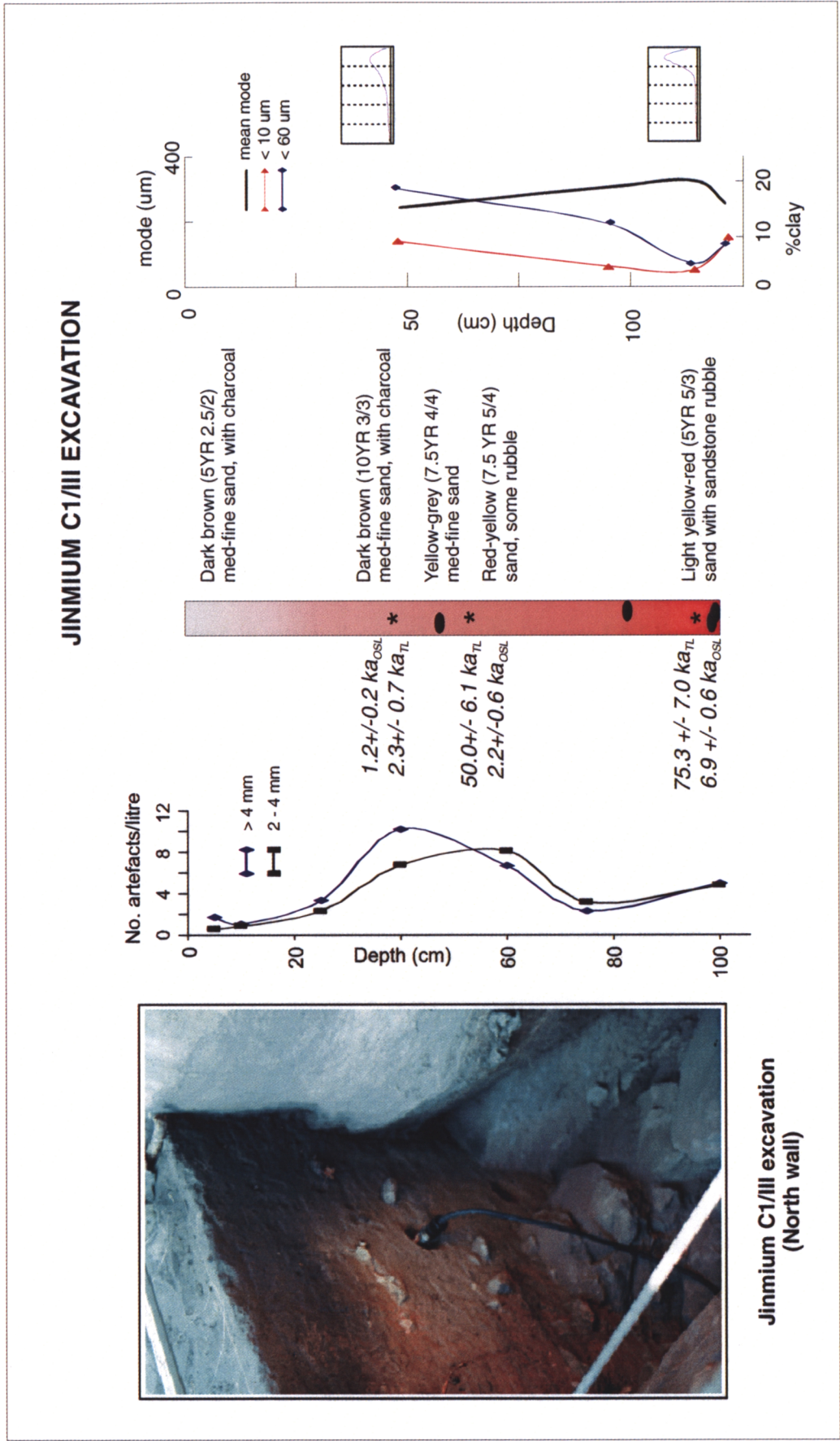


Figure 5.4 Profiles for the Jinmium C1 rock shelter. Dates are sourced from Fullagar et al. (1996) and Roberts et al. (1998a), and artefact numbers were kindly supplied by R. Fullagar (pers. comm., 2001).

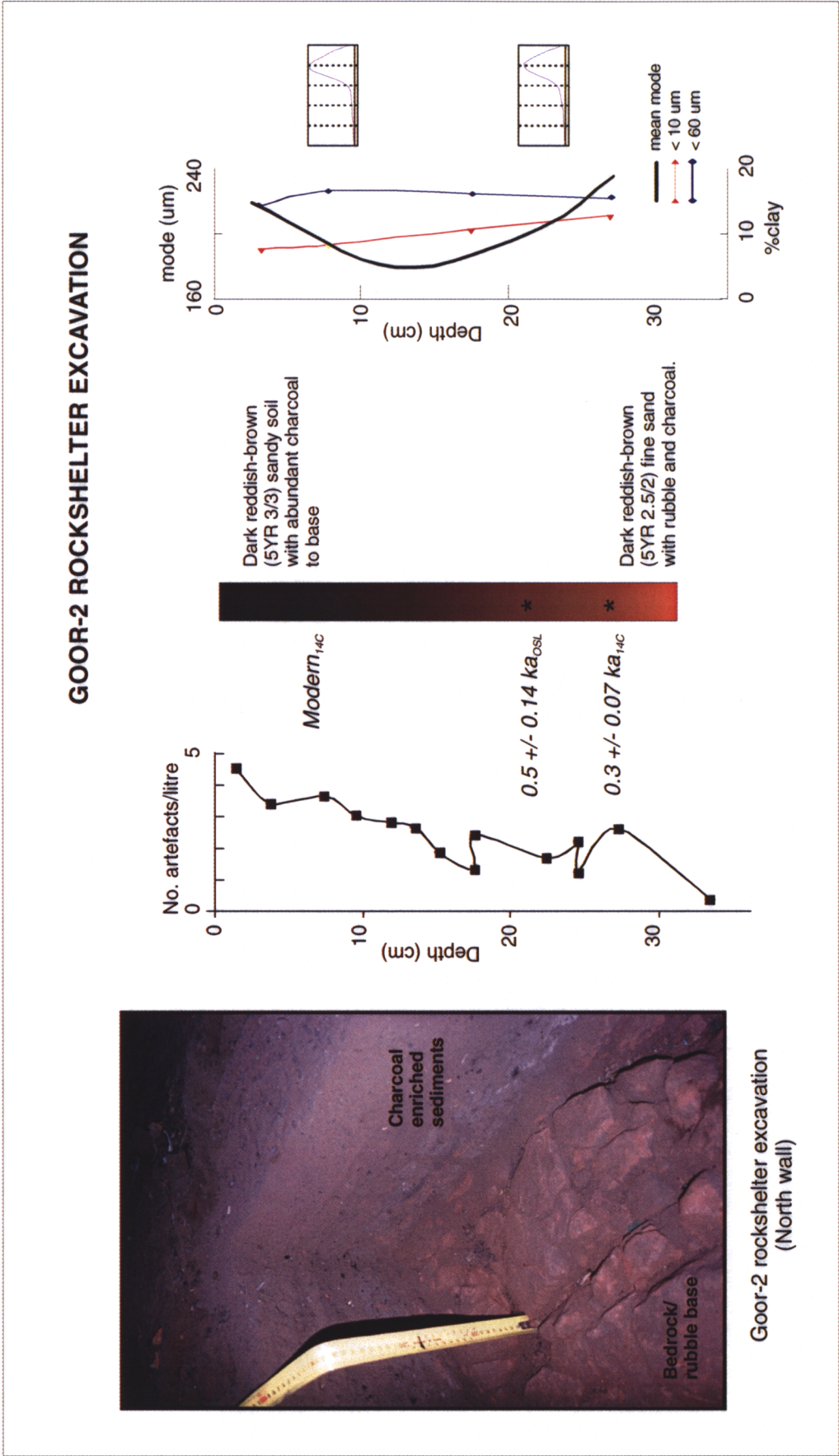


Figure 5.5 Profiles for the Goorurarmum, the rock shelter excavation. Luminescence dates are derived from Chapter Six, and radiocarbon dates are detailed in Chapter Seven. Artefact numbers were kindly supplied by R. Fullagar (pers. comm., 2001).

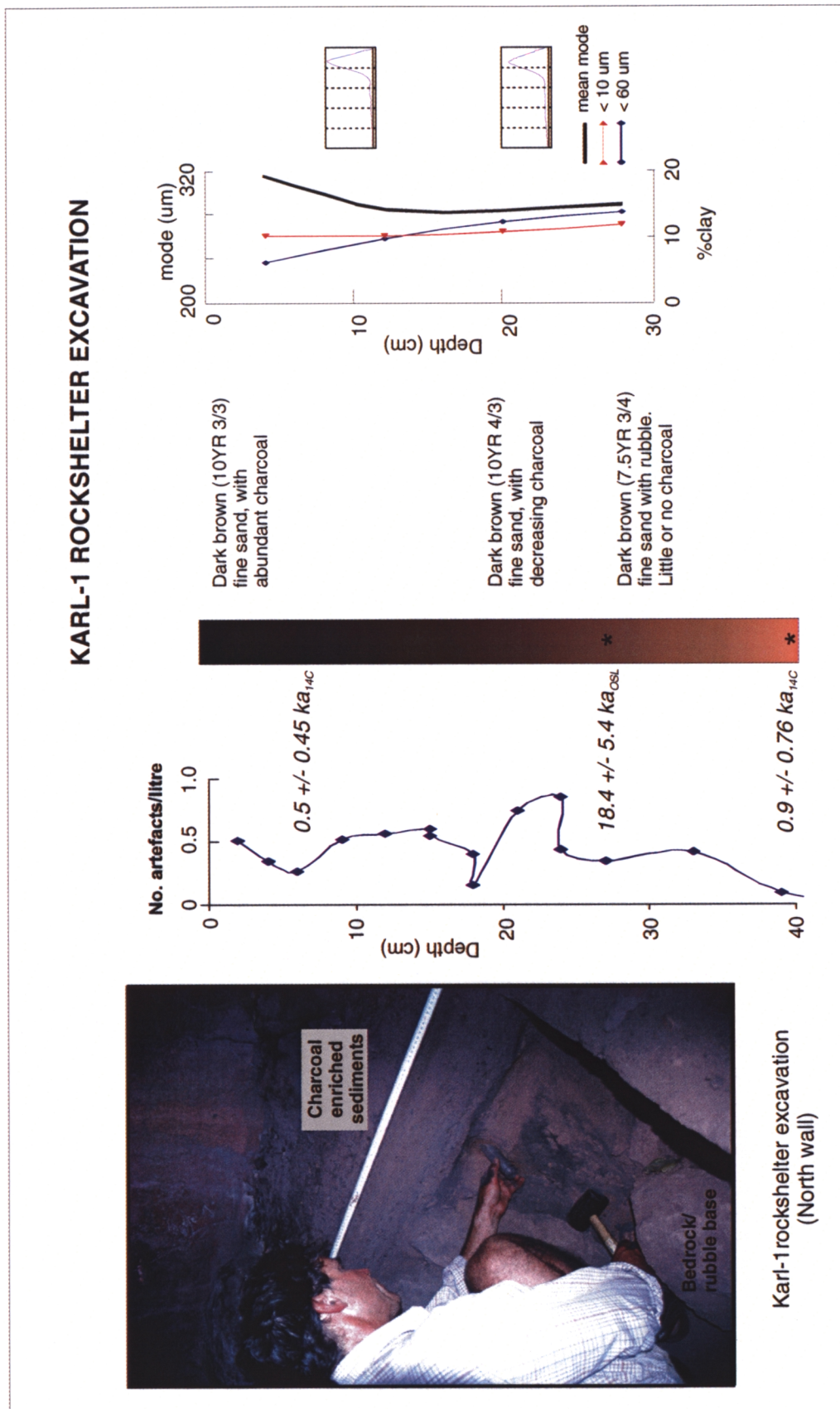


Figure 5.6 Profiles for the Karlinga rock shelter excavation. Luminescence dates are derived from Chapter Six, and radiocarbon dates are detailed in Chapter Seven. Artefact numbers were kindly supplied by R. Fullagar (pers. comm., 2001).

The Goorurarmum (Goor-2) rock shelter sediments comprise moderately sorted, med-fine (~ 201 µm), dark-reddish brown sands (5YR 3/3 to 2.5/2), with a relatively high percentage of charcoal (~ 5%) down to the base of the 30 cm deep profile (Fig. 5.5). These sediments lie on an indurated sandstone base of bedrock and/or rubble. No significant grain size change is observed. Artefact density decreases towards the base of the profile. The luminescence ages are discussed in Chapters Six (refer 6.6.2.3) and radiocarbon ages in Chapter Seven (refer 7.2.1).

The Karlinga (Karl-1) rockshelter sediments comprise well-sorted, dark brown (10YR 3/3 to 7.5 YR 3/4) med-fine sands (~ 260 µm), also with charcoal decreasing towards the base of the 30 - 40 cm profile (~ 5%) as evident from the colour change of the sands (Fig. 5.6). These sands infill and lie over a base of boulders and rubble material. Again the luminescence ages are discussed in Chapters Six (refer 6.6.2.3) and radiocarbon ages in Chapter Seven (refer 7.2.1).

5.3.1.2 Sand Sheets

Sediments within the Goorurarmum amphitheatre comprise medium-fine (~ 160 µm), moderately sorted, unimodal sands with pebble and cobble material gradually increasing near the bedrock/rubble base. There is little or no stratigraphic differentiation throughout the sand sheet profile. In the Goorurarmum sand sheet excavation (Goor-1), the sediment colours range from red-brown sands (10YR 4/2 to 7.5YR 5/4) near the surface, to increasingly red (5YR 5/6) sands towards the bedrock/rubble base at about 2.4 metres depth (Fig. 5.7). The darker hue and colour near the surface probably results from recent burning. The luminescence ages are discussed in Chapters Six (refer 6.6.2.1) and radiocarbon ages in Chapter Seven (refer 7.2.1). A kilometre north, towards the coastal mudflats, the surface sediments from Gu-5 are a lighter brown (10YR 6/4) and at 2 m depth show deep red (10R 6/8) mottling.

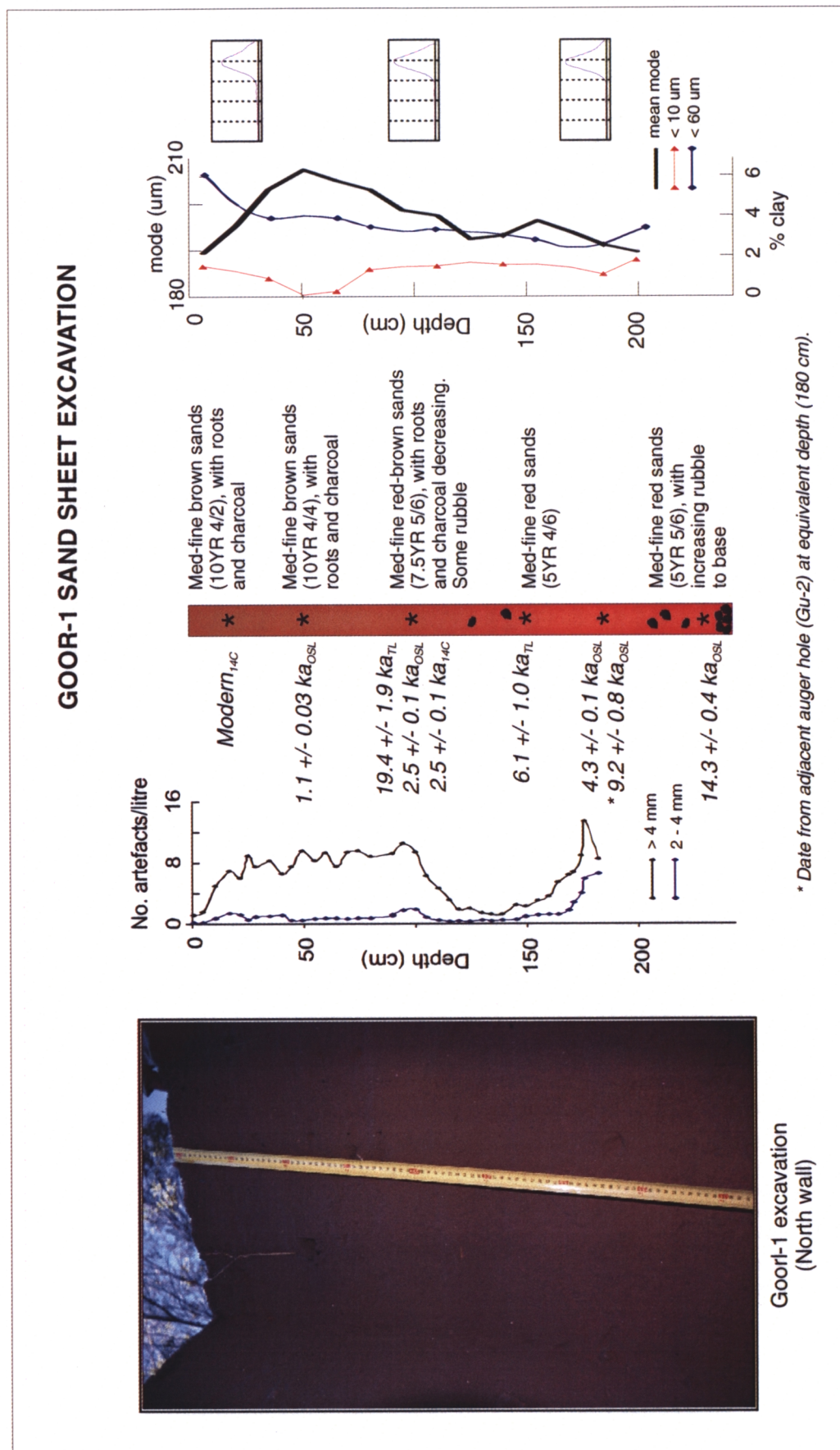


Figure 5.7 Profiles for the Goorurarmum sand sheet excavation. Luminescence dates are derived from Chapter Six, and radiocarbon dates are detailed in Chapter Seven. Artefact numbers were kindly supplied by R. Fullagar (pers. comm., 2001).

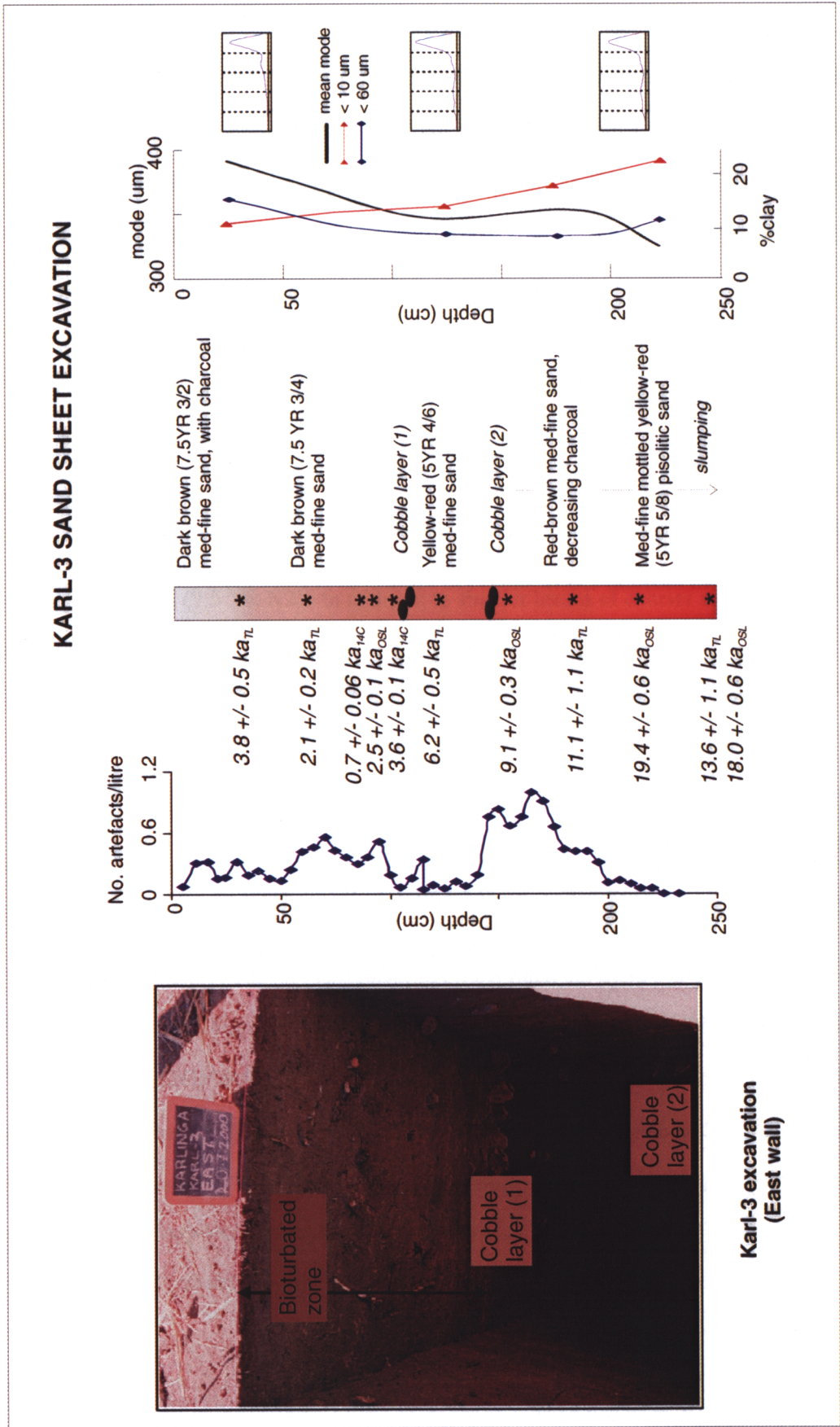


Figure 5.8 Profiles of the Karlunga sand sheet excavation. Luminescence dates are derived from Chapter Six, and radiocarbon dates are detailed in Chapter Seven. Artefact numbers were kindly supplied by R. Fullagar (pers. comm., 2001).

West toward Jinmium, the sediments become less red and increasingly yellow with decreasing elevation. At the surface the sediments are orange-yellow (5YR 4/6 - 5/6), and at depth show varying degrees of red-yellow mottling (10R 4/6 and 7.5YR 6/8). Situated at a higher elevation (~ 15 m AHD), the sediments near Jinmium are typically lighter red (2.5YR 4/6) at the surface and become dark red at depth (10R 4/6), with pisolites developing at the base of the profile (Fig. A3.2), reflecting past fluctuations in the water table. The sediments around Jinmium (~ 380 µm) are slightly coarser and more angular than those at Goorurarmum. North of Jinmium and with decreasing relative level, the sediments again become light red to yellow (5YR 4/6) and are underlain at shallow depths (< 2 m) by darker red sediments (10R 4/6) or pisolitic material.

Around the main Karlinga escarpment, the sediments are dominantly coarse (360 µm), poorly sorted, and ranging from medium brown sands (10YR 4/2) to slightly lighter sands at depth (10YR 7/2). In the Karlinga sand sheet excavation (Karl-3) the sediments are darker (7.5YR 3/2) at the surface, progressing through yellow-red and mottled yellow-orange sands (5 YR 4/6) with red (2.5YR 3/6) pisolitic material at the base of the 2.5 m excavation pit (Fig. 5.8).

Rubble layers, comprising (imbricated?) cobbles 5 - 10 cm thick, were encountered at depths of 1 m and 1.5 m (Fig. 5.8). Again, the luminescence ages are discussed in Chapters Six (refer 6.6.2.1) and radiocarbon ages in Chapter Seven (refer 7.2.1).

Traversing further south-east from the main Karlinga escarpment towards the Keep River, and with decreasing relative level, the sediments become more yellow-orange (10YR 5/8) and show a greater degree of slumping due to a higher water table at depth (Fig. A3.3). One auger hole, KN7, revealed a layer of red pisolitic sands at about 2 m depth indicating the presence of a fluctuating water table at some time in the past. At the lowest relative level, saturated brown sandy clay in KN8 reflected a swamp-land.

5.3.1.3 Creeks

It was observed after the 2000 wet season, that the sand deposits in the creeks which drained into the Karlinga and Goorurarmum sand sheets were significantly coarser than those of the respective sand sheets. Grain size analysis of a creek sample from each of these sites ($\sim 450\ \mu\text{m}$ at Karlinga and $\sim 320\ \mu\text{m}$ at Goorurarmum) confirmed this observation, and indicates some process of preferential sorting and preservation within the sand sheets.

The sediments within the KR99 Creek Profile (Fig. 5.9) are similar to those found nearer to the main Karlinga site but are finer ($\sim 300\ \mu\text{m}$) with a significant clay fraction ($<10\ \mu\text{m}$). These creek sediments progress down the profile from dark grey-brown (10YR 3/2) pebbly sands, through brown-white sands (5YR 5/4 - 8/1) and more abruptly into dark grey sands (5YR 5/1) with black streaks (7.5 YR N2). In addition to smaller lenses of coarser and dark brown sands, these changes possibly reflect changing energy levels in the adjacent creek at various times in the past. The luminescence ages are discussed in Chapters Six (refer 6.6.2.2).

The sediments adjacent to Sandy Creek comprise well-sorted, fine sands ($\sim 150\ \mu\text{m}$) with a sub-dominant clay fraction ($< 10\ \mu\text{m}$). The sediment colours range from fine yellow-brown sands (10YR to 7.5 YR 4/4) at the surface to more orange (10YR 5/6) about 2 m depth. Interestingly the water table was encountered progressively higher up the profile along the traverse from Sandy Creek towards the billabong near the auger core SC-3. In the nearby Sandy Creek Gorge, the creek section revealed strongly leached, highly differentiated lateritic soils and gleyed-podzolic soils with sinuous root mottles (Fig. 5.10) which are representative of one or more palaeosol horizons. The brown sandy sediments (7.5 YR 4/4) at the surface progressed downward into very well-sorted red clayey sands (2.5 YR 4/6) with small black pisolites, into very well-sorted streaky red-grey (7.5 YR 3/8-6/6) clayey sand with dark red mottles (2.5 YR 3/6).

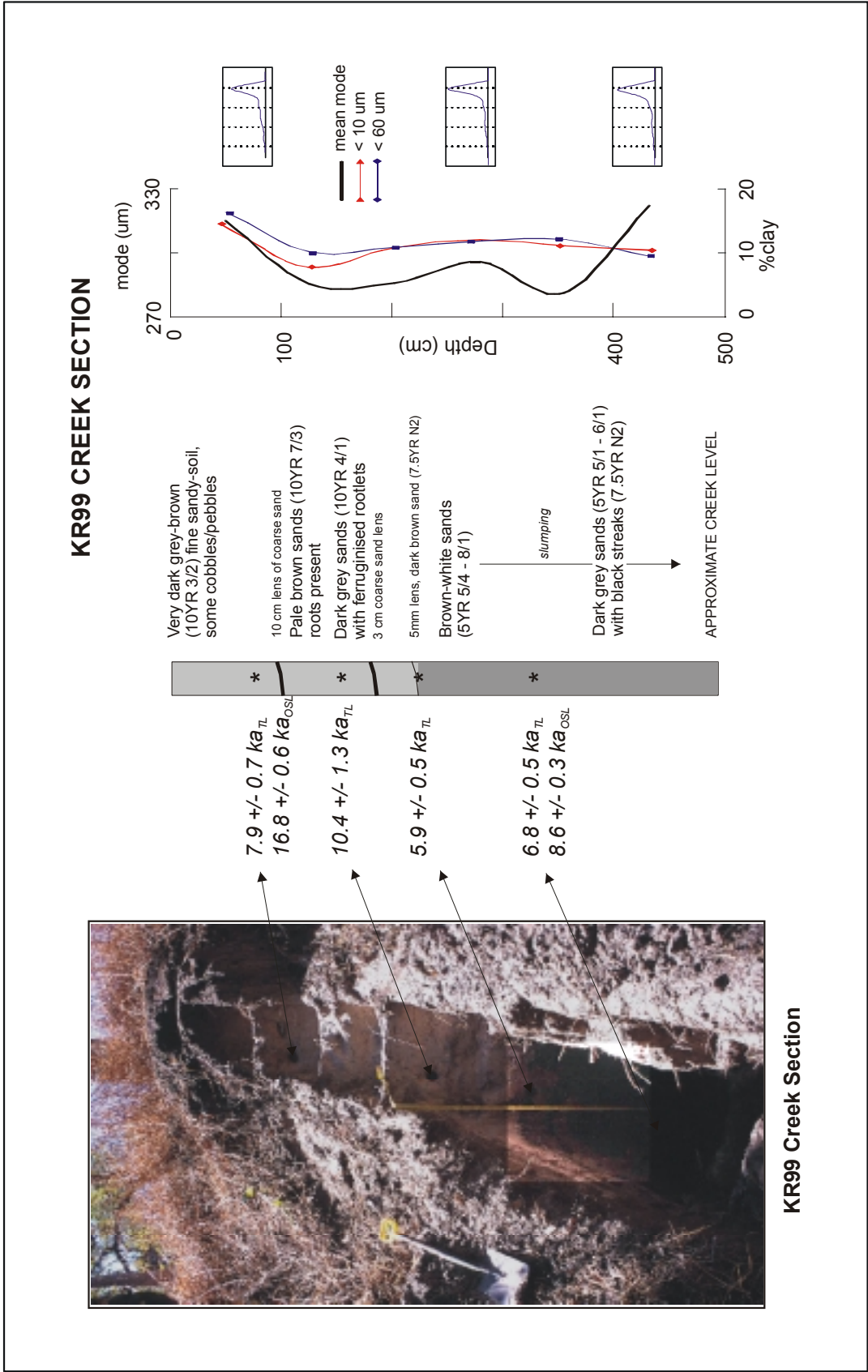


Figure 5.9 Profiles of the creek near the site of KR99. Luminescence dates are derived from Chapter Six.

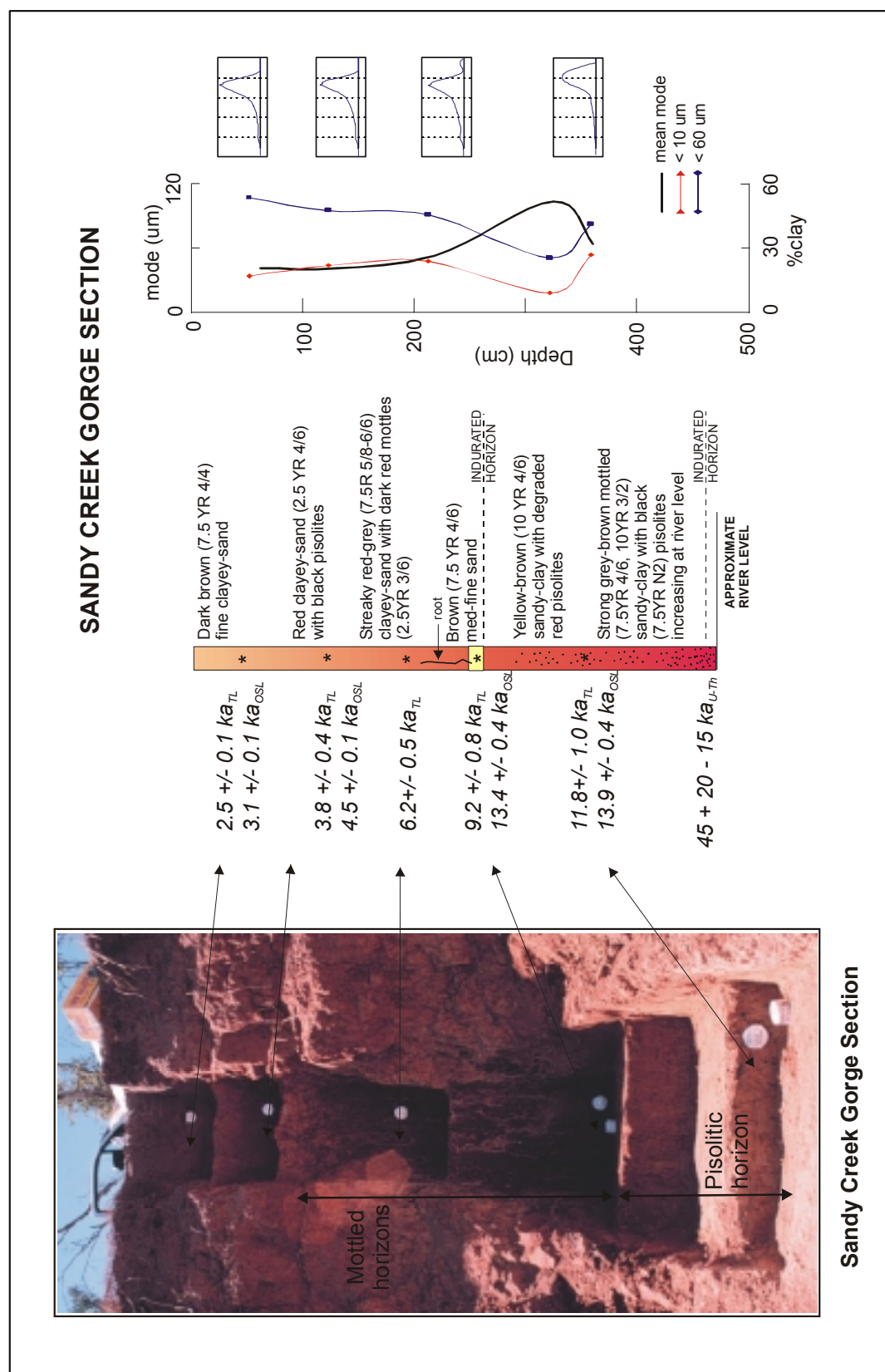


Figure 5.10 Profiles of the creek at Sandy Creek Gorge. Luminescence dates are derived from Chapter Six.

At about 3 m depth in the Sandy Creek Gorge profile, a narrow band (~ 20 cm) of coarser sands was observed (Fig. 5.10). With increasing depth the sediments progressed from brown clayey-sands (7.5 YR 4/6) with degraded red pisolites to well-sorted mottled sandy-clay (7.5 YR 4/6, 10YR 3/2) with hard black pisolites (7.5 YR 3/2). The pisolitic material (5 - 8 mm diameter) increased in abundance to form a distinct horizon within the bed of Sandy Creek reflecting the presence of a fluctuating water table at some time in the past.

Also evident on the bank of Sandy Creek Gorge were two unconformable horizons of a hard, indurated silicate material (Fig. 5.11) at about 320 cm and 500 cm depth. These horizons were not observed in the section cut in the creek bank, indicating they are either an isolated outcrop or represent a later event. The luminescence ages are discussed in Chapters Six (refer 6.6.2.2).

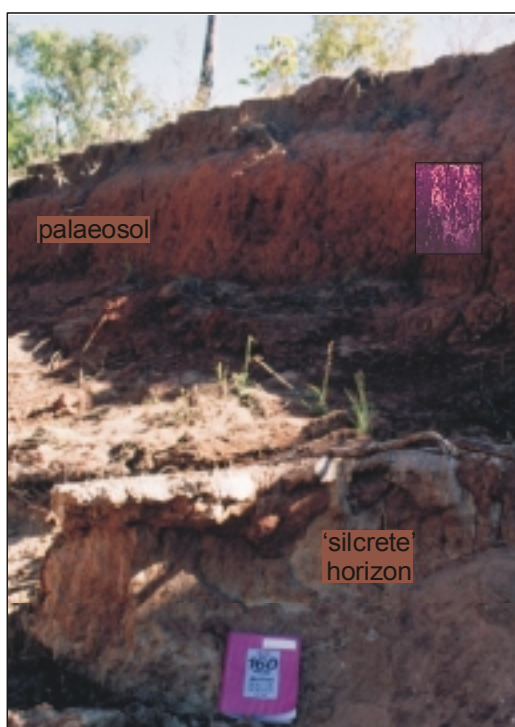


Figure 5.11 An indurated silicate horizon situated adjacent to the main creek bank profile at Sandy Creek Gorge (refer text for further description).

5.3.2 Sediment Micromorphology

5.3.2.1 Bedrock

The sampled bedrock from the escarpments overlooking Jinmium, Goorurarmum and Karlinga generally comprises medium-grained quartz sandstone cemented with clay, and stained by limonite (Fig. 5.12a – f). Evidence of pressure-solution is evident from the interlocking of grains and occasional quartz overgrowths. Porosity is generally less than 10%.

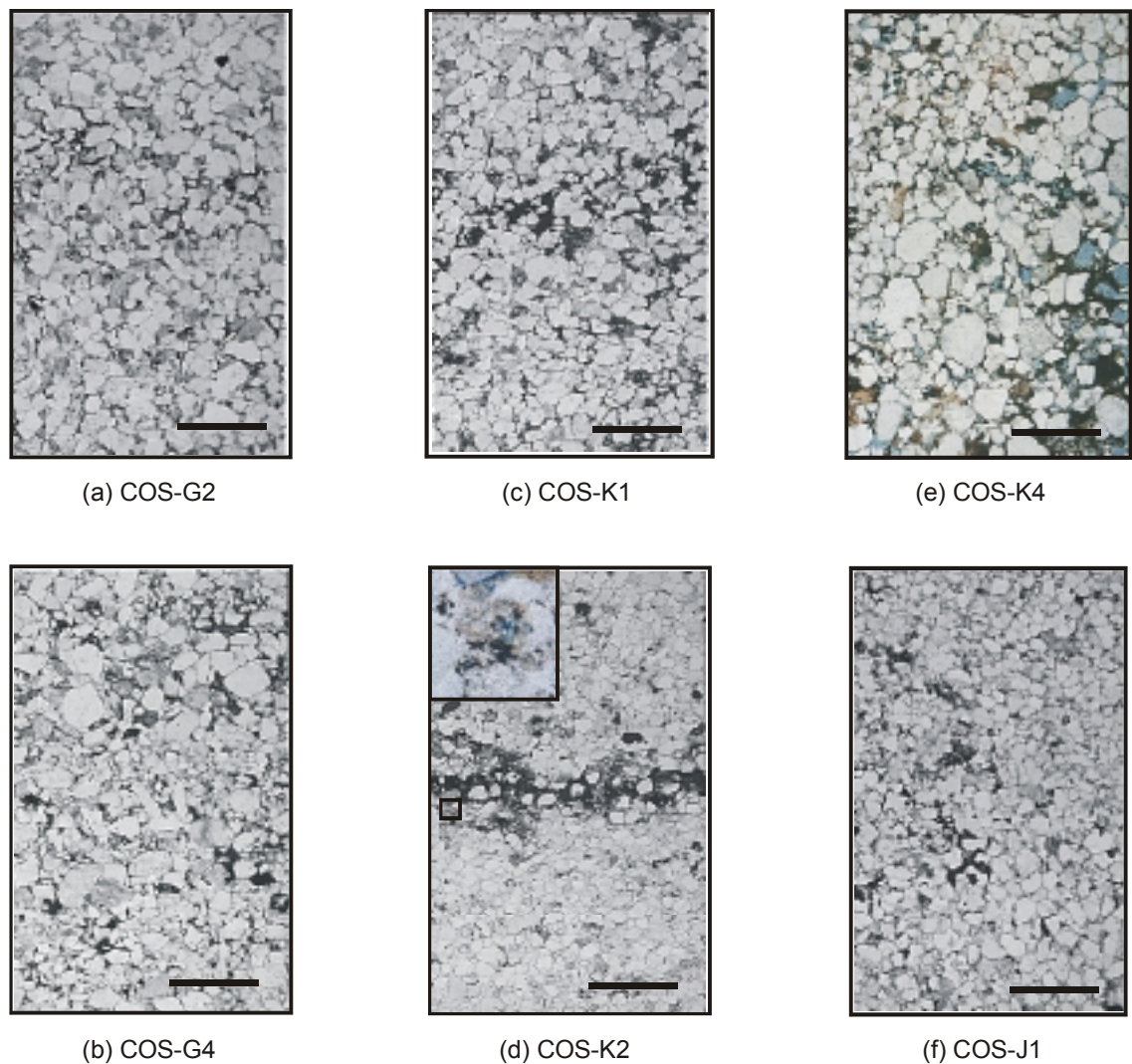


Figure 5.12a – f Thin section of escarpment bedrock sampled from (a and b) Goorurarmum, (c - e) Karlinga and (f) Jinmium (scale bar = 250 μ m).

Moderately-sorted, sub-rounded to sub-angular quartz grains range from 0.2 - 0.4 mm in diameter. Monocrystalline, non-undulose quartz is dominant, with lesser amounts (< 10 %) of polycrystalline quartz and vein quartz (possibly from conglomerates). Thin banding evident in hand specimens is comprised either of alternating fine and medium grained laminae and/or high concentrations of heavy minerals, mainly iron oxides (e.g. Fig. 5.12). Minor amounts of lithics include tourmaline, chlorite, zircon, sphene and epidote.

5.3.2.2 Sand Sheets

Sediments from the Goorurarmum excavation comprise medium to fine, sub-rounded, moderately-sorted quartz. Thin section reveals the quartz comprises both monocrystalline and larger clasts of polycrystalline quartz (Fig. 5.13). Iron-staining generally occurs around the boundaries of the quartz grains, and also as overgrowths in some quartz grains. Although minimal, there is indication of an increase in the fine clays with depth, and illuviation of clays in the voids and around quartz grains. Porosity is about 40 %, and there is no obvious evidence of compaction or bedding. Apart from the much greater porosity and an absence of lithics, the sediments are very similar to the bedrock sampled in this area.

Sediments from the Karlinga excavation are obviously coarser in thin section than those from Goorurarmum, but are of a similar composition and porosity. Compared to the bedrock samples from this area, the sediments from this locality showed the greatest similarity with the escarpment bedrock directly north of the site (COS-K4), rather than with bedrock overlooking the main Karlinga site (COS-K1 and K2). The strong dark red colour in matrix exemplified in the buried sediments at Karlinga (Fig. 5.14), show the incorporation of iron oxides with clay in these horizons. This may indicate the process of rubefaction (reddening).

Goorurarmum
Excavation No. 2

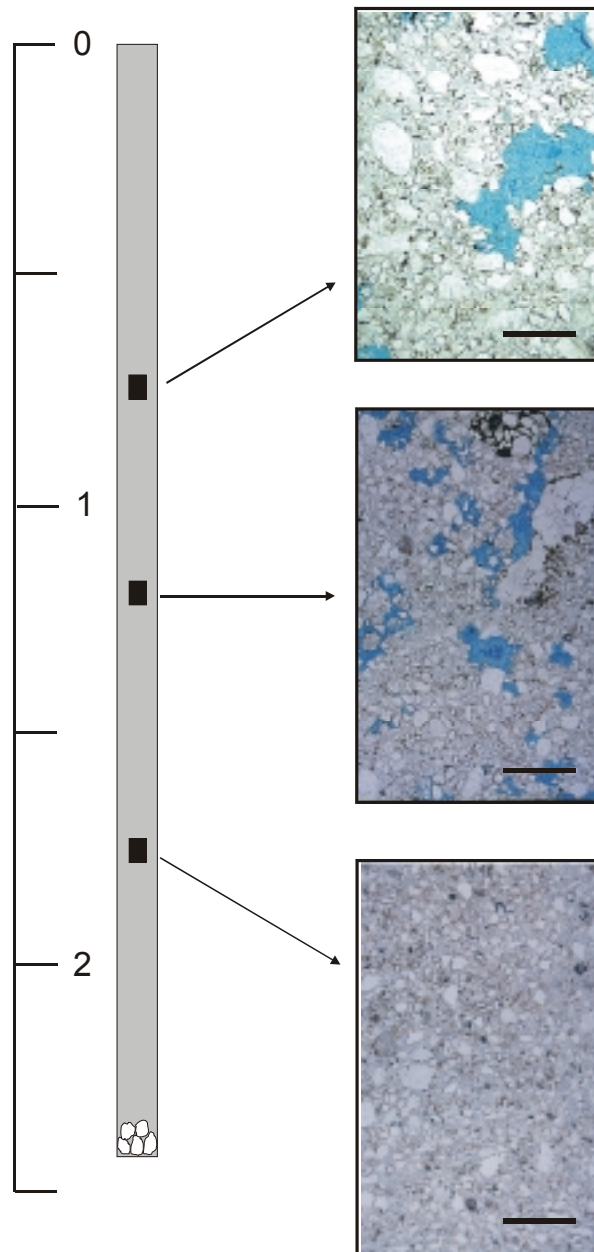


Figure 5.13 Thin section of Goorurarmum (Goor-1) sand sheet sediments, taken at 75 cm, 120 cm, and 175 cm respectively (scale bar = 100 μm).

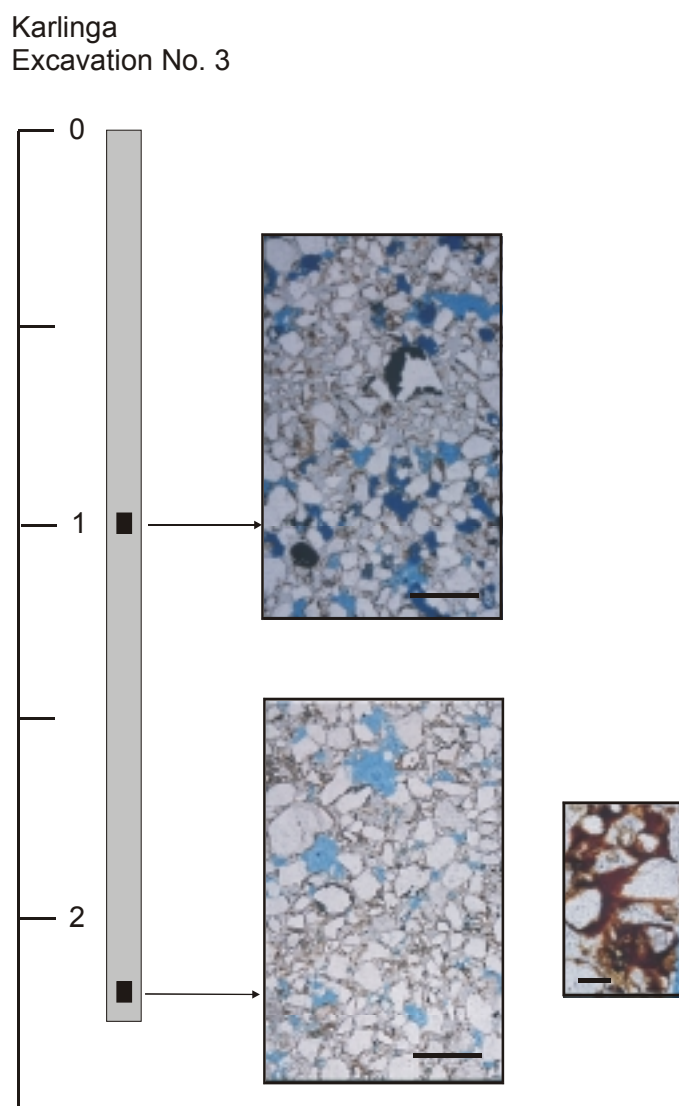


Figure 5.14 Thin section of the Karlinga (Karl-3) sand sheet sediments, taken at 100 cm and 240 cm respectively (scale bar = 100 μ m). Inset shows limonite staining in sediment matrix, which may indicate the process of rubefaction (reddening).

SEM analyses of sand sheet sediments

SEM/EDRXA analyses also indicate that Fe_2O_3 , present as iron oxides and oxyhydroxides (limonite), is intimately mixed with Al_2O_3 as phyllosilicate clay minerals. Together these are present as grain cutans, infilling grain fractures, diffuse impregnations of the groundmass, and on the walls of root channels. The composition of the clay minerals is kaolinite and illite,

determined from presence of Al_2O_3 , SiO_2 and K_2O in EDRXA traces and bulk XRD analyses. The cutans are not present in surface sands appear to form post-depositionally (Fig. 5.15).

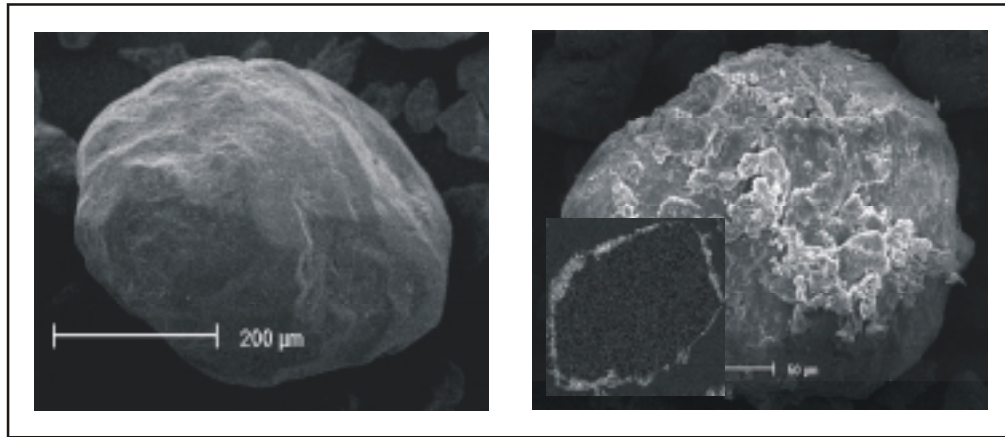


Figure 5.15 Post depositional formation of iron-clay cutans as evidenced from the contrasting images of quartz grains (a) before burial, and (b) after burial. Inset of (b) shows a cross-section of a quartz grain highlighting the Fe_2O_3 - and Al_2O_3 - rich cutan.

With continued burial, some of the quartz grains show increasing evidence of deterioration (Fig. 5.16). There is little or no presence of pitting or etching that would be indicative of aeolian weathering. Rather features such as grain angularity and adhering particles are more typical of *in situ* weathering. The few etched grains observed indicate some sediment populations probably derive from dissolution of bedrock material, and have subsequently acquired iron-enriched clay cutans through burial diagenesis.

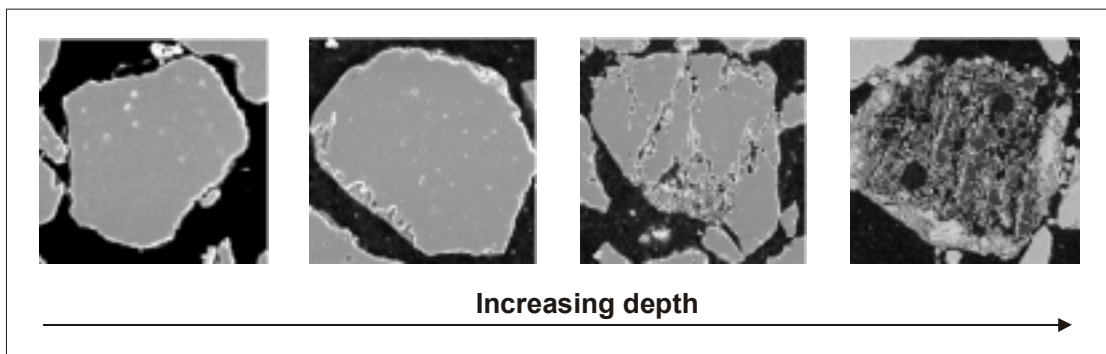


Figure 5.16 General observation of deterioration of quartz grains from with depth in sand sheet profiles.

Fig. 5.17 shows examples of the more angular grains that are present within some of the sands from the various rock-shelter and sand sheet excavations. No clear evidence of fracturing was discernable on these grains to clearly distinguish them as possible flaked material (microliths) amongst the general population of moderate to poorly sorted sands in the sand sheets throughout the Keep River region. However, a more thorough study distinguishing such microlithic flakes is presently being undertaken by George Susino (in prep.). The presence of cutans on these angular grains indicates that they have probably undergone a similar period of burial as other grains with which they are associated.

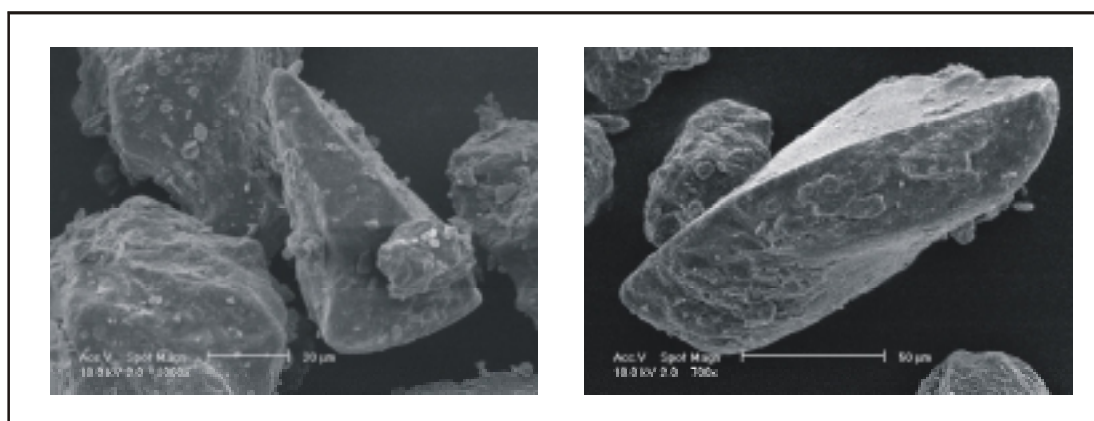


Figure 5.17 Example of shard-like grains sampled from the Karlinga (Karl-3) and Goorurarmum (Goor-1) excavations.

SEM analyses of pisolites

The iron-rich concretions observed at the base of one site near Jinmium (JG4) and at Sandy Creek Gorge consist of goethite, quartz and kaolinite. In thin section, the pisolites at the Jinmium site (Fig. 5.18) are homogeneous. In contrast, the pisolites from Sandy Creek Gorge (Fig. 5.19) comprise up to 15 bands of iron-rich material that probably reflect periodic change in physicochemical conditions during formation. The unrounded shape and poorly sorted matrix of the pisolites at Sandy Creek Gorge indicate they are probably *in situ*.

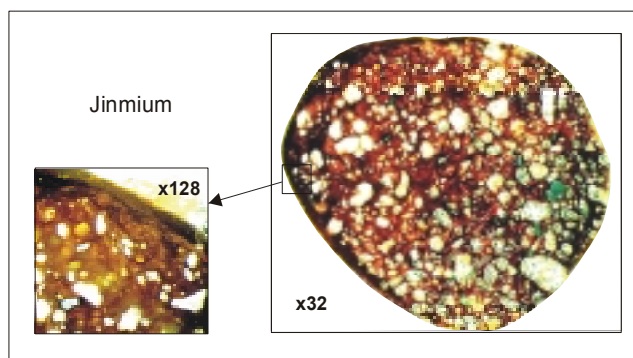


Figure 5.18 Cross section of pisolitic material taken from the base of the profile (450 cm) of auger JG4, near Jinmium. The sample has a thin crust and a matrix of poorly sorted quartz and clay.

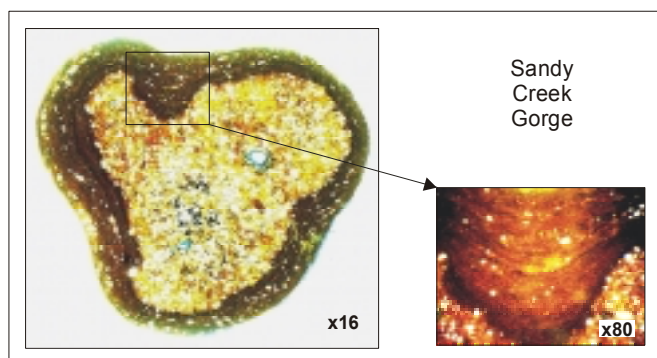


Figure 5.19 Cross section of pisolitic material taken from the base of the profile (540 cm) of Sandy Creek Gorge. The sample has a thick crust, and a matrix of poorly sorted quartz and clay minerals.

5.3.2.3 Creeks

Impregnated samples were not taken from the main profile of Sandy Creek Gorge, but a thin section was made of the adjacent indurated horizon (Fig. 5.20). Thin section reveals very fine grained, iron-stained quartz surrounding larger degraded clasts, comprised of lithics including iron oxides, chlorite and zircon (Fig. 5.20). Despite extensive investigation, the nearest identification was with what has been termed ‘creek rock’ in parts of North Queensland (Bob Henderson, pers. comm., 2001).

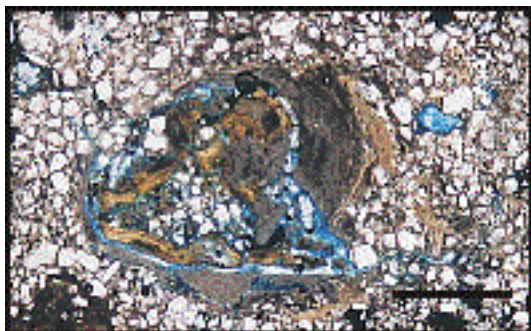


Figure 5.20 Magnification (x 50) of indurated silicate material adjacent to Sandy Creek Gorge profile, showing the fine grained, iron-stained quartz surrounding larger degraded opaline-like clasts (scale bar = 100 μ m).

Sediments from the KR99 creek section reveal an increase in lithics, and degree of sorting, and a slight decrease ($\sim 10\%$) in porosity down the profile. The sediments generally consist of medium to coarse, sub-rounded, moderate to poorly sorted mono-crystalline quartz; the coarse clasts generally comprising polycrystalline quartz with occasional inclusions. The obvious change in colour in the field section at about 3 m depth is also obvious in thin section where there is a distinct increase in iron staining around the quartz (Fig. 5.21).

KR99
Creek Section

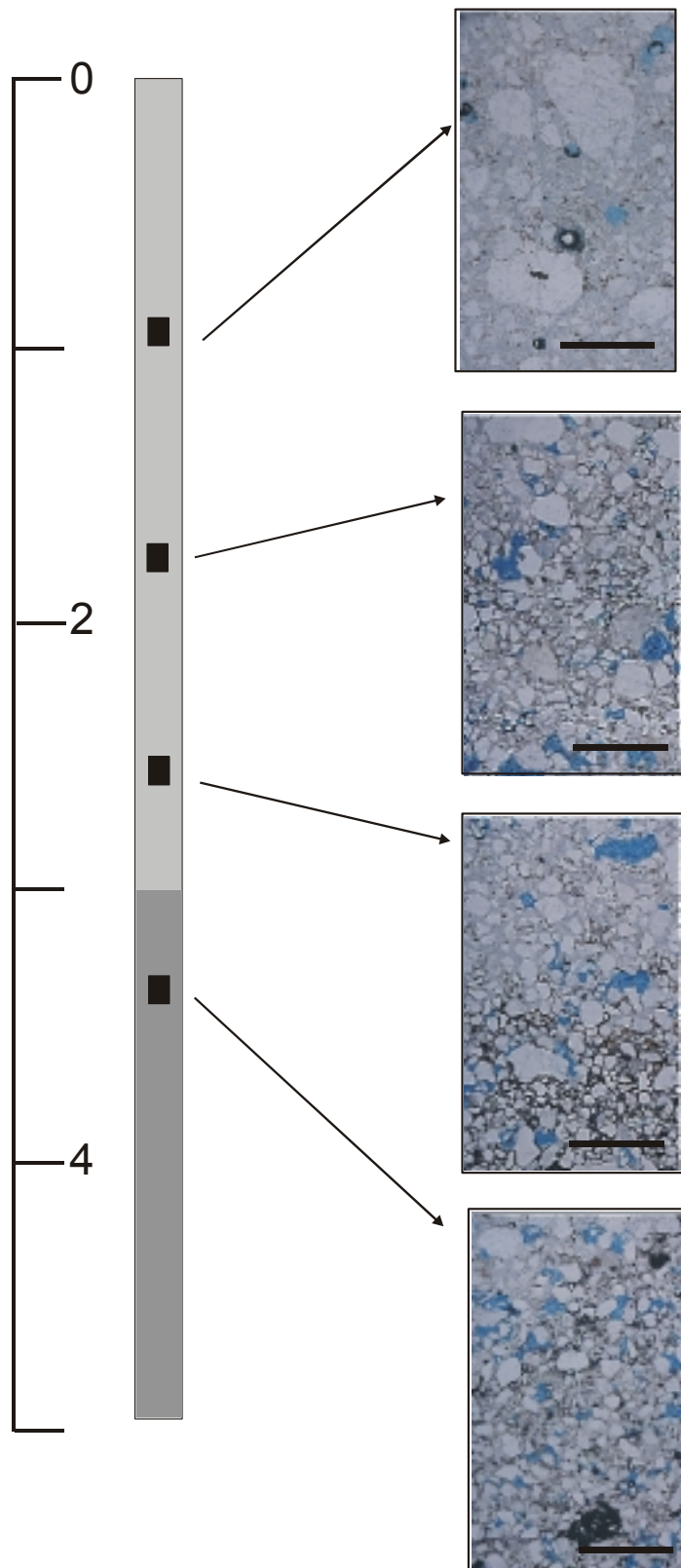


Figure 5.21 Thin section of KR99CP sediments, taken at 95 cm, 180 cm, 255 cm and 340 cm respectively (scale bar = 100 µm).

5.3.3 Sediment Geochemistry

Mineralogical analyses indicate the sand sheet sediments are dominated by quartz, with lesser amounts of kaolinite and minor accessory minerals. The mineralogy of sediments elsewhere in the Keep River region is similar, with the addition of micaceous (muscovite) and hydrated clay minerals (illite, smectite, montmorillonite) in the cracking clay soils. The average bedrock and sediment geochemistry is given in Table 5.1. Statistical analyses are given in Appendix A3.5.3.

5.3.3.1 Bedrock and Rubble Geochemistry

The dominance of quartz in all the bedrock samples is indicated by the high percentage of SiO_2 (95 wt. %), with minor amounts of clay and organics indicated by low concentration of Al_2O_3 (2.0 wt. %), and LOI (1.5 wt. %). The greatest geochemical variation is shown in the relative percent of Fe_2O_3 (0.08 to 1.6 wt. %), with the higher concentrations reflecting the redness of the bedrock sample. The overall geochemistry of the rubble samples is more like that of the sand sheet sediments than the escarpment bedrock samples, although the degree of difference between the bedrock and all other sediment samples is not significant except perhaps at Jinmium. At this site the bedrock geochemistry is distinguished by higher relative concentrations of SiO_2 , Al_2O_3 , Fe_2O_3 and P_2O_5 (refer Appendix 3.5.3). The similar sediment mineralogy and geochemistry of the escarpment bedrock and sand sheet samples supports the microscopic evidence that the sediments have not undergone any significant transport.

Table 5.1 Summary (mean and standard deviation, SD) of sediment geochemistry for each location, and for all combined sediment samples compared to bedrock (in bold). Results indicate the very similar geochemistry of all samples.

		SiO ₂	TiO ₂	Al ₂ O ₃	Fe ₂ O ₃	MgO	CaO	Na ₂ O	K ₂ O	P ₂ O ₅	LOI
Jinmium C1/III	Mean	93.67	0.17	2.83	0.85	0.18	0.13	0.55	0.18	0.06	1.72
rock-shelter	SD	2.74	0.08	1.63	0.31	0.02	0.13	0.39	0.11	0.02	0.78
Jinmium A5	Mean	87.87	0.30	5.79	1.69	0.11	0.05	0.08	0.18	0.03	3.61
sand sheet	SD	5.21	0.12	2.89	0.69	0.02	0.01	0.02	0.06	0.01	1.74
Jinmium-	Mean	93.50	0.18	3.16	0.98	0.15	0.06	0.44	0.17	0.02	1.68
Goorurarmum	SD	2.47	0.02	1.14	0.49	0.00	0.01	0.14	0.06	0.00	0.58
Goor-1	Mean	94.75	0.12	1.59	1.04		0.09		0.11	0.06	1.91
sand sheet	SD	2.90	0.02	0.82	0.66		0.04		0.02	0.04	1.41
Goor-2	Mean	88.25	0.11	2.04	1.19	0.15	0.72	0.14	0.18	0.25	6.77
rock-shelter	SD	1.60	0.02	0.72	0.12	0.05	0.36	0.14	0.05	0.09	1.51
Karl-1	Mean	91.34	0.15	1.80	0.91	0.13	0.17	0.19	0.18	0.08	4.66
rock-shelter	SD	1.05	0.04	0.42	0.15	0.04	0.08	0.15	0.04	0.02	1.14
Karl-3	Mean	92.42	0.21	2.59	0.91	0.14	0.16	0.26	0.14	0.04	3.07
sand sheet	SD	2.39	0.02	0.29	0.15	0.01	0.16		0.02	0.01	2.22
Karlinga	Mean	93.83	0.23	2.27	0.78		0.05		0.12	0.04	2.31
sand sheet	SD	0.99	0.05	0.31	0.19		0.01		0.02	0.02	0.91
KR99CP	Mean	95.48	0.14	1.73	0.21		0.11	0.32	0.11	0.03	1.98
	SD	2.41	0.05	0.54	0.21		0.10		0.02	0.02	1.67
Sandy Creek	Mean	93.84	0.34	2.62	1.00	0.14	0.07	0.36	0.70	0.02	0.98
	SD	0.79	0.03	0.13	0.19	0.01	0.01		0.02	0.00	0.06
Sandy Creek	Mean	86.16	0.63	6.11	2.20	0.29	0.10	0.44	1.35	0.03	2.98
Gorge	SD	4.51	0.14	1.95	0.88	0.09	0.03	0.16	0.34	0.01	1.52
Sediment	Mean	91.60	0.22	3.01	1.58	0.16	0.13	0.29	0.27	0.06	2.71
	SD	6.13	0.15	2.14	3.58	0.07	0.19	0.21	0.33	0.06	1.91
Bedrock	Mean	95.21	0.10	2.12	0.69		0.06	0.39	0.11	0.07	1.46
	SD	1.21	0.04	0.62	0.54		0.02	0.09	0.02	0.05	0.34

5.3.3.2 Rock-shelter Geochemistry

There is no significant difference in grain size between the rock shelters and the adjacent sand sheets, except at Karlinga where the rock-shelter ($\sim 260 \mu\text{m}$) sediments are finer grained than the adjacent sand sheet ($\sim 360 \mu\text{m}$). This is marginally reflected in the higher relative concentration of SiO_2 and lower relative concentration of Al_2O_3 in the sand sheet sediments.

Within the three rock shelters of Jinmium (CI/III), Goorurarmum (Goor-2) and Karlinga (Karl-1), the relative concentrations of P_2O_5 and LOI are significantly higher than the adjacent sand sheets (Table 5.1). However, the correlation between P_2O_5 and LOI is not significant, possibly indicating the presence of P_2O_5 with both organic and inorganic components. Organic phosphatic additions could be derived from either human or animal activity. The Goor-2 rock-shelter sediments are also distinguished by lower relative concentrations of SiO_2 and higher concentrations of CaO . The high CaO content is probably sourced from gypsum salts (refer Fig. 5.23). The Jinmium rock shelter has lower relative concentrations of Al_2O_3 and Fe_2O_3 than the adjacent sand sheets, possibly reflecting low clay content. There is no correlation of any of these distinguishing elements (SiO_2 , Al_2O_3 , CaO , P_2O_5 , and LOI) with artefact distribution in any of the shelters, but this may partly be an effect of the low number of geochemical analyses compared to artefact analyses.

5.3.3.3 Sand sheet Geochemistry

The three main modal sizes in the sand sheet sediments are coarse sands ($250 - 500 \mu\text{m}$), medium-fine sand ($125 - 180 \mu\text{m}$) and clay ($< 10 \mu\text{m}$). Depth profiles of the sediment grain size and geochemistry in the sand sheets and rock shelters (Appendix Figs. 3.7 – 3.10) show that, in general, the mean modal size follows the trend of SiO_2 (as quartz), and the $< 60 \mu\text{m}$ fraction and more especially the $< 10 \mu\text{m}$ fraction follows the trend of Al_2O_3 , K_2O and Fe_2O_3 (as oxyhydroxides), and the organic (LOI) content generally mirrors that of SiO_2 .

Mineralogical analyses indicate the sand sheet sediments are dominated by quartz, with lesser amounts of kaolinite and minor accessory minerals. Statistical analyses indicate that there is a much greater difference between the four sites of Goorurarmum, Jinmium, Karlinga and Sandy Creek Gorge than there is within the sites. This difference is manifest in the difference in grain size (Appendix 3.4.3) and to a lesser extent in the geochemistry (Appendix 3.5.3). The sediments around Karlinga are generally coarser and the relative concentration of SiO_2 higher, whilst the sediments surrounding Jinmium are distinguished by slightly higher relative concentrations of Al_2O_3 and Fe_2O_3 , and those at Goorurarmum by higher relative concentrations of CaO , P_2O_5 , and to a minor extent organic (LOI) content.

Iron minerals, evident from the red and yellow colour of many of the sediments, generally occur below the level of detection by XRD (2 %), thus no mineralogical distinction could be made between the mottles and sediment matrix. The exception is in the deep red sands between Jinmium and Goorurarmum where relative percentages of hematite and goethite are above 5 %. The positive association of Fe_2O_3 with Al_2O_3 ($r = 0.77$) and K_2O ($r = 0.53$) indicates iron oxide and oxyhydroxide minerals are closely associated with clay minerals, and confirms microscopic observations of illuviation of clays in the voids and around quartz grains. In general, shallow yellow sediments (< 2 m) are observed at lower depositional levels whereas deep red sediments were measured to the limit of the auger depth (6 m), and are observed at slightly higher relative levels.

5.3.3.4 Creek Geochemistry

The sediments at Sandy Creek Gorge have a significantly higher relative concentration of Al_2O_3 and K_2O and smaller grain size. The relative enrichment of potassium in the Sandy Creek sediments reflects the preferential removal of other cations and silica, and illitisation of sediments, and is clearly shown in a triplot of Al_2O_3 - $\text{Na}_2\text{O}+\text{CaO}$ - K_2O (Fig. 5.22). This trend is typical of many clayey palaeosols that are predominantly illitic in composition, and which contain large root traces of the kind formed under forests (Retallack, 1990). A depth profile of grain size and geochemistry at Sandy Creek Gorge (Fig. 5.10) indicates at least three horizons, distinguished by the marked change in SiO_2 and Al_2O_3 , with the SiO_2 -enriched middle horizon corresponding to the coarse sandy horizon observed in the field at about 3 m depth.

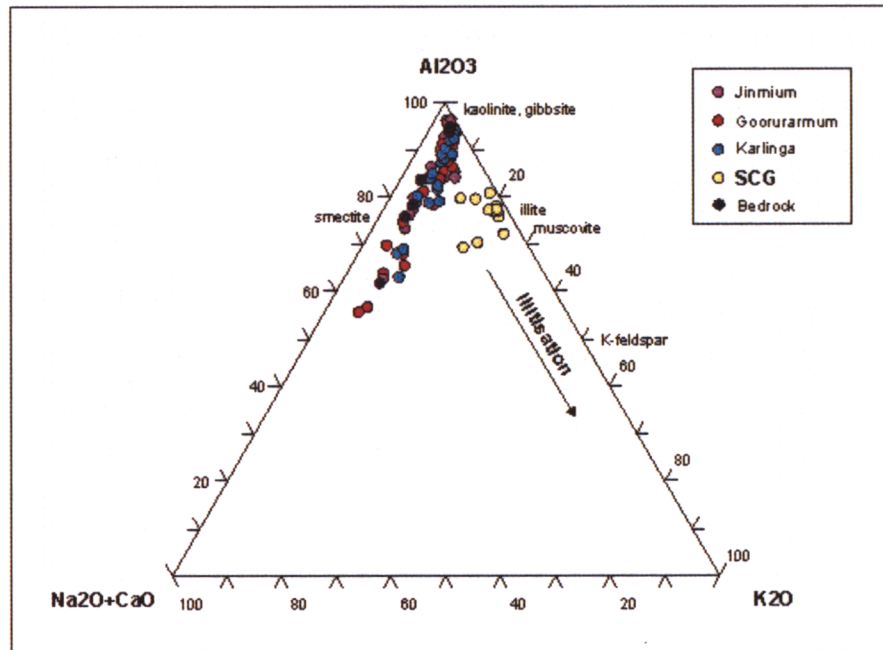


Figure 5.22 Triplot of major elements Al_2O_3 - $\text{Na}_2\text{O}+\text{CaO}$ - K_2O for each of the four major sites and bedrock samples indicating obvious discrimination of the Sandy Creek Gorge sediments on the basis of high relative K_2O concentration. The enrichment of K_2O reflects the process of illitisation and is typical of clayey palaeosols (Retallack, 1990).

5.4 Discussion

The following discussion considers how the characteristics of sandy deposits in the Keep River region reflect source and transport processes, depositional environment, and post-depositional processes, and how these may have influenced the formation and preservation of archaeological deposits.

5.4.1 Depositional Processes – Source and Transport Processes

In the Arnhem Land plateau, Roberts (1991) argued that although the geological rate of weathering and erosion has been constant over the Quaternary period, fluctuations in hydrological activity have changed the dominance of particular sediment sources. In the Keep River region, not only has the rate of escarpment denudation been relatively constant (Chapter Four), but petrographic evidence indicates that the source and sedimentary processes have not significantly altered during the period of sand sheet formation in any of the site catchments of Jinmium, Goorurarmum, and Karlinga. However, the rate of depositional processes may have been more erratic.

The distribution and mixing of the three modal sizes namely coarse sand ($\sim 360 \mu\text{m}$), med-fine sand ($\sim 180 \mu\text{m}$) and clay ($< 10 \mu\text{m}$), reflects the influence of the escarpments and rivers as sources and/or as agents of sedimentary processes. Nearer the escarpments, the dominantly unimodal (Fig. 5.23), moderately sorted and sub-rounded quartz sediments reflect a single major source and/or local transport process. Towards the major rivers and creeks the sediments are multi-modal (Fig. 5.23) and well-rounded reflecting the contribution and transport of material from more than one source, although these sources have not changed through time. Essentially the depositional environment becomes less endogenous with increasing distance from the escarpments.

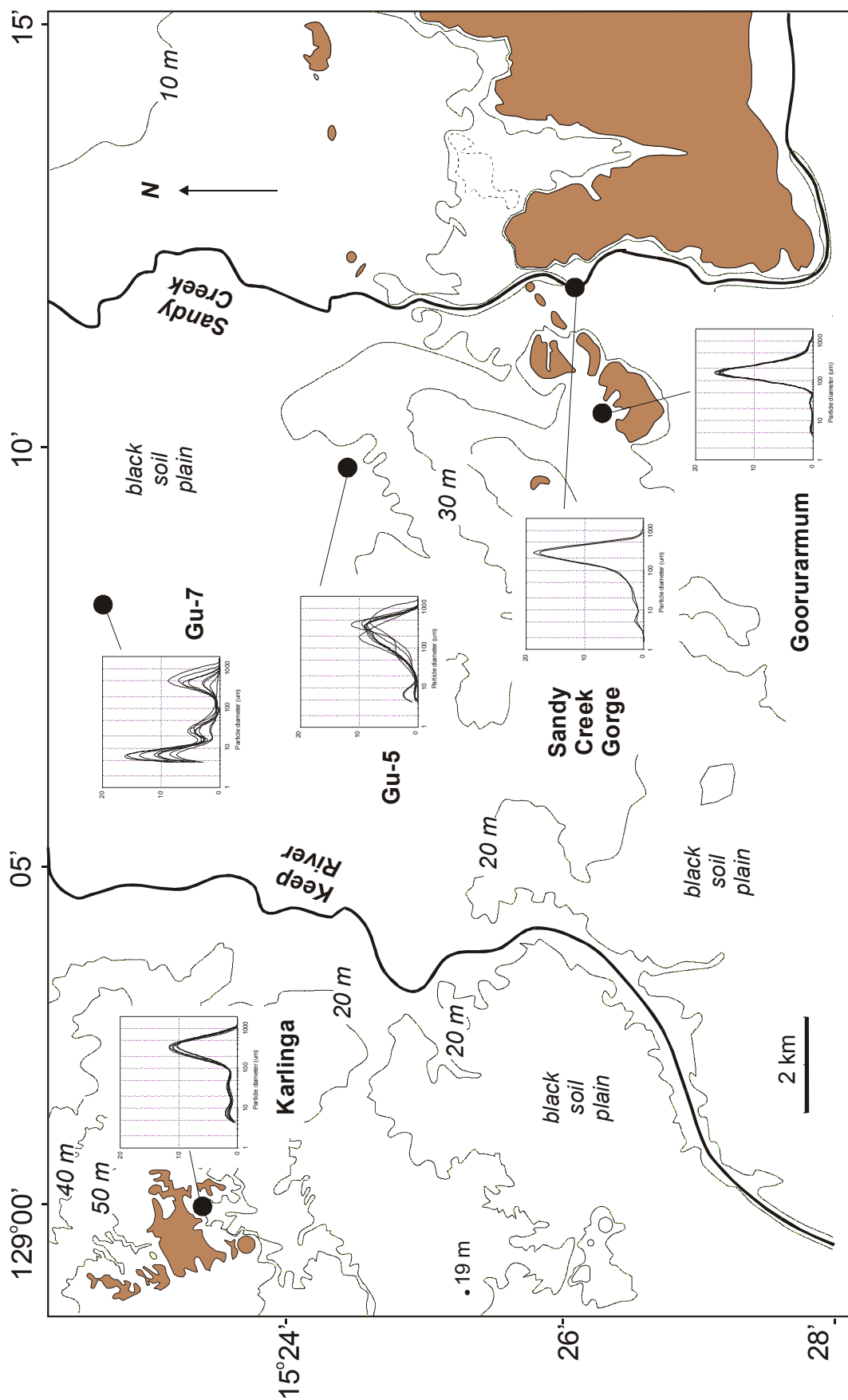


Figure 5.23 Grain size map, indicating typical grain size distribution for the different depositional sand sheet and mud flat environments.

Walsh (2000: 384) observes that sediment populations of 360 μm , 250 μm and 60-70 μm are observed in other parts of north-east Kimberley, and argues that all three modes are indicative of widespread aridity. It is questionable whether grain size can be used as a proxy for climate. In any case, the similarity of the 360 μm and 250 μm modes in the Keep River region most likely reflects a common type of sandstone source as exists throughout the rest of the Kimberley region. The 60 - 70 μm fraction noted elsewhere in the north-east Kimberley apparently represents aeolian dust (McTainsh, 1989), derived from the Quaternary Dust Path which originated in Central Australia and passed off the Kimberley coast into the Indian Ocean (Bowler, 1976). The virtual absence of the 60 - 70 μm mode within the Keep River sand sheets might indicate that this region lies outside this dust path. More likely, the absence of this mode reflects a similar absence in the local sandstone source and/or selective reworking and transport of silt from the sand sheets in the upper catchments onto the black soil plains via river systems. It is possible that ants and termites are also a contributor to selective reworking as some species prefer silt and clay size material to sand when re-arranging soil particles (Lobry de Brun and Conacher, 1990). The mud in the estuaries that form the black soil plains is derived from the shelf as a result of the high energy tidal range that operates in northern Australia (Woodroffe et al., 1989; Chappell and Woodroffe, 1997).

The moderately poor sorting observed in each of the sand sheet sediments probably reflects the degree of sorting in the bedrock source more than any particular transport process. As found previously (Aldrick and Moody, 1977), the similar petrology and geochemistry of the sand sheet and bedrock sediments limits determination of a specific source at any particular site. Rather the similar geochemistry of the bedrock and sediment samples supports microscopic observations that the sand sheet sediments are locally derived and have not undergone significant transport. Coarser sands may be concentrated in small creeks and fans debouching onto the sand sheets due to lower competence of flow. The unconsolidated sands are closely packed, and the absence of well sorted, layered deposits and poor differentiation along slope indicates the sand sheet sediments are most likely transported mainly by sheet flow rather than by major flood events (Courty et al., 1989, Coventry et al., 1988). The surface of the sand

sheets are protected by a lag, a few grains thick, of the coarsest particles that can be easily shifted by wind or water.

High water tables, seasonal saturation and/or bioturbation may further inhibit the formation or preservation of any obvious lamination in any of the sand sheet sediments. There is evidence from root and burrow traces that some mechanical disturbance does occur in the uppermost sediments, but ferruginisation of these remnant traces indicates this disturbance is essentially limited to the upper metre. Consideration of biogenic processes on archaeological site formation is given in Chapter Seven (see also Ward and Larcombe, in press).

5.4.2 Environment of Deposition (Site Formation)

Typically, the sand sheet and rock-shelter stratigraphy comprise loose charcoal-enriched surface sands, overlying slightly more compact sands, which themselves overlie rubble and/or a bedrock base. The Jinmium archaeological deposit, according to Roberts (pers. comm., 2002), is constrained in a ‘basin’ of crumbling saprolite. However, the distinction needs to be made between saprolite as *in situ* decomposed bedrock and *incorporated* bedrock material that is broken down within a sedimentary profile. It is not possible from the close geochemical similarity of bedrock and loose sand to positively distinguish saprolite or buried rubble in the sand sheets. However, the observed exfoliation of modern surfaces (Fig. 5.24) indicates that much of the rubble in the Jinmium deposit, including the ‘sandstone pavement’ depicted in Fullagar et al. (1996), probably derives from previously exfoliated material rather than underlying saprolite (see also Bednarik, 2002: 1215). Robbins et al. (2000: 1090) describe a similar scenario of rock breakdown and burial in the White Paintings rock shelter, in the northwest Kalahari Desert, during a period of increased moisture and rock breakdown at the shelter.

The precipitation of gypsum ($\text{CaSO}_4 \cdot 2\text{H}_2\text{O}$), particularly within and around the rock shelters, is seen to increase the breakdown of sandstone (Fig. 5.25) and exacerbate the exfoliation of rock-art. This is supported by the higher concentration of CaO in the rock-shelter sediments. Thin sections of the escarpment bedrock confirm the breakdown of the escarpment sandstone through the removal of intergranular cement, as described by Young and Young (1992).



Figure 5.24 Throughout the Keep River region, large slabs of bedrock can be observed in the process of mass exfoliation; this example has a petroglyph on the surface. The frequency of mass exfoliation of these sandstone surfaces may provide some indication of the age of the engraving.



Figure 5.25 Salt (gypsum) weathering within the Goorurarmum (Goor-2) rock shelter effecting mass exfoliation and disintegration of the shelter walls.

5.4.3 Post-Depositional (Diagenetic) Processes

5.4.3.1 Sediment Colour

Sandy sediments across northern Australia often appear homogenous, with the only changes in the form of colour (e.g. Jones and Johnson, 1985; Allen and Barton, 1989; O'Connor, 1999). Dark hues may partly result from organic matter. Pigmentation of sediments (or lack thereof) is often due to the nature of iron oxide and hydroxide minerals, and may be characteristic of the sedimentary environment (Table 5.2). The red and yellow sediments observed in the Keep River region (Fig. 5.24) are common throughout northern Australia (Coventry and Williams, 1984), and result from different degrees of leaching and deposition of iron and silica. A strong relationship may develop between morphological features of the soils (including mottling, gleying, and clay content) and the depth and duration of profile saturation (Coventry and Williams, 1984).

Good drainage and aeration of the sand sheet sediments at higher relative levels and lower water table levels is evident from the hematite-rich deep red (10R 4/6 or 2.5 YR 3/6) and reddish brown (7.5YR 5/4) colours found typically around Jinmium and Goorurarmum. At lower relative levels and higher water tables such as typically found around the Karlinga area, the poor drainage results in reduction and leaching of iron minerals to give the goethite-rich yellow (7.5YR 6/8) and orange-yellow (5YR 4/6) colours (Table 5.2). Although hematite may be less abundant than goethite, it is in fact the hematite content that usually determines the redness of a soil (Schwertmann, 1993).

Table 5.2 Pigmentation of sediments is due mainly to the nature and grain size of iron oxide and hydroxide minerals, and may provide information on the pedoenvironment (from Schwertmann, 1993: 54).

Iron oxide, Formula, Colour	Pedoenvironments	Soils
Goethite FeOOH 10YR - 2.5Y	Wherever weathering takes place	All soils with Fe release
Hematite Fe_2O_3 10R - 5YR	High soil temperature, low water activity, rapid biomass turnover, high Fe-release rate from rocks	Aerobic soils of the tropics and sub-tropics with dry seasons(?)
Lepidocrocite Fe-OOH 5YR - 7.5YR Value > 6	Anaerobic/aerobic systems Noncalcareous	Aquic subgroups in temperate regions (pseudogleys)
Ferrihydrite $\text{Fe}_5\text{OH}_8.4\text{H}_2\text{O}$ 5YR - 7.5YR Value < 6	Rapid oxidation in humic environments	Gleys
Maghemite Fe_2O_3 2.5YR - 5YR	Usually a product of fires	Mainly tropical and subtropical soils

Care must be taken to show whether sediment reddening is inherited from the parent rock or has been acquired post-depositionally, particularly as it may influence the properties of the sediment for luminescence dating. Whilst field observations indicate that some degree of redness is retained through transportation, the comparison of 'fresh' and buried quartz grains at high magnification (Fig. 5.15) corroborates the post-depositional accretion of iron-rich clay coatings, and Roberts (1997: 862) corresponding evaluation of the Jinmium sediments. The association of iron with aluminosilicate minerals as fine clay coatings or within pore spaces indicates that clay coatings are a co-requisite for iron staining (Sullivan and Koppi, 1998). The deposition of clay itself is favoured by the weathering of ash (high in K) (Courty et al., 1989), which is abundant from the frequent bushfires in the Keep River region.

As previously indicated (refer 2.3.2), one of the concerns expressed in relation to the Jinmium site was that the TL ages of > 100 ka were not supported by the weathering colours of the sandy soils (Roberts et al., 1998a). Rubefaction reflects the *intensity* as much as the *duration* of such pedogenic development and, as such, is not useful as an indicator of soil development and proxy chronosequence. The timespan necessary to obtain a homogenous rubefied (red) layer is on the order of a few hundred to a few thousand years depending on the environment (Schwertmann, 1993). Interpretations based on hue of sediments may therefore only be useful for comparison of palaeosols with a common burial history (Retallack, 1997).

Correspondingly, the absence of post-depositional red staining of the sand in the Jinmium rock-shelter (C1) trench compared to that developed in the supposedly coeval sand aprons (Roberts, 1997: 863) is not necessarily evidence for any inconsistency in the luminescence ages. Rather the colour differences between the rock shelter and adjacent sand sheets might indicate slightly divergent post-depositional histories.



red sands



yellow sands
and pisolites

Figure 5.24 Examples of the coloured sands found throughout the Keep River region, including the red sands around Jinmium (JG-1) and yellow sands overlying a red pisolitic horizon around Karlinga (KN-7).

According to Fullagar et al. (1996), the sand sheet sediments surrounding the Jinmium rock shelter show a colour change from yellow-grey to a deep weathered red at about 60 cm depth. Red soils occurring in an area where only yellow-brown soils are presently forming can usually be recognised as palaeosols (Schwertmann, 1993), providing some credence to the 100 ky BP luminescence ages obtained from the base (~ 5 m) of this sand sheet profile. In contrast, the sediments within the Jinmium rock shelter show a high degree of mottling including yellow-grey (7.5YR 4/4), red-yellow (7.5YR 5/4), and light yellow-red sand (5YR 5/3) respectively in the horizons overlying the sandstone rubble base. This discolouration probably results from incomplete weathering and poor drainage of the rock-shelter rubble and sandy sediments, and may be complicated by the hydrophobic nature of the charcoal-enriched sandy sediments.

The hydrophobic character of charcoal-enriched sediments may be related to organic compounds (e.g. waxes) associated with organic material rather than the charcoal itself (Ross Coventry, pers. comm., 2002). Little is known about the fluid dynamics of hydrophobic sandy sediments, but water is probably concentrated along preferential pathways, such as root burrows at the sediment/bedrock/rubble interface, rather than through the sediment as a whole (Peter Ridd, pers. comm., 2002). Where water is concentrated for longer periods, it will not only enhance sandstone decomposition but may also result in greater attenuation of dose rates and potentially influence luminescence age determinations (e.g. Goldberg, 2002). The hydrodynamic and sedimentary environment, and luminescence dating thereof, is likely to be more predictable with increasing distance from the escarpments and rock-shelters.

5.4.3.2 Mottles and Concretions

The site of KR99CP is positioned at the head of a large creek, and it is possible that the creek previously drained into a small alluvial swamp. The mottled greyish, brownish and yellowish colours revealed by the creek sediments at Karlinga (KR99CP, Fig. 5.9) are indicative of the incomplete decay of organic matter that probably accumulated in waterlogged (swamp) conditions. The relatively abrupt change from dark (7.5 YR N2) to lighter (5YR 5/4 - 8/1)

coloured sands is certainly indicative of a long-standing water table. Whilst such waterlogging may have allowed the carbonaceous palaeosol to develop, periodic drying of the swamp sediments (possibly through seepage) may have minimized peat accumulation (Rapp and Hill, 1998: 35). Subsequent sand deposition probably filled out the swamp (refer 6.6.2.2 for chronology), reducing its extent to the present creek that runs alongside the cliff. Periods of alternating high energy and low sedimentation are indicated by short but successive intervals of coarse sands in the creek profile (Fig. 5.9). The fact that the stratified organic layers are preserved in the earlier creek sediments indicates that initial bioturbation may have been reduced at this site (possibly as a result of rapid sedimentation), and/or that bioturbation is presently concentrated in the upper metre.

The reddish-grey streaked (10YR 3/2 - 10R 7/1) or *pseudogley* horizons observed in the Sandy Creek Gorge profile also indicate that previous hydrological changes have allowed temporary waterlogging of these sediments and localised iron movement due to changing redox conditions (Courty et al., 1989). The sinuous root mottles which extend up to a metre deep, along with the presence of *in situ* ferric nodules and concretions, may indicate the former existence of a dry rainforest or vine thicket community that once existed along Sandy Creek (Fig. 5.25). If it were wooded grassland, as exists presently, the root mottles would be expected to be less than 2 mm in diameter and much shallower (Retallack, 1997). Palaeobotanical studies indicate that rainforest trees (Atchison, 2000) and vine thicket communities (Jon Luly, pers. comm., 2002) were more extensive in some parts of the Keep River region (see 7.1.2 for further discussion). Atchison (2000) also indicates that present monsoon rainforest patches are small and isolated on dolomite outcrops – although not all dolomite outcrops have monsoon rainforest. The indurated silicified horizon at Sandy Creek Gorge may therefore represent a degraded detrital dolomite outcrop upon which an isolated rainforest community once existed. Groundwater may have effected the process of dedolomitisation and replacement of carbonate by silica (Folk, 1968).

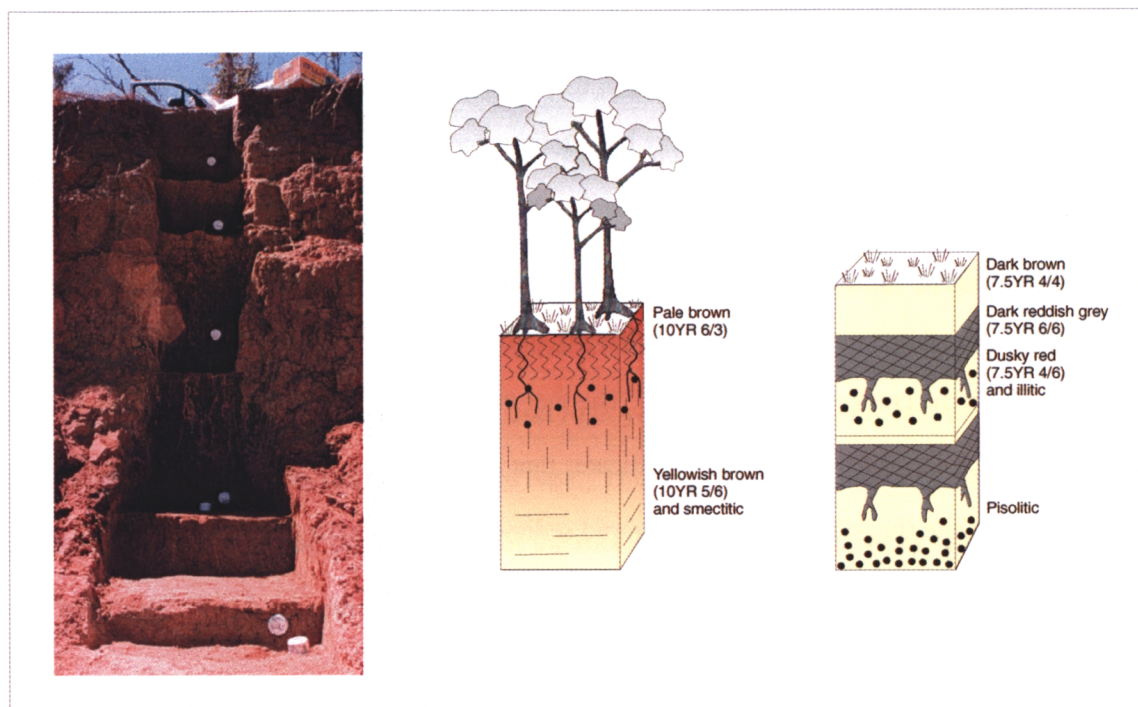


Figure 5.25 Hypothetical interpretation of the present sedimentary features observed at Sandy Creek Gorge. A soil horizon(s) formed (a) initially under an ancient rainforest or vine thicket community undergoes (b) post-depositional burial gley of organic matter, dehydration of ferric oxyhydroxides, compaction and illitisation of smectite clay (modified from Retallack, 1990).

The occurrence of sand sheets over laterite and ferruginous nodules is not unusual (Newsome, 2000) and, throughout the Keep River region, ferruginous mottles and pisoliths are found in association with red and yellow sands. Caution is however advised in the use of such concretions as palaeoenvironmental indicators (Young et al., 1987; Nanson et al., 1991), particularly as such ferruginous weathering may be ongoing in the present climate. Indeed, the apparent continuity between the pisolitic and overlying ferruginised deposits indicates that time rather than climate has had a greater effect on stratigraphic differentiation of sandy sediments in the Keep River region. The time factor is the subject of the following chapter.

5.5 Conclusions

The analyses of bedrock, rock shelter and sand sheet material indicates that *basic* sediment characterisation is not especially useful in differentiating depositional facies and processes, or distinguishing cultural and natural deposits in these unconsolidated sandy sediments. This essentially reflects the similarity of the quartz sandstone bedrock and quartz-rich sand sheets, and the fact that aboriginal people didn't significantly alter their environment. Thus despite earlier criticisms (refer 2.4.1), the stratigraphy of these sandy sediments may be better defined from the geochronology (Chapter Six).

Poorly-sorted, medium to coarse sand sheet sediments, are derived locally through mass wasting, salt weathering and granular disintegration of local escarpment bedrock. Post-depositional processes in the sand sheets include the loss or gain of organic matter, silicate clay minerals and iron oxides, changes in sediment colour, and the development of mottles or concretions. The pigmentation of the sediments reflects topographic and groundwater levels, rather than the degree of maturation or stratification of the sand sheet sediments. Palaeosol horizons in two creek profiles are distinguished by sediment mottling and illitisation, and potentially mark significant palaeoenvironmental and palaeoclimatic changes during the Quaternary (refer 6.6.2).

Microscopic analyses of rock-shelter and sand sheet sediments do not reveal any distinct anthropogenic signatures, such as laminated sediments, organic residues, or ash from fires. Attempts to obtain comparative micro-morphological (thin section) analyses of the charcoal-enriched rock shelter sediments were unsuccessful, due to their hydrophobic nature. The present work may, however, provide a useful foundation on which to do more detailed geological or archaeological studies related to specific field problems or site formation studies in the Keep River region.

CHAPTER SIX

Luminescence Dating and U-Series Dating of Sand Sheets and Archaeological Sites

If there is one issue on which nearly all archaeologists can agree, it is the importance of chronology. - Dean (1978): 223

6.1 Introduction

As previously outlined, the Keep River region was made known to the archaeological and public community through the controversy surrounding the luminescence dating of material from the excavations at the site of Jinmium. This chapter extends the luminescence dating in the Keep River region to other occupation deposits (rock-shelter sites and sand sheet sediments), and non-occupation deposits (creek bank profiles), and uses both thermoluminescence (TL) and optically stimulated luminescence (OSL) dating techniques. The luminescence ages are later combined with previous luminescence and radiocarbon ages (Chapter Seven) to provide a broad overview of the chronostratigraphy for this region, and an outline of some of the geomorphological processes which may occur within sandy sites, such as Jinmium.

6.2 Geoarchaeological Application of Luminescence Dating in the Keep River region

Luminescence dating techniques have found many applications in both archaeology (Roberts, 1997; Feathers, 1997a,b) and geomorphology (Duller, 1996; Stokes, 1999). Although mainly used as a dating tool, luminescence techniques are also being applied to specific studies of sedimentary processes, including bioturbation (Bateman et al., 2002), transport (Heimsath et al., 1999), and surface exposure dating (Habermann, et al., 2000). These applications illustrate how luminescence dating techniques may both provide chrononological context and understanding of geomorphological processes.

Dating of rock-shelter deposits may not be straightforward because sediments are commonly derived by various means and from various proveniences. These transported sediment grains may not have been adequately bleached at the time of deposition, and the complexity of the stratigraphy can further complicate dose rate determinations (Feathers, 1997b). In the Keep River region, there is not only major discrepancy within the apparent age of some of the archaeological deposits but also between the archaeological sequences and the rock art. The original stratigraphy of the rock-shelter excavations (C1/II and III) (Fig. 6.1), shows the juxtaposition of 2.3 ky BP and 50 ky BP horizons, which contrasts with the Holocene age of sediments in the adjacent sand sheet excavation (C1/IV) (Fig. 6.2). These initial estimates were contradicted by subsequent elemental carbon and OSL age estimates (COOR numbers in Fig. 6.1) on large and small aliquots and single grains of sand (Spooner, 1998, Roberts et al., 1998a), although the reliability of these elemental carbon results also is uncertain (John Head, pers. comm., 2002). If the entire deposit is of Holocene age, as Roberts et al. (1998a) and others (Galbraith et al., 1999; Watchman et al., 2000) propose, and if the deposits reflect the age of the rock art (refer 7.4.2), then either the extant regional rock art sequence is much younger than is widely accepted, or the Aboriginal production of cupules and old paintings has left no signature in the excavated deposit.

In any case, all agree that the true luminescence history of the site is complex. Regardless of the physics of luminescence dating techniques, further research is needed to refine relationships between the visible rock art and the sedimentary and cultural deposits, especially since both young and old chronologies depend on some degree of taphonomic disturbance of the archaeological sediments. Consequently, the focus of this study is on the depositional processes that form the rationale for luminescence techniques. Duplicate excavation samples however, do allow for some comparison and estimate of reproducibility between OSL and TL dating and the implications this has for the application of the two techniques in these sorts of environments.

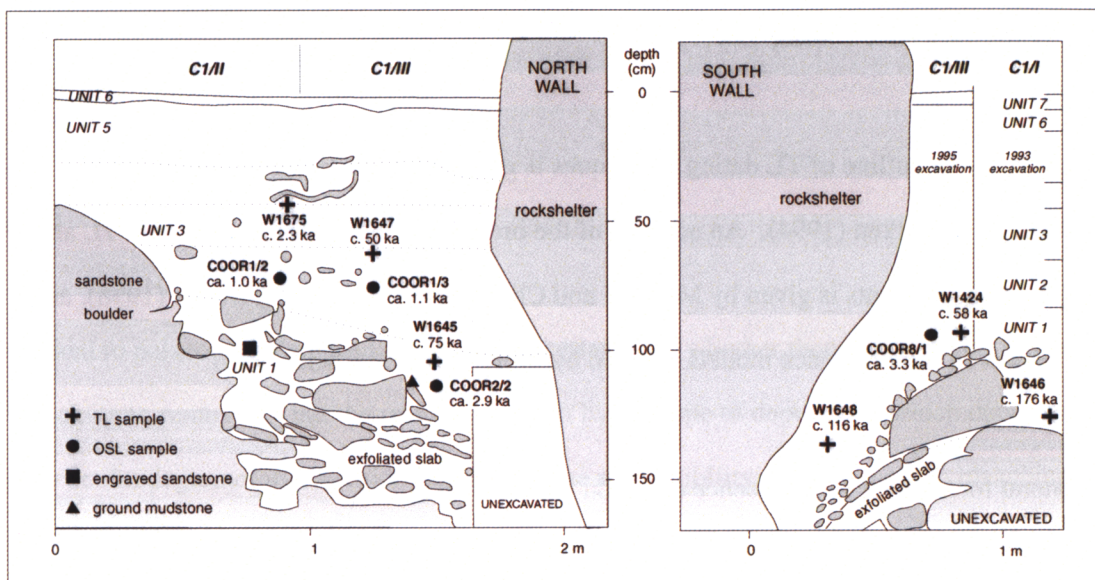


Figure 6.1 Stratigraphic sections of the north (C1/II and C1/III) and south (C1/III) faces of the Jinmium pit, adapted from Fullagar et al. (1996, Figs. 5 and 6). Crosses indicate TL ages (Fullagar et al., 1996), dots indicate single-grain OSL ages (Roberts et al., 1998a).

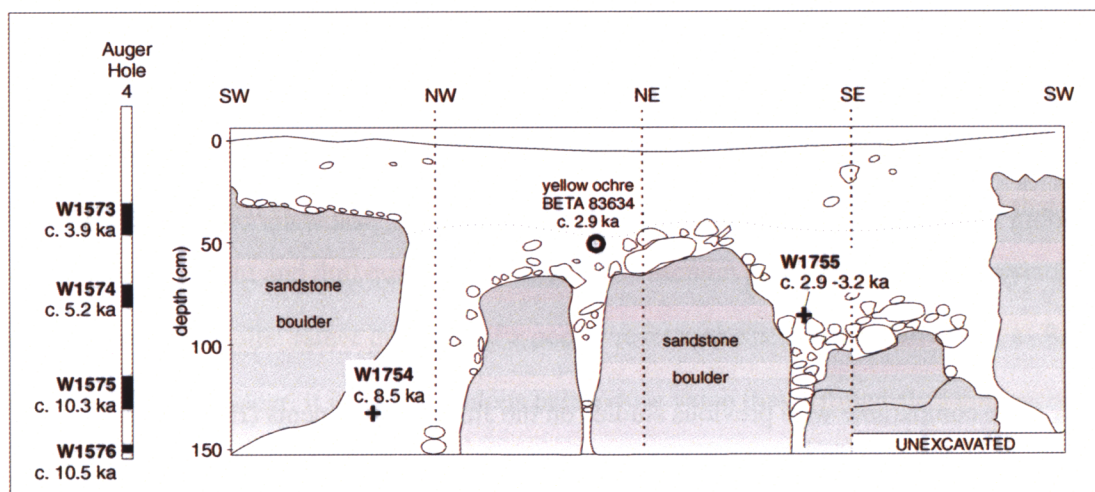


Figure 6.2 Stratigraphic section of the excavation pit C1/IV and auger hole 4 (A4) at Jinmium. Adapted from Fullagar et al. (1996, Fig. 7). Crosses indicate TL ages (Fullagar et al., 1996).

6.3 Luminescence Dating Theory

A comprehensive outline of TL dating techniques is given by Aitken (1985; 1989), and of optical dating by Aitken (1994). An account of the procedures and protocols for both TL and OSL dating of sediments is given by Mejdahl and Christiansen (1994) and Wintle (1998), and a recent review of luminescence models is given by McKeever and Chen (1998).

The general form of the luminescence equation is:

$$\text{Age} = \text{Palaeodose/Dose Rate}$$

Palaeodose (also known as equivalent dose, or archaeological dose) is the radiation dose needed to induce luminescence equal to that acquired subsequent to the most recent bleaching event, and includes a residual fraction of luminescence retained in a sedimentary sample after bleaching (Aitken, 1998). The dose rate (also known as the annual dose or radiation flux) is the rate at which radiation (measured from ^{232}Th , ^{238}U , and ^{40}K) is absorbed by sediments.

Uncertainties in the age therefore depend on the uncertainty in the palaeodose and the dose rate – including U-disequilibrium, mobility of U, Th and K isotopes, past water contents (Prescott and Fox, 1990; Olley et al., 1996).

In order to be comparable with previous studies on the Jinmium sediments (Fullagar et al., 1996; Spooner, 1998; Roberts et al., 1998a; Galbraith et al., 1999; Roberts et al., 1999; McCoy et al., 2000), this study makes use of both TL and OSL techniques to determine the luminescence age of sediments in the Keep River region. Despite lacking the interpretable structure of TL glow curves for thermal stability (Wintle, 1996), OSL dating is advantageous because it measures only the rapidly bleached signal (equivalent to the 325 °C peak used by TL), and so circumvents the need to assess the residual signal remaining at burial, giving greater accuracy and precision (< 5 %) for dating sunlight-exposed sediments than TL (Spooner, 1998). However, the use of the rapidly bleached signal implies that OSL is perhaps

less robust when used in disturbed sites. Both techniques are subject to the same uncertainties in the determination of the dose rate.

6.3.1 Determining Palaeodose

Critical to palaeodose determination is the uncertainty of whether there has been sufficient bleaching to remove all but the residual fraction by the time of deposition, which depends not only on the degree of illumination but also on the susceptibility of the sample to bleaching. While it is not clear whether the presence of impurities, such as organic or oxide coatings, hinders bleaching of quartz (Smith et al., 1997), it is only likely to be important if such impurities were obtained prior to transport (pre-depositional) (Roberts, 1991). Field observation indicates that most of the original oxide coating is removed by abrasion during transport, but upon burial a subsequent oxyhydroxide coating may form over time, and is evident from sediment characterisation (Fig. 5.15).

Despite the exposure of the sand sheets at Jinmium to full sunlight, incomplete bleaching was argued (Roberts et al., 1998a; Spooner, 1998) to account for the more ancient chronology presented by Fullagar et al. (1996). A recent study by McCoy et al. (2000) observed that the distribution of bright and dull quartz grains from the Jinmium excavation site does resemble that of a well reset site, rather than that of a poorly reset rock-shelter site. However, as Roberts et al. (1999) make clear, it is the anomalous palaeodose value that distinguishes unbleached grains, not the brightness sensitivity.

A more intrinsic problem in palaeodose determinations arises from the various possible depositional histories (refer 6.3), and potential mixing of younger and older sediments (Smith et al., 1997; Roberts et al., 1998b). As indicated by Roberts et al. (1999), older sediments may derive from *in-situ* disintegration of overlying bedrock or underlying saprolite (Fig. 6.3b), and neither would be distinguishable from partially bleached grains (Fig. 6.3d).

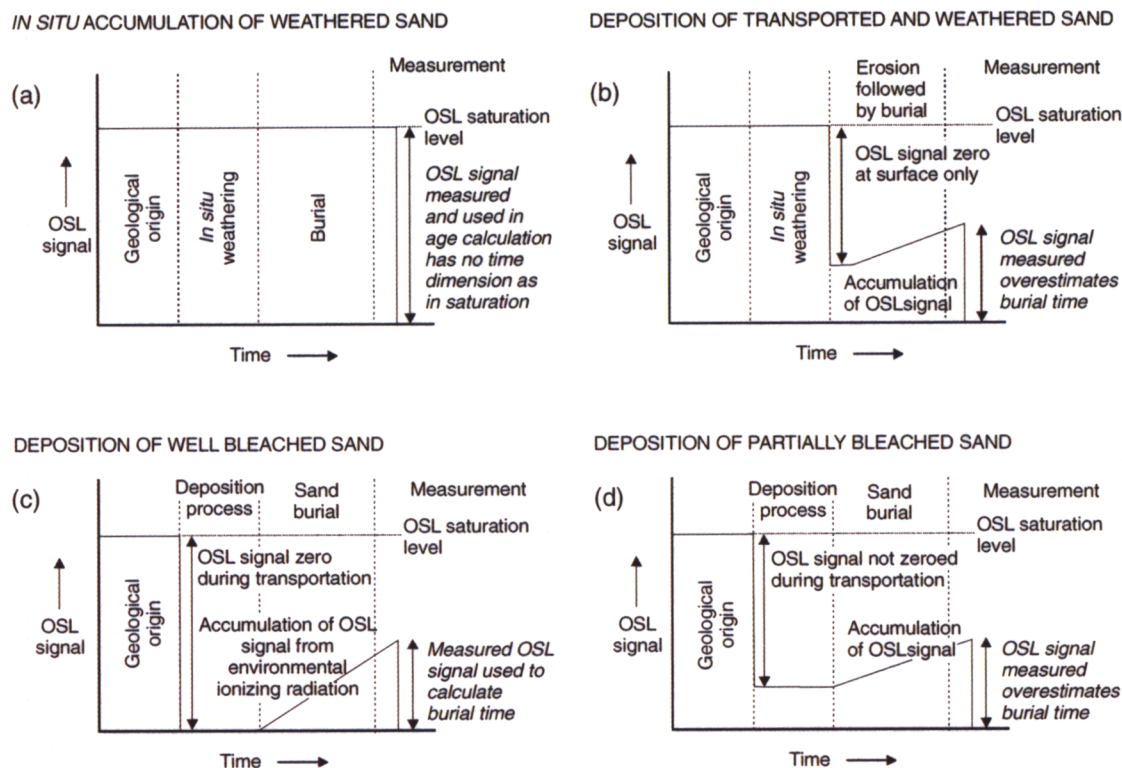


Figure 6.3 Schematic diagrams illustrating theoretical OSL signal histories including (a) *in situ* decay of unbleached saprolite, (b) deposition of well-bleached over unbleached sediment sands, (c) deposition of well-bleached transported sediments, and (d) deposition of partially-bleached sediments (modified from Frederick, et al., 2002). An understanding of the geomorphological context remains critical to differentiating luminescence history.

Using conventional multiple-grain TL methods, such mixing was thought to overestimate the average age of sediments in the Jinmium rock shelter (Spooner, 1998). This argument was supported by subsequent single-aliquot and single-grain OSL dating (Galbraith et al., 1999; Roberts, et al., 1999). Unfortunately, similar OSL analyses were not undertaken on samples from the adjacent sand sheet to indicate whether any of the features of the rock-shelter sediments were characteristic of the wider area.

Recent tests of single-grain OSL techniques are attempting to distinguish dose populations in natural deposits (Roberts, et al., 2000). These single-grain studies assume, as in standard multiple-aliquot studies (Olley et al., 1999), that the minimum palaeodose (or lowest 10 % of

are likely to have been bleached to the greatest extent (Roberts et al., 1999). However, studies have shown that young material may be incorporated into older sediments through bioturbation (Bateman et al., 2002), or intruded into older deposits through dessication cracks (Jon Olley, pers. comm., 2001), hence the minimum palaeodose may not always be stratigraphically accurate. Nevertheless, a recent study of burrow structures indicates that exhumation of material by bioturbation may not be significant, as the bulk of grains retain a significant palaeodose value corresponding to the depth and antiquity of the material exhumed (Bateman et al., 2002). Thus while single-grain dating improves the statistical distribution of palaeodose determinations, it does not identify the reason for the variability (McCoy et al., 2000), and an understanding of the geomorphological context remains critical to the reliability of dated sequences.

6.3.2 Determining Dose Rate

The dose rate is derived mainly from the decay of the lithogenic radionuclides uranium (^{238}U), thorium (^{232}Th), and potassium (^{40}K), and from cosmic rays, and is attenuated by water content of the sedimentary deposit (Olley et al., 1997). Cosmic rays contribute a small amount to the overall radiation flux level, and this only becomes significant when very low flux levels are in operation ie low K, Th and U values (Aitken, 1994). Estimates of dose rate cannot account for the long-term variations in the environment; thus a major uncertainty in dose rate comes from problems in the estimated measurement of both water content and in the disequilibrium in the U-Th decay series (Olley et al., 1996). Whilst water content does not directly contribute to the dose rate, its presence modifies the radiation flux level (Aitken, 1994). Thus radioactive disequilibrium may be significant where a site is wet or has been wet for any significant period (Prescott and Hutton, 1995). In the Keep River region, the land surface can be wet for 4 to 5 months of the year, during and after the wet season (Kinhill, 2001), although this may have been greater or less in the past. Although present uncertainties in dose rate calculations are unlikely to be above the 15 % threshold associated with luminescence dating (Roberts, 1996),

the error contribution from the dose rate becomes more significant as the precision in palaeodose determinations increases.

At Jinmium, as in most luminescence dating applications, it was assumed for simplicity that the dose rate had not changed over the period of burial (Fullagar et al., 1996). Evidence of large changes in water content and probable radioactive mobility throughout much of the Keep River region is manifested in the colouration and mottling of the sands by iron oxides and hydroxides (refer Chapter Five). Dissolution and re-precipitation of uranium and thorium in association with amorphous- and crystalline-iron and manganese oxides and hydroxides is typical of lateritic weathering environments (Short et al., 1989; von Gunten et al., 1999), and such element mobility may effect dose rate determinations. Studies at Allen's Cave, Nullarbor Plain, have shown that sediment heterogeneity has the potential to induce significant differences in the dose rate of individual grains and hence age determinations (Olley et al., 1997). At Ngarrabullgan, Cape York, disparate multiple-aliquot OSL ages between closely spaced samples were considered to be a result of the mixing of sediments from an underlying mottled zone (either saprolite or an ancient palaeosol) and more recently bleached sediments (Roberts, 1997: 859). Regardless of any possible influence of the mottled zone on the dose rate, the age of occupation at Ngarrabullgan was revised from ~ 60 ky BP to 30 ky BP. Such results highlight the importance of understanding the relationships between pedogenic features, disequilibria and burial dose rates in semi-arid monsoonal sediments of northern Australia.

This study prefaces luminescence age calculations with a preliminary investigation of the potential correlation between the degree of mottling of the sediments and radioactive disequilibrium, using a combination of high-resolution gamma and alpha-particle spectrometry. For a more detailed study of post-depositional processes and the potential impact on luminescence dating refer to Roberts (1996). In conjunction with these U/Th studies, U-series dating of pisolitic material from Sandy Creek Gorge and the sand sheets at Jinmium is also undertaken.

The application of luminescence (TL and OSL) dating is used here to:

- Obtain age estimates and determine the chronostratigraphy for the sand sheets and creeks around Jinmium, Goorurarmum, Karlinga and Sandy Creek, and for the rock-shelter excavations at Goorurarmum and Karlinga.
- Investigate the effect of weathering and diagenesis on dose rate estimates
- Discuss the geoarchaeological implications of the above results.

6.4 Methodology

Both TL and OSL techniques were used for age determinations of sand sheet sediments and creek profiles (including auger samples and excavation profiles). The Jinmium rock-shelter site is even more exposed than that of either Goorurarmum or Karlinga, but the aspect of the Jinmium site is apparently insufficient (more probably due to sediment mixing rather than lack of solar exposure) to allow the TL signal to be completely reset (Roberts et al., 1998a; 1999). In any case, optical dating is preferred for the rock-shelter sites.

6.4.1 Field work

Luminescence samples were taken from the excavation pits only after all archaeological investigation and sampling had been completed. Sampled excavation pits include those from Goorurarmum (KR31) rock shelter (Goor-2) and sand sheet (Goor-1), and from the Karlinga rock shelter (Karl-1) and sand sheet (Karl-3). Luminescence samples were also taken from non occupation sites in the sand sheets (auger holes) and from the creek sections at Sandy Creek Gorge and near the rock shelter KR99.

Samples for TL and OSL dating were collected in separate tubing, the former in opaque polyethylene tubes and the latter in smaller steel tubes to minimise light penetration. Eight duplicate samples were taken for comparative TL and OSL analyses, two from each excavation profile at Goorurarmum and Karlinga, and four from the Sandy Creek Gorge profile. Details of

methodology used to take luminescence samples from auger holes and excavation pits are described in Appendix A3.1. Excavation profiles, creek profiles and core descriptions were done *in situ*, and collected samples were transported to UOW for analyses.

A total of 36 TL samples were collected around Karlinga, Goorurarmum, Jinmium and Sandy Creek Gorge in the 1999 and 2000 field trips, in order to discern the temporal and spatial variation in depositional age within and between each of the sites. Of the 36 samples collected, 33 were analysed. A total of 19 OSL samples were also collected but limitations with the OSL facilities at UOW constrained the total number of samples analysed to 15. Of the total 48 dated samples, 12 that had various degrees of mottling or red staining were specifically selected for dose rate measurements, and to help determine disequilibrium in the uranium and thorium decay series in relation to iron content, water table and depth. Pisolithic material from the base of the Sandy Creek Gorge profile (540 cm) and JG-1 auger (450 cm) was also obtained for U-series dating.

6.4.2 Laboratory work

TL analyses were undertaken by David Price at UOW, using the combined additive and regenerative method on the 90 – 125 μm quartz fraction as outlined in Nanson et al. (1991). Full details for TL determinations are given in Appendix A4.2. The following outlines the methods used for determination of palaeodose and dose rate in OSL dating, and full details are given in Appendix 4.3.

OSL determinations were also undertaken on the 90 - 125 μm quartz fraction, in order to be comparable with TL measurements and with previous studies (Fullagar et al., 1996; Spooner, 1998, Roberts et al., 1998a; Galbraith et al., 1999; Roberts et al., 1999; McCoy et al., 2000). Grain size analyses (Appendix 3.2.2) indicated that the 90 - 125 μm constituted about 10% of the dry mass. OSL sample processing was undertaken personally, under the direction of Dr. Jon Olley (C.S.I.R.O., Canberra) and Dr. Bert Roberts (UOW).

6.4.2.1 Palaeodose

The technique for palaeodose determinations derived from the studies of Galbraith et al., (1999), but followed the most recent and robust protocol of single-aliquot-regenerative-dose (SAR) outlined by Murray and Wintle (2000), and modified from Murray and Roberts (1998). Each of the 15 samples was split into three portions: one for grain size, another for palaeodose determinations (single- and multiple-aliquot), and the third for dose rate determinations. Luminescence measurements were made at two laboratories (University of Wollongong, and CSIRO Land and Water in Canberra) using automated Risø TL/OSL (TL-DA-12) readers (Bøtter-Jensen and Duller, 1992). Samples were optically stimulated by a tungsten-halogen lamp filtered to between 420 and 550 nm using GG-420 filter in combination with an interference filter. Luminescence was detected by a Thorn-EMI 9235QA photomultiplier tube fitted with 2.5 mm of U-340 filter. Beta irradiations were delivered using calibrated $^{90}\text{Sr}/^{90}\text{Y}$ sources ($0.024 - 0.030 \text{ Gy s}^{-1}$). Riso software version 4.65 was used at both laboratories.

The sequence of protocols were made on most samples, comprised an IR check for feldspars (using 2 aliquots), a multiple-aliquot run (SARA, Mejdahl and Bøtter-Jensen, 1994) before and after sun bleaching (24 aliquots), a single-aliquot preheat plateau test (24 aliquots), two runs (24 aliquots) using a single-aliquot regenerative-dose (SAR, Murray and Roberts, 2000), and a double-regenerative test for 12 aliquots. The initial SARA run established a check of linearity and preliminary estimation of the true palaeodose, which allowed a single regenerative dose to be used in subsequent SAR determinations. A single regenerative dose may be unreliable if it is over 10 % of the true palaeodose (Folz and Mercier, 1999), or in the non-linear region of the OSL dose-response curve (Galbraith et al., 1999). A plot of palaeodose values from the SARA and SAR protocols indicates that there is good linear agreement ($r^2 = 0.92$) indicating that use of a single regenerative dose is reasonable. Where this was not the case (i.e. generally for palaeodose values over 20 Gy), multiple regenerative doses were applied which bracket the true palaeodose ($R_1 < N < R_2$) (refer Appendix A4.3.2).

6.4.2.2 Dose Rate Measurement

Twelve samples were selected for radionuclide analyses (α , ^{232}Th , ^{238}U , and ^{40}K). Three samples were taken from each of two profiles; the first was a 2.5 metre auger core taken from the Jinnium sand sheets (JG-2), which grades from red sands to pisolitic red sands. The second profile was a 3.5 metre section taken from Sandy Creek Gorge that includes streaky red and grey horizons considered to be representative of a series of palaeosols. Another six samples, with various degrees of mottling or redness, were chosen for determination of dose rate and subsequent OSL determinations.

U-series dating was also undertaken on pisolitic material from the base of the above two profiles. Facilities for all U-series determinations were provided by ANSTO, with sample processing and chemistry based on methods outlined by Short et al. (1989) and Gilmore and Hemingway (1995). Measurement of isotopic concentrations of ^{236}U and ^{238}Th are made using high-resolution gamma spectroscopy (Canberra Industries GR5022 fitted with a NaI annulus) and alpha-particle spectrometry (EG & G Octete PC Alpha Spectrometer), with analytical uncertainties of 5 % based on counting statistics, variability in machine response and uncertainty in blank corrections. Details of chemical separations are outlined in Appendix A4.4. The results will be compared with thick-source alpha counting conducted for TL age determinations on similar deposits, at the University of Wollongong.

6.5 Results

Section diagrams of all rock-shelter, sand sheet and creek excavations are presented in Chapter Five (section 6.3.1). A summary of TL age determinations for all auger cores and excavations is given in Table 6.1, and detailed in Appendix A4.2.1. OSL age determinations are similarly summarised in Table 6.2, and detailed in Appendix A4.3.3 and A4.4.2 respectively. An outline of how radial plots are constructed is given in Appendix A4.3.2. The chronostratigraphic results are presented in the discussion below.

6.5.1 Thermoluminescence (TL) dating

6.5.2

Table 6.1 Thermoluminescence (TL) age estimates, grouped according to location. All palaeodose estimates are calculated from the 375°C peak, except those marked with an asterix (*). The latter are derived from stepped plateaux (using the 325°C peak), hence the corresponding age determinations should be considered maximum values.

Sample Code	Sample Source	Sample Depth (cm)	Palaeodose (Grays)	Dose Rate ($\mu\text{Gy/yr}$)	TL age (ky BP)
Goorurarmum					
Gr-1	Auger	90	2.0 ± 0.3	908 ± 29	2.2 ± 0.3
Goor-1	Excavation	95	23.7 ± 2.2	1220 ± 30	19.4 ± 1.9
Goor-1	Excavation	155	5.9 ± 1.0	962 ± 28	6.1 ± 1.0
Gu-2	Auger	180	11.1 ± 0.9	1206 ± 31	9.2 ± 0.8
Jinmium					
JG1	Auger	210	22.4 ± 1.9	1428 ± 31	15.7 ± 1.4
JG2	Auger	390	49.3 ± 4.3	1216 ± 28	40.5 ± 3.7
JG2	Auger	560	84.7 ± 6.1	1112 ± 29	76.1 ± 5.8
JG4	Auger	420	40.7 ± 2.9	1053 ± 27	38.7 ± 2.9
JG4	Auger	590	93.2 ± 8.0	1275 ± 29	73.1 ± 6.5
Karlinga					
Ka-2	Auger	235	9.1 ± 0.9	968 ± 30	9.4 ± 1.0
Ka-4	Auger	200	6.3 ± 0.5	1075 ± 31	5.8 ± 0.5
Ka-4	Auger	360	27.5 ± 2.8	1856 ± 34	14.8 ± 1.5
KN2	Auger	100	4.2 ± 0.4	956 ± 28	4.4 ± 0.4
KN3	Auger	145	7.4 ± 0.6	1034 ± 29	7.1 ± 0.6
KN3	Auger	230	15 ± 2.0	1171 ± 27	12.8 ± 1.7
KN4	Auger	115	6.0 ± 0.5	1081 ± 30	5.6 ± 0.5
Karl-3	Excavation	30	6.0 ± 0.5	1055 ± 29	3.8 ± 0.5
Karl-3	Excavation	60	3.1 ± 0.3	1464 ± 25	2.1 ± 0.2
Karl-3	Excavation	120	8.1 ± 0.7	1291 ± 29	6.2 ± 0.5
Karl-3	Excavation	180	13.4 ± 1.3	1206 ± 29	11.1 ± 1.1
Karl-3	Excavation	240	17.6 ± 0.5	1297 ± 26	13.6 ± 1.1
KR99CP	Profile	95	6.8 ± 0.6	857 ± 28	7.9 ± 0.7
KR99CP	Profile	175	13.9 ± 1.6	1338 ± 33	10.4 ± 1.3
KR99CP	Profile	225	11.3 ± 0.9	1913 ± 43	5.9 ± 0.5
KR99CP	Profile	320	12.9 ± 1.0	1885 ± 42	6.8 ± 0.5
Sandy Creek					
SC1	Auger	55	6.8 ± 0.6	1130 ± 28	6.0 ± 0.5
SC1	Auger	200	14.1 ± 1.6	1564 ± 29	9.0 ± 1.0
SC2	Auger	200	10.9 ± 0.8	1421 ± 29	7.6 ± 0.6
SC3	Auger	200	10.6 ± 0.8	1477 ± 27	7.2 ± 0.5
SCG	Profile	57	$3.0 \pm 0.2^*$	1333 ± 25	2.3 ± 0.5
SCG	Profile	126	13.3 ± 1.3	3469 ± 65	3.8 ± 0.4
SCG	Profile	214	$22.7 \pm 1.8^*$	3652 ± 58	6.2 ± 0.5
SCG	Profile	321	21.5 ± 1.8	1817 ± 55	11.8 ± 1.0
SCG	Profile	357	27.0 ± 2.1	3113 ± 66	8.7 ± 0.7

Jinmium

The sediments sampled between the major sites of Jinmium and Goorurarmum yield significantly older depositional ages than those sampled elsewhere in the Keep River region, with similar estimates of ~ 40 ky BP (W2969 and W2971) at about 400 cm depth (Table 6.1), and ~ 75 ky BP (W2972 and W2970) around 550 - 600 cm (Table 6.1). These results are in broad agreement with previous age determinations of the sand sheets around Jinmium (Fullagar et al., 1996).

Goorurarmum

TL determinations on sediment samples from the Goorurarmum catchment indicate the sand sheets are generally well bleached. The temperature plateau comparisons extend between 300 and 500°C, which indicate good TL resetting prior to final deposition (David Price, pers. comm., 2000). However, the TL ages of the two samples taken from the Goorurarmum (Goor-1) excavation are the inverse of their order of depth at 19.4 ± 1.9 ky BP at 95 cm (W3033) and 6.1 ± 1.0 ky BP at 155 cm (W3034) (Fig. 5.7). The older sample exhibited a truncated temperature plateau (Fig. 6.4 and Fig. 6.7), which indicates that this sediment was not completely reset at the time of deposition or contained older material. Additionally these samples displayed different secondary (laboratory generated) TL glow curve characteristics (Fig. 6.5), indicating a mixed provenance of quartz grains (Price, 1994b). These quartz grains may derive from different geographical sources or from different formation sequences in a single bedrock outcrop. The overall results indicate that the sand sheets around Goorurarmum have been accumulating for at least 10 ky BP.

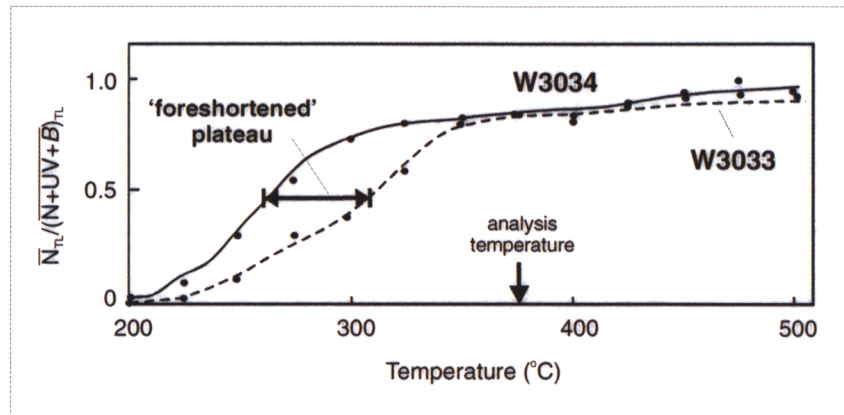


Figure 6.4 Examples of the temperature plateau for Goor-1 samples taken at 95 cm (W3033) and 155 cm (W3034). Note the foreshortened temperature plateau in W3033, which is similar to those found in samples from the original Jinmium rock shelter excavation (Fullagar et al., 1996).

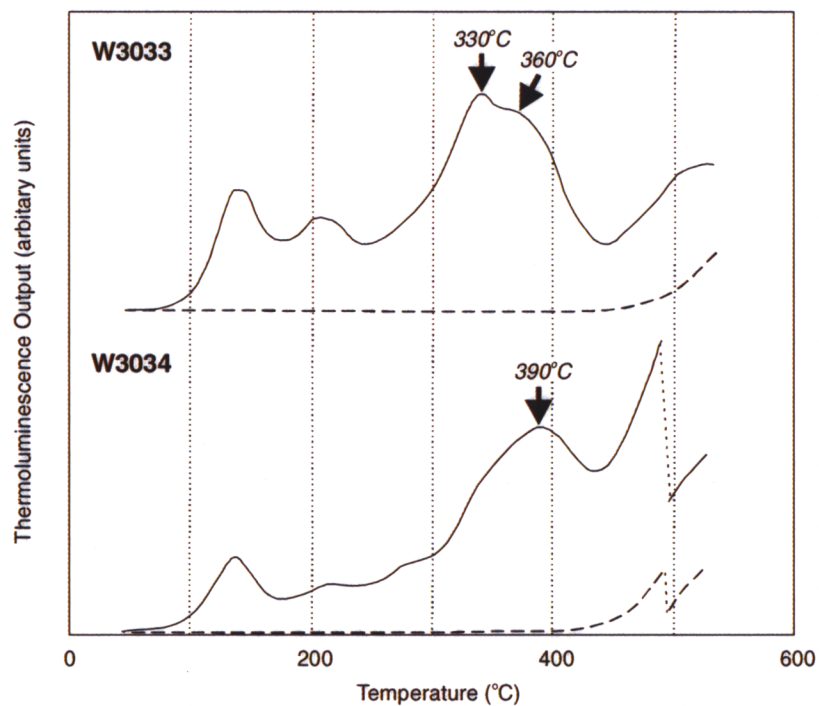


Figure 6.5 Examples of differing second glow curves for Goorurarmum (W3033 and W3034), indicating differing provenance of the sedimentary material.

Karlinga

TL determinations of the Karlinga sand sheet sediments indicate that they are generally well bleached, and as for Goorurarmum, the temperature plateaux extend between 300 and 500°C, which indicates the sediments are well-bleached prior to final deposition. The sample Ka-4 (W2793) taken near the edge of the Karlinga sand sheet (Fig. 5.2) at about 360 cm depth, had a relatively high water content (13 %) and radiation flux ($\sim 2000 \mu\text{Gy.yr}^{-1}$) compared to other samples from this site (refer Appendix A4.2.1). This probably reflects the position of the water table at the time of field sampling. The calculated age of the sample, using this high water content, is 14.8 ± 1.5 ky BP (Table 6.1).

Of the five samples taken from the Karlinga north excavation (Karl-3), two in the upper metre (Fig. 5.8) show an age reversal (3.8 ± 0.5 ky BP at 30 cm and 2.1 ± 0.2 ky BP at 60 cm), which may be attributed to bioturbation. The oldest age of 13.6 ± 1.1 ky BP in the deepest sample (Table 6.1) is consistent with above age estimate for the sand sheets around Karlinga.

North of this excavation site, two samples KN-2 (W2973) and KN-3 (W2974) exhibit quite different second glow-curve characteristics (e.g. Fig. 6.6), which is indicative of a sediment population(s) of differing provenance than other sediments around Karlinga (Price, 1994b). At the creek site east of Karlinga (KR99CP), the samples exhibit acceptable TL characteristics but fall into two age groups, the deeper of which have the more recent age. At 95 cm and 175 cm depth, the TL ages were 7.9 ± 0.7 ky BP (W3040) and 10.4 ± 1.3 ky BP (W3041) respectively (Fig. 5.9). At 225 cm and 320 cm the TL ages were 5.9 ± 0.5 ky BP (W3042) and 6.8 ± 0.5 ky BP (W3043) respectively (Fig. 5.9). Despite attempts to remove slumped material and sample from parallel horizons (Fig. 5.3), the results may represent a slumped or cross-channel sequence.

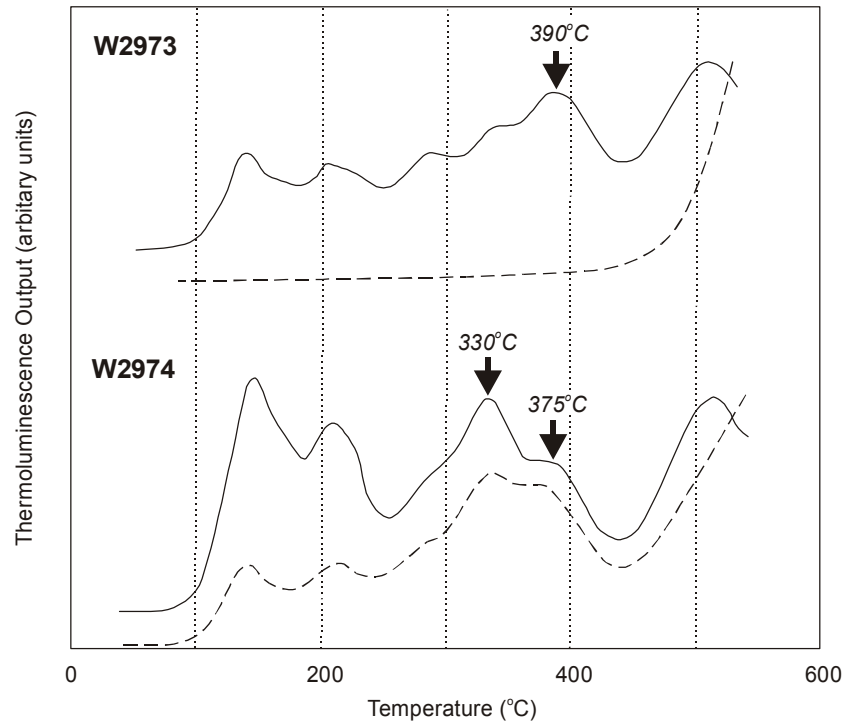


Figure 6.6 Examples of differing glow curves for auger samples KN-2 (W2973) and KN-3 (W2974), indicating a different provenance for sediments from these two sites.

Sandy Creek

With one exception (W2980), the samples from Sandy Creek transect exhibited stepped temperature plateaux characteristics (Fig. 6.7). This may indicate the samples have been insufficiently bleached or were re-exposed enough to minimise the entire TL energy spectrum between 300 and 500°C (Price, 1994a). These samples were analysed at both 325°C and 375°C, with the ages computed at the lower temperature more likely to represent the timing of the last period of sediment mobility, although according to David Price (pers. comm., 2000) this may still retain a percentage of previously acquired signal and therefore should be regarded as a maximum value. Samples taken nearest to Sandy Creek (SC1), at 55 cm and 200 cm, yielded identical ages of 3.6 ± 0.4 ky BP at 325°C (Table 6.1).

Taken at a further distance from Sandy Creek, the SC2 auger at 200 cm returned an age of 6.0 ± 0.5 ky BP using the 325°C peak and 7.6 ± 0.6 ky BP using the 375°C peak, indicating that any previous TL signal has been effectively minimised (David Price, pers. comm., 2000). The

sample taken the furthest away (~ 1 km) from Sandy Creek (SC3), exhibited a single temperature plateau extending between 275°C and 500°C, indicating that the age of 7.2 ± 0.5 ky BP at 200 cm represents a reliable estimate of the depositional age (David Price, pers. comm., 2000).

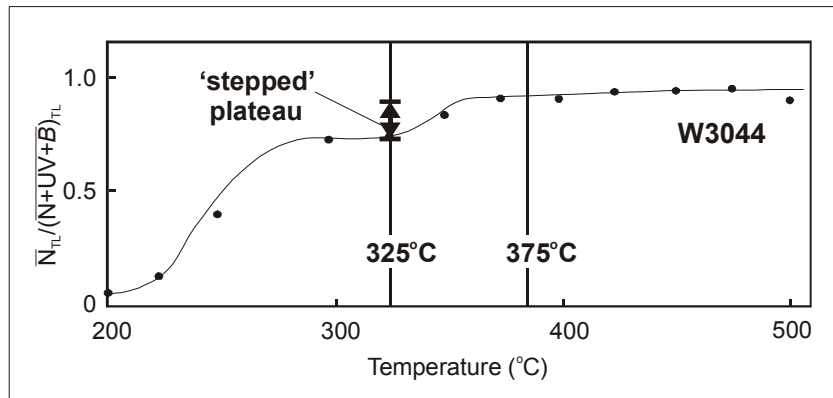


Figure 6.7 Example of the stepped temperature plateau that is typical of the Sandy Creek sediments, this sample (W3044) was taken from Sandy Creek Gorge at 57 cm.

Samples taken at Sandy Creek Gorge also reveal stepped plateau characteristics, with the exception of the sample taken from the lowest depth at 357 cm. Two samples, SCG-57 and SCG-214, were analysed only at 325°C, and returned an age of 2.3 ± 0.5 ky BP and 6.2 ± 0.5 ky BP respectively (Table 6.1). The sample taken at 126 cm returned an age of 3.0 ± 0.3 ky BP using the 325°C peak and 3.8 ± 0.4 ky BP using the 375°C peak. The samples taken at 321 cm returned an age of 9.2 ± 0.8 ky BP using the 325°C peak and 11.8 ± 1.0 ky BP using the 375°C peak. The sample taken at 357 cm exhibited acceptable TL characteristics and an apparently reliable TL age of 8.7 ± 0.7 ky BP (David Price, pers. comm., 2000). The age profile for this site is significantly less than was anticipated from the presence of the palaeosol horizons. Comparative dates are derived below from OSL dating and U-series ages of pisolites taken from the base of this sequence.

6.5.2 Optically Stimulated Luminescence (OSL) dating

Table 6.2 OSL age determinations, grouped according to location, and calculated using central age palaeodose and dose rate determined from thick-source alpha-counting (TSAC) and high-resolution gamma spectrometry for the two rock-shelter samples (*).

Sample Code	Sample Depth (cm)	Palaeodose (Grays)	Dose Rate (uGy/yr)	OSL age (ky BP)
<i>Goorurarmum</i>				
Goor-2	20	0.4 ± 0.01	760 ± 41*	0.53 ± 0.14
Goor-1	50	1.3 ± 0.03	1220 ± 30	1.1 ± 0.03
Goor-1	100	3.1 ± 0.05	1220 ± 30	2.5 ± 0.07
Goor-1	175	5.2 ± 0.08	1206 ± 31	4.3 ± 0.13
Goor-1	220	17.2 ± 0.23	1206 ± 31	14.3 ± 0.41
<i>Karlinga</i>				
Karl-1	27	19.7 ± 0.27	1064 ± 75*	18.5 ± 1.38
Karl -3	90	3.4 ± 0.05	1378 ± 40	2.5 ± 0.08
Karl -3	150	11.4 ± 0.18	1249 ± 34	9.1 ± 0.29
Karl -3	210	24.2 ± 0.28	1252 ± 40	19.4 ± 0.64
Karl -3	240	23.4 ± 0.55	1297 ± 26	18.0 ± 0.56
KR99CP	95	14.4 ± 0.28	857 ± 28	16.9 ± 0.64
KR99CP	320	16.2 ± 0.32	1885 ± 42	8.6 ± 0.25
<i>Sandy Creek</i>				
SCG	57	4.2 ± 0.06	1333 ± 25	3.1 ± 0.07
SCG	126	15.8 ± 0.22	3490 ± 65	4.5 ± 0.10
SCG	321	24.5 ± 0.30	1828 ± 55	13.4 ± 0.44
SCG	357	43.2 ± 0.59	3113 ± 66	13.9 ± 0.35

6.5.2.1 Palaeodose

Goorurarmum

Figure 6.8a shows the T_r/T_n ratios obtained from samples from the Goorurarmum rock shelter (Goor-2) and sand sheet (Goor-1) excavation. Sensitivity changes are indicated by a slight increase in the T_r/T_n ratio with preheat temperature, but the corresponding palaeodose estimates

are unchanged (Fig. 6.8b), indicating that the test dose OSL signal corrects sufficiently for changes in OSL sensitivity between the natural and regenerative dose cycles.

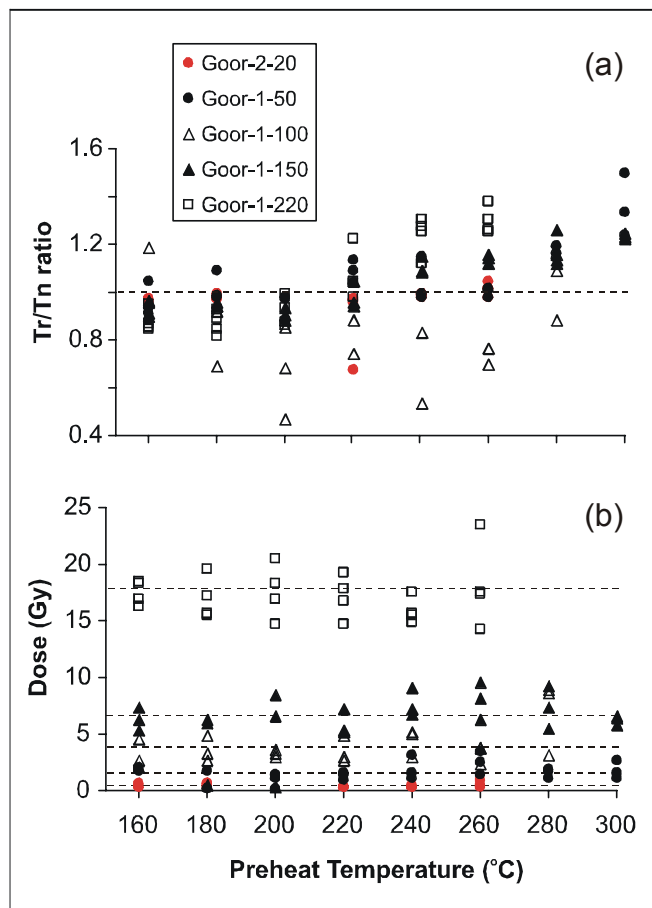


Figure 6.8 (a) Test dose OSL (T_r/T_n) ratios and (b) palaeodose estimates obtained at preheat temperatures ranging from 160 – 300°C using an SAR protocol applied to 24 single aliquots of quartz from the Goorurarmum rock shelter, and from four different depths (50, 100, 150, 220 cm) of the Goorurarmum sand sheet excavation. The dashed line in (a) corresponds to a unit test dose OSL ratio ($T_r/T_n = 1$) that indicates no change in sensitivity between the natural and regenerative cycles. The dashed lines in (b) correspond to the average palaeodose for each sample.

The palaeodose estimates of the Goor-1 sand sheet excavation at 50, 100, 175 and 220 cm depths are in respective stratigraphic order of 0.4, 3.1, 5.2 and 17.2 Gy. The deepest sample at

220 cm gives a value over three times that at 150 cm, and despite the low dispersion shown using either MAA or SAR protocols, the possibility of some bedrock contamination cannot be ruled out.

Insufficient bleaching may be detected by scatter in D_E results, shown on radial plots by the spread greater than accommodated with ± 2 band projected from y-axis. The low dispersion in the radial plots (Fig. 6.9) of the Goorurarmum rock shelter (Goor-2-20) sediments indicate they are surprisingly well bleached. Further confidence of laboratory protocol and palaeodose estimates was obtained from a double-regenerative test in which a known regenerative dose is repeated (on a 0.5 mm aliquot) to give a similar palaeodose estimate that is accommodated within ± 2 sigma band projected from the y-axis (inset of Fig. 6.9).

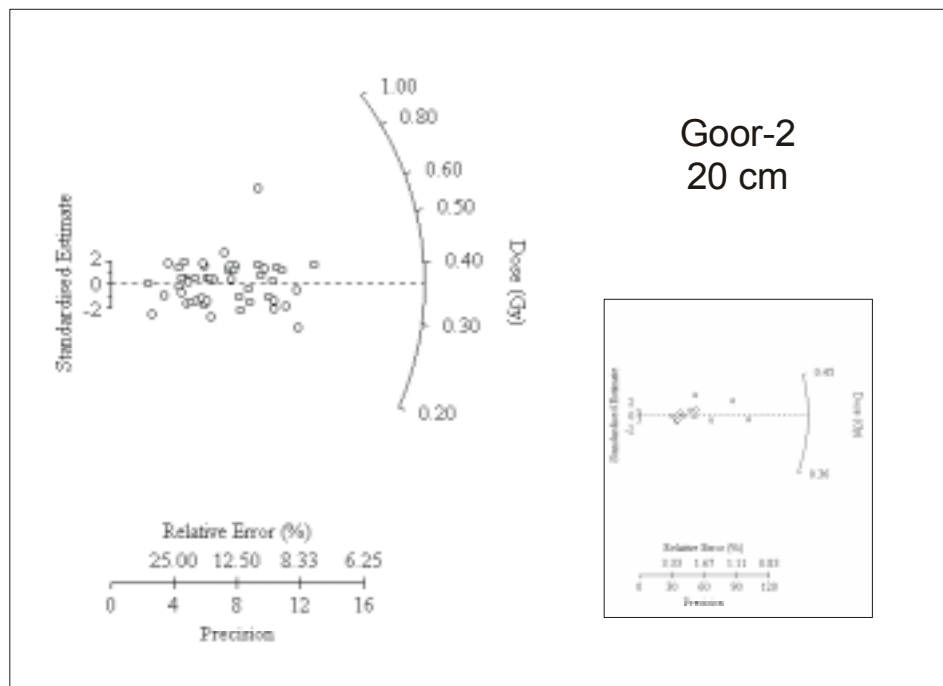


Figure 6.9 Radial plot of palaeodose estimates for the Goorurarmum rock shelter at 20 cm depth. Inset shows palaeodose estimates for a double-regenerative test using a single regenerative dose of 0.4 Gy on 12 aliquots using a mask size of 0.5 mm.

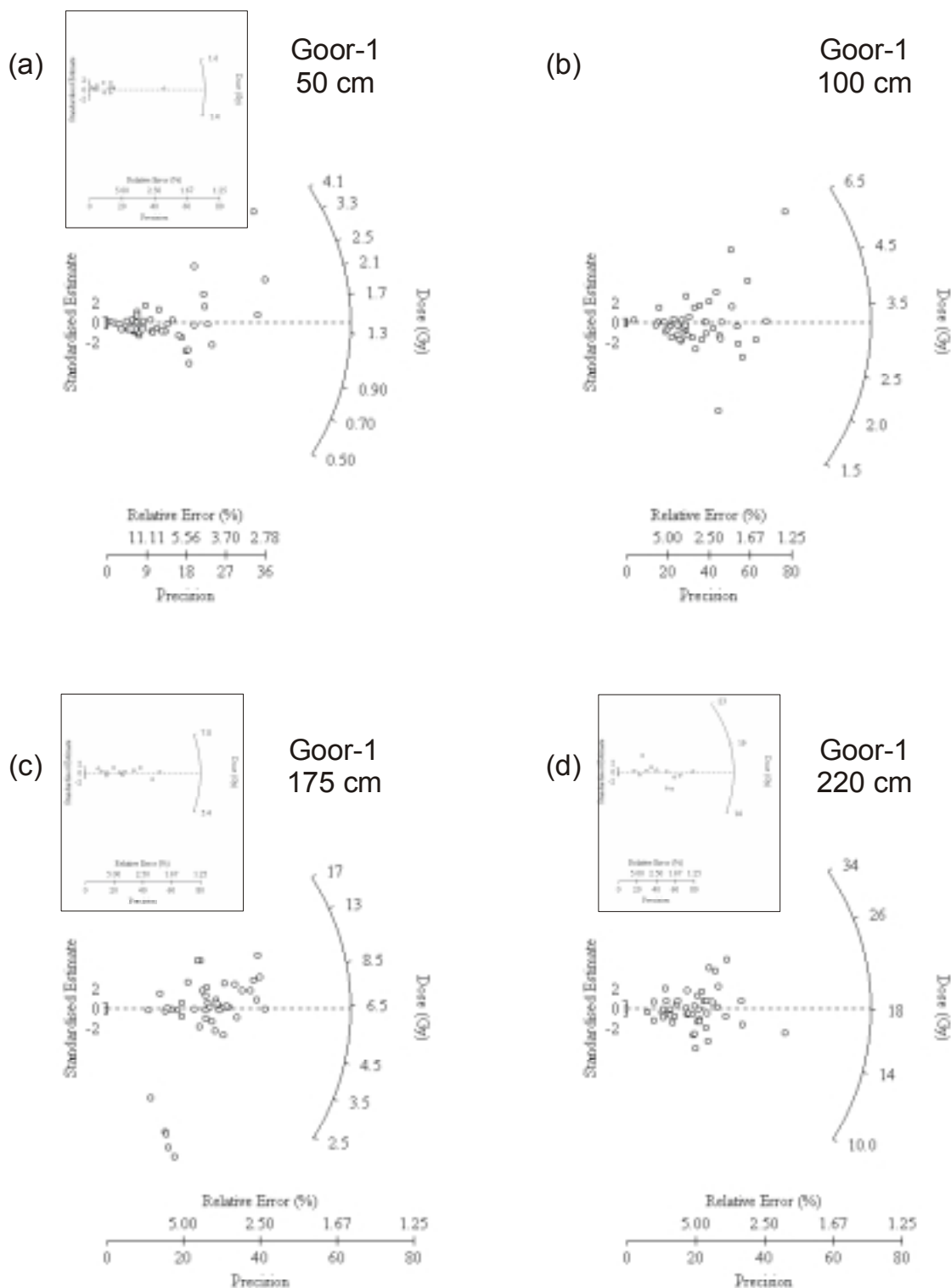


Figure 6.10 Radial plots of palaeodose estimates for the Goorurarmum sand sheet samples at (a) 50, (b) 100, (c) 175 and (d) 220 cm. Inset shows palaeodose estimates for a double-regenerative test using a single regenerative dose of 1.5 Gy at 50 cm, 6.7 Gy at 175 cm and 17.5 Gy at 220 cm.

Samples from the sand sheet excavation show much greater dispersion in palaeodose estimates, which increase with depth (6.10a - d). The OSL palaeodose estimate of 3.1 ± 0.05 Gy at 100 cm is significantly less than the corresponding TL estimate of 23.7 ± 2.2 Gy. This large discrepancy can be explained if the sample was deposited as a result of a rapid depositional event allowing the OSL (325°C) peak to be completely reset but not the TL (375°C) peak.

A lesser difference is also evident between the TL (11.1 ± 0.9 Gy) and OSL (5.2 ± 0.08 Gy) palaeodose estimate for Goor-1 at 175 cm. The sample may comprise a mixed population of poorly bleached and well bleached quartz, accounting for the large scatter in palaeodose values evident from the radial plot (Fig. 6.10c). The scatter observed at 220 cm may be similarly explained, and is further supported by the outliers in the double-regenerative test (inset Fig. 6.10d). Thus the palaeodose estimate of 17.2 ± 0.23 Gy at 220 cm may be a slight overestimate and should therefore be taken as a maximum.

Karlinga

Compared to the Goorurarmum rock shelter, the Karlinga rock-shelter samples show significantly greater scatter, as evident in the dispersion shown in double-regeneration plot (inset of Fig. 6.11) indicating they are less well bleached. The Karlinga rock-shelter sediments may derive from local bedrock material that has not been fully bleached at deposition. In addition, the rock shelter sediment show little temperature sensitivity but have a significantly lower T_r/T_n ratio (0.74 ± 0.053) (Fig. 6.12) than those from the Goorurarmum (Goor-2) rock shelter (0.97 ± 0.073). This low sensitivity probably indicates the rapidly bleached traps (325°C) are saturated but the slowly bleached traps (375°C) are empty, and are sensitised by exposure on the OSL machine (Jon Olley, pers. comm., 2001). A partial analysis of the Karlinga rock-shelter sample by TL provided a palaeodose estimate of 40.25 Gy (D. Price, pers. comm., 2002), which is evidently much higher than the OSL palaeodose estimate and most likely indicates that these rock-shelter sediments have seen very little exposure to light. A minimum palaeodose of around 14 Gy may be a more accurate indicator of the depositional age

of the sediments at 27 cm depth, although this value is not much less than the central palaeodose estimate of 19.7 ± 0.27 Gy.

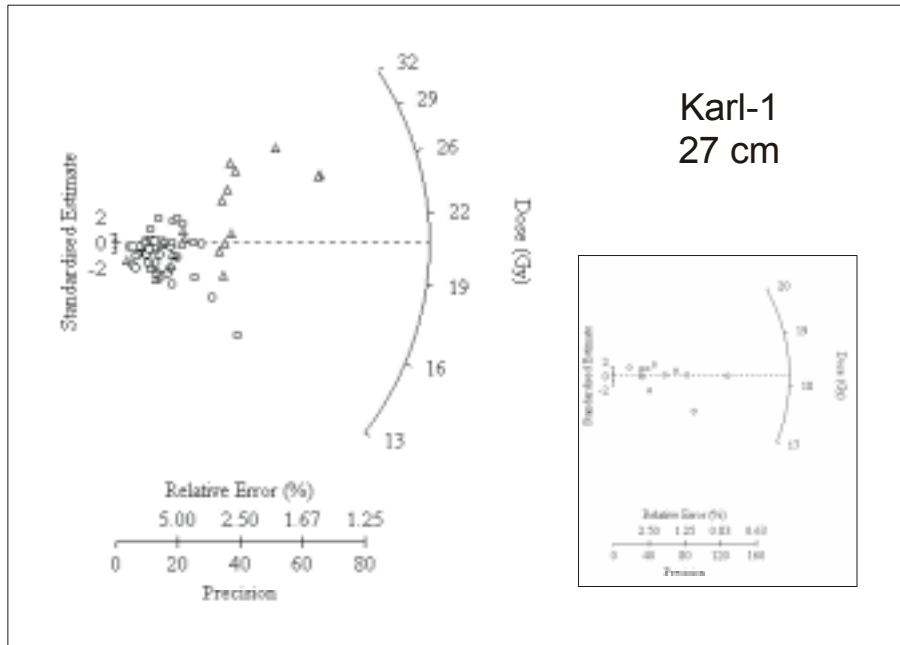


Figure 6.11 Radial plot of palaeodose estimates for the Karlinga (Karl-1) rock shelter. Circles represent estimated palaeodose values using a single regenerative value ($D_e = R_1$), and the diamonds estimated palaeodose values using bracketed regenerative values ($R_1 < D_e < R_2$) for the SAR protocol. Inset shows palaeodose estimates for a double-regenerative test using a single regenerative dose of 18 Gy on 12 aliquots using a mask size of 0.5 mm.

With the exception of the deepest samples at 210 cm and 240 cm, the samples from the Karlinga sand sheet excavation (Karl-3) also show little OSL sensitivity with temperature, and have an average T_r/T_n ratio less than 1.0 (Fig. 6.12). All of the samples from the Karl-3 excavation show a significant amount of dispersion that increases with depth, as evident from the increasing standard error (Table 6.2). These samples probably comprise a mixed population of well-bleached and poorly bleached quartz. The palaeodose estimates of the Karl-3 samples at 90, 150, 210 and 240 cm depths are also in respective stratigraphic order of 3.4, 11.4, 24.2 and 23.4 Gy. No bedrock material was encountered during sampling but the water table was reached on the lowest sample at 240 cm.

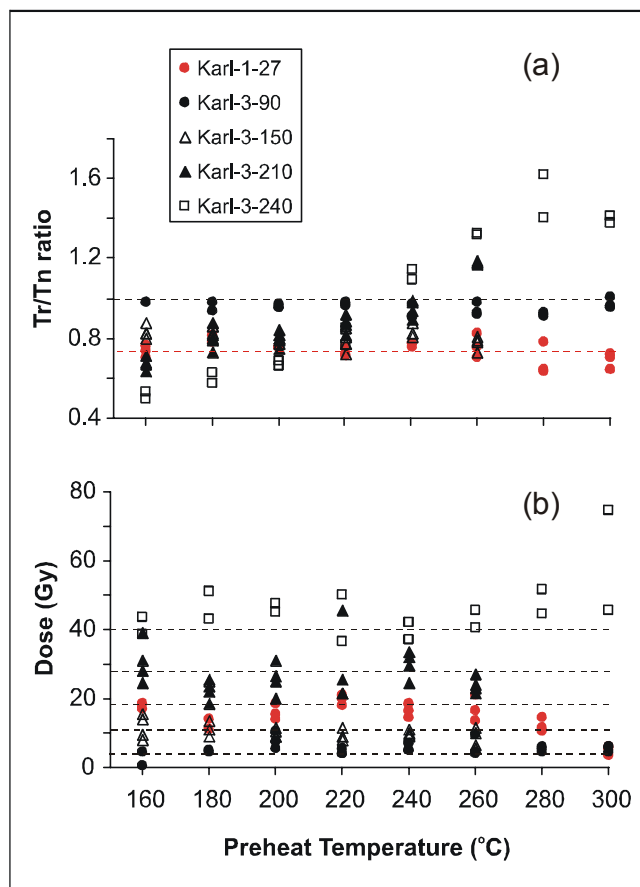


Figure 6.12 As for 6.10, for samples from the Karlinga rock shelter (Karl-1 at 27 cm) and Karlinga sand sheet excavation (Karl-3) from depths of 90, 150, 210 and 240 cm.

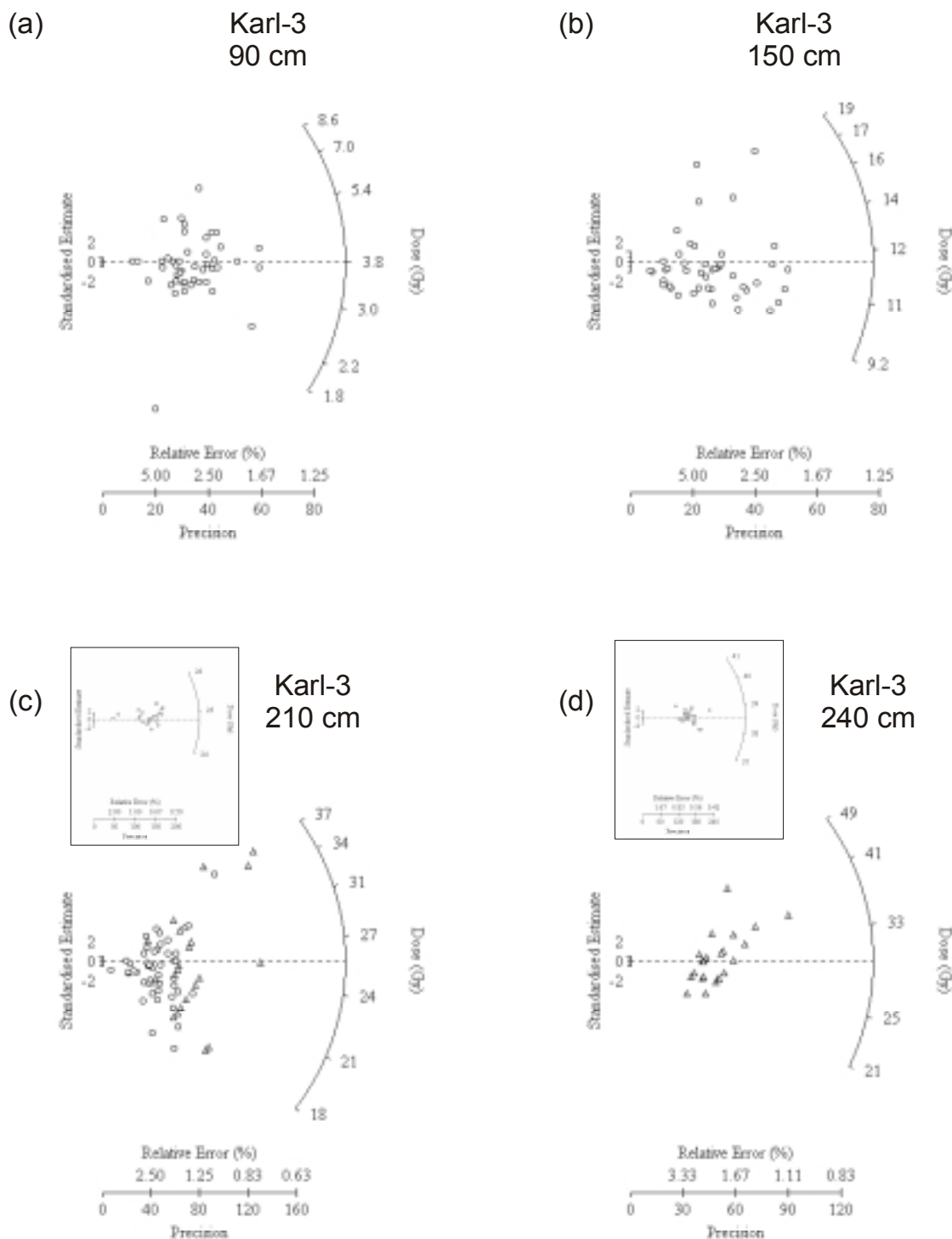


Figure 6.13 Radial plot of palaeodose estimates for the Karlinga (Karl-3) sand sheet excavation at (a) 90, (b) 150, (c) 210 and (d) 240 cm. Circles represent estimated palaeodose values using a single regenerative value ($D_e = R_1$), and the diamonds estimated palaeodose values using bracketed regenerative values ($R_1 < D_e < R_2$) for the SAR protocol. Inset shows palaeodose estimates for a double-regenerative test for a regenerative dose of 25 Gy at 210 cm and 40 Gy at 240 cm.

Karlinga Creek

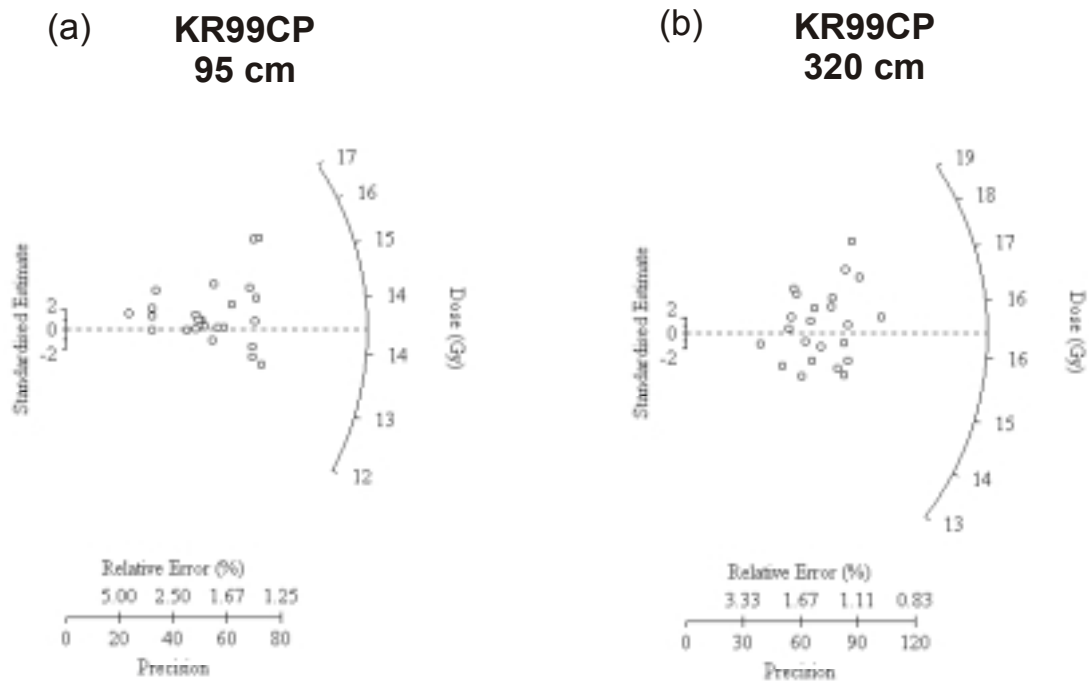


Figure 6.14 Radial plot of palaeodose estimates for the Karlinga Creek site (KR99CP) at (a) 95 cm and (b) 320 cm.

The Karlinga Creek samples show increasing sensitivity (T_r/T_n ratio) with preheat temperature, but there is negligible thermal transfer in the corresponding palaeodose estimates (refer Appendix A4.3.3). As in the sand sheet, the dispersion in palaeodose estimates indicates the sediments probably comprise a mixed population of well-bleached and poorly bleached grains. The estimated palaeodose of 14.4 ± 0.3 Gy and 16.2 ± 0.3 Gy at 95 cm and 320 cm respectively, are both greater than the corresponding palaeodose values of 6.8 ± 0.6 Gy and 12.9 ± 1.0 Gy estimated from TL dating.

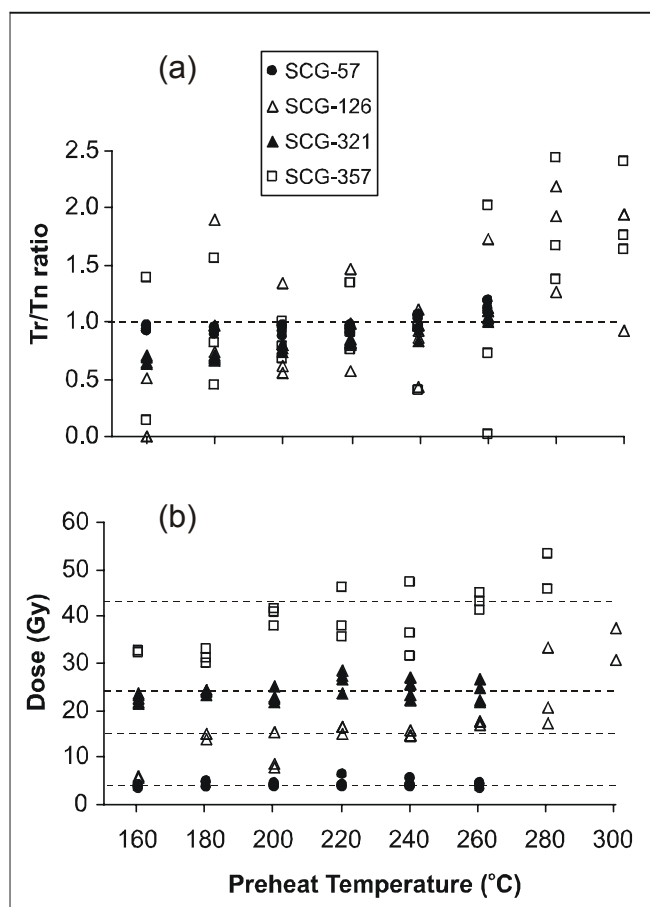
Sandy Creek

Figure 6.15 As for 6.10, for samples taken from depths of 57, 126, 321 and 357 cm at Sandy Creek Gorge.

All the Sandy Creek Gorge samples show a sensitivity change with temperature (Fig. 6.15a), but again the average palaeodose at the corresponding range of temperatures (160 to 300°C) implies negligible thermal transfer (Fig. 6.15b). The palaeodose estimates for samples at 57, 126, 310 and 357 cm increase respectively from 4.2, 15.8, 24.5 to 43.2 Gy. The deepest sample at 357 cm shows the greatest degree of dispersion using either MAA and SAR protocols (refer Appendix A4.3.3). This dispersion, also shown in the radial plot diagrams (Fig. 6.16), indicates the probable presence of incompletely bleached grains in this alluvial sample. As such, the estimated palaeodose value should be considered a maximum.

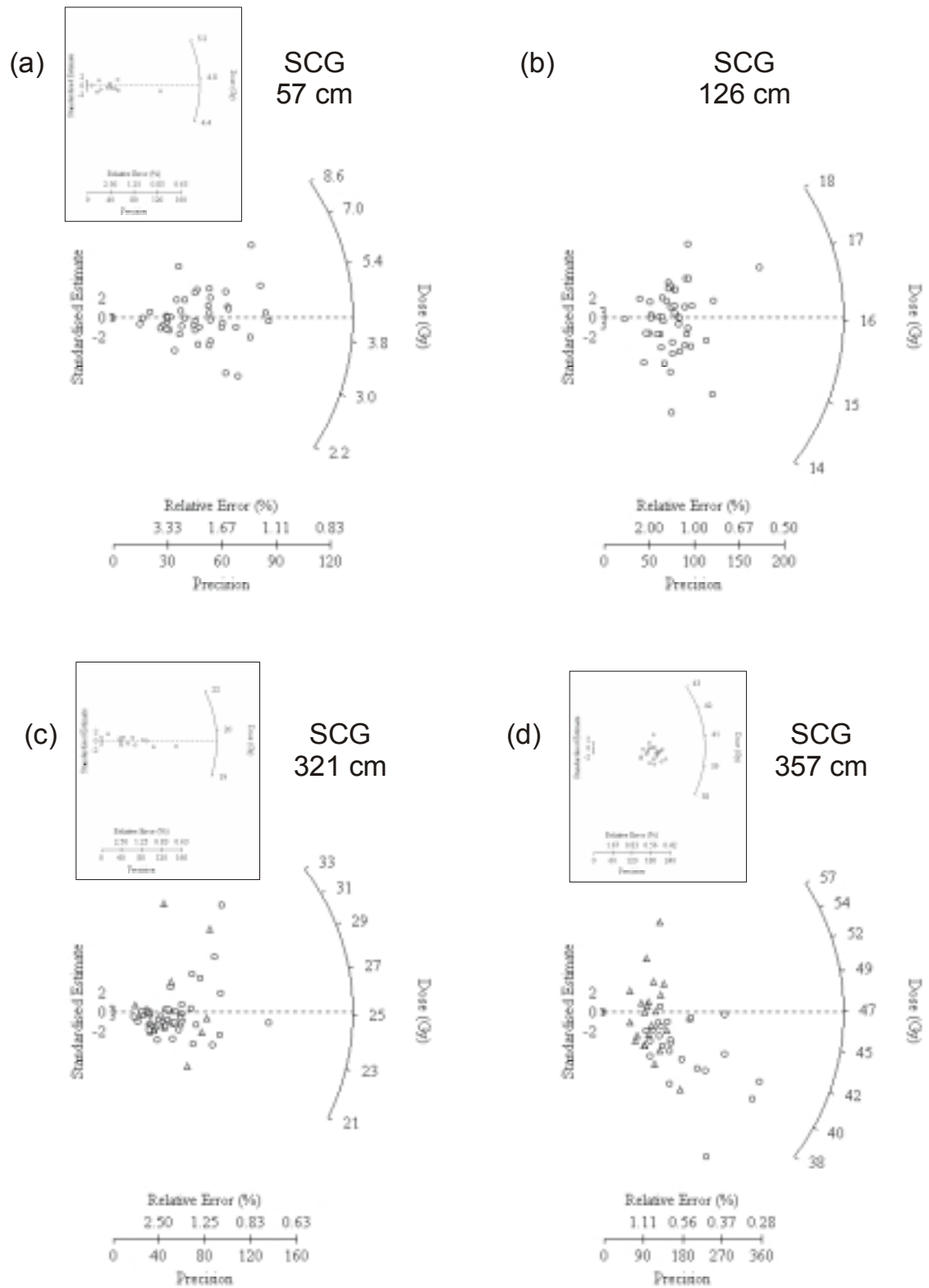


Figure 6.16 As for Figure 6.13 for samples from Sandy Creek Gorge at (a) 57, (b) 126, (c) 321 and (d) 357 cm. A regenerative dose of 4.7 Gy at 57 cm, 24.4 Gy at 321 cm and 40 Gy at 357 cm was used for double-regenerative tests (shown inset).

6.5.2.2 Dose Rate

Comparisons of ^{238}U and ^{228}Th data calculated by high-resolution gamma spectroscopy (HRGS) and alpha-particle spectrometry (APS) indicate the former values are 2 to 6 times higher for ^{238}U and approximately 0.6 times less for ^{228}Th (Table A6.3). The reason for this is unknown but may be attributed to differences in U and Th chemistry (Andrew Jenkinson, pers. comm., 2002), or may reflect problems in the radiochemistry methods, or the analytical programs used to calculate the individual radionuclide concentrations (Bert Roberts, pers. comm., 2002). More significantly, the estimated values for U, Th and K obtained by HRGS and APS provide dose rates that are 30 – 50 % of that estimated from thick-source alpha counting (TSAC). Although the absolute numbers may be imprecise, the radionuclide ratios should be reliable and can be used to provide some estimate of disequilibria. Thus dose rates estimated from TSAC where available are used for age calculations (Table 6.2) and use of TSAC results is justified by the secular equilibrium which generally prevails in the U-series (mean $^{238}\text{U}/^{226}\text{Ra}$ is 1.1 ± 0.39 and $^{210}\text{Pb}/^{226}\text{Ra}$ is 0.9 ± 0.22) and Th-series (mean $^{228}\text{Th}/^{228}\text{Ra}$ ratio is 0.9 ± 0.19). By mainly using TSAC, the only variable in comparisons of TL and OSL techniques is the palaeodose, which in any case is the most likely source of any major age discrepancy.

Dose rate calculations were individually assessed, for the samples where TSAC was not undertaken. For the Karlinga sand sheet samples at 90, 150 and 210 cm, dose rates were calculated from the average value of that estimated from bracketing sample depths – i.e the dose rate for Karl-3 at 90 cm is the average of the dose rate estimated by TSAC at 60 cm and 120 cm depth. If instead the HRGS results were used, the calculated ages for these three samples would be almost double that estimated using the bracketed dose rate values, and also inconsistent with the chronostratigraphy determined by TL dating. For the Goorurarmum sand sheet sample (Goor-1 at 220 cm), the 100% error in U, Th and K concentrations estimated from HRGS would render any subsequent age calculations meaningless. The average dose rate of 1.13 ± 0.312 Gy/ka is used in preference, and is estimated from TSAC for the shallower depths from the same Goorurarmum site.

The mean dose rate for all samples calculated using TSAC, excluding the Sandy Creek Gorge samples, is $1.3 \pm 0.29 \text{ Gy.ky}^{-1}$. The mottled sediments from Sandy Creek Gorge have a higher dose rate of $3.0 \pm 0.83 \text{ Gy.ky}^{-1}$, which reflects the higher U, Th and K concentrations in these samples. The 12 samples selected for HRGS and APS, which include the highly mottled sediments from Sandy Creek Gorge, show no apparent correlation between the degree of mottling and relative disequilibria in either the U-series or Th-decay series. Rather virtually all the samples indicate relative secular equilibrium, although the excess of ^{234}U over ^{230}Th and ^{228}Th over ^{232}Th does indicate some post-depositional migration and precipitation of ^{234}U and ^{228}Th with amorphous iron oxides and oxyhydroxides.

For the two rock-shelter samples, Karl-1 (27 cm) and Goor-2 (20 cm), the dose rates were estimated from HRGS, acknowledging some degree of uncertainty with the results. Whilst the K concentrations values do not significantly affect the total dose rate, the low ^{40}K values in other samples measured by HRGS compared to the equivalent K concentration estimated by flame photometry (for TL determinations) indicate that U and Th concentrations may also be underestimated. The radionuclide ratios indicate secular equilibrium in the U-series for both samples. However, in the Karl-1 sample possible disequilibrium and redistribution of Ra in the Th-series is indicated from a low $^{228}\text{Th}/^{228}\text{Ra}$ ratio (0.41), which may result in an underestimate of the dose rate and an overestimate of the luminescence age. Thus the total dose rates estimated for Karl-1 ($1.06 \pm 0.075 \text{ Gy/ka}$) and Goor-2 ($0.67 \pm 0.169 \text{ Gy/ka}$) may be too low, and the age for these sites may be overestimated and should be taken as a maximum and with a maximum 15 % error.

6.5.3 Comparison of OSL and TL results

As indicated above, similar palaeodose estimates were obtained from OSL determinations, using MAA and SAR protocols ($R^2 = 0.92$), for values less than about 20 Gy. The correlation between OSL and TL palaeodose determinations is poor. As indicated above (refer 6.5.2.1), the large disparity between the palaeodose estimate of 19.4 Gy by TL and 3.1 Gy by OSL for Goor-1 at 100 cm depth probably reflects the effect of a depositional event associated with limited sunlight exposure which reset the rapidly bleached 325°C TL peak but not the more robust 375°C TL peak (resulting in a foreshortened plateau) (Fig. 6.4). Thus excluding Goor-1-100 cm and Karl-3-90 cm (whose TL value is an approximate calculation), OSL palaeodose estimates are approximately 20 % greater than the corresponding TL estimate. For SCG-357, the OSL palaeodose estimate (~ 43 Gy) is almost double that of the corresponding TL estimate (~27 Gy). The OSL signal is more readily bleached during transport and deposition hence the greater TL age over the OSL age is unusual and not easily explained.

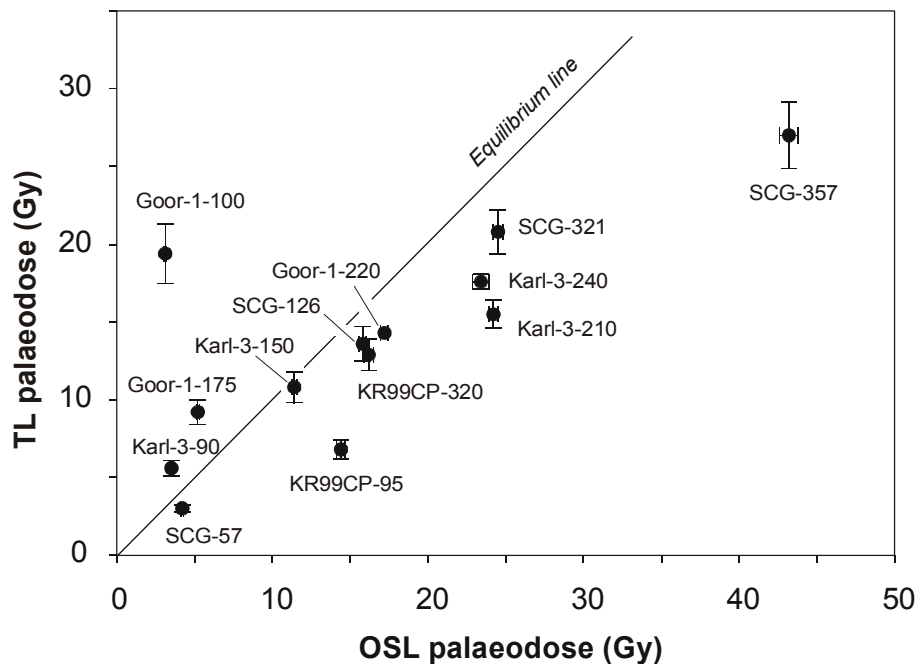


Figure 6.17 Comparison of TL and OSL palaeodose estimates. Samples should plot along the equilibrium line if there is a good correspondence between the two methods.

A poor correlation between TL and OSL palaeodose estimates may result where inadvertently bleaching by the laboratory illumination induces a stepped TL plateau, and only the 325°C TL peak is used for age calculations. Otherwise the 325°C TL and OSL palaeodoses should be similar although not exactly the same because of a contribution to the former from the underlying 375°C TL peak. The palaeodose value calculated using the 375°C TL peak of all samples with stepped-plateau is also approximately 20 % greater than that calculated at 325°C. The step or depression of the plateaux may be attributed to partial exposure during transport in the field, releasing electrons trapped at lower energy (325°C) levels but insufficient to release those stored at deeper (375°C) levels (Price, 1994a). Alternatively, the use of yellow light (500 nm) filters in the TL laboratory may be removing a proportion of the 325°C signal (Spooner and Prescott, 1986; Smith, 1988; Spooner, et al., 1988) as demonstrated by Roberts (1997) (Fig. 6.18).

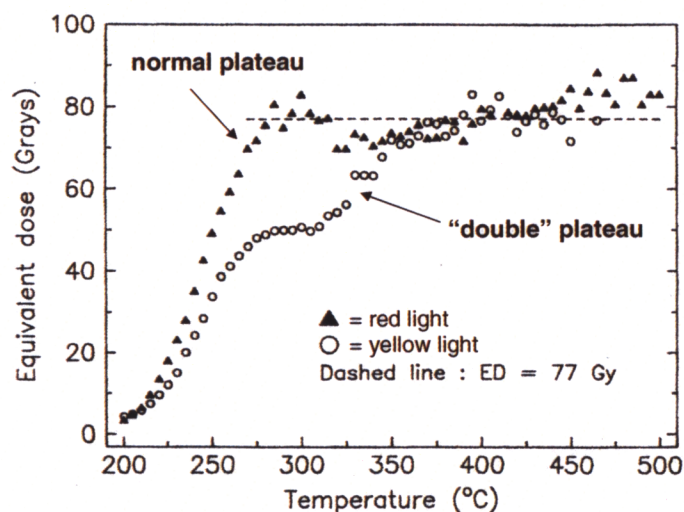


Figure 6.18 Palaeodose ‘plateau test’ for aliquots of sample KTL167 processed under red (filled triangle) and yellow (open circle) light from Roberts (1997: 854, his figure 9(b)). Note the “double” or stepped plateau and partial erasure of 325°C peak under yellow illumination, compared to the full plateau under red illumination.

It might be questioned why only some samples prepared under yellow lights show significant loss of the 325°C TL signal, and why some samples without stepped TL plateau (e.g. SC3) still produce a lower palaeodose estimate than the corresponding OSL palaeodose estimate. It is possible that yellow lights are affecting all samples and that the 20% difference between TL

possible that yellow lights are affecting all samples and that the 20% difference between TL and OSL estimates is simply more apparent in samples of older age (Fig. 6.17). Two tests were conducted to see if there is a significant loss of the 325°C TL/OSL signal due to the use of yellow lights in the laboratory, or due to something inherent in the sample.

The first test involved a TL test on two samples, one with a stepped plateau (SCG-321) and one without (Goor-1-220). After being given a known dose of 100 Gy, three aliquots of each sample were exposed to red and another three to yellow light for 3 hours. If the yellow laboratory illumination had no effect, the TL glow curves for the ‘red light’ sample should be the same as the corresponding ‘yellow light’ sample. The results indicate that the 325°C peaks are diminished in both samples after 3 hours exposure to yellow light (Fig. 6.19). However, because the 375°C peak is dominant in both samples to start, the diminution in the 325°C peak is only slight. Consequently the age estimated from the 375°C peak should be fairly reliable. Further tests may be able to separate these overlapping peaks and accurately estimate the effect of yellow light exposure on each.

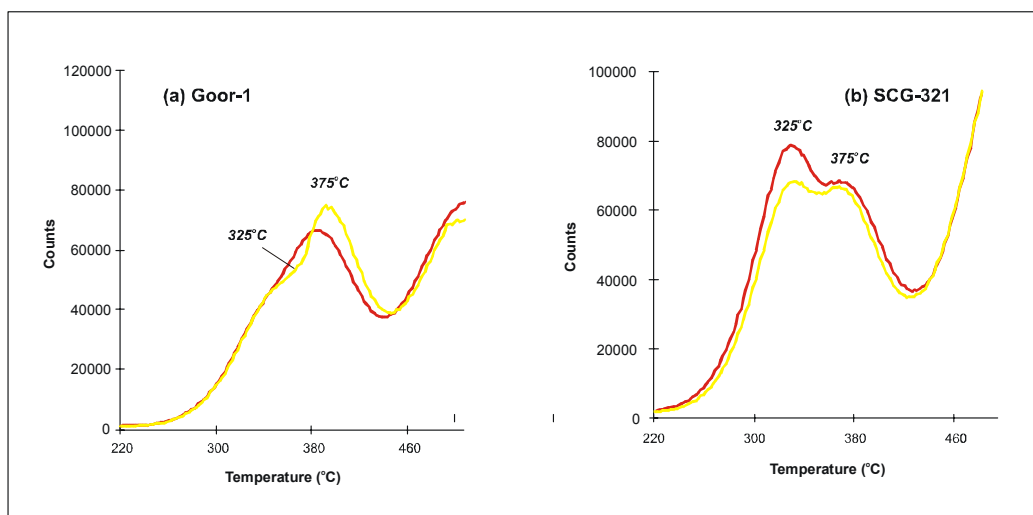


Figure 6.19 Comparative glow curves for two samples (a) Goor-1 at 220 cm and (b) SCG at 321 cm, exposed to red (red curve) and yellow light (yellow curve) for 3 hours. The latter sample has an initial stepped TL plateau. After 3 hours exposure to yellow illumination

the 325°C peak is diminished relative to the sample exposed under red illumination.

Refer text for details.

The second test involved exposing aliquots of the same two samples to yellow light for different lengths of time to see if the OSL signal is proportionately diminished. This test assumes that the decline in the 325°C TL peak and OSL signal result from emptying of the same electron source traps (Aitken, 1998). After being bleached to the background count rate (using blue LEDs) and then given a known beta-dose of 20 Gy, three aliquots of each sample were exposed to yellow light for 1, 10, 100, 1000 and 10,000 seconds respectively (Fig. 6.20). Another three aliquots of each sample were exposed to red light for 10,000 seconds (~ 3 hrs) as a control (Fig. 6.20). The exposure times assumed a rapid decline (e.g. exponential) in the OSL signal with yellow light exposure. The SAR protocol (Murray and Wintle, 2000; Murray and Roberts, 1998) was used to calculate the doses.

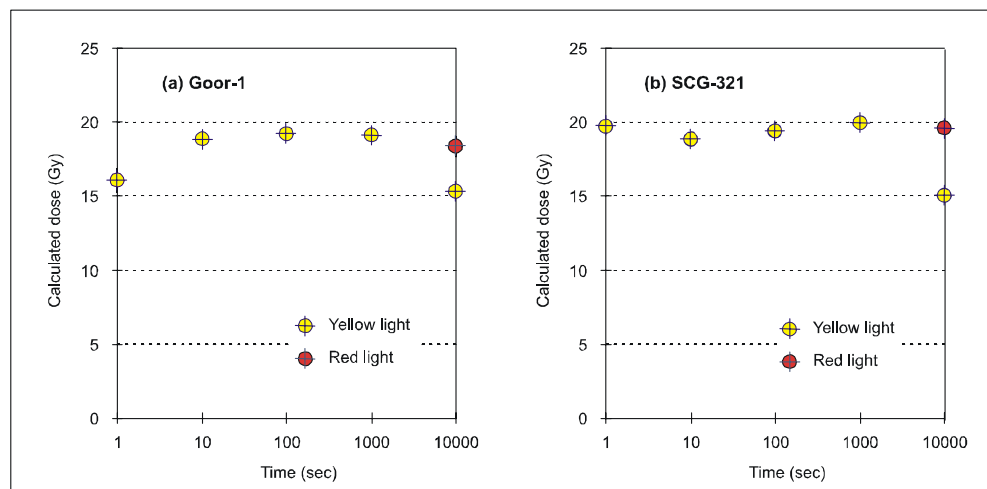


Figure 6.20 Results of exposure test undertaken on a sample from (a) Goor-1 at 220 cm and (b) SCG at 321 cm. Samples were exposed to yellow illumination for 1, 10, 100, 1000 and 10,000 seconds, respectively, and compared to a control sample exposed to red illumination for 10,000 seconds. A significant decrease in the palaeodose value is measured after 10,000 seconds exposure to yellow illumination. Refer text for details.

The results show that whilst exposures of less than 1000 seconds to yellow light have no discernable effect, a 20–25% loss of the 325°C TL peak is measurable at 10,000 seconds (Fig. 6.20). This is longer than the estimated maximum exposure time of one hour for samples

prepared and dated in the TL laboratory (David Price, pers. comm., 2003) (although this was unknown before the experiment) but some loss of the 325°C TL peak may be expected to occur within this time. Again, a more reliable estimate of age may be calculated from the 375°C peak (provided the sample was well bleached at the time of deposition) or from the OSL samples, which were prepared under red light. Agreement between these paired ages would confirm that the sample had been sufficiently bleached at the time of burial.

In summary, the results of the above tests indicate that prolonged exposure (~ 3 hrs) of samples to yellow illumination in the laboratory can result in a significant loss of the 325°C TL peak, which may induce a stepped-plateau in some samples. The stepped-plateau present in several of the Sandy Creek and Sandy Creek Gorge samples indicate that they have either been partially exposed in the field, or subject to prolonged exposure in the TL laboratory. It is unknown why only the samples from the one locality of Sandy Creek Gorge show these stepped plateaux. The majority of samples in the Keep River region have a dominant 375°C TL peak, which means that the adverse effects of yellow illumination and corresponding age determinations based on this peak are minimised. Thus the discrepancy between the OSL and TL age determinations (almost all of which are calculated from the 375°C TL peak) may only be partially explained by yellow light exposure. Additional discrepancy may be due to contamination of younger age grains, which may be masked in TL analyses by the large number of grains comprised in each aliquot. Hence, OSL age calculations which are based on small aliquots (10 - 20 grains) arguably provide a more reliable indication of the depositional age and dispersion of a population(s) of grains.

6.5.4 U-series dating of pisolites

Uranium series analysis of the pisolites from one of the auger holes near Jinmium gives an estimated age > 350 ky BP at 420 - 450 cm. This means that the pisolites come from an open system, which results in an excess of ^{230}Th , and cannot be dated (Fig. 6.21). It is noted that the raw concentration of thorium (8.90 ± 0.260 ppm) is approximately twice that of the pisolites taken from Sandy Creek Gorge, and the uranium (0.996 ± 0.039 ppm) concentration is approximately one-sixth the value, indicating quite different groundwater influences.

The pisolites taken from Sandy Creek Gorge at about 550 cm depth give an estimated age of 45 ky BP ± 20 - 15 ky BP (Fig. 6.21). This age is significantly more than expected from the luminescence dating of the underlying sediments, which give an age of 9 ky BP from TL determinations or 13 ky BP from OSL determinations at about 360 cm depth. The pisolites from this site are considered to be *in situ* (refer 5.2.2.2). From the chronological evidence alone, at least one diastem in the sequence is assumed (Fig. 5.10).

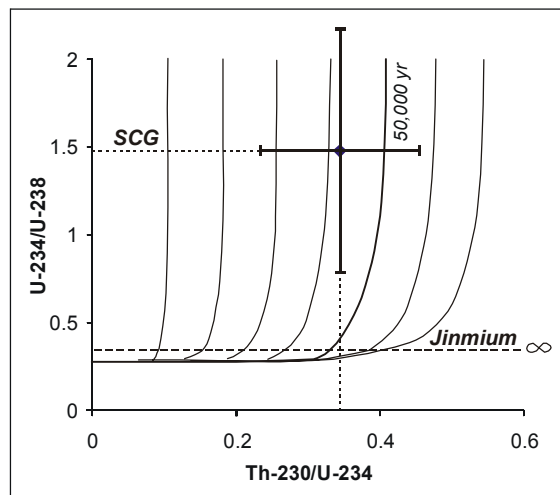


Figure 6.21 Isochron plot of U-series dating of pisolitic material from Jinmium and Sandy Creek Gorge, indicating an open and closed system for the former and latter sites respectively.

6.5.5 Age-depth Curves

Age determinations from past and present TL, OSL and U-series dating are combined to provide age-depth curves for individual sites (Fig. 6.22), and collated for the Keep River region as a whole (Fig. 6.23). In theory, age-depth curves can allow calculation of the rates of accumulation of various components of the deposit (e.g. sediment, stone artefacts, shell) which when compared may provide some insight into the history of human occupation and the of the site environment and its surroundings (Hughes and Djohadze, 1980).

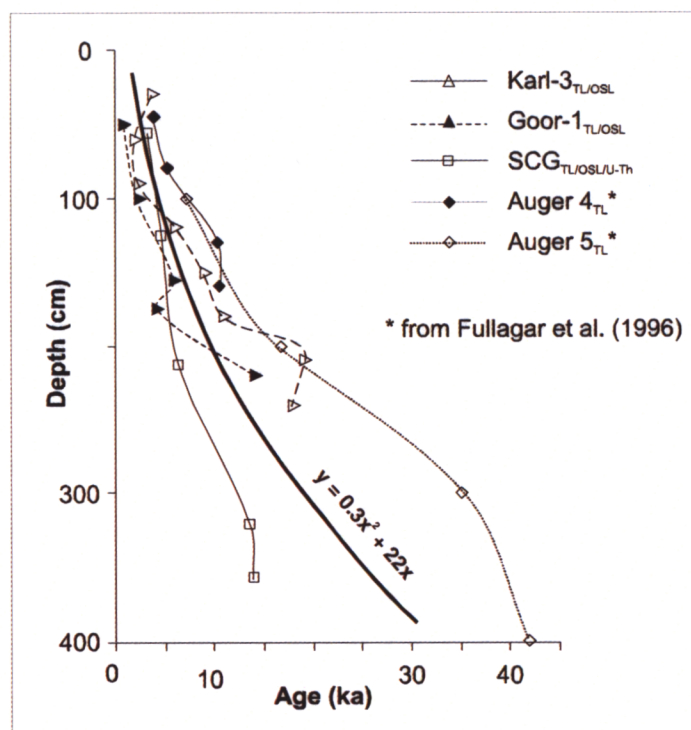


Figure 6.22 Age-depth curve for the sand sheets at Karlinga (Karl-3), Goorurarmum (Goor-1), Jinmium (Auger 4 and 5, from Fullagar et al., 1996), and for Sandy Creek Gorge. A line of best fit for all data shows a progressive increase in sedimentation from about 30 ka.

Age-depth curves of sand sheet and creek profiles from this study show relatively similar trends for each site (Fig. 6.22), allowing a general sedimentation rate to be calculated. Whilst the inflection point or curve-fitting is in effect subjective, the overall trend indicates that the sedimentation rate increases progressively from about 120 - 150 mm.ka⁻¹ during the early Pleistocene to about 200 mm.ka⁻¹ during the Holocene. The rates are slightly less if the creek

sand sheet has the lowest overall sedimentation rate ($\sim 100 \text{ mm.ka}^{-1}$), whilst Sandy Creek Gorge has the highest overall sedimentation rate ($\sim 250 \text{ mm.ka}^{-1}$) and probably reflects the difference in alluvial transport and deposition of these sediments.

Figure 6.23 shows an age-depth curve of all luminescence ages (and the U-series age on the pisolites) determined from this and previous studies in the Keep River region. It is apparent that the regional trend follows that shown at the individual site level (Fig. 6.22) with a progressive increase in sedimentation rate from less than 100 mm.ka^{-1} in the early Pleistocene to over 200 mm.ka^{-1} during the Holocene. If only Holocene ages are considered, the age-depth curve reveals a constant sedimentation rate of $\sim 250 \text{ mm.ka}^{-1}$. The results however reveal a great degree of spread, and any local or short-term geochronological discontinuities may not be revealed by this general extraction of the data.

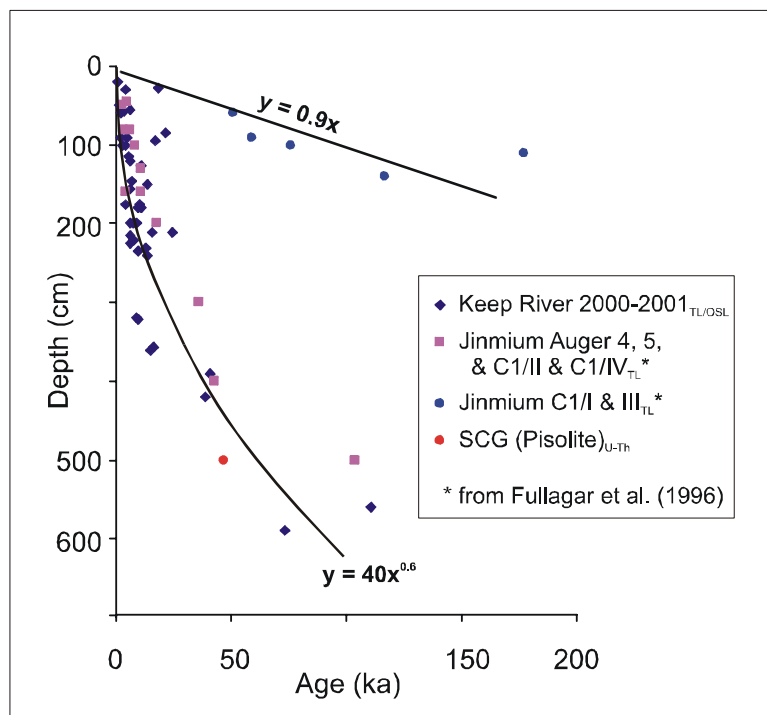


Figure 6.23 Age-depth curve combining all present and previously published (Fullagar et al., 1996) luminescence and U-series ages from the Keep River region. A line of best fit is drawn for the original Jinmium (C1) excavation and another for all other data (refer text for explanation).

The other obvious trend is the digression from the main curve of the original TL ages determined from the C1/I and C1/III excavation at Jinmium, which indicates they have been deposited at a significantly lower sedimentation rate and by a different process than sediments elsewhere in the region, or that something is aberrant in the luminescence ages themselves. This is equally applicable of the sediment trend shown from the Karlinga rock shelter (15 mm.ka⁻¹), although this was calculated from only a single OSL age. These results are discussed further below and in Chapter Seven.

6.6 Discussion

The following discussion presents a broad overview and diagrammatic summary of the chronostratigraphy of the rock shelters, sand sheets and creek profiles in the Keep River region as determined from past (Fullagar et al., 1996; Roberts, 1998a) and present results of TL and OSL dating.

6.6.1 Sedimentation Rates and Processes

The collective age/depth curve indicates that the sedimentation rate throughout the Keep River region has increased progressively from 100 mm.ka⁻¹ during the late Pleistocene up to 250 mm.ka⁻¹ during the Holocene. The range of accumulation rates at the individual site scale is similar to those determined from the collective age/depth curve. The difference in accumulation rates between individual sites largely reflects the depositional environment, such that higher accumulation rates (250 mm.ka⁻¹) are observed in higher energy river and creek sites, and lower accumulation rates (100 mm.ka⁻¹) are observed on the lower energy sand sheet sites. It is likely that sedimentation rates are likely to differ again for individual units (if these can be distinguished) within each site. The sedimentation rate of the excavation sequences on the sand sheets which comprise occupation records is similar to those which do not, hence the increase in sedimentation in the Holocene most likely results from natural processes, such as enhanced monsoonal activity in this part of northern Australia (Hubbard, 1995; Nott and Price,

1994) and/or the post-glacial marine transgression (Woodroffe, 1993). It is not possible to discern from the available ages if rate of sedimentation changed significantly over the late Holocene or in the past 200 years since European occupation. At Nauwalabila, in Arnhem Land, Hope et al. (1995) also noted a progressive increase in sediment accumulation over 60 ka, and tentatively argued for an apparent cessation of sedimentation over the past 2 ka. High resolution dating is needed to confirm whether the long-term increase in sedimentation reflects a more regional trend.

There is an indication from the luminescence data that episodic rapid deposition of individual or isolated units does occur. As indicated above, the discrepancy in the OSL (~ 3 Gy) and TL (~ 19 Gy) palaeodose estimates from a sample from the Goorurarmum sand sheet (Goor-1) at 100 cm may reflect a rapid depositional event such as localised mass wasting of escarpment bedrock, or dump of sediment during a storm. The event age may be indicated by the OSL age of ~2.5 ky BP. Foreshortened plateaux were also noted in the original Jinmium rock shelter and upper part of the nearby sand sheet (Auger 4) (Fullagar et al., 1996). These foreshortened plateaux were considered to result from partial re-exposure *following* deposition (Fullagar et al., 1996: 768). Alternatively, it is possible that these sediments also represent a similar rapid depositional event to that at Goorurarmum.

Thus accumulation rates for smaller excavated areas may be higher than those calculated for an entire site, with deposition beginning and ending over discrete periods (e.g. Stein et al., 2002) and also over discrete areas. Thus the calculated accumulation rates do not always represent continuous human occupation characterised by gradual accumulation of material, but rather short-duration occupations that were repeated infrequently in the same area (Stein et al., 2002). Accordingly, where there are enough data points to allow it, estimations of archaeological accumulation rates should be calculated from the duration of accumulation between any two points in time rather than from the total period of accumulation (e.g. Stein et al., 2002; Ward and Larcombe, 2003).

6.6.2 Chronostratigraphy

6.6.2.1 Chronostratigraphy of the Sand Sheets

The chronology and first evidence of stone, seed and ochre in each of the sand sheet profiles which contain evidence of occupation is summarised in Fig. 6.24. The following discussion concentrates on the chronostratigraphy. Further analysis of the rate of artefact accumulation and sediment accumulation for each of the archaeological excavation sites is given in Chapter Seven (refer 7.3.3).

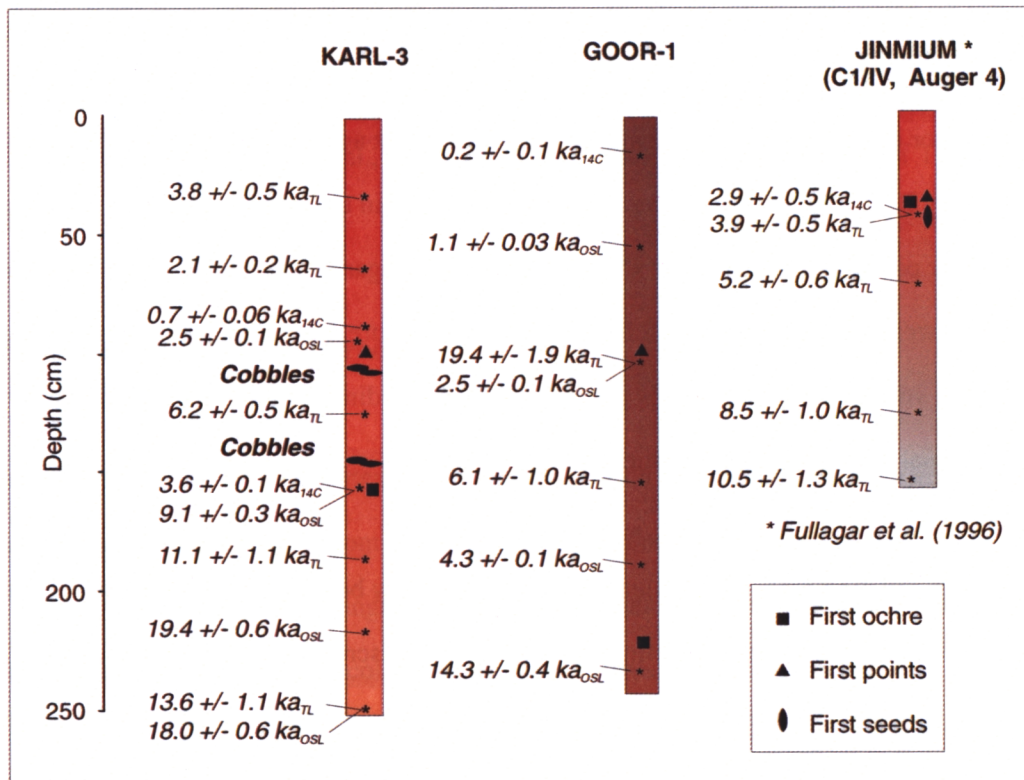


Figure 6.24 Ages and archaeological evidence from the three sand sheet excavations with occupation records in the Keep River region, including Karlinga (Karl-3), Goorurarmum (Goor-1) (this study) and Jinmium (Auger 4) (Fullagar et al., 1996).

In the Karlinga sand sheet excavation (Karl-3), the lowermost luminescence age of 13.6 ky BP (TL) or 18 ky BP (OSL) represents a minimum age for the beginning of sand sheet formation as there was no contact made with the underlying bedrock. Assuming that the respective OSL

estimate of depositional age than the TL age (refer 6.5.3), then there is either a major change and/or hiatus in sedimentation sometime between 18 ky BP and 9 ky BP. There is also a less distinct change or hiatus in sedimentation between 6 ky BP and 3 ky BP. There is no significant change in the stratigraphy to represent a sedimentary hiatus, although the presence of two cobble layers between each of these two possible chronological ‘hiccups’ may be significant boundary markers (e.g. Robbins et al., 2000). These cobble layers were not found in adjacent profiles, so are unlikely to represent a lag deposit, and may represent an anthropogenic feature. The peaks in artefact (stone tool) density occur above and below these cobble layers, around 2.5 ky BP and 10 ky BP (Fig. 5.8).

The sand sheet excavation at Goorurarmum (Goor-1) effectively abuts the escarpment, and contact is made with an underlying bedrock horizon at about 2.5 m, which is dated to $14.3 \text{ ky} \pm 0.4 \text{ ky BP}$ (Fig. 6.21). It is possible that the base of the Goorurarmum excavation represents an LGM surface. Between 14 ky BP and 6 ky BP there is either an increase in sedimentation or there is a chronological hiatus that is not evident from the stratigraphy. However, a TL age of $9.2 \pm 0.1 \text{ ky BP}$ at 180 cm in an adjacent auger (Gu-2) effectively fills this chronological gap, and highlights the discontinuous nature of sedimentation on the sand sheets. The inversion between the OSL age of $4.3 \pm 0.1 \text{ ky BP}$ at 180 cm and the TL age of $6.1 \pm 0.1 \text{ ky BP}$ at 155 cm may indicate some secondary mixing of the sediment profile. Either way the results indicate a slightly faster rate of sedimentation than the Karlinga or Jinmium sand sheets, with up to 180 cm deposited over 6 ka (Fig. 6.21). The indication of a rapid depositional event at 100 cm or around 2.5 ka (refer 6.6.1) may have exacerbated this process. The peak in artefact density occurs in upper 50 cm or around 1 ky BP (Fig. 5.7).

The chronology obtained from the Jinmium sand sheet excavation and adjacent auger hole (Auger 4) (from Fullagar et al., 1996) indicates a relatively constant rate of sedimentation from about 10.5 ky BP. Fullagar et al. (1996) note that stone artefacts are found throughout the deposit, but no peak is documented. Between Jinmium and Goorurarmum, luminescence dating indicates that the sand sheets are older than 76 ky BP (Fig. 6.25), the basal age limited to the 6

m length of auger. The results from this study lend support to the luminescence chronology determined by Fullagar et al. (1996) for the sand sheet sediments near the Jinmium site, which provided an age of 103 ± 14 ky BP at 5 m depth (Fig. 6.25). Thus the most recent phase of sand sheet accumulation in the Keep River region may be of the equivalent age (but not depth, Fig. 7.6) to those in Arnhem Land, which began to develop at 220 - 230 ky BP and 100 - 120 ky BP: these ages coinciding with the start of the last penultimate and last interglacials respectively (Roberts, 1991).

The Jinmium and Goorurarmum catchments are at a similar or slightly lower relative level as the Karlinga catchment and only a few kilometres further inland. Hence it may be presumed that sequences older than 20 ky BP do exist around Karlinga but were not sampled or dated in this study (Fig. 6.26). Alternatively it is possible that the palaeosurface over which these sand sheets have accumulated at Karlinga occurs at a higher relative level, so that only the more recent (Holocene) period of sedimentation is preserved and is preserved differentially. In contrast, the older (early Pleistocene) sediments around Jinmium represent a topographic low. Compared to the redder sands near Jinmium, the more leached sands at Karlinga (refer 5.4.3.1) also indicate that the water table, and hence a less permeable barrier, occurs at a higher relative level at this site.

The implication is that in the absence of any obvious regional chronological hiatuses, the spatial range of the chronostratigraphy is essentially limited by the relative level of the present surface and underlying palaeosurface topography (refer 4.5.2). There is a greater representation of Holocene age sediments in all of the sand sheet excavations. The collective ages hint at a possible continuity, albeit spatially variable, between Pleistocene and Holocene levels. Such dynamic spatial (not temporal) distribution of sedimentation is likely to impress upon the preservation of archaeological deposits.

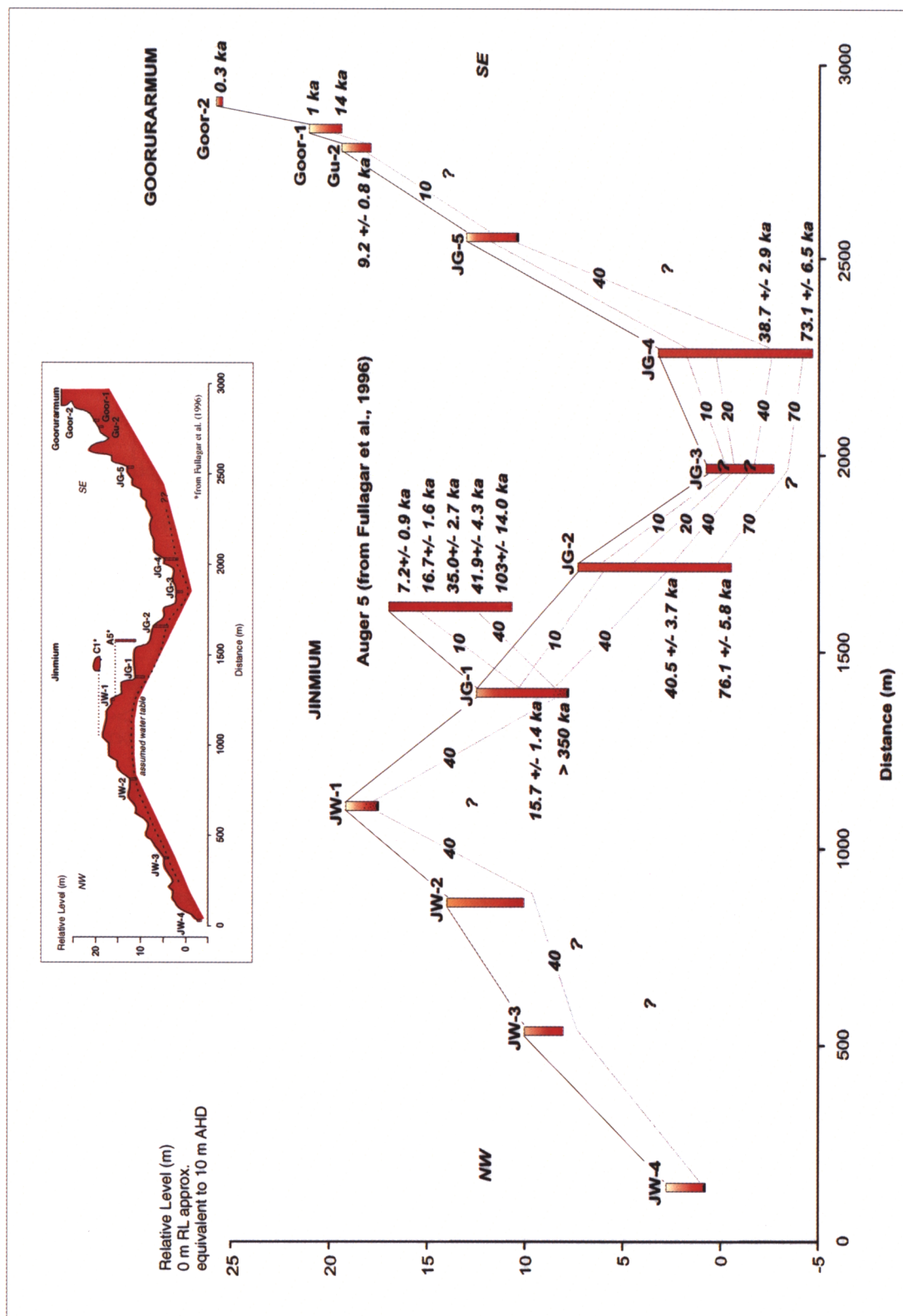


Figure 6.25 Chronostratigraphy of the Jinmium-Gooruramum transect (including dates from Fullagar et al., 1996).

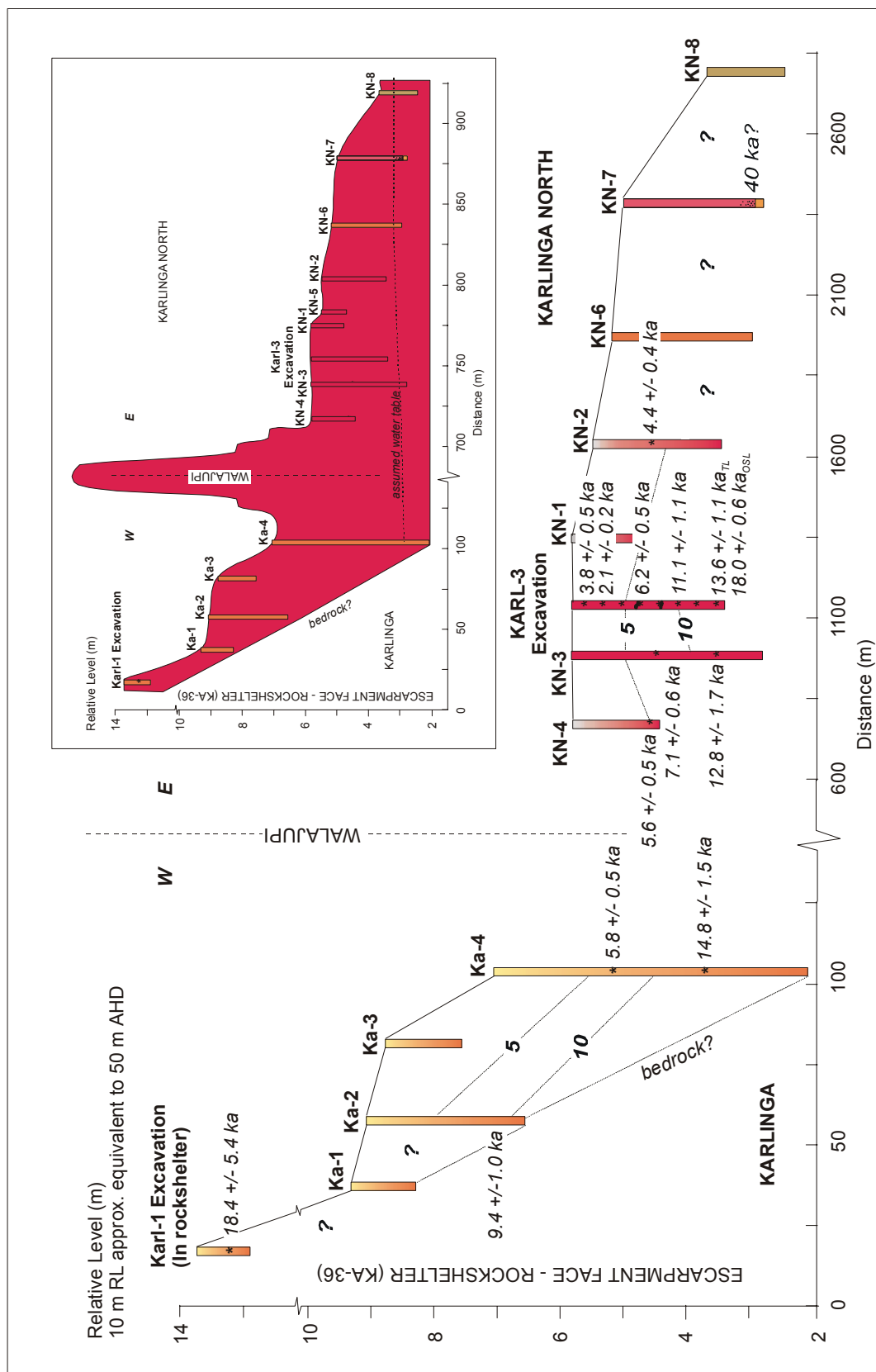


Figure 6.26 Chronostratigraphy of the Karlinga to Karlinga North transect.

6.6.2.2 Chronostratigraphy of Karlinga Creek and Sandy Creek

The calculated luminescence ages at the Karlinga creek site (KR99CP) (Fig. 5.9) imply there is an age inversion of the sediments. An age inversion might occur if well-bleached sediments were deposited at night (Bert Roberts, pers. comm., 2002), and although this may occur occasionally for one or two facies it is unlikely for an entire stratigraphic sequence.

Alternatively, inverted luminescence ages might partly be explained by water contents and dose rate calculations (Feathers and Bush, 2000). Neither the TL (Tables 6.1) and OSL (Table 6.2) palaeodose values, nor the dose rate values indicate a significant inversion. The best conclusion from these data is that ages of all four samples are similar, and reflect a mixed population of presumably water-laid and partially-bleached sediments. The combined palaeodose (mean value 12.6 ± 3.27 Gy) and dose rate (mean value 1.6 ± 0.52 Gy.yr⁻¹) values give a mean depositional age of 7.7 ± 3.16 ky BP. The sedimentary characteristics of this creek site are indicative of infilling of a small alluvial swamp (refer 5.4.3.2), which from the luminescence ages, may have occurred sometime after ~ 10 ky BP.

In Sandy Creek Gorge, the age of the pisolitic palaeosol which forms the creek bed is estimated from U-series dating to be about 45 ky BP (Fig. 6.27). Similar ages were found for pisolitic deposits in Arnhem Land (Roberts, 1991), whilst slightly older ages of 66 ± 12 ky BP were obtained from pisolites in the Gilbert River, northern Australia (Nanson et al., 1991).

According to Nanson et al. (1991), the induration of such ferricrete accumulations cannot occur during periods of sediment deposition, hence their presence provides a chronological marker of stratigraphic discontinuity. In the chronostratigraphic sections between Jinmium and Gooruramum (Fig. 6.25) and between Karlinga and Karlinga North (Fig. 6.26) the pisolitic deposits, wherever documented, are tentatively marked at 40 ky BP. However, not all pisolitic deposits are necessarily *in situ* and further dating is required before any regional interpretations can be made.

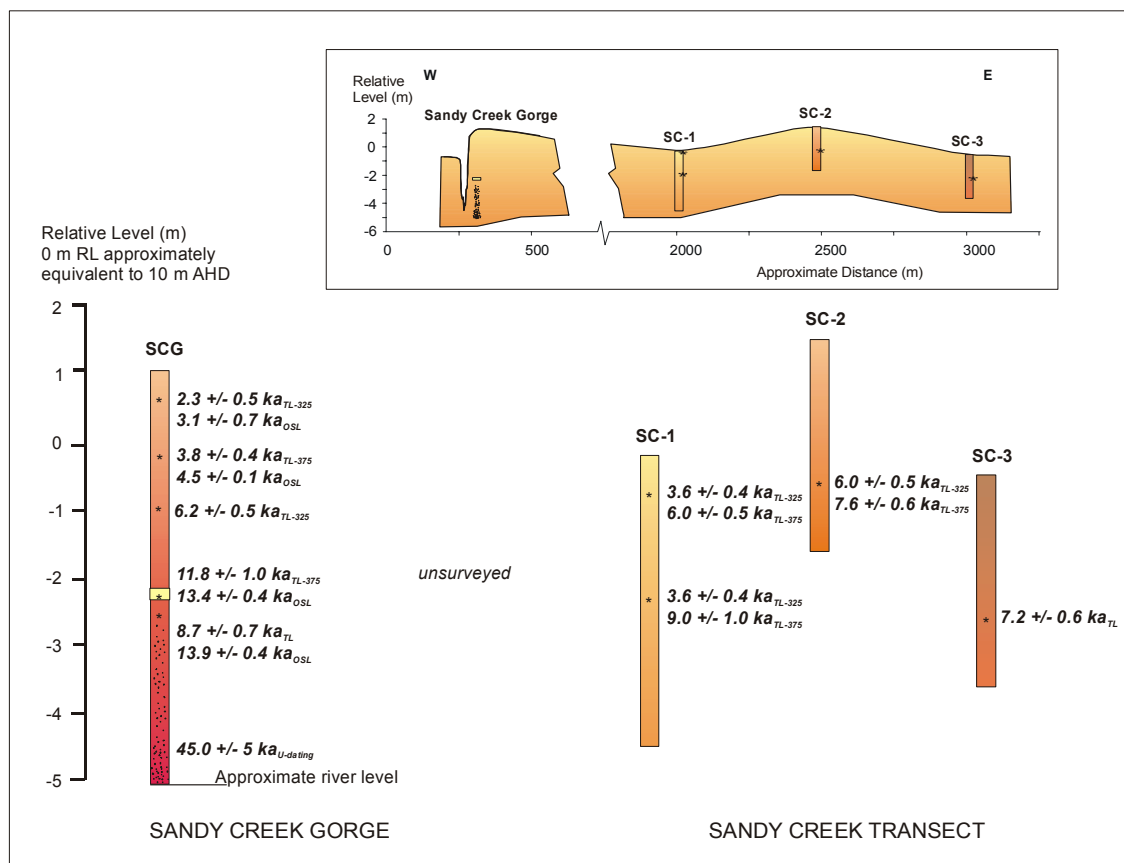


Figure 6.27 Chronostratigraphy of Sandy Creek Gorge and Sandy Creek transect. It should be noted that the TL age estimates are mainly derived from stepped plateaux and therefore represent maximum values.

At Sandy Creek Gorge, the pisolitic palaeosol is overlain by alluvial sediments dated by OSL from about 14 ky BP (Fig. 6.27). At shallower depths of 200 cm, comparative OSL ages of 6 – 8 ka are obtained for sand deposits at Sandy Creek Gorge and alongside Sandy Creek (Fig. 6.27). The majority of these show stepped TL plateaux (hence partial bleaching) which may signify the rapid deposition of these sediments. Stepped plateaux have also been observed in marine sediments from the Shoalhaven River by Price et al. (1999), which were to result from a rapid depositional event, such as a major storm or a tsunami.

The rapid deposition of the Sandy Creek sediments, may perhaps be compared with the infilling of Magela Creek in Arnhem Land at about 8 ky BP. Infilling of the Magela Creek occurred with sand supplied by gullyng of nearby sand aprons in association with the enhanced

monsoonal activity to the region during the post-glacial marine transgression (Roberts, 1991). Evidence of enhanced alluvial activity between 12 and 6 – 5 ka is also indicated from dated overbank deposits at Cabbage Creek, just south of Kununurra (Wende et al., 1997). Thus the proposed infilling of the Karlinga Creek site, alongside the rapid deposition of the sediments around Sandy Creek, may be indicative of a more regional event.

It is possible that as these smaller floodplain creeks became infilled, alluvial activity may have been concentrated in the main Keep River, just as it was in the main Magela Creek in Arnhem Land (Nanson et al., 1993: 298). This may have resulted in preferential preservation of some Pleistocene sequences, and follows Gregory's (1998) conclusion that the major aspect of archaeological preservation in the Ord-Victoria region is fluvial. The further implication is that at the regional scale continuous archaeological sequences may be preserved near major rivers, but at the site specific scale archaeological sequences may be better preserved away from major rivers. Consequently, just as the ecology in the Keep River region retains both continuity and change (Atchison, 2000), so to does the geoarchaeology (refer 2.3).

6.6.2.3 Chronostratigraphy of Rock-shelter Excavations

OSL determinations indicate that the rock-shelter sediments at Goorurarmum are well bleached and have accumulated over much less time (0.5 ± 0.14 ky BP) than those at Karlinga (18.5 ± 1.4 ky BP). Given the large boulders protecting the opening of the Karlinga rock shelter, the poorer bleaching characteristics are not unexpected. However, the significantly old age at Karlinga at such a shallow depth of 27 cm is surprising. The quartz grains in the Karlinga rock shelter have a consistently low regeneration ratio ($T_r/T_n \gg 1$) (refer 6.5.2.1), and are analogous to the weakly luminescent ('dim') grains in the Jinmium rock-shelter previously described by Roberts et al. (1999: 392). These weakly luminescent grains are probably derived from the slow disintegration of the overlying and surrounding bedrock and as such will not provide a reliable age estimate or sedimentation rate of these rock-shelter sediments using either TL or OSL dating techniques. Moreover the 18.5 ky BP age is inconsistent with the much younger

radiocarbon estimates of charcoal samples from the same sediments (refer 7.2.1), and also with other luminescence and radiocarbon ages for rock-shelter excavations undertaken in the Keep River region (Fig. 6.28 and Fig. 7.7). The divergence of luminescence dates on the age-depth curve (Fig. 6.23) further support the view that the sediments in both the Karlinga and Jinnium (C1) rock-shelter excavation probably include material from the overlying bedrock.

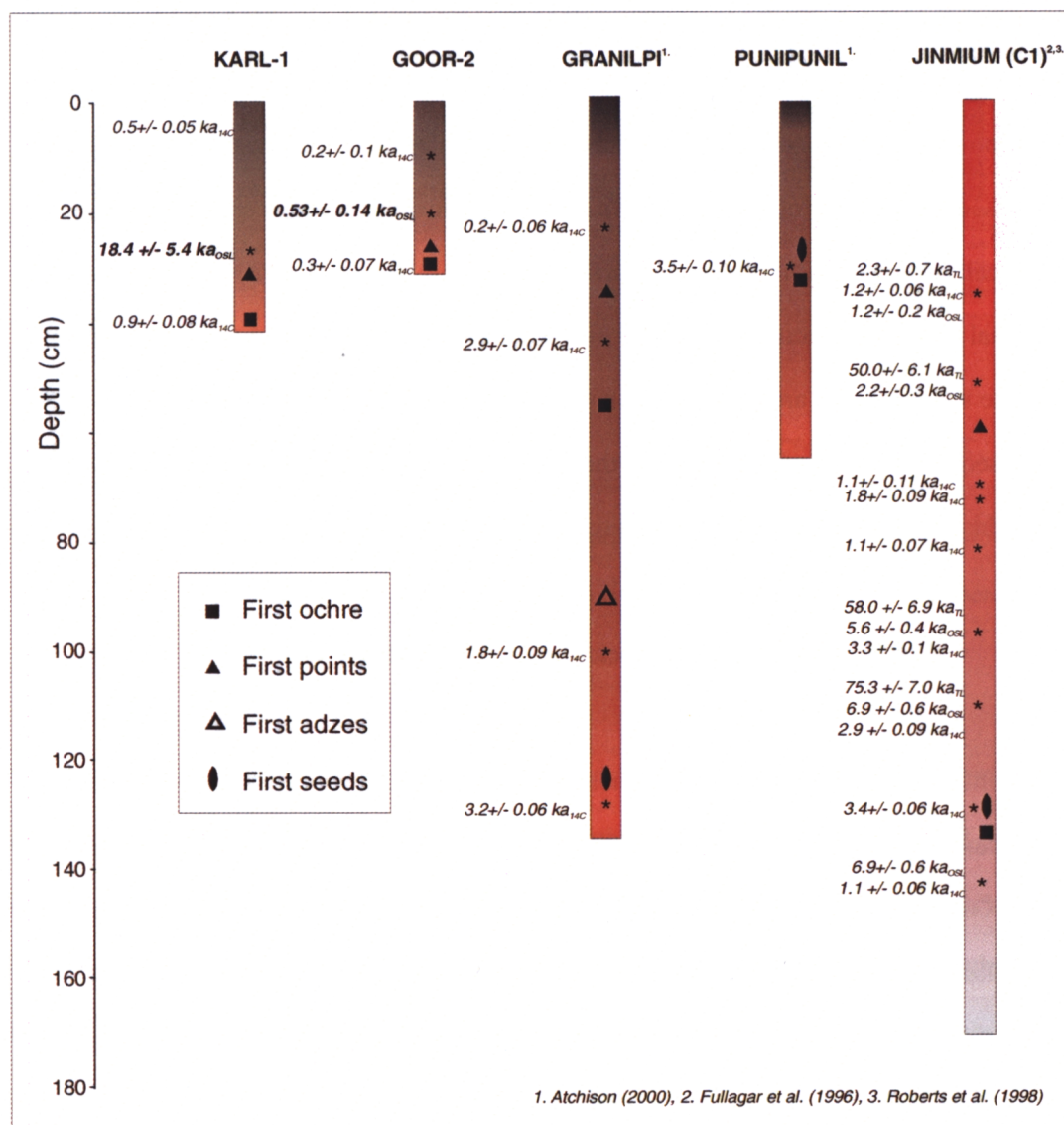


Figure 6.28 Ages and archaeological evidence from five rock-shelter excavations from past and present research in the Keep River region, including Karlinga (Karl-1), Goorurarmum (Goor-2) (this study), Punipunil (PP1), Granilpi (G1) (Atchison, 2000, Atchison et al., in prep.), and Jinnium (C1) (Fullagar et al., 1996; Roberts et al., 1998; Atchison et al., in prep.). The OSL ages for the Jinnium profile represent central age estimates from single-grain dating (from Roberts et al., 1998).

Roberts et al. (1998) argue that the true age of the Jinmium rock-shelter sediments should be bracketed by the minimum and central age estimates of 1.9 to 6.9 ky BP from single-grain OSL analyses. Thus, disregarding the 18.5 ky BP estimate for the Karlinga rock shelter, the rock shelters in the Keep River region are all late Holocene in age (Fig. 6.28). The earliest preservation of archaeobotanical (Atchison, 2000; Atchison et al., in prep.) and stone artefact records (Fullagar et al., 1996) is also around 4 ka. The OSL age of the sediments in the Goorurarmum and Karlinga rock shelters are younger than that indicated from presence of points (Fig. 6.28), indicating that representative sediments from the period of point production have been reworked or lost, or that the points themselves have been moved or reworked. The seed and stone artefact chronology for Granilpi and Jinmium are considered to generally support the young sediment chronology provided by the OSL and radiocarbon dates (Atchison, 2000; Atchison et al., in prep.), despite any apparent disturbance or contamination (Roberts et al., 1998).

The luminescence ages of the surrounding sand sheets sediments correspond with the main regional trend and validate the Pleistocene age of the surrounding sand sheet sediments. So both the Jinmium and Karlinga rock-shelters comprise sediments and associated cultural sequences that are much younger than those outside the rock shelter. The presence of older and deeper deposits outside rock shelters has also been noted in Kakadu (Allen and Barton, 1989), and north Queensland (Morwood, 1981; Morwood et al., 1995). Thus, contrary to the view that enclosed rock-shelters offer greater potential for older sequences (Lourandos and David, 1998), better preservation of older sequences may actually be found in more open sites. However, the antiquity of the rock art record is not necessarily predicated by either the luminescence age of the rock shelter or the adjacent sand sheet sediments (refer also Bednarik, 2002). Further discussion of the stone-artefact and rock art record is given in Chapter Seven (refer 7.3).

6.7 Conclusions

Useful age determinations are gained from both TL and OSL analyses of rock-shelters and sand sheets of the main archaeological sites of Goorurarmum, Jinmium and Karlinga and also from the non-archaeological site of Sandy Creek Gorge. Whilst OSL ages are considered more reliable estimates of depositional age, TL plateaux and glow curves are useful for discerning depositional processes - normal TL plateaux indicate well-bleached sediment, foreshortened TL plateaux may indicate episodic rapid deposition (e.g. mass wasting), stepped TL plateaux may indicate partial bleaching (e.g. storm event) or partial re-exposure, and differing glow curves within or between sequences may indicate differing provenance of source sediments (refer also Price, 1994b). Attempts to obtain a more accurate assessment of radionuclide mobility and dose-rate by high-resolution techniques have been problematic. Radionuclide ratios indicate secular equilibrium in the uranium- and thorium-series decay chains, and justify using TSAC results for age calculations.

Whilst a young age (~ 500 yrs) for the Goorurarmum rock shelter is acceptable, the Pleistocene age (~ 18 ky BP) of the Karlinga rock shelter is less certain. The sedimentary record in the Keep River region is temporally and spatially discontinuous. The sand sheets around Jinmium and Goorurarmum have possibly been accumulating since the last interglacial (~100 ky BP), whereas only the last glacial (~ 20 ky BP) is represented in the sand sheets around Karlinga (although the latter have not been dated to the bedrock base). Sedimentation rate has progressively increased from 100 mm.ka⁻¹ during the Pleistocene to 200 mm.ka⁻¹ during the Holocene, in both unoccupied and unoccupied sediment sequences indicating this increase is probably due to environmental rather than anthropogenic processes. The geomorphic relationship between the rock shelters and adjacent sand sheets remains to be accurately determined, as does the age relationship between these sedimentary records and the rock art.

CHAPTER SEVEN

Connecting the Local and Regional Sedimentary and Archaeological Records

The success of geoarchaeological investigation and indeed of archaeological research in general, depends ultimately on open and mutual exchange of information across the artificial boundaries of various disciplines.

-Hassan, 1978: 211.

7.1 Introduction

This chapter brings the geochronological and sedimentary investigations of the escarpments and sand sheets into the context of the local and regional archaeological records. Some of the issues outlined in Chapter Two are revisited, including issues of quantifying, identifying and interpreting change in the archaeological records. Archaeological information for the Keep River region is sourced from published and unpublished research in the areas of archaeobotany, rock-art studies, and archaeological excavation and analysis. The occupation record for the Keep River region is then evaluated in the more regional context of the Kimberley and adjacent Arnhem Land regions. General thesis conclusions and suggestions for further research are presented in Chapter Eight.

7.2 Quantifying Change - Comparison of Chronological Records

Stratigraphic resolution is determined by the temporal spacing between preserved depositional events, and defined within the resolving power of each dating technique. The following section compares the chronological records obtained from *in situ* cosmogenic dating, luminescence dating and radiocarbon dating in the Keep River region; contributing to a more general discussion of the local and regional geochronology in section 7.6.

7.2.1 Comparison of *in situ* Cosmogenic and Luminescence Dating Results

The results from *in situ* cosmogenic dating, luminescence dating and sediment characterisation can be used to provide an indication of sedimentary processes across the sand sheets from the erosional sources to sediment sinks. The slow denudation (5 mm.k^{-1}) of the sandstone escarpments provides the main source of sediment to the adjacent sand sheets, which periodically accrete over a previously exposed palaeosurface. The accumulation of sand over this palaeosurface is temporally and spatially discontinuous with greater accommodation space for sediment accumulation away from the escarpment. Accordingly the age of the sediments near the escarpments and within rock shelters is younger than that further from escarpments. The rate of sediment accumulation is slowest near the low-energy escarpments ($< 100 \text{ mm.k}^{-1}$) and greater near the high-energy creeks and rivers ($> 200 \text{ mm.k}^{-1}$) where there are a greater number of sediment sources.

Between the escarpments and the creeks, the sand sheets are in-transit zones for sediment storage. The minimum accumulation rates of the sand sheets are 133 mm.k^{-1} at JG1 (based on TL age at 210 cm) and $7 - 10 \text{ mm.k}^{-1}$ at JG2 (based on TL ages at 390 and 560 cm), which are 5 – 20 times greater than the cosmogenic rate of $5 - 20 \text{ mm.k}^{-1}$ for the same profiles. Turnover rates by termites in similar sandy terrain has been estimated to be in the order of $20 - 50 \text{ mm.k}^{-1}$ (Williams, 1968; Holt et al., 1980; Colin et al., 2001), which may amount to 20 – 50 % of apparent accumulation rates. Such mixing will induce significant scatter in both the cosmogenic (refer 4.4.2) and OSL data (refer 6.5.2.1) and will make OSL ages appear too young and the apparent sedimentation rate higher than the actual net rate. Thus some of the inconsistency between the estimated sediment accumulation rate of the sand sheets from luminescence dating and *in situ* cosmogenic dating may be due to mixing. It is reasonable to expect that the scale of such mixing will be greater over longer-term timescales.

The differences also reflect the chronometric sensitivity of each technique - *in situ* cosmogenic dating which measures over timescales of 100 ka to 2 Ma is much less sensitive to more disparate

episodes of erosion, transport, deposition and preservation of sediment horizons than luminescence dating which measures over timescales of 10 ka to 200 ka. However, there is some overlap. If the regional age-depth curve of luminescence ages (from Fig. 6.23) is extended over longer timescales using a logarithmic axis (Fig. 7.1), the trend is towards lower accumulation rates. Based on this figure, Holocene accumulation rates range from 100 - 250 mm.ka⁻¹, for the LGM to Holocene period, 50 – 100 mm.ka⁻¹, and since the last interglacial (Stage 5), 20 – 50 mm.ka⁻¹. Estimates from cosmogenic isotope dating are consistent with these trends.

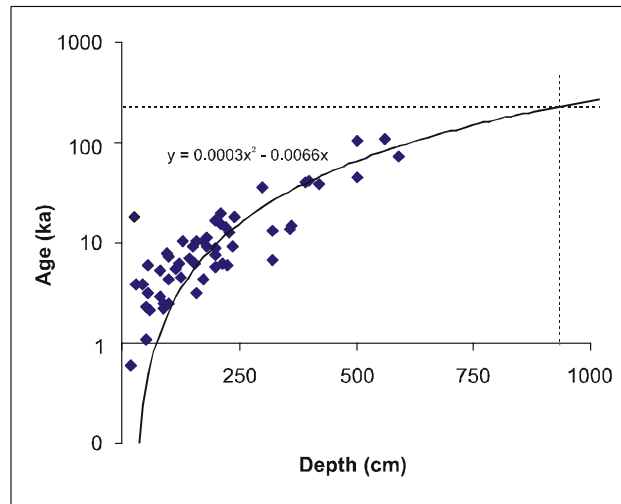


Figure 7.1 Equivalent plot to the regional age-depth curve depicted in Figure 6.23 (excluding Jinnium rock shelter ages), using a logarithmic axis for age (ka). The plot indicates a trend towards lower accumulation rates over longer term timescales.

Over human timescales, sedimentation on the sand sheets is likely to be out of equilibrium with both these longer term estimates. In the Selima sand sheets, Egypt, stratigraphic, archaeological and radiometric dating of materials indicated a dynamic equilibrium over timescales of only tens of years, with sediment supply matched by transport across the sand sheet, contrasting with slow vertical accretion over timescales of hundreds to thousands of years (Maxwell and Haynes, 2001). It is clear that in the Keep River region there must also be some disequilibrium of longer and shorter term dynamics otherwise the bedrock would eventually be buried by the faster accumulating sand

sheets (refer 4.6). Essentially *in situ* cosmogenic dating is used to provide a geomorphological story. The remainder of this chapter considers the archaeological record from timescales provided only by luminescence and radiocarbon dating.

7.2.2 Comparison of Radiocarbon and Luminescence Dating Results

Direct comparison of age estimates from radiocarbon dating with those from TL and OSL dating (Table 7.1) indicate a correspondence between 6 of the 12 samples. With the exception of Spit 17 in the Karl-3 excavation (Table 7.1), there is a good correspondence between radiocarbon ages and luminescence ages in the first metre of both the Goorurarmum and Karlinga sand sheet deposits. The correspondence between radiocarbon and luminescence ages to this depth in these sand sheets attests to the minimal disturbance and general homogeneity of the organic and inorganic material being dated. The major discrepancies occur between luminescence and carbon samples from the Karlinga rock shelter (Karl-1) and from the Karlinga sand sheet (Karl-3). The results for OZG337 and OZG338 derive from NaOH soluble extracts of charcoal, and should be reliable (Head, pers. comm., 2003). Some inconsistency is not unexpected for the two radiocarbon results OZG339 and OZG240 (Table 7.1), which derive from fine grained organic material and may be more mobile in the sediment profile (Head, pers. comm., 2003). Nor is it unexpected for there to be a poor correlation between OSL and radiocarbon ages in either of the rock-shelters, where the OSL age is extrapolated from only a single OSL estimate (particularly for Karl-1 where the OSL is considered to be unreliable). The only inexplicable radiocarbon age is that from Spit 17 in the Karl-3 excavation (^{14}C 0.7 ± 0.09 ka *c.f.* OSL 2.5 ± 0.12 ka), which may simply reflect local contamination by young charcoal.

Table 7.1 Comparison of radiocarbon dating results with measured and extrapolated luminescence age estimates for equivalent depths in the rock shelter and adjacent sand sheets at Goorurarmum and Karlinga. Extrapolated luminescence ages are essentially estimated from a line drawn through dated samples of known depth in the same sequence back to the origin. Samples with a ‘Wk.’ lab code comprise < 125 um material, whereas samples with an ‘OZ’ lab code comprise finer grained or degraded carbon material.

Sample Name	Depth (cm)	Laboratory Code	$\delta^{13}\text{C}$	Age (Cal BP)	Measured OSL Age (BP)	Extrapolated TL/OSL Age (BP)
Goor 1 – Spit 4	16	Wk 10779	-25.5 ± 0.2	Modern	-	200 ± 10
Goor 1 – Spit 21	100	Wk 10780	-25.8 ± 0.2	2536 ± 105	2530 ± 70	-
Goor 1 – Spit 21	100	OZG337		2780 ± 40	2530 ± 70	-
Goor 1 – Spit 35	175	OZG339		3680 ± 50	5200 ± 80	
Goor 2 – Spit 3	7	Wk 10781	-25.6 ± 0.2	Modern	-	185 ± 10
Goor 2 – Spit 11	27	Wk 10782	-23.4 ± 0.2	286 ± 71	-	720 ± 40
Karl 1 – Spit 3	6	Wk 10783	-26.3 ± 0.2	484 ± 45	-	5600 ± 300
Karl 1 – Spit 12	39	Wk 10784	-25.8 ± 0.2	917 ± 76	-	36 300 ± 1800
Karl 1 – Spit 12	39	OZG338		4080 ± 40	-	36 300 ± 1800
Karl 3 – Spit 17	85	Wk 10788	-24.4 ± 0.2	708 ± 57	2500 ± 120	-
Karl 3 – Spit 20	100	Wk 10789	-24.7 ± 0.2	3619 ± 122	-	3600 ± 180
Karl 3 – Spit 31	155	OZG340		2810 ± 40	11 400 ± 170	-

The results of all past and present radiocarbon data and luminescence data for occupation deposits over the past 20 ka are shown in Fig. 7.2. It is apparent that, whether calculated from radiocarbon or luminescence dating, most occupation deposits preserved in the Keep River region are Holocene in age. Radiocarbon ages are generally younger for the same depth than luminescence ages, which

may in part reflect the different age range of multiple sediment populations as measured by multiple and single-aliquot luminescence dating.

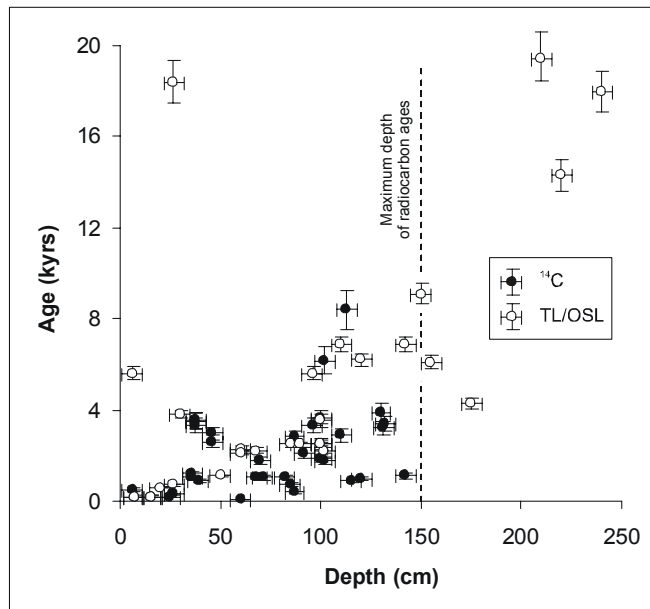


Figure 7.2 Comparison of luminescence ages and radiocarbon ages (including Atchison, 2000; Roberts et al., 1998) for archaeological sites in the Keep River region over the past 20 ka. Note, radiocarbon ages do not extend beyond 150 cm.

No radiocarbon ages have been obtained at depths greater than 150 cm (Fig. 7.2) and this most likely reflects *in situ* weathering processes beyond these depths, such as water table changes, rather than any sampling bias (J. Head, pers. comm., 2002). At Nauwalabila, for example, Fifield et al. (2001) observed that beyond this depth radiometric ^{14}C ages were unreliable, coincident with the appearance of pisoliths, which themselves indicate a previous fluctuating water table. Similarly, in the Jinmium rock-shelter excavation, fruit seeds were noticeably weathered and declined in number with depth indicating that this record was influenced more by preservation factors rather than cultural processes (Atchison et al., in prep.). The implication is that some of the deeper radiocarbon ages in the Keep River region may be less reliable and should be assessed in the context of the

material dated and the sedimentary environment. This does not imply that all radiocarbon ages beyond 150 cm are meaningless, and less so if careful extraction procedures (e.g. Bird et al., 1999; Fifield et al., 2001) are used. However, in occupation sequences deeper than 150 cm where radiocarbon dates appear unreliable or unobtainable, other dating techniques may be required.

7.3 Identifying Change

In contrast to the stratigraphic resolution determined from the duration between preserved depositional events, depositional resolution is determined by the temporal span of physical records preserved within the sediment horizons (Kowalewski and Bambach, 2001). In effect, depositional resolution represents the archaeological record (e.g. artefacts, seeds). The typical temporal range of both types of resolution is comparable over hundreds to thousands of years, but whereas stratigraphic resolution is controlled more by geomorphic and climatic factors and depositional resolution is controlled primarily by temporal mixing through bioturbation and taphonomic processes (Kowalewski and Bambach, 2001). The following is a step towards quantify depositional resolution in the Keep River sand sheets.

7.3.1 Depositional Resolution

The appearance of undisturbed sediments is no guarantee of stratigraphic integrity (Richardson, 1992). The movement of stone artefacts in seemingly cohesive sandy deposits has been estimated to be in the order of 50 - 80 mm in Nauwalabila I (Jones and Johnson, 1985) and up to 30 cm in Kenniff Cave (Richardson, 1992). Hughes and Lampert (1977: 136) indicate that a zone of 20 cm or so that has been affected by deliberate occupational disturbance (e.g. trampling) could easily cover hundreds or thousands of years. Given that well over half the dated archaeological sites in the Kimberley including the Keep River region relate to sandy deposits of a metre or less, these

estimates translate to at least 20 – 30 % of the entire deposit or timespan measured. For Kenniff Cave, this amounted to a temporal resolution no better than 2.5 ka (Richardson, 1992). For deeper sites such as the Karlinga sand sheets, the resolution is probably shorter than 1 ka years, but for shallow sites such as the Karlinga rock shelter, the entire artefact chronology may be questionable. Temporal mixing of hundreds or thousands of years is probably the rule rather than the exception (Kowalewski et al., 1998).

The extent of bioturbation is an important factor on archaeological and chronological interpretations (refer 2.4.2). The introduction of points around 3 ky BP in the Keep River region (Fullagar et al., 1996: 764; Atchison, 2000; Boer-Mah, 2002: 38) represents a useful chronological marker, which if it differs significantly from the chronology (e.g. from radiocarbon or luminescence dating) may indicate the extent of disturbance in the sediment profile. There is no reason to assume that points would appear at exactly the same time at all sites – the temporal differences may well include dating and taphonomic error, but may also include real regional variability. Nevertheless, excepting the Karlinga rock-shelter where there is some doubt the OSL age estimates, the date of introduction of points in the occupation sequences of the sand sheets (Fig. 6.24) and rock-shelters (Fig. 6.28) averaged from luminescence and radiocarbon dating of the sediments is 3.3 ± 0.15 ka. The correspondence between the point and sediment chronology indicates that the degree of disturbance is within the ~ 10 % error of temporal resolution provided by these two measures. For Holocene sedimentation rates around 200 mm.ka^{-1} this translates to a disturbance rate of about 20 mm.ka^{-1} , which is equivalent to previous estimates of termites reworking (Holt et al., 1980; Colin et al., 2001).

As such, the estimated rate of bioturbation is less than the estimated rate of sand sheet accumulation of $100 - 200 \text{ mm.ka}^{-1}$ from luminescence dating, and is supported by the largely sequential radiocarbon and luminescence chronology shown in the occupation profiles (Chapter Six). Preservation of stratified organic layers in at least one of the creeks studied indicates that

bioturbation may also be reduced in more wet or stagnant environments (5.4.3.2). However, bioturbation may be more significant over horizontal surfaces rather than vertically (e.g. Fanning and Holdaway, 2002), and the possibility that bioturbation does influence some aspects of the archaeological record cannot be discounted.

Other secondary mixing processes may influence the archaeological record. For example, in the Goor-1 sand sheet there is an indication of grain-size sorting through illuviation such that the modal grain size will decrease as finer material is concentrated in deeper horizons (Fig. 7.3). The similar pattern of mean grain size and artefact numbers (2 – 4 mm fraction) with depth in the Goor-1 profile (Fig. 7.3) also indicates that the possibility of some preferential sorting of the archaeological record through secondary mixing processes cannot be entirely overlooked.

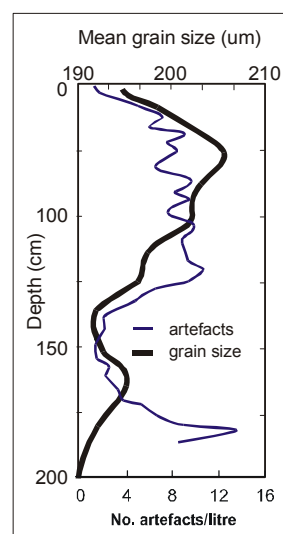


Figure 7.3 Profile of mean grain size and artefact (2 – 4 mm) numbers with depth in the Goorurarmum (Goor-1) sand sheet. Both these trends may reflect natural processes.

A more accurate measure of the integrity of the artefact record and the scales over which disturbance processes overlap with it may be better defined from micro- and meso-scale

sedimentary features. Preliminary petrographic and microscopic observations of sedimentary quartz from this study showed more evidence of diagenetic alteration than post-depositional transport (refer Fig. 5.15). Assuming any of the crypto-crystalline quartz grains in the occupational sequences represent cultural material from flaked stones, the presence of iron-rich clay coatings indicates that they have undergone the same diagenetic processes and have probably been buried for the same period as the surrounding grains. The identification of microdebitage in sandy archaeological sites, including the Keep River region, is the subject and expertise of present doctoral research by Susino (in prep.).

7.4 Interpreting Change

7.4.1 Cultural versus Natural Processes - The Stone Tool Record

A major quandary in using abundance estimates of artefact material as evidence of apparent discard rates or of site use, is deciding what unit of measurement to use. From a broad methodological perspective, the production of a few large stone tools may have left little (albeit relatively weighty) debris whereas the adoption of microlithic technology and unifacial and bifacial point manufacture may have increased the number, but not necessarily the weight, of flaked stone pieces. Other percussion techniques, such as quartz bipolar flaking, may produce more flake debitage than point production, depending on the raw materials used (Fullagar, pers. comm., 2003). In addition to these cultural processes, stone artefacts may be broken, burnt and weathered by natural processes that will affect interpretations of assemblage size and composition (Hiscock, 2002). A more careful consideration may be to correlate, where possible, changes in stone artefacts with other artefact material such as ochre, charcoal, bone, and shell, and/or with the total number of occupation sites in an area (e.g. Fullagar et al., 1996). Alternatively, data may be normalised to remove changes in, for example, sediment accumulation (Ward and Larcombe, 2003). Variations in sedimentation rate,

whether due to cultural or natural processes, are an important consideration when evaluating the intensity of site use as a function of the density of artefacts or fauna (Farrand, 2001: 547).

Figure 7.4 shows the rate of artefact accumulation in the Goorurarmum sand sheet excavation (Goor-1), measured both by number and weight, as a function of sedimentation rate. The onset of occupation or artefact accumulation is not specifically defined, and for calculation purposes, the uppermost spit is given a nominal age of 10 years. The uppermost spit is given a nominal age of 10 years.

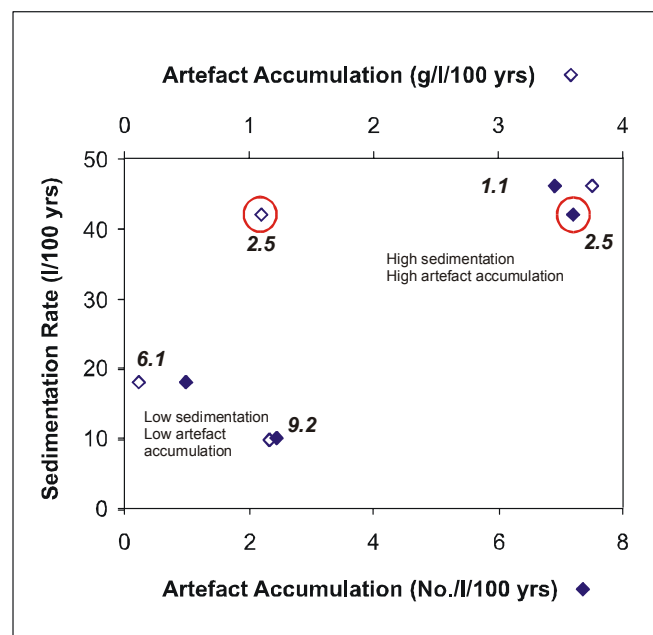


Figure 7.4 Plot of artefact accumulation rate against sedimentation rate (litres/100 years) for the archaeological excavation site of Goor-1. Artefact accumulation is measured both as the number of artefacts per unit time (closed diamonds) and weight per unit time (open diamonds) and normalized against total volume of sediment. Numbers refer to the lowest age (ky BP) of each sediment interval. The circled points indicate the large differences where there are low artefact numbers but a high artefact weight (e.g. a single core stone).

At 2.5 ky BP the artefact weight indicates a much smaller increase in the rate of artefact accumulation with increasing sedimentation than the artefact numbers (Fig. 7.4). The general increase in both the rate of artefact accumulation and sedimentation may simply reflect high preservation with rapid rates of burial and visa-versa for low rates of burial. Data from the Karlinga sand sheet excavation (Fig. 7.5) shows a similar general correspondence in the rate of artefact accumulation and rate of sedimentation.

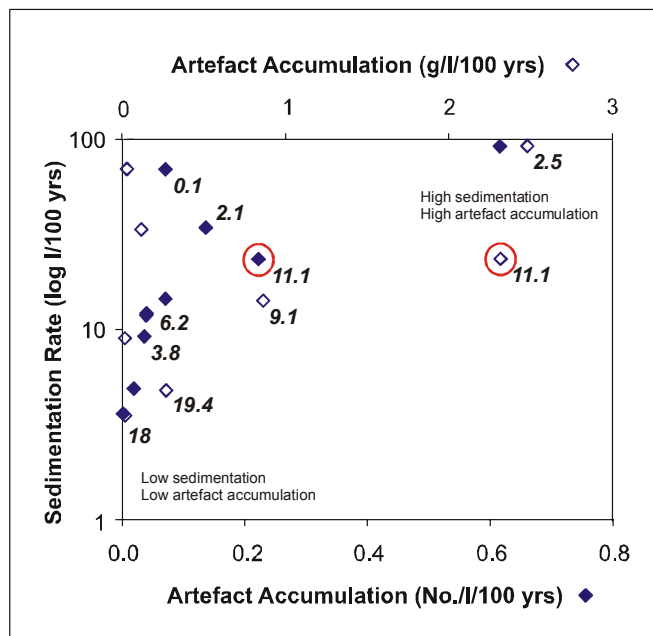


Figure 7.5 As for Figure 7.4, for the archaeological excavation site of Karl-3. Note, for clarity, the rate of sedimentation is plotted on a log scale. Numbers refer to the lowest age (ky BP) of each sediment interval. The circled points indicate the large differences where there are low artefact numbers but a high artefact density (e.g. a single core stone).

The onset of occupation or artefact accumulation again is not specifically defined, and the uppermost spit is given a nominal age of 100 years. The rate of change at 2.5 ky BP is calculated from 0.1 ky BP rather than 3.8 ky BP as the latter gives a negative value for both sediment accumulation and artefact accumulation. For the deepest part of the sequence, only the OSL ages of

18 ky BP and 19.4 ky BP are used. The results show a peak in the rate of sedimentation and artefact accumulation around 11.1 ky BP (Fig. 7.5), with weight indicating a significantly higher rate of artefact accumulation than the artefact concentrations. After 11.1 ky BP, the sedimentation and artefact rates fluctuate (Fig. 7.5).

The implication from both excavation records is that high sedimentation rate and high artefact numbers do not necessarily indicate greater discard per unit time, but rather greater preservation per unit time (refer also Farrand, 2001). In other words there is no reason to invoke a cultural explanation for any increase or decrease in the rate of artefact accumulation, because these can be explained readily from sedimentary processes. As pointed out by Hiscock (1984: 133-135), when offering explanations for variability in the archaeological record, post-depositional factors and taphonomic processes, must be considered first before explanations of human behaviour can be considered.

Comparison between these and other sites may begin to reveal patterns in the archaeological and sedimentary record that are indicative of wider landscape processes. For example, in both records the artefact and sediment accumulation rates around 2.5 ka, when the climate is drier, are significantly greater than those earlier around 9 and 6 ka, when wetter monsoonal conditions prevailed (refer 3.5). The low artefact and sediment accumulation rates around 18 ka in the Karlinga sand sheet may be associated with the more arid conditions during the LGM. Local environmental and/or cultural factors may also be important as the correlation of artefact and sediment accumulation rates with climatic conditions is far from absolute.

7.4.2 Rock Shelters - The Rock Art Record

Basal OSL ages for the Goorururumum rock shelter and adjacent sand sheet excavation are 0.3 ± 0.07 ka and 14.3 ± 0.4 ka respectively. The near-basal OSL ages for the Karlinga rock shelter and more distant sand sheet excavation are 18.4 ± 5.4 ka and 18.0 ± 0.6 ka respectively. An 18 ka age for the Karlinga sediments would imply a considerable hiatus period for these shallow sediments. Hiatuses are not easily recognised in rock shelter and cave sediments and these can give a false impression of continuity (Farrand, 2001). However, the more conservative radiocarbon age of 4.1 ± 0.04 ka (Table 7.1) is favoured for the Karlinga rock shelter as this corresponds better with the presence of stone points just above the radiocarbon sample depth (Fig. 6.28).

From these ages it is apparent the sand sheets preserve a much older record (or time span) than the rock shelters in the Keep River region, demarcating the rock shelters as temporary storage systems for sediments and archaeological material (*c.f.* Lourandos and David, 1998). In effect ancient sedimentary material is constantly overwhelmed by younger material through natural and cultural processes, and the inefficiency of the rock shelter as a sediment trap (*c.f.* Fullagar et al., 1996). Often the evolution of stratigraphic sequences is either bedrock controlled or is strongly dependent on the morphology of the floor created by the earliest phase of roof fall (O'Connor et al., 1999). The evolution of stratigraphic sequences on the sand sheets may be similarly controlled by bedrock morphology (refer 4.5.2 and 6.6.2.1).

As a consequence of this differential preservation, younger rock shelter sediments may theoretically be linked with younger rock art, whilst the older sand sheet sediments may be linked with more ancient rock art. Figure 7.6 illustrates possible depositional relationships between the rock art and adjacent sediments, in which previously buried bedrock surfaces, and older surfaces may have been re-exposed by erosion of all or part of any overlying sediments. In Scenario A, the exposed rock art

may relate to the contemporary sediment horizon (Period 1), or to an unrepresented (eroded) horizon (Periods 2 and 3). In Scenario B, the rock relates to an exposed contemporary horizon (Period 1) or subsequently to a buried horizon (Period 2). Re-exposure of the buried horizon (Period 3) would modify the luminescence age, although representative radiocarbon estimates or artefact material may still provide an accurate age of the rock art.

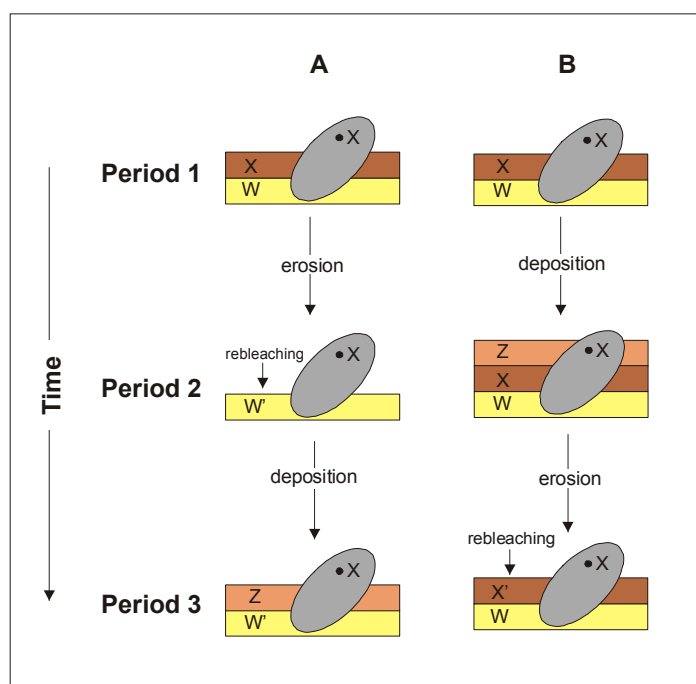


Figure 7.6 Possible scenarios for sedimentation and rock-art dating. Horizon 'w' represents a sterile surface, over which is deposited an archaeological horizon 'x' that is contemporaneous with the rock art surface (x). In scenario A, the archaeological horizon 'x' is eroded, re-exposing horizon 'w' which is older than the rock art surface. Horizon 'z' is subsequently deposited over horizon 'w', and is younger than the art surface. Neither surface relates to the age of the rock art. In scenario B, the younger horizon 'z' is deposited immediately over horizon 'x'. Subsequent erosion of horizon 'z' would re-expose horizon 'x'. Luminescence dating of the modified surface (x') would underestimate the age of the rock art.

From AMS ^{14}C radiocarbon of associated oxalate crusts, the minimum age of the cupules in the Keep River region is mid-Holocene and possibly older than 5.8 ky BP (Watchman et al., 2000). Thus, the cupules were made at or prior to the onset of sand deposition in the rock shelter (Spooner, 1998; Roberts et al., 1998a; 1999; Atchison, 2000). Watchman et al. (2000: 8) speculated that late Pleistocene-early Holocene sediments dating to the time of cupule formation may have been eroded as they have in other parts of the Kimberley (refer 7.4.3 below). However, this hiatus period is not noted in the Keep River region so the cupules could have been made at any time. Thus in the absence of longer sedimentary records in the rock shelters, and until a more accurate age of the rock art is provided, the association of rock art and shelter sediments will remain hypothetical. Samples of rock crusts have been taken from several sites with Bradshaw-style paintings, such as that depicted in Fig. 1.7(a), for such analyses. Given the preservation of occupation sequences of up to 18 ka in the adjacent sand sheets, it is possible that equivalent age sediments to the rock art do exist in the Keep River region. More detailed archaeological studies of the rock shelters in the Keep River are provided by Atchison (2000) and a comparison of rock shelters and open occupation sites is provided by Boer-Mah (2002).

7.4.3 Open Sites – The Climatic Record

The dynamics of the landscape may provide an important palaeoenvironment context for the archaeological record (refer 2.5.3). From geomorphic evidence around Lake Gregory (Fig. 7.9), Wyrwoll and Miller (2001) established that the summer monsoon was not operational from the period of the LGM until about 14 ky BP. If true, it might be expected that sites in the Keep River region older than 14 ky BP should show a corresponding facies change in the sediments (John Head, pers. comm., 2002). However, they do not. Most of the sandy sediments in the Keep River region are petrographically, mineralogically and geochemically uniform (refer Chapter Five) and do not show evidence of palaeoclimatic or palaeoenvironmental changes. This is not so improbable

given the consistent transport processes (runoff, mass transport, sheet flow), low source variability (mostly quartz sandstones), and extreme weathering regime (which preserves only resistant inorganic minerals) of at least the past 100 ka. In addition, secondary mixing processes may obliterate any stratigraphic differentiation which might have been present (Ward and Larcombe, 2003). Vegetation may destroy stratigraphic integrity, and indeed the presence of vegetation is thought to contribute to the sheet-like nature of sand deposits that would otherwise form dunes (Woodroffe et al., 1992).

The geomorphic and chronological evidence from Sandy Creek Gorge indicates that there was a decline in a forest community (e.g. *Melaleuca*, rainforest or vine thicket) around 13 ky BP (OSL age). The degraded indurated horizon at Sandy Creek Gorge may represent a past equivalent of the contemporary association of isolated monsoon rainforest patches with dolomite outcrops (Atchison, 2000) (refer 5.4.3.2). Pollen records from the nearby Flying Fox Springs site, in the Keep River National Park, also indicate the persistence of a vine-thicket community along the surrounding floodplains dominated by *Guettarda* sp. until a few hundred or one thousand years ago, after which *Melaleuca* sp. became dominant (J. Luly, pers. comm., 2000). The Flying Fox swamp itself also indicates a change in vegetation at about 12 ky BP, from fire-infested grassland to pandanas and sedges (J. Luly, pers. comm., 2000). Further west in north Queensland, charcoal collections indicate expansion of Eucalyptus woodlands between 13 and 8 ky BP, with reinvasion of rainforest during the Holocene (Hopkins et al., 1993). These vegetation changes may all be part of more regional trends across northern Australia, which are associated with rising sea-levels (refer Fig. 3.12) and major climatic changes (Torgersen, et al., 1988).

Other major palaeoclimatic and palaeoenvironmental phases in northern Australia include the post-glacial marine transgression from 18 – 6 ky BP, and the concomitant increase in estuarine conditions, including the ‘big swamp’ phase around 8 - 7 ky BP (Woodroffe, 1993), the gradual

return of the summer monsoon around 7 ky BP (Schulmeister, 1999), and the pluvial maximum and increased freshwater conditions around 4 ky BP (Schulmeister, 1999). It is improbable that there should be a sedimentary expression of all these events in all sites throughout the Keep River region. The facies changes at Sandy Creek Gorge, for example, are not reflected in the sand sheet sediments of the same age anywhere else in the Keep River region probably because the finer grained nature of the Sandy Creek Gorge sediments allow better expression or preservation of the mottled palaeosols (refer 6.4.3.2). For many sandy sites in northern Australia, finding the event ‘signature’ is perhaps more of a forensic exercise.

7.5 Continuity and Discontinuity in the Keep River Region

No site yet excavated in the Kimberley shows a clear continuity of occupation between Pleistocene and Holocene levels (Walsh, 2000: 36). Then again, there is no depositional context in which sedimentation is continuous both through time and across space (Sadler, 1981). Temporal continuity is essentially defined within the stratigraphic and depositional resolution of the sedimentary record (Kowalewski and Bambach, 2001). Whilst *in situ* cosmogenic dating indicates sedimentation is cumulative over timescales of many hundreds of thousands of years (refer 7.2), luminescence dating indicates continuity over many tens to hundreds of years but from combined rather than individual site records (refer 6.5.5).

It might be argued that the Karl-3 sand sheet excavation does combine Pleistocene and Holocene time periods, but more detailed sampling may reveal more episodic and discontinuous depositional events. The closest sampling interval in this study was 20 cm in the Karl-3 excavation. Given a progressive change in the rate of sedimentation from $\sim 100 \text{ mm.k}^{-1}$ during the Pleistocene to $\sim 200 \text{ mm.k}^{-1}$ during the Holocene, the maximum chronological resolution provided from this sampling interval is 1 – 2 ka. Unfortunately when considered over shorter periods, such as only the past 10

ka, the greater scatter in the data means that the chronological resolution is even less definitive. Thus the (analytical) precision of radiometric dating is often unnecessary because time-averaging blurs many short-term events, processes or discontinuities. The shorter term dynamics that exist in the natural and cultural records may only be discerned from high-resolution dating (e.g. Kowalewski, et al., 1998; Otte et al., 2002), but this ideal is generally limited by financial constraints.

The higher frequency sampling and analysis of cultural records potentially provides a more comprehensive indication of short-term and site specific changes, provided the influence of taphonomic processes is acknowledged. For example, in many of the excavation sequences stone artefacts are present to the base of the profile (refer site profiles in Chapter Five), but time-averaged assemblages of these records indicates that sedimentation is intermittent and localised (refer 7.4). Where there are discontinuities in the cultural record, such as the break in seed deposition evident in the Granilpi and Punipuni rock-shelter sequences (Atchison, 2000: 184), these may be bridged from adjacent excavations. Once the temporal and spatial discontinuities within the sedimentary and archaeological evidence can be quantified (and they may not be equivalent), the formation history of the archaeological landscape may then be defined. Atchison (2000) argued that although the archaeobotanical record in the Keep River region is spatially and temporally variable at both a regional and site-specific scale, the landscape retains elements of both continuity and change.

In order to better understand the changes in human use of the landscape it is first necessary to undertake studies aimed at deciphering the diverse formation processes within the context of the depositional environment. If human activity and land-use was concentrated within or at the boundary of any particular facies environment then the record of that land-use may conceivably be temporally continuous, but would be spatially variable. If land-use remains geographically constant regardless of facies change, then the cultural record may be both temporally and spatially

continuous. The former scenario may be typical of riverine or other open environments such as the Keep River region, whereas the latter may be more typical of inland rock-shelter environments. In this context, Barton et al. (2002) argue for a middle-ground approach, which focuses beyond the site but within the geographic range of many human activities. Barton et al. (2002) suggested that a more nomadic existence would be better observed over larger spatial and longer temporal scales, whereas a more sedentary existence would be better observed over local spatial and shorter timescales.

7.6 Placing the Keep River Record into a Regional Perspective

It is evident (assuming the more widely accepted age determinations are valid) that the earliest evidence for occupation is in Arnhem Land (~ 60 ky BP), then in the western Kimberley region (~ 40 ky BP), and finally in the eastern Kimberley region, including the Keep River area. From the period 7 – 6 ky BP, the cultures of Arnhem Land and the Kimberley started to become distinct (Lewis, 1988). In these regions, this period is considered to be one of increasing cultural innovation and ecological change, but the nature and timing of changes in the Kimberley remains unknown (Lewis, 1988). The following attempts to place the occupation record of the Keep River into a more regional context with Arnhem Land and the Kimberley.

7.6.1 Age-depth Curves for the Kimberley and Arnhem Land region

Before interpretations concerning prehistoric human behaviour between regions can be properly addressed, it is important to know whether the archaeological time period being studied is equally preserved within these regions (Waters and Khuen, 1996). In terms of regional representation, there is no clear correlation between age and depth (Fig. 7.7). In parts of western Kimberley (O'Connor, 1995, 1996), occupation sequences are generally older for the same depth than those in Arnhem

Land (Roberts et al., 1990, 1998b), indicating a much slower sediment accumulation rate. In contrast, the higher sediment accumulation rates of the Keep River sand sheets ($100 - 200 \text{ mm.ka}^{-1}$) have generally preserved relatively young and shallow occupation deposits. These regional differences may be an effect of the proximal distance of the coastline, with older (Pleistocene) sequences better preserved inland and at higher topographic levels, and better resolution of recent (Holocene) sedimentation in more lowland coastal sequences.

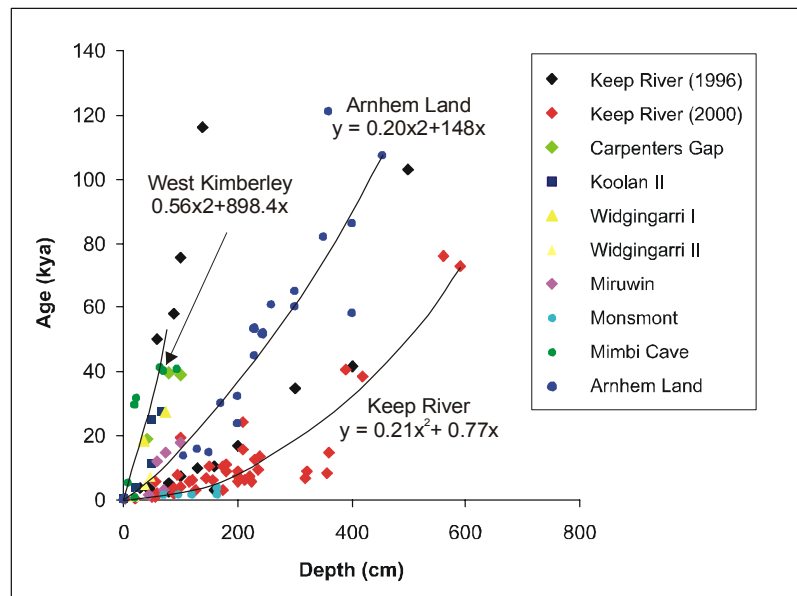


Figure 7.7 Age-depth data for archaeological sites (rock-shelters and sand sheets) in the Kimberley and Arnhem Land regions (data from Atchison, 2000; Balme, 2000; Dortch and Roberts, 1996; Harrison and Frink, 2000; Morwood and Hobbs, 1995; McConnell and O'Connor, 1997; O'Connor, 1996).

7.6.2 The Holocene Record and Intensification

Figure 7.8 plots the chronological record for the Keep River against the available ages for other archaeological sites in the Kimberley and nearby Arnhem Land region. The chronological evidence for the Keep River region, including nearby Miruwin (Dortch and Roberts, 1996), indicates probable occupation from the LGM but a significantly greater preservation of Holocene sites. Most archaeological sites excavated in the Keep River and surrounding region have been rock shelter sites, and of these rock-shelter sites, most are Holocene in age with occupation beginning about 4 - 3.5 ka (Fig. 7.8). The chronological results from this study support archaeobotanical evidence of fruit seed processing in the Goorurarmum - Jinmium catchment area from at least 3.5 ky BP (Atchison, 2000), introduction of stone points in the Keep River region around 3 ky BP (Fullagar et al., 1996: 764; Atchison, 2000; Boer-Mah, 2002: 38), and an increase in preserved rock art at from about 4 ky BP (Watchman et al., 2000; Ouzman et al., 2002). In the nearby Wardaman country, there is also an apparent increase in the amount of rock art at about 4 ky BP (Watchman, 2001).

Regionally, this period from 4 - 3.5 ka is generally regarded as one of increased cultural change with alterations in stone artefacts (new types), use of processed plants, regional art styles, and increased occupation of older sites (Hiscock, 1984). Whilst *qualitative* changes can be observed in the processing of plants (e.g. Atchison, 2000; Atchison et al., in prep.) and reduction of stone tools (Fullagar et al., 1996; Boer-Mah, 2002), it is questionable whether the *quantitative* changes in the number of archaeological deposits actually indicates increased numbers and more intensive use of sites (Lourandos, 1996), or reflects the preferential preservation of archaeological deposits dated to this period (refer 7.4.1).

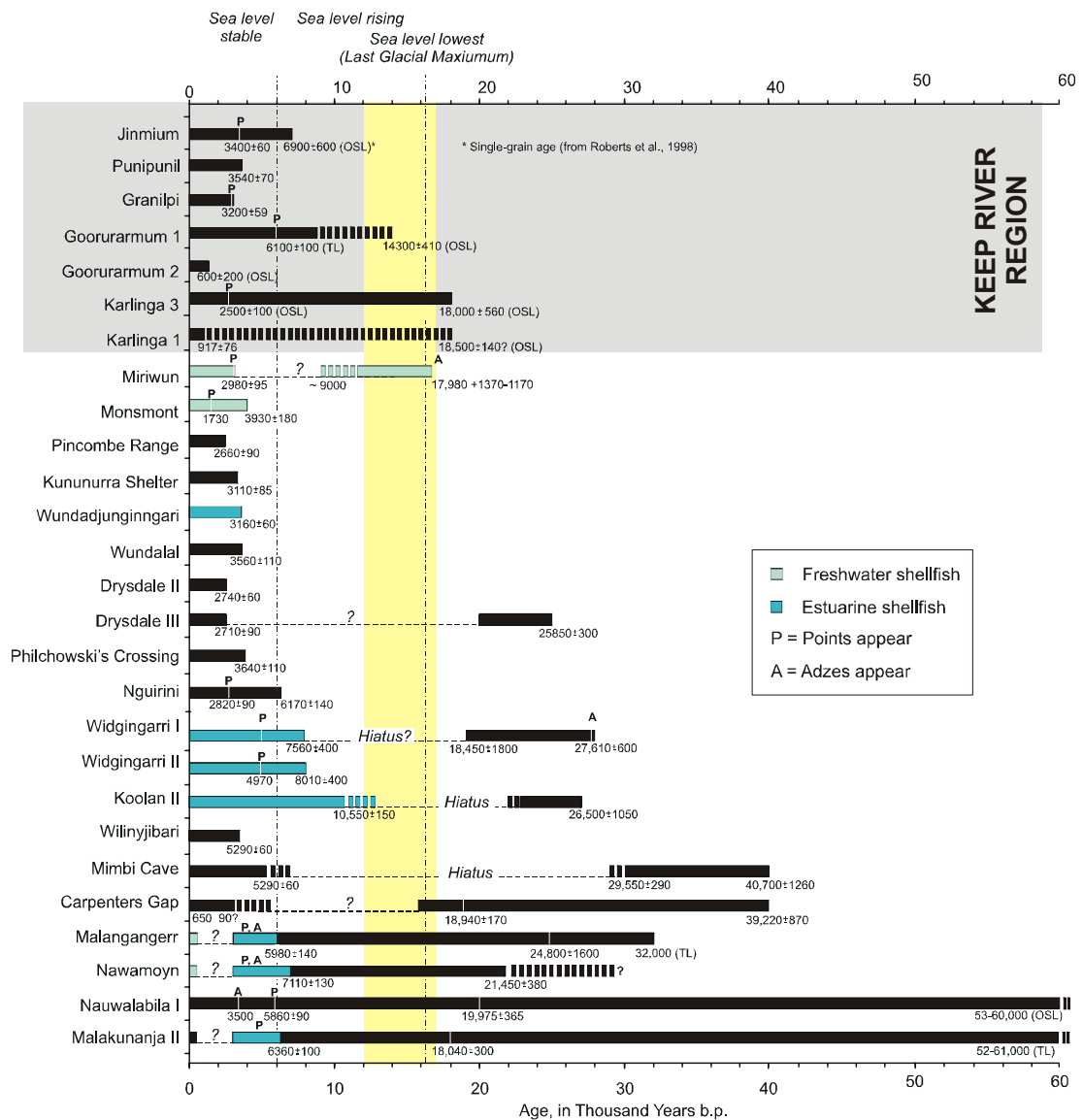


Figure 7.8 Dated archaeological sites in the Kimberley and Arnhem Land region (data from Atchison, 2000; Balme, 2000; Dortch and Roberts, 1996; Harrison and Frink, 2000; Morwood and Hobbs, 1995; McConnell and O'Connor, 1997; O'Connor, 1996 and Walsh, 2000 and references therein). All ages are calibrated ^{14}C ages, or are marked by subscript as luminescence age (TL or OSL). Chronological gaps (stippled line) are defined as a cultural hiatus according to the authors, or as a question mark if unknown. The yellow band marks the period (~17 to 12 ky BP) where no ages have apparently been registered for northwest Australia (Veth, 1995: 744). The dated introduction of stone points (P) and adzes (A) are marked.

The sediment chronology throughout the Keep River region indicates that open sites are much older than the adjacent rock shelters. However, the apparent ‘intensification’ of late Holocene sites in the Keep River region may be a product of both research and preservation, rather than of cultural change. In terms of research the total number of excavated rock shelter sites (~ 8) is significantly greater than the number of open sites (~ 3), which translates as a greater emphasis on Holocene geomorphic environments. Poor preservation in semi-arid monsoonal climates will also result in a biased record in favour of younger sites, particularly where older records are located within a fluctuating water table zone (refer 7.2.2). Progressively increasing sedimentation rates will also favour preservation of Holocene records (refer 7.4.1). A similar problem exists in North America, with problems in the poor preservation and dating of pre-Clovis sites (Marshall, 2001) and justification of ‘intensification’ of Clovis sites around 4.3 – 3 ka (Dent, 1995).

The implication is that rock shelter sites could have been occupied earlier but the associated sedimentary record was either removed or was never present. The removal of sediments may have occurred during wetter monsoonal periods before (e.g. Nott and Price, 1994) and after (e.g. Wyrwoll and Miller, 2001) the LGM. The absence of sediment deposition may indicate that the sand sheets had to build up to the level of the rock shelters before there was any intrusion into the rock shelters, as demonstrated in Sandy Creek rock shelter, North Queensland (Morwood et al., 1995). In any case, before comparing any cultural trends it is just as important to consider whether archaeological time periods are equally preserved *within* regions as it is *between* regions (Waters and Khuen, 1996).

7.4.3 The Pleistocene Record and the east Kimberley Refuge

In the other parts of the Kimberley, including Widgingarri I and II, Koolan 2 (O'Connor, 1996), Carpenter's Gap (O'Connor, 1995), Mimbi Cave (Balme, 2000) and Drysdale (in Walsh, 2000), the period from ~17 to 12 ky BP is regarded as a cultural hiatus (refer 2.6). It is unclear whether each of the major chronological hiatuses evident in these excavations (Fig. 7.8) actually represent a 'cultural hiatus' during which time the site was seldom used and little sediment accumulated, or represent a natural hiatus in which any late Pleistocene-early Holocene sediments were removed by geomorphic processes. There is additional interpretive inconsistency at Carpenter's Gap which apparently provides evidence for a continuous cultural presence for the past 40 ka (McConnell and O'Connor, 1997; Balme, 2000), but at the same time reveals a disconformity above the LGM levels, which may more not represent a cultural or natural hiatus (Wallis, 2001: 105).

In the Keep River region there is an archaeological record which extends back to the LGM, and which includes the cultural hiatus period (Fig. 7.8). The Keep River record may perhaps be compared with that from nearby Miriwun which also extends back to the LGM (Fig. 7.8). It has been postulated that riverine sites in this region were favoured for occupation during the LGM (Veth, 1995; Dortch and Roberts, 1996). Unlike the southwest Kimberley, which likely experienced arid conditions during the LGM and Pleistocene-Holocene transition, the uplands of the Mitchell Plateau (west of the Ord River) and the east Kimberley provided reliable networks of water during the climatic oscillations of the last 40 ka (Veth, 1995). The Keep River system itself may have been one of these reliable networks (Fig. 7.9), which formed part of the alleged east Kimberley 'refuge' (Veth, 1989).

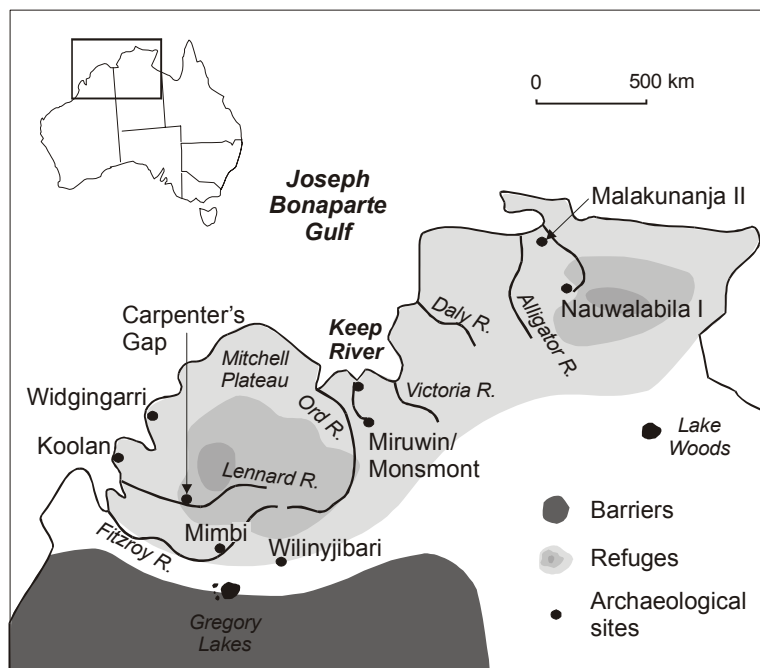


Figure 7.9 Location of the Keep River region in the context of the biogeographic refuge, defined by Veth (1989: 81) as an extensive system of piedmont/montane uplands and riverine gorges which provided reliable networks of water during the climatic oscillations of the last 40 ka.

The Ord, of which the Keep River may have at times been part, is the most likely catchment in the general region to have retained permanent water at this time (Walsh, 2000: 36). Under the arid conditions operating at the LGM, this region of the Kimberley contained seasonal herbaceous vegetation with open forest along stream courses, an attractive and suitable landscape for the migration of early peoples (Van Andel and Veevers, 1967: 108). Indications of perched water and swamp conditions at the LGM at Fox Creek (in what is now the Keep River National Park) (J. Luly, personal communication, 2002) may support the region as a refuge for plants, animals and people.

Thus existing data are consistent with the Keep River region as a refuge area but supporting archaeological evidence is limited by the preservation factor of sedimentation. As in the Polop Alto valley, in eastern Spain, the evidence for human activity and landuse is a cumulative, but

discontiguous palimpsest of the most durable behavioral residues whose distributions have been affected by diverse natural and cultural formation processes (Barton et al., 2002). If the Keep River and the Ord River regions provide reliable water but the sedimentary record is discontiguous (refer 6.6.2), then it might be predicted that a continuous occupation record exists but has not yet been found archaeologically. In this respect, the nature and completeness of the buried archaeological record parallels that of the sedimentary record (Waters and Khuen, 1996).

7.7 Conclusions

The continuity of the geoarchaeological record in the Keep River region is dependent on the temporal and spatial resolution within which both the sedimentary and archaeological records are defined. *In situ* cosmogenic dating indicates *net* sedimentation is cumulative at the regional scale and over many tens of millennia, whereas luminescence and radiocarbon dating indicates more stochastic sedimentation at the local scale and over centuries to millennia. Superimposed on this temporal variability is spatially discontiguous sedimentation and geomorphically biased preservation – whilst more ancient Pleistocene sequences are preserved in the sand sheets, only Holocene sequences are preserved in the rock shelters.

The archaeological record potentially provides better resolution of shorter term dynamics of centuries or greater, although analyses and interpretations need to be defined within the context of the depositional environment. Comparison of stone points and sediment chronology indicates that although bioturbation may be important, the rate of bioturbation is probably only 20 mm.ka⁻¹ and less than the rate of sediment accumulation (100 – 200 mm.ka⁻¹). Other taphonomic factors which may influence the archaeological record include secondary reworking and *in situ* disintegration. Some artefact accumulation rates may be explained as a function of sedimentation rates and differential preservation, with changes in sedimentation reflecting regional climatic conditions. A

Holocene age for the rock art is consistent with a Holocene age of the preserved rock shelter sediments, but links between any existent ancient rock art and adjacent sand sheet sediments need to be geomorphologically defined.

Overall, in order to more clearly define temporal and spatial resolution in sandy deposits, decipher the various processes of site formation and patterns of artefact preservation, substantiate the Keep River region as part of the East Kimberley refuge, and also substantiate late Holocene ‘intensification’, more work is needed to understand past and present relationships between the sediments and the physical and climatic environment, both locally and throughout northern Australia. Although no single site provides the necessary detail of both cultural and natural dynamics, these may be pieced together from representative archaeological and non-archaeological sites.

CHAPTER EIGHT

Conclusions and Suggestions for Further Research

If we define archaeology quite broadly as the application of all current knowledge and techniques to the study of all past knowledge and techniques, then archaeologists are compelled to communicate with their disciplinary neighbours.

- Boddington et al. (1987: 3)

8.1 Introduction

The following discussion summarises the major results of the thesis bearing in mind the initial aims of the thesis (refer 1.5). These aims include a consideration of a geoarchaeological approach to archaeological studies in northern Australia, and the environmental context of the Keep River region; estimations of denudation rates of the sandstone escarpments and accumulation rates of the adjacent sand sheet accumulation using both *in situ* cosmogenic dating and luminescence dating; an analyses of the rock-shelter, sand-sheet and creek sediments; and finally an evaluation of the chronological and contextual relationship between the landscape and its archaeological record at the site specific and regional level. The chapter themes are further explored in suggestions for further research.

8.2 Summary and Major Conclusions

A range of empirical and observational data generated from within this study and from external sources were used to establish the geomorphic context and provide a geoarchaeological interpretation of archaeological sites in the Keep River region. Specifically this includes describing the landscape context (regional environment and landscape processes), the stratigraphic context (chronostratigraphy), site formation (cultural and natural processes), and the archaeological context (landscape use and modification). The main geomorphic focus is on the sand sheets, which

represent both the landscape on which people lived and the link between the sandstone escarpments and rock shelters.

The Keep River region is a good example of an ancient (Ma) landscape located in a presently semi-arid monsoonal environment, consisting of palimpsest features formed over time under different environmental regimes, upon which are etched the more recent (ka) geomorphic and human landscapes. The regional geological, geomorphological, palaeoclimatic and ecological context of the Keep River region underpin the geochronologic and geoarchaeological interpretations but are somewhat constrained by the limited record for northwest Australia. In particular, the origin of sand sheets is uncertain. In Arnhem Land there is geomorphological evidence for recurring periods of sand sheet accumulation and denudation over the past quarter of a million years, in association with climatic interglacial and glacial cycles (Roberts, 1991). There is also evidence in that region of northern Australia becoming progressively drier over that time (Nanson et al., 1993). Although the climate in the Keep River region has remained essentially semi-arid monsoonal, it too has probably gradually become more arid and the denudation of sand sheets less extensive. *In situ* cosmogenic dating and luminescence dating indicates that the bulk of the present sand sheets have accumulated in the past 100 ka, but it is likely that, as in Arnhem Land, this is simply the latest episode in a series.

Measurement of in-situ cosmogenic ^{10}Be and ^{26}Al in the local eroding plateau surfaces and depth profiles of genetically linked sand sheets provided useful quantitative measures of long term (10^3 – 10^5 ka) processes in the Keep River region. Spatially averaged rates of plateau denudation range from 4 - 7 mm.k $^{-1}$ and are consistent with regional estimates. These denudation rates are used primarily for burial dating. Cosmogenic burial dating of two sediment profiles from the Jinmium sand sheet indicates net vertical accumulation of sediment ranging from 10 to 20 mm.k $^{-1}$ over the past few hundred thousand years. A high ^{10}Be concentration at the base of one sediment profile indicates the sand sheets have probably accumulated over a previously exposed pediment.

Disparity of longer and shorter term dynamics is indicated from the significantly greater accumulation rates measured from luminescence dating ($100 - 200 \text{ mm.k.a}^{-1}$) compared to that estimated from burial dating. This partly reflects the chronometric sensitivity of each dating technique to sedimentary processes, in particular mixing, and the timescales over which the measure of these processes are integrated.

The processes of weathering and sedimentation within the sand sheets of the Keep River region have been investigated using evidence from grain size, mineralogy, geochemistry and micro-morphology. Sediment characterisation provides limited information of landscape change because the sandstone source material and depositional and post-depositional processes in the genetically linked sands have remained relatively constant over the past 100 ka. The exploratory analyses indicate that the sediments are locally sourced, with little geochemical differentiation between the bedrock (source) and the sand sheets and rock-shelters (sinks). The sand-sheet sediments represent a mixture of sediment populations derived from local drainage basins. The rock-shelter sediments have higher relative concentrations of calcium (CaO), phosphate (P_2O_5) and organics (LOI) than the surrounding sand-sheet sediments, reflecting higher levels of charcoal, guano and organic matter. Post-depositional reddening of the sediments, evident both at the macro (cm) and micro (μm) scale reflect the relative position of groundwater rather than depositional age. Ongoing processes of weathering and diagenesis are evident in the form of mixing, and in the development of mottles and concretions. At least one palaeosol horizon dating to $13.9 \pm 0.4 \text{ ky BP}$ is evident at the Sandy Creek Gorge site, with deep root mottles, pisolites, potassium-enriched sediments, and peculiar indurated silicate deposits all indicating the prior existence of a forest community at this site, which now supports grassland. The facies changes evident in the finer-grained sediments in Sandy Creek Gorge are not evident in the contemporaneous but more unconsolidated sand sheet sediments elsewhere in the Keep River region.

The chronostratigraphy of the rock shelters, sand sheets and creek profiles in the Keep River region has been investigated using both thermoluminescence (TL) dating and optically stimulated

luminescence (OSL) dating. For both the sand sheets and creeks the U- and Th- decay series indicate relative equilibrium. However, the lateritic nature of the sediments indicates past or present changes in the hydrological environment and potential radioactive mobility cannot be disregarded. The mean dose rate determined from thick-source alpha counting (TSAC) is $1.3 \pm 0.29 \text{ Gy.ky}^{-1}$ with significantly higher values of $3.0 \pm 0.83 \text{ Gy.ky}^{-1}$ for the mottled sediments at Sandy Creek Gorge, reflecting higher concentrations of U, Th and K in these samples. The palaeodose analyses indicate that the sand sheets are generally well-bleached but the rock-shelter and creek sediments show evidence of partial bleaching during deposition. Foreshortened and stepped TL temperature plateaux relating to some sand sheet and creek profiles may be indicative of stochastic depositional events, which may be more widespread but are seldom preserved or deciphered in the relatively uniform sand sheet sediments. Oddly, OSL palaeodose estimates may be up to 20 % greater than the corresponding TL estimate and tests indicate the potential for partial loss of the 325°C TL signal under prolonged yellow light illumination (2 - 3 hrs). Consequently, OSL ages are considered more reliable estimates of depositional age.

The Jinmium, Goorurarmum and Karlinga rock-shelters all comprise sediments and associated cultural sequences that are mid-Holocene in age. Basal OSL ages for the Goorurarmum and Karlinga rock shelter are $0.3 \pm 0.07 \text{ ky BP}$ and $18.4 \pm 5.4 \text{ ky BP}$, although a radiocarbon age of $4080 \pm 40 \text{ ky BP}$ for the latter is preferred. In contrast, the sand sheets provide cultural sequences from the LGM and non-cultural sequences extending beyond 100 ka. Basal OSL ages for the Goorurarmum and Karlinga sand sheet excavation are $14.3 \pm 0.4 \text{ ky BP}$ and $18.0 \pm 0.6 \text{ ka}$ respectively. The cumulative chronological record for the Keep River region indicates temporal continuity between the Pleistocene and Holocene sequences, but within and between sites the sedimentary record is temporally and spatially discontinuous. The intermittent and localised accumulation of sediment results in the formation of time averaged assemblages of material remains. Both individual site records and regionally combined records indicate a progressive increase in the rate of sediment accumulation from $\sim 100 \text{ mm.ka}^{-1}$ in the late Pleistocene to over 200 mm.ka^{-1} in the Holocene. Preservation of organic horizons in a creek site at Karlinga are indicative

of infilling of a small alluvial swamp around 10 ka. The increase in sedimentation most likely results from enhanced monsoonal activity following the post-glacial marine transgression rather than human activity.

The preceding geoarchaeological results were integrated with the information from radiocarbon analyses, palaeobotanical studies, rock-art studies and regional archaeology. Luminescence dating from this study supports previous chronological estimates for the commencement of seed processing (Atchison, 2000; Atchison et al., in prep.), the introduction of stone points (Fullagar et al., 1996; Boer-Mah, 2002), and an increase in rock art (Watchman et al., 2000; Ouzman et al., 2002) around 3 – 4 ka. Whether these trends reflect ‘intensification’ or preferential preservation of archaeological material is illustrated by showing a correlation between the rates of sedimentation and the rates of stone artefact accumulation in two sand sheet excavations. Stratigraphic and depositional resolution defines the integrity of the sedimentary and archaeological records. Combined radiocarbon and luminescence dating indicates that whilst occupation from the Last Glacial Maximum (LGM) cannot be discounted (at least in the Karlinga area), the majority of occupation records preserved in the Keep River region are Holocene. However, this partly reflects sampling bias as more rock shelter sites (8) have been sampled in this region than open sites (2). Present records indicate a possible connection of the Keep River region with the east Kimberley ‘refuge’, which provided reliable networks of water during the climatic oscillations of the last 40 ka.

Few individual sites can provide a complete record of both palaeoenvironmental and archaeological changes (e.g. Thomas et al., in press). Discrete records were obtained in this study from non-occupational (riverine) and occupational (rock shelters, sand sheets) sites, but the chronostratigraphic coincidence is not always obvious in these unconsolidated sandy sediments. The issues and interpretations outlined above are not unique to the Keep River region, or to northern Australia. The issues and interpretations outlined above are not unique to the Keep River region, or to northern Australia. The human-landscape story is well hidden in the sandstone

landscapes of the Keep River region, at least according to the chronological and sedimentological methods used in this study. Higher resolution analyses may discern landscape changes that are more responsive to human-environmental interactions. This geoarchaeological study in the Keep River region has offered the opportunity to at least begin to relate past and ongoing chronological, palaeobotanical, rock art, stone artefact, ethnographic studies, and explore associations between the changing environment and the archaeological record. The following suggestions for further research are a continuation of these explorations.

8.3 Suggestions for Further Research

8.3.1 Regional Environment

In dry savannas throughout the world, detailed information on Quaternary landscape evolution remains rather incomplete, due to the absence of productive sedimentary archives (Heinrich and Moldenhauer, 2002). Consequently, it becomes difficult to understand the various influences on the stratigraphic and archaeological record, and to consider long-term human-environmental interactions. The stratigraphic and depositional resolution in the Keep River region provides an indication of landscape dynamics over timescales of hundreds to thousands of years. It would be useful to obtain an understanding of landscape processes over timescales of only tens of years, as exemplified in the Selima sand sheets, Egypt (Maxwell and Haynes, 2001).

The period around 4 ka corresponds to the pluvial maximum (Schulmeister, 1999) and is followed by a drier, albeit more variable climate (refer 3.5.3). The period around 4 ka is regarded as one of ‘intensification’. Did the pluvial conditions facilitate a larger cultural network via the drainage basins connecting Arnhem Land and the Kimberley (Lewis, 1988), and an expansion of the classic Bradshaw rock art into the Keep River region? What are the chronostratigraphic connections between these drainage basins? Whilst providing more favourable conditions for occupation, do

pluvial conditions decrease the preservation of these records? Part of the answer may derive from combined proxies of both dry and wet occupation sites (e.g. Thomas et al., in press) and from more detailed research of formation processes in these sandy sediments. The geoarchaeological paradigm is that some archaeological questions can be answered, at least in part, by appropriately framed geological studies (Stein and Farrand, 1985).

8.3.2 *In situ* Cosmogenic Isotope Dating

Future prospects for exposure age dating have been outlined generally by Watchman and Twidale (2002). Although the research for this thesis indicates a relatively consistent plateau denudation rate of $5 - 6 \text{ mm.k}^{-1}$ for northwest Australia, continued sampling and analyses of sandstone and other rock formations would improve the resolution within and between geomorphic regions. Using plateau denudation rates this study has derived estimates for erosion of the escarpment faces around $50 - 100 \text{ mm.k}^{-1}$, but it would be more valuable to obtain direct measurements of vertical escarpment retreat rates from *in situ* cosmogenic dating. These estimates may in turn provide a more accurate assessment of the potential rates of erosion of rock art, and allow determination of the relative contributions of source material from the plateaux and escarpment faces to the adjacent sand sheets.

Whilst the theory and application of burial dating is still relatively undeveloped, early research heralds significant potential for geoarchaeological studies. Burial dating of sand sheets in the Keep River region indicates that modelling of accumulation rates can be obtained over depths of less than 10 m and time periods of 100 ka or more. With improved modelling of both the neutron and muon components, better resolution may be obtained from deeper and older sediment profiles, particularly with the inclusion of underlying bedrock, allowing differentiation not only of allochthonous and autochthonous sediment accumulation, but also of periods of erosion and accumulation. With further understanding of shielding factors, similar advances may be made in open rock shelters, and closed cave systems, particularly where combined with higher-resolution luminescence dating.

Northern Australia is particularly well-suited for such research given the geological antiquity, relatively open landscape, and the purity of the siliceous sands.

8.3.3 Luminescence Dating

The results of luminescence dating of the sand sheets have improved the chronological understanding of each of the archaeological sites studied. TL dating is acceptable for well-bleached sites but OSL dating is preferred for rock shelter and riverine sites. Whilst OSL dating techniques are increasingly preferable for dating because of developments in the use of small aliquot and single-grain OSL analyses and remaining problems with use of yellow illumination in TL, this study illustrates that there remains potential for using the characteristic TL spectra to identify differences in sedimentary provenances and processes, such as events of rapid deposition. In order to distinguish cultural and non-cultural processes, including changes in sedimentation rate, higher resolution dating is needed from occupation and non-occupation deposits. In addition, basal ages from the sand sheets are required to obtain more accurate estimates of volumetric rates of accumulation.

Members of the uranium- and thorium-series differ greatly in their chemical mobility and are subject to post-depositional migration, which potentially affects the accuracy of the geological dose-rate (Roberts, 1996; Roberts and Plater, 1999). Although this study did not find any significant degree of disequilibrium despite the presence of sediment mottling, a more accurate measure of disequilibrium in lateritic sandy sediments of northern Australia is needed. Detailed examination of selected sediment phases, particularly the amorphous- and crystalline-iron and manganese oxides and oxyhydroxides, may help identify and quantify the degree of post-depositional radionuclide migration and *in situ* chemical weathering. Further examination of the different chemical behaviour of radioisotopes of the uranium- and thorium-series should also provide a more accurate assessment of post-depositional environmental conditions, such as water-table fluctuations and exposure to oxidized and/or reduced waters.

8.3.4 Sediment Characterisation

Preliminary investigations from this study indicate that discriminating cultural and non-cultural processes in sandy sediments of semi-arid monsoonal environments require a more detailed investigation than undertaken in this study. The intensely weathered nature of the sandstone landscape of the Keep River region means that many indicators of weathering (e.g. heavy minerals, carbonate or organic content) is of limited use. Basic sediment characterisation (e.g. grain size, mineralogy, major element chemistry) can provide useful contextual information, and further sediment characterisation might include more details such as minor element chemistry, sediment pH, moisture, magnetic characteristics, compaction and micromorphology.

Whilst this study was able to obtain resin impregnated samples from the sand sheets, comparative micromorphological studies of the rock shelter sediments is necessary. Resin impregnation of samples in the field is preferable, but this research has shown that this may suffer because of the hydrophobic nature of charcoal-enriched sediments, particularly in the rock shelters. Future studies may need to consider use of polyester resins rather than the epoxy resins used in this study. Unlike epoxy resins, polyester resins are not exothermic and can be diluted with acrylic monomers that reduce surface tension and facilitate better the impregnation of loose sediments (Magee, pers. comm., 2003).

The analysis and interpretation of palaeosols at Sandy Creek Gorge indicate that palaeosols may be a prospective source of stratigraphic and palaeoenvironmental information. Palaeosols have been used as a source of stratigraphic and palaeoenvironmental information to archaeology in many parts of the world (Holliday, 1989; Bettis, 1992; Evans, 1995) but remain relatively unexploited in Australian research (Bowman, 1987), despite the recognition of discrete paleosols and relict features (exposed silcrete, ferricrete, etc.) throughout the landscape (Firman, 1994; Young and Young, 1992), and the recognition of silcrete as a component of stone artefact assemblages in some parts of the continent (Hughes et al., 1973; Sullivan and Simmons, 1979).

8.3.5 Archaeological Comparisons

Geoarchaeological investigations provide a means for reconstructing prehistoric and ancient landscapes, depositional environments, and paleoclimatic regimes. Despite arguments that archaeological and geological records preserve and overlap differently over space and time (Dincauze, 2000), studies are showing that environmental and archaeological changes can be explored using multi-proxy data from different environmental contexts.

Many archaeological issues relate specifically to the nature of basic physical, chemical, biological and human properties and processes, to morphological and sedimentological changes on timescales ranging from months to millennia, and at spatial scales ranging from tens of metres to tens of kilometres. Consequently, there remains a great need to quantify all these processes in semi-arid monsoonal sandy terrains in Australia and elsewhere (e.g. Ward and Larcombe, 2003).

Theoretically, according to Lourandos (1997: 194), arid and semi-arid landscapes allow fairly good visibility of archaeological sites, and of the possible historical events that occurred within them. In practice, however, neither archaeological sites nor their formation history are obvious. Indications arising from this study are that semi-arid monsoonal sandy environments comprise a discontinuous palimpsest record of the most durable sedimentary residues (mainly inorganic minerals) and of cultural residues (mainly stone artefacts). The distributions of both these residues have been influenced by diverse natural and cultural formation processes, which remain largely unknown and unquantified. Whilst it is virtually impossible to account for all the various individual processes, and combinations of processes that influence archaeological site formation, it is useful to move towards investigating and quantifying some of the most significant processes (Ward and Larcombe, 2003).

References

- Aharon, P. (1983) Surface ocean temperature variations during Late Wisconsinan stages: $^{16}\text{O}/^{18}\text{O}$ isotopic evidence from Papua New Guinea. In Chappell, J. and Grindrod, A. (Eds.) *Proceedings of the first CLIMANZ Conference*. RSPS, Canberra.
- Aitken, M.J. (1985) *Thermoluminescence Dating*. Academic Press, New York. 359pp.
- Aitken, M.J. (1989) Luminescence dating: A guide for non-specialists. *Archaeometry*, 31(2), 147-159.
- Aitken, M.J. (1994) Optical dating: a non-specialist review. *Quaternary Geochronology (Quaternary Science Reviews)*, 13, 503-508.
- Aitken, M.J. (1998) *An Introduction to Optical Dating. The Dating of Quaternary Sediments by the Use of Photon-stimulated Luminescence*. Oxford University Press.
- Aldrick, J.M. and Moody, P.W. (1977) Report on the soils of the lower Weaber and Keep Plains, N.T. Department of the Northern Territory Animal Industry and Agricultural Branch. Technical Bulletin, No. 19. 110pp.
- Allen, J. (1989) When did humans first colonise Australia. *Search*, 20, 149-154.
- Allen, J. (1994) Radiocarbon determinations, luminescence dating and Australian archaeology. *Antiquity*, 68, 339-343.
- Allen, H. and Barton, G. (1989) Ngarradj Warde Djobkeng: White Cockatoo Dreaming and the prehistory of Kakadu. Oceania Monograph 37, Oceania Publications, Sydney.
- Allen, J. and Holdaway, S. (1995) The contamination of Pleistocene radiocarbon determinations in Australia. *Antiquity*, 69, 101-112.
- Allen, J. and O'Connell, J.F. (1995) Transitions. Pleistocene to Holocene Australia and Papua New Guinea. *Antiquity*, Special Number 265. 862pp.
- Atchison, J. (2000) Continuity and change: a late Holocene and post contact history of Aboriginal environmental interaction and vegetation process from the Keep River region, Northern Territory. Unpublished PhD thesis, University of Wollongong.
- Atchison, J. and Fullagar, R. (1998) Starch residues on pounding implements from Jinnium rock-shelter. In: R. Fullagar (ed.) *A Closer Look: Recent Studies of Australian Stone Tools*. Sydney: Archaeological Computing Laboratory, Archaeology (Prehistoric and Historical), University of Sydney.
- Atchison, J., Head, L. and Fullagar, R. (in prep.) Archaeobotany of fruit seed processing in a monsoon savanna environment: evidence from the Keep River region, Northern Territory, Australia.

- Attenbrow, V., David, B. and Flood, J. (1995) Menngge-ya and the origin of points: new insights into the appearance of points in the semi-arid zone of the Northern Territory. *Archaeology in Oceania*, 30, 105-120.
- Bailey, R.M. (2000) The slow component of quartz optically stimulated luminescence. *Radiation Measurements*, 32, 233-246.
- Balme, J. (2000) Excavations revealing 40,000 years of occupation at Mimbi Caves, south central Kimberley, Western Australia. *Australian Archaeology*, 51, 1-5.
- Balme, J. and Beck, W.E. (2002) Starch and charcoal: useful measures of activity areas in archaeological rockshelters. *Journal of Archaeological Science*, 29, 157-166.
- Barham, T., Bates, M. and Macphail, R.I. (1995) *Archaeological Sediments and Soils: Analysis, Interpretation and Management*. Archetype Books, London.
- Barton, C.M. and G.A. Clark (1993). Cultural and natural formation processes in late Quaternary cave and rockshelter sites of western Europe and the Near East. In: Goldberg, P., Nash, D.T. and Petraglia, M.D. (eds.). *Formation Processes in Archaeological Context*. Prehistory Press, Madison. pp 33-52.
- Barton, M.C., Bernabeu, J., Aura, J.E., Garcia, O. and La Roca, N. (2002) Dynamic landscapes, artifact taphonomy, and landuse modelling in the Western Mediterranean. *Geoarchaeology*, 17(2), 155-190.
- Bateman, M., Frederick, C.D., Jaiswal, M.K. and Singhvi, A.K. (2002) Getting to grips with bioturbation using luminescence. Unpublished poster presentation. 10th International ESR and luminescence dating conference, Reno.
- Bednarik, R.G. (2002) The dating of rock art: a critique. *Journal of Archaeological Science*, 29, 1213-1233.
- Bettis III, E.A. (1992) Soil morphologic properties and weathering zone characteristics as age indicators in Holocene alluvium in the upper Midwest. In V.T. Holliday (ed.). *Soils in archaeology: landscape evolution and human occupation*. Washington: Smithsonian Institution Press. Pp. 119-144.
- Bierman, P.R. (1994) Using *in situ* produced cosmogenic isotopes to estimate rates of landscape evolution: A review from the geomorphic perspective. *Journal of Geophysical Research*, 99 (B7), 13885- 13896.
- Bierman, P.R. and Turner, J. (1995) ¹⁰Be and ²⁶Al evidence for exceptionally low rates of Australian bedrock erosion and the likely existence of pre-Pleistocene landscapes. *Quaternary Research*, 44, 378-382.

References

- Bierman, P.R. and Caffee, M. (2002) Geomorphology/surface processes – cosmogenic exposure and erosion history of Australian bedrock landforms. *Geological Society of America Bulletin*, 114(7), 787-804.
- Bierman, P., Larsen, P., Clapp, E. and Clark, D. (1996) Refining estimates of ^{10}Be and ^{26}Al Production rates. *Radiocarbon*, 38(1), 149.
- Bird, M.I., Ayliffe, L.K., Fifield, L.K., Turney, C.S.M., Cresswell, R.G., Barrows, T.T. and David, B. (1999) Radiocarbon dating of “old” charcoal using a wet oxidation, stepped combustion procedure. *Radiocarbon*, 40(2), 127-140.
- Boaretto, E., Berkovits, D., Hass, M., Hui, S.K., Kaufman, S., Paul, M., Weiner, S. (2000) Dating of prehistoric cave sediments and flints using ^{10}Be and ^{26}Al in quartz from Tabun Cave (Israel): Progress Report. *Nuclear Instruments and Methods in Physics Research B*, 172, 767-771.
- Boddington, A., Garland, A.N. and Janaway, R.C. (1987) *Death, Decay and Reconstruction: Approaches to Archaeology and Forensic Science*. Manchester University Press.
- Boer-Mah, T.S. (2002) Beyond the Dripline: Comparison of Rock Shelters and Excavated Open Sites in the Keep River region, Northern Territory, Australia. Unpublished Honours thesis, University of Sydney.
- Bowdler, S. and O'Connor, S. (1991) The dating of the Australian small tool tradition, with new evidence from the Kimberley, W.A. *Australian Aboriginal Studies*, 1, 53-62.
- Bowler, J.M. (1976) Aridity in Australia: age, origins and expression in aeolian landforms and sediments. *Earth Science Reviews*, 12, 279-310.
- Bowler, J.M. (1998) Willandra Lakes revisited: environmental framework for human occupation. *Archaeology in Oceania*, 33, 120-155.
- Bowler, J. (2000) Pluvial aspects of the LGM: evidence from SE Australia. In: Magee, J. and Craven, C. (eds.) *Quaternary Studies Meeting, Regional Analysis of Australian Quaternary Studies: Strengths, Gaps and Future Directions*. 7-9 Feb. Geology Department, Australian National University. Pp. 11-12.
- Bowler, J.M. and Magee, J.W. (2000) Redating Australia's oldest human remains: a skeptic's view. *Journal of Human Evolution*, 38, 719-726.
- Bowler, J.M., Jones, R., Allen, H. and Thorne, A.G. (1970) Pleistocene human remains from Australia: A living site and human cremation from Lake Mungo, western New South Wales. *World Archaeology*, 2, 39-60.
- Bowler, J., Hope, G.S., Jennings, J.N., Singh, G. and Walker, D. (1976) Late Quaternary climates of Australia and New Guinea. *Quaternary Research*, 6, 359-394.

- Bowler, J.M., Wyrwoll, K.-H. and Lu, Y. (2001) Variations of the northwest Australian summer monsoon over the last 300,000 years: the palaeohydrological record of the Gregory (Mulan) Lakes System. *Quaternary International*, 83-85, 63-80.
- Bowman, G.M. (1987) Pedochronology: potential for age determination of archaeological sites. In: Ambrose, W.R. and Mammery, J.M.J. (Eds.). *Archaeometry: Further Australasian Studies*. RSPAS, ANU, Canberra.
- Braucher, R., Bourles, D.L., Colin, F., Brown, E.T. and Boulange, B. (1998) Brazilian laterite dynamics using in situ-produced ^{10}Be . *Earth and Planetary Science Letters*, 163, 197-205.
- Braucher, R., Bourles, D.L., Brown, E.T., Colin, F., Muller, J.-P., Braun, J.-J., Delaune, M., Minko, A.E., Lescouet, C., Raisbeck, G.M. and Yiou, F. (2000) Application of in situ-produced cosmogenic ^{10}Be and ^{26}Al to the study of lateritic soil development in tropical forest: theory and examples from Cameroon and Gabon. *Chemical Geology*, 170, 95-111.
- Brook, E.J., Brown, E., Kurz, M., Raisbeck, G. and Yiou, F. (1995) Constraints on age, erosion and uplift of Neogene glacial deposits in the Transantarctic Mountains determined from in-situ produced ^{10}Be and ^{26}Al . *Geology*, 23, 1063 – 1066.
- Brown, E.T. and Bourles, D.L. (2002) Use of a new ^{10}Be and ^{26}Al inventory to date marine terraces, Santa Cruz, California, USA. Comment and reply. *Geology*, 30(12), 1147-1148.
- Brown, E.T., Edmond, J.M., Raisbeck, G.M., Yiou, F., Kurz, M.D., Brook, E.J. (1991) Examination of surface exposure ages of Antarctic moraines using in-situ produced ^{10}Be and ^{26}Al . *Geochimica et Cosmochimica Acta*, 55, 2269.
- Brown, E.T., Bourles, D.L., Colin, F., Sanfo, Z., Raisbeck, G.M. and Yiou, F. (1994) The development of iron crust lateritic systems in Burkina Faso, West Africa examined with *in-situ*-produced cosmogenic nuclides. *Earth and Planetary Science Letters*, 124, 19-33.
- Brown, E.T., Stallard, R.F., Larsen, M.C., Raisbeck, G.M. and Yiou, F. (1995) Denudation rates determined from the accumulation of in situ-produced ^{10}Be in Luquillo Experimental Forest, Puerto Rico. *Earth and Planetary Science Letters*, 129, 193-202.
- Brown, E.T., Stallard, R.F., Larsen, M.C., Bourles, D.L., Raisbeck, G.M. and Yiou, F. (1998) Determination of predevelopment denudation rates of an agricultural watershed (Cayaguas River, Puerto Rico) using in-situ-produced ^{10}Be in river-borne quartz. *Earth and Planetary Science Letters*, 160, 723-728.
- Brown, E.T., Trull, T.W., Jean-Baptist, P., Raisbeck, G., Bourles, D., Yiou, F. and Marty, B. (2000) Determination of cosmogenic production rates of ^{10}Be , ^3He , and ^3H in water. *Nuclear Instruments and Methods in Physics Research B*, 172, 873-883.

References

- Butzer, K.W. (1982) *Archaeology as Human Ecology: Method and Theory for a Contextual Approach*. Cambridge University Press, Melbourne. 364pp.
- Camuti, K.S., McGuire, P.T. (1999) Preparation of polished thin sections from poorly consolidated regolith and sediment materials. *Sedimentary Geology*, 128, 171-178.
- Canti, M.G. (2003) Earthworm activity and archaeological stratigraphy: a review of products and processes. *Journal of Archaeological Science*, 30, 135-148.
- Cerling, T.E. and Craig, H. (1994) Geomorphology and in-situ cosmogenic isotopes. *Annual Review in Earth Planetary Sciences*, 22, 273-317.
- Chaloupka, G. (1993) *Journey in Time*. Reed Books, Sydney.
- Chappell, J. (1978) Chronological methods and the ranges and rates of Quaternary physical changes. In: Walker, D. and Guppy, J.C. (Eds.) *Biology and Quaternary environments*. Australian Academy of Sciences, Canberra. Pp. 1-34.
- Chappell, J. (1994) Upper quaternary sea levels, coral terraces, oxygen isotopes and deep-sea temperatures. *Journal of Geography*, 107(7), 828-840.
- Chappell, J. (2000) Late Holocene diversion and extinction of 3 large tidal rivers in northern Australia: a singular climatic event? Quaternary Studies Meeting, ANU. In: Magee, J. and Craven, C. (eds.) *Quaternary Studies Meeting, Regional Analysis of Australian Quaternary Studies: Strengths, Gaps and Future Directions*. 7 -9 Feb. Geology Department, Australian National University. P. 13
- Chappell, J. and Woodroffe, C.D. (1997) Macrotidal estuaries. In: Carter, R.W.G. and Woodroffe, C.D. (Eds.) *Coastal Evolution*. Cambridge University Press. Pp. 187-218.
- Chappell, J., Head, J. and Magee, J. (1996) Beyond the radiocarbon limit in Australian archaeology and Quaternary research. *Antiquity*, 70, 543-52.
- Chappell, J., Fifield, K. and Alimanovitch, A. (2001) Determination of long-term erosion rates on blocky, weathering-limited terrain. Seventh Australasian Conference on Isotopes in the Environment, Robertson, NSW. P.7
- Chen, X.Y., Chappell, J. and Murray, A.S. (1995) High (ground) water levels and dune development in central Australia: TL dates from gypsum and quartz dunes around Lake Lewis (Napperby), Northern Territory. *Geomorphology*, 11, 311-322.
- Child, D., Elliott, G., Misfud, C., Smith, A.M. and Fink, D. (2000) Sample Processing for Earth Science Studies at ANTARES. *Nuclear Instruments and Methods*, B172, 856-860.
- Clarke, R.L. (1983) Pollen and charcoal evidence for the effects of Aboriginal burning on the vegetation of Australia. *Archaeology in Oceania*, 18(1): 32-37.

References

- Clarke, D.H., Bierman, P. and Larsen, P. (1995) Improving in situ cosmogenic chronometers. *Quaternary Research*, 44 (3), 366-376.
- Colin, F., Gurarus, E, Bourles, D., Braucher, R., Brown, E., Aran, R., Gilkas, R., Meunier, J.D. and Varajao, C. (2001) The application of in-situ produced ^{10}Be to the study of Australian stone line induced by termites. *Eos Transactions*, AGU, 82 (47). Fall Meeting Supplementary Abstract, B22F-03.
- Courty, M.A., Goldberg, P. and Macphail, R. (1989) *Soils and Micromorphology in Archaeology*. Cambridge University Press, Cambridge. 344pp.
- Coventry, R.J. and Williams, J. (1984) Quantitative relationships between morphology and current soil hydrology in some alfisols in semi-arid tropical Australia. *Geoderma*, 33, 191-218.
- Coventry, R.J., Moss, A.J. and Verster, E. (1988) Thin surface soil layers attributable to rain-flow transportation on low-angle slopes: An example from semi-arid tropical Queensland, Australia. *Earth Surface Processes and Landforms*, 13, 431-430.
- David, B. and Lourandos, H. (1999) Landscape as mind: land use, cultural space and change in north Queensland prehistory. *Quaternary International*, 59, 107-123.
- Davidson, D.A. and Shackley, M.I. (1976). *Geoarchaeology*. London: Duckworth.
- Davidson, D.A., Carter, S.P. and Quine, T.A. (1992) An evaluation of micromorphology as an aid to archaeological interpretation. *Geoarchaeology*, 7(1), 55-65.
- Dean, J.S. (1978) Independent dating in archaeological analysis. *Advances in Archaeological Method and Theory*, 1, 223-255.
- DeDeckker, P. (1986) What happened to the Australian aquatic biota 18,000 years ago? In P. DeDeckker and W.D. Williams (Eds.) *Limnology in Australia*. Junk, The Hague.
- Dent, R.J. Jr. (1995) *Chesapeake Prehistory: Old Traditions, New Directions*. Plenum Press, New York.
- Derbyshire, E. (1976) *Geomorphology and Climate*. John Wiley & Sons, London. Pp. 1-24.
- Dickinson, W.R., Burley, D.V., Nunn, P.D., Anderson, A., Hope, G., De Biran, A., Burke, C. & Matararaba, S. (1998). Geomorphic and Archaeological Landscapes of the Sigatoka Dune Site, Viti Levu, Fiji: Interdisciplinary Investigations. *Asian Perspectives*, 37(1), 1-31
- Dincauze, D.F. (2000) *Environmental Archaeology. Principles and Practice*. Cambridge University Press. 587 pp.
- Dodson, J. (1992) *The Naïve Lands: Prehistory and Environmental Change in Australia and the Southwest Pacific*. Melbourne. Longman Cheshire.
- Dorn, R.I. and F.M. Phillips (1991). Surface exposure dating: review and critical evaluation. *Physical Geography*, 12, 303-333.

References

- Dortch, C. (1977) Early and late stone industrial phases in Western Australia. In: Wright, R.V.S. (Ed.) *Stone Tools as Cultural Markers: Change, Evolution and Complexity*. Australian Aboriginal Studies, Canberra. Pp. 104-132.
- Dortch, C.E. and Roberts, R.G. (1996) An evaluation of radiocarbon chronologies at Miriwun rock shelter and the Monsmont site, Ord Valley, east Kimberley, Western Australia. *Australian Archaeology*, 42, 24-34.
- Dow, D.B. and Gemuts, I. (1969) Geology of the Kimberley region, Western Australia: the East Kimberley. *Bureau of Mineral Resources Australia Bulletin*, 106.
- Du, M., Yang, H., Chang, Q., Minami, K. and Hatta, T. (1998) Caesium-137 fallout depth distribution in different soil profiles and significance for estimating soil erosion rate. *Sciences of Soils*, 3, 3.
- Duller, G.A.T. (1996) Recent developments in luminescence dating of Quaternary sediments. *Progress in Physical Geography*, 20(2), 127-145.
- Dunai T.J. (2000) Scaling factors for production rates of in situ produced cosmogenic nuclides: A critical re-evaluation. *Earth and Planetary Science Letters*, 176 (1), 157-169.
- Dunne, J., Elmore, D. and Muzikar, P. (1999) Scaling factors for the rates of production of cosmogenic nuclides for geometric shielding and attenuation at depth on sloped surfaces. *Geomorphology*, 27, 3-11.
- Eisenberg, E. (1998) *The Ecology of Eden*. Picador, London.
- Evans, L.J. (1995). The use of paleosols in dating Quaternary deposits. In: Rutter, N.W. and Catto, N.R. (Eds.) *Dating Methods for Quaternary Deposits*. Newfoundland: Geological Association of Canada, Memorial University of Newfoundland. pp. 269-281.
- Fanning, P and Holdaway, S. (2002) Temporal limits to the archaeological record in arid western NSW, Australia: Lessons from OSL and radiocarbon dating of hearths and sediments. In: Jones, M. and Sheppard, P. (Eds.), *Proceedings of the 7th Australasian Archaeometry Conference*, Auckland. February 2001. Pp. 91-111.
- Farrand, W.R. (1985). Rockshelter and cave sediments. In: Stein, J.K. and Farrand, W.R. (eds.) *Archaeological Sediments in Context*. Center for the Study of Early Man, Institute for Quaternary Studies, University of Maine, Orono. Pp. 21-40.
- Farrand, W.R. (1993). Discontinuity in the stratigraphic record: snapshots from Franchthi Cave. In: Goldberg, P., Nash, D.T. and Petraglia, M.D. (eds.) *Formation Processes in Archaeological Context*. Prehistory Press, Madison. Pp. 85-96.
- Farrand, W.R. (2001). Sediments and stratigraphy in rockshelters and caves: A personal perspective on principles and pragmatics. *Geoarchaeology*, 16 (5), 537-557.

References

- Feathers, J.K. (1997a) The application of luminescence dating in American archaeology. *Journal of Archaeological Method and Theory*, 4(1), 1-65.
- Feathers, J.K. (1997b) Luminescence dating of sediment samples from white paintings rockshelter, Botswana. *Quaternary Science Reviews (Quaternary Geochronology)*, 16, 321-331.
- Feathers, J.K. and Bush, D.A. (2000) Luminescence dating of Middle stone age deposits at Die Kelders. *Journal of Human Evolution*, 38, 91-119.
- Ferring, C.R. (1992). Alluvial pedology and geoarchaeological research. In: Holliday, V.T. (ed.) *Soils in Archaeology Landscape Evolution and Human Occupation*. Smithsonian Institution Press, Washington. Pp. 1-40.
- Fifield, L.K., Bird, M.I., Turney, C.S.M., Hausladen, P.A., Santos, G.M. and di Tada, M.L. (2001). Radiocarbon dating of the human occupation of Australia prior to 40 ka – success and pitfalls. *Radiocarbon*, 43(2B), 1139-1145.
- Fink, D., McKelvey, B., Hanna, D. and Newsome, D. (2000) Cold rocks, hot sands: *In-situ* cosmogenic applications in Australia at ANTARES. *Nuclear Instruments and Methods in Physics Research B*, 172, 838-846.
- Firman, J.B. (1994) Paleosols in laterite and silcrete profiles. Evidence from the South East Margin of the Australian Precambrian Shield. *Earth Science Reviews*, 36, 149-177.
- Flannery, T. (1994) *The Future Eaters*. Reed, Sydney.
- Flemming, A., Summerfield, M.A., Stone, J.O., Fifield, L.K. and Cresswell, R.G. (1999) Denudation rates for the southern Drakensberg escarpment, SE Africa, derived from *in-situ*-produced cosmogenic ^{36}Cl : initial results. *Journal of the Geological Society, London*, 156, 209-212.
- Flood, J. (1970) A point assemblage from northern Australia. *Archaeology and Physical Anthropology in Oceania*, 5, 25 – 27.
- Flood, J. (1997) *Rock Art of the Dreamtime: Images of Ancient Australia*. Harper Collins, New York.
- Folk, R.L. (1968) Petrology and sedimentary rocks. Hamphills University Station, Texas.
- Folz, E. and Mercier, N. (1999) A single-aliquot OSL protocol using bracketing regenerative doses to accurately determine equivalent doses in quartz. *Radiation Measurements*, 30 (4), 477-485.
- Fox, A. (1983) *Kakadu Man and Landscape*. Heritage Australia.
- Frankel, D. (1990) Time inflation. *New Scientist*, 127(1724), 52-53.
- Frankel, D. (1993). Pleistocene chronological structures and explanations: a challenge. In: Smith, M.A., Spriggs, M. and Fankhauser, B. (Eds.). *Sahul in Review: the Archaeology of Australia, Papua New Guinea and Island Melanesia*. Prehistory, Research School of Pacific Studies. Australian National University Press, Canberra. Pp. 24-33

References

- Frankel, D. (1988) Characterising change in prehistoric sequences: a view from Australia. *Archaeology in Oceania*, 23, 41-48.
- Frankel, D. (1995) The Australian transition: real and perceived boundaries. *Antiquity*, 69, 649-655.
- Frederick, C.D., Bateman, M.D. and Rogers, R. (2002) Evidence for eolian deposition in the sandy uplands of east Texas and the implications for archaeological site integrity. *Geoarchaeology*, 17(2), 191-217.
- Freidel, M.H. (1994) How spatial and temporal scale effect the perception of change in rangelands. *The Rangeland Journal*, 16, 16-25.
- French, C.A.I. and Whitelaw, T.M. (1999) Soil erosion, agricultural terracing and site formation processes at Markiani, Amorgos, Greece: the micromorphological perspective. *Geoarchaeology*, 14, 151-189.
- Fullagar, R. and L. Head (1999) Aboriginal landscapes of the northwest Northern Territory, Australia. In: Layton, R., Ucko, P. and Austin, D. (eds.) *Frontiers of Landscape Archaeology*. London: Routledge. pp 322-335.
- Fullagar, R.L.K., Price, D.M. and Head, L.M. (1996) Early human occupation of northern Australia: archaeology and thermoluminescence dating of Jinmium rock-shelter, Northern Territory. *Antiquity*, 70, 751-773.
- Fullagar, R., Head, L., Ward, I., Mulvaney, K. and Tacon, P. (2000) Archaeological research in the Keep River region, Northern Territory. *Australian Archaeology*, 49, 45-46.
- Galbraith, R.F., Roberts, R.G., Laslett, G.M., Yoshida, H. and Olley, J.M. (1999) Optical dating of single and multiple grains of quartz from Jinmium rock shelter, Northern Australia: Part I, Experimental design and statistical models. *Archaeometry*, 41(2), 339-364.
- Gilbert, G. K. (1877) Geology of the Henry Mountains (Utah), US Geographical and Geological Survey of the Rocky Mountain Region, Washington DC.
- Gillespie, R. and Roberts, R.G. (2000) On the reliability of age estimates for human remains at Lake Mungo. *Journal of Human Evolution*, 38, 727-732.
- Gladfelter, B.G. (1985). On the interpretation of archaeological sites in alluvial settings. In: Stein, J.K. and Farrand, W.R. (eds.) *Archaeological Sediments in Context*. Center for the Study of Early Man, Institute for Quaternary Studies, University of Maine, Orono. pp. 41-52.
- Goldberg, P. (2002) Micromorphology and site formation at Die Kelders Cave I, South Africa. *Journal of Human Evolution*, 38, 43-90.

- Goldberg, P. and Arpin, T.L. (1999) Micromorphological analysis of sediments from Meadowcroft rockshelter, Pennsylvania: Implications for radiocarbon dating. *Journal of Field Archaeology*, 26(3), 325-342.
- Goldberg, P., Lev-Yadun, S. and Bar-Yosef, O. (1994) Petrographic thin sections of archaeological sediments: a new method for palaeobotanical studies. *Geoarchaeology*, 9(3), 243-257.
- Gosden, C. and Head, L. (1994) Landscape – a usefully ambiguous concept. *Archaeology in Oceania*, 29, 113-116.
- Gosse, J.C. and Phillips, F.M. (2001) Terrestrial in situ cosmogenic nuclides: theory and application. *Quaternary Science Reviews*, 20, 1475-1560.
- Goudie, A. (1986) *The Human Impact on the Natural Environment*. Cambridge.
- Gould, R.A. (1969) Puntutjarpa rockshelter: A reply to Messrs Glover and Lampert. *Archaeology and Physical Anthropology in Oceania*, 4, 229-237.
- Granger D.E. and Muzikar P.F. (2001) Dating sediment burial with in situ-produced cosmogenic nuclides: Theory, techniques, and limitations. *Earth and Planetary Science Letters*, 188 (1-2), 269-281.
- Granger, D.E. and Smith, A.L. (2000) Dating of buried sediments using radioactive decay and muogenic production of ^{26}Al and ^{10}Be . *Nuclear Instruments and Methods in Physics B*, 172, 822-826.
- Grave, P. & Kealhofer, L. (1999) Assessing bioturbation in archaeological sediments using soil morphology and phytolith analysis. *Journal of Archaeological Science*, 26, 1239-1248.
- Gregory, R.L. (1998) Aboriginal settlement patterns in the Ord-Victoria River region, Unpublished PhD thesis, Anthropology Dept., Northern Territory University, Darwin.
- Grun, R., Spooner, N., Thorne, A., Mortimer, G., Simpson, J.J., McCulloch, M.T., Taylor, L. and Curnoe, D. (2000) Age of the Late Mungo 3 skeleton, reply to Bowler and Magee and to Gillespie and Roberts. *Journal of Human Evolution*, 38, 733-741.
- Habermann, J., Schilles, T., Kalchgruber, R. and Wagner, G.A. (2000) Steps towards surface exposure dating using luminescence. *Radiation Measurements*, 32, 847-851.
- Harbor, J. (1999) Editorial. *Geomorphology*, 27, 1-2.
- Harrison, R. and Frink, D.S. (2000) The OCR carbon dating procedure in Australia: New dates from Wilinyjibari Rockshelter, southeast Kimberley, Western Australia. *Australian Archaeology*, 51, 6-15.
- Hart, D.M. (1995) Litterfall and decomposition in the Pilliga State Forests, NSW, Australia. *Australian Journal of Ecology*, 20, 19-25.

References

- Hassan, F.A. (1978) Sediments in Archaeology: Methods and Implications for palaeoenvironmental and cultural analysis. *Journal of Field Archaeology*, 5(2), 197-213.
- Hassan, F.A. (1985). Fluvial systems and geoarchaeology in arid lands: with examples from North Africa, the Near East, and the American Southwest. In: Stein, J.K. and Farrand, W.R. (eds.) *Archaeological Sediments in Context*. Center for the Study of Early Man, Institute for Quaternary Studies, University of Maine, Orono. Pp. 53-68.
- Head, J. (1979) Structure and properties of fresh and degraded wood: their effects on radiocarbon activity measurements. Unpublished M.Sc thesis, Australian National University, Canberra.
- Head, L. (1989) Prehistoric aboriginal impacts on Australian vegetation: an assessment of the evidence. *Australian Geographer*, 20(1), 37-46.
- Head, L. (1994). Both ends of the candle? Discerning human impact on the vegetation. *Australian Archaeology*, 39, 82-86.
- Head, L. (1996) Rethinking the prehistory of hunter-gatherers, fire and vegetation change in northern Australia. *The Holocene*, 6(4), 481-487.
- Head, L. (1999a) The Northern Myth Revisited? Aborigines, environment and agriculture in the Ord River Irrigation Scheme, Stages One and Two. *Australian Geographer*, 30(2), 141-158.
- Head, L. (1999b) Second Nature: Hunter-Gatherers, Land and the Past in Australia. In: Bennett, B. (ed.) *Australia in Between Cultures*. Papers from the Australian Association of the Humanities Symposium, Australian Academy of Humanities. Pp. 153-162.
- Head, L. (2000) *Second Nature. The History and Implications of Australia and Aboriginal Landscape*. Syracuse Press.
- Head, L. and Fullagar, R. (1997) Hunter-gatherer archaeology and postoral contact: Perspectives from the northwest Northern Territory, Australia. *World Archaeology*, 28, 418-428.
- Head, L., Atchison, J. and Fullagar, R. (2002) Country and garden: ethnobotany, archaeobotany and Aboriginal landscapes near the Keep River, northwestern Australia. *Journal of Social Archaeology*, 2, 173-196.
- Heimsath, A.M., Dietrich, W.E., Nishizumi, K. and Finkel, R.C. (1999) Cosmogenic nuclides, topography, and the spatial variation of soils depth. *Geomorphology*, 27, 151-172.
- Heimsath A.M., Chappell J., Dietrich, W.E., Nishiizumi, K. and Finkel R.C. (2000) Soil production on a retreating escarpment in southeastern Australia. *Geology*, 28 (9), 787-790.
- Heinrich, J. and Moldenhauer, K-M. (2002) Climatic and anthropogenic induced landscape degradations of West African dry Savanna environments during the Later Holocene. *Quaternary International*, 93/94, 127-137.

References

- Hiscock, P. (1981) Comments on the use of chipped stone artefacts as a measure of “intensity of site usage”. *Australian Archaeology*, 13, 30-34.
- Hiscock, P. (1984) A preliminary report on the stone artefacts from Colless Creek Cave. *Queensland Archaeological Research*, 1, 120-151.
- Hiscock, P. (1990) A study in scarlet: taphonomy and inorganic artefacts. In: Solomon, S., Davidson, I. And Watson, D. (eds.) *Problem Solving in Taphonomy: Archaeological and Palaeontological Studies from Europe, Africa and Oceania*. TEMPUS, Vol. 2, pp. 34-44.
- Hiscock, P. (2002) Quantifying the Size of Artefact Assemblages. *Journal of Archaeological Science*, 29(4), 251-258.
- Hiscock, P. and Kershaw, A.P. (1992) Palaeoenvironments and prehistory of Australia’s tropical Top End. In: Dodson, J. (ed.) *The Naïve Lands: Prehistory and Environmental Change in Australia and the Southwest Pacific*. Melbourne. Longman Cheshire. Pp. 43-75.
- Hoelzmann, P., Keding, B., Berke, H., Kropelin, S. and Kruse, H-J. (2001) Environmental change and archaeology: lake evolution and human occupation in the Eastern Sahara during the Holocene. *Palaeogeography, Palaeoclimatology, Palaeoecology*. 169, 193-217.
- Holdaway, S.J., Fanning, P.C. and Witter, D. (2000) Prehistoric Aboriginal occupation of the rangelands. Interpreting the surface archaeological record of far western New South Wales, Australia. *The Rangelands Journal*, 22, 58-71.
- Holdaway, S.J., Fanning, P.C., Jones, M., Shiner, J., Witter, D.C. and Nicholls, G. (2002) Variability in the Chronology of Late Holocene Aboriginal Occupation on the Arid Margin of Southeastern Australia. *Journal of Archaeological Science*, 29(4), 351-363.
- Holliday, V.T. (1989) Paleopedology in Archaeology. *Catena Supplement*, 16, 187-206.
- Holt, J.A., Coventry, R.J. and Sinclair, D.F. (1980) Some aspects of the biology and pedological significance of mound-building termites in a red and yellow earth landscape near Charters Towers, north Queensland. *Australian Journal of Soil Research*, 18: 97-109.
- Hope, G. (1984) Australian Environmental Change. Timing, Directions, Magnitudes, and Rates. In: Martin, P.S. and Klein, R.G. (eds.) *Pleistocene Extinctions: Prehistoric Revolution*. University of Arizona Press, Tuscon. Pp. 681 – 691.
- Hope, G. (1989) Climatic implications of timberline changes in Australasia from 30,000 yr B.P. to present. In: Donnelly, T.H. and Wasson, R.J. (Eds.) *CLIMANZ 3*. CSIRO, Division of Water Resources, Canberra.

References

- Hope, G., Hughes, J. and Russell-Smith, J. (1985) Geomorphological fieldwork and the evolution of the landscape of Kakadu National Park. In: Jones, R. (Ed.) *Archaeological Research in Kakadu NP*. NPWS Special Publication. 13. Pp. 229-240.
- Hopkins, S., Ash, J., Graham, A.W., Head, J. and Hewett, R.K. (1993) Charcoal evidence of the spatial extent of the Eucalyptus woodland expansions and rainforest contractions in North Queensland during the late Pleistocene. *Journal of Biogeography*, 20(4), 357-372.
- Horton, D.R. (1993) Here be dragons: a view of Australian Archaeology. In: Smith, M.A., Spriggs, M. and Fankhauser, B. (eds.) *Sahul in Review. Pleistocene Archaeology in Australia, New Guinea and Island Melanesia*. Department of Prehistory, R.S.P.A.S., Australian National University, Canberra. Pp. 11-16.
- Howard, A.J. and M.G. Macklin (1999). A generic geomorphological approach to archaeological interpretation and prospection in British river valleys: a guide for archaeologists investigating Holocene landscapes. *Antiquity*, 73, 527-541.
- Hubbard, N.N. (1995) In search of palaeoclimates: Australia, 18,000 yr BP. *Palaeogeography, Palaeoclimatology, Palaeoecology*, 116, 167-188.
- Hughes, P.J. (1983a) Geoarchaeology in Australia. In: Connah, G. (ed.). *Australian Field Archaeology. A Guide to Techniques*. Canberra: Australian Institute of Aboriginal Studies. Pp. 109-117.
- Hughes, P. (1983b) Colless Creek rockshelter archaeological site northwestern Queensland – 18 ka. In: Chappell, J. and Grindrod, J. (Eds) *CLIMANZ I*. Australian National University, Canberra. Pp. 59-61.
- Hughes, P.J. and Djohadze, V. (1980) Radiocarbon dates from archaeological sites on the south coast of New South Wales and the use of age/depth curves. *Occasional Papers in Prehistory*, 1, 21.
- Hughes, P.J. and Lampert, R.J. (1982) Prehistoric population change in southern coastal New South Wales. In: Bowdler, S. (ed.) *Coastal archaeology in eastern Australia*. Department of Prehistory, RSPAS, Australian National University. Pp. 16-28.
- Hughes, P.J. and Sullivan, M.E. (1981) Aboriginal burning and late Holocene geomorphic events in eastern NSW. *Search*, 12, 277-278.
- Hughes, P.J. and Sullivan, M.E. (1982) Geoarchaeology in Australia. In: Ambrose, W. and Duerden, P. (eds.) *Archaeometry: An Australasian Perspective*. RSPAS, ANU, Canberra.
- Hughes, P.J. & Sullivan, M.E. (1986). 'Aboriginal landscape'. In: Russell, J.S. and Isbell, R.F. (Eds.). *Australian Soils: the Human Impact*. St. Lucia: University of Queensland Press. Pp. 117-133.
- Hughes, P.J., Sullivan, M.E. and Lampert, R.J. (1973). The use of silcrete by Aborigines in southern coastal New South Wales. *Search*, 12, 277-278.

References

- Huntley, D.J., Godfrey-Smith, D.I. and Thewalt, M.L.W. (1995) Optical dating of sediments. *Nature*, 313, 105-107.
- Ivy-Ochs, S., Wust, R., Kubik, P.W., Muller-Beck, H. and Schluchter, C. (2001) Can we use cosmogenic isotopes to date stone artefacts? *Radiocarbon*, 43(2B), 759-764.
- Jones, R. (1985) *Archaeological Research in Kakadu NP*. NPWS Special Publication. No. 13.
- Jones, R. and Johnson, I. (1985) Deaf Adder Gorge: Lindner Site, Nauwalabila I. In: Jones, R. (Ed.) *Archaeological Research in Kakadu NP*. NPWS Special Publication. 13. Pp. 165-227.
- Johnson, B.J., Miller, G.H., Fogel, M.L., Magee, J.W., Gagan, M.K. and Chivas, A.R. (1999) 65,000 years of vegetation change in Central Australia and the Australian Summer monsoon. *Science*, 284, 1150-1152.
- Johnson, D.L., Mandel, R.D., Leach, J.D. and Petraglia, M. (2002) Formation Processes in Regional Perspective. *Geoarchaeology*, 17(1), 3 – 5.
- Keeley, H.C.M. and Macphail, R.I. (1981) A soil handbook for archaeologists. *Institute of Archaeology Bulletin*, 18, 225-243.
- Kemp, E.M. (1981) Pre-Quaternary fire in Australia. In: Gill, A.M., Groves, R.H. and Noble, I.R. (Eds.) *Fire and the Australian Biota*. Australian Academy of Science, Canberra. Pp. 1 –22.
- Kershaw, A.P. (1986) The last two glacial-interglacial cycles from northeastern Australia: implication for climate change and Aboriginal burning. *Nature*, 322, 47-49.
- Kershaw, A.P., Moss, P.T. and Van der Kaars, S. (1997) Environmental change and the Human Occupation of Australia. *Anthropologie*, XXXV/2 – 3, 35-43.
- Kershaw, P.A., Clark, J.S., Gill, M.A. and D’Costa, D.M. (2000) A history of fire in Australia. In: Bradstock, R., Williams, J. and Gill, A.M. (Eds.) *Flammable Australia: the Fire Regimes and Biodiversity of a Continent*. Cambridge University Press.
- Kershaw, A.P., van der Kaars, S., Moss, P.T. and Wang, X. (2002) Palynological evidence for environmental change in the Indonesian-northern Australian region over the last 140,000 to 300,000 years. In Kershaw, A.P., David, B., Tapper, N.J., Penny, D. and Brown, J. (eds.) *Bridging Wallace's Line: The Environmental and Cultural History and Dynamics of the Southeast Asian - Australian Region*. Catena Verlag, Reiskirchen, Germany.
- Kinhill PTY LTD (2001) Ord River Irrigation Area, Stage 2. Proposed development of the M2 area. Environmental Review and Management Program. Environmental Impact Study.
- Kohl, C.P. and Nishiizumi, K. (1992) Chemical isolation of quartz for measurement of *in-situ* produced cosmogenic nuclides. *Geochimica et Cosmochimica Acta*, 56, 3583 – 3587.

References

- Kowalewski, M., and Bambach, R.K., (2001) Diastems and time-averaging: The limits of resolution in stratigraphy and paleontology. *Geological Society of America Abstracts with Programs*, 33, A32.
- Kowalewski, M., Goodfriend, G.A. and Flessa, K.W. (1998) High-resolution estimates of temporal mixing within shell beds: the evils and virtues of time averaging. *Palaeobiology*, 24(3), 287-304.
- Kubik P.W., Frank M., Schluchter C., Ivy-Ochs S. and Masarik J. (1998) ^{10}Be and ^{26}Al production rates deduced from an instantaneous event within the dendro-calibration curve, the landslide of Kofels, Otz Valley, Austria. *Earth and Planetary Science Letters*, 161(1-4), 231 - 241.
- Lal, D. (1991) Cosmic ray labeling of erosion surfaces: in situ nuclide production rates and erosion models. *Earth and Planetary Science Letters*, 104, 424-439.
- Lal, D. and Arnold, J.R. (1995) Tracing quartz through the environment. *Proceedings of the Indian Academy of Sciences (Earth Planetary Science)*, 94(1), 1985.
- Lal, D., Nishiizumi, K. and Arnold, J. (1987) In situ cosmogenic ^3H , ^{14}C and ^{10}Be for determining the net accumulation and ablation rates of ice sheets. *Journal of Geophysical Research*, 92, 4947-4952.
- Lawson, E.M., Elliot, G., Fallon, J., Fink, D., Hotchkis, M.A.C., Hua, Q., Jacobsen, G.E., Lee, P., Smith, A.M., Tuniz, C. and Zoppi, U. (2000) AMS at ANTARES – the first 10 years. *Nuclear Instruments and Methods in Physics Research B*, 172, 95-99.
- Lees, B.G. (1992a) Geomorphological evidence for Late Holocene climatic change in northern Australia. *Australian Geographer*, 23(1), 1-10.
- Lees, B.G. (1992b) Recent terrigenous sedimentation in Joseph Bonaparte Gulf, Northwestern Australia. *Marine Geology*, 103, 199-213.
- Lees, B.G., Lu, Y. and Head, J. (1990) Reconnaissance thermoluminescence dating of northern Australian dunefields. *Quaternary Research*, 34, 169-185.
- Lees, B.G., Yanchou, L. and Price, D.M. (1992) Thermoluminescence dating of dunes at Cape St. Lambert, East Kimberleys, northwestern Australia. *Marine Geology*, 106, 131-139.
- Lewis, D. (1988) The rock paintings of Arnhem Land, Australia: social ecological and material culture change in the post-glacial period. *BAR International Series*, 415.
- Lewis, D. (1997) Bradshaws: the view from Arnhem Land. *Australian Archaeology*, 44, 1-16.
- Lobry de Brun, L.A. and Conacher, A.J. (1990) The role of termites and ants in soil modification: a review. *Australian Journal of Soil Research*, 28, 55-93.
- Lourandos, H. (1996) Change in Australian prehistory: scale, trends and frameworks of interpretation. *Tempus*, 6, 15-21.
- Lourandos, H. (1997) *Continent of Hunter-Gatherers: New Perspectives in Australian Prehistory*. Cambridge: Cambridge University Press.

References

- Lourandos, H. and David, B. (1998) Comparing long-term archaeological and environmental trends: north Queensland, arid and semi-arid Australia. *The Artefact*, 21, 105-112.
- MacLeod, I.D., Haydock, P. and Ford, B. (1997) Conservation Management of West Kimberley rock art: micro-climate studies and decay mechanisms. In: Kenneally, K.F., Lewis, M.R., Donaldson, M. and C. Clement (eds.) *Aboriginal Rock Art of the Kimberley*. Occasional Paper No.1 Kimberley Society, Perth, Western Australia. Pp. 39-46.
- Macphail, R.I., Courty, M.A. and Goldberg, P. (1990) Soil Micromorphology in Archaeology. *Endeavour*, 14(4), 163-171.
- Mardaga-Campbell, M. and Campbell, J.B. (1985) Lithic occurrences and stratigraphic problems at Turtle Rock (Harvey Ranges) North Queensland. *Queensland Archaeological Research*, 2, 98-131.
- Markewich, H.W., Wysocki, D.A., Pavich, M.J., Rutledge, E.M., Millard, H.T., Rich, F.J., Maat, P., Rubin, M. and McGeehin, J.P. (1998) Palaeopedology plus TL, ^{10}Be , and ^{14}C dating as tools in stratigraphic and palaeoclimatic investigations, Mississippi River Valley, U.S.A. *Quaternary International*, 51/52, 143-167.
- Marshall, E. (2001) Pre-Clovis sites fight for acceptance. *Science*, 291, 1730-1732.
- Masarik, J., Kollar, D. and Vanya, S. (2000) Numerical simulation of in situ production of cosmogenic nuclides: Effects of irradiation geometry. *Nuclear Instruments and Methods in Physics Research B*, 172, 786-789.
- Masarik, J., Frank, M., Schafer, J.M. and Wieler, R. (2001) Corrections of in situ cosmogenic nuclide production rates for geometric field intensity variations during the past 800,000 years. *Geochimica et Cosmochimica Acta*, 65(17), 2995-3003.
- Mathews, W., French, C.A.I., Lawrence, T., Cutler, D.F. and Jones, M.K. (1997) Microstratigraphic traces of site formation processes and human activities. *World Archaeology*, 29(2), 281-308.
- Maxwell, T.A. and Haynes, C. V. Jr. (2001) Sand sheet dynamics and Quaternary landscape evolution of the Selima sand sheet, southern Egypt. *Quaternary Science Reviews*, 20, 1623-1647.
- McBeaty, S. (1990) Consider the humble termite: termites as agents of post-depositional disturbance at African archaeological sites. *Journal of Archaeological Science*, 17, 111-144.
- McConnell, K. (1997) Palaeoethnobotanical remains of Carpenter's Gap Site 1, the Kimberleys, Western Australia. Unpublished M.A thesis. Division of Archaeology and Natural History, RSPAS, Australian National University.
- McConnell, K. and O'Conner, S. (1997) 40,000 year record of food plants in the Southern Kimberley Ranges, Western Australia. *Australian Archaeology*, 45, 20-31.

References

- McCoy, D.G., Prescott, J.R. and Nation, R.J. (2000) Some aspects of single-grain luminescence dating. *Radiation Measurements*, 32, 859-864.
- McKeever, S.W.S. and Chen, R. (1998) Luminescence models. *Radiation Measurements*, 27 (5/6), 625-661.
- McTainsh, G.H. (1989) Quaternary aeolian dust processes and sediments in the Australian region. *Quaternary Science Reviews*, 8, 235-253.
- Mejdahl, V. and Botter-Jensen, L. (1994) Luminescence dating of archaeological material using a new technique based on single aliquot measurements. *Quaternary Science Reviews (Quaternary Geochronology)*, 13, 551-554.
- Mejdahl, V. and Christiansen, H.H. (1994) Procedures used for luminescence dating of sediments. *Quaternary Science Reviews (Quaternary Geochronology)*, 13, 403-406.
- Miller, G.H., Magee, J.W., Johnson, B.J., Fogel, M.L., Spooner, N.A., McCulloch, M.T. and Ayliffe, L.K. (1999) Pleistocene Extinction of *Genyornis newtoni*: Human impact on Australian megafauna. *Science*, 283, 205-208.
- Morwood, M.J. (1981) Archaeology of the Central Queensland Highlands: the stone component. *Archaeology in Oceania*, 16, 1-52.
- Morwood, M.J. (1986) The archaeology of art: excavations at Maidenwell and Gatton Shelters, S.E. Queensland. *Queensland Archaeological Research*, 3, 88-132.
- Morwood, M.J. and Hobbs, D.R. (1995) Themes in the prehistory of tropical Australia. *Antiquity*, 69, 747-768.
- Morwood, M.J., Hobbs, D.R. and Price, D.M. (1995) Excavations at Sandy Creek 1 and 2. *Tempus*, 3, 71-85.
- Mory, A.J. and Beere, G.M. (1988) Geology of the onshore Bonaparte and Ord Basins in Western Australia. *Geological Survey of Western Australia*, Bulletin 134.
- Moss, P. and Kershaw, P. (2000) The last glacial cycle from the humid tropics of northeastern Australia: comparison of a terrestrial and marine record. *Palaeogeography, Palaeoclimatology, Palaeoecology*, 155, 155-176.
- Mulvaney, D.J. (1961) The Stone Age of Australia. *Proceedings of the Prehistoric Society*, XXXVII, 56-107
- Mulvaney, D.J. (1972) Australian Archaeology. A Guide to Field and Laboratory Techniques. In: Mulvaney, D.J. (Ed.) *Australian Institute of Aboriginal Studies*. Pp.1-4.
- Mulvaney, K. J. (1996) What to do on a rainy day: reminiscences of Mirriuwung and Gadjerong artists. *Rock Art Research*, 13, 3-20.

- Mulvaney, J. and Kamminga, J. (1999) *Prehistory of Australia*. Allen & Unwin, Sydney.
- Murray, A.S. and Roberts, R.G. (1998) Measurement of the equivalent dose in quartz using regenerative-dose single-aliquot protocol. *Radiation Measurements*, 29, 503-515.
- Murray, A.S. and Wintle, A.G. (2000) Luminescence dating of quartz using an improved single-aliquot regenerative protocol. *Radiation Measurements*, 32, 57-73.
- Nanson, G.C. (1986). Episodes of vertical accretion and catastrophic stripping: a model of disequilibrium floodplain development. *Geological Society of America Bulletin*, 97, 1467-1475.
- Nanson, G.C. and Tooth, S. (1999) Arid-zone rivers as indicators of climate change. In: Singhvi, A.K. and Derbyshire, E. (eds.) *Palaeoenvironmental Reconstruction in Arid Lands*. Oxford, New Delhi. Pp. 175-216.
- Nanson, G.C., Price, D.M. and Short, S.A. (1992) Wetting and drying of Australia over the past 300 ka. *Geology*, 20, 791-794.
- Nanson, G.C., East, T.J. and Roberts, R.G. (1993) Quaternary stratigraphy, geochronology and evolution of the Magela Creek catchment in the monsoon tropics of northern Australia. *Sedimentary Geology*, 83, 277-302.
- Nanson, G.C., Young, R.W., Price, D.M. and Rust, B.R. (1988) Stratigraphy, sedimentology, and late-Quaternary chronology of the Channel Country of western Queensland. In: Warner, R.F. (ed.) *Fluvial geomorphology of Australia*. Pp. 151-175. Academic Press, Sydney.
- Nanson, G.C., Price, D.M., Short, S.A., Young, R.W. and Jones, B.G. (1991) Comparative Uranium-Thorium and thermoluminescence dating of weathered Quaternary alluvium in the tropics of northern Australia. *Quaternary Research*, 35, 347-366.
- Newsome, D. (2000) Origin of sand plains in Western Australia: a review of the debate and some recent findings. *Australian Journal of Earth Sciences*, 47, 695-706.
- Nkem, J.N., Lobry de Brun, L.A., Grant, C.D. & Hulugalle, N.R. (2000) The impact of ant bioturbation and foraging activities on surrounding soil properties. *Pedobiologica*, 44 (5), 609-621.
- Nishiizumi, K., Winterer, E.L., Kohl, C.P., Klein, J., Middleton, R., Lal, D. and Arnold, J.R. (1989) Cosmic ray production rates of ^{10}Be and ^{26}Al in quartz from glacially polished rocks. *Journal of Geophysical Research*, 94, 17907.
- Nishiizumi K., Kohl, C.P., Arnold, J.R., Klein, J., Fink D. and Middleton R. (1991) Cosmic ray produced ^{10}Be and ^{26}Al in Antarctic rocks: exposure and erosion history. *Earth and Planetary Science Letters*, 104 (2-4), 440-454.

References

- Nishiizumi, K., Kohl, C.P., Arnold, J.R., Dorn, R., Klein, J., Fink, D., Middleton, R. and Lal, D. (1993) Role of in situ cosmogenic nuclides ^{10}Be and ^{26}Al in the study of diverse geomorphic processes. *Earth Surface Processes and Landforms*, 18, 407-425.
- Nishiizumi, K., Finkel, R.C., Klein, J. and Kohl, C.P. (1996) Cosmogenic production of ^7Be and ^{10}Be in water targets. *Journal of Geophysical Research*, 101, 22,225-22,232.
- Nott J. (1994a) Long-term landscape evolution in the Darwin region and its implications for the origin of landsurfaces in the north of the Northern Territory. *Australian Journal of Earth Sciences*, 41(5), 407-415.
- Nott, J. (1994b) The influence of deep weathering on coastal landscape and landform development in the monsoonal tropics of northern Australia. *Journal of Geology*, 102 (5), 509-522.
- Nott, J. and Price, D. (1994) Plunge pools and palaeoprecipitation. *Geology*, 22, 1047-1050.
- Nott, J. and Price, D. (1999) Waterfalls, floods and climate change: evidence from tropical Australia. *Earth and Planetary Science Letters*, 171, 267-276.
- Nott, J. and Roberts, R.G. (1996) Time and process rates over the past 100 m.y.: A case for dramatically increased landscape denudation rates during the late Quaternary in northern Australia. *Geology*, 24(10), 883-887.
- Nott, J., Bryant, E. and Price, D. (1999) Early-Holocene aridity in tropical northern Australia. *The Holocene*, 9(2), 231-236.
- O'Connor, S. (1995) Carpenter's Gap rockshelter 1: 40,000 years of Aboriginal occupation in the Napier Ranges, Kimberley, WA. *Australian Archaeology*, 40, 58-59.
- O'Connor, S. (1996) Thirty-thousand years in the Kimberley: results of excavation of three rockshelters in the coastal West Kimberley, W.A. *Tempus*, 3, 26-49.
- O'Connor, S. (1999) 30,000 years of Aboriginal Occupation: Kimberley, North West Australia. Department of Archaeology and Natural History and Centre for Archaeological Research, The Australian National University, Canberra.
- O'Connor, S., Veth, P. and Barham, A. (1999) Cultural versus natural explanations for lacunae in Aboriginal occupation deposits in northern Australia. *Quaternary International*, 59, 61-70.
- Olley, J.M., Murray, A. and Roberts, R. (1996) The effects of disequilibria in the uranium and thorium decay chains on burial dose rates in fluvial sediments. *Quaternary Science Reviews (Quaternary Geochronology)*, 15, 751-760.
- Olley, J.M., Roberts, R.G. and Murray, A.S. (1997) Disequilibrium in the Uranium decay series in sedimentary deposits at Allen's Cave, Nullabor Plain, Australia: Implication for the dose rate determinations. *Radiation Measurements*, 27(2), 433-443.

References

- Olley, J., Caitcheon, G.G. and Roberts, R.G. (1999) The origin of dose distributions in fluvial sediments, and the prospect of dating single grains from fluvial deposits using optically stimulated luminescence. *Radiation Measurements*, 30, 207-217.
- Otte, M., Bayon, I.L., Noiret, P., Bar-Yosef, O., Yalcinkaya, I., Kartal, M., Leotard, J-M. and Pettitt, P. (2002) Sedimentary deposition rates and carbon-14: the epi-palaeolithic sequence of Okuzini Cave (Southwest Turkey). *Journal of Archaeological Science*, 30, 325-341.
- Ouzman, S., Tacon, P., Mulvaney, K. and Fullagar, R. (2002) Extraordinary engraved bird track from North Australia: extinct fauna, Dreaming Being and/or aesthetic masterpiece? *Cambridge Archaeological Journal*, 12(1), 103-112.
- Parnell, J.J., Terry, R.E and Nelson, Z. (2002) Soil Chemical Analysis Applied as an Interpretive Tool for Ancient Human Activities in Piedras Negras, Guatemala. *Journal of Archaeological Science*, 29(4), 379-404.
- Paterson, S.J. (1970) Geomorphology of the Ord-Victoria area, Lands of the Ord-Victoria River Area, Western Australia and Northern Territory. *Land Research Series*, No. 28. Melbourne, CSIRO.
- Patterson, W.A., Edwards, K.J., and Maguire, D.J. (1987) Microscopic charcoal as a fossil indicator of fire. *Quaternary Science Reviews*, 6, 3-23.
- Pavich, M.J., Brown, L., Klein, J. and Middleton, R. (1986) ^{10}Be accumulation in a soil chronosequence. *Earth and Planetary Science Letters*, 68, 198-204.
- Peterson, N. (1971) Open sites and the ethnographic approach to the archaeology of hunter-gatherers. In: Mulvaney, D.J. and Golson, J. (Eds.) *Aboriginal Man and Environment in Australia*. Canberra: ANU Press. Pp. 239-248.
- Phillips, W.M. (2000) Estimating cumulative soil accumulation rates with *in situ*-produced cosmogenic nuclide depth profiles. *Nuclear Instruments and Methods in Physics Research B*. 172, 817-821.
- Phillips, F.M., Flinsch, M., Elmore, D. and Sharma, P. (1997) Maximum ages of the Coa valley (Portugal) engravings measured with Chlorine-36. *Antiquity*, 71, 100-104.
- Prescott, J.R. and Fox, P.J. (1990) Dating quartz sediments using the 325°C TL peak: new spectral data. *Ancient TL*, 8, 32-34.
- Prescott, J.R. and Hutton, J.T. (1995) Environmental dose rates and radioactive disequilibrium from some Australian luminescence dating sites. *Quaternary Science Reviews*, 14, 439-448.
- Price, D.M. (1994a) TL dating of fluvial quartz sands: a comparison of ages obtained at 325 °C and 375 °C. *Ancient TL*, 12(2), 20-23.

References

- Price, D.M. (1994b) TL signatures of quartz grains of different origin. *Radiation Measurements*, 23(2/3), 413-417.
- Price, D.M., Bryant, E.A. and Young, R.W. (1999) Thermoluminescence evidence for the deposition of coastal sediments by tsunami wave action. *Quaternary International*, 56, 123-128.
- Pulleine, R. (1928). The Tasmanians and their Stone-culture. *Australasian Association for the Advancement of Science*, 19, 294-314.
- Pye, K. and Gardner, R. (1981): Nature, origin and palaeoenvironmental significance of red coastal and desert dune sands. *Progress in Physical Geography*, 5, 514-534.
- Rapp, G. Jr. And Hill, C.L. (1998) *Geoarchaeology. The Earth Science Approach to Archaeological Interpretation*. Yale University Press, London. 274pp.
- Readhead, M.L. (1984) Thermoluminescence dating of some Australian sedimentary deposits. Unpublished PhD thesis, Australian National University.
- Renfrew, C. (1976) Archaeology and the Earth Sciences. In. Davidson, D.A. and Shackley, M.L. (eds.) *Geoarchaeology: Earth Science and the Past*. Westview Press, Colorado. Pp. 1-5.
- Retallack, G.J. (1990) *Soils of the Past. An Introduction to Paleopedology*. Unwin Hyman. Sydney. 520pp.
- Retallack, G.J. (1997) *A Colour Guide to Paleosols*. John Wiley & Sons. Brisbane. 175pp.
- Reynolds, K.S. and Catt, J.A. (1987) Soils and vegetation history of abandoned enclosures in the New Forest, Hampshire, England. *Journal of Archaeological Science*, 14, 507-527.
- Richardson, N. (1992) Conjoin sets and stratigraphic integrity in a sandstone shelter: Kenniff Cave (Queensland, Australia). *Antiquity*, 66, 408-418.
- Robbins, L.H., Murphy, M.L., Brook, G.A., Ivester, A.H., Campbell, A.C., Klein, R.G., Milo, R.G., Stewart, K.M., Downey, W.S. and Stevens, N.J. (2000) Archaeology, palaeoenvironment, and chronology of the Tsodilo Hills White Paintings Rock Shelter, Northwest Kalahari, Botswana. *Journal of Archaeological Science*, 27, 1085-1113.
- Roberts, H.M. (1996) Post-depositional migration of uranium – and thorium-series radionuclides: The potential impact on luminescence ages. Abstract from PhD thesis, University of Liverpool. (<http://www.aber.ac.uk/~qecwww/papers/helen/phd.html>).
- Roberts, H.M. and Plater, A.J. (1999) U- and Th-series disequilibria in coastal infill sediments from Praia da Rocha (Algarve Region, Portugal): a contribution to the study of late Quaternary weathering and erosion. *Geomorphology*, 26, 223-238.
- Roberts, R.G. (1991) Sediment budgets and Quaternary history of the Magela Creek catchment, tropical Northern Australia. Unpublished PhD thesis, Wollongong, Australia.

- Roberts, R.G. (1997) Luminescence dating in archaeology: from origins to optical. *Radiation Measurements*, 27(5/6), 819-892.
- Roberts, R.G. and Jones, R. (1991). The test of time: physical dating methods in archaeology. *Australian Natural History*, 23(11), 858-865.
- Roberts, R.G. and Jones, R. (2001) Chronologies of carbon and silica: evidence concerning the dating of the earliest human presence in Northern Australia. In: Tobias, P.V., Raath, M.A., Moggi-Cecchi, J. and Doyle, G.A. (eds.) *Humanity from African Naissance to Coming Millennia*. Pp. 239-248.
- Roberts, R.G., Jones, R. and Smith, M.A. (1990) Thermoluminescence dating of a 50,000 year-old human occupation site in northern Australia. *Nature*, 345, 153-156.
- Roberts, R.G., Jones, R. and Smith, M.A. (1994a) Beyond the radiocarbon barrier in Australian prehistory. *Antiquity*, 68, 611-616.
- Roberts, R.G., Jones, R., Spooner, N.A., Head, M.J., Murray, A.S. and Smith, M.A. (1994b) The human colonisation of Australia: optical dates of 53,000 and 60,000 years bracket human arrival at Deaf Adder Gorge, Northern Territory. *Quaternary Geochronology (Quaternary Science Reviews)*, 13, 575-583.
- Roberts, R., Walsh, G., Murray, A., Olley, J., Jones, R., Morwood, M., Tuniz, C., Lawson, E., Macphail, M., Bowdery, D. and Naumann, I. (1997) Luminescence dating of rock art and past environments using mud-wasp nests in northern Australia. *Nature*, 387, 696-699.
- Roberts, R., M. Bird, J. Olley, R. Galbraith, E. Lawson, G. Laslett, H. Yoshida, R. Jones, R. Fullagar, G. Jacobsen and Q. Hua. (1998a). Optical and radiocarbon dating at Jinmium rock shelter, northern Australia. *Nature*, 393, 358-362.
- Roberts, R., Yoshida, H., Galbraith, R., Laslett, G., Jones, R. and Smith, M. (1998b) Single-aliquot and single-grain optical dating confirm thermoluminescence age estimates at Malakunanja II rock shelter in northern Australia. *Ancient TL*, 16(1), 19-24.
- Roberts, R.G., Galbraith, R.F., Olley, J., Yoshida, H. and Laslett, G.M. (1999) Optical dating of single and multiple grains of quartz from Jinmium rock shelter, northern Australia: Part II, Results and Implications. *Archaeometry*, 41(2), 365-395.
- Roberts, R.G., Galbraith, R.F., Yoshida, H., Laslett, G.M. and Olley, J.M. (2000) Distinguishing dose populations in sediment mixtures: a test of single-grain optical dating procedures using mixtures of laboratory-dose quartz. *Radiation Measurements*, 32, 459-465.
- Roberts, R.G., Flannery, T.F., Ayliffe, L., Yoshida, H., Olley, J.M., Prideaux, G.J., Laslett, G.M., Baynes, A., Smith, M.A., Jones, R. and Smith, B.L. (2001) New ages for the last Australian megafauna: continent-wide extinction about 46,000 years ago. *Science*, 292, 1888-1892.

References

- Ross, A. (1982) Problems of disentangling human and palaeoclimatic influences upon the Australian landscape. In: Thom, B.J. and Wasson, R.J. (eds.) *Holocene Research in Australia. 1978-1982*. Vol 33, 29-36.
- Ross, A., Donnelly, T. and Wasson, R. (1992) The peopling of the arid zone: human-environment interactions. In: Dodson, J. (ed.) *The Naïve Lands. Prehistory and Environmental Change in Australia and the South-west Pacific*. Longman Cheshire pub., Melbourne. Pp. 76 – 113.
- Sadler, P.M. (1981) Sediment accumulation rates and the completeness of the stratigraphic section. *Journal of Geology*, 89, 569-584.
- Saunders, I. And Young, A. (1983) Rates of surface processes on slopes, slope retreat and denudation. *Earth Surface Processes and Landforms*, 8, 473-501.
- Shackley, M.S. (1998) Gamma rays, x-rays and stone tools: some recent advances in archaeological geochemistry. *Journal of Archaeological Science*, 25, 259-270.
- Schick, K.D. (1987) Experimentally-derived criteria for assessing hydrological disturbance of archaeological sites. In: Nash, D.T. and Petraglia, M.D. (Eds.) *Natural Formation Processes and the Archaeological Record*. BAR International Series 352. British Archaeological Reports, Oxford. Pp. 86-107.
- Schulmeister, J. (1992) A Holocene pollen record from lowland tropical Australia. *The Holocene*, 2, 107-116.
- Schulmeister, J. (1999) Australasian evidence for mid-holocene climate change implies precessional control of Walker Circulation in the Pacific. *Quaternary International*, 57/58, 81-91.
- Schwartz, D. (1996) Archeologie prehistorique et processus de formation des “stone-lines” en Afrique Centrale (Congo-Brassaville et zones peripheriques). *Geo-Eco-Trop*, 20,(1-4), 15-38.
- Schwertmann, U. (1993) Relations between iron oxides, soil colour, and soil formation. *Soil Science Society of America, Special Publication*, 31, 51-69.
- Short, S.A., Lowson, R.T., Ellis, J. and Price, D.M. (1989) Thorium-uranium disequilibrium dating of Late Quaternary ferruginous concretions and rinds. *Geochimica et Cosmochimica Acta*, 53, 1379-1389.
- Skarpe, C. (1992) Dynamics of savanna ecosystems. *Journal of Vegetation Science*, 3, 293-300.
- Smith, B.W. (1988) More cautions on laboratory illumination. *Ancient TL*, 6, 9.
- Smith, M.A. (1989) The case for a resident human population in the Central Australian Ranges during full glacial aridity. *Archaeology in Oceania*, 24, 93-105.
- Smith, M.A. (2003) 23 °C: Archaeology and Environmental History of the Southern Deserts. Conference Program and Abstracts, Canberra, January 2003.

- Smith, M.A. and Sharp, N.D. (1993) Pleistocene sites in Australia, New Guinea and Island Melanesia: geographic and temporal structure of the archaeological record. In: Smith, M.A., Spriggs, M. and Fankenhauer, B. (eds.) *Sahul in Review: the Archaeology of Australia, New Guinea and Island Melanesia*. R.S.P.A.S., Australian National University Press, Canberra. Pp. 37-59.
- Smith, M.A., Prescott, J.R. and Head, M.J. (1997) Comparison of ¹⁴C and luminescence chronologies at Puriŋjarra rock shelter, central Australia. *Quaternary Science Reviews (Quaternary Geochronology)*, 16, 299-320.
- Spooner, N.A. (1998) Human occupation at Jinmium, northern Australia, 116,000 years ago or much less? *Antiquity*, 72, 173-178.
- Spooner, N.A. and Prescott, J.R. (1986) A caution on laboratory illumination. *Ancient TL*, 4(3), 46-48.
- Spooner, N.A., Prescott, J.R. and Hutton, J.T. (1988) The effect of illumination wavelength on the bleaching of the thermoluminescence (TL) of quartz. *Quaternary Science Reviews*, 7, 325-329.
- Stace, H. C. T. (1968) *A Handbook of Australian Soils*. Glenside, South Australia: Rellim Technical Publications for the Commonwealth Scientific and Industrial Research Organization and the International Society of Soil Science.
- Stein, J.K. (1985) Interpreting sediments in cultural settings. *Peopling of the Americas*, 1, 5-19.
- Stein, J.K. (2001) A review of site formation processes and their relevance to geoarchaeology. In: Goldberg, P., Holliday, V.T. and Ferring, C.R. (eds.) *Earth Sciences and Archaeology*. Pp. 37-51.
- Stein, J.K., Deo, J.N. and Phillips, L.S. (2002) Big sites – short time: accumulation rates in archaeological sites. *Journal of Archaeological Science*, 30, 297-316.
- Stern, N. (1994) The implications of time-averaging for reconstructing the land-use patterns of early tool-using hominids. *Journal of Human Evolution*, 27, 89-105.
- Stokes, S. (1999) Luminescence dating applications in geomorphological research. *Geomorphology*, 29, 153-171.
- Stone, J. (2000) Air pressure and cosmogenic isotope production. *Journal of Geophysical Research*, 105, 23, 23752 – 23759.
- Straus, L.G., Eriksen, B.V., Erlandson, J.M. & Yesner, D.R. (1996) *Humans at the End of the Ice Age. The Archaeology of the Pleistocene-Holocene Transition*. Plenum Press, New York. Pp. 303-318.
- Sullivan, M. (1996) Northern Australian Landscapes. In: Veth, P. and Hiscock, P. (eds.) *Archaeology of Northern Australia*. *Tempus*, 4, 1-8.
- Sullivan, M.E. and Simmons, S. (1979) Silcrete: A classification for flaked stone artefact assemblages. *The Artefact*, 4, 51-60.

References

- Sullivan, L.A. and Koppi, T.J. (1998) Iron Staining of quartz beach sand in Southeastern Australia. *Journal of Coastal Research*, 14(3), 992-999.
- Susino, G. J. (1999) Microdebitage and the Archaeology of Rock Art: an Experimental Approach. Unpublished Thesis, School of Geosciences, University Of Sydney.
- Susino, G.J. (in prep.) Analysis of lithic artefact microwaste for spatial, chronological and environmental modelling of archaeological sites. PhD thesis, University of Wollongong.
- Taçon, P., R. Fullagar, S. Ouzman and K. Mulvaney (1997) Cupule engravings from Jinmium-Granilpi (northern Australia) and beyond: exploration of a widespread and enigmatic class of rock markings. *Antiquity*, 71, 942-65.
- Tacon, P.S.C., Mulvaney, K., Fullagar, R. and Head, L. (1999) 'Bradshaws' - an eastern province? *Rock Art Research*, 16(2), 127-128.
- Terberger, T. and Street, M. (2002) Hiatus or continuity? New results for the question of pleniglacial settlement in Central Europe. *Antiquity*, 76, 691-698.
- Thomas, D.S.G., Brook, G., Shaw, P., Bateman, M., Haberyan, K., Appleton, C., Nash, D., McLaren, S. and Davies, F. (2003) Late Pleistocene wetting and drying in the NW Kalahari: an integrated study from the Tsodilo Hills, Botswana. *Quaternary International*, 104, 53-67.
- Tipper, J.C. (1998). The influence of field sampling area on estimates of stratigraphic completeness. *Journal of Geology*, 106(6), 727-738.
- Torgersen, T., Luly, J., De Deckker, P., Jones, M.R., Searle, D.E., Chivas, A.R. and Ullman, W.J. (1988) Late Quaternary environments of the Carpentaria Basin, Australia. *Palaeogeography, Palaeoclimatology, Palaeoecology*, 67, 245-261.
- Traves, D.M., Dunn, P.R. and Jones, P.J. (1970) Outline of the geology of the Ord-Victoria River area, Lands of the Ord-Victoria River Area, Western Australia and Northern Territory. Land Research Series. No. 28. Melbourne, CSIRO.
- Trull, T.W., Brown, E.T., Marty, B., Raisbeck, G.M. and Yiou, F. (1995) Cosmogenic ^{10}Be and ^3He accumulation in Death Valley Pleistocene beach terraces: Implications for cosmic ray exposure dating of young surfaces in hot climates. *Chemical Geology*, 119, 191 - 207.
- Tuniz, C., Bird, R., Fink, D. and Herzog, G. (1998) Accelerator Mass Spectrometry : Ultrasensitive Analysis For Global Science. CRC PRESS, Boca Raton, Florida, USA. 371 pp.
- Turney, C.S.M. and Bird, M.I. (2002) Determining the timing and pattern of human colonisation in Australia: Proposals for radiocarbon dating 'early' sequences. *Australian Archaeology*, 54, 1-5.

References

- Turney, C.S.M., Bird, M.I., Fifield, L.K., Roberts, R.G., Smith, M.A., Dortch, C.E., Grün, R., Lawson, E., Ayliffe, L.K., Miller, G.H., Dortch, J. and Cresswell, R.G. (2001) Early human occupation at Devil's Lair, southwestern Australia 50,000 years ago, *Quaternary Research*, 55, 3-13.
- Van Andel, T.H. and Veevers, J.J. (1967) Morphology and Sediments of the Timor Sea. *Bureau of Mineral Resources Bulletin*, No. 83. 173 pp.
- Van der Kaars, W.A. (1991) Palynology of eastern Indonesian marine piston-cores: A Late Quaternary vegetational and climatic record for Australasia. *Palaeogeography, Palaeoclimatology, Palaeoecology*, 85, 239-302.
- Van der Kaars, S., Wang, X., Kershaw, P., Guichard, F. and Setiabudi, D.A. (2000) A Late Quaternary palaeoecological record from the Banda Sea, Indonesia: patterns of vegetation, climate and biomass burning in Indonesia and northern Australia. *Palaeogeography, Palaeoclimatology, Palaeoecology*, 155, 135-153.
- Van Nest, J. (2002) The good earthworm: how natural processes preserve upland Archaic archaeological sites of Western Illinois, U.S.A. *Geoarchaeology*, 17(1), 53-90.
- Veth, P. (1989) Islands of the interior: a model for the colonisation of Australia's arid zone. *Archaeology in Oceania*, 24(3), 81-92.
- Veth, P. (1994) The Aboriginal occupation of the Montebello Islands, north-west Australia. *Australian Aboriginal Studies*, 2, 39-50.
- Veth, P. (1995) Aridity and settlement in northwest Australia. *Antiquity*, 69, 733-746.
- Veth, P. (1999) The occupation of arid coastlines during the terminal Pleistocene of Australia. In: Hall, J. and McNiven, I.J. (eds.) *Australian Coastal Archaeology*. Pp. 65-72. Archaeology and Natural History Publications, RSPAS, Australian National University.
- Veth, P., Spriggs, M., Jatmiko, A. and O'Connor, S. (1998) Bridging Sunda and Sahul: the archaeological significance of the Aru Islands, southern Moluccas. In: Bartstra, G-T. (Ed.) *Bird's Head Approaches. Irian Jaya Studies – A Programme for Interdisciplinary Research*. A.A. Balkema, Rotterdam. Ch. 9. Pp. 157-177.
- Von Gunten, H.R., Roessler, E., Lowson, R.T., Reid, P.D. and Short, S.A. (1999) Distribution of uranium- and thorium series radionuclides in mineral phases of a weathered lateritic transect of a uranium ore body. *Chemical Geology*, 160, 225-240.
- Wallis, L. (2001) Environmental history of northwest Australia based on phytolith analysis at Carpenter's Gap 1. *Quaternary International*, 83-85, 103-117.
- Walsh, G. (2000) *Bradshaw Art of the Kimberley*. Takarakka Nowan Kas Publications, Melbourne.

References

- Walsh, P.J. (1993) Catastrophic Flooding, Northern Territory. Honours thesis, University of Wollongong, Australia.
- Wang, X., van der Kaars, S., Kershaw, P., Bird, M. and Jansen, F. (1999) A record of fire, vegetation and climate through the last three glacial cycles from Lombok Ridge core G6-4, eastern Indian Ocean, Indonesia. *Palaeogeography, Palaeoclimatology, Palaeoecology*, 147, 241-256.
- Ward, I. and Larcombe, P. (2003) A Process-Orientated Approach to Archaeological Site Formation: Application to Semi-Arid Northern Australia. *Journal of Archaeological Science*, 30, 1223-1236.
- Ward, I., Patterson, C. and Watchman, A. (1999) The environment and condition of multi-layered Aboriginal paintings at Kennedy-A in the wet tropics, north Queensland. *Rock Art Research*, 16(1), 25-35.
- Ward, I., Larcombe, P. & Veth, P. (2000) A New Process-Based Model For Wreck Site Formation. *Journal of Archaeological Science*, 26(5), 561-567.
- Wasson, R.J. (1983) Termination of dune building in the Strzelecki Desert, South Australia: 15-10 KA. In: Chappell, J. and Grindrod, A. (Eds.) CLIMANZ 1, ANU Canberra. p. 86.
- Wasson, R.J. (1986) Geomorphology and Quaternary history of the Australian continental dunefields. *Geographical Review of Japan*. 59B(1), 55-67.
- Watchman, A. (1998) Some observations on the radiocarbon and cosmogenic isotope dating of petroglyphs, Foz Coa, Portugal. *Antiquity*, 72, 197-200.
- Watchman, A. (1999) A review of the history of dating rock varnish. *Earth Science Reviews*, 49(1), 261-279.
- Watchman, A. (2001) Wargata Mina to Gunbilmurrung: The direct dating of Australian rock art. In A. Anderson, I. Lilley and S. O'Connor (Eds.) *Histories of old ages: Essays in honour of Rhys Jones*. Canberra: Centre for Archaeological Research and Pandanus Books, the Australian National University. pp. 315-325.
- Watchman, A.L. and Twidale, C.R. (2002). Relative and 'absolute' dating of land surfaces. *Earth Science Reviews*, 58, 1-49.
- Watchman, A., Walsh, G.L., Morwood, M.J. and Tuniz, C. (1997) AMS radiocarbon age estimates for early rock paintings in the Kimberley, N.W. Australia: preliminary results. *Rock Art Research*, 14(1), 18-26.
- Watchman, A., Tacon, P., Fullagar, R. and Head, L. (2000) Minimum ages for pecked rock markings from Jinmium, north western Australia. *Archaeology in Oceania*, 35, 1-10.
- Waters, M.R. (1992) *Principles of Geoarchaeology*. University of Arizona Press.

References

- Waters, M.R. and Kuehn, D.D. (1996) The geoarchaeology of place: the effect of geological processes on the preservation and interpretation of the archaeological record. *American Antiquity*, 61(3), 483-497.
- Webb, E. (1992) Sand traps for the unwary – problems in the interpretation of sedimentological analyses. *Quaternary Archaeological Research*, 9, 43-49.
- Webb, E.R. (1998) Problems with radiometric “time”: dating the initial human colonisation of Sahul. *Radiocarbon*, 40(2), 749-758.
- Weiner, S., Goldberg, P. and Bar-Yosef, O. (2002) Three-dimensional distribution of minerals in the sediments of Hayonim Cave, Israel: Diagenetic processes and archaeological implications. *Journal of Archaeological Science*, 29, 1289-1308.
- Wende, R., Nanson, G.C. and Price, D.M. (1997) Aeolian and fluvial evidence for Late Quaternary environmental change in the east Kimberley of Western Australia. *Australian Journal of Earth Sciences*, 44, 519-526.
- White, J.P. and O’Connell, J.F. (1982) *A prehistory of Australia, New Guinea and Sahul*. Academic Press.
- Whitehead, B.R. and Fahey, G.M. (1985) Geology of Keep River National Park. Technical Report No. 1, Dept. Mines and Energy, Northern Territory Geological Survey.
- Williams M.A.J. (1968) Termites and soil development near Brock's Creek, Northern Territory, Australia. *Science*, 31, 153-154.
- Williams, J. and Coventry, R.J. (1979) The contrasting soil hydrology of red and yellow earths in a landscape of low relief. In: *The Hydrology of Areas of Low Precipitation*. Proceedings of the Symposium, Canberra. (IAHS-AISH Pub. No. 128). Pp. 385-396.
- Williams, J. and Coventry, R.J. (1981) The potential for groundwater recharge through red, yellow, and grey earth profiles in central north Queensland. In: *Groundwater Recharge*. Australian Water Resources Council, Conference Series, No. 2. Pp. 169-181.
- Williams-Thorpe, O., Jenkins, D.G., Jenkins, J. and Watson, J.S. (1995) Chlorine-36 dating and the bluestones of Stonehenge. *Antiquity*, 69, 1019-1020.
- Wintle, A.G. (1996) Archaeologically-relevant dating techniques for the next century. *Journal of Archaeological Science*, 3, 123-138.
- Wintle, A.G. (1998) Luminescence dating: laboratory procedures and protocols. *Radiation Measurements*, 27 (5/6), 769-817.
- Wintle, A.G. and Murray, A. (1999) Luminescence sensitivity changes in quartz. *Radiation Measurements*, 30, 107-118.

References

- Woodroffe C.D. (1993) Late Quaternary evolution of coastal and lowland riverine plains of Southeast Asia and northern Australia, an overview. *Sedimentary Geology*, 83(3-4), 163-175.
- Woodroffe, C., Thom, B.G., Chappell, J., Wallensky, E., Grindrod, J. and Head, J. (1987) Relative sea-level in the South Alligator River Region, Northern Australia, during the Holocene. *Search*, 18, 198-200.
- Woodroffe, C.D., Chappell, J., Thom, B.G. and Wallensky, E. (1989) Depositional model of a macrotidal estuary and floodplain, South Alligator River, northern Australia. *Sedimentology*, 36, 737-756.
- Woodroffe, C.D., Bryant, E.A., Price, D.M. and Short, S.A. (1992) Quaternary inheritance of coastal landforms, Coburg Peninsula, Northern Territory. *Australian Geographer*, 23(2), 101-114.
- Wyrwoll, K.H., McKenzie, N.L., Pederson, B.J. and Tapley, I.J. (1986) The Great Sandy Desert of Northwestern Australia: the last 7000 years. *Search*, 17, 208-210.
- Wyrwoll, K.H., McKenzie, N.L., Pederson, B.J. and Tapley, I.J. (1992) The Holocene palaeohydrology and climate history of the northern Great Sandy Desert – Fitzroy trough: with special reference to the history of the northwest Australian monsoon. *Climatic Change*, 22, 47-65.
- Wyrwoll, K.-H. and Miller, G.H. (2001) Initiation of the Australian summer monsoon 14,000 years ago. *Quaternary International*, 83-85, 119-128.
- Yosukame, Y. (2001). Shore-line reconstruction around Australia during the Last Glacial Maximum and Late Glacial Stage. *Quaternary International*, 83-85, 9-18.
- Yosukame, Y., DeDeckker, P., Lambeck, K., Johnson, P. and Fifield, L.K. (2001) Sea-level at the Last Glacial Maximum: evidence from northwestern Australia to constrain ice volumes for oxygen isotope stage 2. *Palaeoceanography, Palaeoclimatology, Palaeoecology*, 165, 281-297.
- Young, R.W. (1983) The tempo of geomorphological change: evidence from southeastern Australia. *Journal of Geology*, 91, 221-230.
- Young, R.W. (1986) Tower Karst in sandstone: Bungle Bungle massif, northwestern Australia. *Zeitschrift für Geomorphologie*, 30(2), 189-202.
- Young, R.W. (1988) Quartz etching and sandstone Kaarst: examples from the East Kimberleys, northwestern Australia. *Zeitschrift für Geomorphologie*, 32(4), 409-423.
- Young, R.W. (1992) Structural heritage and planation in the evolution of landforms in the East Kimberley. *Australian Journal of Earth Sciences*, 39, 141-151.
- Young, R.W. and Young, A. (1992) *Sandstone Landforms*. Springer-Verlag, Germany.
- Young, R.W., Nanson, G.C. and Jones, B.G. (1987) Weathering of Late Pleistocene alluvium under a humid temperate climate: Cranebrook Terrace, Southeastern Australia. *Catena*, 14, 469-484.

APPENDIX ONE - SURVEYING

Surveying was conducted using a SOKKIA electronic total station (model SET5F), connected to a SOKKIA digital note pad (model SDR33), enabling all survey readings and additional notes to be stored electronically. The location and number of stations was dictated by the required resolution and site visibility (dictated by topography and vegetation density). Survey stations and site locations were determined from Global Positioning Systems (GPS).

Table A1.1 Location of cosmogenic sample sites and auger sites as determined from GPS measurement.

No.	SITE	Latitude (°S)	Longitude (°E)	No.	SITE	Latitude (°S)	Longitude (°E)
1	COS-K1	15.365	129.019	17	KN2	15.366	129.023
2	COS-K3	15.364	129.020	18	KN3-5	15.366	129.023
3	COS-K4	15.364	129.020	19	KN6	15.367	129.023
4	COS-K5	15.364	129.020	20	KN7	15.369	129.023
5	COS-K6	15.367	129.018	21	KN8	15.360	129.059
6	COS-K7	15.367	129.018	22	SCG	15.440	129.201
7	COS-K8	15.373	129.013	23	SC1	15.421	129.195
8	COS-K9	15.373	129.013	24	SC2	15.421	129.197
9	COS-J1	15.432	129.162	25	SC3	15.421	129.198
10	COS-J2	15.432	129.162	26	JN1	15.427	129.157
11	COS-J3	15.432	129.162	27	JN2	15.423	129.155
12	COS-G1	15.448	129.179	28	JN3	15.421	129.150
13	COS-G2	15.448	129.179	29	JN4	15.418	129.147
14	COS-G3	15.444	129.177	30	JG3	15.436	129.166
15	COS-G4	15.444	129.177	31	JG4	15.439	129.169
16	KR99/Ck	15.372	129.017	32	JG5	15.444	129.174

APPENDIX TWO - COSMOGENIC ISOTOPE DATING

Field methods are outlined in Chapter Four (refer 4.3). The following include field details of sample sites, raw results for Al and Be chemistry analyses, and raw results for ^{10}Be and ^{26}Al AMS analyses.

2.1 ANSTO Sample Forms

SAMPLE ID	IW-GUR2-2000 (OZ0785)	IW-GUR4-2000 (OZ0787)
Geographic Locality	Goorurarmum, Northern Territory	Goorurarmum, Northern Territory
Grid Ref (Lat/Long)	15°26.86'S / 129°10.73'E	15°26.65'S / 129°10.59'E
Altitude (asl)	190 m	40 m
Rock Type / Lithology	Sandstone (red)	Sandstone (red)
Glacial Stage / Age	-	
Site Description	Escarpment	Escarpment
Surface position	Saddle of escarpment	Top of escarpment overlooking rockshelter
Surface character	Case-hardened ironstone	Case-hardened ironstone
Depth / Thickness	5 cm	5 cm
Topographic Shading	Low	Low
Till Cover	None	None
Surface slope	18°	14°
Mass at ANSTO / retained	~ 2 kg	~ 1 kg
Comment	Sample 1 of 6	Sample 2 of 6

SAMPLE ID	IW-JIN1-2000 (OZ714)	IW-JIN2-2000 (OZ0715)
Geographic Locality	Jinmium	Jinmium
Grid Ref (Lat/Long)	15°25.93'S / 129°09.73'E	15°25.94'S / 129°09.73'E
Altitude (asl)	30 m	40 m
Rock Type / Lithology	Sandstone (yellow)	Sandstone (white)
Glacial Stage / Age		
Site Description	Sandstone outcrop	Sandstone outcrop
Surface position	Top of outcrop	Top of outcrop
Surface character	Smooth exposed surface	Tafoni
Depth / Thickness	5 cm	5 cm
Topographic Shading	Low	Low
Till Cover	None	None
Surface slope	20°	2°
Mass at ANSTO / retained	~ 1 kg	~ 1kg
Comment	Sample 3 of 6	Sample 4 of 6

SAMPLE ID	IW-KAR1-2000 (OZ717)	IW-KAR5-2000 (OZ0721)
Geographic Locality	Karlinga	Karlinga
Grid Ref (Lat/Long)	15°21.91'S / 129°01.16'E	15°21.84'S / 129°01.20'E
Altitude (asl)	74 m	60 m
Rock Type / Lithology	Sandstone (yellow)	Sandstone (red)
Glacial Stage / Age		
Site Description	Escarpment	Pillar on escarpment
Surface position	Top of escarpment overlooking excavation	Base of pillar
Surface character	Case-hardened surface	Case-hardened surface
Depth / Thickness	5 cm	5 cm
Topographic Shading	Low	High
Till Cover	None	None
Surface slope	4°	8°
Mass at ANSTO / retained	~ 1 kg	~ 1 kg
Comment	Sample 5 of 6	Sample 6 of 6

SAMPLE ID	IW-JG1 (OZ731 to 738)	IW-JG2 (OZ931 to 940)
Geographic Locality	Jinmium	Jinmium
Grid Ref (Lat/Long)	15°25.40'S / 129°09.28'E	15°25.43'S / 129°09.28'E
Altitude (asl)	10 m	5 m
Rock Type / Lithology	Red Sand	Red Sand
Glacial Stage / Age		
Site Description	Sand sheet adjacent to Jinmium outcrop	Sand sheet ~ 1 km from Jinmium outcrop
Surface position	Core	Core
Surface character	Well-drained sand	Well-drained sand
Depth / Thickness	300 cm	600 cm
Interval Sampling	30 cm	30 cm
Topographic Shading	Medium	Medium
Surface slope	< 4°	< 4°
Mass at ANSTO / retained	0 kg	0 kg
Comment (Samples analysed)	30, 60, 90, 150, 180, 210, 270, 300 cm (Total 8)	30, 60, 90, 150, 210, 300, 360, 450, 540, 600 cm (Total 10)

A2.2 Chemistry Results

Table A2.1 Chemical analyses of beryllium (Be) and aluminium (Al) in cosmogenic bedrock and sediment samples. (Be carrier concentration = 1.017 mg.g^{-1}).

OZ No.	Sample ID	Initial Quartz (g)	Final Quartz (g)	Fraction Etched %	MASS Quartz Dissolved (g)	ICP Al (ppm)	Actual Mass Al added (mg)	Mass Be Carrier (mg)	Actual Mass Be added (mg)
0714	JIN1-2000	282.68	202.00	28.5%	80.182	101.80	0	0.4828	0.4747
0715	JIN2-2000	292.12	206.00	29.5%	80.552	89.80	0	0.5114	0.5028
0717	KAR1-2000	277.35	214.22	22.8%	80.343	158.10	0	0.4854	0.4773
0721	KAR5-2000	277.35	213.26	23.1%	80.054	93.40	0	0.5088	0.5003
0731	J1-30-2000	124.00	98.36	20.7%	50.032	121.30	0	0.4490	0.4415
0732	J1-60-2000	111.00	85.81	22.7%	52.664	121.30	0	0.4062	0.3994
0733	J1-90-2000	76.00	53.96	29.0%	50.746	109.50	0	0.4245	0.4174
0734	J1-150-2000	67.00	44.21	34.0%	50.419	116.80	0	0.4362	0.4289
0735	J1-180-2000	110.00	89.83	18.3%	50.555	123.60	0	0.4397	0.4323
0736	J1-210-2000	84.00	61.14	27.2%	50.820	126.10	0	0.4585	0.4509
0737	J1-270-2000	83.00	58.80	29.2%	52.354	149.50	0	0.3970	0.3903
0738	J1-300-2000	56.00	32.91	41.2%	40.260	112.10	0	0.4051	0.3984
0785	GUR2-2000	292.04	227.57	22.1%	79.935	112.20	0	0.4946	0.4864
0787	GUR4-2000	245.84	183.79	25.2%	79.999	119.30	0	0.4824	0.4743
0931	J2-30-2001	119.8	99.45	17.0%	78.034	145.10	0	0.4445	0.4371
0932	J2-60-2001	146.25	122.84	16.0%	74.534	164.60	0	0.4442	0.4368
0933	J2-90-2001	128.64	107.62	16.3%	80.198	164.80	0	0.4381	0.4307
0934	J2-150-2001	124.35	93.34	24.9%	80.470	145.80	0	0.4609	0.4532
0935	J2-210-2001	140.64	113.80	19.1%	79.091	213.2	0	0.4559	0.4483
0936	J2-300-2001	113.02	68.00	39.8%	67.332	113.2	0	0.4480	0.4405
0937	J2-360-2001	106.83	79.03	26.0%	77.969	146.5	0	0.4440	0.4366
0938	J2-450-2001	127.73	103.50	19.0%	102.094	203.7	0	0.4473	0.4398
0939	J2-540-2001	117.14	94.53	19.3%	92.941	202.6	0	0.4573	0.4496
0940	J2-600-2001	145.97	96.00	34.2%	80.153	132.1	0	0.4474	0.4399

AMS ¹⁰Be Radioisotope Results for all Bedrock and Sediment Samples

TOWNSHIP EXPOSURE ASSES													
WORLD MAP, KERP RIVER DISTRICT, NARRAGANSETT, NORTHEAST TERRITORY													
		10Be half-life =		1.51E+05 y						err=		0	
		lambda =		4.59E-07 y-1						err=		7.5	
		High lat sea level P(10Be)=		5.100 atp-s						err=			
QZ	SAMPLE	10Be/9Be	ERR	ERR	SAMPLE	CARRIER	10Be CONC	ALT	LAT	LACF	SITE PROC	10Be Min	Max Erosion
#	NAME	ABS RATIO	(abs)	(%)	MASS	MASS	atoms/g-Q	(m)	(deg)	(Lat)	rate	age	rate
		(1E-15)			(g)	(mg)	(10E)				(at/g-yr)	(ka)	(mm / ka)
0714	IW-JM1-2000	911	15.8	1.7	80.2	0.475	0.380	30	15.43	0.933	3.23	154.6	4.72
0715	IW-JM2-2000	593	13.2	2.2	80.6	0.503	0.347	40	15.43	0.939	3.25	77.3	7.06
0717	IW-KAR1-2000	1290	21.4	1.7	80.3	0.477	0.512	135	15.37	0.983	3.49	152.2	3.52
0721	IW-KAR2-2000	738	16.2	2.2	80.1	0.500	0.384	120	15.37	0.975	3.44	90.1	6.04
0785	IW-GUR2-2000	773	10.7	1.4	79.9	0.486	0.314	190	15.45	0.710	3.82	88.6	6.14
0787	IW-GUR4-2000	1791	36.1	2.0	80.0	0.474	0.706	70	15.45	0.952	3.33	223.3	2.36
0731	IW-J1-30-2000	865	41.6	4.6	50.0	0.442	0.534	30					
0732	IW-J1-40-2000	840	38.2	4.1	52.7	0.399	0.479	30					
0733	IW-J1-60-2000	857	26.2	2.7	50.7	0.417	0.528	30					
0734	IW-J1-150-2000	1054	23.3	2.2	50.4	0.429	0.589	30					
0735	IW-J1-180-2000	953	28.7	3.0	50.6	0.432	0.545	30					
0736	IW-J1-210-2000	899	40.3	4.4	50.8	0.451	0.539	30					
0737	IW-J1-270-2000	1186	30	2.6	52.4	0.390	0.591	30					
0738	IW-J1-300-2000	1085	45.9	4.3	40.3	0.398	0.705	30					
0931	IW-J2-30	1590	44.0	2.8	78.0	0.437	0.584	40					
0932	IW-J2-60	1607.1	23.5	1.5	74.5	0.437	0.629	40					
0933	IW-J2-90	1766.4	25.3	1.4	80.2	0.431	0.634	40					
0934	IW-J2-150	1678.9	24.0	1.4	80.5	0.453	0.632	40					
0935	IW-J2-210	1807.2	33.5	1.8	78.1	0.448	0.685	40					
0936	IW-J2-300	1370.8	22.2	1.6	67.3	0.440	0.599	40					
0937	IW-J2-360	1573.4	34.6	2.2	78.0	0.437	0.599	40					
0938	IW-J2-450	2177.4	34.5	1.6	152.1	0.440	0.827	40					
0939	IW-J2-540	1805.1	59.2	3.3	82.9	0.450	0.584	40					
0940	IW-J2-600	1435.2	39.0	2.7	80.2	0.440	0.528	40					

A2.4 AMS ²⁶Al Radioisotope Results for all Bedrock and Sediment Samples

25AI EXPOSURE AGES WORLD WARD, KEEF RIVER DISTRICT-JANBUSS, NORTHERN TERRITORY																																																																																																																																																																																																																																																																																																																																																																																																																																																																																																																																																																																																																																																																																																																																																																																																																																																																																																																																																																																																																																																																																																																																																																																																																																																																																																																																																			
CZ #	SAMPLE NAME	25AI/Al ABS RATIO	No : ents	ERR (abs)	ERR (%)	ppm Al	native Al	25AI CONC (atoms/g-G)	ALT (m)	LAT (deg)	LACF	SITE PROD rate	Min exposure age [ka]	Max Erosion rate [mm / ka]	QuasD Error [mm / ka]																																																																																																																																																																																																																																																																																																																																																																																																																																																																																																																																																																																																																																																																																																																																																																																																																																																																																																																																																																																																																																																																																																																																																																																																																																																																																																																																				
																																																																																																																																																																																																																																																																																																																																																																																																																																																																																																																																																																																																																																																																																																																																																																																																																																																																																																																																																																																																																																																																																																																																																																																																																																																																																																																																																			</

APPENDIX THREE - SEDIMENT CHARACTERISATION

A number of relative and absolute techniques were used to characterise the sediment stratigraphy, including petrographic descriptions, thin section descriptions, grain size analyses, and geochemistry. The techniques and raw results are given below. Statistical analysis of the grain size and geochemistry are also included.

A3.1 Petrographic Descriptions

The following petrographic descriptions are grouped according to location, and include:

- Figure A3.1 Petrographic description of auger cores (Gu-1 to 4) and excavation pits (Goor-1 and 2) taken within the Goorurarmum amphitheatre, and auger cores (Gu-6 to 8) taken at ~ 1 km intervals north towards the coast.
- Figure A3.2 Petrographic description of auger cores taken north-west of Jinmium (JN-1 to 4) and between Jinmium and Goorurarmum (JG-1 to 5).
- Figure A3.3 Petrographic description of (a) the creek bank profile excavated adjacent to the archaeological site of Kr99, and (b) auger cores (Ka-1 to 4) and excavation pit (Karl-1) taken within the Karlinga amphitheatre.
- Figure A3.4 Petrographic description of auger cores (KN-1 to 8) and the sand sheet excavation (Karl-3) taken north of Karlinga, and
- Figure A3.5 Petrographic description of (a) auger cores (SC-1 to 3) taken adjacent to Sandy Creek, and (b) creek bank profile excavated at Sandy Creek Gorge.

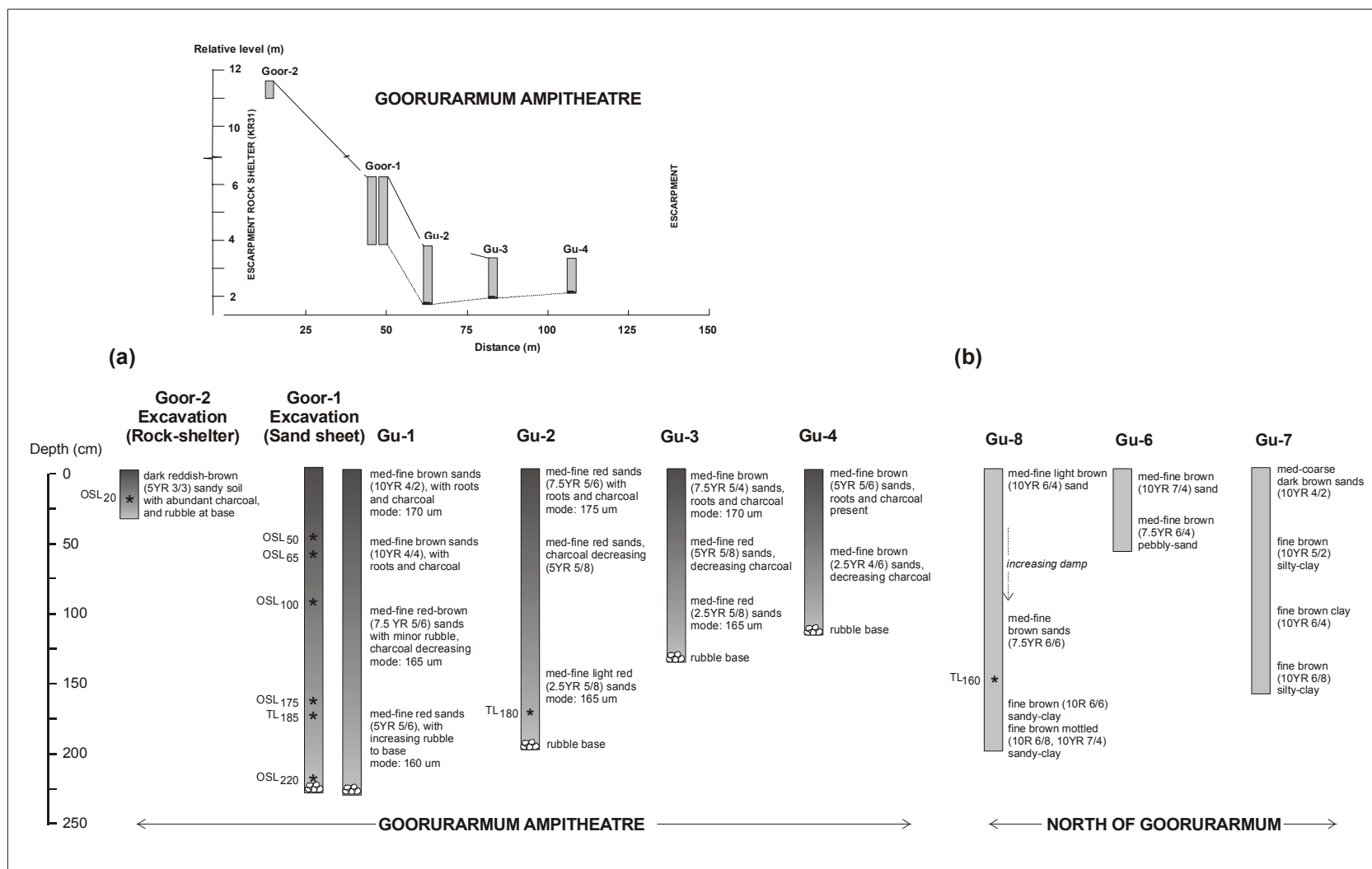


Figure A3.1 Petrographic description of (a) auger cores (Gu-1 to 4) and excavation pits (Goor-1 and 2) taken within the Goorurarmum ampitheatre, and (b) auger cores (Gu-6 to 8) taken at ~ 1 km intervals north towards the coast.

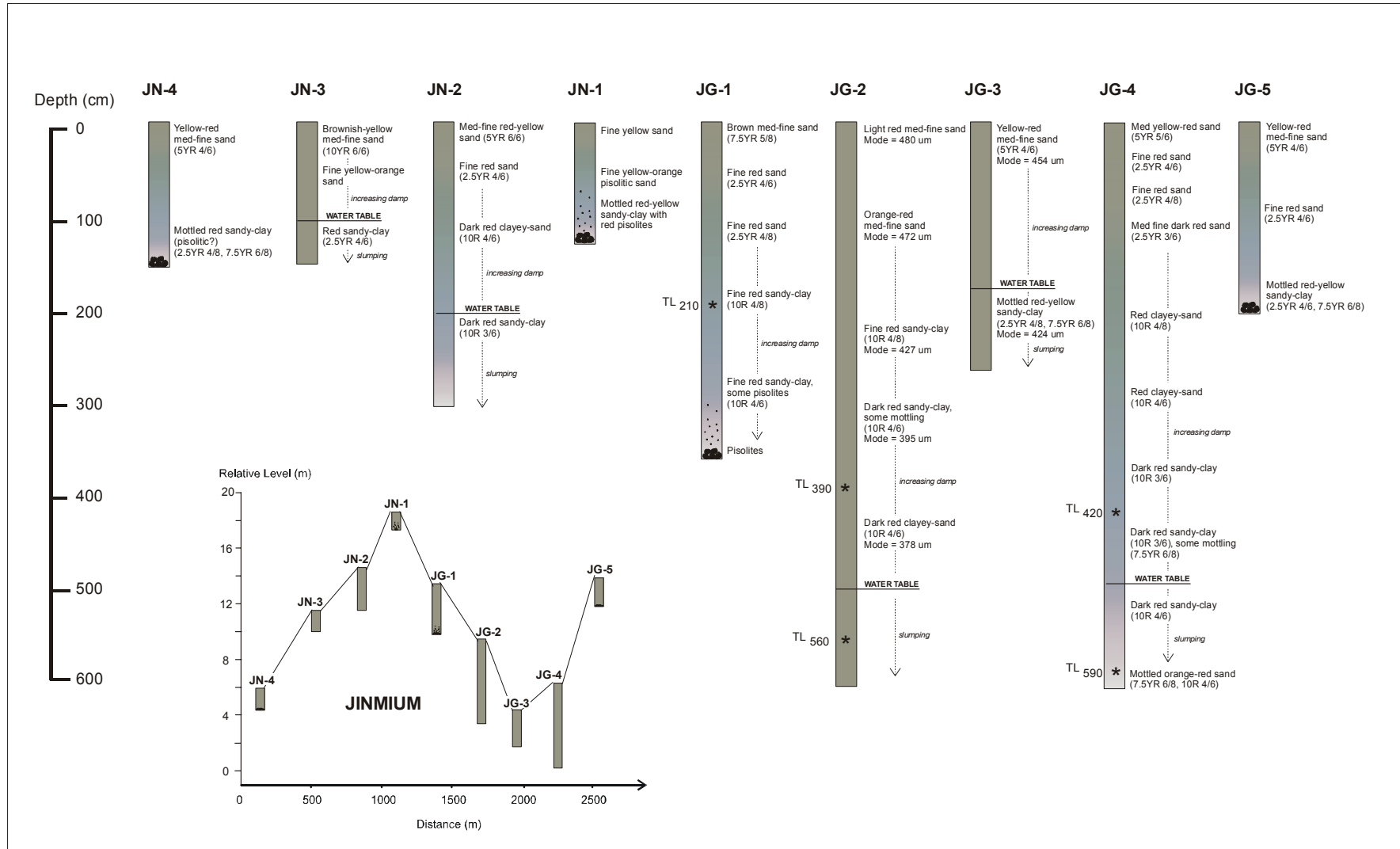


Figure A3.2 Petrographic description of auger cores taken north-west of Jinmium (JN-1 to 4) and between Jinmium and Goorurarmum (JG-1 to 5).

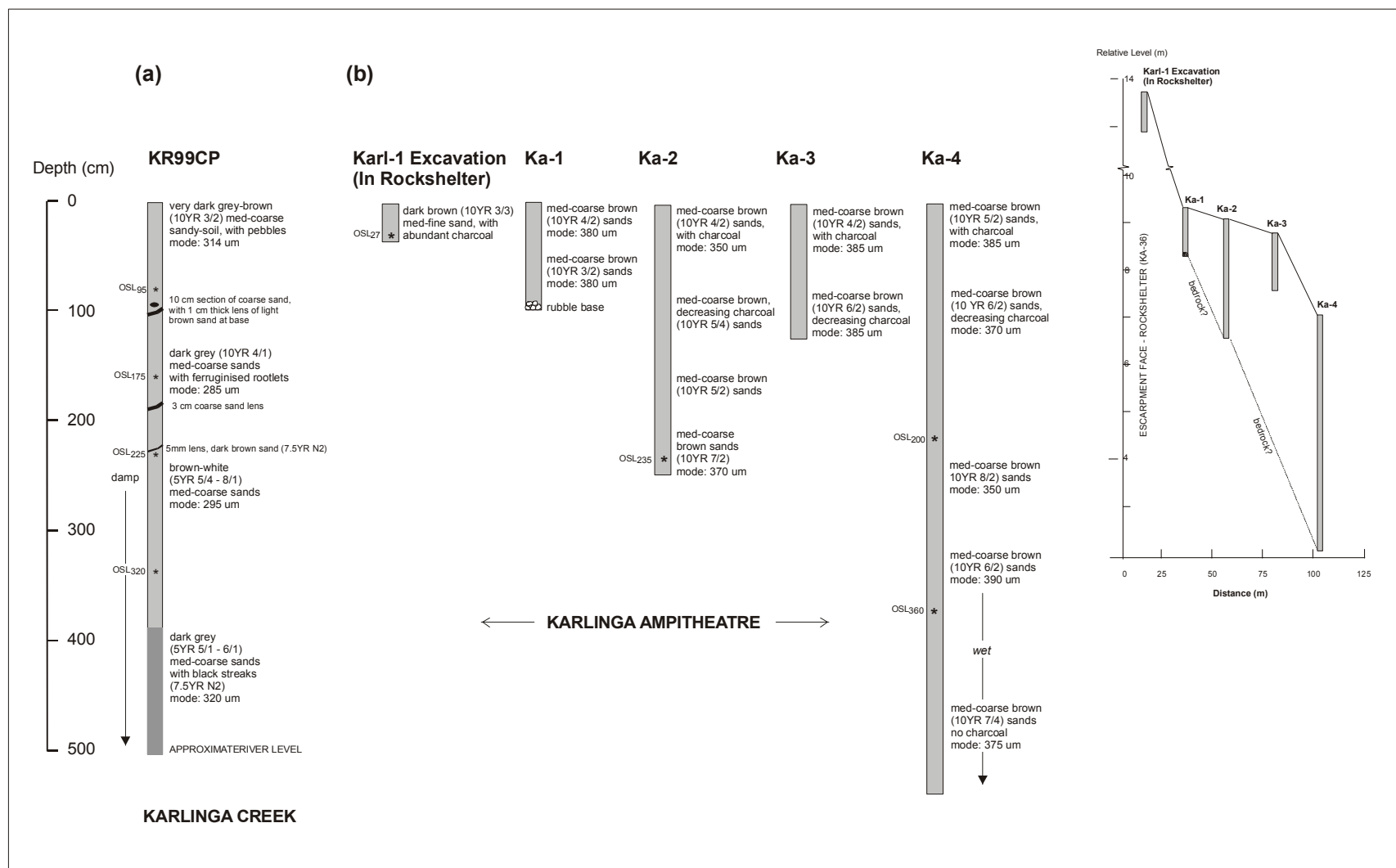


Figure A3.3 Petrographic description of (a) the creek bank profile excavated adjacent to the archaeological site of Kr99, and (b) auger cores (Ka-1 to 4) and excavation pit (Karl-1) taken within the Karlinga amphitheatre.

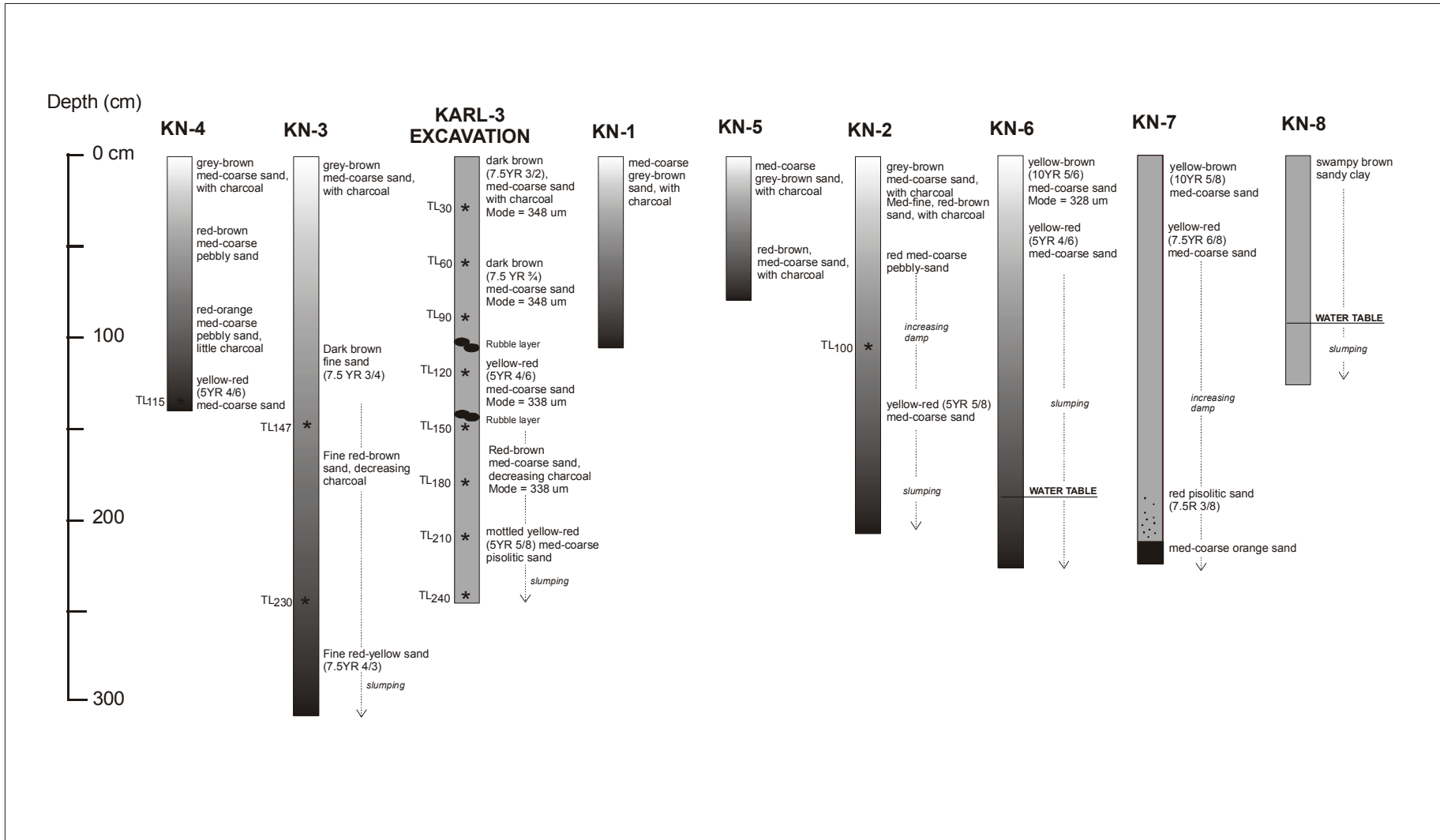


Figure A3.4 Petrographic description of auger cores (KN-1 to 8) and the sand sheet excavation (Karl-3) taken north of Karlinga.

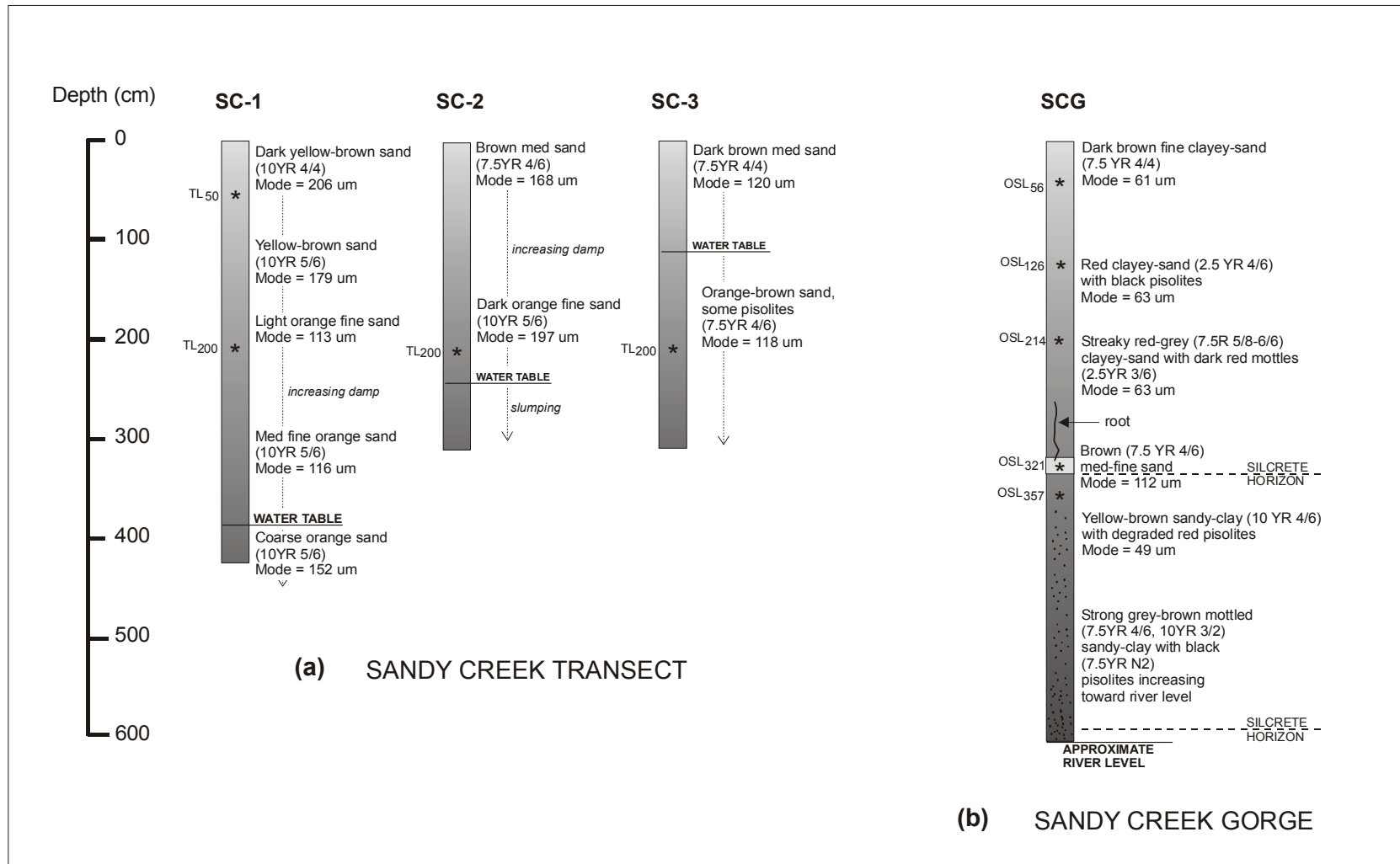


Figure A3.5 Petrographic description of (a) auger cores (SC-1 to 3) taken adjacent to Sandy Creek, and (b) creek bank profile excavated at Sandy Creek Gorge.

A3.2 Soil Micromorphology

The sampling, and preparation of thin sections from unconsolidated regolith and sedimentary material has always remained problematic. Prior to sectioning and resin impregnation, fragile materials often require drying, and subsequent polishing techniques can involve use of powders which can become embedded in the resin, or use of metal laps which can cause plucking and surface deformation (Camuti and McGuire, 1999: 172). In this study, attempts were made to minimise these problems using a modification of the procedure outlined by Camuti and McGuire (1999).

Undisturbed, oriented blocks of sediment were obtained using Kubiena tins, pushed gently into the walls of the excavation pits, or creek sections (Fig. A6.1). The recovery of these samples was achieved by pouring water above the section that was to be sampled, assuming that this mimicked the natural seepage of water through the sedimentary profile. Although theoretically it would be more ideal to impregnate sediment samples *in situ*, to minimise disturbance of the potential micromorphology, this was impractical in such a remote location. In addition, without the use of vacuum facilities, incomplete impregnation and loss of sample may occur, particularly in partly wet sediments. Samples were then sealed with tape and stored upright in polyethylene bags, and packed carefully for transport back to UOW.



Figure A3.6 Sampling of sand sheet sediments using Kubiena tin pressed into soaked excavation pit wall (Goor-1).

Thin sections of the block samples were prepared by drying them overnight in an oven at around 60°C, and then impregnating under vacuum with low viscosity epoxy resin (3 parts Araldite LC191 to 1 part Hardener LC249). Fifty percent resin penetration was obtained, and it is suggested that future resin impregnation would be improved by first heating the resin to 60 °C. The hardened sections were then sliced in half with a rock saw, one half for preparation of thin sections and the other for resin-mounted stubs. The smoothed surface of one half was mounted on glass slides (5 x 7 cm) and ground down to 20-30 µm, using a light lubricating oil and 600 µm, 400 µm and 3 µm grit respectively. Resin mounted stubs were similarly prepared by reimpregnating and polishing oriented blocks in moulds.

A3.2.1 Chemical Mapping (SEM/EDXA)

Chemical mapping of a polished cross-section of a rock crust, mounted in low viscosity epoxy resin, was achieved using a JEOL JXA-840A Scanning Electron Microprobe (SEM). To obtain a 256 x 256 pixel energy dispersive spectrum (EDS) bitmap a standard set of elements ranging from Z = 11 to 26 was programmed in 'Moran Scientific' and scanned at 60 millisecond/point at a beam current of 5 nA, for a total period of 90 minutes.

A3.3 XRD

Mineralogy was determined from smear-mounted slides of bulk ground and sieved (< 63 µm) sediment samples, run from 1.3 to 60° 2θ on a Siemens x-ray diffractometer (XRD) fitted with a post-diffraction curved graphite crystal monochromator using CuKα radiation. Analyses were run through a trace-match program to identify mineral phases using standard mineral patterns.

A3.4 Grain size Analyses

A3.4.1 Methods

The Malvern Mastersizer uses a laser light scattering technique, which employs “conventional” and “reverse” Fourier optics to measure grain size, based on laser beam obscuration (a measure of unscattered light energy). Using the 1000 mm lens, the particle sizer is able to measure grain sizes in the 4 μm - 2000 μm size range. (Note: Although the Mastersizer housed at UOW has a lower range of 0.1 μm to 880 μm with the same 1000 μm lens, the modal size of virtually all the sediments falls in the middle of this range). The primary output is presented as a volume size distribution, with an accuracy of $\pm 2\%$ based on volume and median diameter (manufacturers' specifications). The Malvern Mastersizer based at James Cook University (JCU) and at UOW was used to measure grain size of samples from the 1999 and 2000 field trip respectively. Although the latter has a lower range of 0.1 μm to 880 μm , the modal size of virtually all the sediments within the sandsheets falls within the middle of this range.

After sieving through 1000 μm mesh, a sub-sample of sediment (1 - 2 g) was dispersed in 1 litre of undistilled tapwater. Before a measurement was made, each sample was subjected to 15 seconds of ultrasound to disperse any flocs. The Malvern software normalises the output of the grain size result to 100 %, including the grains that are either larger or smaller than the lens range. A significant sediment mode is defined as a peak $> 2\%$ on the volume grain size distribution curve. The area under the curve between 4 and 10 μm is proportional to the total amount of sediment $< 10 \mu\text{m}$ and is referred to as the $< 10 \mu\text{m}$ mode.

A3.4.2 Grain size Results

Table A3.1 Grain size analyses for samples taken around Jinmium.

JINMIUM	Assumes a single size mode			Gives size of most common mode	XX % is finer than this size					
Sample	mean	standard deviation	skewness deviation	kurtosis deviation	mode1	mode2	mode3	25%	50%	75%
	um	um	um	um	um	um	um	um	um	um
TL7-105	283.48	207.17	0.615	-0.4317	388.94			108.92	250.75	423.08
TL8	295.77	207.527	0.48	-0.4399	338.84	6.13		141.29	273.74	431.33
TL10	354.46	206.849	0.246	-0.6136	420.5	7.49		202.37	342.02	498.07
TL16	231.88	199.228	0.887	0.0517	325.44			63.02	184.85	355.04
MEAN	291.40	205.19	0.56	-0.36	368.43	6.81		128.90	262.84	426.88
SDEV	50.336	3.987	0.268	0.286	44.180	0.962		58.568	64.851	58.490
A5 - spit 3	275.87	223.744	0.553	-0.7193	432.29	58.24		62.01	246.05	439.3
A5 - spit 5	240.45	222.706	0.792	-0.474	447.54	54.64		45.04	166.44	402.81
A5 - 1.5m	174.73	198.148	1.316	0.8243	389.65	40.73	1.2	28.9	73.94	285.47
A5 - 2.5m	164.82	195.768	1.486	1.3153	416.93	42.61	1.22	28.97	67.8	251.43
A5 - 3.5m	159.89	185.428	1.591	1.8053	381.81	50.44	1.16	32.8	75	228.1
A5 - 4.5m	139.1	163.97	1.855	3.1366	201.43	51.53	1.13	31.77	69.44	184.41
MEAN	192.48	198.29	1.27	0.98	378.28	49.70	1.18	38.25	116.45	298.59
SDEV	53.379	22.776	0.497	1.447	90.139	6.811	0.040	13.083	74.023	101.058
JG2 - 0	466.48	165.124	0.094	-0.3109	479.55			350.7	458.72	577.86
JG2 - 50	300.69	226.111	0.375	-0.9138	472.38	75.51	0.36	80.96	290.41	472.1
JG2 - 150	312.04	235.684	0.302	-1.0361	496.84	78.02	0.35	78.3	308.24	495.42
JG2 - 250	235.92	216.376	0.772	-0.3991	426.69	0.35	2.49	46.01	175.84	389.79
JG2 - 350	199.19	207.928	1.023	0.1229	394.63	2.46	0.35	20.85	120.73	333.08
JG2 - 450	194.42	207.269	1.01	0.1114	378	0.32	2.21	9.21	119.23	328.46
JG2 - 450	190.28	206.578	1.077	0.2511	384.17	0.33		11.43	109.07	319.24
JG2 - 550	220.38	218.439	0.852	-0.3124	432.43	85.47	6.4	27.61	145.83	375.02
MEAN	264.93	210.44	0.69	-0.31	433.09	34.64	2.03	78.13	216.01	411.37
SDEV	93.970	20.931	0.378	0.475	45.849	42.234	2.357	113.620	124.997	93.922
JG3 - 0	310.81	213.052	0.447	-0.7191	453.61			122.51	288.95	465.37
JG3 - 100	307.81	214.653	0.446	-0.7014	439.55	2.24		120.24	285.76	462.08
JG3 - 200	233.57	216.545	0.781	-0.3601	424.26	5.06	0.34	39.43	176.84	384.65
MEAN	284.06	214.75	0.56	-0.59	439.14	3.65		94.06	250.52	437.37
SDEV	43.754	1.749	0.193	0.202	14.679	1.994		47.325	63.826	45.684
JG4-100	229.44	198.233	0.903	0.0801	326.2			57.7	182.06	351.75
JG4-200	204.76	178.611	1.164	0.9484	235.88			65.22	157.35	296.29
JG4-300	238.23	183.799	0.933	0.4244	275.78			98.25	199.3	340.89
JG4-400	159.71	162.989	1.455	1.9673	205.52	33.68		30.63	109.12	234.38
JG4-590	150.26	175.929	1.55	1.9244	218.36	27.74		20.87	72.84	226.17
MEAN	196.48	179.91	1.20	1.07	252.35	30.71		54.53	144.13	289.90
SDEV	39.957	12.794	0.295	0.858	49.047	4.200		30.578	52.357	58.331

Table A3.2 Grain size analyses for samples taken around Goorurarmum.

Sample	Assumes a single size mode				Gives size of most common mode			XX % is finer than this size		
	mean	standard deviation	skewness deviation	kurtosis deviation	mode1	mode2	mode3	25%	50%	75%
	um	um	um	um	um	um	um	um	um	um
GOORURARMUM										
Goor. Ck	313.75	167.116	0.497	0.0661	327.65	29.92		198	295	414
Goor1-1-spit 1	216.67	159.977	1.387	1.9617	169.81	19.9		108.92	174.72	279.87
Goor-1-spit 5	199.01	147.579	1.511	2.7742	191.62	17.64		103.31	163.99	254.08
Goor-1-spit 9	199.07	124.825	0.868	0.6274	179.93	17.2		112.67	175.67	264.87
Goor-1-spit 19	197.43	122.439	1.084	1.2492	195.11			112.81	171.38	255.81
Goor-1-spit 37	197.9	138.599	1.601	3.3195	158.49			108.96	164.67	247.99
MEAN	202.02	138.68	1.29	1.99	178.99	18.25		109.33	170.09	260.52
SDEV	7.354	14.061	0.274	0.979	13.600	1.183		3.459	4.916	11.082
Goor-2-spit 1	246.39	184.4	1.004	0.5025	210.28			109.54	199.04	345.88
Goor-2-spit 5	222.48	174.459	1.225	1.1524	170.77			97.38	173.2	303.34
Goor-2-spit 9	237.57	188.533	1.049	0.4889	195.15			94.65	184.36	339.7
Goor-2-spit 11	216.82	177.981	1.146	0.9449	227.01			85.24	170.8	305.18
MEAN	230.82	181.34	1.11	0.77	200.80			96.70	181.85	323.53
SDEV	11.764	5.471	0.086	0.286	20.679			8.673	11.166	19.399
Gu-1/1	189.08	134.12	2.64	11.11	161			113	161	228
Gu-1/2	195.12	136.08	2.47	9.2	159			116	163	232
Gu-1/3	203.02	140.01	2.57	10.32	163			121	169	243
Gu-1/4	207.1	144.87	2.51	9.08	163			122	170	244
Gu-1/5	204.78	139.63	2.46	9.06	162			121	170	244
Gu-1/6	202.86	139.09	2.44	9.28	162			120	169	243
Gu-1/7	198.22	139.15	2.71	11.13	161			119	165	234
Gu-1/8	197.1	134.55	2.57	10.52	160			118	165	236
Gu-1/9	192.04	130.51	2.53	9.72	158			117	162	227
Gu-1/10	192.88	129.27	2.45	9.1	158			118	163	229
Gu-1/11	196.09	140.1	2.79	11.28	157			118	162	228
Gu-1/12	193.54	131.95	2.9	12.86	160			120	163	227
Gu-1/13	190.74	125.77	2.75	11.43	158			119	162	223
Gu-1/14	189.31	127.99	2.5	9.55	157			116	160	224
MEAN	196.56	135.22	2.59	10.26	159.93			118.43	164.57	233.00
SDEV	5.889	5.561	0.144	1.169	2.129			2.409	3.502	7.706
Gu-2/1	230.05	164.55	1.25	1.86	176			118	190	309
Gu-2/2	298	259.27	1.69	2.7						
Gu-2/3	232.1	168.42	1.38	2.38	173			120	189	307
Gu-2/4	218.56	151.23	1.27	1.86	170			118	181	286
Gu-2/5	214.44	156.98	1.56	3.44	171			115	177	277
Gu-2/6	204.01	147.49	1.84	4.98	166			114	169	254
Gu-2/7	205.93	151.51	1.94	5.47	164			115	169	254
Gu-2/8	190.13	150.47	1.77	4.8	163			101	160	242
Gu-2/9	226.09	162.1	1.4	2.36	169			119	183	295
MEAN	224.37	168.00	1.57	3.32	169.00			115.00	177.25	278.00
SDEV	30.773	34.964	0.255	1.416	4.472			6.047	10.566	25.646
Gu-3/1	237.9	178.84	1.42	2.28	172			116	188	318
Gu-3/2	239.54	175.13	1.34	1.96	170			118	190	322
Gu-3/3	237.28	170.08	1.42	2.29	169			120	189	313
Gu-3/4	228.12	162.29	1.57	3.06	170			119	183	294
Gu-3/5	218.8	159.06	1.59	3.13	165			113	175	281
Gu-3/6	212.44	165.15	1.79	3.97	161			107	167	267
Gu-3/7	207.68	158.18	1.82	4.19	156			107	163	258
Gu-3/8	220.07	164.09	1.71	3.45	159			113	171	276
MEAN	225.23	166.60	1.58	3.04	165.25			114.13	178.25	291.13
SDEV	12.30	7.46	0.18	0.82	5.95			5.08	10.65	24.42

Table A3.2 Grain size analyses for samples taken around Goorurarmum (continued).

Sample	Assumes a single size mode				Gives size of most common mode			XX % is finer than this size		
	mean	standard deviation	skewness deviation	kurtosis deviation	mode1	mode2	mode3	25%	50%	75%
	um	um	um	um	um	um	um	um	um	um
Gu-5/1	258.79	195.08	1.03	0.79	364			104	211	374
Gu-5/2	256.5	198.17	1.06	0.87	356			101	209	371
Gu-5/3	275.14	204.96	1.05	0.84	359			116	226	391
Gu-5/4	258.33	188.3	1.04	0.87	346			112	213	367
Gu-5/5	269.2	206.11	1.05	0.74	374			107	215	389
Gu-5/6	237.79	183.03	1.53	2.54	184			108	185	314
Gu-5/7	295.02	229.31	0.8	0.19	404			111	255	438
Gu-5/8	401.15	340.18	0.89	0.15	463			124	328	602
MEAN	281.49	218.14	1.06	0.87	356.25			110.38	230.25	405.75
SDEV	51.10	51.26	0.21	0.74	79.13			7.23	44.05	86.34
Gu-6/1	278.18	202.64	0.65	-0.17	386	84		93	259	414
Gu-6/2	342.94	252.7	0.86	0.51	399			132	311	488
Gu-6/3	306.1	228.61	0.86	0.58	382	84		109	279	441
Gu-6/4	298.4	222.27	0.79	0.31	386			103	273	435
MEAN	306.41	226.56	0.79	0.31	388.25			109.25	280.50	444.50
SDEV	27.053	20.640	0.099	0.338	7.411			16.540	21.992	31.225
Gu-7/1	318.14	329	0.77	-0.36	488	7		9	274	542
Gu-7/2	208.63	269.53	1.1	0.08	7	504		7	22	409
Gu-7/3	29.51	80.08	6.16	44.89	6	28		6	8	22
Gu-7/4	43.46	107.2	3.89	16.7	7	26		6	9	22
Gu-7/5	72.33	145.84	2.73	7.14	7	27	405	7	13	37
Gu-7/6	77.12	160.04	2.57	6.02	7	26	431	7	10	31
Gu-7/7	142.73	212.23	1.48	1.19	7	421	27	7	18	285
Gu-7/8	140.1	212.85	1.64	1.78	7	446	30	8	25	233
MEAN	129.00	189.60	2.54	9.68	67.00			7.13	47.38	197.63
SDEV	96.766	83.193	1.777	15.289	170.110			0.991	91.782	202.630
Gu-8/1	173.97	140.268	1.387	2.1483	147.85			78.73	140.18	232.03
Gu-8/2	158.58	120.234	1.495	2.9091	137.32			79.86	132.14	205.93
MEAN	166.28	130.25	1.44	2.53	142.59			79.30	136.16	218.98
SDEV	10.882	14.166	0.076	0.538	7.446			0.799	5.685	18.455

Table A3.3 Grain size analyses for samples taken around Karlinga.

Sample	Assumes a single size mode				Gives size of most common mode			XX % is finer than this size		
	mean	standard deviation	skewness deviation	kurtosis deviation	mode1	mode2	mode3	25%	50%	75%
	um	um	um	um	um	um	um	um	um	um
Karl-1-0	271.86	178.42	0.72	0.69	301			151	256	373
Karl-1-2	267.47	162.735	0.377	-0.2383	316.17	35.62	8.51	157.11	257.15	368.05
Karl-1-12	262.25	170.513	0.478	-0.0949	287.24	31.92		145.47	250.65	365.01
Karl-1-18	256.43	183.639	0.609	0.0012	287.63	35.73	6.8	121.32	240.64	365.29
Karl-1-36	250.91	186.894	0.558	-0.1279	289.66	6.22		105.01	239.77	364.36
MEAN	261.78	176.44	0.55	0.05	296.34	27.37	7.66	135.98	248.84	367.14
SDEV	8.381	9.849	0.130	0.370	12.432	14.212	1.209	22.001	8.263	3.566
Ka-1/1	290.06	227	0.73	0.2	378			86	267	431
Ka-1/2	294.48	230.47	0.78	0.29	364			101	266	433
Ka-1/3	285.83	208.03	0.69	0.23	346			130	264	411
Ka-1/4	286.03	209.63	0.81	0.52	326			133	259	406
Ka-1/5	273.55	192.57	0.71	0.39	322			133	254	388
MEAN	250.75	178.02	0.60	0.19	293.87			118.41	234.28	356.28
SDEV	77.581	57.165	0.195	0.280	93.614			36.924	71.725	114.060
Ka-2/1	302.86	211.2	0.72	0.36	351			151	279	426
Ka-2/2	335.28	213.57	0.5	0.01	391			187	320	467
Ka-2/3	329.59	215.56	0.58	0.1	376			180	307	460
Ka-2/4	317.63	229.33	0.74	0.32	363			152	288	452
Ka-2/5	329.05	235.75	0.78	0.38	360			159	295	465
Ka-2/6	324.87	225.31	0.7	0.25	364			164	297	458
Ka-2/7	318.33	213.79	0.68	0.28	357			169	294	443
Ka-2/8	310.3	189.85	0.53	0.21	345			183	293	424
Ka-2/9	299.69	195.78	0.86	0.85	306			167	270	405
Ka-2/10	294.8	216.81	0.71	0.18	368			126	270	427
MEAN	316.24	214.70	0.68	0.29	358.1			163.8	291.3	442.7
SDEV	13.878	14.003	0.112	0.227	22.363			18.140	15.621	21.093
Ka-3/1	303.93	225.34	0.64	-0.02	386			118	283	445
Ka-3/2	325.68	235.27	0.58	-0.17	416			138	304	476
Ka-3/3	336.95	242.32	0.69	0.2	406			155	311	484
Ka-3/4	307.8	229.67	0.68	0.06	381			126	283	449
Ka-3/5	316.8	216.85	0.69	0.24	365			162	291	445
Ka-3/6	304.88	209.73	0.73	0.42	342			158	280	425
MEAN	316.01	226.53	0.67	0.12	382.67			142.83	292.00	454.00
SDEV	13.190	11.941	0.052	0.209	26.964			18.269	12.744	21.964
Ka-4/1	239.8	230.9	0.99	0.46	367	7	30	29	194	381
Ka-4/2	268.98	219.34	0.7	-0.03	375			55	247	411
Ka-4/3	287.76	216.21	0.71	0.21	361			114	266	419
Ka-4/5	286.57	225.12	0.98	1.08	326			113	256	407
Ka-4/7	279.15	234.12	0.74	-0.01	389	7		50	253	429
Ka-4/9	292.94	188.81	0.61	0.17	351			153	277	409
Ka-4/11	269.39	205.8	0.76	0.37	342			96	249	393
Ka-4/14	287.69	225.44	0.78	0.37	342	7		98	265	417
Ka-4/16	321.39	230.36	0.61	0	392			146	301	464
Ka-4/19	246.36	219.27	0.93	0.51	339	6		42	216	377
Ka-4/21	228.63	216.58	0.88	0.26	362	7		22	198	370
Ka-4/23	265.35	222.37	0.73	0.15	360	7		41	249	403
Ka-4/25	287.32	233.09	0.68	0.02	373	6		57	270	431
MEAN	273.95	220.57	0.78	0.27	359.92			78.15	249.31	408.54
SDEV	24.927	12.435	0.129	0.303	19.662			44.206	30.628	25.330
Kalinga Ck	457.17	193.009	-0.097	-0.5169	553.83			316.73	456.98	600.46
	485.45	190.771	-0.205	-0.4386	636.69			349.89	488.84	629.22
MEAN	471.31	191.89	-0.151	-0.48	595.26			333.31	472.91	614.84
SDEV	19.997	1.583	0.076	0.055	58.591			23.448	22.528	20.336

Table A3.3 Grain size analyses for samples taken around Karlinga (continued).

Sample	Assumes a single size mode				Gives size of most common mode			XX % is finer than this size		
	mean	standard deviation	skewness deviation	kurtosis deviation	mode1	mode2	mode3	25%	50%	75%
	um	um	um	um	um	um	um	um	um	um
KARL-3-0	231.15	206.499	0.895	-0.0771	370.89			54.07	172.69	365
KARL-3-30	257.66	205.655	0.54	-0.4926	347.78	43.58	0.33	54.58	244.04	397.01
KARL-3-90	266.65	205.383	0.494	-0.4928	347.97	2.7	0.34	77.11	253.89	404.52
KARL-3-120	277.06	212.938	0.553	-0.5389				83.65	253.02	422.73
KARL-3-150	253.73	192.006	0.463	-0.4687	337.59	2.27		81.66	244.18	382.48
KARL-3-210	240.52	197.866	0.581	-0.3636	325.38	2.29	0.35	49.05	225.56	371.42
KARL-3-240	207.16	183.367	0.544	-0.6258	307.79	2.51	45.51	15.26	197.49	337.19
MEAN	247.70	200.53	0.58	-0.44	339.57	10.67	11.63	59.34	227.27	382.91
SDEV	23.543	10.114	0.144	0.177	21.606	18.398	22.585	24.167	31.112	28.269
KR99/Ck/1	231.69	200.265	0.73	-0.1797	313.57	47.16	0.34	40.1	205.26	360.91
KR99/Ck/2	242.51	165.85	0.497	-0.2475	285.16	7.69		117.48	230.85	346.04
KR99/Ck/3	239.04	172.039	0.536	-0.1171	285.24	6.21	0.53	98.89	232.38	343.64
KR99/Ck/4	236.82	173.195	0.414	-0.5028	295.21	6.16	0.53	79.69	234.17	351.42
KR99/Ck/5	224.62	167.42	0.579	-0.2201	280.69	5.99	0.53	82.04	212.4	329.37
KR99/Ck/6	269.66	196.521	0.569	-0.1897	320.51	2.68	5.23	113.61	254.08	389.1
MEAN	240.72	179.22	0.55	-0.24	296.73	12.65	1.43	88.64	228.19	353.41
SDEV	15.489	15.153	0.105	0.135	16.580	16.988	2.125	28.426	17.354	20.306

Table A3.4 Grain size analyses for samples taken around Sandy Creek Gorge.

Sample	Assumes a single size mode				Gives size of most common mode			XX % is finer than this size		
	mean	standard deviation	skewness deviation	kurtosis deviation	mode1	mode2	mode3	25%	50%	75%
	um	um	um	um	um	um	um	um	um	um
SC1/1	166.16	107.12	0.377	-0.3916	205.78	7.36		87.92	160.21	235.39
SC1/2	138.77	98.625	0.554	-0.2486	179.41	6.1	0.35	61.39	128.58	202.54
SC1/3	109.77	72.439	0.899	0.9695	113.29			59.83	99.29	147.98
SC1/4	144.32	88.367	0.775	0.4936	152.22			81.42	131.27	193.62
SC1/5	163.5	163.105	1.584	2.3809	116.1	0.36		49.77	110.46	224.02
MEAN	144.50	105.93	0.84	0.64	153.36	4.61		68.07	125.96	200.71
SDEV	22.744	34.474	0.463	1.120	40.068	3.731		15.966	23.236	33.838
SC2/1	146.58	127.873	1.252	1.4644	167.76	6.28	0.34	52.49	114.51	207.96
SC2/2	165.65	159.727	1.383	1.7889	196.62	6.48	0.34	46.72	118.81	239.62
MEAN	156.12	143.80	1.32	1.63	182.19	6.38	0.34	49.61	116.66	223.79
SDEV	13.485	22.524	0.093	0.229	20.407	0.141	0.000	4.080	3.041	22.387
SC3 - 50	145.11	146.279	1.773	3.6054	120.32	5.69	0.51	44.78	104.16	194.87
SC3 - 160	157.06	161.194	1.723	2.9263	113.94			46.83	105.07	207.63
SC3 - 200	135.79	146.691	1.787	3.5608	118.2	7.3	0.51	27.4	92.69	185.58
MEAN	145.99	151.39	1.76	3.36	117.49	6.50	0.51	39.67	100.64	196.03
SDEV	10.662	8.495	0.034	0.380	3.249	1.138	0.000	10.675	6.900	11.070
SCG-57	49.96	40.48	1.049	0.9744	60.82	0.34		18.14	41.99	72.11
SCG-126	49.04	42.189	1.007	0.7238	63.35	0.35		13.19	40.77	73.36
SCG-214	62.54	99.245	4.376	22.6879	62.61	520.37	0.34	11.21	39.18	74.31
SCG-321	115.9	96.954	1.097	0.8024	111.75			42.66	90.96	167.31
SCG-357	73.91	106.256	2.628	7.9838	48.61	0.34		9.22	34.97	86.77
MEAN	70.27	77.02	2.03	6.63	69.43	130.35		18.88	49.57	94.77
SDEV	27.470	32.766	1.478	9.494	24.403	260.013		13.698	23.287	40.977

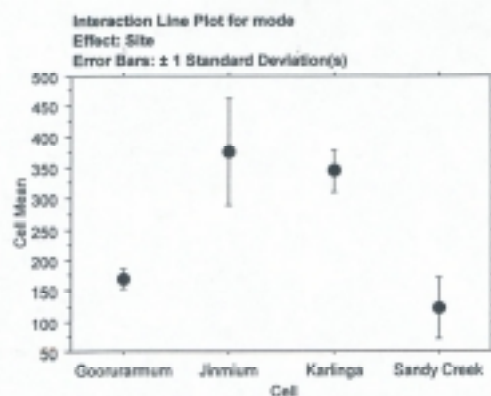
Table A3.5 Summary of all grain size analyses for each of the site areas.

Appendixes

SUMMARY Sample	Assumes a single size mode				Gives size of most common mode			XX % is finer than this size		
	mean	standard deviation	skewness deviation	kurtosis deviation	mode1	mode2	mode3	25%	50%	75%
	um	um	um	um	um	um	um	um	um	um
SC1	145	106	1	1	153	5		68	126	201
SC2	156	144	1	2	182	6		50	117	224
SC3	122	114	2	4	124	6		35	88	170
SCG	70	77	2	7	69	130		19	50	95
Mean	123	110	1	3	132	37		43	95	172
CI/III	291	205	1	0	368	7		129	263	427
Auger5	192	198	1	1	378	50		38	116	299
JG2	265	210	1	0	433	35		78	216	411
JG3	284	215	1	-1	439	4		94	251	437
JG4	196	180	1	1	252	31		55	144	290
Mean	246	202	1	0	374	25		79	198	373
Goor. Ck	314	167	0	0	328	30		198	295	414
Goor-1	202	139	1	2	179	18		109	170	261
Goor-2	231	181	1	1	201			97	182	324
Gu-1	197	135	3	10	160			118	165	233
Gu-2	224	168	2	3	169			115	177	278
Gu-3	225	167	2	3	165			114	178	291
Mean	216	158	2	4	175	18		111	174	277
Gu-5	281	218	1	1	356			110	230	406
Gu-6	306	227	1	0	388			109	281	445
Gu-7	129	190	3	10	67			7	47	198
Gu-8	166	130	1	3	143			79	136	219
Mean	221	191	1	3	239			77	174	317
Karlinga Ck.	471	192	0	0	595			333	473	615
KR99/Creek	241	179	1	0	297	13	1	89	228	353
Mean	356	186	0	0	446	13	1	211	351	484
Karl. Nth	270	184	0	0	328	2	1	134	267	388
KARL-1	259	186	1	3	286			121	222	359
KARL-3	270	188	1	2	314			127	241	378
Ka-1	284	182	0	0	388			176	301	431
Ka-2	316	215	1	0	358			164	291	443
Ka-3	316	227	1	0	383			143	292	454
Ka-4	274	221	1	0	360			78	249	409
Mean	284	200	1	1	345	2	1	135	266	409
Granilpi	248	165	1	3	268			10	31	112
Mean	240	176	1	2	281	24	1	104	202	331

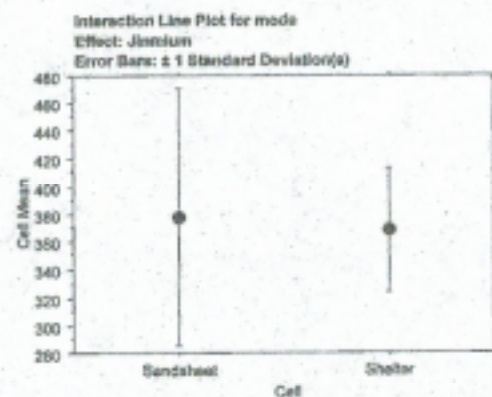
Towards the mangrove and salt flats, the multi-modal sediments comprise three distinct modes dominated by a mud fraction ($< 10 \mu\text{m}$) that is mixed with a silt fraction ($\sim 30 \mu\text{m}$), and a coarse sand fraction ($\sim 460 \mu\text{m}$) probably representing overwash. A detailed analysis of these sediments was not undertaken.

A3.4.3 Statistical analyses of grain size results



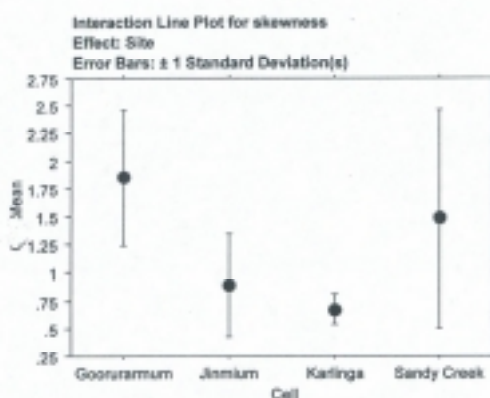
Fisher's PLSD for mode
Effect: Site
Significance Level: 5 %

	Mean Diff.	Crit. Diff.	P-Value	
Gooruramum, Jinmium	-206.914	23.888	<.0001	S
Gooruramum, Karlinga	-175.414	20.070	<.0001	S
Gooruramum, Sandy Cre...	47.485	28.885	.0014	S
Jinmium, Karlinga	31.501	22.736	.0070	S
Jinmium, Sandy Creek	254.380	30.591	<.0001	S
Karlinga, Sandy Creek	222.879	27.713	<.0001	S



Fisher's PLSD for mode
Effect: Jinmium
Significance Level: 5 %

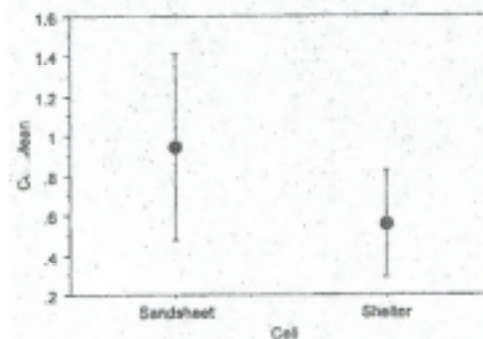
	Mean Diff.	Crit. Diff.	P-Value
Sandsheet, Shelter	9.459	98.678	.8442



Fisher's PLSD for skewness
Effect: Site
Significance Level: 5 %

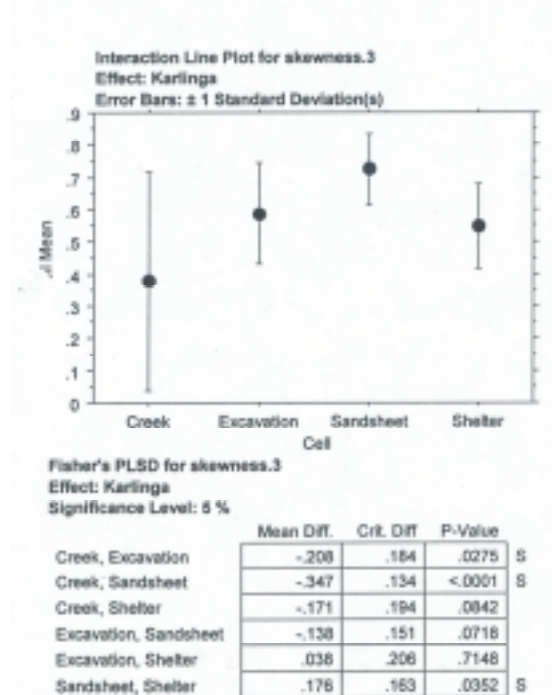
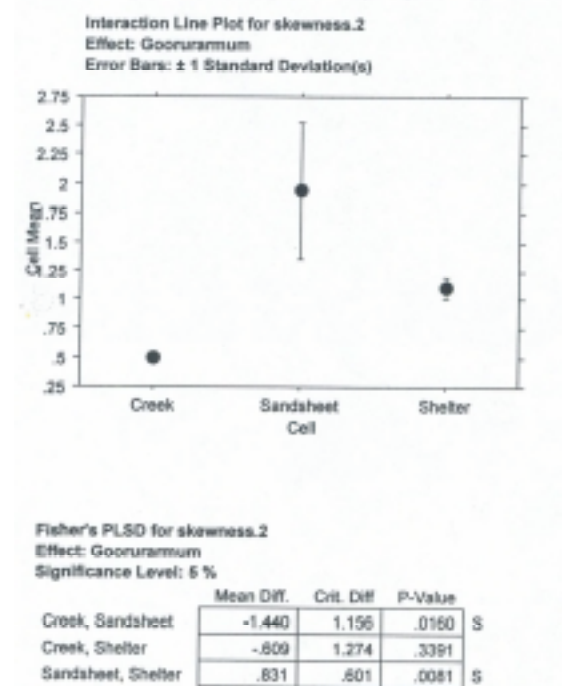
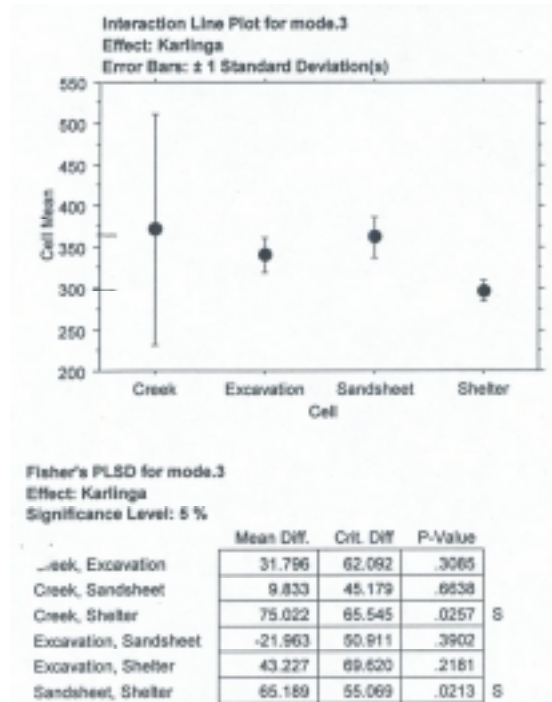
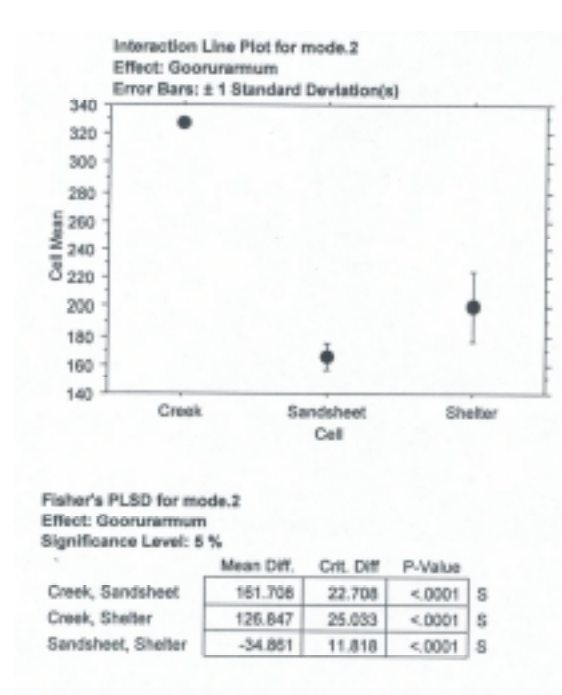
	Mean Diff.	Crit. Diff.	P-Value	
Gooruramum, Jinmium	.957	.259	<.0001	S
Gooruramum, Karlinga	1.181	.218	<.0001	S
Gooruramum, Sandy Cre...	.368	.311	.0207	S
Jinmium, Karlinga	.214	.246	.0883	
Jinmium, Sandy Creek	-.589	.332	.0005	S
Karlinga, Sandy Creek	-.813	.390	<.0001	S

Interaction Line Plot for skewness
Effect: Jinmium
Error Bars: ± 1 Standard Deviation(s)



Fisher's PLSD for skewness
Effect: Jinmium
Significance Level: 5 %

	Mean Diff.	Crit. Diff.	P-Value
Sandsheet, Shelter	.387	.502	.1240



A3.5 Geochemistry

Bulk chemical analyses of major elements were performed by X-ray fluorescence (XRF) at James Cook University (JCU).

A3.5.1 X-ray Fluorescence (XRF) Results

Table A3.7 Major element chemistry for Keep River samples (AAC Job No. 4148).

Method : ACXRF001		JOB NO. 4148-01												
		Client I Ward												
Analyte	SiO2	TiO2	Al2O3	Fe2O3T	MnO	MgO	CaO	Na2O	K2O	P2O5	SO3	LOI	SUM	
LINE	KA1,2	KA1,2	KA1,2	KA1,2	KA1,2	KA1,2	KA1,2	KA1,2	KA1,2	KA1,2	KA1,2			
CRYSTAL	InSb	LIF100	PET	LIF100	LIF100	OVO55	LIF100	OVO55	LIF100	GE	GE			
KV	40	50	40	50	50	40	50	30	50	40	40			
mA	60	50	60	50	50	60	50	90	50	60	60			
TIME(SEC)	45	90	65	90	90	40	50	65	25	35	240			
UNITS	%	%	%	%	%	%	%	%	%	%	%	%	%	
SAMPLE	LAB #													
Karl-1 Spit 1	4148-01	89.7	0.10	1.77	0.73	bd	0.21	0.25	0.49	0.27	0.06	0.04	5.9	99.5
Karl-1 Spit 3	4148-02	91.6	0.12	1.36	0.80	bd	bd	0.19	bd	0.16	0.08	0.01	5.1	99.5
Karl-1 Spit 5	4148-03	90.8	0.13	1.32	0.73	0.01	0.13	0.27	0.16	0.15	0.09	0.01	5.6	99.4
Karl-1 Spit 7	4148-04	91.8	0.15	1.60	0.93	0.01	0.10	0.16	0.11	0.15	0.08	0.01	4.0	99.1
Karl-1 Spit 9	4148-05	91.1	0.17	1.87	1.01	0.01	0.11	0.18	0.05	0.17	0.12	0.01	5.4	100.2
Karl-1 Spit 11	4148-06	93.1	0.19	2.19	1.11	0.01	0.11	0.08	0.18	0.19	0.08	0.02	2.9	100.2
Karl-1 Spit 13	4148-07	91.3	0.20	2.46	1.04	bd	0.09	0.05	0.14	0.15	0.05	bd	3.6	99.1
Karl-1 Spit 13 (rubble)	4148-08	92.8	0.15	2.07	0.92	0.01	0.09	0.06	0.20	0.12	0.04	0.01	2.8	99.3
KARL-3 Spit 1	4148-09	87.7	0.22	2.46	1.10	bd	0.14	0.48	bd	0.16	0.06	0.01	7.4	99.7
KARL-3 Spit 12	4148-10	93.1	0.19	2.31	0.97	bd	bd	0.11	bd	0.12	0.04	bd	2.1	99.0
Jinmium 1	4148-11	94.1	0.18	2.14	0.80	bd	bd	0.07	bd	0.11	0.02	bd	1.5	99.0
Jinmium 3	4148-12	93.5	0.17	2.55	0.94	0.01	0.09	0.07	0.08	0.11	0.02	0.01	2.1	99.6
Jinmium 5	4148-13	91.1	0.22	4.15	1.29	0.01	0.09	0.06	0.11	0.14	0.02	0.01	2.2	99.4
JG4 200cm	4148-14	90.3	0.19	3.80	1.41	bd	bd	0.07	0.41	0.22	0.03	0.03	2.8	99.2
JG5 200cm (rubble)	4148-15	76.6	0.12	3.11	16.46	0.01	0.12	0.02	0.05	0.08	0.15	0.06	2.8	99.5
SC3 50cm	4148-16	93.5	0.32	2.60	1.14	bd	0.15	0.08	bd	0.68	0.02	0.07	1.0	99.6
SC3 50cm	4148-17	94.2	0.31	2.62	0.87	bd	0.14	0.08	0.36	0.69	0.02	0.08	1.0	100.4
SC3 100cm	4148-18	94.7	0.32	2.42	0.84	bd	bd	0.06	bd	0.69	0.02	0.01	0.9	100.0
SC3 200cm	4148-19	92.6	0.37	2.77	1.27	bd	0.13	0.06	bd	0.73	0.02	0.01	1.0	99.0
SC3 200cm	4148-20	94.1	0.36	2.69	0.89	bd	bd	0.06	bd	0.73	0.02	0.01	1.0	99.8
TL16	4148-21	89.0	0.31	6.11	1.22	bd	0.19	0.37	bd	0.37	0.07	0.01	2.8	100.5
TL8	4148-22	91.2	0.28	4.67	1.39	bd	bd	0.07	bd	0.23	0.08	0.01	1.9	99.9
Au-5 60cm (rubble)	4148-23	91.1	0.11	3.42	2.99	bd	bd	0.05	bd	0.11	0.04	0.03	1.6	99.5
KA-4/1 0-15cm	4148-24	93.0	0.16	2.26	0.57	bd	bd	0.15	bd	0.14	0.03	0.01	3.4	99.7
KA-4/13 270-280cm	4148-25	94.0	0.22	3.43	0.23	bd	bd	0.06	bd	0.15	0.03	0.01	1.6	99.7
KA-4/5 1-1.25m	4148-26	97.5	0.11	1.05	0.10	bd	bd	0.05	bd	0.08	0.02	0.01	0.8	99.7
Auger 5 1.5m	4148-27	87.8	0.29	6.10	1.80	bd	bd	0.04	bd	0.18	0.03	bd	3.6	99.8
Jinmium A5 2.5m	4148-28	84.9	0.37	7.69	2.14	0.01	0.12	0.04	0.06	0.22	0.03	0.01	4.8	100.3
Jinmium A5 3.5m	4148-29	82.0	0.44	8.73	2.39	0.01	0.13	0.05	0.08	0.23	0.03	0.01	5.3	99.4
Jinmium A5 4.5m	4148-30	81.7	0.46	9.14	2.50	bd	0.13	0.04	bd	0.25	0.03	0.01	5.9	100.1
Goor-1 Spit 1	4148-31	93.9	0.11	1.10	0.73	bd	bd	0.18	bd	0.12	0.04	bd	3.3	99.5
Goor-1 Spit 5	4148-32	95.3	0.12	1.36	0.86	bd	bd	0.14	bd	0.11	0.04	0.01	1.7	99.7
Goor-1 Spit 9	4148-33	95.8	0.12	1.39	0.89	bd	bd	0.11	bd	0.11	0.04	0.01	1.4	99.9
Goor-1 Spit 19	4148-34	96.4	0.11	0.98	0.70	bd	bd	0.06	bd	0.09	0.03	bd	0.7	99.1
Goor-1 Spit 37	4148-35	95.1	0.14	1.32	1.19	bd	bd	0.06	bd	0.10	0.05	bd	1.9	99.8
Goor-1 Spit 44 (rubble)	4148-36	87.6	0.15	3.51	2.65	bd	bd	0.06	bd	0.12	0.17	0.01	5.0	99.3
Goor-2 Spit 1	4148-37	88.4	0.10	1.50	1.04	bd	0.23	0.94	bd	0.19	0.32	0.02	6.6	99.4
Goor-2 Spit 3	4148-38	90.5	0.11	1.47	1.13	bd	0.13	0.68	0.30	0.16	0.26	0.01	5.3	100.1
Goor-2 Spit 5	4148-39	89.3	0.13	1.71	1.16	bd	0.13	0.77	bd	0.17	0.25	bd	6.1	99.8
Goor-2 Spit 7	4148-40	87.9	0.12	2.07	1.22	bd	0.15	0.71	bd	0.25	0.24	0.01	7.3	99.9
Goor-2 Spit 9	4148-41	85.9	0.08	2.11	1.19	0.01	0.07	0.07	0.03	0.09	0.09	0.01	9.5	99.1
Goor-2 Spit 11	4148-42	87.5	0.13	3.40	1.41	0.02	0.18	1.14	0.09	0.21	0.36	0.01	5.8	100.3
Goor-2 Spit 12 (bedrock?)	4148-43	92.1	0.15	3.03	1.71	bd	0.15	0.54	0.28	0.19	0.21	0.03	1.9	100.3
bd = below detection														

bd = below detection

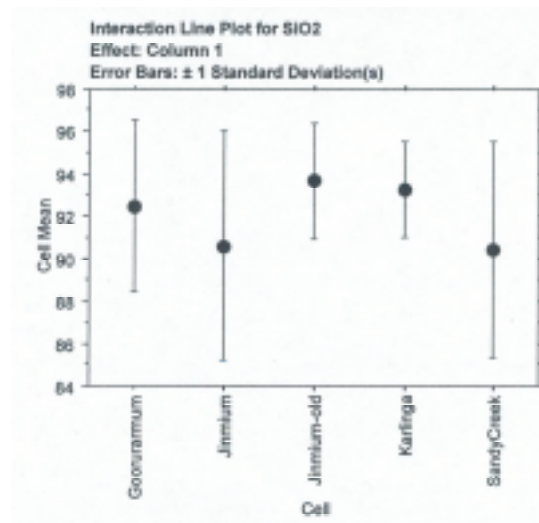
Table A3.8 Major element chemistry for Keep River samples (AAC Job No. 3923).

Method : ACXRF001

JOB NO. 3923-00

		Client I Ward												
Analyte	SiO2	TiO2	Al2O3	Fe2O3T	MnO	MgO	CaO	Na2O	K2O	P2O5	SO3	LOI	SUM	
LINE	KA1,2	KA1,2	KA1,2	KA1,2	KA1,2	KA1,2	KA1,2	KA1,2	KA1,2	KA1,2	KA1,2			
CRYSTAL	InSb	LIF100	PET	LIF100	LIF100	OVO55	LIF100	OVO55	LIF100	GE	GE			
KV	40	50	40	50	50	40	50	30	50	40	40			
mA	60	50	60	50	50	60	50	90	50	60	60			
TIME(SEC)	45	90	65	90	90	40	50	65	25	35	240			
UNITS	%	%	%	%	%	%	%	%	%	%	%	%		
SAMPLE	LAB #													
TL2	3923-01	93.8	0.15	2.34	0.66	bd	bd	0.06	bd	0.11	0.06	0.03	2.3	99.4
TL16	3923-02	91.4	0.16	2.82	0.73	bd	0.16	0.35	1.00	0.32	0.10	0.08	2.3	99.4
TL5	3923-03	94.1	0.14	2.50	0.83	bd	bd	0.09	0.39	0.13	0.06	0.07	1.8	100.1
TL6	3923-04	94.4	0.16	2.61	0.86	bd	bd	0.05	bd	0.12	0.06	0.01	2.0	100.3
TL7	3923-05	96.8	0.11	1.47	1.02	bd	bd	0.08	0.27	0.10	0.06	0.01	0.9	100.9
TL8	3923-06	94.8	0.17	2.25	0.55	bd	bd	0.06	bd	0.12	0.03	0.03	1.1	99.1
TL10	3923-07	97.5	0.07	0.72	0.43	bd	bd	0.05	bd	0.08	0.02	0.02	0.4	99.3
GU/2/1	3923-08	92.2	0.14	2.79	1.01	bd	0.13	0.07	0.38	0.18	0.05	0.04	2.2	99.2
KA/2/15	3923-09	97.1	0.08	1.00	0.10	bd	bd	0.06	bd	0.07	0.02	0.02	0.6	99.1
KA/4/8	3923-10	96.0	0.13	1.46	0.11	bd	bd	0.09	0.43	0.15	0.02	0.04	0.9	99.3
KA/4/18	3923-11	92.4	0.30	4.10	0.35	bd	bd	0.05	bd	0.20	0.04	0.02	1.8	99.3
GU/5/7	3923-12	97.9	0.17	0.97	0.18	bd	bd	0.06	0.30	0.14	0.02	0.02	0.5	100.3
GOOR1-50	3923-13	96.7	0.10	1.37	0.53	bd	bd	0.09	bd	0.10	0.04	bd	1.3	100.2
GOOR1-170	3923-14	97.6	0.11	0.98	0.50	bd	bd	0.06	bd	0.09	0.03	0.01	0.6	100.0
GOOR1-220	3923-15	94.4	0.16	2.32	1.35	bd	bd	0.07	bd	0.15	0.07	0.02	1.3	99.8
JG1-420	3923-16	50.2	0.45	12.70	30.33	bd	0.09	0.16	bd	0.27	0.10	0.01	6.5	100.7
JG2-0	3923-17	98.2	0.03	0.55	0.16	bd	bd	0.05	bd	0.05	0.01	0.02	0.5	99.6
JG2-50	3923-18	96.3	0.10	2.46	0.48	bd	bd	0.05	bd	0.14	0.02	0.04	0.9	100.6
JG2-100	3923-19	91.9	0.19	3.47	1.10	bd	0.13	0.05	0.32	0.16	0.02	0.02	3.0	100.3
JG2-300	3923-20	90.2	0.30	5.23	1.68	bd	0.16	0.05	bd	0.21	0.03	0.03	2.3	100.2
JG2-500	3923-21	90.8	0.31	4.78	1.55	bd	0.14	0.05	bd	0.18	0.02	0.02	2.1	100.0
JG3-0	3923-22	97.5	0.12	0.99	0.30	bd	bd	0.06	bd	0.10	0.02	0.03	0.8	100.0
JG3-90	3923-23	97.3	0.15	1.86	0.33	bd	bd	0.04	bd	0.11	0.01	0.01	0.6	100.4
JG3-210	3923-24	93.1	0.21	3.00	0.82	bd	bd	0.06	0.59	0.20	0.02	0.07	1.7	99.8
JG4-100	3923-25	95.4	0.11	1.91	0.72	bd	bd	0.06	0.47	0.15	0.02	0.01	1.2	100.0
JG4-400	3923-26	89.6	0.24	5.73	1.88	bd	0.15	0.07	bd	0.30	0.02	0.03	2.3	100.3
JG4-590	3923-27	88.9	0.28	5.46	1.84	bd	0.15	0.07	0.36	0.29	0.03	0.01	2.6	100.0
JG5-RED	3923-28	85.1	0.15	3.26	7.07	bd	bd	0.04	bd	0.13	0.07	0.01	3.2	99.1
JG5-YELLOW	3923-29	94.2	0.10	2.55	0.58	bd	bd	0.04	bd	0.08	0.04	0.01	2.8	100.4
KARL3-30	3923-30	92.6	0.19	2.44	0.72	bd	bd	0.16	bd	0.13	0.03	0.01	3.1	99.3
KARL3-90	3923-31	93.5	0.20	2.45	0.73	bd	bd	0.08	bd	0.12	0.04	0.02	2.6	99.8
KARL3-150	3923-32	94.1	0.23	2.81	0.98	bd	0.13	0.06	0.26	0.16	0.04	0.01	1.5	100.4
KARL3-210	3923-33	93.5	0.25	3.06	0.96	bd	bd	0.05	bd	0.16	0.05	bd	1.6	99.6
KN2-100	3923-34	93.3	0.17	2.05	0.69	bd	bd	0.05	bd	0.10	0.03	0.02	3.0	99.4
KN3-145	3923-35	94.2	0.24	2.80	0.79	bd	bd	0.06	bd	0.16	0.07	0.02	1.6	99.9
KN3-230	3923-36	92.6	0.21	2.26	0.79	bd	bd	0.06	bd	0.13	0.05	0.02	3.6	99.7
KN4-115	3923-37	95.2	0.20	2.10	0.55	bd	bd	0.05	bd	0.10	0.03	0.01	1.6	99.9
KN7-100	3923-38	93.8	0.31	2.13	1.07	bd	bd	0.05	bd	0.12	0.03	0.01	1.8	99.3
KR99CP-50	3923-39	92.9	0.15	2.01	0.45	bd	bd	0.23	bd	0.12	0.05	0.01	3.9	99.8
KR99CP-125	3923-40	97.7	0.08	1.11	0.07	bd	bd	0.05	bd	0.08	0.02	0.01	0.6	99.8
KR99CP-200	3923-41	95.8	0.18	2.08	0.12	bd	bd	0.06	0.32	0.12	0.02	0.01	1.5	100.1
SC1-100	3923-42	93.1	0.22	2.05	0.72	bd	bd	0.08	bd	0.51	0.02	bd	2.8	99.5
SC1-300	3923-43	96.1	0.23	1.46	0.51	bd	bd	0.06	bd	0.49	0.02	0.01	0.7	99.6
SCG-57	3923-44	89.2	0.65	4.81	1.57	bd	0.22	0.11	0.46	1.40	0.04	0.02	2.1	100.7
SCG-126	3923-45	85.8	0.70	6.41	2.23	bd	0.27	0.10	bd	1.63	0.03	0.01	2.5	99.8
SCG-214	3923-46	82.9	0.78	7.71	2.90	bd	0.35	0.10	bd	1.68	0.04	bd	3.3	99.7
SCG-321	3923-47	93.7	0.37	2.79	0.97	bd	0.15	0.06	bd	0.76	0.02	0.01	1.1	99.9
SCG-357	3923-48	83.0	0.71	7.39	3.40	bd	0.36	0.07	0.59	1.17	0.04	0.02	3.2	100.0
SCG-SIL	3923-49	82.3	0.59	7.53	2.10	bd	0.39	0.14	0.28	1.46	0.03	0.02	5.6	100.4
G2	3923-50	97.2	0.07	0.89	0.47	bd	bd	0.06	0.38	0.10	0.05	0.04	0.9	100.2
G4	3923-51	95.3	0.13	2.57	0.34	bd	bd	0.07	0.30	0.11	0.05	0.03	1.3	100.1
J1	3923-52	94.3	0.14	2.27	0.67	bd	bd	0.06	0.51	0.14	0.10	0.05	1.8	100.0
J2	3923-53	95.9	0.05	2.50	0.08	bd	bd	0.05	bd	0.09	0.03	0.01	1.6	100.3
K1	3923-54	94.6	0.11	2.28	0.94	bd	bd	0.09	0.38	0.14	0.17	0.03	1.5	100.2
K5	3923-55	94.0	0.08	2.22	1.61	bd	bd	0.05	bd	0.09	0.03	0.01	1.6	99.8

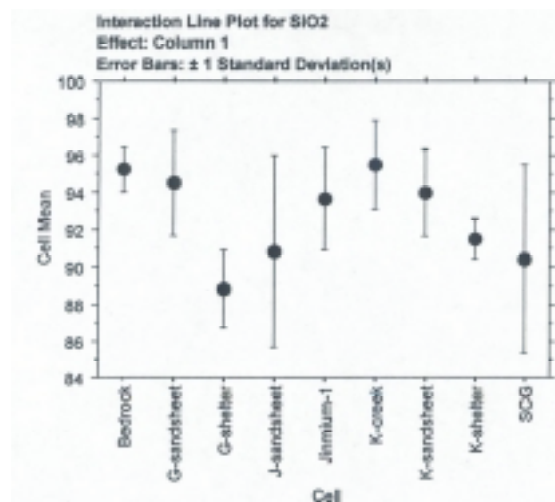
A3.5.2 Statistical analyses of geochemistry



Fisher's PLSD for SiO₂
Effect: Column 1
Significance Level: 5 %

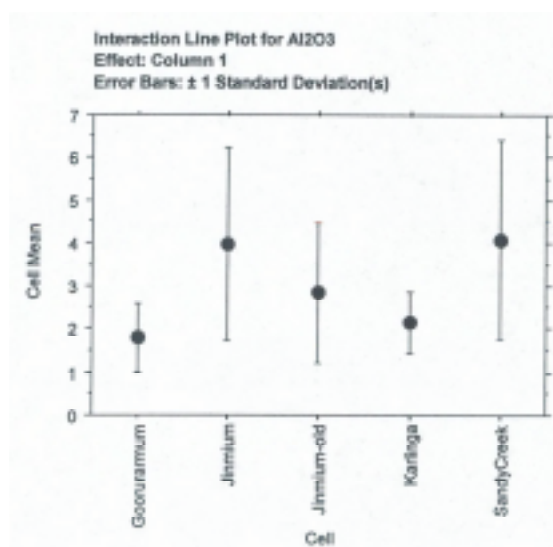
	Mean Diff.	Crit. Diff.	P-Value
Gooruramum, Jinmium	1.918	2.588	.1443
Gooruramum, Jinmium-old	-1.177	3.365	.4887
Gooruramum, Karlinga	-.801	2.510	.5272
Gooruramum, SandyCreek	2.079	3.007	.1730
Jinmium, Jinmium-old	-3.095	3.190	.0571
Jinmium, Karlinga	-2.719	2.271	.0195
Jinmium, SandyCreek	.161	2.811	.9096
Jinmium-old, Karlinga	.376	3.128	.8118
Jinmium-old, SandyCreek	3.256	3.539	.0709
Karlinga, SandyCreek	2.880	2.739	.0398

6 cases were omitted due to missing values.



Fisher's PLSD for SiO₂
Effect: Column 1
Significance Level: 5 %

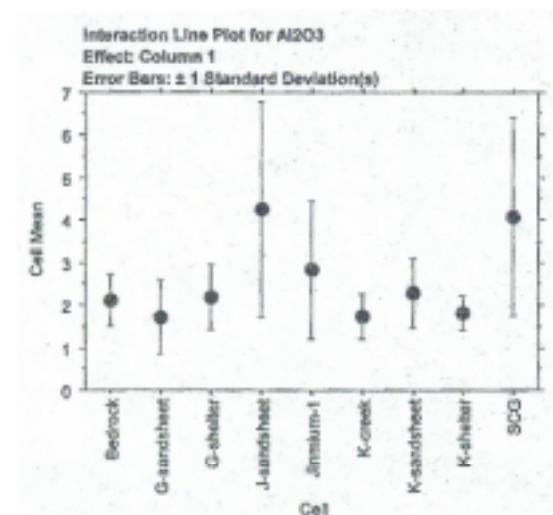
	Mean Diff.	Crit. Diff.	P-Value
Bedrock, G-sandsheet	.714	3.643	.6975
Bedrock, G-shelter	6.403	3.925	.0017
Bedrock, J-sandsheet	4.361	3.325	.0108
Bedrock, Jinmium-1	1.539	3.718	.4126
Bedrock, K-creek	-.266	4.988	.9151
Bedrock, K-sandsheet	1.234	3.325	.4626
Bedrock, K-shelter	3.690	3.810	.0675
Bedrock, SCG	4.795	3.482	.0075
G-sandsheet, G-shelter	5.668	3.476	.0016
G-sandsheet, J-sandsheet	3.647	2.782	.0108
G-sandsheet, Jinmium-1	.825	3.241	.8140
G-sandsheet, K-creek	-.983	4.644	.8749
G-sandsheet, K-sandsheet	.520	2.782	.7113
G-sandsheet, K-shelter	2.975	3.346	.0806
G-sandsheet, SCG	4.081	2.967	.0075
G-shelter, J-sandsheet	-2.042	3.142	.1999
G-shelter, Jinmium-1	-4.863	3.555	.0079
G-shelter, K-creek	-6.671	4.868	.0078
G-shelter, K-sandsheet	-5.169	3.142	.0016
G-shelter, K-shelter	-2.713	3.651	.1432
G-shelter, SCG	-1.607	3.307	.3365
J-sandsheet, Jinmium-1	-2.822	2.880	.0547
J-sandsheet, K-creek	-4.629	4.399	.0394
J-sandsheet, K-sandsheet	-3.127	2.351	.0098
J-sandsheet, K-shelter	-.672	2.997	.6571
J-sandsheet, SCG	.434	2.568	.7375
Jinmium-1, K-creek	-1.808	4.703	.4467
Jinmium-1, K-sandsheet	-.306	2.880	.8334
Jinmium-1, K-shelter	2.150	3.428	.2157
Jinmium-1, SCG	3.256	3.059	.0373
K-creek, K-sandsheet	1.502	4.399	.4989
K-creek, K-shelter	3.958	4.776	.1031
K-creek, SCG	5.064	4.518	.0285
K-sandsheet, K-shelter	2.456	2.997	.1070
K-sandsheet, SCG	3.561	2.568	.0071
K-shelter, SCG	1.108	3.170	.4898



Fisher's PLSD for Al2O3
Effect: Column 1
Significance Level: 5 %

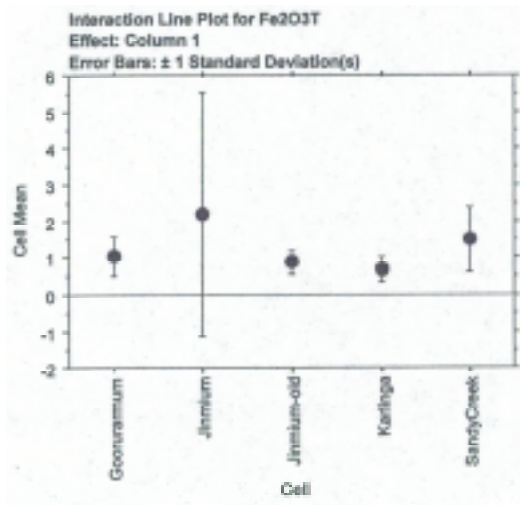
	Mean Diff.	Crit. Diff.	P-Value	
Gooruramum, Jinnium	-2.178	1.027	<.0001	S
Gooruramum, Jinnium-old	-1.047	1.336	.1228	
Gooruramum, Karlinga	-.358	.996	.4770	
Gooruramum, SandyCreek	-2.311	1.194	.0002	S
Jinnium, Jinnium-old	1.131	1.266	.0794	
Jinnium, Karlinga	1.820	.901	.0001	S
Jinnium, SandyCreek	-.133	1.116	.8129	
Jinnium-old, Karlinga	.689	1.241	.2730	
Jinnium-old, SandyCreek	-1.264	1.405	.0772	
Karlinga, SandyCreek	-1.553	1.067	.0006	S

6 cases were omitted due to missing values.



Fisher's PLSD for Al2O3
Effect: Column 1
Significance Level: 5 %

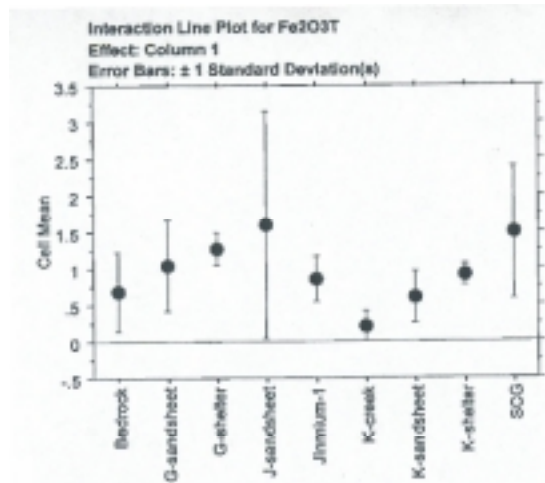
	Mean Diff.	Crit. Diff.	P-Value	
Bedrock, G-sandsheet	.410	1.676	.8281	
Bedrock, G-shelter	-.063	1.805	.9452	
Bedrock, J-sandsheet	-2.140	1.530	.0057	S
Bedrock, Jinnium-1	-.711	1.710	.4110	
Bedrock, K-creek	.386	2.294	.7372	
Bedrock, K-sandsheet	-.164	1.530	.8318	
Bedrock, K-shelter	.292	1.752	.7415	
Bedrock, SCG	-1.974	1.682	.0163	S
G-sandsheet, G-shelter	-.472	1.660	.6585	
G-sandsheet, J-sandsheet	-2.550	1.280	.0002	S
G-sandsheet, Jinnium-1	-1.120	1.491	.1389	
G-sandsheet, K-creek	-.021	2.135	.9842	
G-sandsheet, K-sandsheet	-.574	1.280	.3753	
G-sandsheet, K-shelter	-.116	1.639	.8792	
G-sandsheet, SCG	-2.384	1.365	.0006	S
G-shelter, J-sandsheet	-2.077	1.445	.0054	S
G-shelter, Jinnium-1	-.648	1.635	.4329	
G-shelter, K-creek	.451	2.239	.6886	
G-shelter, K-sandsheet	-.101	1.445	.6865	
G-shelter, K-shelter	.364	1.679	.6769	
G-shelter, SCG	-1.512	1.521	.0144	S
J-sandsheet, Jinnium-1	1.429	1.325	.0348	S
J-sandsheet, K-creek	2.528	2.024	.0150	S
J-sandsheet, K-sandsheet	1.976	1.082	.0006	S
J-sandsheet, K-shelter	2.432	1.379	.0007	S
J-sandsheet, SCG	.166	1.181	.7811	
Jinnium-1, K-creek	1.099	2.163	.3153	
Jinnium-1, K-sandsheet	.547	1.325	.4141	
Jinnium-1, K-shelter	1.002	1.577	.2097	
Jinnium-1, SCG	-1.264	1.407	.0777	
K-creek, K-sandsheet	-.552	2.024	.5887	
K-creek, K-shelter	-.097	2.197	.9305	
K-creek, SCG	-2.363	2.078	.0264	S
K-sandsheet, K-shelter	.456	1.379	.5129	
K-sandsheet, SCG	-1.811	1.181	.0031	S
K-shelter, SCG	-2.266	1.458	.0027	S



Fisher's PLSD for Fe2O3T
Effect: Column 1
Significance Level: 5 %

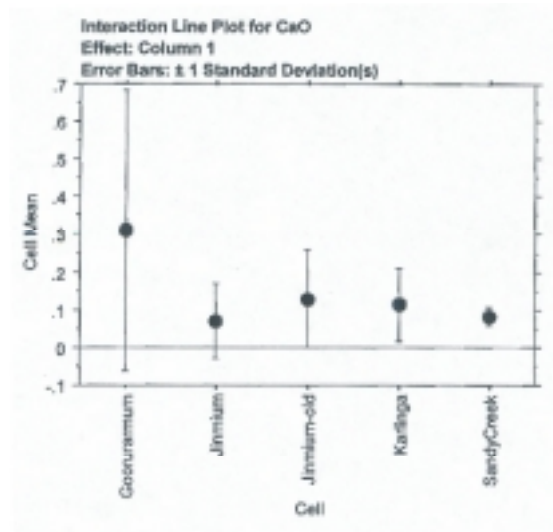
	Mean Diff.	Crit. Diff.	P-Value	
Gooruramum, Jinmium	-1.162	1.126	.0432	S
Gooruramum, Jinmium-old	.189	1.464	.7980	
Gooruramum, Karlinga	.375	1.092	.4967	
Gooruramum, SandyCreek	-.450	1.309	.4965	
Jinmium, Jinmium-old	1.351	1.388	.0563	
Jinmium, Karlinga	1.537	.986	.0027	S
Jinmium, SandyCreek	.713	1.223	.2499	
Jinmium-old, Karlinga	.186	1.381	.7867	
Jinmium-old, SandyCreek	-.639	1.540	.4120	
Karlinga, SandyCreek	-.825	1.192	.1727	

6 cases were omitted due to missing values.



Fisher's PLSD for Fe2O3T
Effect: Column 1
Significance Level: 5 %

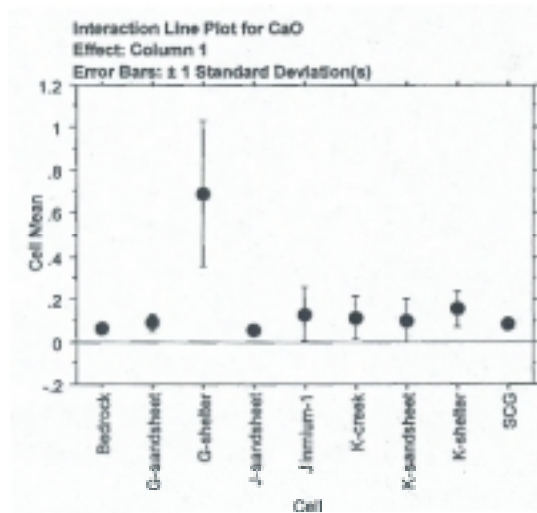
	Mean Diff.	Crit. Diff.	P-Value	
Bedrock, G-sandsheet	-.356	.868	.4171	
Bedrock, G-shelter	-.561	.935	.2204	
Bedrock, J-sandsheet	-.912	.793	.0246	S
Bedrock, Jinmium-1	-.169	.886	.7046	
Bedrock, K-creek	.472	1.189	.4323	
Bedrock, K-sandsheet	.074	.793	.8522	
Bedrock, K-shelter	-.224	.906	.6253	
Bedrock, SCG	-.808	.830	.0561	
G-sandsheet, G-shelter	-.225	.826	.5910	
G-sandsheet, J-sandsheet	-.556	.663	.0990	
G-sandsheet, Jinmium-1	.187	.772	.6322	
G-sandsheet, K-creek	.826	1.107	.1407	
G-sandsheet, K-sandsheet	.430	.663	.2002	
G-sandsheet, K-shelter	.132	.797	.7423	
G-sandsheet, SCG	-.452	.707	.2071	
G-shelter, J-sandsheet	-.332	.749	.3811	
G-shelter, Jinmium-1	.411	.847	.3371	
G-shelter, K-creek	1.052	1.160	.0748	
G-shelter, K-sandsheet	.655	.749	.0855	
G-shelter, K-shelter	.357	.870	.4168	
G-shelter, SCG	-.227	.788	.5677	
J-sandsheet, Jinmium-1	.743	.886	.0343	S
J-sandsheet, K-creek	1.384	1.048	.0103	S
J-sandsheet, K-sandsheet	.987	.560	.0007	S
J-sandsheet, K-shelter	.688	.714	.0567	
J-sandsheet, SCG	.104	.612	.7358	
Jinmium-1, K-creek	.641	1.121	.2566	
Jinmium-1, K-sandsheet	.244	.686	.4817	
Jinmium-1, K-shelter	-.054	.817	.8961	
Jinmium-1, SCG	-.639	.729	.0851	
K-creek, K-sandsheet	-.397	1.048	.4532	
K-creek, K-shelter	-.695	1.138	.2277	
K-creek, SCG	-1.280	1.077	.0204	S
K-sandsheet, K-shelter	-.296	.714	.4066	
K-sandsheet, SCG	-.883	.612	.0052	S



Fisher's PLSD for CaO
Effect: Column 1
Significance Level: 5 %

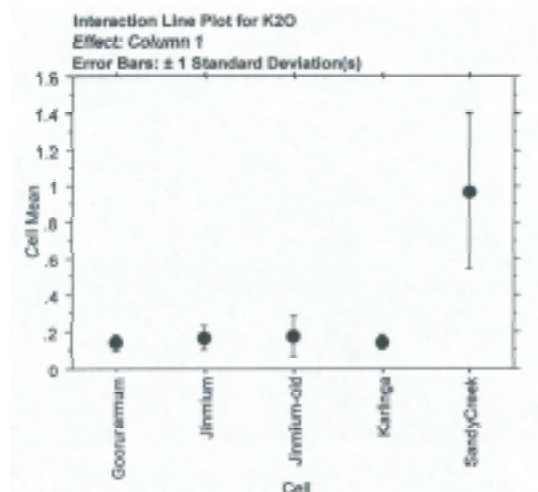
	Mean Diff.	Crit. Diff.	P-Value	
Gooruramum, Jinmium	.238	.115	<.0001	\$
Gooruramum, Jinmium-old	.179	.149	.0194	\$
Gooruramum, Karlinga	.194	.111	.0008	\$
Gooruramum, SandyCreek	.228	.133	.0010	\$
Jinmium, Jinmium-old	-.059	.141	.4125	
Jinmium, Karlinga	-.044	.101	.3920	
Jinmium, SandyCreek	-.009	.125	.8857	
Jinmium-old, Karlinga	.015	.139	.8298	
Jinmium-old, SandyCreek	.050	.157	.5318	
Karlinga, SandyCreek	.035	.121	.5735	

6 cases were omitted due to missing values.



Fisher's PLSD for CaO
Effect: Column 1
Significance Level: 5 %

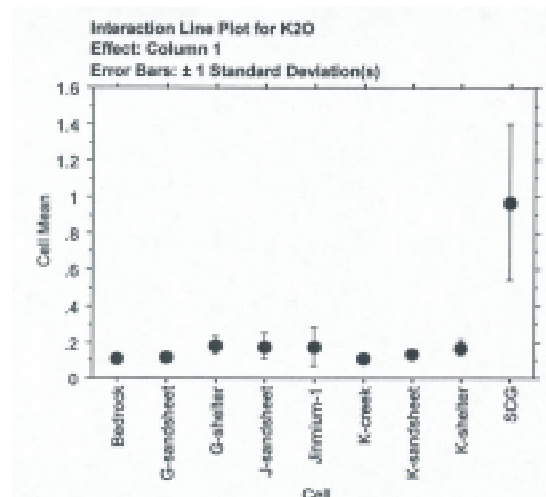
	Mean Diff.	Crit. Diff.	P-Value	
Bedrock, G-sandsheet	-.027	.118	.6529	
Bedrock, G-shelter	-.630	.127	<.0001	\$
Bedrock, J-sandsheet	.012	.107	.8293	
Bedrock, Jinmium-1	-.058	.120	.2643	
Bedrock, K-creek	-.050	.161	.5383	
Bedrock, K-sandsheet	-.033	.107	.5451	
Bedrock, K-shelter	-.092	.123	.1418	
Bedrock, SCG	-.018	.112	.7480	
G-sandsheet, G-shelter	-.603	.112	<.0001	\$
G-sandsheet, J-sandsheet	.038	.090	.3981	
G-sandsheet, Jinmium-1	-.041	.105	.4365	
G-sandsheet, K-creek	-.023	.150	.7575	
G-sandsheet, K-sandsheet	-.006	.090	.8926	
G-sandsheet, K-shelter	-.065	.108	.2345	
G-sandsheet, SCG	.008	.096	.8609	
G-shelter, J-sandsheet	.541	.101	<.0001	\$
G-shelter, Jinmium-1	.582	.115	<.0001	\$
G-shelter, K-creek	.580	.157	<.0001	\$
G-shelter, K-sandsheet	.597	.101	<.0001	\$
G-shelter, K-shelter	.538	.118	<.0001	\$
G-shelter, SCG	.611	.107	<.0001	\$
J-sandsheet, Jinmium-1	-.079	.093	.0927	
J-sandsheet, K-creek	-.062	.142	.3900	
J-sandsheet, K-sandsheet	-.044	.076	.2472	
J-sandsheet, K-shelter	-.103	.097	.0365	\$
J-sandsheet, SCG	-.030	.083	.4752	
Jinmium-1, K-creek	.018	.152	.8163	
Jinmium-1, K-sandsheet	.035	.093	.4556	
Jinmium-1, K-shelter	-.024	.111	.6686	
Jinmium-1, SCG	.050	.099	.3206	
K-creek, K-sandsheet	.017	.142	.8099	
K-creek, K-shelter	-.042	.154	.5821	
K-creek, SCG	.032	.146	.8655	
K-sandsheet, K-shelter	-.059	.097	.2293	



Fisher's PLSD for K2O
Effect: Column 1
Significance Level: 5 %

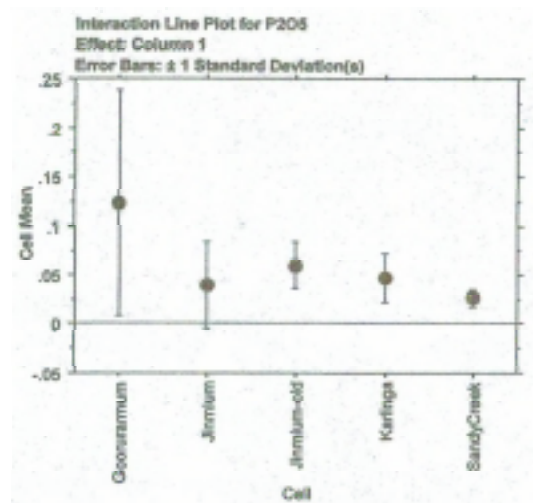
	Mean Diff.	Crit. Diff.	P-Value	
Goonuramum, Jinnium	-.024	.108	.6571	
Goonuramum, Jinnium-old	-.036	.140	.6155	
Goonuramum, Karlinga	-3.571E-4	.105	.9946	
Goonuramum, SandyCreek	-.831	.125	<.0001	S
Jinnium, Jinnium-old	-.011	.133	.8652	
Jinnium, Karlinga	.024	.095	.6182	
Jinnium, SandyCreek	-.857	.117	<.0001	S
Jinnium-old, Karlinga	.035	.130	.5926	
Jinnium-old, SandyCreek	-.795	.148	<.0001	S
Karlinga, SandyCreek	-.830	.114	<.0001	S

cases were omitted due to missing values.



Fisher's PLSD for K2O
Effect: Column 1
Significance Level: 5 %

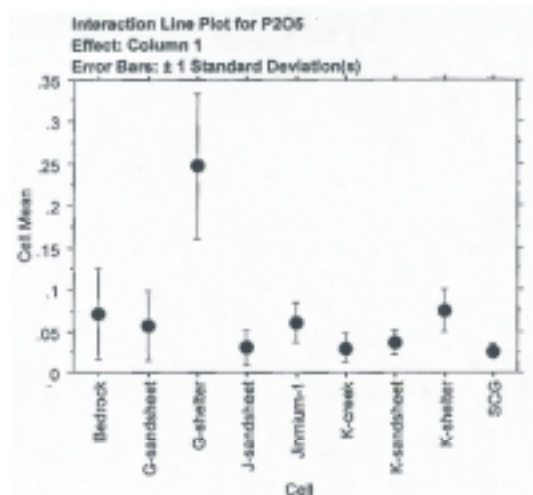
	Mean Diff.	Crit. Diff.	P-Value	
Bedrock, G-sandsheet	-.005	.177	.9525	
Bedrock, G-shelter	-.068	.161	.4789	
Bedrock, J-sandsheet	-.066	.162	.4190	
Bedrock, Jinnium-1	+.064	.181	.4647	
Bedrock, K-creek	.005	.243	.9674	
Bedrock, K-sandsheet	-.021	.182	.7060	
Bedrock, K-shelter	-.068	.185	.5334	
Bedrock, SCG	-.859	.170	<.0001	S
G-sandsheet, G-shelter	-.063	.169	.4612	
G-sandsheet, J-sandsheet	-.061	.135	.3748	
G-sandsheet, Jinnium-1	-.059	.158	.4626	
G-sandsheet, K-creek	.010	.226	.9278	
G-sandsheet, K-sandsheet	-.016	.135	.8174	
G-sandsheet, K-shelter	-.053	.163	.5194	
G-sandsheet, SCG	-.854	.144	<.0001	S
G-shelter, J-sandsheet	.002	.153	.9770	
G-shelter, Jinnium-1	.004	.173	.9694	
G-shelter, K-creek	.073	.237	.5400	
G-shelter, K-sandsheet	.047	.153	.5410	
G-shelter, K-shelter	.010	.176	.9112	
G-shelter, SCG	-.791	.161	<.0001	S
J-sandsheet, Jinnium-1	.002	.140	.9748	
J-sandsheet, K-creek	.071	.214	.5109	
J-sandsheet, K-sandsheet	.045	.114	.4366	
J-sandsheet, K-shelter	.008	.148	.9158	
J-sandsheet, SCG	-.783	.125	<.0001	S
Jinnium-1, K-creek	.069	.229	.5512	
Jinnium-1, K-sandsheet	.043	.140	.5457	
Jinnium-1, K-shelter	.006	.167	.9474	
Jinnium-1, SCG	-.786	.148	<.0001	S
K-creek, K-sandsheet	-.026	.214	.8090	
K-creek, K-shelter	-.063	.233	.5895	
K-creek, SCG	-.864	.220	<.0001	S



Fisher's PLSD for P205
Effect: Column 1
Significance Level: 5 %

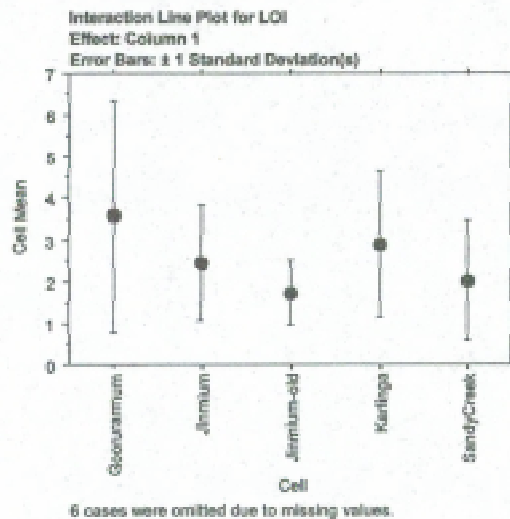
	Mean Diff.	Crit. Diff.	P-Value	
Goosaramum, Jinmium	.064	.036	<.0001	S
Goosaramum, Jinmium-old	.064	.047	.0091	S
Goosaramum, Karlinga	.076	.035	<.0001	S
Goosaramum, SandyCreek	.097	.042	<.0001	S
Jinmium, Jinmium-old	-.021	.045	.3585	
Jinmium, Karlinga	-.006	.032	.6207	
Jinmium, SandyCreek	.013	.040	.5145	
Jinmium-old, Karlinga	.013	.044	.6626	
Jinmium-old, SandyCreek	.034	.050	.1799	
Karlinga, SandyCreek	.021	.039	.2817	

6 cases were omitted due to missing values.



Fisher's PLSD for P205
Effect: Column 1
Significance Level: 5 %

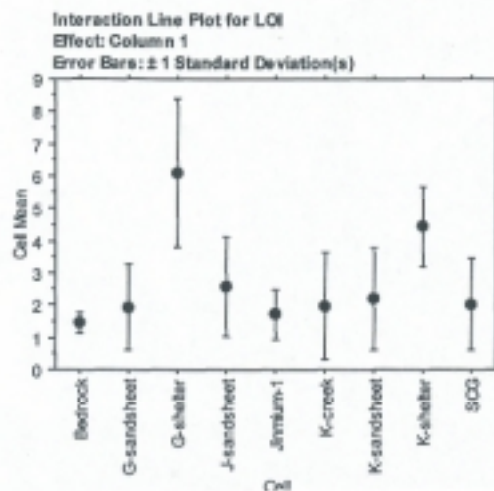
	Mean Diff.	Crit. Diff.	P-Value	
Bedrock, G-sandsheet	.016	.035	.3743	
Bedrock, G-shelter	-.175	.038	<.0001	S
Bedrock, J-sandsheet	.041	.032	.0114	S
Bedrock, Jinmium-1	.012	.036	.5163	
Bedrock, K-creek	.042	.048	.0864	
Bedrock, K-sandsheet	.036	.032	.0291	S
Bedrock, K-shelter	-.003	.036	.8562	
Bedrock, SCG	.046	.033	.0060	S
G-sandsheet, G-shelter	-.191	.033	<.0001	S
G-sandsheet, J-sandsheet	.025	.026	.0583	
G-sandsheet, Jinmium-1	-.004	.031	.7963	
G-sandsheet, K-creek	.026	.044	.2482	
G-sandsheet, K-sandsheet	.020	.027	.1414	
G-sandsheet, K-shelter	-.019	.032	.2416	
G-sandsheet, SCG	.030	.028	.0397	S
G-shelter, J-sandsheet	.217	.030	<.0001	S
G-shelter, Jinmium-1	.187	.034	<.0001	S
G-shelter, K-creek	.217	.047	<.0001	S
G-shelter, K-sandsheet	.211	.030	<.0001	S
G-shelter, K-shelter	.172	.035	<.0001	S
G-shelter, SCG	.221	.032	<.0001	S
J-sandsheet, Jinmium-1	-.029	.027	.0349	S
J-sandsheet, K-creek	.001	.042	.9802	
J-sandsheet, K-sandsheet	-.006	.022	.6184	
J-sandsheet, K-shelter	-.044	.028	.0026	S
J-sandsheet, SCG	.004	.024	.7215	
Jinmium-1, K-creek	.030	.045	.1888	
Jinmium-1, K-sandsheet	.024	.028	.0866	
Jinmium-1, K-shelter	-.015	.033	.3660	
Jinmium-1, SCG	.034	.029	.0240	S
K-creek, K-sandsheet	-.006	.042	.7737	
K-creek, K-shelter	-.045	.046	.0537	
K-creek, SCG	.004	.043	.8601	
K-sandsheet, K-shelter	-.039	.029	.0065	S
K-sandsheet, SCG	.010	.025	.4228	
K-shelter, SCG	.049	.030	.0019	S



Fisher's PLSD for LOI
Effect: Column 1
Significance Level: 5 %

	Mean Diff.	Crit. Diff.	P-Value	
Goornaramum, Jinmium	1.125	1.142	.0538	
Goornaramum, Jinmium-old	1.639	1.488	.0159	S
Goornaramum, Karlinga	.685	1.108	.2237	
Goornaramum, SandyCreek	1.540	1.328	.0235	S
Jinmium, Jinmium-old	.714	1.409	.3162	
Jinmium, Karlinga	-.441	1.002	.5838	
Jinmium, SandyCreek	.415	1.241	.5076	
Jinmium-old, Karlinga	-1.156	1.381	.0898	
Jinmium-old, SandyCreek	-.299	1.563	.7046	
Karlinga, SandyCreek	.657	1.210	.1627	

6 cases were omitted due to missing values.



Fisher's PLSD for LOI
Effect: Column 1
Significance Level: 5 %

	Mean Diff.	Crit. Diff.	P-Value	
Bedrock, G-sandsheet	-.485	1.510	.5249	
Bedrock, G-shelter	-4.621	1.626	<.0001	S
Bedrock, J-sandsheet	-1.124	1.378	.1085	
Bedrock, Jinmium-1	-.267	1.541	.7314	
Bedrock, K-creek	-.528	2.067	.6125	
Bedrock, K-sandsheet	-.748	1.378	.2833	
Bedrock, K-shelter	-2.977	1.579	.0003	S
Bedrock, SCG	-.566	1.443	.4376	
G-sandsheet, G-shelter	-4.137	1.441	<.0001	S
G-sandsheet, J-sandsheet	-.639	1.153	.2731	
G-sandsheet, Jinmium-1	.216	1.343	.7478	
G-sandsheet, K-creek	-.044	1.924	.9640	
G-sandsheet, K-sandsheet	-.264	1.153	.6605	
G-sandsheet, K-shelter	-2.482	1.387	.0006	S
G-sandsheet, SCG	-.061	1.230	.8957	
G-shelter, J-sandsheet	3.497	1.302	<.0001	S
G-shelter, Jinmium-1	4.355	1.473	<.0001	S
G-shelter, K-creek	4.093	2.017	.0001	S
G-shelter, K-sandsheet	3.873	1.302	<.0001	S
G-shelter, K-shelter	1.645	1.513	.0335	S
G-shelter, SCG	4.056	1.370	<.0001	S
J-sandsheet, Jinmium-1	.857	1.193	.1568	
J-sandsheet, K-creek	.596	1.823	.5175	
J-sandsheet, K-sandsheet	.376	.974	.4451	
J-sandsheet, K-shelter	-1.853	1.242	.0039	S
J-sandsheet, SCG	.558	1.064	.2998	
Jinmium-1, K-creek	-.262	1.949	.7902	
Jinmium-1, K-sandsheet	-.481	1.193	.4247	
Jinmium-1, K-shelter	-2.710	1.420	.0003	S
Jinmium-1, SCG	-.298	1.268	.6401	
K-creek, K-sandsheet	-.220	1.823	.8111	
K-creek, K-shelter	-2.449	1.979	.0159	S

A3.5.3 Graphical Comparison of Grain Size and Geochemistry.

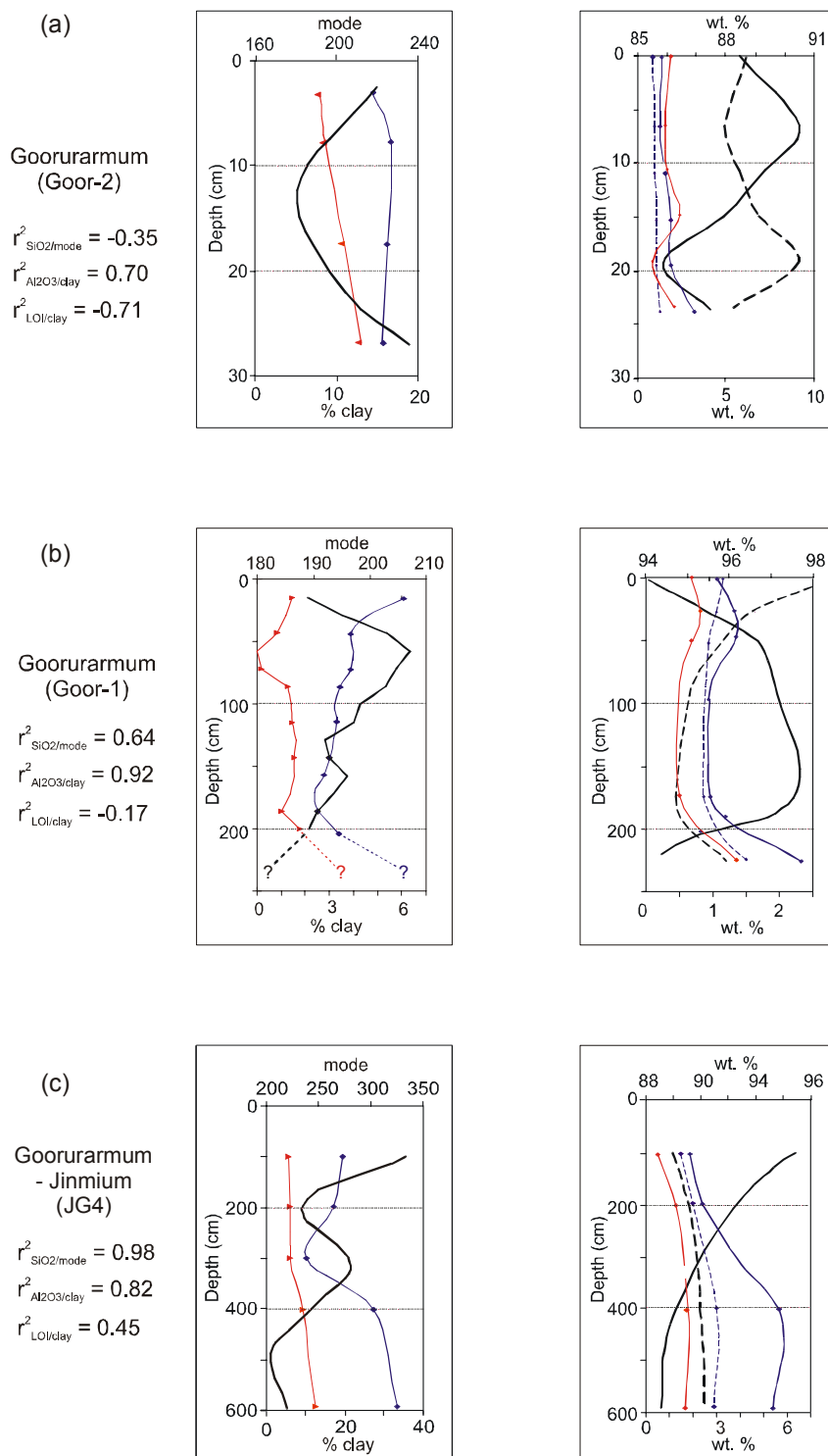


Figure A3.7 Profiles of grain size mode (black), < 60 μm (blue) and < 10 μm (red) and major element chemistry SiO_2 (black), Al_2O_3 (blue), K_2O (blue dashed), and LOI (black dashed) in (a) Goor-2 rock shelter excavation, (b) Goor-1 sand sheet excavation and (c) auger core JG4.

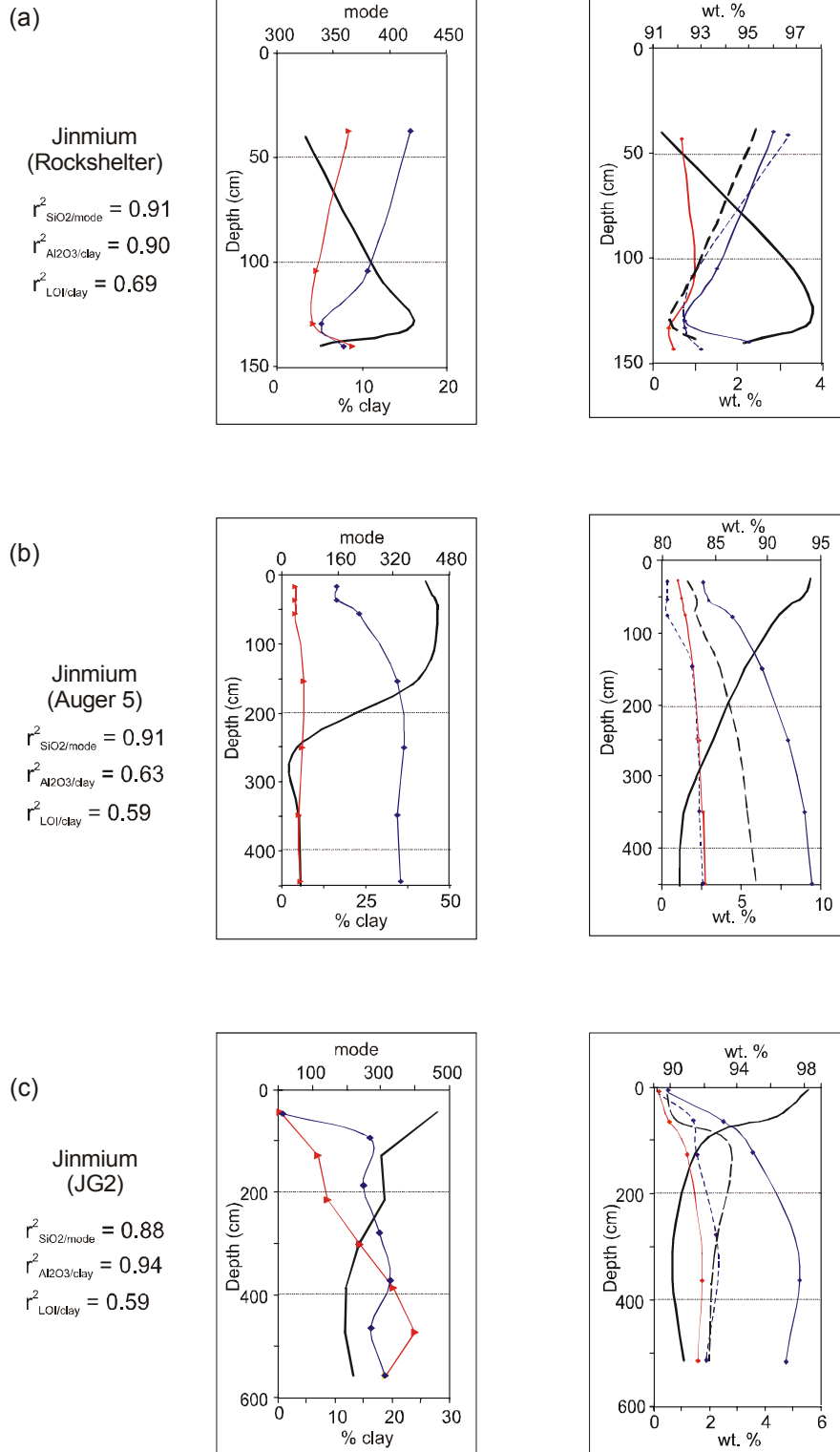


Figure A3.8 Profiles of grain size mode (black), $< 60 \mu\text{m}$ (blue) and $< 10 \mu\text{m}$ (red) and major element chemistry SiO_2 (black), Al_2O_3 (blue), K_2O (blue dashed), and LOI (black dashed) in (a) Jinmium (CI/1) rock shelter excavation and auger cores (b) Auger 5, and (c) JG-2.

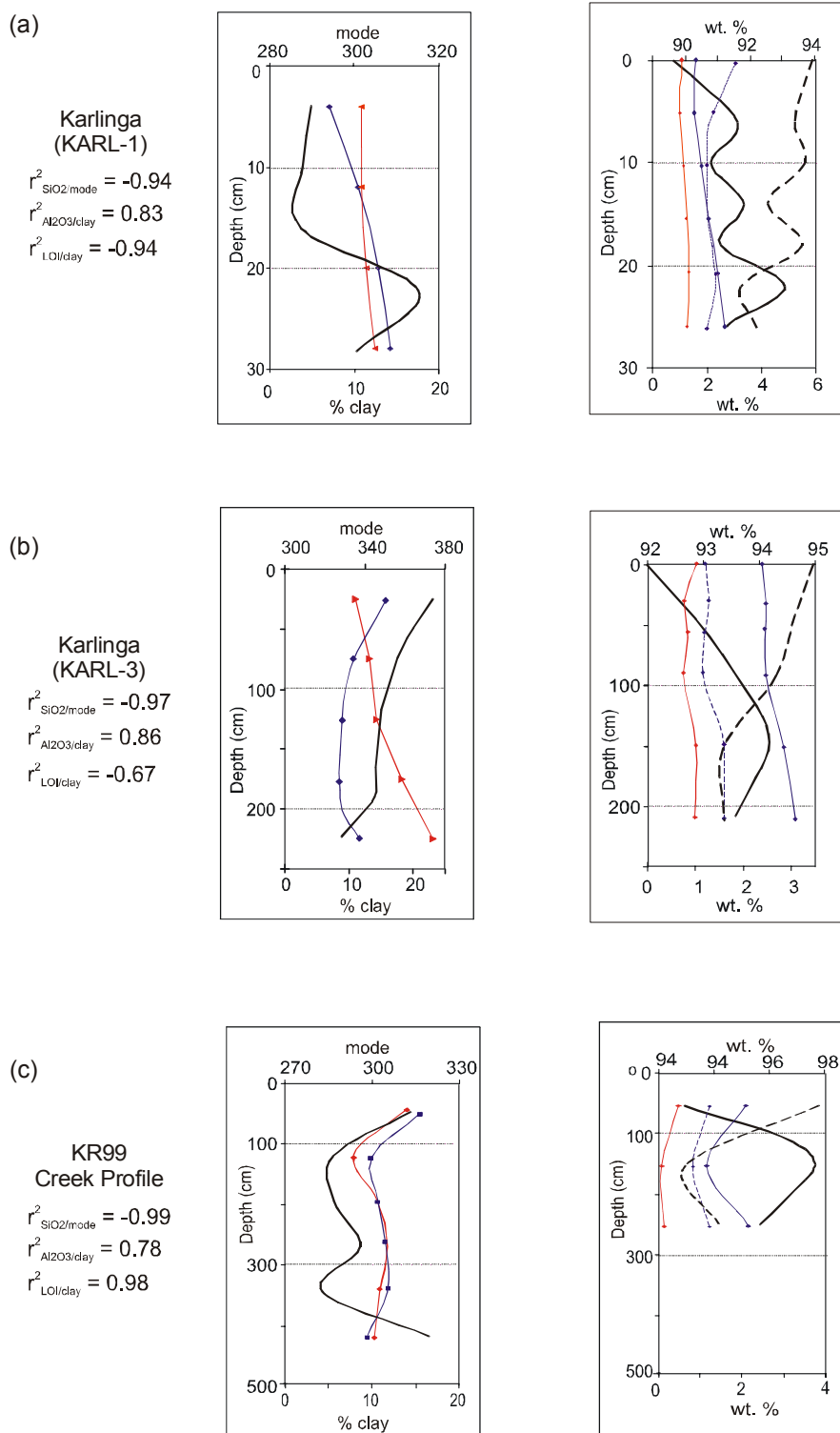


Figure A3.9 Profiles of grain size mode (black), < 60 μm (blue) and < 10 μm (red) and major element chemistry SiO_2 (black), Al_2O_3 (blue), K_2O (blue dashed), and LOI (black dashed) in the (a) Karl-1 rock shelter excavation, (b) Karl-3 sand sheet excavation, and (c) KR99 creek profile.

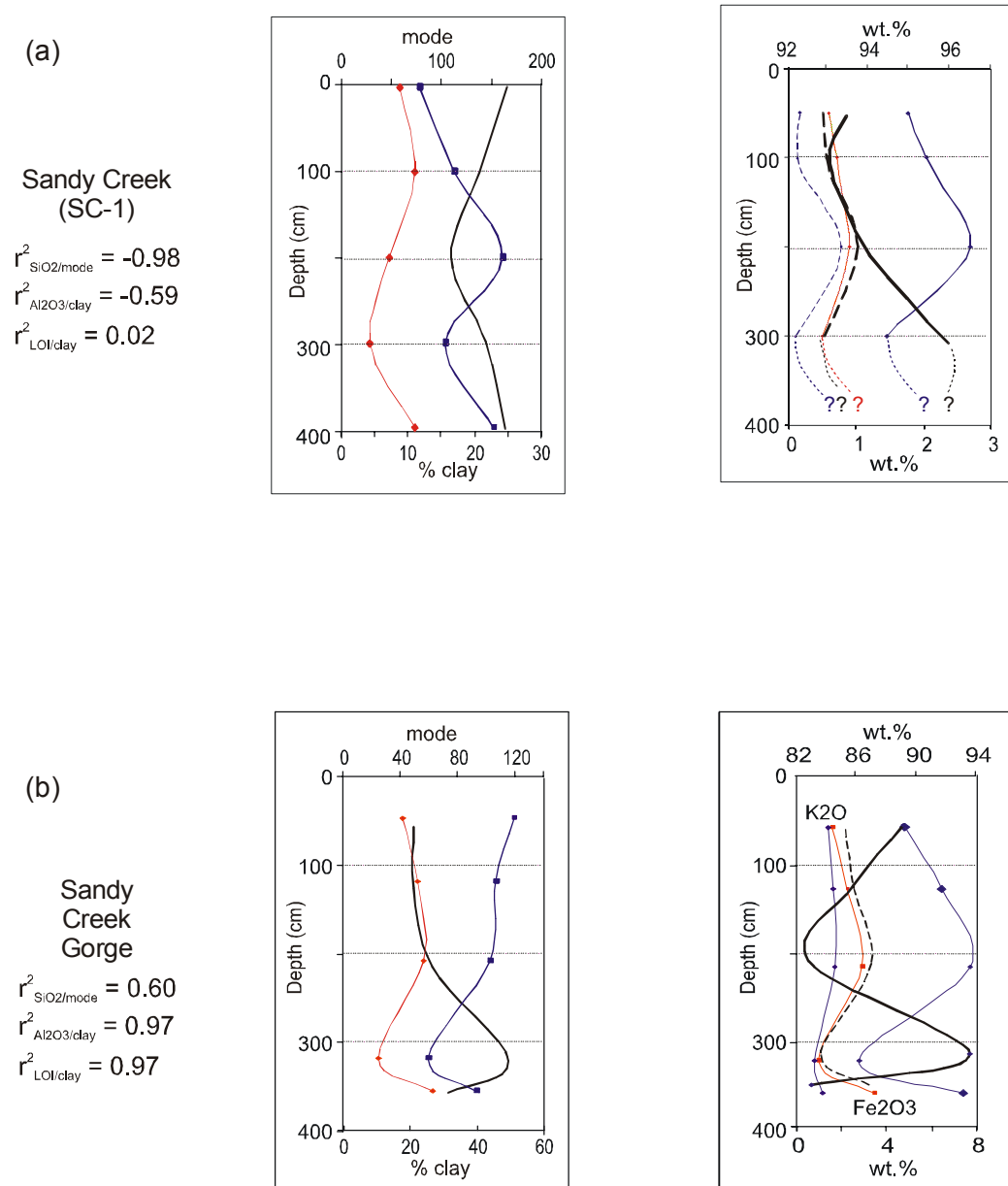


Figure A3.10 Profiles of grain size mode (black), < 60 μm (blue) and < 10 μm (red) and major element chemistry SiO_2 (black), Al_2O_3 (blue), K_2O (blue dashed), and LOI (black dashed) in the (a) auger core SC-1 and (b) Sandy Creek Gorge (SCG) creek bank profile.

APPENDIX FOUR - LUMINESCENCE DATING

A4.1 Field Sampling

Luminescence samples were collected in separate tubing, opaque polyethylene tubes were used for TL samples, and smaller steel tubes used for OSL samples to minimise light penetration. Luminescence samples were obtained from auger holes and excavation pits by gently hammering the tubes into the sections (Figure A4.1), and quickly sealing them with a cap and tape after removal. Marked samples were then sealed in black polyethylene bags to prevent light exposure, and taken back to UOW for analyses.



Figure A4.1 Collection of luminescence samples involved gently hammering a PVC or steel tube (both depicted) into the excavation pit wall.

A4.2 Thermoluminescence (TL) Determinations

Sample preparation was done under yellow (> 470 nm) light. Samples were separated into a portion for moisture content, a second for palaeodose determinations using the 90 – 125 μm quartz fraction, and the third for radionuclide analyses (U, Th and ^{40}K). The latter employed calibrated thick source alpha counting (TSAC) in the determination of the sample U and Th specific activity levels, and atomic emission spectroscopy (AES) to determine the sample potassium contents, as outlined in Fullagar et al. (1996).

TL palaeodose analyses in this study use the combined additive and regenerative method as described by Redhead (1984), and as used in the original Jinmium study (Fullagar et al., 1996). TL measurements were made using an EMI 9635QB photomultiplier fitted with a Corning 7-59 transmitting filter and a Chance Pilkington heat filter. The two principle peaks used to date the sediments comprise the more sensitive, rapidly bleached (RBP) peak at 325°C and the more stable, slowly bleached (SBP) peak at 375°C . If incomplete bleaching is suspected from the ‘plateau test’, the best measurement is found from regeneration of the RBP. Conversely, if the plateaux are foreshortened by partial exposure, as was suspected for the Jinmium rock-shelter sediments, the best measurement may be found from regeneration of the SBP. Characterisation and problems associated with the use of the SBP in luminescence dating are outlined in Huntley et al. (1995), and Bailey (2000). The validity of using the 375°C quartz peak for these samples is outlined in Price (1994a). The resultant ages are not corrected for surface residual TL, as there is no suitable analogue for this purpose. In this situation it is normal to assume that the TL level at the time of deposition is that value reached following a minimum 24 hour sample exposure beneath a laboratory ultraviolet lamp (Philips MLU 300W). This may, in some circumstances, provide an overcorrection to the age but in the present application, based upon the quality of the TL data, this affect is thought minimal (Price, written communication, 2000).

Table A4.1 Thermoluminescence (TL) results.

Jinmium-Goorurarmum									
Specimen No.	W3033	W3034	W2789	W2790	W2968	W2969	W2970	W2971	W2972
Sample Location	Goorurarmum	Goorurarmum	Goorurarmum	Goorurarmum	Jin-Goor	Jin-Goor	Jin-Goor	Jin-Goor	Jin-Goor
Sample Reference	Goor-1	Goor-1	Gu-2	Gu-8	JG1	JG2	JG2	JG4	JG4
Sample Depth (cm)	95	155	180	160	210	390	560	420	590
Plateau Region (C)	350-500	300-500	300-500	300-500	300-500	300-500	300-500	300-500	300-500
Analysis Temp. (C)	375	375	375	375	375	375	375	375	375
Palaeodose (Grays)	23.7+/-2.2	5.9+/-1.0	11.1+/-0.9	15.8+/-1.5	22.4+/-1.9	49.3+/-4.3	84.7+/-6.1	40.7+/-2.9	93.2+/-8.0
K content (%)	0.245+/-0.005	0.175+/-0.005	0.165+/-0.005	0.175+/-0.005	0.235+/-0.005	0.195+/-0.005	0.170+/-0.005	0.235+/-0.005	0.265+/-0.005
Rb content (ppm assumed)	50+/-25	50+/-25	50+/-25	50+/-25	50+/-25	50+/-25	50+/-25	50+/-25	50+/-25
Moisture content (% by weight)	4.0+/-3	1.3+/-3	3.4+/-3	14.8+/-3	5.7+/-3	7.2+/-3	12.8+/-3	10.8+/-3	9.3+/-3
Specific Activity (Bq/kg U+Th)	40.0+/-1.3	30.7+/-0.8	44.7+/-1.3	28.5+/-0.9	54.2+/-1.5	47.4+/-1.1	47.5+/-1.4	39.4+/-1.1	49.2+/-1.4
Cosmic Contribution (uGy/yr assumed)	185+/-25	150+/-25	150+/-25	150+/-25	150+/-25	128+/-25	113+/-25	126+/-25	110+/-25
Annual Radiation Dose (uGy/yr)	1220+/-30	962+/-28	1206+/-31	795+/-25	1428+/-31	1216+/-28	1112+/-29	1053+/-27	1275+/-29
TL age (ka)	19.4+/-1.9	6.1+/-1.0	9.2+/-0.8	19.9+/-1.9	15.7+/-1.4	40.5+/-3.7	76.1+/-5.8	38.7+/-2.9	73.1+/-6.5
				18.0+/-1.7*					
Karlinga									
Specimen No.	W2791	W2792	W2793	W2973	W2974	W2975	W2976		
Sample Location	Karlinga	Karlinga	Karlinga	Karlinga	Karlinga	Karlinga	Karlinga		
Sample Reference	Ka-2	Ka-4	Ka-4	KN2	KN3	KN3	KN4		
Sample Depth (cm)	235	200	360	100	145	230	115		
Plateau Region (C)	300-500	300-500	300-500	300-500	300-500	300-500	300-500		
Analysis Temp. (C)	375	375	375	375	375	375	375		
Palaeodose (Grays)	9.1+/-0.9	6.3+/-0.5	27.5+/-2.8	4.2+/-0.4	7.4+/-0.6	15+/-2.0	6.0+/-0.5		
K content (%)	0.105+/-0.005	0.105+/-0.005	0.190+/-0.005	0.130+/-0.005	0.115+/-0.005	0.130+/-0.005	0.110+/-0.005		
Rb content (ppm assumed)	50+/-25	50+/-25	50+/-25	50+/-25	50+/-25	50+/-25	50+/-25		
Moisture content (% by weight)	1.4+/-3	1.1+/-3	13+/-3	3.5+/-3	4.5+/-3	11.6+/-3	1.3+/-3		
Specific Activity (Bq/kg U+Th)	34.9+/-1.1	39.9+/-1.2	87.5+/-2.0	32.3+/-0.9	38.3+/-1.1	50.4+/-1.2	38.5+/-1.2		
Cosmic Contribution (uGy/yr assumed)	146+/-25	150+/-25	129+/-25	185+/-25	170+/-25	147+/-25	180+/-25		
Annual Radiation Dose (uGy/yr)	968+/-30	1075+/-31	1856+/-34	956+/-28	1034+/-29	1171+/-27	1081+/-30		
TL age (ka)	9.4+/-1.0	5.8+/-0.5	14.8+/-1.5	4.4+/-0.4	7.1+/-0.6	12.8+/-1.7	5.6+/-0.5		
			13.6+/-1.4*						
Specimen No.	W3035	W3036	W3037	W3038	W3039	W3040	W3041		W2788
Sample Location	Karlinga	Karlinga	Karlinga	Karlinga	Karlinga	Karlinga Ck.	Karlinga Ck.		Graniipi
Sample Reference	Karl-3	Karl-3	Karl-3	Karl-3	Karl-3	KR99CP	KR99CP		Gr-1
Sample Depth (cm)	30	60	120	180	240	95	175		90
Plateau Region (C)	300-500	300-500	300-500	300-500	300-500	300-500	300-500		300-500
Analysis Temp. (C)	375	375	375	375	375	375	375		375
Palaeodose (Grays)	6.0+/-0.5	3.1+/-0.3	8.1+/-0.7	13.4+/-1.3	17.6+/-0.5	6.8+/-0.6	13.9+/-1.6		2+/-0.3
K content (%)	4.0+/-0.5	0.205+/-0.005	0.255+/-0.005	0.220+/-0.005	0.265+/-0.005	0.135+/-0.005	0.145+/-0.005		0.110+/-0.005
Rb content (ppm assumed)	50+/-25	50+/-25	50+/-25	50+/-25	50+/-25	50+/-25	50+/-25		50+/-25
Moisture content (% by weight)	1.5+/-3	1.7+/-3	2.8+/-3	2.9+/-3	10.9+/-3	0.1+/-3	0.0+/-3		1.4+/-3
Specific Activity (Bq/kg U+Th)	30.3+/-0.9	52.5+/-1.6	45.4+/-1.1	41.5+/-1.1	49.9+/-1.0	25.3+/-0.8	49.9+/-1.0		29.7+/-0.9
Cosmic Contribution (uGy/yr assumed)	185+/-25	185+/-25	150+/-25	150+/-25	146+/-25	185+/-25	150+/-25		185+/-25
Annual Radiation Dose (uGy/yr)	1055+/-29	1464+/-25	1291+/-29	1206+/-29	1297+/-26	857+/-28	1338+/-33		908+/-29
TL age (ka)	3.8+/-0.5	2.1+/-0.2	6.2+/-0.5	11.1+/-1.1	13.6+/-1.1	7.9+/-0.7	10.4+/-1.3		2.2+/-0.3
Sandy Creek									
Specimen No.	W2977	W2977	W2977	W2977	W3044	W3045	W3046	W3047	W3047
Sample Location	Sandy Creek	Sandy Creek	Sandy Creek	Sandy Creek	Sandy Creek	Sandy Creek	Sandy Creek	Sandy Creek	Sandy Creek
Sample Reference	SC1	SC1	SC2	SC3	Gorge	Gorge	Gorge	Gorge	Gorge
Sample Depth (cm)	55	200	200	200	SCG	SCG	SCG	SCG	SCG
Plateau Region (C)	stepped	stepped	stepped	stepped	stepped	stepped	stepped	stepped	stepped
Analysis Temp. (C)	325 (a)	325 (a)	325 (a)	375	325	325	325	325	375
	375 (b)	375 (b)	375 (b)						
Palaeodose (Grays)	4.1+/-0.4 (a)	5.7+/-0.6 (a)	8.7+/-0.8 (a)	10.6+/-0.8	3.0+/-0.2	10.5+/-1.1(a)	22.7+/-1.8	16.8+/-1.4 (a)	27.0+/-2.1
	6.8+/-0.6 (b)	14.1+/-1.6 (b)	10.9+/-0.8 (b)			13.3+/-1.3(b)		21.5+/-1.8 (b)	
K content (%)	0.330+/-0.005	0.600+/-0.005	0.500+/-0.005	0.550+/-0.005	1.50+/-0.05	1.70+/-0.05	1.50+/-0.05	0.85+/-0.05	1.30+/-0.05
Rb content (ppm assumed)	50+/-25	50+/-25	50+/-25	50+/-25	100+/-25	100+/-25	100+/-25	100+/-25	100+/-25
Moisture content (% by weight)	2.9+/-3	7.1+/-3	13.9+/-3	12.0+/-3	3.2+/-3	8.1+/-3	9.7+/-3	12.6+/-3	8.2+/-3
Specific Activity (Bq/kg U+Th)	30.1+/-0.9	43.2+/-1.3	46.5+/-1.5	45.5+/-1.5	78.7+/-2.4	87.6+/-2.7	94.2+/-1.7	49.3+/-1.4	90.7+/-2.8
Cosmic Contribution (uGy/yr assumed)	185+/-25	150+/-25	150+/-25	150+/-25	185+/-25	150+/-25	150+/-25	140+/-25	131+/-25
Annual Radiation Dose (uGy/yr)	1138+/-28 (a)	1574+/-29 (a)	1431+/-29 (a)	1477+/-27	1333+/-25	3469+/-65	3652+/-58	1817+/-55	3113+/-66
	1130+/-28 (b)	1564+/-29 (b)	1421+/-29 (b)						
TL age (ka)	3.6+/-0.4 (a)	3.6+/-0.4 (a)	6.0+/-0.5 (a)	7.2+/-0.5	2.25+/-0.5	3.0+/-0.3 (a)	6.2+/-0.5	9.2+/-0.8 (a)	8.7+/-0.7
	6.0+/-0.5 (b)	9.0+/-1.0 (b)	7.6+/-0.6 (b)			3.8+/-0.4 (b)		11.8 +/-1.0 (b)	

A4.3 Optically Stimulated Luminescence (OSL) Determinations

A4.3.1 Preparatory grain-size size separation and grain-mounting

All sample preparations were done under red (> 590 nm) light. Samples were divided into three portions: one for grain size, porosity and moisture content, the second for palaeodose determinations, and the third for radionuclide analyses (α , U/Th and ^{40}K). Grains of 90-125 μm were separated by wet-sieving to afford direct comparison with TL ages of the same size fraction. Heavy liquid separation ($> 2.7 \text{ g cm}^{-3}$) was not undertaken, due to the paucity of heavy minerals ($< 2 \%$), and minimal influence on age determinations as outlined by Roberts et al. (1999). Similarly mineralogical analyses (XRD) indicate the virtual absence of feldspar, and are supported by IR tests on all samples (refer below). HF digestions remove outer rind of the quartz, and most residual silicate minerals (clay minerals and feldspars). Grains were mounted on 10 mm stainless-steel discs, using a silicon oil spray with single-aliquot using ~ 1 mg (~ 800 grains). All runs are done using 3 mm masks, except the two final SAR runs which use a 1 mm mask.

A4.3.2 Palaeodose Determinations

A sequence of runs were made on most samples, which comprised an IR check for feldspars (Figure A3.2), a multiple-aliquot run (MAR) before and after sun bleaching (24 aliquots), a single-aliquot preheat plateau test (24 aliquots), and two single-aliquot runs (SAR) using a single calculated regenerative dose.

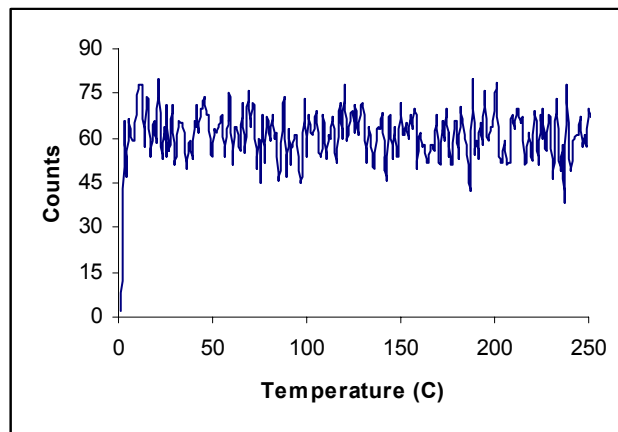


Figure A4.2 Typical IR test result indicating no presence of peaks that would otherwise result from feldspar or heavy mineral contamination.

Multiple-aliquot Regenerative Protocol (SARA)

The multiple-aliquot protocol SARA (single aliquot regeneration and added dose) of Mejdahl and Bøtter-Jensen (1994) involves the application of up to 5 different beta doses to each of 4 aliquots on top of the natural radiation dose prior to regeneration. A graph of regeneration equivalent dose (D_e) against the amount of radiation dose added (Gy) is plotted, and a regression line is extrapolated back to the x-axis to estimate the true equivalent dose.

1. Optical stimulation of the natural aliquot for 0.1 sec, held at 125 °C.
2. Application of regenerative doses (D_{1-5}) for 44 s at 220 °C
3. Optical stimulation of the regenerative doses (D_{1-5}) for 100 s, held at 125 °C.

Where growth is non-linear, the shape of the curve is estimated by repeating the same procedure after bleaching in sunlight for a minimum of 2 hours (after which the curve should pass through the origin). The slope of the curve indicates sensitivity change during analysis, such that a slope > 1 indicates decreased sensitivity and < 1 indicates increased sensitivity.

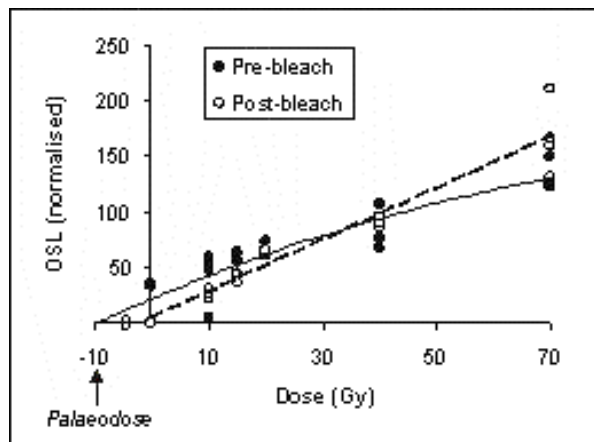


Figure A4.3 Example of MARA plot (KARL-1-27), before and after sun bleaching, showing extrapolation of curve back to x-axis to estimate true palaeodose.

Single-aliquot Regenerative Protocol (SAR)

Single-aliquot and single-grain palaeodoses were estimated using the single-aliquot regenerative-dose (SAR) protocol first suggested by Murray and Roberts (1998), and modified by Murray and Wintle (2000). The following is an outline of the SAR protocol used in this study, and full details are provided in the original papers.

- 1a. A 'preheat plateau' test is made by preheating of the 'natural' aliquot (or grain) at temperatures of 160-280 °C for 10 s, with temperature increasing in 20 °C steps, followed by cooling to < 60 °C.
- 1b. Once the optimal temperature has been estimated, a single temperature may be used.
2. Optical stimulation of the natural aliquot (or grain) for 100-125 s, held at 125 °C (to produce the L_N series).

A preheat allows the meaningful comparison of a natural signal with one or more induced by laboratory irradiation, by ensuring that the signals are obtained from the same stable source trap

(i.e. stable over the geological or archaeological period of interest), with minimal contamination from shallow traps. The responses of the shallow 110 °C TL peak and the OSL signal are used to monitor the sensitivity changes in the OSL signal caused by preheating, the details of which are outlined by Murray and Roberts (1998) and Wintle and Murray (1999). In the SAR protocol proposed by Murray and Wintle (2000), the OSL rather than the 110 °C TL peak is used to correct for changes in luminescence sensitivity.

3. Application of a test-dose (0.1 - 1 Gy), followed by a cut heat to 160 °C.
4. Optical stimulation of the test-dose, again for 100-125 s at 125 °C (to produce the T_N series).

Note the palaeodose has been shown to be relatively insensitive to the size of the test dose, whilst the degree of recuperation is small even at test doses up to 12 times D_E (Murray and Wintle, 2000).

5. Application of the regenerative dose (R_1), of the same order as L_N , followed by the same preheat as in step 1.
6. Optical stimulation of the regenerative dose (D_1) for 100-125 s at 125 °C.
7. Application of a second test-dose (T_2), the same as step 3, followed by a cut heat to 160 °C.
8. Optical stimulation of the test-dose for 100-125 s at 125 °C (to produce the T_R series).

Steps 1 – 8 are adequate when L_N lies in the initial linear region of the OSL dose-response curve, but may need modification when L_N lies in the non-linear region (Galbraith et al., 1999). This follows the argument of Folz and Mercier (1999) that the measured palaeodose agrees well with the known value if the main regeneration dose is within 10 % of the true palaeodose. In the case of non-linear response, the same grains are put through another cycle of irradiation,

preheat and measurement (i.e. using steps 5 – 12) using regenerative doses which bracket the natural dose ($R_1 < N < R_2 < R_1$).

9. Application of a second regenerative dose (D_2), the same as step 5, followed by the same preheat.
10. Optical stimulation of the regenerative dose for 100-125 s at 125 °C.
11. Application of a third test-dose (T_3), the same as step 3, followed by a cut heat to 160 °C.
12. Optical stimulation of the test-dose for 100-125 s at 125 °C.

The repeat regeneration dose ('double-regenerative' dose) provides a regenerated OSL response, with which the natural OSL can be compared, and is a check for repeatability (i.e. R_2/R_1). It also allows a check on the assumption that the test-dose OSL signals should mimic the behaviour of the regenerative dose OSL signals (i.e. no change in sensitivity). Sensitivity change during stimulation does not affect the determination of D_E because changes of the natural and regenerated signals are similar (Murray and Wintle, 2000).

Radial Plots

Radial plots (Figure A4.4) are used to graphically display estimates of palaeodose determined using the SAR protocol outlined above. A full description of the radial plot is detailed in Galbraith et al. (1999), and a summary is given here.

In the radial plot, the y-axis displays the length of a 'two sigma' error bar, and the x-axis displays the precision and relative standard error. In Figure A4.4, the palaeodose estimate of 52.3 Gy has a standard error of 2.5%, and the second estimate of 38.7 Gy has an error of 5% but has a lower precision. If the individual estimates are consistent with a common dose,

ideally about 95% of the points should fall within a single radial band. Roberts et al. (1999) indicate that a relative standard deviation of $\pm 15 - 30\%$ about the mean palaeodose may be a more realistic guide of dispersion in a natural sample. If the data arise from two distinct populations, then the points should fall mainly within two such radial bands (Roberts et al., 1999).

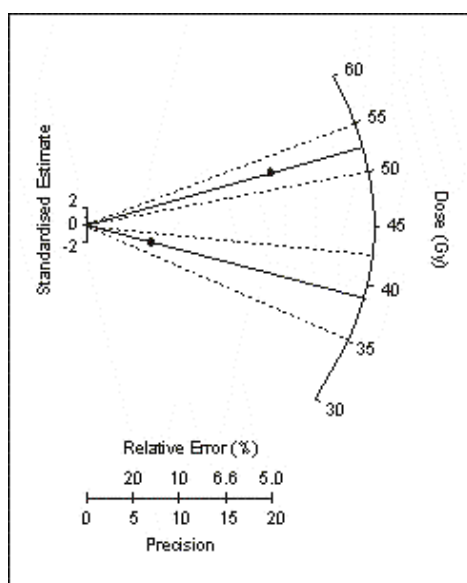


Figure A4.4 Illustration of a radial plot with two hypothetical points that have different palaeodoses and associated uncertainties (from Galbraith et al., 1999: 356).

A.4.3.3 OS� Results

Table A4.2 provides a summary of all 16 OS� analyses. Summary diagrams for all samples (Figures A4.5 – 4.20), including:

- (a) MARA test,
- (b) preheat plateau test,
- (c) sensitivity test, and
- (d) double-regeneration test, and

tabulated results for (e) SAR analyses, are given below.

Table A4.2 Summary of OSL analyses.

Specimen No.	1	2	3	4	5	
Sample Location	Karlinga	Karlinga	Karlinga	Karlinga	Karlinga	
Sample Reference	KARL-1	KARL-3	KARL-3	KARL-3	KARL-3	
Sample Depth (cm)	27	90	150	210	240	
Plateau Region (C)	160-280	160-300	160-260	160-260	160-260	
Analysis Temp. (C)	240	220	240	220	240	
Palaeodose (Grays)						
Mean	19.42+/-0.651	3.85+/-0.245	11.60+/-0.553	24.84+/-0.733	29.5+/-1.35	
Central Age	19.65+/-0.271	3.48+/-0.051	11.44+/-0.178	24.24+/-0.276	23.40+/-0.549	
Full growth curve	21.5+/-7.23	nd	nd	26.1+/-7.01	29.5+/-6.49	
Minimum	7.80	0.14	7.91	12.85	19.20	
n samples	69	45	46	70	24	
K content (%)	0.18+/-0.04	0.120+/-0.005	0.160+/-0.005	0.160+/-0.005	0.265+/-0.005	
40K (Bq/kg)	8.03 +/- 2.33	4.49 +/- 1.01	5.21 +/- 1.1	2.42 +/- 0.95	nd	
Moisture content	5+/-3	5+/-3	5+/-3	5+/-3	10+/-3	
(% by weight)						
Specific Activity	(a) 46.5+/-1.42	(a) 29.1+/-0.28	(a) 30.7+/-0.31	(a) 32.7+/-0.19	nd	
(Bq/kg U+Th)	nd	(b) 49.0+/-1.9	(b) 43.4+/-1.6	(b) 45.7+/-1.52	(b) 49.9+/-1.0	
Cosmic Contribution	180+/-25	180+/-25	150+/-25	150+/-25	146+/-25	
(uGy/yr assumed)						
Annual Radiation Dose	(a) 0.79+/- 0.04	(a) 0.73+/- 0.04	(a) 0.77+/-0.04	(a) 0.78+/- 0.04	nd	
(Gy/yr)	nd	(b) 1.38+/-0.04	(b) 1.25+/-0.034	(b) 1.25+/-0.04	(b) 1.29+/-0.03	
(a) Central Age (ka)	25.10+/-1.48	(a) 4.80+/-0.29	(a) 14.80+/-0.87	(a) 31.18+/-1.72	nd	
(b) TSAC Age (ka)	nd	(b) 2.53+/-0.08	(b) 9.13+/-0.29	(b) 19.36+/-0.64	18.04+/-0.56	
Specimen No.	6	7	8	9	10	
Sample Location	Goorurarmum	Goorurarmum	Goorurarmum	Goorurarmum	Goorurarmum	
Sample Reference	GOOR-2	GOOR-1	GOOR-1	GOOR-1	GOOR-1	
Sample Depth (cm)	20	50	100	175	220	
Plateau Region (C)	160-300	nd	nd	stepped	160-280	
Analysis Temp. (C)	240	240	nd	220	220	
Palaeodose (Grays)						
Mean	0.37+/-0.016	1.39+/-0.114	3.27+/-0.168	6.47+/-0.453	18.12+/-0.63	
Central Age	0.36+/-0.009	1.34+/-0.026	3.09+/-0.046	5.21+/-0.08	17.22+/-0.225	
Minimum	0.13	0.62	1.16	0.23	11.50	
n samples	48	48	45	44	59	
K content (%)	0.18+/-0.05	0.100+/-0.005	0.100+/-0.005	0.090+/-0.005	0.150+/-0.005	
40K (Bq/kg)	7.86+/-1.11	nd	nd	nd	2.72+/-2.49	
Moisture content	5+/-3*	5+/-3*	5+/-3*	5+/-3*	5+/-3*	
(% by weight)						
Specific Activity	(a) 29.9+/-0.57	nd	nd	nd	(a) 29.4+/-1.27	
(Bq/kg U+Th)		(b) 40.0+/-1.3	(b) 40.0+/-1.3	(b) 44.7+/-1.3	(b) nd	
Cosmic Contribution	180+/-25	180+/-25	150+/-25	150+/-25	150+/-25	
(uGy/yr assumed)						
Annual Radiation Dose	(a) 0.76+/-0.04	nd	nd	nd	(a) 0.73+/-0.06	
(uGy/yr)		(b) 1.22+/-0.03	(b) 1.22+/-0.03	(b) 1.21+/-0.03	(b) 1.21+/-0.03	
(a) Central Age (ka)	(a) 0.53+/-0.14	nd	nd	nd	(a) 23.7+/-2.06	
(b) TSAC Age (ka)	nd	(b) 1.10+/-0.03	(b) 2.53+/-0.07	(b) 4.32+/-0.13	(b) 14.28+/-0.41	
Specimen No.	11	12	13	14	15	16
Sample Location	Sandy Ck. Gorge	Sandy Ck. Gorge	Sandy Ck. Gorge	Sandy Ck. Gorge	Karlinga	Karlinga
Sample Reference	SCG	SCG	SCG	SCG	KR99CP	KR99CP
Sample Depth (cm)	57	126	321	357	95	320
Plateau Region (C)	stepped	stepped	stepped	nd		
Analysis Temp. (C)	240	220	240	nd	220	220
Palaeodose (Grays)						
Mean	4.30+/-0.179	15.92+/-0.178	24.80+/-0.617	43.89+/-1.262	14.46+/-0.155	16.2+/-0.217
Central Age	4.17+/-0.058	15.84+/-0.216	24.51+/-0.302	43.18+/-0.590	14.44+/-0.279	16.17+/-0.315
Full growth curve	nd	nd	25.1+/-4.22	46.0+/-5.19	13.29	14.58
Minimum	2.46	12.58	19.40	31.05	23	23
n samples	47	48	60	46	0.135+/-0.005	0.165+/-0.005
K content (%)	1.4+/-0.005	1.63+/-0.005	0.76+/-0.005	1.17+/-0.005	50+/-25	50+/-25
40K (Bq/kg)	56.7+/-1.61	68.2+/-1.80	48.0+/-1.09	58.2+/-9.61		
Moisture content	5+/-3*	5+/-3*	5+/-3*	5+/-3*	5+/-3*	5+/-3*
(% by weight)						
Specific Activity	(a) 60.9+/-0.21	(a) 66.0+/-0.17	(a) 70.9+/-0.18	nd	(a) nd	(a) nd
(Bq/kg U+Th)	(b) 78.7+/-2.4	(b) 87.6+/-2.7	(b) 94.2+/-1.7	(b) 49.3+/-1.4	(b) 25.3+/-0.8	(b) 80.0+/-2.4
Cosmic Contribution	185+/-25	150+/-25	140+/-25	140+/-25	180+/-25	140+/-25
(uGy/yr assumed)						
Annual Radiation Dose	(a) 1.43+/-0.05	(a) 1.56+/-0.05	(a) 1.46+/-0.05	nd	(a) nd	(a) nd
(uGy/yr)	(b) 1.33+/-0.03	(b) 3.49+/-0.07	(b) 1.83+/-0.06	(b) 3.11+/-0.07	(b) 857+/-28	(b) 1885+/-42
(a) Central Age (ka)	(a) 2.94+/-0.12	(a) 10.16+/-0.39	(a) 16.80+/-0.65	nd	nd	nd
(b) TSAC Age (ka)	(b) 3.13+/-0.07	(b) 4.54+/-0.11	(b) 13.41+/-0.44	(b) 13.87+/-0.35	(b) 16.85+/-0.640	(b) 8.58+/-0.254

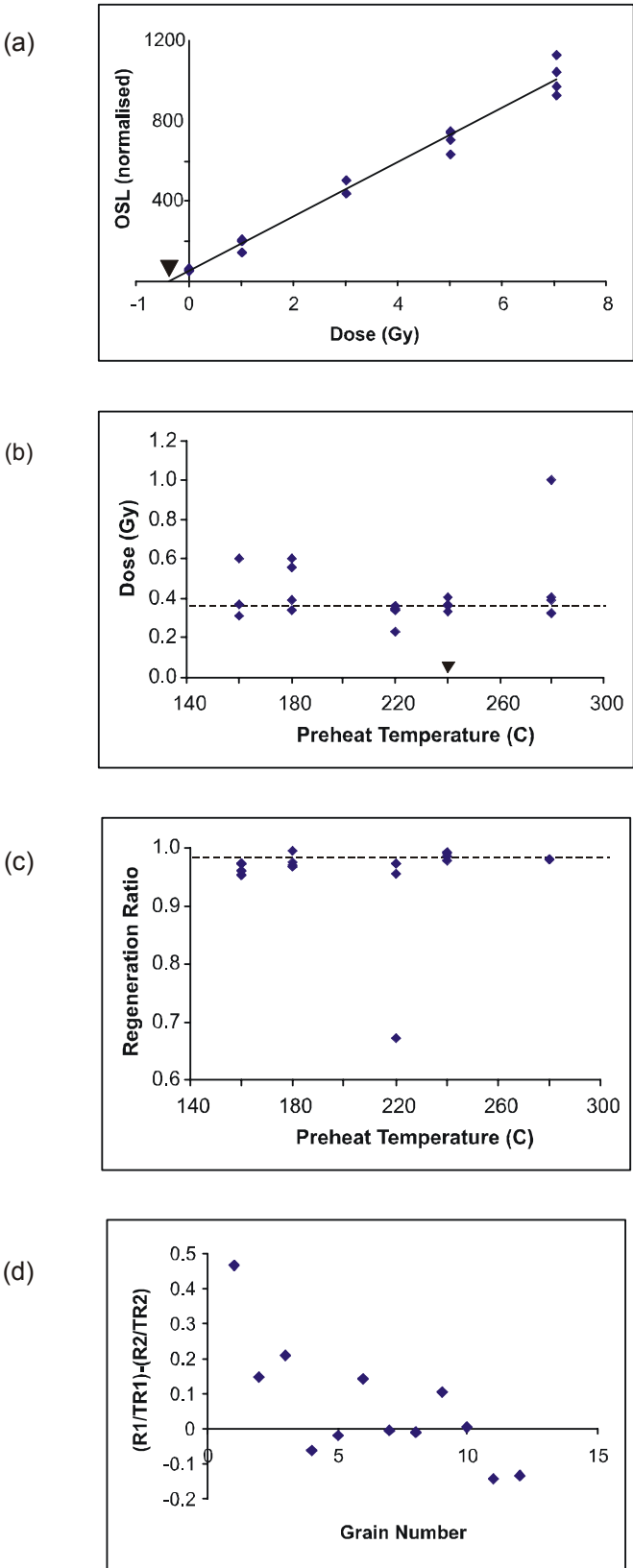


Figure A4.5 OSL results for Goor-2 rock shelter excavation at 20 cm, including: (a) MARA test, (b) preheat plateau test, (c) sensitivity test, and (d) double-regenerative test. Table A4.3 SAR analyses for Goor-2 rock shelter excavation at 20 cm.

Table A4.3 SAR analyses for Goorurarmum rock shelter (Goor-2) excavation.

wt028r1.DAT

goor-2-20, 1mm mask, Dose = 0.1/0.4Gy (2/9 sec)

DOSE RATE (Gy/min) : 2.547

used acquisition (ch) : 1 (1)-> 25 (25)residue (ch) : 226 (226)-> 250 (250)

No.	Nat.(1st)	Natural	Test N	Regen.	Test R	Tr/Tn	Err	Beta (Gy)	PD (Gy)	Err	(%)
1	226	2187	749	2598	533	0.71	0.107	0.382	0.23	0.036	15.7
2	310	3859	1055	4440	1017	0.96	0.090	0.382	0.32	0.032	9.8
3	324	3975	1118	4141	932	0.83	0.079	0.382	0.31	0.030	10.0
4	350	4477	1188	5066	1207	1.02	0.083	0.382	0.34	0.029	8.6
5	310	3781	1305	5190	1217	0.93	0.073	0.382	0.26	0.022	8.4
6	172	2005	363	1885	449	1.24	0.276	0.382	0.50	0.115	22.9
7	261	2784	701	3032	750	1.07	0.138	0.382	0.38	0.050	13.4
8	235	2124	633	2144	637	1.01	0.145	0.382	0.38	0.058	15.3
9	189	1827	398	2014	385	0.97	0.221	0.382	0.34	0.079	23.5
10	318	4045	1220	4777	1136	0.93	0.078	0.382	0.30	0.027	8.8
11	256	2684	874	3437	870	1.00	0.107	0.382	0.30	0.034	11.4
12	242	2410	559	2575	613	1.10	0.172	0.382	0.39	0.064	16.3
13	218	2015	404	2218	465	1.15	0.241	0.382	0.40	0.086	21.5
14	140	1292	280	1338	445	1.59	0.422	0.382	0.59	0.162	27.6
15	217	2208	584	2343	433	0.74	0.135	0.382	0.27	0.050	18.7
16	254	2437	483	2862	698	1.45	0.234	0.382	0.47	0.079	16.8
17	239	2522	680	2321	478	0.70	0.117	0.382	0.29	0.050	17.2
18	226	2838	887	2945	753	0.85	0.097	0.382	0.31	0.038	12.1
19	450	5580	1347	5447	1418	1.05	0.078	0.382	0.41	0.032	7.8
20	185	1792	471	1879	478	1.01	0.198	0.382	0.37	0.075	20.3
21	253	2777	699	2601	713	1.02	0.132	0.382	0.42	0.056	13.6
22	175	1522	449	1639	374	0.83	0.180	0.382	0.30	0.067	22.5
23	318	3883	946	4664	1086	1.15	0.108	0.382	0.37	0.036	9.9
24	220	1901	469	2120	667	1.42	0.233	0.382	0.49	0.084	17.1
1	366	3979	1005	4108	1111	1.11	0.100	0.382	0.41	0.039	9.6
2	315	3396	707	3585	856	1.21	0.148	0.382	0.44	0.056	12.7
3	276	3246	891	3674	1017	1.14	0.115	0.382	0.39	0.041	10.6
4	333	3754	1022	4344	1223	1.20	0.106	0.382	0.40	0.037	9.4
5	300	3663	916	3893	1050	1.15	0.112	0.382	0.41	0.042	10.3
6	245	2417	648	2848	527	0.81	0.130	0.382	0.26	0.044	16.6
7	288	3106	731	2868	783	1.07	0.134	0.382	0.44	0.058	13.1
8	134	1023	353	1238	294	0.83	0.231	0.382	0.26	0.077	29.1
9	176	1779	393	1895	433	1.10	0.241	0.382	0.40	0.089	22.6
10	304	2403	655	2691	546	0.83	0.129	0.382	0.28	0.046	16.1
11	428	4147	622	2735	431	0.69	0.127	0.382	0.40	0.075	18.7
12	338	3866	1166	4138	941	0.81	0.075	0.382	0.29	0.028	9.8
13	266	2858	945	3085	729	0.77	0.089	0.382	0.27	0.033	12.2
14	261	3018	648	2544	736	1.14	0.152	0.382	0.52	0.072	14.0
15	284	2790	700	2865	784	1.12	0.139	0.382	0.42	0.054	13.0
16	178	1512	500	1930	421	0.84	0.165	0.382	0.25	0.052	20.5
17	130	940	223	954	207	0.93	0.383	0.382	0.35	0.148	42.4
18	231	1833	592	1931	430	0.73	0.135	0.382	0.26	0.051	19.4
19	215	2217	558	2613	665	1.19	0.183	0.382	0.39	0.062	16.0
20	331	3699	894	3691	1003	1.12	0.115	0.382	0.43	0.046	10.8
21	382	4042	929	3961	817	0.88	0.096	0.382	0.34	0.039	11.3
22	575	7495	819	4471	1101	1.34	0.140	0.382	0.86	0.092	10.7
23	158	1335	493	1427	182	0.37	0.135	0.382	0.13	0.049	37.2
24	213	2073	387	1861	492	1.27	0.261	0.382	0.54	0.115	21.2
Ave.	267	2865	722	2980	719	1.01	0.154		0.37	0.059	16.2
Stdev.	86.0	1226.3	282.6	1137.3	300.6	0.225	0.0751		0.114	0.0300	7.25

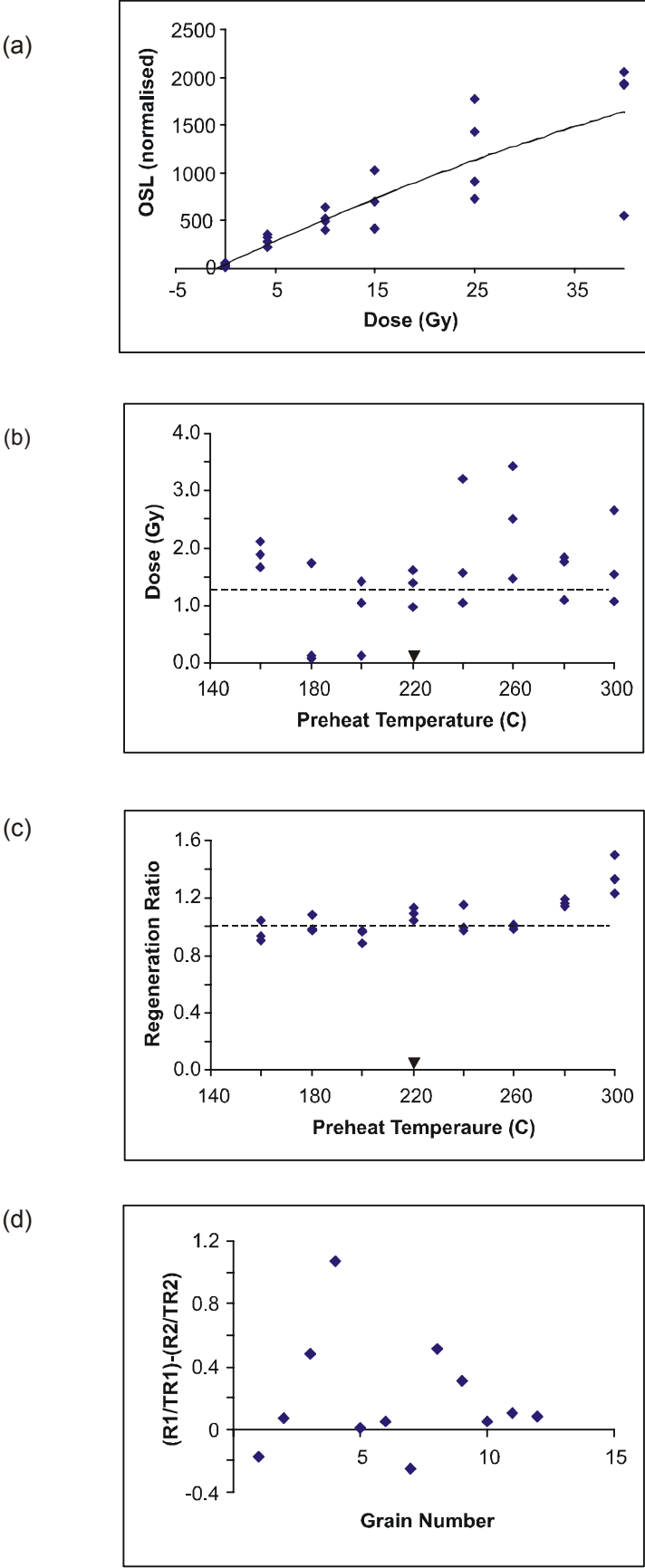


Figure A4.6 OSL results for Goor-1 sand sheet excavation at 50 cm, including: (a) MARA test, (b) preheat plateau test, (c) sensitivity test, and (d) double-regenerative test.

Table A4.4 SAR analyses for Goorurarmum sand sheet excavation (Goor-1) at 50 cm.

wt030r1 and wt030r2.DAT

goor-1-50, 1 mm mask, Dose = 0.5/2 Gy (12/48 sec)

DOSE RATE (Gy/min) : 2.547

used acquisition (ch) : 1 (1)-> 25 (25)residue (ch) : 226 (226)-> 250 (250)

No.	Nat.(1st)	Natural	Test N	Regen.	Test R	Tr/Tn	Err	Beta (Gy)	PD (Gy)	Err	(%)
1	120	253.5	135.6	433	119.4	0.8806	0.2886	1.951	1.006	0.059	3.7
2	479	1949.1	858.6	3237.2	843.3	0.9822	0.0652	1.951	1.154	0.143	5
3	250	892.7	121.3	412.3	112.7	0.9284	0.3312	1.951	3.921	0.197	4.2
4	117	235.8	138.3	440.5	121.1	0.8755	0.2788	1.951	0.914	0.137	8.8
5	190	533.1	323.5	1291.8	366.9	1.1344	0.1509	1.951	0.913	0.124	8.3
6	105	171.1	98.5	481.4	115.1	1.1678	0.4502	1.951	0.81	0.117	8.3
7	298	1016.8	377.1	1471.9	368.4	0.977	0.1225	1.951	1.317	0.066	6.8
8	145	364.2	214.2	861.7	255.1	1.1911	0.2219	1.951	0.982	0.095	3.9
9	294	1058.5	217.6	813	184.9	0.8499	0.1813	1.951	2.159	0.06	7.5
10	191	481.7	196	646.5	207.2	1.0573	0.2212	1.951	1.537	0.154	7.7
11	340	1322.7	468.5	1878.4	517.2	1.1039	0.1103	1.951	1.517	0.044	4.4
12	151	337.1	157.5	745.3	184.3	1.1702	0.2948	1.951	1.032	1.201	144.3
13	553	2499.9	1580.2	5768.2	1484.8	0.9397	0.0416	1.951	0.795	0.125	11.9
14	222	604.6	394.2	1095.4	232.7	0.5902	0.0933	1.951	0.636	0.182	21.4
15	205	749.1	512.7	1891.1	479.7	0.9357	0.0926	1.951	0.723	0.097	6.2
16	248	811.7	389.3	1422.1	360.2	0.9254	0.114	1.951	1.03	0.063	7.5
17	295	1074.2	332.7	1351.4	438.9	1.319	0.1635	1.951	2.046	0.171	11.5
18	243	850.8	391.2	1321.1	347.4	0.8879	0.1107	1.951	1.116	0.098	5.9
19	161	411.3	372.9	1215.3	349.6	0.9374	0.124	1.951	0.619	0.033	3.2
20	149	429.3	211.5	718.2	240.1	1.1349	0.2224	1.951	1.324	0.095	10.3
21	158	403	171.7	626.3	182.7	1.0641	0.2541	1.951	1.336	0.058	5.8
22	205	643.7	352.5	1430.7	388.5	1.1019	0.1378	1.951	0.967	0.092	4.2
23	171	504.6	339.9	1342.7	359.3	1.0573	0.1401	1.951	0.775	0.043	5.3
24	348	1360.4	601	2666	650.2	1.0818	0.0901	1.951	1.077	0.081	4.5
										0.085	7.4
1	890	3906.3	2607.2	7749.4	2843.8	1.0908	0.0336	2.886	1.587	1.447	36.9
2	1015	4473.3	1516.9	4453.8	1485.8	0.9795	0.044	2.886	2.839	0.322	35.2
3	1677	7940.5	1849	5347.8	2011.5	1.0879	0.0412	2.886	4.661	0.139	15.3
4	252	953	687.8	2089.5	816.3	1.1868	0.0865	2.886	1.562	0.347	42.9
5	274	996.8	750.2	2339.6	911.5	1.2151	0.0825	2.886	1.494	0.179	13.6
6	296	966.8	753.6	2370	903.7	1.1991	0.0807	2.886	1.412	0.208	21.2
7	295	1065.1	1151.6	3443.1	1261.3	1.0953	0.0568	2.886	0.978	0.48	22.2
8	1297	5669.6	2359.6	6853.5	2407.6	1.0203	0.0346	2.886	2.436	0.351	22.9
9	240	837.2	1089	3130	1126	1.034	0.0568	2.886	0.798	0.165	10.9
10	355	1280.9	832.3	2155.5	974.3	1.1706	0.074	2.886	2.007	0.283	27.5
11	497	2161.1	2229.8	6597.8	2326.5	1.0434	0.0358	2.886	0.986	0.041	5.2
12	71	22.6	80.3	55.8	57.2	0.7122	0.4332	2.886	0.832	0.11	17.4
13	203	561.2	524.5	1487.8	508.4	0.9693	0.0923	2.886	1.055	0.083	11.4
14	114	228.3	273.2	779.2	274	1.0032	0.1618	2.886	0.848	0.14	13.6
15	451	1721	1145	3530.1	1276.2	1.1145	0.0574	2.886	1.568	0.275	13.4
16	256	889.3	1044	3172.8	1084.3	1.0386	0.0583	2.886	0.84	0.153	13.8
17	250	836.3	508.4	1480.8	463	0.9107	0.0916	2.886	1.484	0.099	16
18	457	1905.3	1234.5	3594.8	1336.3	1.0824	0.0532	2.886	1.656	0.289	21.9
19	864	3755.5	3717.2	11595.9	4140.2	1.1138	0.0276	2.886	1.041	0.347	26
20	206	602.2	656.6	1980.4	688.9	1.0492	0.0831	2.886	0.921	0.137	14.1
21	363	1449.9	1437	4262.6	1441.8	1.0033	0.0459	2.886	0.985	0.119	15.3
22	1090	4566.3	2003	6376	2144.7	1.0707	0.0388	2.886	2.213	0.1	9.2
23	335	1387	1848	5017.8	1850.5	1.0014	0.0392	2.886	0.799	0.043	5.3
24	851	3441	1877.3	5592.6	1917.7	1.0215	0.0391	2.886	1.814	0.081	4.5
Ave.	379.9	1470.3	856.9	2687.9	899.2	1.03	0.128		1.39	0.195	15.4
Stdev.	335.33	1594.36	798.79	2379.35	859.58	0.130	0.1031		0.792	0.2561	20.93

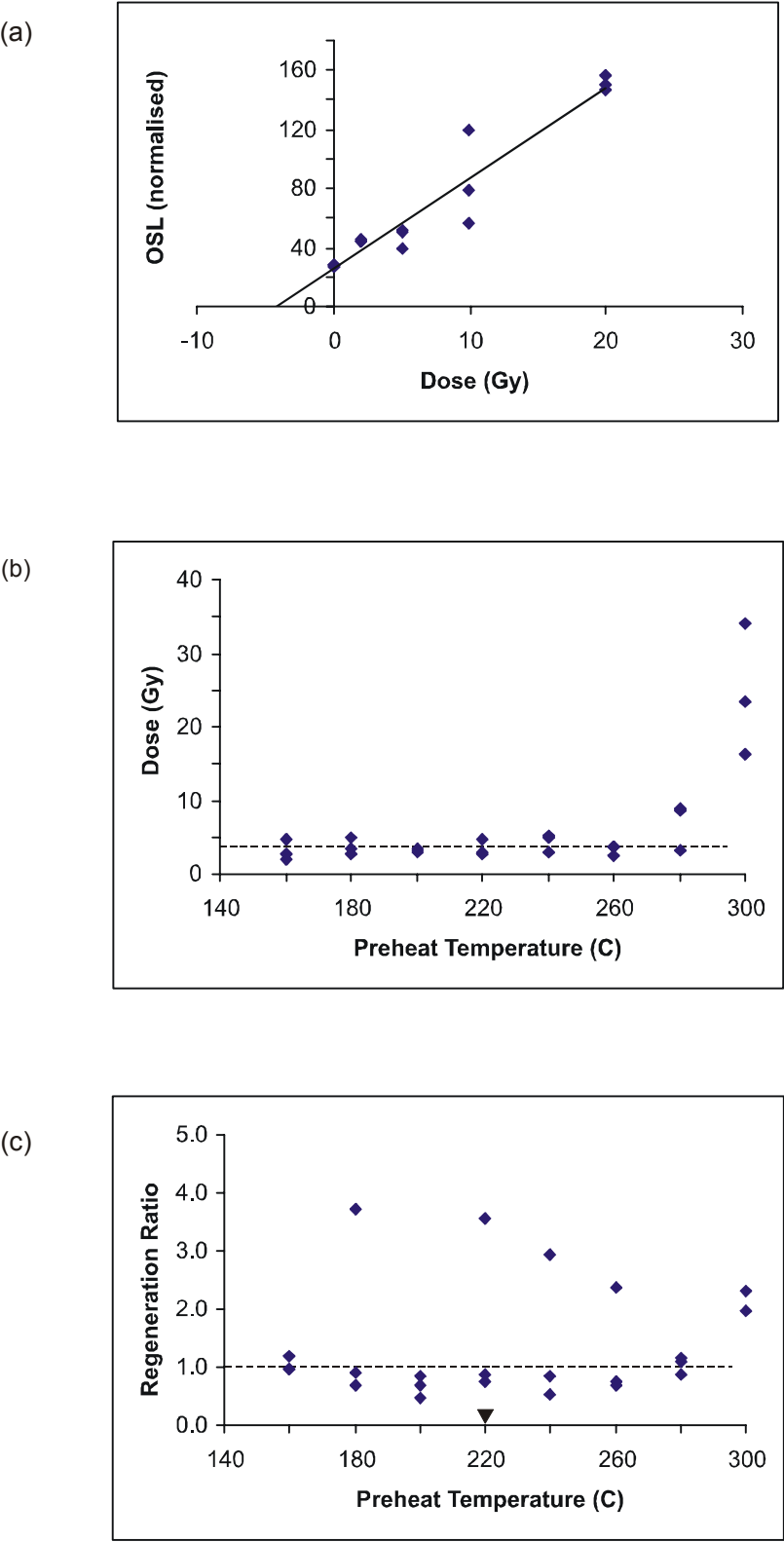


Figure A4.7 OSL results for Goor-1 sand sheet excavation at 100 cm, including:
(a) MARA test, (b) preheat plateau test, and (c) sensitivity test.

Table A4.5 SAR analyses for Goorurarmum sand sheet excavation (Goor-1) at 100 cm.

iw1202.DAT

goor-1-100, 1/3.4 Gy (24/84 sec). 1 mm mask

DOSE RATE (Gy/min) : 2.4387

used acquisition (ch) : 1 (1)-> 25 (25)residue (ch) : 226 (226)-> 250 (250)

No.	Nat.(1st)	Natural	Test N	Regen.	Test R	Tr/Tn	Err	Beta (Gy)	PD (Gy)	Err	(%)
1	5406	18835	4602	15286	4574	0.994	0.022	3.41	4.18	0.104	2.50
2	787	2531	954	3039	1043	1.094	0.062	3.41	3.11	0.2	6.40
3	7826	30162	11253	37796	11414	1.014	0.014	3.41	2.76	0.044	1.60
4	1336	4641	2071	6844	2207	1.066	0.037	3.41	2.47	0.099	4.00
5	12204	45604	7095	22558	6890	0.971	0.017	3.41	6.70	0.132	2.00
6	4269	14976	3768	12027	3641	0.966	0.024	3.41	4.11	0.116	2.80
7	186	511	124	580	197	1.592	0.420	3.41	4.79	1.332	27.80
8	2260	7432	3662	11852	3620	0.989	0.025	3.41	2.12	0.063	3.00
9	2132	6819	2635	8088	2561	0.972	0.030	3.41	2.80	0.099	3.50
10	1895	6879	2771	9369	2788	1.006	0.030	3.41	2.52	0.086	3.40
11	3495	12098	4489	15164	4509	1.004	0.023	3.41	2.74	0.071	2.60
12	1942	7267	2434	8780	2424	0.996	0.032	3.41	2.81	0.102	3.60
13	68	26	-7	-2	17	-2.564	-10.141	3.41	115.48	1488.149	12.89
14	10115	39583	12535	41647	12555	1.002	0.013	3.41	3.25	0.048	1.50
15	4099	15394	5255	17421	5117	0.974	0.020	3.41	2.94	0.07	2.40
16	29055	98058	15345	49044	15146	0.987	0.012	3.41	6.74	0.088	1.30
17	3728	12941	4235	14327	4349	1.027	0.024	3.41	3.17	0.083	2.60
18	1694	5380	1008	3389	973	0.965	0.056	3.41	5.23	0.326	6.20
19	752	2420	852	3119	907	1.065	0.066	3.41	2.82	0.195	6.90
20	949	3113	1329	4535	1382	1.040	0.048	3.41	2.44	0.129	5.30
21	999	3407	1200	4047	1349	1.124	0.054	3.41	3.23	0.176	5.50
22	2695	10024	2933	9520	2888	0.984	0.029	3.41	3.54	0.116	3.30
23	8921	28679	6376	15783	4717	0.740	0.015	3.41	4.59	0.105	2.30
24	5301	19561	1015	3126	1005	0.990	0.056	3.41	21.16	1.272	6.00
2	3974	24533	10447	37039	10610	1.016	0.016	3.41	2.30	0.041	1.80
3	1213	5836	2517	6757	2222	0.883	0.039	3.41	2.60	0.129	5.00
4	3174	17106	4394	14446	4414	1.005	0.028	3.41	4.06	0.123	3.00
5	3527	18883	7432	23802	7449	1.002	0.020	3.41	2.72	0.06	2.20
6	5493	30404	8998	28456	9227	1.026	0.018	3.41	3.74	0.073	1.90
7	3813	23506	10057	32227	10493	1.043	0.017	3.41	2.60	0.048	1.90
8	4048	18387	3603	12352	3630	1.008	0.032	3.41	5.12	0.176	3.40
9	1110	7078	2642	8016	3007	1.138	0.044	3.41	3.43	0.149	4.40
10	1145	7015	3364	11027	3417	1.016	0.034	3.41	2.21	0.083	3.70
11	1301	6801	2512	7753	2387	0.950	0.040	3.41	2.85	0.133	4.70
12	1524	10712	3438	10829	3455	1.005	0.033	3.41	3.39	0.125	3.70
13	2291	11178	3847	11610	3499	0.910	0.029	3.41	2.99	0.105	3.50
14	1215	7302	3250	11350	3332	1.025	0.035	3.41	2.25	0.087	3.90
15	1915	9926	8680	28385	8430	0.971	0.018	3.41	1.16	0.026	2.20
16	3042	18711	5712	19180	5544	0.971	0.023	3.41	3.23	0.084	2.60
17	3086	18597	7219	25866	7763	1.075	0.021	3.41	2.64	0.058	2.20
18	7785	53138	11485	36748	10686	0.930	0.014	3.41	4.59	0.078	1.70
19	2369	11979	5269	17453	5568	1.057	0.026	3.41	2.48	0.068	2.80
20	3590	23064	7698	24484	7732	1.004	0.019	3.41	3.23	0.07	2.20
21	909	5589	2658	8361	2565	0.965	0.039	3.41	2.20	0.1	4.50
22	1421	8398	3013	9784	3072	1.020	0.037	3.41	2.99	0.12	4.00
23	1750	9776	4226	14530	4518	1.069	0.030	3.41	2.46	0.077	3.20
24	4416	27527	9935	30626	9924	0.999	0.016	3.41	3.07	0.057	1.90
Ave.	3749	16421	4901	15924	4877	0.938	-0.178	3.41	6.04	31.81	4.04
StDev.	4585	16816	3596	11743	3574	0.533	1.486	0.00	16.55	217.05	4.05

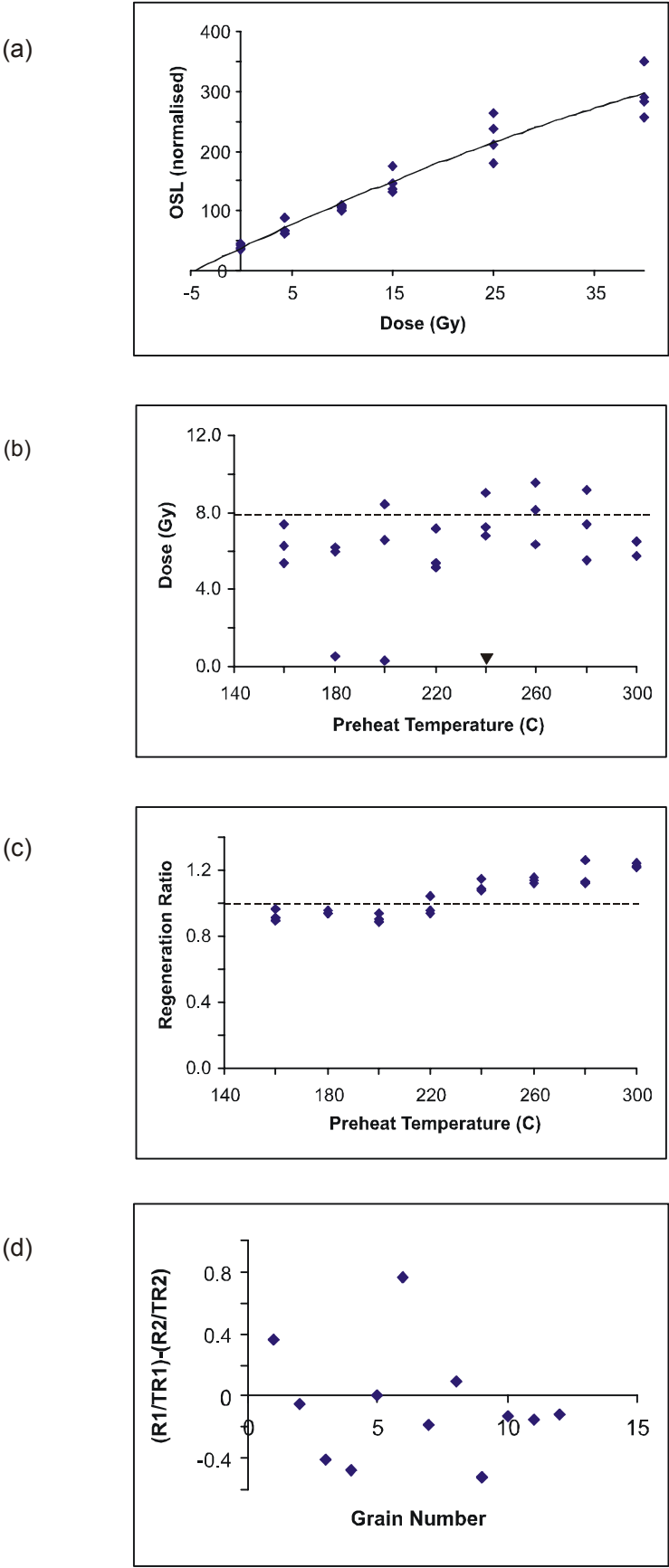


Figure A4.8 OSL results for Goor-1 sand sheet excavation at 175 cm, including: (a) MARA test, (b) preheat plateau test, (c) sensitivity test, and (d) double-regenerative test.

Table A4.6 SAR analyses for Goorurarmum sand sheet excavation (Goor-1) at 175 cm.

ag1341r1.DAT

COOR-1-175, Ingrid Ward's sample, 1/4Gy, IWSAR

DOSE RATE (Gy/min) : 1.104

used acquisition (ch) : 1 (1)-> 25 (25)residue (ch) : 226 (226)-> 250 (250)

No.	Nat.(1st)	Natural	Test N	Regen.	Test R	Tr/Tn	Err	Beta (Gy)	PD (Gy)	Err	(%)
1	6157	26141	4423.6	16496.3	4388.4	0.992	0.0221	3.974	6.248	0.152	2.4
2	2621	11406	2598.7	9562.1	2466.5	0.9491	0.0282	3.974	4.5	0.148	3.3
3	563	2370.6	428.2	1708.4	452.9	1.0577	0.0887	3.974	5.833	0.527	9
4	1305	5486.2	979.8	3842.4	1044.6	1.0662	0.0531	3.974	6.05	0.328	5.4
5	3256	14938	2012.7	371.8	1830.7	0.9096	0.0313	3.974	145.236	11.017	7.6
6	8049	34609.1	5001.1	717.4	4822.8	0.9643	0.02	3.974	184.893	9.096	4.9
7	4315	18613.3	1648.1	273.4	1837.2	1.1147	0.0405	3.974	301.639	28.247	9.4
8	4399	19256.4	224.3	13126.5	3408	15.191	1.4799	3.974	88.57	8.688	9.8
9	2265	9573.6	1803.9	6498.7	1878.2	1.0412	0.0366	3.974	6.096	0.236	3.9
10	1834	7911.1	1172.2	4078.7	1068.9	0.9119	0.0426	3.974	7.03	0.357	5.1
11	3211	13845.5	2073.9	8329.7	2257.2	1.0884	0.0351	3.974	7.19	0.253	3.5
12	6588	28848	3754.9	13749.9	3449.9	0.9188	0.0225	3.974	7.661	0.204	2.7
13	2530	10620.2	2109.8	8025.8	2097.3	0.9941	0.0328	3.974	5.228	0.19	3.6
14	3405	14361.2	2508.6	8734.1	2459.2	0.9803	0.0295	3.974	6.406	0.212	3.3
15	2490	11233.8	1268.5	4705.6	1355	1.0682	0.0464	3.974	10.135	0.475	4.7
16	8071	34933.6	4161.6	15406	3951.5	0.9495	0.0219	3.974	8.557	0.214	2.5
17	6349	27151	3971.8	15167.2	3868	0.9739	0.0227	3.974	6.929	0.177	2.5
18	4583	20660.7	1629.5	5958.2	1604.2	0.9844	0.0373	3.974	13.567	0.553	4.1
19	1160	5022.2	877.7	3104.3	844.7	0.9624	0.0526	3.974	6.188	0.369	6
20	3646	15994.5	2643	9989	2679.1	1.0136	0.0291	3.974	6.451	0.203	3.1
21	2942	12656.6	1659.2	6401.6	1756.9	1.0589	0.0391	3.974	8.321	0.333	4
22	1048	4334.8	756.4	2819.6	708	0.9361	0.0568	3.974	5.72	0.375	6.6
23	4429	18280.1	1445.8	5672.5	1574.3	1.0889	0.0427	3.974	13.947	0.589	4.2
24	3217	14063.8	1961.4	6275.5	1695.2	0.8643	0.0307	3.974	7.698	0.298	3.9
1	3432	14730.5	2272.5	8237.3	2144.3	0.9436	0.03	3.974	6.706	0.233	3.5
2	172	601.7	2574.7	9437.8	2509	0.9745	0.0288	3.974	0.247	0.014	5.8
3	144	519.9	2037.9	7472.4	2014.2	0.9884	0.0331	3.974	0.273	0.018	6.4
4	210	589.3	2790.6	10191.8	2733.9	0.9797	0.0282	3.974	0.225	0.014	6
5	141	561.5	2066.8	7904	2059.8	0.9966	0.0332	3.974	0.281	0.018	6.3
6	2973	12839.9	1991.7	7086.3	1908.1	0.958	0.0332	3.974	6.899	0.261	3.8
7	1057	4671.1	808.4	2738.7	764.5	0.9457	0.0552	3.974	6.411	0.407	6.4
8	114	362.2	1122.9	4209.3	1063.7	0.9473	0.0453	3.974	0.324	0.028	8.6
9	4992	20550.7	2446.3	9381.2	2466.7	1.0083	0.0304	3.974	8.779	0.287	3.3
10	5809	24739.5	3041.8	10750.8	2788.1	0.9166	0.0253	3.974	8.383	0.251	3
11	2863	12382.2	2025.5	7263.3	1943.9	0.9597	0.0327	3.974	6.502	0.242	3.7
12	9458	43412.6	4090.4	14489.4	3668.5	0.8968	0.0211	3.974	10.68	0.272	2.5
13	5234	23603.2	3230.5	12233.7	3260.1	1.0092	0.0264	3.974	7.738	0.22	2.8
14	2201	9342.3	1538.1	5601.8	1421.4	0.9241	0.0369	3.974	6.125	0.267	4.4
15	1300	5703.3	1167.5	3992.6	1101.5	0.9435	0.0436	3.974	5.356	0.272	5.1
16	6921	30071	3774.5	14327.1	3800.8	1.007	0.0241	3.974	8.4	0.219	2.6
17	3683	15893.5	1897.4	6868.2	1796.5	0.9468	0.0334	3.974	8.708	0.332	3.8
18	3612	15930.6	2523.6	10004	2614.9	1.0362	0.0304	3.974	6.558	0.21	3.2
19	3955	17132.4	3024.3	11696.3	2952.4	0.9762	0.0264	3.974	5.683	0.168	3
20	3042	12912.3	2306.4	8469.1	2339.2	1.0142	0.0314	3.974	6.146	0.209	3.4
21	1831	7899.4	1713.9	6146.3	1571.6	0.917	0.0342	3.974	4.684	0.193	4.1
22	2336	9718.5	2167.1	8471.5	2185.2	1.0084	0.0324	3.974	4.598	0.163	3.6
23	1418	6019.7	646.8	2242	586.5	0.9067	0.0611	3.974	9.676	0.698	7.2
24	2191	9436	1875.6	6868.4	1850.3	0.9865	0.0347	3.974	5.386	0.208	3.9
Ave.	3281.7	14207.0	2171.9	7647.9	2188.4	1.28	0.07		20.93	1.43	4.62
Stdev.	2248.23	9899.79	1085.68	4126.48	1020.87	2.052	0.209		53.654	4.575	1.929

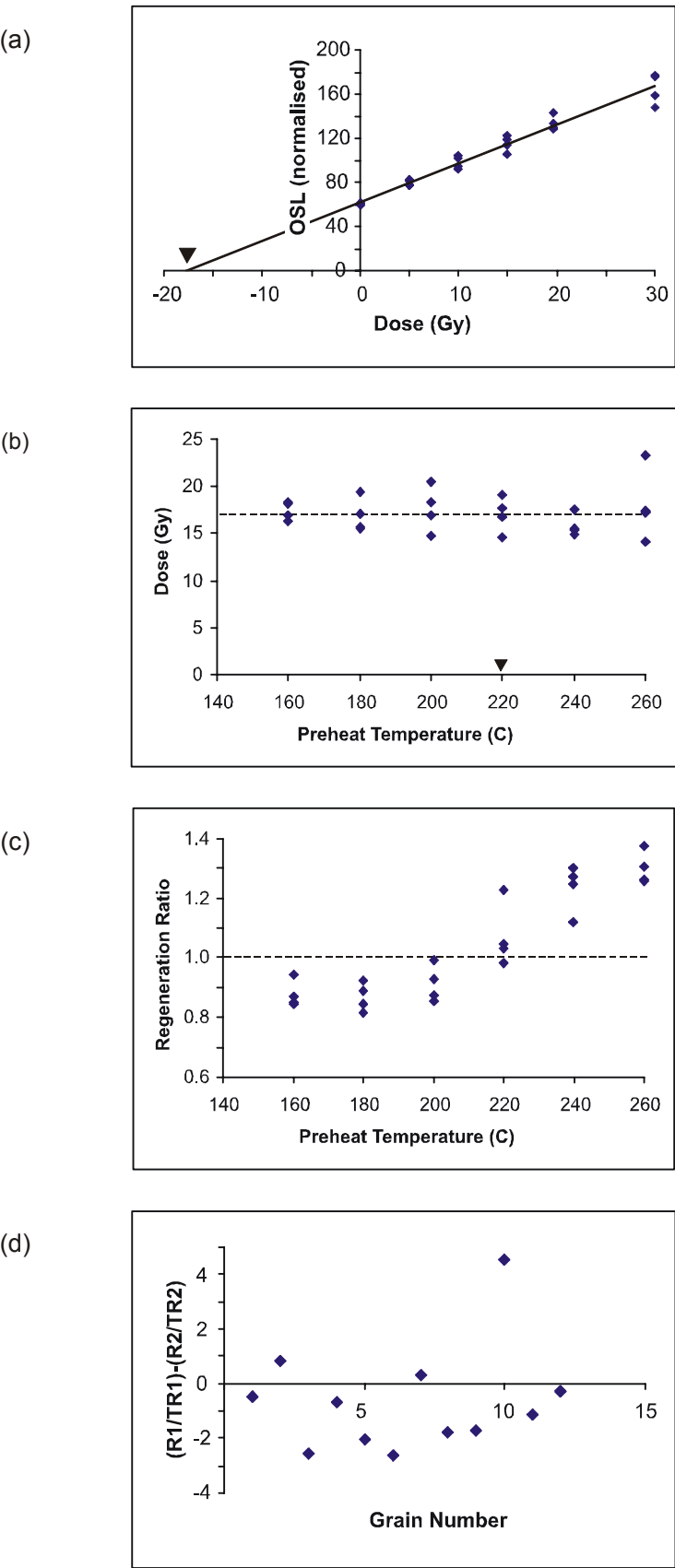


Figure A4.9 OSL results for Goor-1 sand sheet excavation at 220 cm, including: (a) MARA test, (b) preheat plateau test, (c) sensitivity test, and (d) double-regenerative test.

Table A4.7 SAR analyses for Goorurarmum sand sheet excavation (Goor-1) at 220 cm.

wt029r1.DAT

goor-1-220, 1 mm mask, Dose = 1/17 Gy (24/401 sec)

DOSE RATE (Gy/min) : 2.547

used acquisition (ch) : 1 (1)-> 25 (25)residue (ch) : 226 (226)-> 250 (250)

No.	Nat.(1st)	Natural	Test N	Regen.	Test R	Tr/Tn	Err	Beta (Gy)	PD (Gy)	Err	(%)
1	3577	50269	5194	74761	5719	1.10	0.028	17.022	12.60	0.324	2.6
2	2350	35113	2098	29915	2151	1.03	0.053	17.022	20.49	1.065	5.2
3	1359	17621	1610	23428	1835	1.14	0.070	17.022	14.59	0.908	6.2
4	5378	76515	5413	61092	5741	1.06	0.028	17.022	22.61	0.612	2.7
5	1589	21155	1589	23363	1773	1.12	0.070	17.022	17.20	1.098	6.4
6	56	202	106	56	58	0.55	0.649	17.022	33.60	54.723	162.9
7	2613	37609	3987	57797	4337	1.09	0.033	17.022	12.05	0.380	3.1
8	83	47	-26	-65	69	-2.65	-6.453	17.022	32.67	94.398	289
9	80	99	131	68	-20	-0.15	-0.479	17.022	-3.78	12.560	331.9
10	3246	46726	3790	49542	3973	1.05	0.033	17.022	16.83	0.546	3.2
11	10134	157921	11688	126665	10718	0.92	0.015	17.022	19.46	0.328	1.7
12	2478	36438	2525	35736	2881	1.14	0.048	17.022	19.80	0.854	4.3
13	1258	17901	1291	16242	1369	1.06	0.079	17.022	19.90	1.500	7.5
14	4382	68511	4059	46785	3637	0.90	0.030	17.022	22.34	0.755	3.4
15	6483	91785	6301	89308	6858	1.09	0.024	17.022	19.04	0.426	2.2
16	2908	39727	3403	44844	3662	1.08	0.037	17.022	16.23	0.573	3.5
17	1425	19758	1813	23797	2050	1.13	0.063	17.022	15.98	0.910	5.7
18	8376	118294	9514	133975	9929	1.04	0.018	17.022	15.69	0.277	1.8
19	3617	59132	4880	66694	5325	1.09	0.029	17.022	16.47	0.449	2.7
20	4610	68523	5810	70111	5789	1.00	0.025	17.022	16.58	0.417	2.5
21	4634	64515	4892	59950	5091	1.04	0.028	17.022	19.06	0.522	2.7
22	15052	210945	16815	232131	16596	0.99	0.012	17.022	15.27	0.193	1.3
23	2654	42052	1919	26092	1959	1.02	0.056	17.022	28.01	1.546	5.5
24	2611	40091	3465	37968	3464	1.00	0.035	17.022	17.97	0.636	3.5
1	2004	28952	2264	32896	2258	1.00	0.049	18.041	15.84	0.786	5
2	4115	63342	4835	70305	5062	1.05	0.028	18.041	17.02	0.462	2.7
3	6674	100020	7698	110106	7650	0.99	0.020	18.041	16.29	0.330	2
4	12658	188651	9168	110114	8076	0.88	0.017	18.041	27.23	0.521	1.9
5	2717	39332	4161	59725	4453	1.07	0.032	18.041	12.72	0.384	3
6	3316	44627	4092	57254	4420	1.08	0.033	18.041	15.19	0.468	3.1
7	2787	39688	4215	61875	4189	0.99	0.030	18.041	11.50	0.355	3.1
8	1674	22810	2360	29654	2361	1.00	0.046	18.041	13.88	0.657	4.7
9	4745	70136	5535	77394	6334	1.14	0.028	18.041	18.71	0.466	2.5
10	1731	23802	2166	28333	2226	1.03	0.050	18.041	15.58	0.778	5
11	610	7530	901	11017	1026	1.14	0.113	18.041	14.04	1.415	10.1
12	1697	23333	2155	30919	2499	1.16	0.055	18.041	15.79	0.762	4.8
13	3655	55001	4092	55436	4281	1.05	0.032	18.041	18.73	0.575	3.1
14	3547	50374	4340	65359	4721	1.09	0.031	18.041	15.13	0.439	2.9
15	783	11387	1215	16399	1243	1.02	0.082	18.041	12.82	1.045	8.2
16	4574	60160	4061	56082	4616	1.14	0.034	18.041	22.00	0.673	3.1
17	7439	107808	6421	98930	7180	1.12	0.024	18.041	21.98	0.485	2.2
18	3814	59167	5495	82651	6162	1.12	0.027	18.041	14.48	0.362	2.5
19	2597	38447	2829	33100	2753	0.97	0.040	18.041	20.39	0.847	4.2
20	8280	108709	5779	75776	5791	1.00	0.024	18.041	25.94	0.642	2.5
21	2858	41487	3320	48089	3833	1.15	0.039	18.041	17.97	0.618	3.4
22	4733	63972	5257	75955	6432	1.22	0.029	18.041	18.59	0.454	2.4
23	1896	27936	2574	35260	2847	1.11	0.046	18.041	15.81	0.676	4.3
24	7983	107762	5712	83425	6346	1.11	0.026	18.041	25.89	0.613	2.4
1	18075	117409	9460	114927	8135	0.86	0.016	17.884	15.71	0.29	1.8
2	24498	139589	11996	145731	10409	0.87	0.014	17.884	14.86	0.241	1.6
3	9047	62546	5780	67391	4960	0.86	0.022	17.884	14.24	0.367	2.6
4	25605	184245	15785	200753	14021	0.89	0.012	17.884	14.58	0.198	1.4
5	18905	139119	8853	107027	7316	0.83	0.016	17.884	19.21	0.376	2
6	19173	134913	12289	143513	10289	0.84	0.013	17.884	14.08	0.224	1.6
7	30012	185087	16964	213789	14568	0.86	0.011	17.884	13.30	0.173	1.3
8	11877	76666	5489	64377	4774	0.87	0.023	17.884	18.52	0.492	2.7
9	55368	354810	31562	397855	27458	0.87	0.008	17.884	13.88	0.129	0.9
10	7115	40759	2895	36869	2844	0.98	0.038	17.884	19.42	0.771	4
11	12778	82607	7365	85286	6479	0.88	0.019	17.884	15.24	0.337	2.2
12	14320	97860	4949	52758	4194	0.85	0.024	17.884	28.11	0.811	2.9
Ave.	7244	72017	5605	72776	5453	0.93	-0.07		17.75	3.25	16.3
Stdev.	9168	62376	5139	64788	4486	0.508	0.844		5.570	13.933	58.97

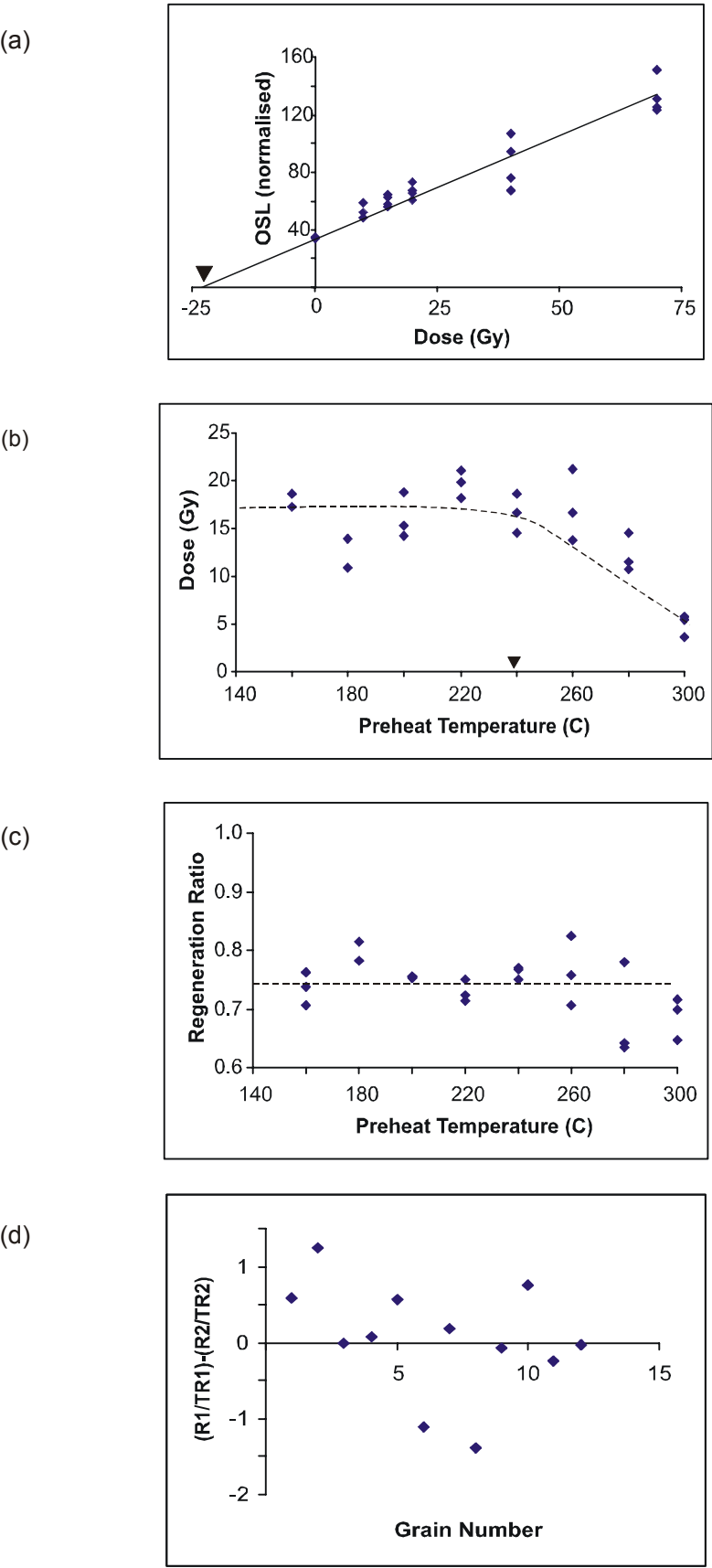


Figure A4.10 OSL results for Karl-1 rock shelter excavation at 27 cm, including: (a) MARA test, (b) preheat plateau test, (c) sensitivity test, and (d) double-regenerative test.

Table A4.8 (a) SAR analyses for the Karlinga rock shelter excavation (Karl-1) at 27 cm.

wt027r1.DAT

karl-1-27, 1 mm mask, Dose = 1/17 Gy (24/401 sec)

DOSE RATE (Gy/min) : 2.547

used acquisition (ch) : 1 (1)-> 25 (25)residue (ch) : 226 (226)-> 250 (250)

No.	Nat.(1st)	Natural	Test N	Regen.	Test R	Tr/Tn	Err	Beta (Gy)	PD (Gy)	Err	(%)
1	1329	5838.1	443.8	4531.8	780.3	0.784866	0.1644	17.022	17.21	3.699	9.6
2	2873	13251.1	1276.9	16152.6	2882.6	1.007813	0.0935	17.022	14.07	1.36	4.3
3	867	3645.3	527.5	7263.7	1209.1	1.023348	0.1763	17.022	8.74	1.566	8
4	5537	24324.2	2345.8	29403	4936.8	0.939554	0.06	17.022	13.23	0.884	3
5	7071	31499.7	2164.8	29982.5	4800.7	0.989955	0.066	17.022	17.70	1.225	3.1
6	4833	22256.1	1220.2	15825.5	2577	0.942857	0.092	17.022	22.57	2.267	4.5
7	3294	15457.8	1173.1	14764.7	2546.7	0.969152	0.0961	17.022	17.27	1.773	4.6
8	5039	22075.1	1624.2	20376.2	3753.8	1.031786	0.081	17.022	19.03	1.553	3.6
9	12204	54665.3	3288.5	40633.7	6609.3	0.897232	0.047	17.022	20.55	1.119	2.4
10	5111	23287.5	1875	23041.5	3703.3	0.881786	0.0645	17.022	15.17	1.155	3.4
11	7172	32370.2	2825.5	36414.3	5939.6	0.938438	0.0534	17.022	14.20	0.845	2.7
12	19092	86307	4368	58208.3	9737.2	0.995179	0.0443	17.022	25.12	1.159	2.1
13	4117	19055.6	1175.6	13180.8	2155.3	0.818438	0.0846	17.022	20.14	2.148	4.8
14	16234	74912.5	3288.7	44354.8	6894.9	0.935982	0.049	17.022	26.91	1.454	2.4
15	3775	16428.1	1534.3	21821.7	3451.4	1.004196	0.0836	17.022	12.87	1.114	3.9
16	4991	23055.2	1577.8	21392	3568.5	1.009688	0.0805	17.022	18.52	1.53	3.7
17	2714	12113.7	1089.8	13457.1	2604.2	1.06683	0.1079	17.022	16.35	1.719	4.7
18	5961	26600.5	1768.8	22279.8	3663.2	0.924554	0.0714	17.022	18.79	1.502	3.6
19	1749	7717.4	566.2	8370.8	1406.5	1.108973	0.1903	17.022	17.40	3.057	7.8
20	6199	28121.1	1554.2	20090.9	3234.2	0.929018	0.0758	17.022	22.13	1.866	3.8
21	2059	9300.3	825.7	8916.1	1556.2	0.841429	0.1064	17.022	14.94	1.958	5.9
22	1725	7368.1	686	8281	1404.8	0.914196	0.131	17.022	13.85	2.051	6.6
23	5769	26087	1595.6	21189.8	3361.2	0.940446	0.0755	17.022	19.71	1.636	3.7
24	3721	16430.5	1311.9	14249.4	2439.4	0.830134	0.0797	17.022	16.29	1.622	4.4
1	2781	12823	631.3	7696.2	604.9	0.9581	0.0821	17.022	27.18	2.364	8.7
2	6813	31943.5	2780	35479.1	2637.3	0.9487	0.0297	17.022	14.54	0.469	3.2
3	1171	5092.8	379.1	4708.1	375.6	0.9908	0.1261	17.022	18.24	2.357	12.9
4	4159	19293.9	796.1	10619.9	773.2	0.9712	0.0689	17.022	30.03	2.165	7.2
5	2181	9613.8	667.8	9067.8	804	1.2039	0.0898	17.022	21.73	1.655	7.6
6	6559	30717.6	1848	25339.9	1885.5	1.0203	0.04	17.022	21.05	0.844	4
7	1607	7427.2	562.5	7095.1	578.8	1.029	0.0932	17.022	18.34	1.692	9.2
8	1499	6583.9	733.4	9396.7	789.3	1.0763	0.0785	17.022	12.84	0.961	7.5
9	4495	20950.1	1822.8	24864.5	2002.1	1.0983	0.042	17.022	15.75	0.621	3.9
10	5703	26267.7	1237.4	17700.7	1324.9	1.0707	0.0531	17.022	27.05	1.367	5.1
11	2969	13057.4	1132.3	14277.7	1131.3	0.9992	0.0542	17.022	15.55	0.866	5.6
12	3268	14085	844.7	10749.8	813.2	0.9627	0.0674	17.022	21.47	1.531	7.1
13	465	1857.8	323.7	3500.5	327.3	1.0112	0.1516	17.022	9.14	1.404	15.4
14	9885	45423	4201.5	54008.7	3771.2	0.8976	0.0221	17.022	12.85	0.327	2.5
15	1952	8774.8	713.1	9694.1	854.7	1.1985	0.0887	17.022	18.47	1.396	7.6
16	2810	12710.9	1246.8	14242	1065.7	0.8547	0.0457	17.022	12.99	0.713	5.5
17	3338	14566.8	1025.2	14212.7	1167.9	1.1392	0.0632	17.022	19.88	1.129	5.7
18	2650	11983.3	786.2	9936.6	741.5	0.9432	0.0701	17.022	19.36	1.465	7.6
19	4237	18731.2	1159.1	15391.9	1191.7	1.0281	0.0552	17.022	21.30	1.169	5.5
20	1809	7847.1	483.7	6439.8	486.8	1.0064	0.1015	17.022	20.87	2.137	10.2
21	4485	20321.8	1406.6	17486.4	1269.7	0.9027	0.0438	17.022	17.86	0.886	5
22	3954	17940.7	1275.2	16270	1225.2	0.9608	0.0487	17.022	18.03	0.936	5.2
23	7193	33782.4	2196.1	28634.3	2261.2	1.0296	0.0364	17.022	20.68	0.751	3.6
24	2405	10751.8	698.5	8791.2	731.5	1.0472	0.0814	17.022	21.80	1.726	7.9
Ave.	4621	20932	1439	18537	2376	0.98	0.08		18.33	1.48	5.63
Stdev.	3618.0	16553.2	943.0	12419.4	1968.8	0.089	0.037		4.51	0.643	2.764

Table A4.8 (b) Bracketed SAR analysis for the Karlinga rock shelter excavation (Karl-1) at 27 cm, analysed with the “Analyst” program.

Analyst data - 0.5 mm aliquot
 WI121 and WI123
 $R1 < N < R2 = 10 < 20 < 30$

Disc#	N.Signal	BG.signal	test_Sign	Signal_C	ED	ED_Err
1	73829	339	3273	0.83	30.9	0.8
2	70632	330	4134	0.78	22.2	0.6
3	44461	358	2899	0.9	20.9	0.6
4	20980	321	2505	0.89	11.9	0.9
5	161432	406	8595	0.95	26.1	0.4
6	33965	319	2313	0.86	23.8	1.1
9	146149	362	7492	1.05	26	0.4
11	64013	355	4778	1.01	17.3	0.5
12	54041	330	3776	0.86	19.9	0.6
1	94190	394	4674	0.96	28.6	0.8
2	98450	713	4318	1	33	0.9
3	44633	315	2890	0.73	22	1
4	23757	327	2082	0.92	16	0.9
5	94502	352	4013	0.83	30.8	0.6
6	13129	362	1148	1.03	21	1.4
7	16363	303	1695	0.95	13.1	1
8	24750	338	1717	1.16	21.2	1
9	21215	333	1813	0.95	18.4	1
10	25726	330	1899	1.08	22.1	1.4
11	4105	291	841	0.94	7.8	2.1
12	52500	358	3057	1	27.2	0.8
Ave.					21.91	0.90
StDev.					6.501	0.392

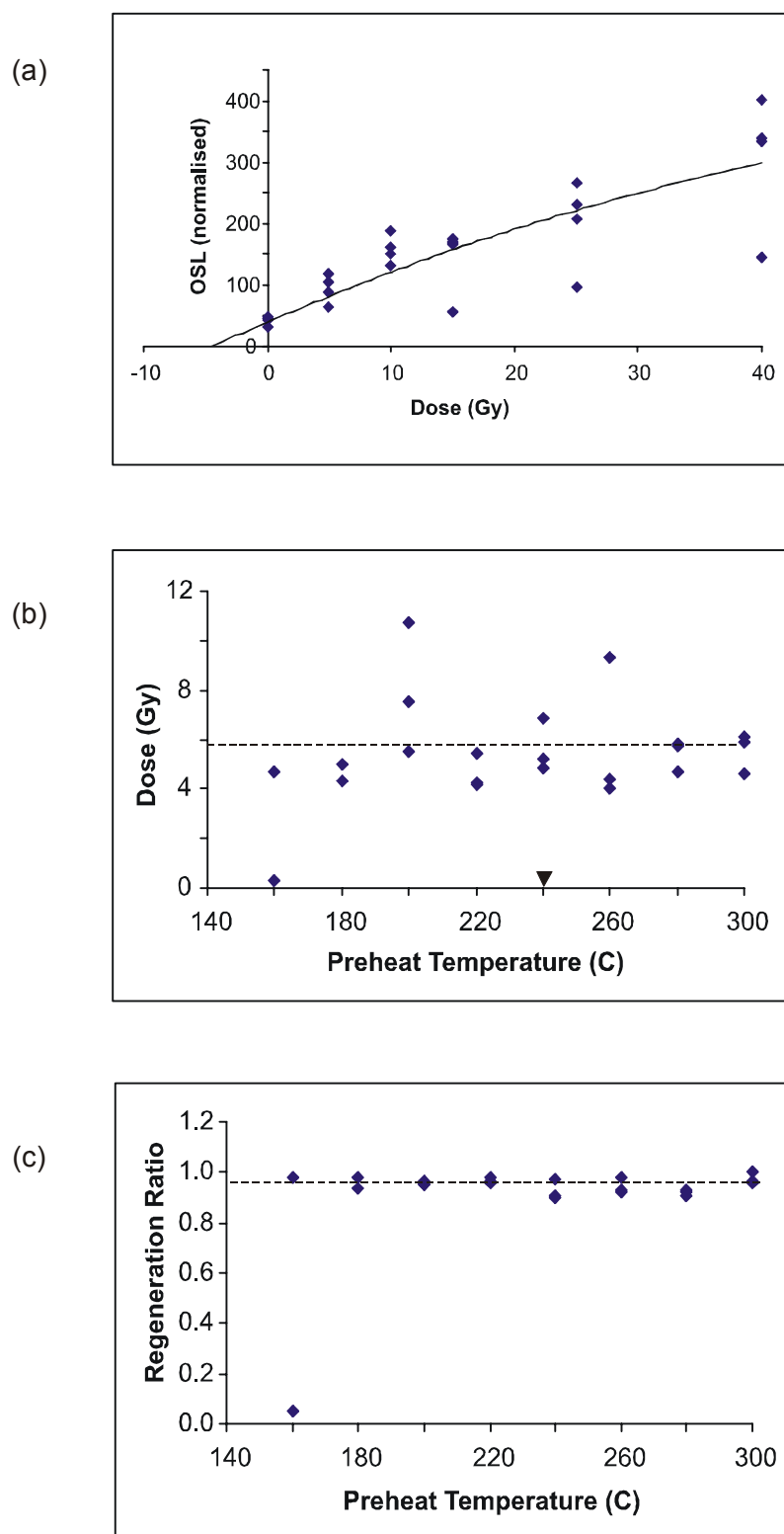


Figure A4.11 OSL results for Karl-3 sand sheet excavation at 90 cm, including: (a) MARA test, (b) preheat plateau test, (c) sensitivity test, and (d) double-regenerative test.

Table A4.9 SAR analyses for the Karlinga sand sheet excavation (Karl-3) at 90 cm.

ag1320R1.DAT

Karl-3-90, 1 mm mask, Dose = 1/4 Gy (54/216 sec), 220C preheat

DOSE RATE (Gy/min) : 1.104

used acquisition (ch) : 1 (1)-> 25 (25)residue (ch) : 226 (226)-> 250 (250)

No.	Nat.(1st)	Natural	Test N	Regen.	Test R	Tr/Tn	Err	Beta (Gy)	PD (Gy)	Err	(%)
1	4519	19328.6	5540	18209.4	4680.1	0.8448	0.0174	3.974	3.564	0.082	2.3
2	3991	17246.7	5045.3	16980.6	4385.7	0.8693	0.0186	3.974	3.509	0.084	2.4
3	7426	28749.2	45.2	10227.6	2461.4	54.5119	23.0262	3.974	608.998	257.343	42.3
4	1696	7204.1	115.7	8392	2077.8	17.9541	3.0625	3.974	61.256	10.496	17.1
5	9447	39542.8	234.2	20602.9	5223.5	22.3045	2.2235	3.974	170.138	17.024	10
6	5814	25664.2	5078.1	15837.9	4114.2	0.8102	0.0177	3.974	5.218	0.126	2.4
7	4700	19305	5098.7	17943.5	4608.8	0.9039	0.019	3.974	3.865	0.091	2.4
8	579	2124.5	667.5	2117.3	620.6	0.9298	0.0624	3.974	3.708	0.277	7.5
9	1974	7852	1885	6569.4	1619.4	0.8591	0.0314	3.974	4.081	0.165	4
10	2983	12108.2	1508.3	5374	1456.7	0.9658	0.0385	3.974	8.648	0.374	4.3
11	4764	20146.2	9278.8	32751.9	8547.3	0.9212	0.0141	3.974	2.252	0.04	1.8
12	2391	10321.6	3917.1	13151.3	3675.4	0.9383	0.0224	3.974	2.927	0.08	2.7
13	5305	22126	5397.9	19036.6	5157.5	0.9555	0.0192	3.974	4.414	0.099	2.2
14	3957	16302.7	2647.1	9451.3	2525.9	0.9542	0.028	3.974	6.542	0.211	3.2
15	3385	14059.8	4176.5	14883.2	3822.8	0.9153	0.0213	3.974	3.437	0.09	2.6
16	1472	5833.2	1532.3	5734.6	1419.5	0.9264	0.0374	3.974	3.745	0.167	4.5
17	1628	7114.4	2418.6	8708.7	2262.1	0.9353	0.0291	3.974	3.037	0.107	3.5
18	1360	5590.4	2521.4	8593.7	2186.7	0.8673	0.0272	3.974	2.242	0.081	3.6
19	437	1653.2	502.7	1725.2	500.7	0.9961	0.0792	3.974	3.794	0.334	8.8
20	4265	17789.3	4408.8	14974.2	3866.9	0.8771	0.02	3.974	4.141	0.105	2.5
21	1497	6135.5	2360.9	8401.8	2226.9	0.9433	0.0297	3.974	2.738	0.098	3.6
22	6232	26097.9	5140.3	17798.3	4566.8	0.8884	0.0187	3.974	5.178	0.12	2.3
23	9522	39576.7	9638.7	34375.2	8883.6	0.9217	0.0138	3.974	4.217	0.071	1.7
24	3012	12372.4	3570.1	12147.4	3135	0.8781	0.0225	3.974	3.555	0.102	2.9
1	7021	29003.4	7518.8	25868.2	6462.3	0.8595	0.0152	3.974	3.83	0.075	2
2	3466	14640.4	5300.4	18085.7	4536.7	0.8559	0.0181	3.974	2.754	0.066	2.4
3	8711	35911.7	3780.4	13022.8	3223.6	0.8527	0.0217	3.974	9.346	0.256	2.7
4	1809	7323.8	2953	10670.3	2667.7	0.9034	0.0255	3.974	2.464	0.079	3.2
5	241	727.7	5034.2	17244.8	4242.8	0.8428	0.0183	3.974	0.141	0.007	5
6	2486	10364.3	3700.4	11876.7	3164.7	0.8552	0.0219	3.974	2.966	0.086	2.9
7	587	2616	1121.3	3657.6	886.6	0.7907	0.0403	3.974	2.248	0.129	5.8
8	2254	9559.1	2563.1	8850.4	2275.1	0.8876	0.0274	3.974	3.81	0.131	3.4
9	1149	4701.4	1647.4	5461.3	1593.7	0.9674	0.037	3.974	3.31	0.144	4.3
10	4766	20883.5	4509.2	13782.2	3749.5	0.8315	0.0191	3.974	5.008	0.128	2.6
11	1625	6768.7	2084.3	7211.8	2131	1.0224	0.0339	3.974	3.814	0.143	3.7
12	1124	4914.1	2086.1	7393.7	1981.5	0.9499	0.0322	3.974	2.509	0.097	3.9
13	3328	13942.6	4771	14816.1	3804.7	0.7975	0.018	3.974	2.983	0.076	2.6
14	1986	8008.5	2661.2	9097.1	2477.8	0.9311	0.0277	3.974	3.258	0.109	3.4
15	2064	8366	3222.4	12354.4	3280.8	1.0181	0.0265	3.974	2.74	0.082	3
16	3903	16145.2	2487	8330.5	2366.8	0.9517	0.0291	3.974	7.331	0.246	3.4
17	1797	7625.3	2750.1	10633.8	2666.6	0.9696	0.0279	3.974	2.763	0.09	3.3
18	1784	7661	2670.5	9426.5	2623.7	0.9825	0.0293	3.974	3.173	0.107	3.4
19	8081	34205.2	9612.3	34269.9	8782.9	0.9137	0.0138	3.974	3.625	0.061	1.7
20	3684	15906.4	4588.2	15526.7	4118.5	0.8976	0.02	3.974	3.655	0.092	2.5
21	2771	11379.2	2899	10226.5	2859.9	0.9865	0.0275	3.974	4.363	0.136	3.1
22	1782	7120.7	2260.8	8155.2	2290.8	1.0133	0.0322	3.974	3.516	0.126	3.6
23	3706	15840.7	2797.8	9640.3	2531.5	0.9048	0.0265	3.974	5.909	0.19	3.2
24	1931	8161.4	2985.3	9912	2536.5	0.8497	0.0244	3.974	2.78	0.09	3.2
Ave.	3425	14292	3515	12906	3360	2.83	0.615		21.11	6.05	4.6
Stdev.	2384.4	9947.9	2255.5	7378.6	1880.9	8.562	3.3467		90.267	37.151	6.12

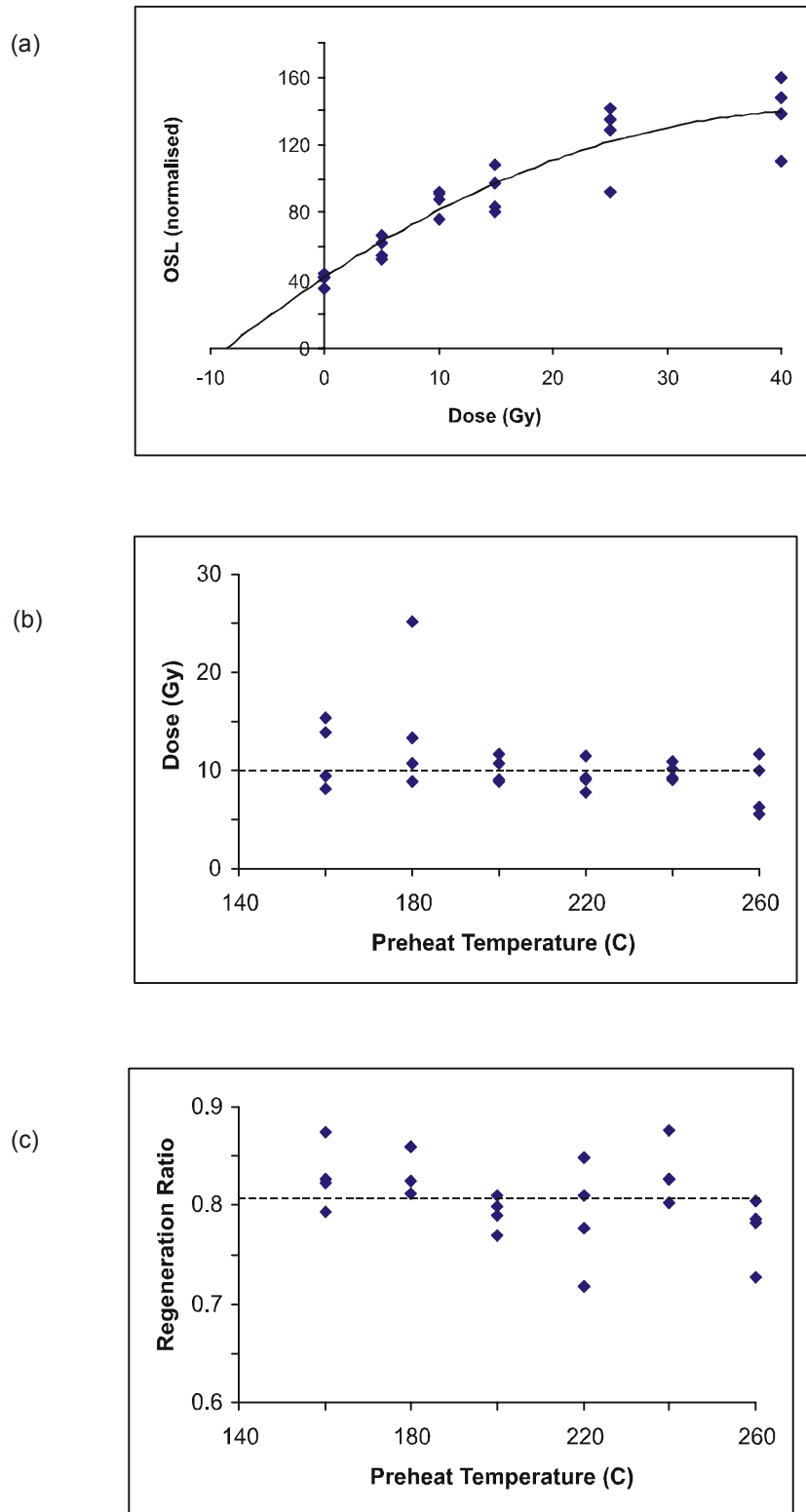


Figure A4.12 OSL results for Karl-3 sand sheet excavation at 150 cm, including:
(a) MARA test, (b) preheat plateau test, and (c) sensitivity test.

Table A4.10 SAR analyses for the Karlinga sand sheet excavation (Karl-3) at 150 cm.

wt026r1.DAT

Karl-3-150

DOSE RATE (Gy/min) : 2.547

used acquisition (ch) : 1 (1)-> 25 (25)residue (ch) : 226 (226)-> 250 (250)

No.	Nat.(1st)	Natural	Test N	Regen.	Test R	Tr/Tn	Err	Beta (Gy)	PD (Gy)	Err	(%)
1	33630	156558	18109.7	144437.2	35946.3	0.99245	0.0186	10.018	10.777	0.217	1
2	28615	132413.6	16405.7	138488.2	34815.8	1.0611	0.0207	10.018	10.164	0.213	1
3	28365	130900.5	14936.3	122827.9	33113.7	1.1085	0.0225	10.018	11.835	0.258	1.1
4	35629	167207.5	18377.5	149351.7	38113.3	1.03695	0.0191	10.018	11.6305	0.23	1
5	34518	162096.7	15797.3	127556.7	31736.1	1.00445	0.0202	10.018	12.788	0.275	1.1
6	5987	27638.5	3821.2	32165.8	8462.5	1.1073	0.0467	10.018	9.532	0.432	2.3
7	43014	206820.3	12001.6	94532.5	22164.6	0.9234	0.0218	10.018	20.239	0.504	1.2
8	14830	70251.5	9090.9	76974.4	18230.5	1.0027	0.0268	10.018	9.1675	0.264	1.4
9	8734	39807.5	4795.7	38730.3	9905.1	1.0327	0.0392	10.018	10.6335	0.432	2
10	24906	116464.3	14893.2	125850.9	31212.2	1.04785	0.0215	10.018	9.715	0.215	1.1
11	14164	64090.4	6617.8	57603.1	15010.9	1.13415	0.036	10.018	12.6415	0.427	1.7
12	19170	88784.9	10227.1	90144.9	21411	1.0468	0.0263	10.018	10.3285	0.277	1.3
13	16023	76302.3	8534.5	68013.8	16729.4	0.9801	0.0278	10.018	11.0155	0.334	1.5
14	10500	48146.2	6191.8	46683.2	11696.1	0.9445	0.0337	10.018	9.7585	0.372	1.9
15	15036	69330.5	8680.8	75889.2	18580.8	1.07025	0.0293	10.018	9.795	0.287	1.5
16	12256	57890.8	6269.1	53171.9	13279.7	1.05915	0.0344	10.018	11.5525	0.4	1.7
17	7343	34509.1	4057.9	33786.2	8649.9	1.0658	0.0438	10.018	10.906	0.479	2.2
18	3099	14156.3	2278.4	18474.4	4697.6	1.0309	0.0616	10.018	7.9135	0.507	3.2
19	22575	105187.9	12111	106514.4	26502.4	1.09415	0.025	10.018	10.825	0.265	1.2
20	22441	106683.4	7966.8	66433.7	17131	1.07515	0.0307	10.018	17.297	0.523	1.5
21	8203	38646.6	4890.3	40585.6	10023.7	1.02485	0.0383	10.018	9.7765	0.391	2
22	11457	53505.1	6037.2	46492.6	11963.3	0.9908	0.0333	10.018	11.423	0.411	1.8
1	4903	22021.1	2147.9	17679.7	4511.2	1.05015	0.0629	10.018	13.104	0.83	3.2
2	9034	40814	4542	35322.2	9173.5	1.00985	0.0394	10.018	11.69	0.488	2.1
3	17744	80574.4	9767.3	82482.9	20861.4	1.0679	0.0272	10.018	10.451	0.286	1.4
4	10904	49114.5	5466.9	43929.2	11001.7	1.0062	0.0355	10.018	11.27	0.425	1.9
5	5397	23701.2	2713.9	25310.2	6250.3	1.15155	0.0601	10.018	10.803	0.598	2.8
6	8420	38783.7	5440	44985.1	11110.2	1.02115	0.0358	10.018	8.82	0.333	1.9
7	12660	56720.8	6048.2	56926.1	14187.8	1.1729	0.038	10.018	11.708	0.404	1.7
8	7370	33950.2	3000	26506.8	6704.4	1.1174	0.054	10.018	14.3375	0.733	2.6
9	4922	22635.5	3327.5	29070.6	7579.3	1.1389	0.0517	10.018	8.884	0.434	2.4
10	5998	25901.8	1924.2	16629.5	4391.1	1.141	0.0717	10.018	17.8045	1.175	3.3
11	1067	4637.6	690.5	5338	1434.7	1.0388	0.1351	10.018	9.0415	1.24	6.9
12	8055	36596.8	3410.7	30435.9	7839.4	1.14925	0.052	10.018	13.844	0.664	2.4
13	2259	10014.5	1296.2	10833.7	2918.5	1.12575	0.0932	10.018	10.4255	0.914	4.4
14	2424	10186	1790.8	13736.9	3917.5	1.0938	0.0778	10.018	8.1255	0.62	3.8
15	2456	11065.2	1417.2	12209.4	3316.2	1.16995	0.0906	10.018	10.6225	0.872	4.1
16	18062	78577.3	3535.6	30811.2	7782.3	1.10055	0.0487	10.018	28.1185	1.301	2.3
17	1746	7990.6	1205.2	10208	2605.5	1.08095	0.0927	10.018	8.4765	0.773	4.6
18	986	3987.3	583.5	5113	1346.5	1.15375	0.1722	10.018	9.0135	1.41	7.8
19	2656	11636.5	1202.8	10571.2	2641.8	1.09825	0.0969	10.018	12.111	1.121	4.6
20	1715	7840.2	1231.4	10127.5	2526.1	1.0257	0.0878	10.018	7.955	0.725	4.6
21	2160	9840.6	1514.5	13686.7	3476.5	1.1477	0.0836	10.018	8.267	0.643	3.9
22	12498	58172.1	3710.8	30806.3	7943.3	1.0703	0.0462	10.018	20.247	0.921	2.3
23	4882	21581.6	2517.8	21346.5	5823.5	1.15645	0.0625	10.018	11.713	0.674	2.9
24	10896	50362.1	5615.8	50252.8	12735.5	1.1339	0.0385	10.018	11.3845	0.413	1.8
Ave.	6634	29863	3088	26430	6753	1.10	0.069		12.01	0.750	3.3
Stdev.	10477.2	49485.2	4983.2	40986.2	10242.4	0.062	0.0319		3.752	0.3126	1.49

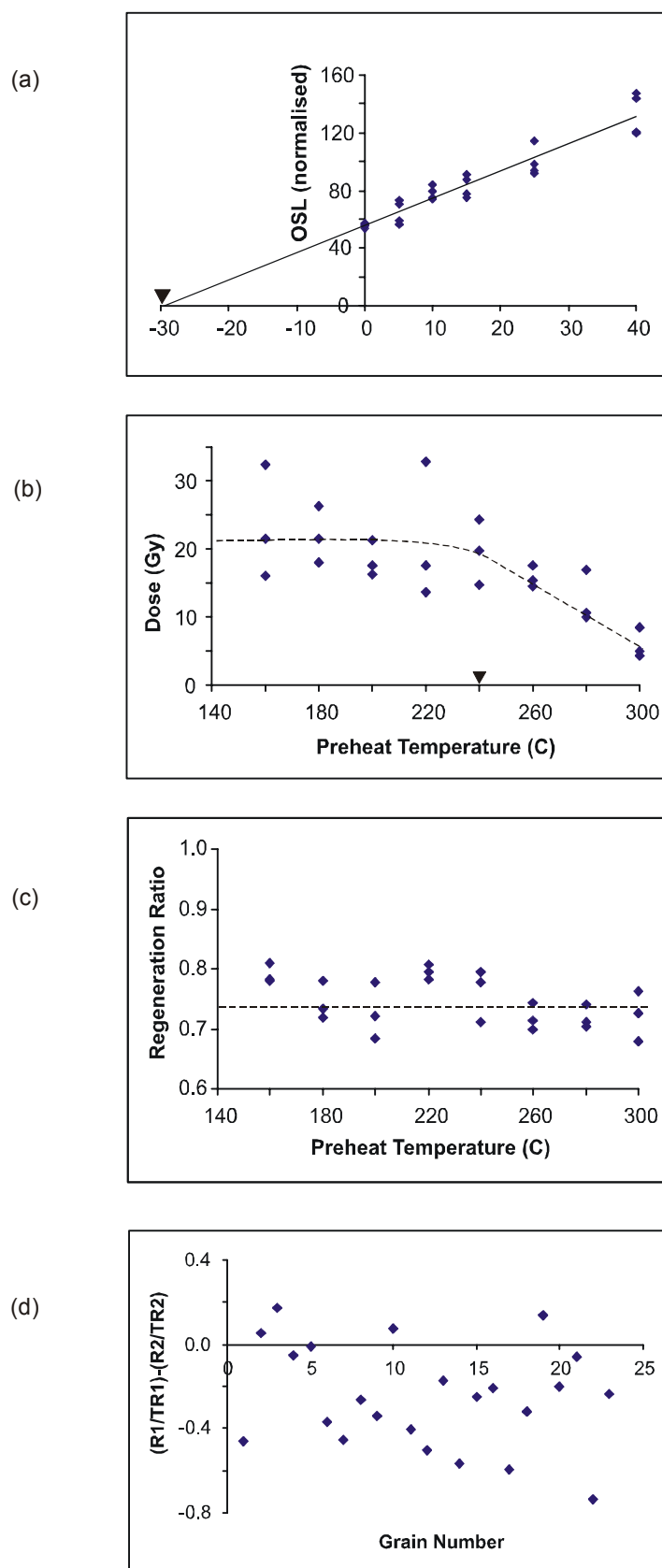


Figure A4.13 OSL results for Karl-3 sand sheet excavation at 210 cm, including: (a) MARA test, (b) preheat plateau test, (c) sensitivity test, and (d) double-regenerative test.

Table A4.11 SAR analyses for the Karlinga sand sheet excavation (Karl-3) at 210 cm.

wt025r1.DAT

karl-3-210, 1 mm mask, Dose = 24/471 sec

DOSE RATE (Gy/min) : 2.547

used acquisition (ch) : 1 (1)-> 25 (25)residue (ch) : 226 (226)-> 250 (250)

No.	Nat.(1st)	Natural	Test N	Regen.	Test R	Tr/Tn	Err	Beta (Gy)	PD (Gy)	Err	(%)
1	11529	155022	7317	99626	6766	0.92	0.020	19.994	28.77	0.63	2.20
2	45501	659854	23795	291799	20005	0.84	0.009	19.994	38.01	0.41	1.10
3	7478	105523	7814	90291	6651	0.85	0.018	19.994	19.89	0.43	2.20
4	5158	80139	5991	64730	4933	0.82	0.021	19.994	20.38	0.53	2.60
5	12366	166862	11157	141777	10405	0.93	0.016	19.994	21.95	0.37	1.70
6	6984	105428	8059	95630	6686	0.83	0.018	19.994	18.29	0.40	2.20
7	6588	106037	6070	65602	4591	0.76	0.020	19.994	24.44	0.65	2.60
8	15606	198060	10655	144854	10147	0.95	0.016	19.994	26.03	0.44	1.70
9	18785	264910	15849	229664	14934	0.94	0.012	19.994	21.73	0.29	1.30
10	18757	225147	11447	150435	10438	0.91	0.015	19.994	27.29	0.45	1.60
11	10336	138423	7024	86185	6216	0.89	0.020	19.994	28.42	0.66	2.30
12	29202	383046	15628	185814	11998	0.77	0.011	19.994	31.64	0.46	1.50
13	14793	190614	12304	164602	11289	0.92	0.014	19.994	21.24	0.34	1.60
14	13019	186982	10927	148336	9991	0.91	0.015	19.994	23.04	0.39	1.70
15	8288	121624	8555	92046	6929	0.81	0.017	19.994	21.40	0.45	2.10
16	14726	191447	9612	124203	8602	0.89	0.016	19.994	27.58	0.51	1.80
17	10198	130567	7940	101191	7043	0.89	0.018	19.994	22.88	0.49	2.10
18	2574	38050	2781	31840	2409	0.87	0.039	19.994	20.70	0.94	4.50
19	19062	226662	9934	132617	8832	0.89	0.016	19.994	30.38	0.56	1.80
20	9663	127591	5693	78430	5281	0.93	0.024	19.994	30.17	0.81	2.70
21	4496	66715	7144	86326	5939	0.83	0.020	19.994	12.85	0.31	2.40
22	12210	153102	8486	109240	7577	0.89	0.018	19.994	25.02	0.52	2.10
23	12513	188886	8390	99775	6674	0.80	0.016	19.994	30.11	0.63	2.10
24	10826	147201	10506	143028	9465	0.90	0.015	19.994	18.54	0.32	1.70
1	10393	50803	4501	73071	4212	0.94	0.0269	24.387	15.867	0.47	2.90
2	10327	54451	3592	53183	3178	0.88	0.0302	24.387	22.091	0.77	3.50
3	14533	63748	4938	68874	4419	0.89	0.025	24.387	20.2	0.58	2.90
4	24784	103321	6387	81624	5083	0.80	0.0195	24.387	24.567	0.61	2.50
5	9708	49086	2944	54069	2939	1.00	0.0383	24.387	22.102	0.86	3.90
6	28173	162895	6838	104816	6265	0.92	0.0201	24.387	34.724	0.77	2.20
7	1482	6948	738	9104	622	0.84	0.1088	24.387	15.686	2.05	13.00
8	25204	103659	10458	164964	9672	0.92	0.0155	24.387	14.172	0.24	1.70
9	22561	97826	4756	82269	4967	1.04	0.0279	24.387	30.285	0.82	2.70
10	15177	76048	5756	78696	5184	0.90	0.0224	24.387	21.225	0.54	2.50
11	35249	184465	11341	154826	10214	0.90	0.0144	24.387	26.168	0.43	1.60
12	17644	94344	6732	93807	5826	0.87	0.0196	24.387	21.226	0.49	2.30
13	17479	87063	6290	102392	5690	0.90	0.0212	24.387	18.758	0.45	2.40
14	21674	104024	5690	78477	4469	0.79	0.0206	24.387	25.389	0.68	2.70
15	30839	146268	10580	150297	8946	0.85	0.0143	24.387	20.068	0.35	1.70
16	41511	165012	7333	111232	6715	0.92	0.0189	24.387	33.129	0.70	2.10
17	31124	152003	12624	176755	10143	0.80	0.0124	24.387	16.85	0.27	1.60
18	58363	294283	13930	218014	13466	0.97	0.0134	24.387	31.822	0.45	1.40
19	17889	104681	6111	85742	5104	0.84	0.0211	24.387	24.867	0.64	2.60
20	16873	87112	4501	71586	4341	0.96	0.0274	24.387	28.621	0.83	2.90
21	6895	31451	2128	29949	2120	1.00	0.0493	24.387	25.514	1.28	5.00
22	25783	129675	5104	82798	4617	0.90	0.0245	24.387	34.55	0.95	2.70
23	6748	33655	2488	36095	2282	0.92	0.0418	24.387	20.856	0.97	4.60
24	9657	45411	2652	43856	2546	0.96	0.0405	24.387	24.242	1.04	4.30
Ave.	17099	141378	7948	107595	7017	0.89	0.023	22	24.24	0.61	2.61
Stdev.	11512.0	105435.7	4197.8	54914.1	3658.0	0.06	0.0153	2.2	5.664	0.308	1.763

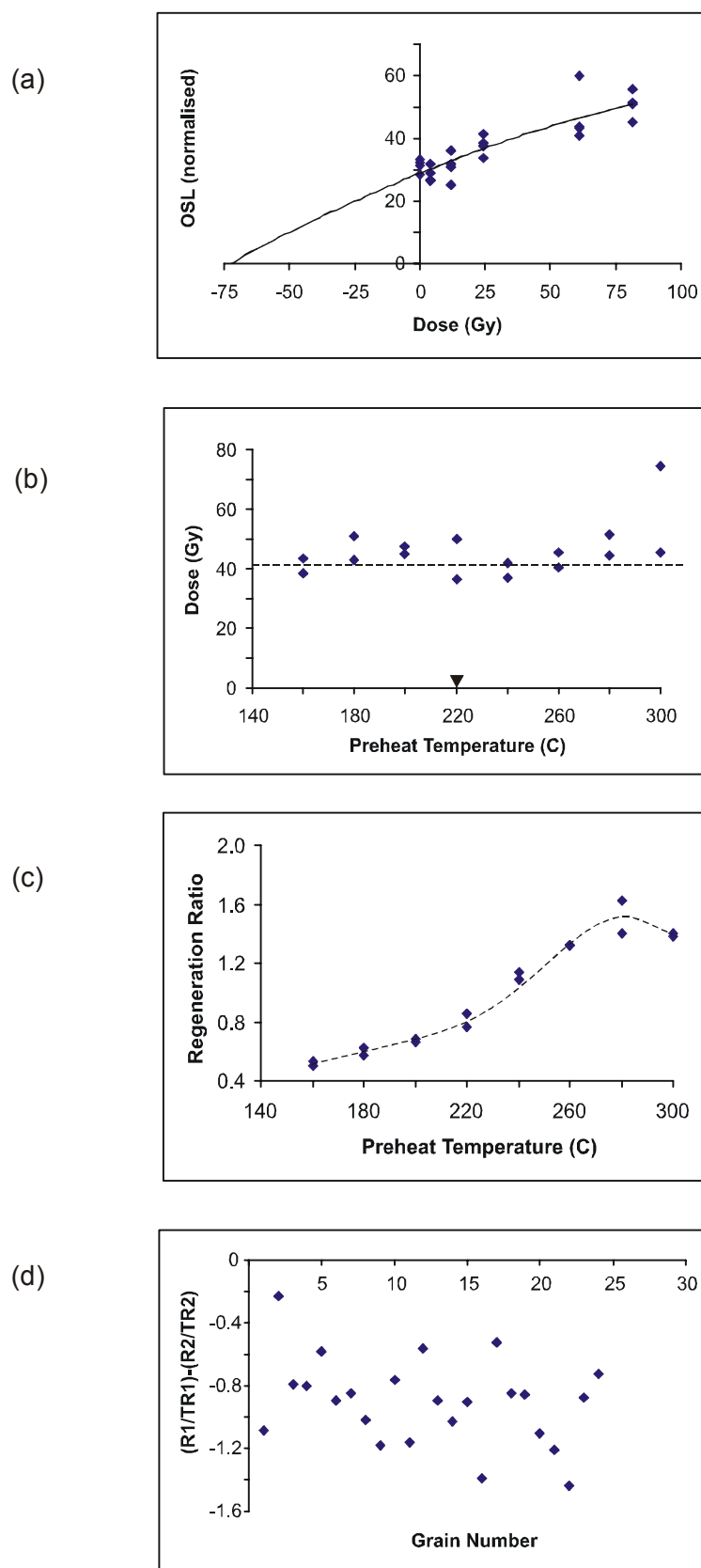


Figure A4.14 OSL results for Karl-3 sand sheet excavation at 240 cm, including: (a) MARA test, (b) preheat plateau test, (c) sensitivity test, and (d) double-regenerative test.

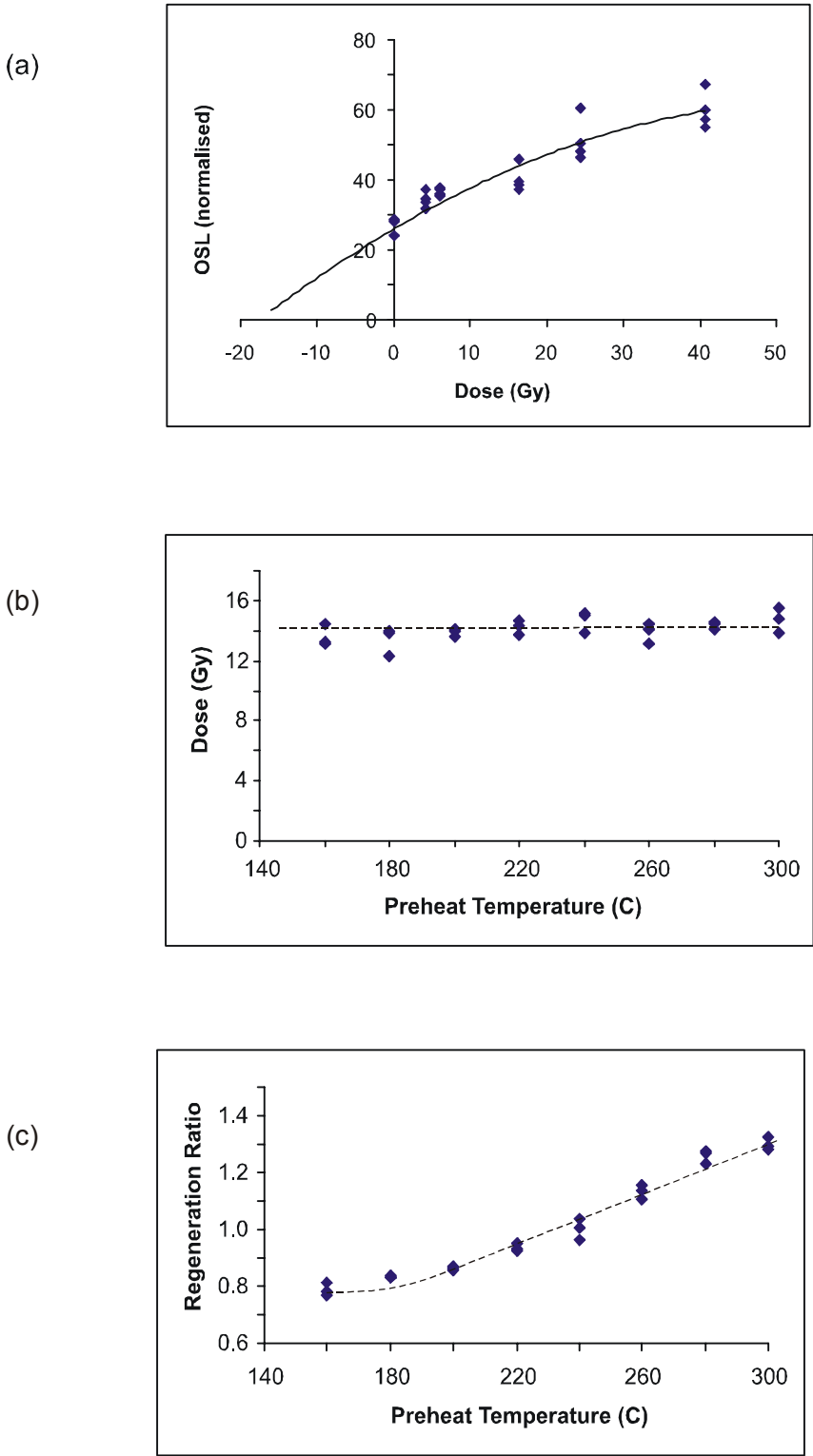


Figure A4.15 OSL results for creek profile near KR99 at 95 cm, including:
(a) MARA test, (b) preheat plateau test, and (c) sensitivity test.

Table A4.12 SAR analyses for the creek bank profile near KR99 at 95 cm depth.

wi111.DAT

kr99cp-95, 1 mm mask, Dose = 1/14.5 Gy (24/360 sec) temp. 240C

DOSE RATE (Gy/min) : 2.4387

used acquisition (ch) : 1 (1)-> 25 (25)residue (ch) : 226 (226)-> 250 (250)

No.	Nat.(1st)	Natural	Test N	Regen.	Test R	Tr/Tn	Err	Beta (Gy)	PD (Gy)	Err	(%)
1	4675	17129.4	1560.7	19942.6	1862.2	1.1932	0.0488	14.632	14.996	0.634	4.2
2	30214	110162	8958.7	110467.3	8958.2	0.9999	0.0156	14.632	14.591	0.236	1.6
3	26679	91680.7	7620	95068.2	7580.8	0.9949	0.0169	14.632	14.038	0.248	1.8
4	18171	64824.4	5760.2	69366.4	5887.2	1.0221	0.0202	14.632	13.976	0.287	2.1
5	33826	119351.4	10957.3	137535.2	11572.8	1.0562	0.0146	14.632	13.411	0.193	1.4
6	19735	74049.5	6501	78170.8	6601.8	1.0155	0.0188	14.632	14.076	0.271	1.9
7	19075	71398.4	5994.9	70576.6	5854.2	0.9765	0.0195	14.632	14.455	0.298	2.1
8	36763	132173.4	12237.5	145800	12263.4	1.0021	0.0133	14.632	13.293	0.183	1.4
9	23913	85411.3	7231.7	90119.7	7140.6	0.9874	0.0174	14.632	13.693	0.25	1.8
10	37557	149263.2	11457.7	136114.4	11432.5	0.9978	0.0137	14.632	16.01	0.228	1.4
11	37623	140646.4	11687.6	123658.6	10471.7	0.896	0.0125	14.632	14.911	0.217	1.5
12	9862	34156.9	2844.2	34559.3	2732.8	0.9609	0.0288	14.632	13.896	0.431	3.1
13	33596	128474.2	11773.2	129405.4	11032.1	0.9371	0.013	14.632	13.612	0.196	1.4
14	19922	75168.5	6425.9	72333.7	6035.5	0.9392	0.0179	14.632	14.282	0.282	2
15	11803	41807	3012	37446.1	2912.8	0.9671	0.0279	14.632	15.798	0.47	3
16	37042	137354.5	11367.3	143050.8	11476.1	1.0096	0.0138	14.632	14.184	0.201	1.4
17	38237	147336.5	11680.9	144205.2	11451	0.9803	0.0133	14.632	14.656	0.207	1.4
18	26594	92922.4	7400.5	86226.2	7165.5	0.9683	0.0169	14.632	15.268	0.276	1.8
19	8779	31087.6	2708.3	33180.3	2891	1.0675	0.0318	14.632	14.634	0.452	3.1
20	19481	71121.3	6038	71363	5922	0.9808	0.019	14.632	14.302	0.288	2
21	16239	57025.7	4970.2	60717	5043.9	1.0148	0.0217	14.632	13.946	0.31	2.2
22	44383	158734.8	12192.9	139056.5	11674.1	0.9574	0.0128	14.632	15.992	0.222	1.4
23	9396	34517.8	2762.7	33657	2764.2	1.0006	0.03	14.632	15.015	0.466	3.1
24	25292	93194.1	8110.5	99563.1	8319.8	1.0258	0.0168	14.632	14.05	0.239	1.7
Ave.	24536	89958	7552	90066	7460	0.998	0.020	14.63	14.46	0.295	2.0
Stdev.	10629	40207	3329	38946	3242	0.038	0.006	0.00	0.77	0.089	0.6

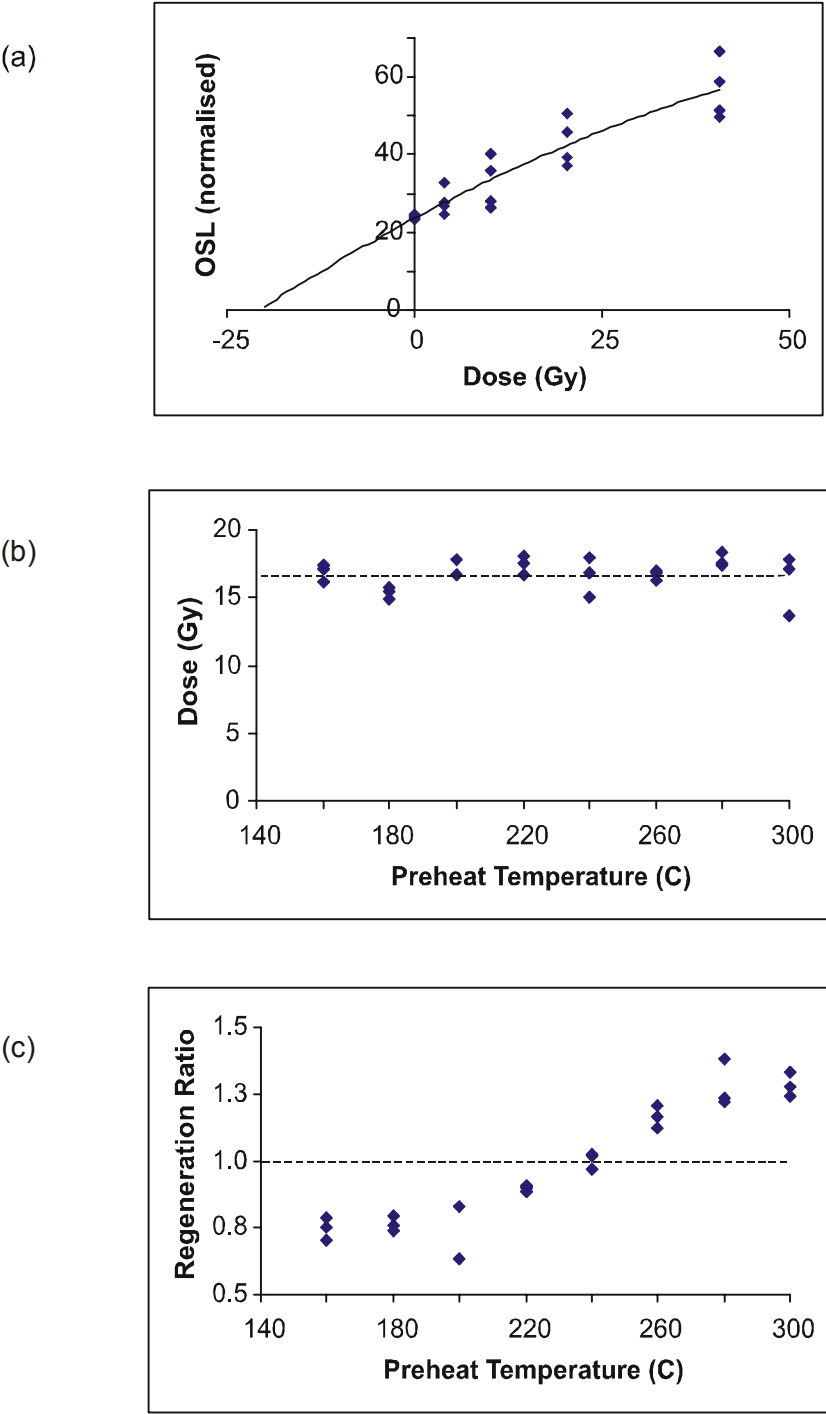


Figure A4.16 OSL results for creek profile near KR99 at 320 cm, including:
(a) MARA test, (b) preheat plateau test, and (c) sensitivity test.

Table A4.13 SAR analyses for the creek bank profile near KR99 at 320 cm depth.

WI112.DAT

kr99c0-320. 1 mm mask, Dose = 16.5 Gy (405sec) 240 C

DOSE RATE (Gy/min) : 2.4387

used acquisition (ch) : 1 (1)-> 25 (25)residue (ch) : 226 (226)-> 250 (250)

No.	Nat.(1st)	Natural	Test N	Regen.	Test R	Tr/Tn	Err	Beta (Gy)	PD (Gy)	Err	(%)
1	17132	136959	10088	122029	9513	0.943	0.016	16.461	17.42	0.30	1.7
2	42670	294874	20429	250065	19272	0.943	0.011	16.461	18.31	0.21	1.1
3	25967	234967	19452	250518	18864	0.970	0.011	16.461	14.97	0.18	1.2
4	40200	324313	25449	317574	24707	0.971	0.009	16.461	16.32	0.16	1
5	22645	146385	12107	150566	11448	0.946	0.014	16.461	15.13	0.23	1.5
6	27634	166641	14236	170589	13800	0.969	0.013	16.461	15.59	0.22	1.4
7	33113	197102	17676	212416	17474	0.989	0.012	16.461	15.10	0.19	1.2
8	35706	222763	18001	237464	18343	1.019	0.012	16.461	15.74	0.19	1.2
9	17836	120639	10619	128072	9983	0.940	0.015	16.461	14.58	0.24	1.7
10	36411	273730	18475	254639	18386	0.995	0.011	16.461	17.61	0.21	1.2
11	35932	310904	22670	282804	21682	0.956	0.010	16.461	17.31	0.19	1.1
12	15333	105324	8559	112701	9007	1.052	0.019	16.461	16.19	0.30	1.8
13	34113	249947	20331	254733	19270	0.948	0.011	16.461	15.31	0.18	1.1
14	18424	123828	9286	115698	9307	1.002	0.017	16.461	17.66	0.31	1.8
15	30013	197116	16048	203890	17110	1.066	0.013	16.461	16.97	0.22	1.3
16	8956	61362	5496	65590	5478	0.997	0.025	16.461	15.35	0.39	2.5
17	19306	126572	9886	115352	9086	0.919	0.016	16.461	16.60	0.30	1.8
18	23781	151315	11965	154183	12142	1.015	0.015	16.461	16.39	0.25	1.5
19	20674	127944	11241	147232	12324	1.096	0.017	16.461	15.68	0.25	1.6
20	28060	188261	15026	189840	15387	1.024	0.013	16.461	16.72	0.22	1.3
21	26668	171735	13182	156507	12243	0.929	0.014	16.461	16.78	0.25	1.5
22	15662	97814	8791	99590	7990	0.909	0.018	16.461	14.70	0.29	2
23	39565	253373	19817	249458	19186	0.968	0.011	16.461	16.19	0.19	1.2
Ave	26774	186255	14732	184413	14435	0.98	0.01	16.46	16.20	0.24	1.47
Stdev.	9038.0	72296.5	5144.3	66596.5	4972.3	0.05	0.00	0.00	1.01	0.05	0.36

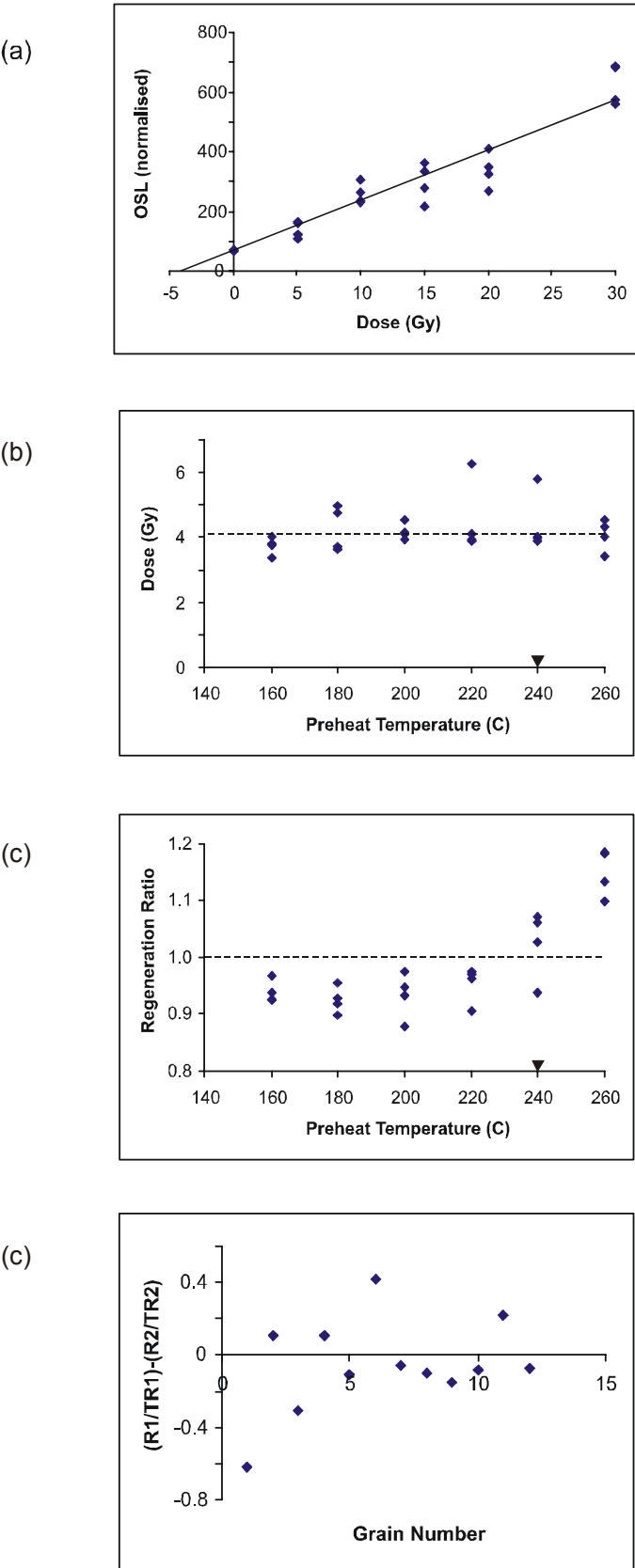


Figure A4.17 OSL results for the creek bank profile at Sandy Creek Gorge at 57 cm, including:

(a) MARA test, (b) preheat plateau test, (c) sensitivity test, and

(d) double-regenerative test.

Table A4.14 SAR analyses for creek bank profile at Sandy Creek Gorge at 57 cm depth.

wt023r1.DAT

scg-57, 1 mm mask, Dose = 1/4Gy (24/94sec) (1/5 Gy in 2002)

DOSE RATE (Gy/min) : 2.547 (2.4387 in 2002)

used acquisition (ch) : 1 (1)-> 25 (25)residue (ch) : 226 (226)-> 250 (250)

No.	Nat.(1st)	Natural	Test N	Regen.	Test R	Tr/Tn	Err	Beta (Gy)	PD (Gy)	Err	(%)
1	3497	16123.1	3068.8	11047	2865.3	0.9337	0.0274	3.821	5.206	0.097	1.8
2	7223	34402.3	6718.4	23740.7	6431.1	0.9572	0.0178	3.821	5.3	0.065	1.2
3	17882	80425.7	3810.9	13899.2	3584	0.9405	0.0243	3.821	20.791	0.32	1.6
4	551	2218.2	576.7	2321.4	629.5	1.0914	0.0952	3.821	3.985	0.24	5.9
5	1776	7971.5	2364	8631.7	2404.3	1.0171	0.034	3.821	3.589	0.079	2.2
6	1257	5383.9	1547	5047.3	1428.8	0.9236	0.0414	3.821	3.764	0.126	3.1
7	1282	5759.5	1373.8	4918.5	1323.8	0.9637	0.0462	3.821	4.311	0.135	3.1
8	3334	15835.6	2649.3	9797.6	2565.7	0.9684	0.0305	3.821	5.98	0.129	2
9	2159	10206.9	2757.6	10093.2	2681	0.9722	0.0297	3.821	3.756	0.079	2
10	2705	12398.2	3722.8	13601	3517.2	0.9448	0.0245	3.821	3.29	0.061	1.7
11	849	3765.6	1076.3	4084.7	1103.4	1.0252	0.0568	3.821	3.611	0.129	3.7
12	359	1262.9	446.5	1504.6	440.5	0.9865	0.1083	3.821	3.164	0.215	8.2
13	1166	4890.4	1176.3	4920.4	1344.3	1.1428	0.0585	3.821	4.339	0.147	3.4
14	1281	5515	1395.4	4971.7	1370.5	0.9821	0.0469	3.821	4.162	0.139	3.1
15	2586	12088.5	2085.4	7853.6	2013.2	0.9653	0.0358	3.821	5.677	0.162	2.5
16	773	3344.4	1005.2	3720.3	963	0.958	0.0569	3.821	3.29	0.126	3.7
17	2292	10131.8	1957.5	7449.8	2039.3	1.0418	0.0388	3.821	5.413	0.135	2.4
18	3003	13249.1	2366.4	8762.8	2378.3	1.005	0.0337	3.821	5.806	0.128	2.1
19	2101	9470.3	2602.5	8990.8	2612.2	1.0037	0.0319	3.821	4.039	0.089	2.1
20	1092	4482.8	1571.9	5320.3	1626	1.0344	0.0451	3.821	3.33	0.106	3.1
21	1732	7798.8	2141.4	8211.2	2170.9	1.0138	0.037	3.821	3.679	0.097	2.4
22	1863	8369	1890.9	6523.3	1815.2	0.9599	0.038	3.821	4.705	0.125	2.6
23	887	3759.6	756.5	2808.5	736.8	0.9739	0.0709	3.821	4.981	0.242	4.5
24	1438	6145.3	1391.8	4991.6	1268.7	0.9116	0.0443	3.821	4.288	0.141	3.1
1	2839	16453	5272	24015	5114	0.97	0.0241	4.877	3.241	0.088	2.7
2	4507	26296	8070	37195	7177	0.89	0.0172	4.877	3.067	0.065	2.1
3	7758	47838	15752	74956	13310	0.85	0.0112	4.877	2.63	0.038	1.5
4	7708	45150	11717	52792	11224	0.96	0.0145	4.877	3.996	0.066	1.6
5	6856	37764	9407	43534	9069	0.96	0.0166	4.877	4.079	0.076	1.9
6	7648	42351	11546	52407	11290	0.98	0.0148	4.877	3.854	0.064	1.7
7	4155	28201	9380	42989	9204	0.98	0.0167	4.877	3.14	0.059	1.9
8	5772	39492	9328	40719	8834	0.95	0.0163	4.877	4.48	0.084	1.9
9	9145	44482	4999	22753	4844	0.97	0.0251	4.877	9.24	0.252	2.7
10	10087	56474	14261	65969	13258	0.93	0.0126	4.877	3.882	0.057	1.5
11	4079	25615	7025	32735	7008	1.00	0.0203	4.877	3.807	0.085	2.2
12	9865	55018	9481	42342	8568	0.90	0.0157	4.877	5.727	0.107	1.9
13	2330	12259	3746	17845	3742	1.00	0.0311	4.877	3.347	0.113	3.4
14	9422	57218	12788	56045	11948	0.93	0.0135	4.877	4.652	0.073	1.6
15	21010	119935	17014	78990	16584	0.97	0.0118	4.877	7.218	0.094	1.3
16	4670	23390	5952	27178	5913	0.99	0.0228	4.877	4.17	0.104	2.5
17	10279	57980	12891	59305	12356	0.96	0.0137	4.877	4.571	0.071	1.6
18	9920	61821	12262	53005	11583	0.94	0.0139	4.877	5.374	0.086	1.6
19	12194	85279	21508	100244	21360	0.99	0.0104	4.877	4.121	0.048	1.2
20	5814	33333	12986	62154	12750	0.98	0.0141	4.877	2.568	0.041	1.6
21	14010	91346	20049	99219	19575	0.98	0.0107	4.877	4.384	0.052	1.2
22	11155	61026	17100	81588	17149	1.00	0.0119	4.877	3.659	0.048	1.3
23	6137	46432	9215	43715	8559	0.93	0.0164	4.877	4.812	0.091	1.9
24	1558	11303	4744	22277	4706	0.99	0.0263	4.877	2.455	0.072	2.9
Ave.	5250	29405	6603	29525	6342	0.97	0.031		4.64	0.11	2.44
Stdev.	4702.6	27612.3	5741.1	27640.9	5510.6	0.05	0.0210		2.671	0.060	1.25

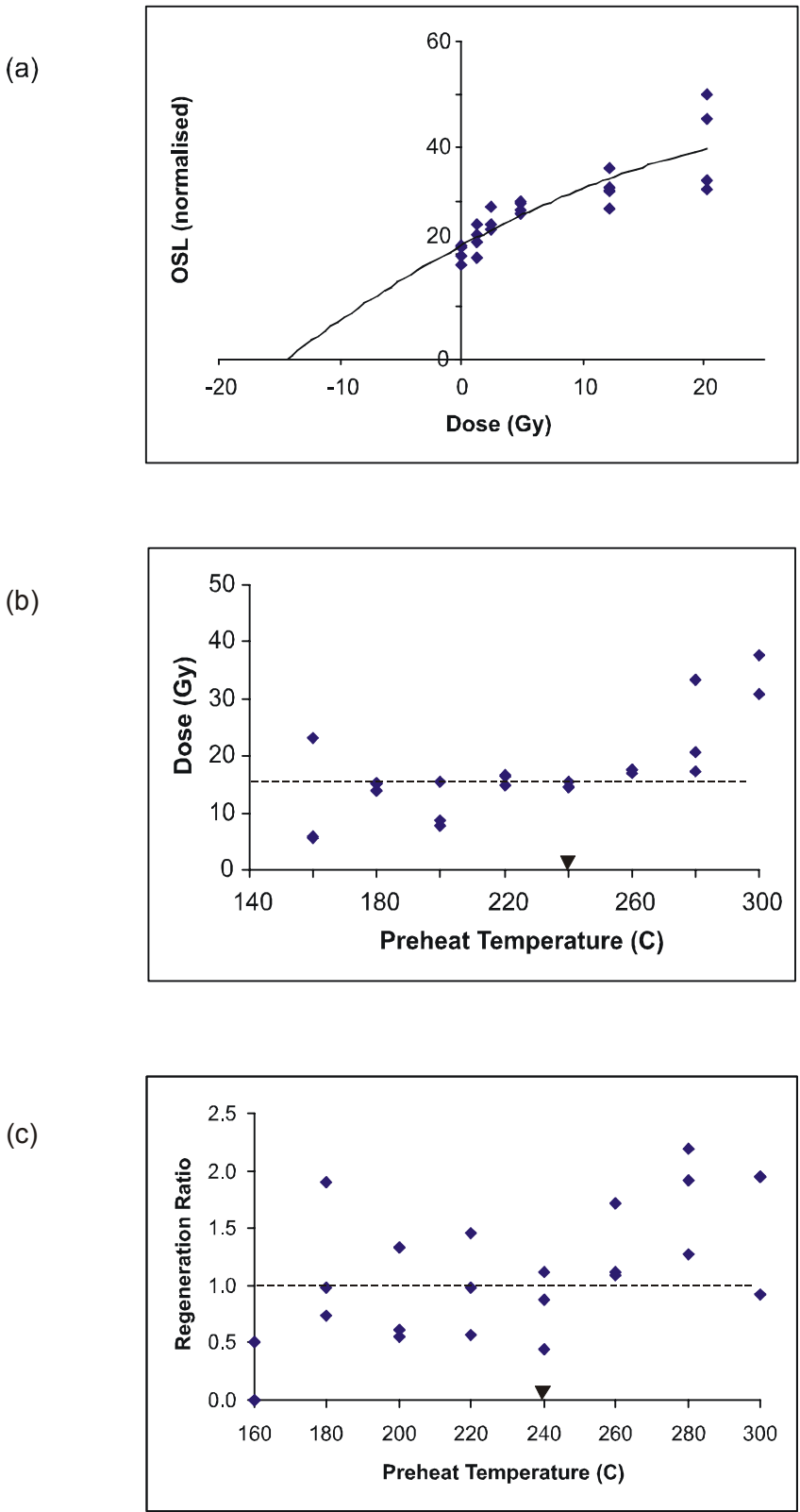


Figure A4.18 OSL results for the creek bank profile at Sandy Creek Gorge at 126 cm, including:
(a) MARA test, (b) preheat plateau test, and (c) sensitivity test.

Table A4.15 SAR analyses for creek bank profile at Sandy Creek Gorge at 126 cm depth.

iw0502.DAT

scg-126, Dose = 1/15 Gy (24/370 sec) 1 mm mask

DOSE RATE (Gy/min) : 2.4387

used acquisition (ch) : 1 (1)-> 25 (25)residue (ch) : 225 (225)-> 250 (250)

No.	Nat.(1st)	Natural	Test N	Regen.	Test R	Tr/Tn	Err	Beta (Gy)	PD (Gy)	Err	(%)
1	143	716	159	538	142	0.895	0.468	15.04	17.90	9.698	54.2
2	16405	96070	7948	93939	7759	0.976	0.019	15.04	15.01	0.300	2.0
3	84699	544909	38162	450148	34423	0.902	0.007	15.04	16.42	0.135	0.8
4	42112	209016	14376	177047	13542	0.942	0.013	15.04	16.72	0.238	1.4
5	18636	117535	8646	104774	8284	0.958	0.018	15.04	16.16	0.303	1.9
6	48242	233492	15026	178561	13401	0.892	0.012	15.04	17.54	0.242	1.4
7	54418	303476	22905	276555	21444	0.936	0.010	15.04	15.45	0.166	1.1
8	18329	121631	8711	106292	8054	0.925	0.017	15.04	15.91	0.303	1.9
9	12990	83526	7146	82702	6210	0.869	0.019	15.04	13.20	0.293	2.2
10	19548	128673	8608	102311	7717	0.896	0.017	15.04	16.96	0.327	1.9
11	41407	249132	16670	193485	14139	0.848	0.011	15.04	16.42	0.219	1.3
12	48280	256119	17607	209395	16346	0.928	0.011	15.04	17.08	0.215	1.3
13	44062	261922	19316	219052	16895	0.875	0.010	15.04	15.73	0.189	1.2
14	3681	41138	2806	33380	2382	0.849	0.035	15.04	15.74	0.665	4.2
15	28904	182883	12913	156344	11584	0.897	0.013	15.04	15.78	0.238	1.5
16	35658	215025	16493	202027	15066	0.914	0.012	15.04	14.62	0.191	1.3
17	36367	214395	16899	197404	15553	0.920	0.012	15.04	15.03	0.195	1.3
18	33304	227272	16039	183443	14157	0.883	0.012	15.04	16.45	0.221	1.3
19	29355	168018	11956	135914	10311	0.862	0.014	15.04	16.03	0.257	1.6
20	42372	240040	17862	196447	16007	0.896	0.011	15.04	16.47	0.208	1.3
21	17330	88567	5826	67752	5172	0.888	0.022	15.04	17.45	0.434	2.5
22	28752	180480	12695	148921	11797	0.929	0.014	15.04	16.94	0.258	1.5
23	54168	283420	22742	249418	20047	0.882	0.009	15.04	15.06	0.166	1.1
24	16353	91622	7305	83287	6613	0.905	0.019	15.04	14.98	0.320	2.1
1	64883	347896	23323	282356	21264	0.912	0.010	15.45	17.35	0.189	1.1
2	29009	173971	15711	200592	14759	0.939	0.012	15.45	12.58	0.167	1.3
3	72354	474136	39021	452587	34166	0.876	0.007	15.45	14.17	0.117	0.8
4	43582	247975	19781	237916	18193	0.920	0.011	15.45	14.81	0.175	1.2
5	23541	147589	11624	140171	10840	0.933	0.014	15.45	15.17	0.241	1.6
6	25294	136480	10679	131371	10057	0.942	0.015	15.45	15.11	0.254	1.7
7	71693	342310	23562	316514	22054	0.936	0.010	15.45	15.64	0.166	1.1
8	54002	278314	19664	239964	17556	0.893	0.010	15.45	15.99	0.193	1.2
9	59302	364155	24142	298105	22135	0.917	0.009	15.45	17.30	0.182	1.1
10	42245	227826	15652	185985	14371	0.918	0.012	15.45	17.37	0.234	1.3
11	143819	1108383	76328	866336	65305	0.856	0.005	15.45	16.91	0.098	0.6
12	57051	370666	26094	312405	23287	0.892	0.009	15.45	16.35	0.167	1
13	49863	308541	21832	270885	20309	0.930	0.010	15.45	16.37	0.182	1.1
14	62202	383012	23671	289489	21502	0.908	0.010	15.45	18.56	0.199	1.1
15	27328	176504	12688	154682	11547	0.910	0.014	15.45	16.04	0.244	1.5
16	48096	269414	19466	242199	18088	0.929	0.011	15.45	15.96	0.189	1.2
17	47512	246089	17620	210826	15789	0.896	0.011	15.45	16.16	0.205	1.3
18	27040	148533	13122	149714	11988	0.914	0.013	15.45	14.00	0.208	1.5
19	51538	280726	18755	215303	15899	0.848	0.010	15.45	17.07	0.212	1.2
20	83348	439739	33577	410607	31220	0.930	0.008	15.45	15.38	0.135	0.9
21	58428	329826	24827	315096	23178	0.934	0.009	15.45	15.09	0.155	1
22	24547	154648	12473	147089	11207	0.899	0.014	15.45	14.59	0.227	1.6
23	27095	184553	15276	194853	14535	0.952	0.012	15.45	13.92	0.187	1.3
24	40201	209164	14507	175115	13565	0.935	0.013	15.45	17.25	0.241	1.4
Ave.	32313	189128	17963	214360	16247	0.91	0.02	15.24	15.92	0.42	2.5
SD.	18887	110410	11695	135676	10173	0.03	0.07	0.21	1.23	1.37	7.64

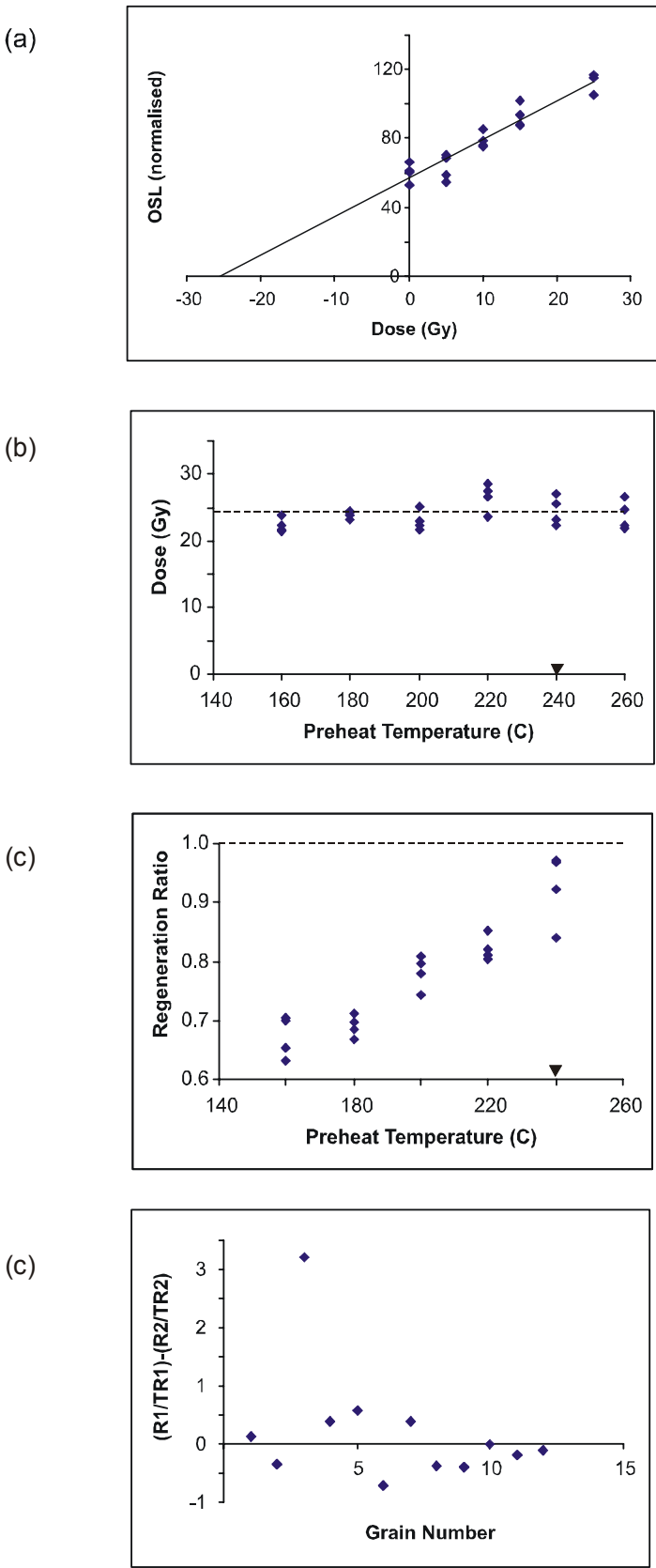


Figure A4.19 OSL results for the creek bank profile at Sandy Creek Gorge at 321 cm, including:
(a) MARA test, (b) preheat plateau test, (c) sensitivity test, and
(d) double-regenerative test.

Table A4.16 SAR analyses for creek bank profile at Sandy Creek Gorge at 321 cm depth.

wt024r1.DAT

scg-321, 1 mm mask, 1/26Gy = 24/612 sec

DOSE RATE (Gy/min) : 2.547

used acquisition (ch) : 1 (1)-> 25 (25)residue (ch) : 226 (226)-> 250 (250)

No.	Nat.(1st)	Natural	Test N	Regen.	Test R	Tr/Tn	Err	Beta (Gy)	PD (Gy)	Err	(%)
1	34763	462501	24314	435118	20390	0.84	0.009	25.979	23.16	0.249	1.1
2	8188	126740	6990	120797	5889	0.84	0.019	25.979	22.96	0.529	2.3
3	25150	378336	17207	284514	14285	0.83	0.011	25.979	28.68	0.378	1.3
4	13587	209291	11703	181182	9101	0.78	0.013	25.979	23.34	0.393	1.7
5	14296	226013	12059	178625	9510	0.79	0.013	25.979	25.92	0.429	1.7
6	10920	164121	9811	157066	8387	0.85	0.016	25.979	23.21	0.438	1.9
7	9628	146506	7521	121989	6141	0.82	0.018	25.979	25.48	0.560	2.2
8	16566	216256	11574	196246	9619	0.83	0.014	25.979	23.79	0.395	1.7
9	7589	114713	6674	103108	5542	0.83	0.020	25.979	24.00	0.579	2.4
10	13788	193816	11773	174261	10044	0.85	0.014	25.979	24.65	0.410	1.7
11	24957	358446	21416	369538	18850	0.88	0.010	25.979	22.18	0.255	1.1
12	51370	679977	24936	420408	20903	0.84	0.009	25.979	35.22	0.371	1.1
13	9605	140228	9122	134722	7869	0.86	0.017	25.979	23.33	0.457	2
14	7871	108687	7397	116950	6782	0.92	0.020	25.979	22.14	0.495	2.2
15	34869	477708	24278	401245	20832	0.86	0.009	25.979	26.54	0.282	1.1
16	11842	166018	9046	126603	6615	0.73	0.015	25.979	24.91	0.504	2
17	13026	174111	8605	136030	7515	0.87	0.017	25.979	29.04	0.580	2
18	9797	142952	7896	135009	6791	0.86	0.018	25.979	23.66	0.499	2.1
19	34047	504715	22823	365191	19165	0.84	0.009	25.979	30.15	0.339	1.1
20	51263	850760	51339	728388	41193	0.80	0.006	25.979	24.35	0.180	0.7
21	19823	320297	15088	221084	11880	0.79	0.011	25.979	29.64	0.432	1.5
22	15781	238259	14200	254659	12672	0.89	0.013	25.979	21.69	0.310	1.4
23	11152	176169	10158	160189	8923	0.88	0.016	25.979	25.10	0.458	1.8
24	19187	282136	14302	242686	12051	0.84	0.012	25.979	25.45	0.374	1.5
1	11614	53864.2	3143.7	57134.3	2739.3	0.8714	0.0265	24.875	20.434	0.633	3.1
2	38931	181797.2	9162.8	158882.3	7802.5	0.8515	0.0141	24.875	24.237	0.409	1.7
3	52529	242163.3	12965.9	227480.5	11537.4	0.8898	0.012	24.875	23.563	0.324	1.4
4	37450	171941.4	9148.9	145275	7524.6	0.8225	0.0136	24.875	24.214	0.411	1.7
5	6728	30982.1	1698.8	28318.6	1339	0.7882	0.0354	24.875	21.45	0.98	4.6
6	18168	85658.4	4518.2	75579	3738.2	0.8274	0.0204	24.875	23.325	0.586	2.5
7	11766	54741	2816.7	50234.2	2603.2	0.9242	0.0287	24.875	25.052	0.794	3.2
8	30209	138568	7049.8	136831.9	5947.5	0.8436	0.0159	24.875	21.252	0.408	1.9
9	8346	37861.1	1913.4	36523.2	1756.6	0.918	0.0362	24.875	23.673	0.95	4
10	12092	54479.5	2940.3	52894	2512.7	0.8546	0.0264	24.875	21.894	0.689	3.1
11	16883	79385.5	4279.5	66902.4	3161.7	0.7388	0.0195	24.875	21.807	0.588	2.7
12	8935	41014	2175	36894.4	1867.2	0.8585	0.0321	24.875	23.739	0.904	3.8
13	11226	52251.6	2520	41530.7	1991.9	0.7904	0.0279	24.875	24.737	0.889	3.6
14	13436	61602	3119.5	52607	2588.3	0.8297	0.0252	24.875	24.168	0.749	3.1
15	22800	105410.4	5506.7	96221.2	4578.3	0.8314	0.018	24.875	22.656	0.502	2.2
16	12660	59071.9	3412.9	56220.5	2850.1	0.8351	0.024	24.875	21.826	0.641	2.9
17	9910	45429.2	2195.4	36570.4	1788.7	0.8147	0.0313	24.875	25.175	0.982	3.9
18	11009	51777.4	2950.4	52631.7	2516.3	0.8529	0.0268	24.875	20.871	0.668	3.2
19	14352	67081.3	4178.7	70376.2	3514.9	0.8411	0.0214	24.875	19.944	0.518	2.6
20	33838	158886.7	8766.8	143696	7224.1	0.824	0.014	24.875	22.664	0.395	1.7
21	28515	132608	6502.5	104977.9	5246.4	0.8068	0.0162	24.875	25.352	0.521	2.1
22	31364	144070.7	7693.8	129579.7	6496.2	0.8443	0.0153	24.875	23.351	0.433	1.9
23	4817	22044.9	1291.9	21372.7	1148.6	0.8891	0.048	24.875	22.811	1.252	5.5
24	21979	104474.5	5643.7	96860.5	4773.3	0.8458	0.0182	24.875	22.692	0.499	2.2
Ave.	19555	188248	9913	161275	8296	0.84	0.019		24.16	0.534	2.3
Stdev.	12476.0	170272.1	8817.3	135634.6	7255.8	0.040	0.0085		2.745	0.2200	0.99

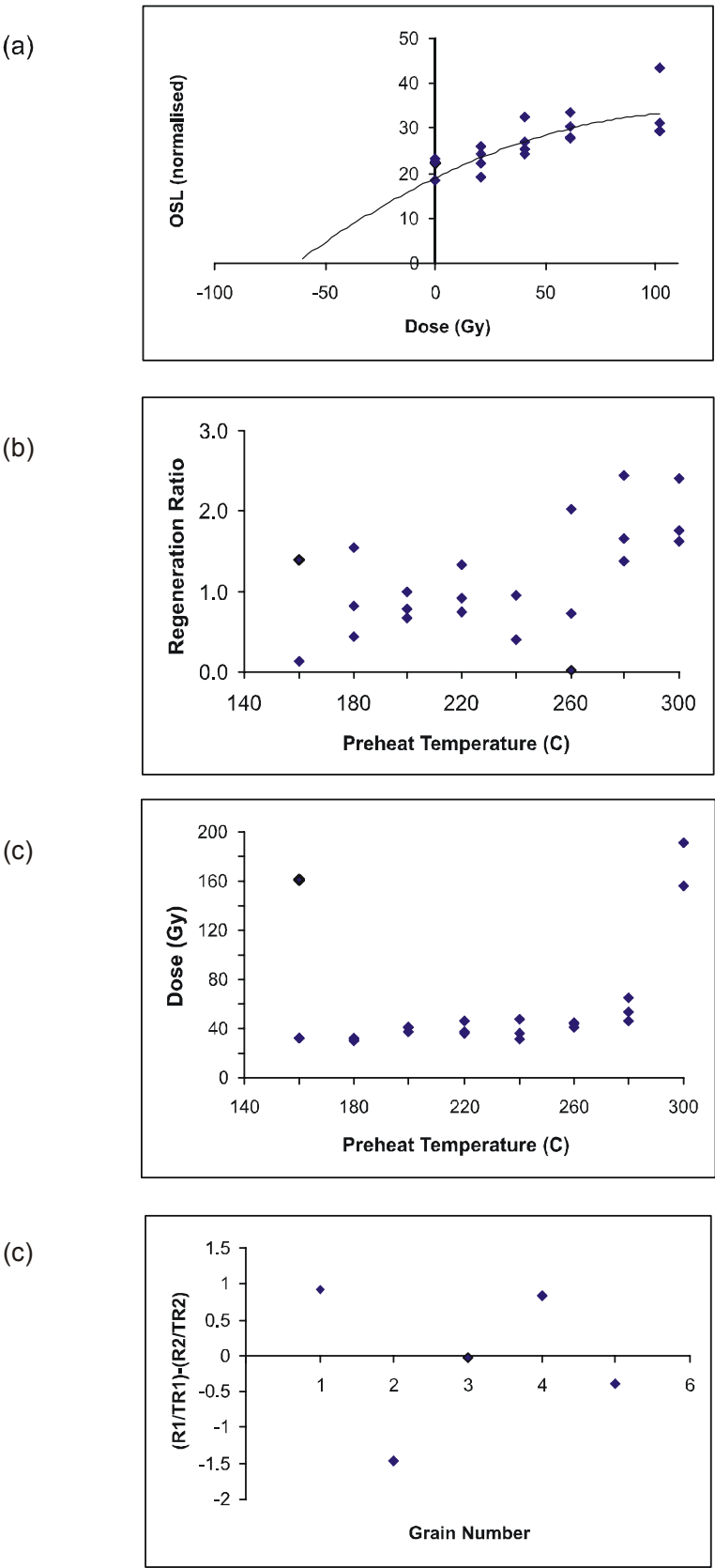


Figure A4.19 OSL results for the creek bank profile at Sandy Creek Gorge at 357 cm, including:
(a) MARA test, (b) preheat plateau test, and (c) sensitivity test.

Table A4.17 (a) SAR analyses for the creek bank profile at Sandy Creek Gorge at 357 cm depth.

iw1502.DAT

scg-357, 1 mm mask, 2/40 Gy (50/900 sec)

DOSE RATE (Gy/min) : 2.4387

used acquisition (ch) : 1 (1)-> 25 (25)residue (ch) : 226 (226)-> 250 (250)

No.	Nat.(1st)	Natural	Test N	Regen.	Test R	Tr/Tn	Err	Beta (Gy)	PD (Gy)	Err	BIN	(%)
1	279755	1741336	124721	1182657	91080	0.7303	0.0033	36.58	39.33	0.184	30	0.5
2	546713	3149720	203258	2116099	158251	0.7786	0.0027	36.58	42.39	0.153	30.75	0.4
3	151466	875463	63703	614450	48043	0.7542	0.0048	36.58	39.31	0.26	31.5	0.7
4	765154	4656182	329961	3200555	255351	0.7739	0.0021	36.58	41.18	0.116	32.25	0.3
5	730889	4173666	303702	3067894	241183	0.7941	0.0023	36.58	39.52	0.116	33	0.3
6	75878	403295	31442	339941	25714	0.8178	0.0074	36.58	35.49	0.333	33.75	0.9
7	119414	708689	47840	530824	38721	0.8094	0.0059	36.58	39.53	0.296	34.5	0.7
8	120489	665007	44018	437592	34896	0.7928	0.0061	36.58	44.07	0.352	35.25	0.8
9	82784	466921	34889	327566	28056	0.8042	0.0069	36.58	41.93	0.374	36	0.9
10	147641	769670	45276	484318	37588	0.8302	0.0062	36.58	48.26	0.371	36.75	0.8
11	288492	1630894	102800	1037849	81684	0.7946	0.0039	36.58	45.68	0.232	37.5	0.5
12	121951	713164	59390	645196	49851	0.8394	0.0054	36.58	33.94	0.226	38.25	0.7
13	185331	884836	63575	631990	50704	0.7975	0.005	36.58	40.85	0.267	39	0.7
14	613950	3085263	192907	2032358	161871	0.8391	0.0029	36.58	46.60	0.169	39.75	0.4
15	334582	2109816	165211	1597744	106190	0.6428	0.0027	36.58	31.05	0.132	40.5	0.4
16	111468	638026	44340	460917	36051	0.8131	0.0062	36.58	41.17	0.322	41.25	0.8
17	313742	1624934	103970	1081202	87055	0.8373	0.0041	36.58	46.03	0.23	42	0.5
18	71161	430631	31211	330921	25598	0.8202	0.0074	36.58	39.04	0.366	42.75	0.9
19	87586	713197	46046	481885	36967	0.8028	0.0059	36.58	43.47	0.33	43.5	0.8
20	182522	871560	56635	577031	45904	0.8105	0.0054	36.58	44.78	0.305	44.25	0.7
21	328848	1963536	143978	1392763	110579	0.768	0.0032	36.58	39.61	0.171	45	0.4
22	186708	1017151	81696	802145	68965	0.8442	0.0046	36.58	39.16	0.22	45.75	0.6
23	77558	365857	26325	277642	22474	0.8537	0.0085	36.58	41.15	0.422	46.5	1
24	167223	951250	65759	627705	49209	0.7483	0.0047	36.58	41.48	0.27	47.25	0.7
Ave.	253804	1442086	100527	1011635	78833	0.796	0.005	36.58	41.04	0.26		0.6
Stdev.	207695	1201038	83958	833148	65133.0	0.0455	0.0018	0	3.970	0.090		0.21

Table A4.18 (b) Bracketed SAR analyses for creek bank profile at Sandy Creek Gorge at 357 cm,
analysed with the “Analyst” program.

Analyst data = 0.5 mm aliquot

WI119

R1 < N < R2 = 20 < 40 < 60 Gy

Disc#	N.Signal	BG.signal	Test_Signa	Signal_Ch	ED	ED_Err
1	1379221	928	56992	0.98	34.8	0.2
2	1315438	838	45788	1.03	38	0.5
3	778884	716	31655	1.01	37.2	0.4
5	1559202	845	42688	0.95	56.5	0.5
6	1567063	970	55248	0.94	43.1	0.4
7	1726066	885	49049	0.9	54.3	0.4
8	691500	578	27917	1.09	35.9	0.5
9	1115203	996	34530	0.95	50.7	0.6
10	1577232	978	54707	0.97	40.5	0.4
11	1463657	928	46580	0.94	50.3	0.5
12	1012424	723	40029	1	34.7	0.3
13	1333036	1037	49738	0.97	38.3	0.3
15	1117082	673	41774	0.95	41.5	0.7
16	1216706	690	38101	0.9	51.5	0.4
17	1763296	886	58828	0.7	43	0.3
18	2023654	1203	61721	0.92	49.1	0.5
19	3036795	1430	57138	0.83	75.9	0.6
20	2194205	1210	68469	0.91	46.7	0.5
21	1305365	930	50990	0.99	36.7	0.4
22	2186396	1318	57541	0.89	68.2	0.7
23	1574561	928	51848	0.95	47.4	0.4
24	1095956	667	28879	0.93	59.7	1
Ave.					47.0	0.5
Stdev.					10.96	0.17

A4.4 Dose Rate Determinations

A4.4.1 Methods

Facilities and academic support for cosmogenic isotope dating were provided by ANSTO. Sample processing includes sample preparation, high-resolution gamma spectroscopy and alpha-particle spectrometry, and data analysis. Sample chemistry follows the methods outlined by Gilmore and Hemingway (1995), and follows a sequential purification and solvent extraction as outlined in the following flow chart. Measurement of isotopic concentrations of ^{236}U and ^{238}Th on all samples were made using high-resolution gamma spectroscopy and alpha-particle spectrometry, with analytical uncertainties of 5 % based on counting statistics, variability in machine response and uncertainty in blank corrections.

PRETREATMENT	Ash
DISSOLUTION	Dissolution
CONCENTRATION	Coprecipitation
CLARIFY	Centrifuge/Filter
SEPARATION	Anion exchange column => Remove Th and Ra
ISOLATION	U Electrodeposition
ANALYSIS	Alpha Spectrometry

The paucity of heavy minerals (< 5%) is unlikely to influence dose rate, hence heavy liquid separation was considered unnecessary. However, for correct evaluation of the past dose rate it is necessary to know the past water content. An average value of $5 \pm 2\%$ is usually used but any underestimate of this value will result in an underestimate of the age by a similar percentage multiplied by about 0.8 (Huntley et al., 1994).

A4.4.2

Raw Results for U and Th Analyses

Client	Ingrid Ward
Project	2001rc0052

ANSTO Sample ID	Client Sample ID		U-238 (alpha) (Th-234/Pa-234m)	U-238 (gamma) (Th-234/Pa-234m)	Ra-226 (Pb-214/Bi-214)	Pb-210	Ra-228 (Ac-228)	Th-228 (alpha) (Bi-212/Tl-208)	Th-228 (gamma) (Bi-212/Tl-208)	K-40
b770	Goor-2-20	Activity (Bq/g)	0.0024700	0.0126675	0.0199813	0.0123053	0.0107302	0.0090435	0.0090400	0.0078591
		Uncertainty (1s)	0.0001800	0.0062379	0.0006060	0.0032325	0.0016465	0.0024677	0.0024700	0.0011063
		Uncertainty (%)	49.2	49.2	3.0	26.3	15.3	27.3		14.1
b771	Goor-1-220	Activity (Bq/g)	0.0027300	0.0097591	0.0149470	0.0129518	0.0183023	0.0034800	0.0034800	0.0027216
		Uncertainty (1s)	0.0001100	0.0086926	0.0010942	0.0060081	0.0032895	0.0056343	0.0056300	0.0024965
		Uncertainty (%)	89.1	89.1	7.3	46.4	18.0	161.9		91.7
b772	Karl-1-27	Activity (Bq/g)	0.0053100	0.0212247	0.0279817	0.0412216	0.0209756	0.0087157	0.0087200	0.0080303
		Uncertainty (1s)	0.0002100	0.0086252	0.0024689	0.0069862	0.0032455	0.0051879	0.0051900	0.0023279
		Uncertainty (%)	40.6	40.6	8.8	16.9	15.5	59.5		29.0
b773	Karl-3-90	Activity (Bq/g)	0.0041200	0.0134923	0.0145478	0.0115563	0.0153018	0.0133823	0.0133800	0.0044929
		Uncertainty (1s)	0.0001600	0.0091579	0.0007277	0.0032181	0.0015170	0.0023106	0.0023100	0.0010066
		Uncertainty (%)	67.9	67.9	5.0	27.8	9.9	17.3		22.4
b774	Karl-3-150	Activity (Bq/g)	0.0041200	0.0256300	0.0131988	0.0138605	0.0176905	0.0162166	0.0162200	0.0052008
		Uncertainty (1s)	0.0001000	0.0087625	0.0009966	0.0033073	0.0014755	0.0023260	0.0023300	0.0010074
		Uncertainty (%)	34.2	34.2	7.6	23.9	8.3	14.3		19.4
b775	Karl-3-210	Activity (Bq/g)	0.0046500	0.0186536	0.0146941	0.0132537	0.0186696	0.0151807	0.0151800	0.0024158
		Uncertainty (1s)	0.0002800	0.0042042	0.0006759	0.0031010	0.0012467	0.0024844	0.0024800	0.0009477
		Uncertainty (%)	22.5	22.5	4.6	23.4	6.7	16.4		39.2
b776	Scg-57	Activity (Bq/g)	0.0062800	0.0306979	0.0263038	0.0249229	0.0347917	0.0338934	0.0338900	0.0567333
		Uncertainty (1s)	0.0003700	0.0059082	0.0011145	0.0043482	0.0018173	0.0026763	0.0026800	0.0016085
		Uncertainty (%)	19.2	19.2	4.2	17.4	5.2	7.9		2.8
b777	Scg-126	Activity (Bq/g)	0.0075800	0.0338592	0.0259596	0.0149653	0.0415429	0.0380043	0.0380000	0.0681482
		Uncertainty (1s)	0.0006200	0.0093015	0.0007187	0.0046756	0.0021630	0.0028713	0.0028700	0.0017950
		Uncertainty (%)	27.5	27.5	2.8	31.2	5.2	7.6		2.6
b778	Scg-357	Activity (Bq/g)	0.0084000	0.0419622	0.0286604	0.0244357	0.0431187	0.0399883	0.0399900	0.0480062
		Uncertainty (1s)	0.0005200	0.0055471	0.0010944	0.0043858	0.0018354	0.0024807	0.0024800	0.0010933
		Uncertainty (%)	13.2	13.2	3.8	17.9	4.3	6.2		2.3
b779	Jg-1-250	Activity (Bq/g)	0.0029100	0.0127951	0.0135480	0.0120093	0.0208191	0.0221625	0.0221600	0.0068166
		Uncertainty (1s)	0.0001700	0.0074326	0.0005096	0.0029718	0.0014989	0.0020806	0.0020800	0.0009605
		Uncertainty (%)	58.1	58.1	3.8	24.7	7.2	9.4		14.1
b780	Jg-1-450	Activity (Bq/g)	0.0032000	0.0102633	0.0144860	0.0133743	0.0248607	0.0137661	0.0137700	0.0059689
		Uncertainty (1s)	0.0001700	0.0082076	0.0005896	0.0036649	0.0016031	0.0025589	0.0025600	0.0009746
		Uncertainty (%)	80.0	80.0	4.1	27.4	6.4	18.6		16.3
b781	Jg-1-550	Activity (Bq/g)	0.0059500	0.0127146	0.0151284	0.0136984	0.0234943	0.0227137	0.0227100	0.0053630
		Uncertainty (1s)	0.0003300	0.0034762	0.0004302	0.0026722	0.0012830	0.0018086	0.0018100	0.0008039
		Uncertainty (%)	27.3	27.3	2.8	19.5	5.5	8.0		15.0

Table A4.18 Alpha-spectrometry and gamma spectroscopy results (supplied by ANSTO).

A4.4.3 U-series dating of pisolites

Chemical preparation for U-series dating of the pisolite samples from Jinnium and Sandy Creek Gorge follow are similar to that used for dose rate determinations. Raw results as provided by ANSTO are presented overleaf.

Environmental Radiochemistry Laboratory

Building 34

Australian Nuclear Science & Technology Organisation

PMB 1 Menai NSW 2234

Tel: (02) 9717 3209

Fax: (02) 9717 9270

Contact Officer: **Henk Heijnis****Ansto**

1-Aug-01

Certificate of Analysis

Client Name:	Ingrid Ward
Client Institution:	Uni of Wollongong
Client Project:	261 (70-90m)
Project Code:	2001RC0052
Sample ID:	ANSTO B769

Sample Description:	Ferricrete Selective
Mass analysed (g):	4.3306
Organic Content (%):	0.0
Uranium conc. (ppm):	0.9958 0.0393
Thorium conc. (ppm):	8.9072 0.2604

Mass of U-236 tracer added (g):	0.10287
Activity of U-236 tracer (dpm):	9.48461
Chemical yield of U-236 tracer (%):	41.3
Count time for uranium spectrum (s):	193240.3

Mass of Th-229 tracer added (g):	0.11245
Activity of Th-229 tracer (dpm):	10.08156
Chemical yield of Th-229 tracer (%):	54.0
Count time for thorium spectrum (s):	166202

Isotope	Gross Counts	Specific Activity (dpm/g)	Specific Act. Error (dpm/g)
U-238	1094	0.73897	0.02919
U-236	3203	tracer	
U-234	1559	1.07890	0.03864

Isotope	Gross Counts	Specific Activity (dpm/g)	Specific Act. Error (dpm/g)
Th-232	3466	2.17605	0.06362
Th-230	1658	1.02616	0.03564
Th-229	3708	tracer	
Th-228	3348	2.02667	0.06063

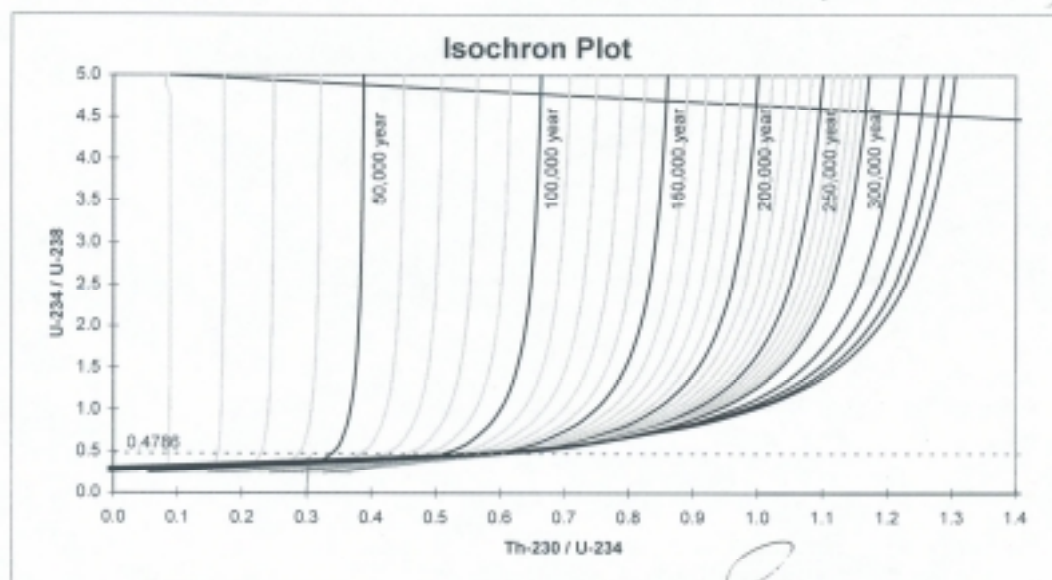
Isotope Ratio	Value	Error
U-234 / Th-232	0.49581	0.02292
U-238 / Th-232	0.33959	0.01669
Th-230 / Th-232	0.47157	0.02141
Th-230 / U-234	0.95111	0.04745
U-234 / U-238	1.46002	0.07785

Calculated Age

Age (year) = > 350 ka plus minus n/a

Precision = 5,000 years

This sample seems to be an c. 100 ka



Environmental Radiochemistry Laboratory

Building 34

Australian Nuclear Science & Technology Organisation

PMB 1 Menai NSW 2234

Tel: (02) 9717 3209

Fax: (02) 9717 9270

Contact Officer: **Henk Heijnis**

1-Aug-01

Certificate of Analysis

Client Name:	Ingrid Ward
Client Institution:	Uni of Wollongong
Client Project:	<i>Sandy Creek Gorge</i>
Project Code:	2001RC0052
Sample ID:	ANSTO B768

Sample Description:	Ferricrete Selective
Mass analysed (g):	5.5944
Organic Content (%):	0.0
Uranium conc. (ppm):	6.2394 0.2089
Thorium conc. (ppm):	4.5364 0.1979

Mass of U-236 tracer added (g):	0.10883
Activity of U-236 tracer (dpm):	10.03413
Chemical yield of U-236 tracer (%):	61.4
Count time for uranium spectrum (s):	74240.8

Mass of Th-229 tracer added (g):	0.11595
Activity of Th-229 tracer (dpm):	10.39976
Chemical yield of Th-229 tracer (%):	57.6
Count time for thorium spectrum (s):	67981.3

Isotope	Gross Counts	Specific Activity (dpm/g)	Specific Act. Error (dpm/g)
U-238	5037	4.63009	0.15350
U-236	2122	tracer	
U-234	10470	9.85300	0.31088

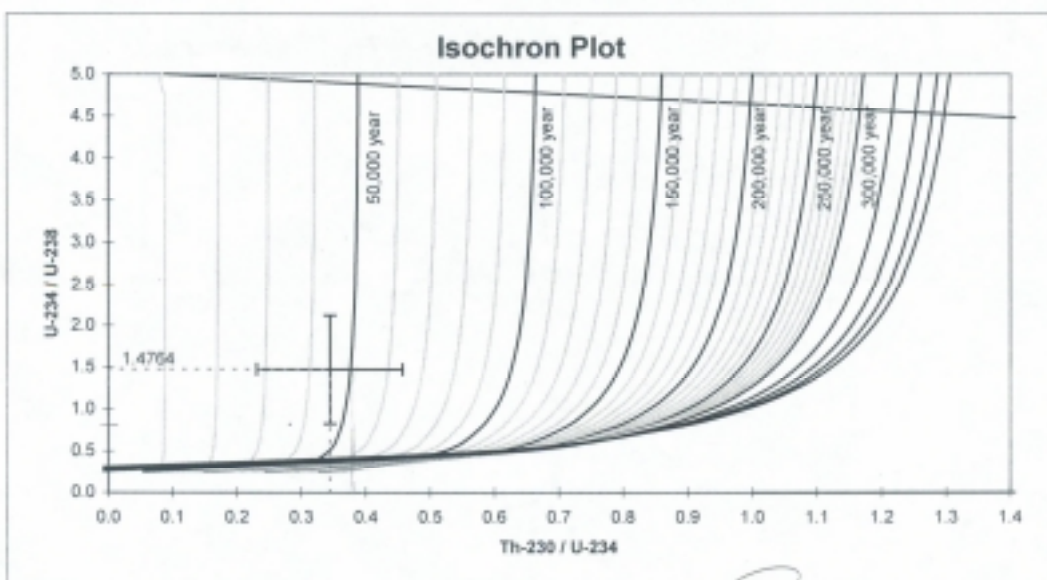
Isotope	Gross Counts	Specific Activity (dpm/g)	Specific Act. Error (dpm/g)
Th-232	995	1.10825	0.04834
Th-230	3544	3.93592	0.13555
Th-229	1669	tracer	
Th-228	1386	1.49233	0.06120

Isotope Ratio	Value	Error
U-234 / Th-232	8.89062	0.47862
U-238 / Th-232	4.17785	0.22890
Th-230 / Th-232	3.55149	0.19738
Th-230 / U-234	0.39946	0.01866
U-234 / U-238	2.12804	0.09739

Calculated Age

Age (year) = 45,000 plus 20,000
 minus 15,000

Precision = 5,000 years



A5 APPENDIX FIVE - ARCHAEOLOGY

A5.1 Radiocarbon Results

Table A5.1 Results of radiocarbon analyses. Charcoal samples were prepared by Dr. John Head, and analysed at Waikato Dating Laboratory ('Wk' lab codes) and at ANSTO, Lucas Heights ('OZG' lab codes).

Lab Code	Sample ID	Sample Material	$\delta^{14}\text{C}$ ‰	$\delta^{13}\text{C}$ ‰	D^{14}C ‰	Modern %	Result BP
Wk10780	Goor-1 Spit 21	Charcoal	-271.9 ± 1.8	-25.8 ± 0.2	-270.7 ± 9.5	-72.9 ± 0.9	2536 ± 105
Wk10781	Goor-2.1 Spit 3	Charcoal	-17.3 ± 4.5	25.6 ± 0.2	-16.1 ± 5.5	98.4 ± 0.5	Modern
Wk10782	Goor-2.1 Spit 11	Charcoal	-31.8 ± 8.5	-23.4 ± 0.2	-34.9 ± 8.5	96.5 ± 0.8	286 ± 71
Wk10783	Karl 1 Spit 3	Charcoal	-60.9 ± 4.3	-26.3 ± 0.2	-58.4 ± 5.3	94.2 ± 0.5	484 ± 45
Wk10784	Karl 1 Spit 12	Charcoal	-109.3 ± 6.8	-25.8 ± 0.2	-107.9 ± 8.4	89.2 ± 0.8	917 ± 76
Wk10788	Karl 3 Spit 17	Charcoal	-83.2 ± 6.5	-24.4 ± 0.2	-84.4 ± 6.5	91.6 ± 0.7	708 ± 57
Wk10789	Karl 3 Spit 20	Charcoal	-362.3 ± 7.9	-24.7 ± 0.2	-362.7 ± 9.6	63.7 ± 1.0	3619 ± 122
OZG337	Goor 1 Spit 21*	Charcoal	-	-25.0	-	70.8 ± 0.3	2780 ± 40
OZG338	Karl 1 Spit 12*	Charcoal	-	-25.0	-	60.2 ± 0.3	4080 ± 40
OZG339	Goor 1 Spit 35	Charcoal	-	-25.0	-	63.2 ± 0.4	3680 ± 50
OZG340	Karl 3 Spit 31	Charcoal	-	-25.0	-	70.5 ± 0.3	2810 ± 40

* Comprises soluble fraction (in NaOH).

A5.2 Stone Artefact Records

Table A5.1 Artefact analyses for Jinmium and Goorurarmum excavations (provided by R. Fullagar, pers. comm., 2002).

Jinmium - CI-1

SPIT	STRATI- GRAPHIC UNITS	Depth (cm)	volume in litres	> 4mm Sum of all artefact counts	> 4mm Sum of all artefact weights (g)	2-4mm Sum of all artefact counts	2-4mm Sum of all artefact weights (g)	Artefact density (g/l)	No. > 4 mm /litre	No. 2 - 4 mm /litre
7		5	54	95	62	33	5	1.24	1.76	0.61
6		10	59	60	26	53	2	0.47	1.02	0.90
5		25	176	584	314	409	16	1.88	3.32	2.32
4		40	92	937	803	624	31	9.07	10.18	6.78
3		60	112	752	657	906	19	6.04	6.71	8.09
2		75	36	82	71	113	30	2.81	2.28	3.14
1		100	71	351	1236	335	7	17.51	4.94	4.72

Goorurarmum - Goor-2

SPIT	STRATI- GRAPHIC UNITS	average depth below surface (m)	estimated corrected thickness (m)	Depth (cm)	volume in litres	weight in kg	estimated area excavated (m)	Sum of all artefact counts	Sum of all artefact weights (g)	Number of artefacts /litre	Artefact density (g/l)
SURFACE		0									
1	4	0.015	0.015	1.5	23.25	35	1.00	104	69.90	4.47	3.01
2	4	0.038	0.023	3.8	18.50	27.75	1.00	63	35.80	3.41	1.94
3	4	0.074	0.036	7.4	22.50	34	1.00	82	50.20	3.64	2.23
4	3	0.097	0.023	9.7	29.50	38.7	1.00	88	63.60	2.98	2.16
5	3	0.119	0.022	11.9	22.30	31.5	1.00	63	25.30	2.83	1.13
6		0.135	0.016	13.5	21.50	26.48	1.00	57	25.70	2.65	1.20
7	2	0.152	0.017	15.2	31.00	39.5	1.00	58	77.60	1.87	2.50
8	2	0.176	0.024	17.6	29.50	36.5	0.50	39	17.40	1.32	0.59
8 termite	2	0.176	0.024	17.6	5.00	7.5	0.50	12	89.70	2.40	17.94
9	2	0.224	0.046	22.4	27.70	31	1.00	47	26.70	1.70	0.96
10	2	0.246	0.022	24.6	9.25	10.5	0.40	20	30.70	2.16	3.32
0 Feature A	2	0.246	0.022	24.6	4.00	5	0.10	9	3.50	2.25	0.88
10 termite	2	0.246	0.022	24.6	6.50	10	0.50	8	4.40	1.23	0.68
11	2	0.273	0.027	27.3	8.50	13	1.00	22	13.10	2.59	1.54
12	1	0.335	0.062	33.5	26.00	40.7	1.00	10	5.90	0.38	0.23

Goorurarmum - Goor-1

SPIT	STRATI- GRAPHIC UNITS	average depth below surface (m)	Depth (cm)	estimated corrected thickness (m)	volume in litres	weight in kg	estimated area excavated (m)	> 4mm Sum of all artefact counts	> 4mm Sum of all artefact weights (g)	2-4mm Sum of all artefact counts	2-4mm Sum of all artefact weights (g)	Artefact density (g/l)	No. > 4 mm /litre	No. 2 - 4 mm /litre	Total Artefact Counts per litre
SURFACE															
1		0.008	0.80	0.008	10	10.5	1.000	2	4.40	11.00	0.60	0.50	0.20	1.10	1.30
2		0.050	5.00	0.042	48.500	71.100	1.000	9	1.90	75.00	3.20	0.11	0.19	1.55	1.73
3		0.101	10.10	0.051	55.200	83.250	1.000	42	11.70	273.00	1204.00	22.02	0.76	4.95	5.71
4		0.164	16.40	0.063	44.900	65.500	1.000	62	24.50	311.00	16.70	0.92	1.38	6.93	8.31
5		0.214	21.40	0.050	50.800	72.500	1.000	62	44.80	304.00	14.30	1.16	1.22	5.98	7.20
6		0.248	24.80	0.034	50.100	73.900	1.000	29	311.60	447.00	20.80	6.63	0.58	8.92	9.50
7		0.288	28.80	0.040	50.200	77.400	1.000	48	30.20	375.00	16.50	0.93	0.96	7.47	8.43
8		0.349	34.90	0.061	57.650	87.850	1.000	62	264.50	474.00	20.50	4.94	1.08	8.22	9.30
9		0.405	40.50	0.056	49.800	74.450	1.000	57	40.80	324.00	13.20	1.08	1.14	6.51	7.65
10		0.445	44.50	0.040	50.600	65.650	1.000	26	107.20	379.00	14.80	2.41	0.51	7.49	8.00
11		0.494	49.40	0.049	48.700	72.500	1.000	25	38.50	464.00	16.80	1.13	0.51	9.53	10.04
12		0.549	54.90	0.055	60.700	88.300	1.000	40	55.60	501.00	18.60	1.22	0.66	8.25	8.91
13		0.597	59.70	0.048	48.900	63.300	1.000	37	53.60	451.00	15.50	1.41	0.76	9.22	9.98
14		0.646	64.60	0.049	55.900	79.900	1.000	40	11.20	420.00	16.40	0.49	0.72	7.51	8.23
15		0.697	69.70	0.051	59.000	79.750	1.000	40	42.70	552.00	19.20	1.05	0.68	9.36	10.03
16		0.745	74.50	0.048	65.200	87.150	1.000	49	35.20	623.00	20.00	0.85	0.75	9.56	10.31
17		0.799	79.90	0.054	53.800	75.350	1.000	41	16.60	471.00	15.90	0.60	0.76	8.75	9.52
18		0.899	89.90	0.041	71.100	89.800	1.000	72	24.40	649.00	19.60	0.62	1.01	9.13	10.14
19		0.899	89.90	0.060	70.750	86.500	1.000	87	392.90	646.00	19.60	5.83	1.23	9.13	10.36
20		0.946	94.60	0.047	45.700	58.050	1.000	82	53.40	481.00	14.30	1.48	1.79	10.53	12.32
21		0.998	99.80	0.052	56.500	77.750	1.000	104	79.60	530.00	18.00	1.73	1.84	9.38	11.22
22		1.048	104.80	0.050	54.550	74.100	1.000	44	36.00	342.00	11.80	0.88	0.81	6.27	7.08
23		1.102	110.20	0.053	65.750	83.700	1.000	32	16.60	301.00	10.40	0.41	0.49	4.58	5.06
24		1.153	115.30	0.052	58.500	76.850	1.000	19	4.60	181.00	6.00	0.18	0.32	3.09	3.42
25		1.197	119.70	0.043	57.000	70.950	1.000	24	12.40	105.00	4.50	0.30	0.42	1.84	2.26
26		1.242	124.20	0.045	59.200	74.650	1.000	17	7.70	117.00	4.30	0.20	0.29	1.98	2.26
27		1.299	129.90	0.057	75.200	97.700	1.000	33	8.10	104.00	4.90	0.17	0.44	1.38	1.82
28		1.340	134.00	0.041	53.300	64.250	1.000	18	13.90	66.00	3.40	0.32	0.34	1.24	1.58
29		1.388	138.80	0.049	56.800	78.600	1.000	27	10.80	68.00	3.60	0.25	0.48	1.20	1.67
30		1.449	144.90	0.061	57.200	81.800	1.000	32	14.00	140.00	8.40	0.39	0.56	2.45	3.01
31		1.491	149.10	0.042	54.000	66.500	1.000	49	15.60	122.00	7.00	0.42	0.91	2.26	3.17
32		1.551	155.10	0.060	58.250	85.000	1.000	65	24.80	174.00	10.10	0.60	1.12	2.99	4.10
33		1.597	159.70	0.046	56.500	79.050	1.000	70	65.50	200.00	11.60	1.36	1.24	3.54	4.78
34		1.641	164.10	0.044	54.250	72.800	1.000	64	135.60	293.00	15.40	2.78	1.18	5.40	6.58
35		1.688	168.80	0.047	60.700	74.500	0.800	110	52.10	384.00	24.40	1.26	1.81	6.33	8.14
36		1.709	170.90	0.021	40.750	53.750	0.800	115	132.00	276.00	19.20	3.71	2.82	6.77	9.60
37		1.740	174.00	0.030	27.000	32.500	0.500	109	76.50	239.00	14.80	3.38	4.04	8.85	12.89
38		1.757	175.70	0.017	10.300	14.500	1.000	61	41.80	138.00	9.90	5.92	5.92	13.40	19.32
39		1.817	181.70	0.060	58.500	99.450	0.660	381	1046.00	492.00	40.90	18.58	6.51	8.41	14.92

Table A5.2 Artefact analyses for Karlinga excavations (provided by R. Fullagar, pers. comm., 2002).

Karlinga - Karl-1

SPIT	STRATI- GRAPHIC UNITS	average depth below surface (m)	Depth (cm)	estimated corrected thickness (m)	volume in litres	weight in kg	estimated area excavated (m)	Sum of all artefact counts	Sum of all artefact weights (g)	No. artefacts /litre	Artefact density (g/l)
1	5	0.02	2.00	0.020	19.50	27.50	1.00	10	28.90	0.51	1.48
2	4	0.04	4.00	0.020	20.50	27.25	1.00	7	74.30	0.34	3.62
3	4	0.06	6.00	0.020	23.00	31.75	1.00	6	19.30	0.26	0.84
4	4	0.09	9.00	0.030	32.85	43.80	1.00	17	35.00	0.52	1.07
5	4	0.12	12.00	0.030	21.25	27.10	1.00	12	8.20	0.56	0.39
6B	4	0.15	15.00	0.020	26.60	34.00	0.80	16	18.50	0.60	0.70
6A	3	0.15	15.00	0.030	5.50	7.00	0.20	3	3.70	0.55	0.67
7B	4	0.18	18.00	0.020	22.50	27.50	0.80	9	8.50	0.40	0.38
7A	3	0.18	18.00	0.020	6.50	9.50	0.20	1	0.20	0.15	0.03
8	3	0.21	21.00	0.030	35.00	49.00	1.00	26	41.40	0.74	1.18
9A	3	0.24	24.00	0.010	7.00	9.50	0.20	6	3.40	0.86	0.49
9B	2	0.24	24.00	0.030	27.25	34.15	0.80	12	8.30	0.44	0.30
10	2	0.27	27.00	0.030	17.25	23.40	0.80	6	4.20	0.35	0.24
11	1	0.33	33.00	0.060	19.00	28.00	0.80	8	7.20	0.42	0.38
12	1	0.39	39.00	0.060	68.50	95.55	0.80	6	5.70	0.09	0.08
13	1	0.45	45.00	0.060	46.50	66.80	0.80	0	0.00	0.00	0.00

Karlinga - Karl-3

SPIT	STRATI- GRAPHIC UNITS	Average depth below surface cm	Estimated corrected thickness cm	Volume in litres	Weight in kg	Estimated area excavated (m)	Sum of all artefact counts	Sum of all artefact weights	No. artefacts/lit re	Artefact Density (g/L)
1	5	5.50	5.50	69.5	84.5	1.00	5	1.3	0.07	0.02
2	5	11.50	6.00	66.000	87.5	1.00	20	6.8	0.30	0.10
3	4	16.50	5.00	60.5	78.5	1.00	19	7.1	0.31	0.12
4	4	21.25	4.75	53	70	1.00	8	2.7	0.15	0.05
5	4	25.00	3.75	49.5	68	1.00	8	3.7	0.16	0.07
6	4	30.00	5.00	44.5	61	1.00	14	8.7	0.31	0.20
7	4	35.00	5.00	48	65	1.00	9	3	0.19	0.06
8	4	40.00	5.00	47.5	64	1.00	11	5.7	0.23	0.12
9	4	45.00	5.00	59	81	1.00	9	3.4	0.15	0.06
10	4	50.00	5.00	60	75	1.00	8	3.2	0.13	0.05
11	4	55.00	5.00	54.5	79	1.00	13	50.4	0.24	0.92
12	4	60.00	5.00	62.5	83	1.00	26	27.1	0.42	0.43
13	4	65.00	5.00	63	90.5	1.00	29	28.9	0.46	0.46
14	3	70.00	5.00	65	92.5	1.00	36	72.2	0.55	1.11
15	3	75.00	5.00	60.5	85.04	1.00	26	39.2	0.43	0.65
16	3	80.00	5.00	58.5	83	1.00	21	22.4	0.36	0.38
17	3	85.00	5.00	58	87.75	1.00	17	413.4	0.29	7.13
18	3	90.00	5.00	57.5	78	1.00	21	11.6	0.37	0.20
19	2	95.00	5.00	64	82	1.00	33	36.2	0.52	0.57
20	2	100.00	5.00	75.5	105	1.00	14	10.1	0.19	0.13
21	2	105.00	5.00	114	92	1.00	7	2.5	0.06	0.02
22	2	110.00	5.00	58.5	77.25	1.00	9	4.7	0.15	0.08
23A	2	115.00	1.25	9	12.5	0.20	3	27.8	0.33	3.09
23B	2	115.00	5.00	63.5	94.5	0.80	3	66.8	0.05	1.05
24	2	120.00	5.00	65	87	1.00	6	1.4	0.09	0.02
25	2	125.00	5.00	77.5	103	1.00	4	25.2	0.05	0.33
26	2	130.00	5.00	67.5	89	1.00	8	15.1	0.12	0.22
27	2	135.00	5.00	55.5	81.5	1.00	4	0.8	0.07	0.01
28	2	140.00	5.00	85.5	108.5	1.00	16	45	0.19	0.53
29	2	145.00	5.00	67.5	86.5	1.00	51	417.7	0.76	6.19
30	2	150.00	5.00	67.5	93.5	1.00	56	1185.8	0.83	17.57
31	2	155.00	5.00	77	96	1.00	51	973.8	0.66	12.65
32	2	160.00	5.00	83.5	102.5	1.00	63	292.1	0.75	3.50
33	1 and 2	165.00	5.00	84	108	1.00	83	246.7	0.99	2.94
34	1 and 2	170.00	5.00	76	97.5	1.00	69	265.8	0.91	3.50
35	1 and 2	175.00	5.00	75	95	1.00	49	184.8	0.65	2.46
36	1	180.00	5.00	73.5	91.5	1.00	32	1562.8	0.44	21.26
37	1	185.00	5.00	74.5	96.5	1.00	31	1212	0.42	16.27
38	1	190.00	5.00	71.5	96.5	1.00	30	80.1	0.42	1.12
39	1	195.00	5.00	72.5	94.5	1.00	22	167.3	0.30	2.31
40	1	200.00	5.00	71.5	96.5	1.00	8	56	0.11	0.78
41	1	205.00	5.00	63.5	85.5	1.00	8	8.5	0.13	0.13
42	1	210.00	5.00	59.5	78	1.00	6	91.2	0.10	1.53
43	1	215.00	5.00	60	84.5	1.00	3	41.8	0.05	0.70
44	1	220.00	5.00	73	111	1.00	4	10	0.05	0.14
45	1	225.00	5.00	56.5	89.5	1.00	0	0	0.00	0.00
46	1	232.75	7.75	62	na	0.25	0	0	0.00	0.00

APPENDIX SIX - PUBLICATIONS

The following manuscript **A Process-Orientated Approach to Archaeological Site Formation: Application to Semi-Arid Northern Australia** by Ingrid Ward and Piers Larcombe is published in the *Journal of Archaeological Science*, 30, 1223-1236.

Please see print copy for Appendix 6
